SOVIET PHYSICS

JETP

A translation of the Journal of Experimental and Theoretical Physics of the USSR.

SOVIET PHYSICS JETP VOL. 37 (10), NO. 6, pp. 1063-1326 JUNE, 1960

RADIOACTIVE DECAY OF Ag^{110m}

N. M. ANTON' EVA, A. A. BASHILOV, and E. K. KULAKOVSKIĬ

Leningrad State University

Submitted to JETP editor April 4, 1959

J. Exptl. Theoret. Phys. (U.S.S.R.) **37**, 1497-1505 (December, 1959)

A magnetic spectrometer study was made of the photoelectron spectrum produced by γ rays from Ag^{110m}, of the β-ray spectrum up to 530 kev, and of the spectrum of the conversion electrons corresponding to nuclear transitions with energies of 116 and 656 kev. The internal-conversion coefficients for 14 nuclear transitions in Cd^{110} and the multipolarity of the radiation were determined from the relative line intensities found in the present work and the data presented in a previous paper.[1] The decay scheme is discussed.

1. EXPERIMENTAL PROCEDURE

THE decay of Ag^{110m} was previously investigated by us[1] and by many others.[2,3] In the present work we investigated the β spectrum and the spectrum of photoelectrons due to γ rays from Ag^{110m} with a magnetic spectrometer of the "Ketron" type.[4] The radius of curvature of the principal trajectory was $\rho_0 = 20$ cm, and the source in the counter slit measured 2 × 30 mm. The divergence angle of the electron beam was 30° in the plane perpendicular to the field and ± 3° in the plane of the field. The corresponding relative half-width of the electron lines was $\Delta H\rho/h\rho = 0.5\%$. The film on the Geiger counter window passed all electrons of energy greater than 8 kev.

In the investigation of the γ radiation we used a photoelectron source with the following arrangement. A copper tube of 2 mm outside diameter and 0.4 mm wall thickness was filled with the investigated radioactive substance. The tube was then wrapped with aluminum foil (0.1 mm) and with foil of the heavy metal (platinum, lead, or bismuth) used as the photoelectron emitter. The photoelectron source was placed at the focus of the magnetic spectrometer.

The spectral sensitivity of a photoelectronic γ spectrometer with a source of this type was investigated by studying the spectrum of photoelectrons due to cascade γ rays from Sc^{46}, Co^{60} and Na^{24} and the γ rays from Sb^{124}, which have lines of well known relative intensity with $E\gamma = 603$ and 1690 kev ($I_{603} : I_{1690} = 2.00 \pm 0.05$, see reference 2). The spectral-sensitivity curve is shown in Fig. 1. The ordinates represent the quantity ϵ, the factor by which the measured relative intensities of the γ lines differ from the actual ones (the curve is normalized to unity at $E\gamma = 1368$ kev Na^{24}). The corrected relative intensities should, in accordance with the calibration curve, be calculated from the following formula

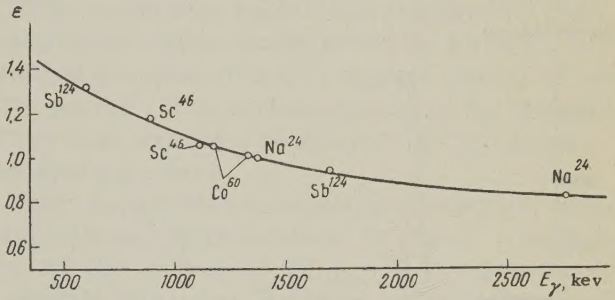

FIG. 1. Spectral sensitivity curve of the photoelectronic γ spectrometer.

$$(I_1/I_2)_{\text{corr}} = (\varepsilon_2/\varepsilon_1)\,(I_1/I_2)_{\text{meas}}.$$

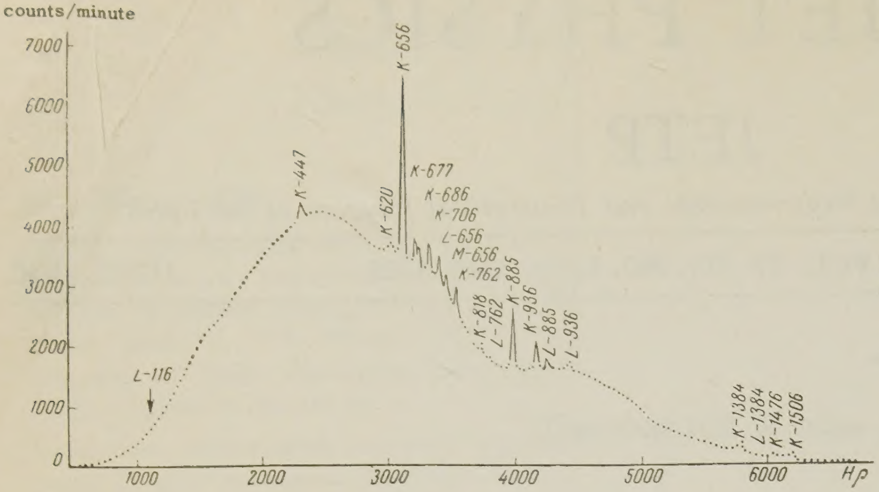

FIG. 2. Overall view of the spectrum of photoelectrons from γ rays of Ag^{110m} (bismuth emitter, σ = 3 mg/cm²).

The accuracy of the calibration curve is 10%.

2. GAMMA RADIATION FROM Ag^{110m}

Figure 2 shows the overall spectrum obtained in this investigation for the photoelectrons knocked out by Ag^{110m} γ rays from the bismuth emitter (3 mg/cm²). Rising above the continuous spectrum are a large number of sufficiently sharp and well resolved photoelectronic peaks. The continuous spectrum is due principally to Compton electrons and partly to fast β particles.

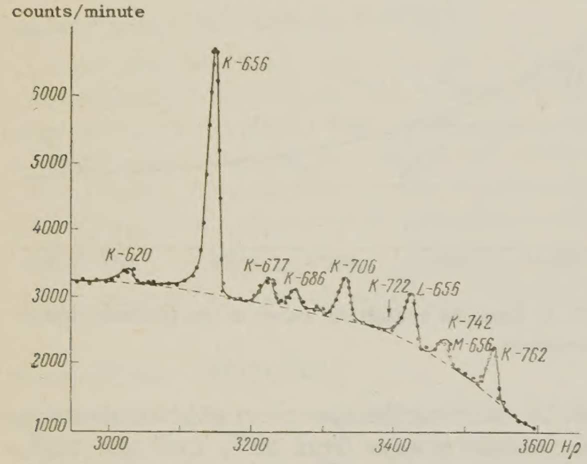

FIG. 3. Portion of the photoelectron spectrum, corresponding to γ rays with energies ranging from ~600 to ~750 kev.

Figure 3 shows the portion of the photoelectron spectrum corresponding to γ rays of energies E_γ = 620, 656, 677, 686, 706, and 762 kev. We note that earlier, in the investigation of the spectrum of conversion electrons,[1] we observed a weak transition with energy E_γ = 742 kev. In the photoelectron spectrum given here, the line K-742 coincides with the rather strong line M-656.

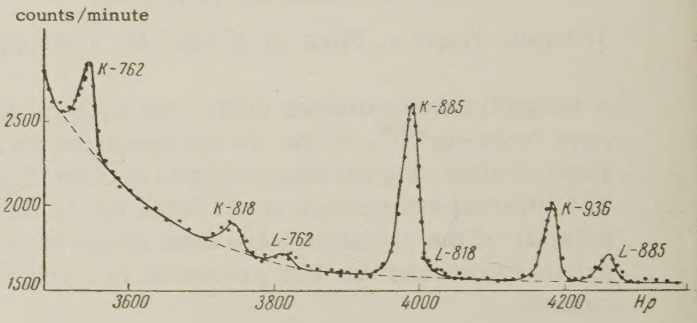

FIG. 4. Portion of the photoelectron spectrum, corresponding to γ rays with energies ranging from ~700 to ~950 kev.

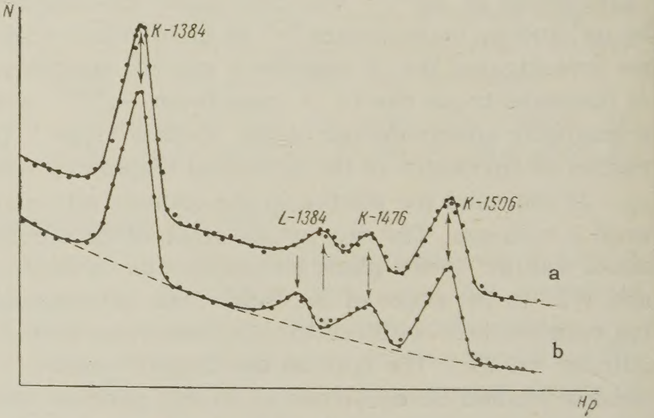

FIG. 5. Portion of the photoelectron spectrum, corresponding to γ rays with energies 1384, 1476, and 1506 kev. The curve a was obtained with a lead emitter, curve b with a platinum emitter. The curves are shifted (along the energy axis) to make the peaks of the corresponding K photoelectron lines coincide.

Figure 4 shows the portion of the photoelectron spectrum corresponding to γ rays with E_γ = 762, 818, 885, and 936 kev. Figure 5 shows the result of two series of measurements for hard γ rays with E = 1384, 1476, and 1506 kev: curve a was obtained with a lead emitter, and curve b with a platinum one. The curves are shifted along the energy axis to make the corresponding K photo-

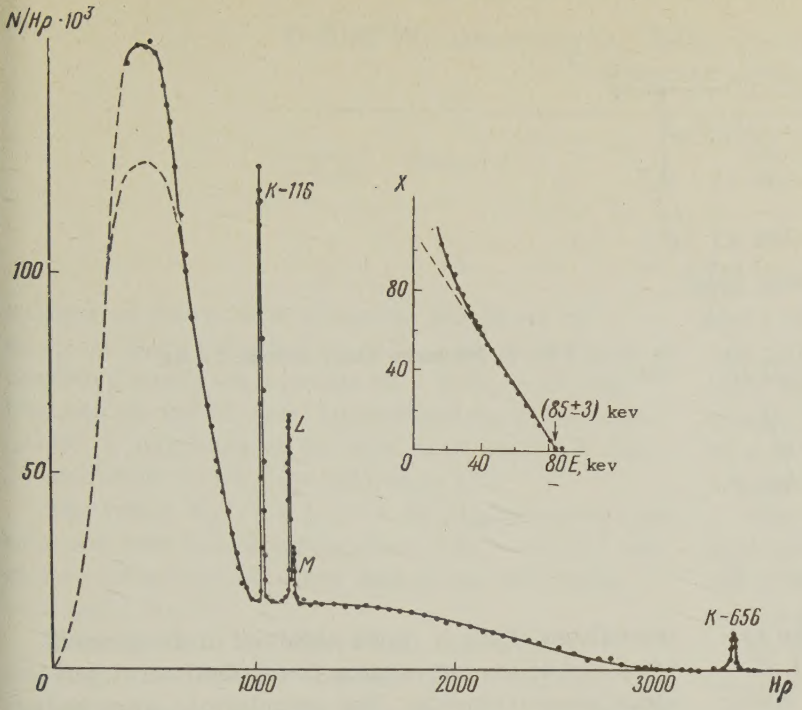

FIG. 6. Beta spectrum of Ag^{110m} up to 600 kev (source with $\sigma \sim 10\ \mu g/cm^2$). In the upper right is shown the Fermi plot for the soft component of the β spectrum ($X = \sqrt{N\delta/E_\beta F}$).

electron peaks coincide (this does not make the positions of the L peaks coincide).

The determined relative intensities of the γ rays from Ag^{110m} are shown in Table I, where they are compared with data by others. The most complete and reliable results were obtained by Dzhelepov and Zhukovskiĭ[5] with the aid of the "Elotron" magnetic spectrometer, which employs recoil electrons. As seen from Table I, the agreement between our data and those of Dzhelepov and Zhukovskiĭ is very good.

TABLE I

γ-line energy, kev	Relative intensities of Ag^{110m} γ rays,			
	Siegbahn,[6] (photo-electrons)	Dzhelepov et al.[5] (recoil electrons)	Knipper[7] (scintillation spectra)	Our data (photo-electrons)
447	—	—	7**	6.4±0.8
620	—	—	10**	3.9±0.5
656	100	100	100	100
677	~17*	13±2	32**	10±1
686	—			7±1
706	~17*	18±2		20±2
742	—	6±2		—
762	⩾17*	23±2	24	25±3
818	~6*	9±1	6**	8±1
885	81	75±4	75	78±8
936	31	32±2	25	37±4
1384	33	28±2	20	26±3
1476	—	6±1	13	5±1
1506	17	15±1		13±1
1560	—	1.3±0.2	—	—

---

*Estimated by Siegbahn from the intensities of the conversion lines under the assumption that all the transitions have equal multipolarity

**Error 50%; error of other values 25%.

3. BETA RADIATION OF Ag^{110m}

In the present investigation we studied the β spectrum up to 530 kev and the conversion lines corresponding to nuclear transitions with energies 116 and 656 kev.

The β-particle source was prepared by thermally sputtering activated silver on a slightly aluminized collodion film with surface density of several $\mu g/cm^2$. The surface density of the sputtered silver also amounted to several $\mu g/cm^2$ (semi-transparent layer).

The β-particle and conversion-electron spectrum obtained by us is shown in Fig. 6. The Fermi plot for the component E_{lim} = 85 kev deviates from a straight line below ~40 kev. In the determination of the area of the β spectrum we therefore extrapolated the distribution curve to the energy region below 40 kev in accordance with the Fermi formula. The Fermi plot for the component of the β spectrum with end-point energy 530 kev is likewise not fully linear.

The data we obtained on the β radiation of

TABLE II. Radiation of Ag^{110m}

E_{rp}, kev	85±3	530±5	400±100*	2200±50 *	2285±25 *
Relative intensity, percent	64	34	(0.2)	0.2	1.5
log fT	5:4	8.1	(4.5)	5.1	4.7

---

*Obtained from the analysis of the β spectrum in reference 1.

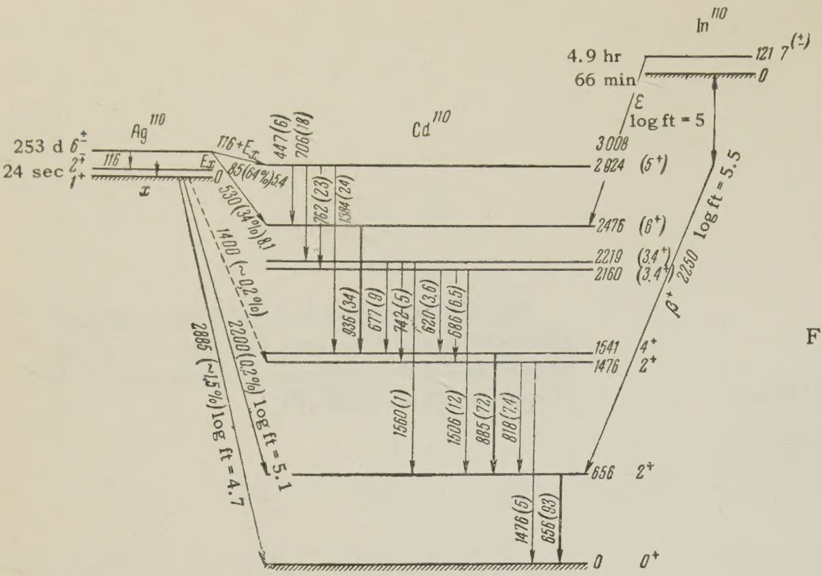

FIG. 7. Proposed decay scheme for Ag^{110}.

Ag^{110m} are given in Table II, together with the results of an analysis of the high-energy region of the β spectrum of Ag^{110m} ($E_\beta > 530$ kev), investigated in our earlier paper.[1] The intensity of the β component with $E_{lim} = 1400$ kev is apparently overvalued, owing to the Compton electrons knocked out by the γ rays with $E_\gamma = 1384 - 1506$ kev from the source material and from the walls of the apparatus. Comparison with literature data[2,3] shows that our data are in good agreement with the most probable results of other authors for β radiation of Ag^{110m} and Ag^{110}.

4. INTERNAL CONVERSION COEFFICIENTS

In the present experiments, the ratio of the number of conversion electrons to the number of β particles was found to be $e_{K-656}/\beta = (2.5 \pm 0.3) \times 10^{-3}$ for a transition with energy 656 kev. If we assume, as is done below in the discussion of the decay scheme, that the number of nuclear transitions with $E_\gamma = 656$ kev amounts to 0.93 per decay (see Fig. 7), we obtain for the coefficient of internal conversion of this transition a value $\alpha_{K-656} = (2.7 \pm 0.3) \times 10^{-3}$. This value coincides, within the experimental accuracy, with the theoretical value of the coefficient of internal conversion for E2 transitions. According to the known systematics of the lower excited levels of even-even nuclei, the first level of the nucleus $_{48}Cd^{110}$ should be of the type 2^+ with a corresponding transition multipolarity E2. Values of 2.5 and 2.2 ± 0.8 are found for $\alpha_{K-656} \times 10^3$ in the literature.[2,3] These are in satisfactory agreement with our data and with the foregoing interpretation of the $E_\gamma = 656$ kev transition.

The coefficients of internal conversion of the remaining γ rays were determined from the relative intensities of the γ lines obtained in the present work and of the conversion lines obtained in previous measurements. The calculations were based here on the theoretical value $\alpha_{K-656} = 2.75 \times 10^{-3}$ for the E2 transition. The results of the calculations of α_K are given in Table III. This table lists also the theoretical values of α_K given by Sliv and Band for transitions of various types. Conclusions regarding the multipolarity of the γ radiation of Ag^{110} are drawn from a comparison of the theoretical and experimental values of α_K. As can be seen from the table, all the observed transitions can be essentially classified as M1, E2, or a mixture of the two.

TABLE III

E, kev	$\alpha_K \cdot 10^3$			
	experiment	theory		
		α_1	α_2	β_1
447	7.3±1.5	2.4	7.9	7.7
620	2.5±0.5	1.1	3.2	3.5
656	2.7±0.3	1.0	2.75±0.05	3.05±0.05
686	3.1±0.6	0.91	2.4	2.7
706	2.2±0.4	0.86	2.3	2.6
762	1.8±0.4	0.73	1.9	2.2
818	1.3±0.3	0.63	1.6	1.8
885	1.2±0.3	0.54	1.3	1.5
936	1.0±0.2	0.49	1.2	1.3
1384	0.65±0.15	0.24	0.50	0.57
1476	0.44±0.10	0.21	0.44	0.49
1506	0.52±0.10	0.20	0.42	0.48

5. THE E = 116 kev ISOMER TRANSITION

The nuclear transition with E = 116 kev corresponds to a de-excitation of the metastable state Ag^{110m}. The lower limit for the coefficient of internal conversion was found to be $\alpha_{K-116} > 60$. Thus, practically all the isomer transitions proceed via emission of conversion electrons. The

TABLE IV. Determination of the type of isomer transition with E = 116 kev in Ag^{110}

Compared quantities	Experiment	Theoretical values					Possible type of transition
		$E4$	$E5$	$M3$	$M4$	$M5$	
$K:L$	2.1 ± 0.1	0.60	0.25	3.6	2.0	1.1	$M4$
α_K	>60	23	134	15	103	740	$M4$, $E5$, $M5$

number of conversion electrons per decay is $e_{K+L+M}/\beta = (1.5 \pm 0.2) \times 10^{-2}$, i.e., the number of isomer transitions amounts to ~ 1.5% of all Ag^{110m} transitions and is equal approximately to the number of β particles of the hard components of the β spectrum (~ 2%, see reference 1).

The value $K/L = 2.1 \pm 0.1$ is in good agreement with our previous determination ($K/L = 2.2$),[1] but differs greatly from other data in the literature (1.3 and 1.2).[2,3]

Table IV lists the theoretical values of K/L and α_K given by Sliv and Band for transitions of various types. From the table we can conclude that the E = 116 kev nuclear transition in the Ag^{110} nucleus is of the M4 type. In explaining this transition, however, we encounter certain difficulties. The point is that the spin of the metastable level of Ag^{110m} has recently been measured[2,3] and found to equal 6. At the same time it follows from the β decay of the ground state of Ag^{110} that the spin of the latter cannot be greater than unity (cf. decay scheme, Fig. 7). To explain the M4 transition with E = 116 kev it is therefore natural to propose that it corresponds to a transition from the metastable level not to the Ag^{110} ground level, but to some excited level x with a low energy and spin 2.* From a consideration of the energy balance of the decay scheme one would expect the energy of the proposed level x to be less than 30 kev. The difficulty in observing low-energy transitions may probably explain why the corresponding transition has not been observed. We note that in the case of Ag^{110} there exists a level with E = 18.5 kev.[2,3]

6. ON THE DECAY SCHEME OF Ag^{110m}

A decay scheme was first proposed for Ag^{110m} by Siegbahn in 1950.[6] In later works somewhat modified and more complete decay schemes were proposed.[2,3,5]

In Fig. 7 we consider one of the possible versions of the decay scheme of Ag^{110m}. This scheme includes all the nuclear transitions observed by us, but does not include the weak transitions noted by Cork and his associates:[9] E_γ = 438, 471, 499, 542, and 575 kev, and also hard radiation with $E_\gamma > 1560$ kev. The version proposed for the level scheme of Cd^{110} differs from that proposed earlier[2,3,5,6] principally in that the $E \approx 1420$ kev level is replaced by a 2160 kev level. This enabled us to fit the transitions E_γ = 620 and 686 kev in the scheme.

The energy balance in the scheme of Fig. 7 is accurate to approximately ±3 kev. The balance of the intensities of β and γ transitions is within the limits of error.

No definite conclusions can be drawn concerning the spins of the Cd^{110} levels. The most reliable estimates can be made regarding the first two levels with energies 656 and 1476 kev. These levels were obtained by Coulomb excitation[2,3] and it is therefore natural to assume that they are vibrational collective levels and that they both must be assigned the quantum characteristics 2^+.

We point out that attempts were made to determine the level spins directly by the method of angular correlations,[2,3] but these led to inconsistent results. Therefore conclusions regarding the quantum characteristics of the remaining excited levels must be drawn principally from data on the β decay and the multipolarity of the nuclear transitions.

It is necessary to account above all for the fact that the multipolarities of all the observed transitions are of the M1 and E2 type, and therefore the parities of all the excited levels of Cd^{110} (Fig. 7) should be the same as the parity of the ground state, which is even. The β transition from the Ag^{110m} metastable state to the upper level of Cd^{110} with energy E = 2925 kev is characterized by log fT = 5.4. Since the spin of the metastable level is $6^{\pm}$,[2,3] the spin of this Cd^{110} level is probably 5, 6, or 7 ($^+$). The value 7 can apparently be discarded, since a transition E_γ = 1384 kev of type M1, E2 is observed from this level to the level E = 1540, which cannot have a spin greater than 4. A spin value of 6 can apparently also be excluded, since there is no transition of noticeable intensity from the 5-hour In^{110m} (the spin measured by Marino et al.[10] is equal to 7) to the Cd^{110} level under consideration.[2,3] The spin of the E = 2925 kev level is probably therefore 5^+.

Furthermore, the β transitions from the Ag^{110m} metastable state to the Cd^{110} level with E = 2476 kev is characterized by log fT = 8.1. The possible values of this level are 4, 5, 6, 7 and 8 $(^{+})$. The values 4 and 5 can apparently be discarded, for the K capture in the 5-hour In^{110} at this level is either allowed or first-forbidden, since log fT = 5.5. Spin values of 7 and 8 must apparently also be discarded, since a transition E = 936 kev of type M1, E2 is observed from this level to the level E = 1540 kev, which cannot have a spin greater than 4. Thus, the spin of the E = 2476 kev level is probably 6^{+}.

---

*An analogous assumption was stated in Zhukovskiĭ's dissertation.[8]

The spins of the 2220 and 2160 kev levels can apparently be 3^{+} or 4^{+}. These spin values agree with the multipolarities of the γ transitions, connected with these levels, and also with the absence of β transitions from the Ag^{110m} metastable state.

In conclusion, the authors consider it their pleasant duty to thank V. K. Adamchuk, who participated in the calibration of the γ spectrometer, and to M. A. Dolgobrodova for aid in measurements of the photoelectron spectrum.

Note added in proof (November 2, 1959). After our article went to press, we learned of new investigations[11,12,13] of Ag^{110m}. In reference 11 the interpretation of the isomer transition in Ag^{110} and the placement of the Cd^{110} levels are similar to ours, but a different spin is assigned to the 2476-kev level. In reference 13, the method of angular γ correlations is used to confirm the characteristics of the Cd^{110} levels proposed by us. However, the classification of the isomer transition in Ag^{110} as a type M5 contradicts our value of K/L = 2.1.

[1] Anton'eva, Bashilov, and Dzhelepov, Dokl. Akad. Nauk SSSR **77**, 41 (1951).

[2] B. S. Dzhelepov and L. K. Peker Схемы распада радиоактивных ядер, (Decay Schemes of Radioactive Nuclei) U.S.S.R. Acad. Sci., 1958, p. 302.

[3] Strominger, Hollander, and Seaborg, Revs. Modern Phys. **30**, 585 (1958).

[4] B. S. Dzhelepov and A. A. Bashilov, Izv. Akad. Nauk SSSR, Ser. Fiz. **14**, 263 (1950).

[5] B. S. Dzhelepov and N. N. Zhukovskiĭ, Nucl. Phys. **6**, 655 (1958).

[6] K. Siegbahn, Phys. Rev. **77**, 233 (1950).

[7] A. Knipper, Proc. Phys. Soc. **71**, 77 (1958).

[8] N. N. Zhukovskiĭ, Dissertation, Radium Inst. Acad. Sci. Leningrad, 1958.

[9] Cork, Rutledge, Branyan, Stoddard, Childs, and LeBlanc, Phys. Rev. **80**, 286 (1950).

[10] Marino, Ewbank, Nierenberg, Shugart, and Silsbee, Phys. Rev. **111**, 286 (1958).

[11] E. G. Funk and M. L. Wiedenbeck, Phys. Rev. **112**, 1247 (1958).

[12] H. W. Taylor and S. A. Scott, Phys. Rev. **114**, 121 (1959).

[13] H. W. Taylor and W. R. Frisken, Phys. Rev. **114**, 127 (1959).

Translated by J. G. Adashko
308

SOVIET PHYSICS JETP VOLUME 37(10), NUMBER 6 JUNE, 1960

INVESTIGATION OF THE THERMAL PROPERTIES OF SUPERCONDUCTORS. III. ANISOTROPY OF THE THERMAL CONDUCTIVITY OF GALLIUM

N. V. ZAVARITSKIĬ

Institute for Physical Problems, Academy of Sciences, U.S.S.R.

Submitted to JETP editor May 13, 1959

J. Exptl. Theoret. Phys. (U.S.S.R.) **37**, 1506-1516 (December, 1959)

The thermal conductivity of gallium in the normal and superconducting states has been measured along different crystallographic directions. The anisotropy observed in the temperature dependence of the electron thermal conductivity in the superconducting state is related to the anisotropy in the gap width in the excitation energy spectrum. The results of measurement of the critical magnetic field of gallium are presented.

INTRODUCTION

EXPERIMENTS thus far carried out have shown that both the electronic specific heat and the electron thermal conductivity of a superconductor decrease exponentially with the temperature. This result agrees with the conclusions of contemporary superconductivity theory[1,2] on the presence of an energy gap separating the ground state of electrons in the superconductor from the excited states. However, while, according to the theory, the width of the gap Δ should be uniquely determined by the critical temperature of the superconductor T_c, comparison of the properties of different metals, given in reference 3, points to a certain change of Δ/T_c from one superconductor to another, a change which can be connected with the ratio T_c/Θ_D (Θ_D = Debye temperature), characterizing the value of the coupling parameter between electrons. It was not, however, made clear in reference 3, nor in other similar researches,[4] to what extent one could attribute a definite value of Δ to each metal, whether perhaps there was not in real superconductors an appreciable anisotropy of the energy spectrum of the excited states of the electrons. The present investigation was undertaken for the purpose of obtaining an answer to this question.

The singularities of the energy spectrum appear most strikingly in the temperature range appreciably below the critical temperature, where the number of excited states is small. The appearance of anisotropy at these temperatures should be expected in the anisotropy of absorption of the electromagnetic field of frequency $\Delta k/h$,* in the anisotropy of ultrasonic absorption, and in the anisotropy of the electronic thermal conductivity of the superconductor K_{es}. The latter effect was chosen for study. This effect had already been observed earlier in a study of tin,[5] but any sort of detailed investigation has been lacking.

Anisotropy of thermal conductivity can appear in the change (with change in crystallographic directions) of both the absolute value of K_{es} and also its temperature dependence. Inasmuch as the anisotropy of the properties of a metal in the normal state already leads to the first effect, the study of the second effect is of greater interest. For this purpose measurements are required in the widest possible temperature range. However, the thermal conductivity of electrons is sharply reduced with decrease in temperature, as a result of which the lattice begins to play the dominant role in the transfer of heat in the region of very low temperatures. Therefore, it was preferable in the measurements to make use of superconductors with a maximum ratio of K_{es}/K_g (K_g = lattice thermal conductivity) or (what amounts to the same thing) with a minimum ratio T_c/Θ_D. Cadmium, zinc, aluminum, gallium and rhenium best satisfy this condition. Of the metals enumerated, there was an especially large anisotropy of properties for gallium which was also chosen for the study of reference 6.

Gallium crystallizes in a rhombic lattice,[7] the axes of which are a = 4.5258 A, b = 4.5198 A, c = 7.6602 A. The position of the atoms in the elementary cell is determined by the coordinates

$$(m\,0\,p),\ (m+{}^1/_2\,{}^1/_2\,\bar{p}),\ (\bar{m}+{}^1/_2\,{}^1/_2\,p),(\bar{m}\,0\,\bar{p}),\ (m\,{}^1/_2\,p+{}^1/_2),$$

$$(m+{}^1/_2\,0\,\bar{p}+{}^1/_2),\quad (\bar{m}+{}^1/_2\,0\,p+{}^1/_2),\quad (\bar{m}\,{}^1/_2\,\bar{p}+{}^1/_2),$$

where m = 0.0785, p = 0.1525.

---

*Here and below, the gap width Δ is given in units of °K.

TABLE I. Characteristics of specimens studied

Specimen*	Diameter of the specimen, mm	K_0, $\frac{w}{deg^2\text{-}cm}$ [Eq. (1)]	$\alpha \cdot 10^4$ cm/w-deg [Eq. (1)]	$\rho_0/\rho_{293\,°K}$	β
a – 1DI	1.8	$1.02 \cdot 10^{-1}$	—	$1.4 \cdot 10^{-2}$	1.30
a – 2PI	1.5	14	5.5	$8.2 \cdot 10^{-5}$	1.49
b – 1DI	1.6	$2.5 \cdot 10^{-1}$	—	$1.25 \cdot 10^{-2}$	1.40
b – 2PI	1.4	22.4	—	$1.4 \cdot 10^{-4}$	1.40
b – 3II	1.7	7.4	—	$4.1 \cdot 10^{-4}$	1.47
c – 1DI	2	$2.35 \cdot 10^{-2}$	—	$1.9 \cdot 10^{-2}$	1.1
c – 2PI	2	6.03	15	$7.4 \cdot 10^{-5}$	1.21
c – 3PI	1.5	6.45	15	$6.9 \cdot 10^{-5}$	1.19
c – 4PII	0.7	4.65	—	$1 \cdot 10^{-4}$	1.22
c – 5DII	1.7	$3 \cdot 10^{-2}$	—	$1.55 \cdot 10^{-2}$	1.17
Series** 2P					
b		72	1.7	$4.3 \cdot 10^{-5}$	1.46
c		6.0	15.5	$7.4 \cdot 10^{-5}$	1.16
b***	1.6	52.5	1.8	$4.9 \cdot 10^{-5}$	—
a		29.5	3.8	$4.8 \cdot 10^{-5}$	1.35
Series 3D					
b		$3.7 \cdot 10^{-2}$		$8.5 \cdot 10^{-3}$	—
c		$3.1 \cdot 10^{-2}$	—	$1.5 \cdot 10^{-2}$	1.17
a	3	$1.8 \cdot 10^{-1}$	—	$7.8 \cdot 10^{-3}$	1.40
b		$3.7 \cdot 10^{-1}$	—	$8.5 \cdot 10^{-3}$	1.53
c		$3.2 \cdot 10^{-2}$	—	$1.45 \cdot 10^{-2}$	1.17
Series 4D					
c	1	$2.5 \cdot 10^{-2}$	—	$1.8 \cdot 10^{-2}$	1.15
a		$1.35 \cdot 10^{-1}$	—	$1 \cdot 10^{-2}$	1.35

*a, b, c are the crystallographic directions along which the specimen was grown; D, P designate the state of the metal used; I, II indicate the method of preparation of the specimen.

**The specimens of a single series are shown in the order of their study.

***The departure of the specimen from the crystallographic direction amounted to 10°.

SPECIMENS AND METHOD OF MEASUREMENT. RESULTS

The samples were made of metal with ~ 0.1 per cent (mainly Si, P, K, Ca, Al, Ti, V) and ~ 0.001 per cent impurity.* The samples were single crystals of length ~ 50 mm and diameters from 0.7 to 3 mm, ground by the method of Kapitza[8] along the principal crystallographic directions of the gallium lattice (with an accuracy ~ 10°). The orientations of the priming wires and the samples were tested by their resistivity † at 20° C and by means of x-rays. The perfection of the single crystals obtained was tested by the angular dependence of the change in a magnetic field of their thermal and electrical conductivity at 4.2° K. The samples were ground either (I) in a graphite mold, or (II) in a tube of paper of thickness 50 μ, which was not removed from the specimen during the course of the measurement. A series of measurements was usually carried out on the samples obtained by the second method, in which one sample was successively recrystallized in all directions. In research with the higher purity gallium, before each crystallization the metal adjacent to places of soldering of the specimen to heaters, thermometers and apparatus (the thermometers were soldered to arms brought out through openings in the walls of the paper tube) was removed (in order to avoid the possibility of contamination). The geometric measurements of specimens prepared in tubes were determined by their resistance at a temperature higher than the melting point of gallium. The fundamental characteristics of all specimens studied are given in Table I.

The method of measurement of thermal conductivity did not differ essentially from that used previously.[10] The results of the measurement of the thermal conductivity of a series of samples are shown in Figs. 1 and 2. The range of measurements for some of these extended only over the part of the temperature range below 1° K, since the sensitivity of the apparatus only permitted a measurement less than several w/cm-deg with sufficient accuracy (~ 10 per cent).

During measurements in a magnetic field, it was noted that the value of the critical magnetic field H_c of gallium, determined by Goodman and Mendoza,[11] at T ~ 0.2°K, was up to ~ 15 per

---

*Samples prepared from a metal with the smaller amount of impurity are marked in what follows by the letter P; samples prepared from metal with the higher impurity, by the letter D.

†In the determination of the orientation of the specimens by means of their resistivity, the data of Powell[9] (see below) on the anisotropy of the electrical conductivity of gallium at 20°C were used.

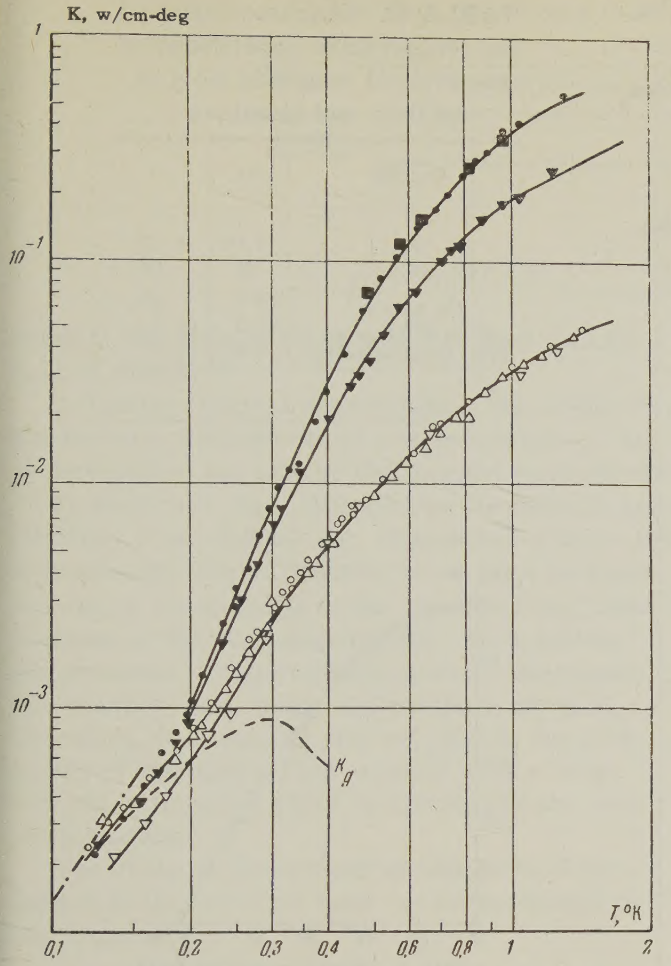

FIG. 1. Thermal conductivity of gallium along the principal crystallographic directions. Samples of the series 3D in the direction: ▼ – a, ●, ■ – b, ○, △ – c (repeated samples are indicated by different signs); △ – sample c–5D. The dot-dash curve is the limiting value of the lattice thermal conductivity, computed by the relation (2); the dashed curve is the lattice thermal conductivity K_g of the specimens c–3D.

cent lower. In view of this fact, additional experiments were undertaken with the view of making more precise the dependence $H_c(T)$. In these experiments, the transition of the specimen from the normal to the superconducting state and return was established by the change in the mutual inductance of coils inside which the specimens were located. The change in the measurement of the temperature was carried out as has been described earlier;[10] the magnetic field generated by the Helmholtz coils was directed along the axis of the specimen. The results of the measurements, which substantiate the data obtained in the determination of thermal conductivity, are shown in Fig. 3. The principal quantities characterizing the dependence $H_c(T)$ are given in Table II, together with the proportionality constant γ between the electron specific heat in the normal state and the temperature, computed on the basis of these measurements. The results of the measurement of H_c for aluminum obtained on the same apparatus are also shown; within the limits of accuracy these are in agreement with the results previously obtained (see the work of Cochrane and Mapother[12]).

DISCUSSION OF RESULTS

As is seen from Figs. 1 and 2, the absolute value of this thermal conductivity of gallium and the law of its temperature dependence are functions of the crystallographic directions. Since this phenomenon has been observed in a large number of samples, prepared in different ways, it is difficult to explain it on a random basis.

1. Thermal conductivity in the normal state. For comparison with the absolute values of the thermal conductivity of specimens grown along the different crystallographic directions, it is most suitable to make use of data obtained at temperatures above the critical. As is well known,[13] the thermal conductivity of electrons* in the normal state K_n can be represented in the region of sufficiently low temperatures by the expression

$$T / K_n = 1 / K_0 + \alpha T^3, \tag{1}$$

where the first term results from the scattering of the electrons on defects in the crystalline lattice ($K_0 = L/\rho_0$, where ρ_0 = residual resistance, L = Lorentz constant), while the second is determined by the scattering of electrons on thermal vibrations. Equation (1) gives a satisfactory description (see Fig. 4) of the change of the thermal conductivity of the specimen in the normal state that we examined. The values of α, K_0 and $\rho_0/\rho_{293°K}$ of α over all samples grown in one crystallographic direction is given in Table III. The average of the values obtained for α and the results of measurement of α in the region of hydrogen temperatures[14] (see Table III) confirm the conclusion of Rosenberg[15] on a certain decrease of this quantity in gallium with decrease in temperature.

The data in Fig. 4 and Table I enable us to compare the role of the various processes in electron scattering. It is shown that in all samples at temperatures below 2°K, the scattering of electrons on thermal vibrations is negligible in comparison with their scattering from lattice defects. This is even more the case in the superconducting state (below 1.08°K). Therefore, we are primarily interested in data on the anisotropy of the quantity K_0 or the value of the residual resistance. They

---

*The lattice thermal conductivity in the normal state in all the specimens that we examined was negligible.

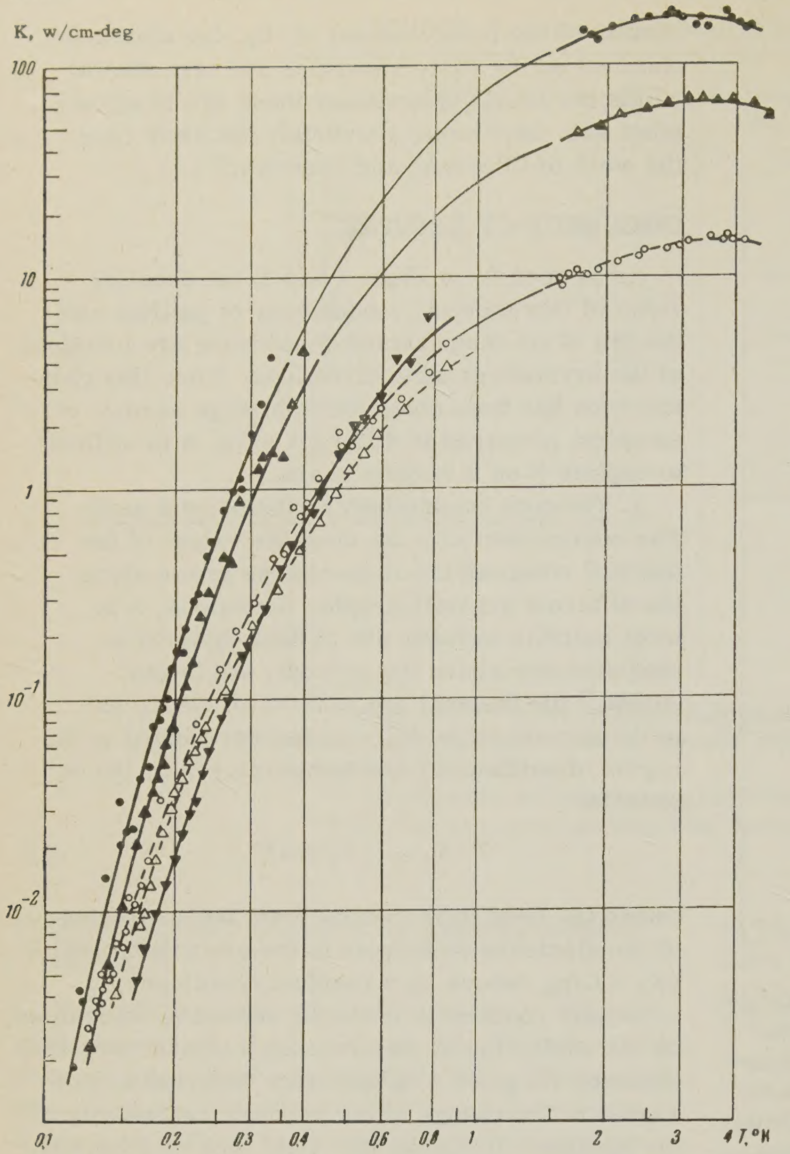

FIG. 2. Thermal conductivity of gallium samples of series 2P in the principal crystallographic directions: ▲ – along a, ● – along b, ○ – along c; ▼ – specimen b–3P; △ – specimen c–4P.

can be obtained from the results of the measurement of a series of samples. In this case, the samples of every orientation are prepared from a single piece of metal and the difference in the values of K_0 cannot be attributed to difference in purity of the initial material. No substantial change in their purity takes place in the process of multiple recrystallization, for proof of which we have the absence of an appreciable change in the ratio $\rho_0/\rho_{293°\,K}$ (see Table I) for specimens of given orientation studied at the beginning and the end of the series. All this allows us to connect the observed anisotropy of the quantity K_0 for a series of specimens with the properties of the metal itself. As is seen from Table III, the anisotropy of the conductivity of gallium in the region of low temperatures is somewhat larger than that

TABLE II. Characteristics of the temperature dependence of the critical magnetic field of gallium and aluminum

Quantity	Ga	Al
T_c	1.08	1.175
$(dH_c/dT)_{T=T_c}$	—92	—163
$H_{c,\,T\to 0°\,K}$	59.5	104
$(dH_c/dT^2)_{T\to 0°\,K}$	56.5	81.5
$10^3\gamma$, ∂ j/g-mole-deg²	0.63	1.3

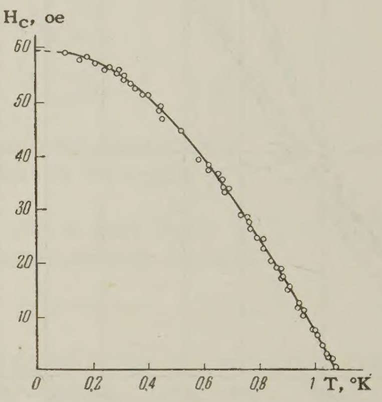

FIG. 3. Critical magnetic field of gallium.

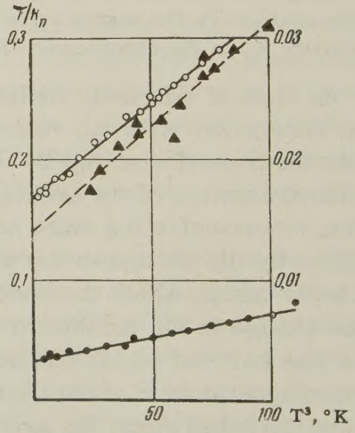

FIG. 4. Temperature dependence of the thermal conductivity of specimens of gallium in the normal state. Series 2P. ● – specimen along a, ▲ – along b, ○ – along c. For the samples a–2P and c–2P, the ordinate is at the left, for the sample b–2P, at the right.

TABLE III. Anisotropy in the conductivity of gallium in the normal state

Crystallographic Direction	Relative anisotropy of the conductivity					$\alpha \cdot 10^4$	
	Region of residual resistance				At 293°K from ref. 9	At 2–4.2 °K	At 7–17°K by reference 14
	Series 2P	Series 3P	Series 4P	Mean value			
c	1	1	1	1	1	15	36.7
a	5	5.7	5.4	5.4	3.2	4.6	14.2
b	12	11.8	—	12	7	1.7	3.5

close to the melting point, which agrees with the data of Powell.[16]

2. Lattice thermal conductivity. The value of the thermal conductivity of a superconductor K_s is determined not only by the thermal conductivity of its electrons K_{es}, but also by the thermal conductivity of the lattice K_g. Separation of these two mechanisms of heat transfer is the first problem arising in the analysis of the results of the measurement of thermal conductivity. As is known,[5] the presence of impurities in a metal decreases the quantity K_{es} more so than the quantity K_g; therefore, it is easy to pick out K_g in the properties of specimens from a metal with a large amount of impurity which is principally the case in this section.

The value of the thermal conductivity of the lattice in the isotropic case can be expressed by the formula

$$K_g = \tfrac{1}{3} Cul, \tag{2}$$

where C is the heat capacity of the lattice per unit volume, u = speed of the phonons, l = free path length. After substitution of numerical values for gallium, we have, under the assumption of a Debye temperature of 330°K,

$$K_g = 0.46 T^3 l \text{ W / cm-deg.} \tag{2a}$$

For specimens with a rough surface, the mean free path of the phonons does not exceed the diameter of the specimen; therefore, substituting the diameter of the specimen in Eq. (2a), we obtain the limiting values for the lattice thermal conductivity, which for specimens of maximum diameter (3 mm) are shown in Fig. 1 (dot-dash line). For temperatures ~0.2°K, the thermal conductivity of the samples is close to this value. For these same specimens the lattice thermal conductivity can play the dominant role in heat conduction. This is also evidenced by the change in the heat conductivity with diameter of the specimen, which is characteristic for the appearance of a lattice thermal conductivity and which is especially evident for the samples c-D at temperatures below 0.3°K.

Since $K_s = K_{es} + K_g$, we can, by making use of the dependence $K_{es}(T)/K_{T_c}$ (see below), determine the value of the lattice thermal conductivity. The results of this calculation for the sample c-3D are given in Fig. 1 (dashed line). The character of the change of the lattice thermal conductivity of gallium with temperature is similar to that observed for other superconductors. Comparison of the absolute value of K_g (at ~0.15°K) for the directions a, b, and c has shown that the lattice thermal conductivity of gallium in the direction b is smaller by a factor of 1.5 – 2 than in the other directions. This result is substantiated by measurements of the thermal conductivity of these specimens in the intermediate state. In all probability the anisotropy of K_g is brought about by the appearance of an anisotropy in the energy spectrum of the phonons of the crystalline lattice for gallium, in the presence of which Eq. (2) takes on a more complicated form.

Since both the lattice and the electron play an important role in the transfer of the heat for contaminated samples, data on their thermal conductivity can be used for the determination of K_{es} only in a limited range of temperatures, where $K_{es} > K_g$. Therefore, in what follows, for the determination of the thermal conductivity of electrons in samples grown along the direction b, a and c out of the more impure metal, only the results of measurements in the temperature intervals above ~0.2, 0.3, and 0.4°K, respectively, were used. Here the correction to the quantity K_g did not exceed ~20 per cent. The situation was somewhat different in the case of samples from metal with lower amounts of impurity, the thermal conductivity of which exceeds by a factor of 10 the thermal conduction of the specimens made out of the more impure metal, over the entire range of measurement. For these specimens, the character of the change of K_s with temperature is determined only by the properties of the electrons of the superconductor; there is no need of a correction for the thermal conductivity of the lattice.

3. Thermal conductivity of electrons. Let us investigate the temperature variation of the thermal

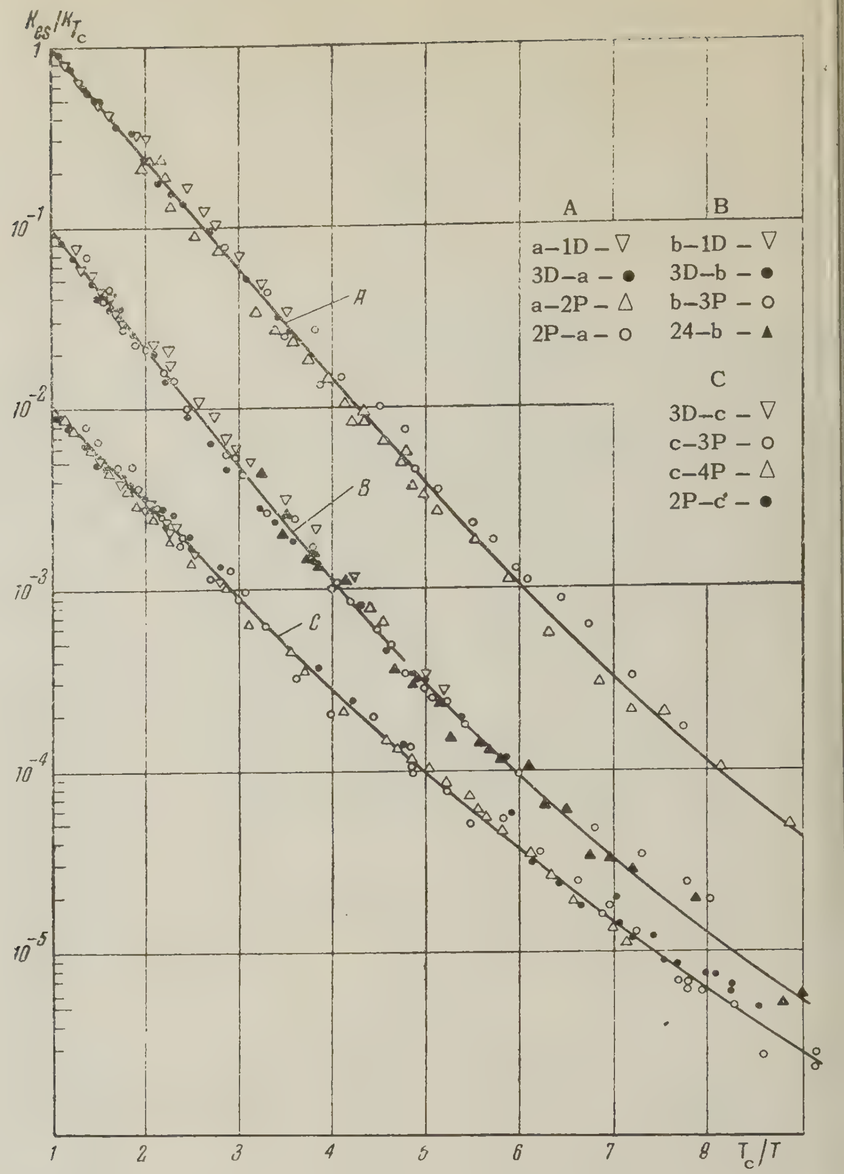

FIG. 5. Temperature variation of the thermal conductivity of electrons of gallium in the superconducting state in the principal crystallographic directions. For curves B and C the zero on the ordinate axis has been displaced by 10 and 100 divisions respectively.

conductivity of the electrons K_{es}. The thermal conductivity of the critical temperature K_{T_c} differs by a factor of more than 100 over the various samples investigated (see Figs. 1 and 2); therefore, we shall study the ratio K_{es}/K_{T_c}. We obtain the value of K_{T_c} for the purest samples by extrapolation of the data on its thermal conductivity in the normal state.

The ratio K_{es}/K_{T_c} is given in Fig. 5 for most of the samples investigated. Over the temperature range from T_c to $\sim 0.25\,T_c$ there is, in first approximation, a direct proportionality between $\log(K_{es}/K_{T_c})$ and T_c/T. The coefficients of proportionality β, obtained for each of the samples investigated, are shown in Table I. For the lowest temperatures $T_c/T \gtrsim 4$, there is a deviation from strict proportionality between $\log(K_{es}/K_{T_c})$ and T_c/T, which is most clearly seen for the samples grown in the direction c.

As is seen from Fig. 5, the dependence of $K_{es}(T)/K_{T_c}$ will T_c/T is a universal one for all samples grown in one direction. Neither the purity of the initial material, nor the method of preparation of the sample, nor its dimensions [although, for example, the amount of impurity in the specimen was varied by a factor of more than 100 (for example, sample b of series 3D, samples b-3, b-P, etc.)] influence this dependence. We recall that in all the samples under investigation the free path length of the electrons is determined by their scattering on lattice defects; therefore, the conclusion just obtained applies only to a similar case. Moreover, if the processes of electron scattering on lattice vibrations also play an important role, then $K_{es}(T)/K_{T_c}$ will change with the purity of the material, since K_{es}/K_n is different for scattering of electrons from lattice vibrations and from lattice defects.[17] From this point of view, one can explain, at least qualitatively, the recent discovery of Graham[18] of the change of $K_{es}(T)$ with purity of the material for very pure tin. Hence there is no longer any necessity for the additional assumptions which Graham made in the treatment of his results.

The dependence of the thermal conductivity of the electrons on the temperature is the same only for samples of a single crystallographic orientation. Samples of different orientation differ not only in the absolute value of the thermal conductivity but also in its temperature dependence. The anisotropy in the laws of temperature variation of K_{es} is most sharply brought out in temperature measurements of the value of the ratio of the thermal conductivity along the different crystallographic directions; these ratios are shown in Fig. 6. In the calculation, the results of averaging K_{es}/K_{T_c} over all specimens along a given crystallographic direction were used. Also, in accord with Table III, it was assumed that at the critical temperature the thermal conductivities along the direction c, a and b bore the relationship 1 : 5.4 : 12.

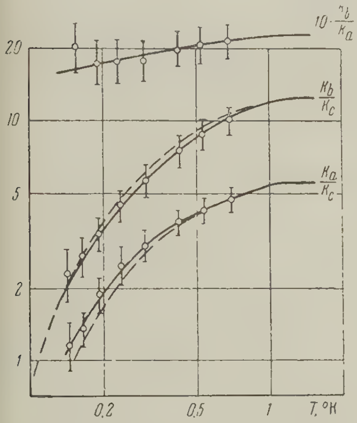

FIG. 6. Temperature dependence of the relative anisotropy of the thermal conductivity of electrons of gallium. The dashed line corresponds to exp(–0.29/T).

The character of the temperature variation of the anisotropy of the thermal conductivity shows that in gallium there is an especially large difference between the laws of change of the thermal conductivity along directions a and c and along b and c. The difference between the temperature variation of the thermal conductivity along the directions a and b lies in the limit of accuracy of our measurements. The greatest change in the anisotropy of the thermal conductivity of the electrons, as can be seen from Fig. 6, takes place in the region of temperatures lying well below the critical temperature. Thus, while the change in the anisotropy between K_a and K_c amounts at most to ~30 per cent in the range from T_c to $0.5\,T_c$, it reaches 200 per cent in the range from $0.5\,T_c$ to $0.2\,T_c$. This character of change is close to exponential dependence. For comparison, the dependence $\exp(-0.29/P)$ is shown in Fig. 6.

There is a qualitative difference between the character of the temperature variation of the anisotropy of the thermal conductivity of electrons in the normal and superconducting states. While in the normal state the value of the anisotropy between the directions a and c or b and c increases with decrease in temperature, in the superconducting state it is decreased. Correspondingly, if in the normal state the thermal conductivity along the axis c is less for the entire range of temperatures than along the other two crystallographic axes, in the superconducting state, such a ratio is maintained only to temperatures ~0.15°K. For lower temperatures, the ratio between the values of the thermal conductivity of the electrons changes along the axes, and it is possible that at temperatures below 0.1°K, the thermal conductivity along the c axis will exceed the thermal conductivity not only along the a axis but even along the b axis.

It is known that the change of the thermal conductivity of the electrons of the superconductor with temperature is primarily brought about by the temperature dependence of the number of excited states. Therefore, the anisotropy of the thermal conductivity can be brought about not only by such effects inherent in the normal state, such as the change in the free path length, or the change in the excitation rates, but also by anisotropies in the density of excited states. This anisotropy occurs in the presence of an anisotropy of the gap width Δ in the energy spectrum of excitations of the superconductor, a gap which separates the excited states from the ground, "superconducting" states of the electrons. In this case, for example, the density of excitations in the directions of minimum and maximum gap width are related as $\exp\{(\Delta_{max} - \Delta_{min})/T\}$. The distinctive peculiarity of the anisotropy connected with this effect is its sharp change in the temperature region $T \ll T_c$, by which the insignificant difference in the gap width is also made evident. The anisotropy of the thermal conductivity of the electrons in gallium has a similar character. Therefore, in what follows we shall connect it with the presence of the anisotropy of Δ in this metal.* In this case the very smooth change in the thermal conductivity along the c axis indicates that this direction corresponds to a minimum Δ. The similar temperature variation of the thermal conductivity along a and b shows that Δ in these directions is essentially the same. In this case, by identifying the temperature variation of the thermal conductivity* along the c axis with $\exp(-\Delta_{\min}/T)$, we obtain the result that $\Delta_{\min} \approx 1.3°K$.

---

*In the present state of the theoretical analysis of the thermal conductivity of an anisotropic superconductor, it is not possible to explain in what measure the anisotropy can be attributed to one of the effects described above.

In the determination of the anisotropy of Δ, it is necessary to assume that not only excitations moving exactly in the direction of the temperature gradient take part in the transfer of energy. Excitations in all directions make an appreciable contribution to the thermal conductivity. This was used in a preliminary communication[6] in the calculation of the connection between the anisotropies of Δ and β; on this basis, an estimate of the anisotropy of Δ was made from experimental results. The data obtained in this case were not very reliable, since a number of simplifications that were to a considerable degree arbitrary were permitted in the calculation. Khalatnikov[19] carried out a rigorous theoretical analysis of the change in the thermal conductivity of an anisotropic superconductor for the range of temperatures in which the density of excitations in the direction of the maximum gap width $\Delta_{\max}$ is negligible in comparison with the density of excitations in the direction of $\Delta_{\min}$. This takes place if $(\Delta_{\max} - \Delta_{\min})/T > 1$. Comparison of the results of the calculation (under the assumption that Δ can be approximated by an ellipsoid of revolution) with experimental data shows that in the case of gallium this region lies below the temperature range covered by our measurements. For the same reason calculation of the thermal conductivity of an anisotropic superconductor in a very wide range of temperatures is necessary for a reliable determination of the anisotropy of Δ. At the present time only approximate estimates of the anisotropy of Δ can be carried out; these show that its magnitude in gallium amounts to 30 per cent of $\Delta_{\min}$.

In conclusion I take this opportunity to express my deep gratitude to Academican P. L. Kapitza and to Professor A. I. Shal'nikov for their constant interest in the work and to V. I. Shishkin for help in carrying out the experiment.

---

*The deviation of the thermal conductivity from strict proportionality of log K_{es} and T_c/T for $T_c/T > 4$ is brought about by the factor multiplying the exponent. The character of this deviation is close to that predicted theoretically.

[1] Bardeen, Cooper, and Schrieffer, Phys. Rev. **108**, 1175 (1957).

[2] Bogolyubov, Tolmachev, and Shirkov, Новый метод в теории сверхпроводимости, (A New Method in the Theory of Superconductivity) Academy of Sciences Press, 1958.

[3] N. V. Zavaritskiĭ, JETP **34**, 1116 (1958); Soviet Phys. JETP **7**, 773 (1958).

[4] B. B. Goodman, Compt. rend. **246**, 3031 (1958); R. R. Richards and M. Tinkham, Phys. Rev. Lett. **1**, 318 (1958).

[5] S. J. Laredo, Proc. Roy. Soc. (London) **A229**, 473 (1955).

[6] N. V. Zavaritskiĭ, Тезисы 5-го Всесоюзного совещания по физике низких температур, (Papers of the Fifth All-Union Conference of the Physics of Low Temperatures), Tbilisi, 1958.

[7] A. J. Bradley, Z. Kristallogr. **91**, 302 (1935).

[8] P. L. Kapitza, Proc. Roy. Soc. (London) **119**, 358 (1928).

[9] R. W. Powell, Proc. Roy. Soc. (London) **A209**, 525 (1951).

[10] N. V. Zavaritskiĭ, JETP **33**, 1085 (1957); Soviet Phys. JETP **6**, 837 (1958).

[11] B. B. Goodman and E. M. Mendoza, Phil. Mag. **42**, 594 (1951).

[12] J. F. Cochran and D. E. Mapother, Phys. Rev. **111**, 132 (1958).

[13] R. E. B. Makinson, Proc. Cambr. Phil. Soc. **34**, 474 (1938).

[14] H. M. Rosenberg, Phil. Trans. Roy. Soc. **247**, 441 (1953).

[15] H. M. Rosenberg, Phil. Mag. **2**, 541 (1957).

[16] M. Olsen-Bär and R. W. Powell, Proc. Roy. Soc. (London) **A209**, 542 (1951).

[17] J. K. Hulm, Proc. Roy. Soc. (London) **A204**, 98 (1950).

[18] G. M. Graham, Proc. Roy. Soc. (London) **A248**, 522 (1958).

[19] I. M. Khalatnikov, JETP **36**, 1818 (1959); Soviet Phys. JETP **9**, 1296 (1959).

Translated by R. T. Beyer
309

SOVIET PHYSICS JETP VOLUME 37(10), NUMBER 6 JUNE, 1960

EFFECT OF THE HYPERFINE STRUCTURE ON POLARIZATION OF NEGATIVE MUONS IN MESIC ATOMS

L. V. EGOROV, A. E. IGNATENKO, and D. CHULTÉM

Joint Institute for Nuclear Research

Submitted to JETP editor June 7, 1959

J. Exptl. Theoret. Phys. (U.S.S.R.) 37, 1517-1523 (December, 1959)

The angular distributions of μ^--meson decay electrons from aluminum, phosphorus, and carbon mesic atoms were studied with scintillation counters. It is shown that the interaction of the hyperfine structure causes a decrease of the μ^--meson polarization. The results of the measurements do not contradict the theoretical predictions if depolarization on the K orbit only of the mesic atom is taken into account. Comparison of the measurement results for phosphorus with those previously obtained for liquid hydrogen shows that the complete depolarization of μ^- mesons observed in hydrogen cannot be explained only by the interaction between the fine and hyperfine structures. To do this, an additional mechanism must be assumed (such as the "jumping" of a μ^- meson from one proton to another with concurrent transition of the hyperfine structure to the ground state). All the experimental data on the depolarization of μ^- mesons in various substances can be explained theoretically if it is assumed that in mesic atoms of metals the electron shell does not affect the depolarization of μ^- mesons. The presence of a fine and hyperfine structure in mesic atoms is confirmed and this again indicates that the electromagnetic properties of mesons and electrons are similar. The decrease in the precession frequency of the mesic-nucleus spin to one half the value of the precession frequency of the free muon spin (observed in experiments with phosphorus) indicates directly that the spin of the negative muon is one-half.

1. INTRODUCTION

MEASUREMENTS[1] of the degree of polarization of μ^- mesons in substances with zero nuclear spin show that the polarization in different mesic atoms is the same, ~17%, within the limits of experimental error. The results of the measurements were qualitatively interpreted in the following manner: the principal mechanisms of depolarization of mesons in such substances are the spin-orbit interaction and the interaction between the magnetic fields of the atomic electron shell and of the μ^- meson during its lifetime on the K orbit. A theoretical analysis of the processes of depolarization of μ^- mesons in various substances is found in the papers by Rose,[2] Dzhrbashyan,[3] Shmushkevich,[4] Dolinskiĭ,[5] and Überall.[6] It must be noted that these authors have obtained different results. In particular, we consider first the results of the calculation of the depolarization of μ^- mesons in substances with zero nuclear spins. Rose, in considering depolarization due explicitly to spin-orbit interaction in cascade transitions, shows that the mean value of the degree of polarization of the μ^- meson on the K shell should be ~50%. This does not agree with the experimental data.[1] Analogous calculations by Shmushkevich (and also by Dzhrbashyan) yield a value of ~17% for the same quantity, in good agreement with the measurement results.[1] At the same time, allowance for the additional depolarization in the field of the electron shell, for example for carbon atoms screened by μ^- mesons, yield a degree of polarization on the K-shell of only ~9%. The fact that this value contradicts experimental data causes Dzhrbashyan to suggest that in condensed matter the influence of neighboring atoms and electrons leads to a cancellation of the magnetic moment of the electron shell. However, comparison of Rose's calculations with the experimental data is evidence in favor of assuming that there is no cancellation of the magnetic moment of the electron shell, and that apparently additional depolarization takes place.

In calculations of the depolarization of μ^- mesons in substances with nuclear spins other than zero, the foregoing mechanisms must be supplemented by including the depolarization due to the hyperfine structure. A theoretical analysis of this mechanism was made by Rose, Dolinskiĭ, and also Überall. For substances with nuclear spin one-half, for example, the depolarization should be reduced to one-third, according to Rose, and to one-half according to Dolinskiĭ and Überall.

It is seen from the above that at the present time we have no quantitative explanation of the depolarization of μ^- mesons in different substances. We have decided to set up several experiments on the effect of the hyperfine structure (due to the spin coupling between the μ^- meson and the nucleus) and the electron shell on the depolarization of μ^- mesons. A study of the depolarization of μ^- mesons in substances with non-zero nuclear spins is also important to determine the feasibility of setting up experiments on hyperfine-structure effects, which manifest themselves in the capture of polarized μ^- mesons.[6,7] In the present article we discuss essentially the results of the investigation of the influence of the hyperfine structure on the depolarization of μ^- mesons in various mesic atoms.

2. BASIC THEORETICAL PREMISES

The interaction with the hyperfine structure will affect the depolarization of μ mesons both in the ground state and in the excited states of the mesic atoms. This can be readily verified by comparing the time τ_l of the μ^- meson at the lower levels with the time τ necessary for spin flip of the μ^- meson under the influence of the nuclear field.

It is found that τ is much smaller than τ_l.[5] We denote by P_0 the degree of polarization of the μ^- meson at the initial instant of its "landing" on the K orbit. According to references 5 and 6, the degree of polarization of the μ meson on the K shell, averaged over the two states of the hyperfine structure, will be

$$P = \frac{1}{3} P_0 \left[1 + \frac{2}{(2J+1)^2}\right], \tag{1}$$

where J is the nuclear spin.

It is seen from this formula that the polarization of the μ^- meson during the instant of its decay or capture by a nucleus depends on the nuclear spin. Thus, for example, for nuclei with $J = 1/2$ the polarization is reduced to one half, and for nuclei with $J \gg 1/2$, it is reduced to one third. We note that in view of the conservation of the spin of the nucleus plus μ^- meson system, the initially unpolarized nucleus acquires a polarization P_{nuc} equal to

$$P_{\text{nuc}} = \frac{4}{3} \frac{J+1}{(2J+1)^2} P_0.$$

A detailed computation of the depolarization due to the hyperfine structure in excited states of a mesic atom is given in the paper by Rose. For example, for substances with nuclear spin $1/2$ the interaction of the hyperfine structure in the ground and excited states, should reduce the polarization to one-third.

It should also be noted that when μ^- mesons are stopped in substances with non-zero nuclear spins, mesic atoms are produced in the two states of the nuclear structure with $F = J \pm 1/2$. The hyperfine splitting in the ground state of the mesic atom is much greater than $\hbar/\tau$, where τ is the lifetime of the μ^- meson. Therefore states with $F = J + 1/2$ and $F = J - 1/2$ form an incoherent mixture.[7] Each state will be characterized by its own gyromagnetic ratio g. Thus, the expressions for g have the following form:[6]

$$g_+ = \frac{1}{J + 1/2} (\mu_\mu + \mu_N); \tag{2}$$

$$g_- = -\frac{1}{J + 1/2} \left(\mu_\mu - \frac{J+1}{J} \mu_N\right), \tag{3}$$

where μ_μ and μ_N are the magnetic moments of the μ^- meson and nucleus respectively.

If the μ^--meson polarization is measured by determining the asymmetry of the decay electrons,[8] then the experimentally observed precession curve will be a superposition of the precession curves of the μ^- mesons decaying from both states of the hyperfine structure. It is obvious that the greater the nuclear spin, the more difficult it is to interpret such a curve.

The objects used for investigation were carbon, aluminum, and phosphorus. Carbon, whose nuclei have zero spin, was used for control experiments. The aluminum and phosphorus were chosen for the investigation of the effects of the hyperfine structure for the following reasons. First, the nuclei of aluminum and phosphorus have greatly different spins, J being $5/2$ for aluminum and $1/2$ for phosphorus. It is therefore easier to verify the theoretical predictions. Secondly, the formation of mesic atoms entails a rearrangement of the electron shell. Therefore, even if the initial spin of the electron shell is zero, the electron shell of the mesic atom may have a spin. The presence of a magnetic moment in the electron shell of the mesic atom may lead to an additional depolarization of the μ mesons on the K orbit, since the time of reorientation of the μ-meson spin under the influence of the magnetic field H of the electron shell ($\tau_e \sim \hbar/\mu H \sim 10^{-10}$ sec) is less than the lifetime of the μ^- meson. One can expect the muon-screened electron shell of the aluminum and phosphorus atoms to be the same, namely closed. Therefore, in the case of aluminum and phosphorus, it is possible to investigate the hyperfine structure effect in "pure form." Finally, Telegdi expressed

Substance	J	$-a_0$	Substance	J	$-a_0$
Carbon	0	0.045 ± 0.005	Aluminum	$^5/_2$	0.007 ± 0.007
Phosphorus	$^1/_2$	0.025 ± 0.005	Hydrogen	$^1/_2$	0.005 ± 0.005

the opinion that the total polarization of μ^- mesons in liquid hydrogen, which we observed earlier,[10] may be connected in principle only with the fine and hyperfine structures. Experience with phosphorus will help answer this question. Actually, the nuclei of phosphorus and hydrogen will have identical spins, and in these mesic atoms there will be no depolarization due to the electron shell. Consequently, the effects of the hyperfine structure should also be equal.

3. EXPERIMENT

The polarization of μ^- mesons was investigated by measuring the anisotropy in the angular distribution of the decay electrons. The experimental conditions and the apparatus used were the same as in previously published papers,[10,1] with exception of the electronic circuitry, which operated in these experiments as follows. In experiments with phosphorus and aluminum, the μ-meson pulse from the anticoincidence $1 + 2 - 3$, delayed by $0.1\,\mu$sec, operated the transmission circuit ("gate") for $0.5\,\mu$sec. Passing through the gates were pulses due to the decay electrons from the $3 + 4 - 2$ anti-coincidence circuit. In experiments with carbon the delay was $0.25\,\mu$sec, and the gate duration $2\,\mu$sec. The coefficient of asymmetry a in the angular distribution of the decay electrons, $J(\theta) = 1 + a \cos\theta$, was determined from an investigation of the dependence of the number of electrons on the intensity H of the magnetic field in which the target was located.

The range of variation of the magnetic field intensity corresponded to that calculated on the basis of (2) and (3) for the values of g. The target used for the phosphorus investigations was made of pressed red-phosphorus powder. This was done to avoid μ-meson transitions between levels of the hyperfine structure through conduction-electron conversion.

The values obtained for a_0 — the asymmetry coefficient for the entire integrated spectrum — are listed in the table.

The values listed for a_0 were corrected for the delay time, for the gate width, for the negative-muon decay, and for the solid angle of the electron detector. The errors indicated included both the standard statistical deviations and the instability of the apparatus. The table lists also the values of a_0 for liquid hydrogen, which we obtained[10] by measuring the number of electrons in the maximum and minimum of the expected precession curve.

4. DISCUSSION OF THE RESULTS

The value of a_0 measured in this investigation for carbon coincided, within the limit of experimental error, with the value measured in the previously published paper.[1] In the experiments with phosphorus there was actually observed a precession of mesic atoms, whose mesic nucleus (the meson plus nucleus system) was in the state F = 1 (see figure). This is direct evidence in favor of the existence of a spin coupling between the μ^- meson and the nucleus in such mesic atoms, i.e., the presence of a hyperfine structure.

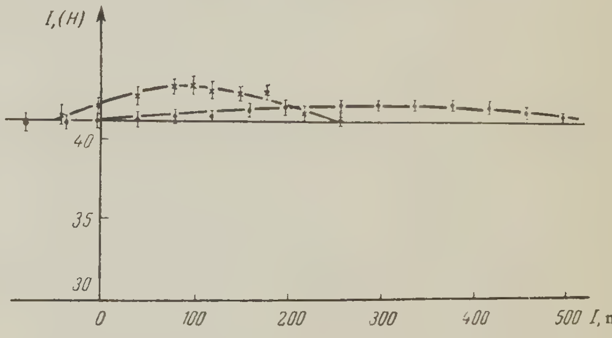

Dependence of the number of the electrons I(H) on the current I (milliamperes) required to magnetize the coil: × – experimental data for graphite, ● – for phosphorus. The solid curves are calculated from the formula

$$I(H) = \int_{t_1}^{t_2} e^{-t/\tau}\,[1 + \cos(2\pi f t + \theta_0)]\,dt$$

with allowance for the delay time t_1, the gate width $t_2 - t_1$, the values of g_+ and g_-, and the lifetime τ of the μ^- mesons.

The experimentally-observed decrease in the frequency of precession of the spin of the phosphorus mesic nucleus, to half the frequency of the precession of the spin of the free μ meson, indicates directly [see Eqs. (2) and (3)] that the spin of the negative muon is ½.*

In experiments with aluminum, no dependence of the electron counting rate on the current in the magnetizing coil was observed. Since the experimentally-observed precession curve is a superposition of the precession curves of μ^- mesons in different hyperfine-structure states, it is impossible to interpret the obtained curve. The value a_0 given in the table for aluminum is an average over two states of the hyperfine structure.

---

*The authors are grateful to Prof. V. Telegdi who called their attention to this conclusion in discussions at the Kiev Conference on High Energy Physics (Kiev, 1959).

Let us compare the measured quantities with the theoretical predictions. Knowing the values of a_0 we can determine[1] the degree of polarization of the μ^- mesons, for example, by comparison with the asymmetry observed in the decay of μ^+ mesons, assuming that the μ decay is invariant under a joint inversion of the space coordinates and charge conjugation. If this condition is satisfied, it is easy to show that the following relation holds

$$a_-/p_- = a_+/p_+, \qquad (4)$$

where p_+ and p_- are the degrees of polarization, a_+ and a_- are the asymmetry coefficients in the angular distributions $1-a_\pm \cos\theta$, integrated over the positron (electron) energies, for positive and negative muons respectively. It is seen from (4) that by comparing the polarization of μ^- mesons in different mesic atoms it is possible to compare the values of a_0. As indicated in Sec. 1, a comparison of Rose's computed results with our experimental data[1] speaks in favor of expecting the polarization of μ^- mesons to be reduced to one third under the influence of the electron shell. Such a reduction in polarization, according to Rose, should also be produced by the interaction of the hyperfine structure for substances with $J = 1/2$. Consequently, taking into account the influence of the electron shell in mesic atoms of carbon and phosphorus, the values of a_0 should be equal, i.e., $a_C = a_P$. In the absence of the influence of the electron shell, according to the theoretical predictions of Dolinskiĭ and Überall, the following relations should hold between the values of a_0 for phosphorus and aluminum: $a_P = (1/2)\,a_C$ and $a_{Al} = (1/3)\,a_C$; according to Rose, $a_P = (1/3)\,a_C$.

If Telegdi's hypothesis that the observed total depolarization of μ^- mesons in liquid hydrogen is connected only with the interaction of the fine and hyperfine structures is correct, then the values of a_0, for reasons indicated in Sec. 2, should be the same for phosphorus and hydrogen, i.e., $a_P = a_H$. Let us clarify now the question of the correspondence between the theoretical expectations and the corresponding relations between the measured values of a_0. Using the normal law of distribution of errors, we can show that the case $a_H = a_P$ must be rejected, since $a_H < a_P$ with a probability of 99.5%; the case $a_{Al} = (1/3)\,a_C$ does not contradict experiment, but according to the experimental data the probability of $a_{Al} > (1/2)\,a_C$ is 5%, and the probability of $a_{Al} < a_C/5$ is 39%. The values of the ratios a_C/a_P were analyzed by the χ^2 criterion. The limits of this ratio with probabilities of 1% (the unbracketed numbers) and 5% (the numbers in the brackets) are as follows:

1.2 (1.4) — (3.0) 3.7 for the case $a_P = {}^1/_2\, a_C$,
1.8 (2.1) — (4.5) 5.5 for the case $a_P = {}^1/_3\, a_C$,
0.6 (0.7) — (1.5) 1.8 for the case $a_P = a_C$.

We see that the experimental value of $a_C/a_P = 1.8$ is in good agreement with the theoretically expected one in the case $a_P = (1/2)\,a_C$, and lies beyond the 1% limits for the cases $a_P = (1/3)\,a_C$ and $a_P = a_C$.

The fact that the measured value of a_C/a_P lies outside the 1% limits for the case $a_P = a_C$ indicates that if the production of mesic atoms is always accompanied by a rearrangement of the electron shell of the initial atom (in view of the change of the effective charge of the nucleus by unity), then the magnetic moment of the electronic shell is apparently cancelled out in mesic atoms of such substances as C, Mg, Zn, Cd, or Pb. In other words, in these mesic atoms there is probably no spin coupling between the electron shell and the μ^- meson. It is obvious that in order to make this conclusion more definite it is necessary to investigate directly the effect of the electron shell on the polarization of μ^- mesons in various mesic atoms. It is necessary to measure for this purpose the values of a_0 for substances placed in a longitudinal magnetic field with intensity sufficient to break the bond between the μ^- meson and the electron shell.

Using the foregoing assumption and the fact that the relations $a_P = a_C$ and $a_P = (1/3)\,a_C$ contradict experiment, while the relations $a_P = (1/2)\,a_C$ and $a_{Al} = (1/3)\,a_C$ do not contradict the experimental data, it can be stated that our results do not contradict the theoretical predictions of Dolinskiĭ and Überall, but do contradict the results of Rose. The circumstance is evidence that when a target of red phosphorus is used, the probability of transition of the μ meson from the upper level of the hyperfine structure to the lower one is small, owing to conduction-electron conversion.

Since the experimental value of a_C/a_P is outside the 1% limit for the case $a_P = (1/3)\,a_C$, it can be stated for μ^- mesons in the lower excited states of the mesic atoms that the interaction of the hyperfine structure is apparently insignificant compared with the interaction on the K orbit.

Finally, the fact that $a_H < a_P$ with probability 99.5% speaks in favor of the fact that the experimentally-observed total depolarization of μ^- mesons in liquid hydrogen cannot be attributed to the interaction of the fine and hyperfine structures; it is necessary to make use of an additional mechanism for this purpose. Such a mechanism can be, for example, the jump of the μ^- meson from one proton to another with simultaneous transition to the lower state of the hyperfine structure.[11] Thus, we can conclude from the foregoing that, assuming that the electron shell does not influence the depolarization of the μ^- mesons in the mesic atoms of metals, the results of the calculations of Shmushkevich, Dzhrbashyan, Dolinskiĭ, and Überall explain all the experimental data on the depolarization of μ^- mesons in various substances, obtained in the present paper and those previously published by us.[1,10]

It is known that the main source of our present information on the properties of mesic atoms have been experiments on x-rays from mesic atoms. The available experimental data were obtained essentially for the energy levels. Such phenomena as the fine and hyperfine structures of mesic atoms remained uninvestigated. This is explained by the fact that with the existing intensities of μ^- meson beams in accelerators, the energy resolution of γ spectrometers presently available to experimenters is insufficient to resolve a fine line, let alone a hyperfine structure. The investigations performed on the mechanism of depolarization of μ^- mesons in various substances have not only confirmed experimentally the presence of a fine and hyperfine structure in mesic atoms, but have also permitted us to disclose certain features of these phenomena. The presence of a fine and hyperfine structure in μ^--mesic atoms once more shows the similarity in the electromagnetic properties of μ^- mesons and electrons.

In conclusion, the authors consider it their duty to thank V. P. Dzhelepov and L. I. Lapidus for discussing the results of this investigation, to I. S. Shapiro, É. I. Dolinskiĭ, L. D. Blokhintsev, and A. Z. Dolginov for numerous discussions and many valuable remarks, to S. N. Sokolov for great help in the reduction of the experimental data, and also to Mr. Überall for furnishing us with a copy of his paper prior to publication.

---

[1] Ignatenko, Egorov, Khalupa, and Chultém, JETP **35**, 1131 (1958), Soviet Phys. JETP **8**, 792 (1959).

[2] M. E. Rose, Depolarization Processes for Negative Mu-mesons, preprint, Oak Ridge Nat. Lab., (1958).

[3] V. A. Dzhrbashyan, JETP **36**, 277 (1959), Soviet Phys. JETP **9**, 188 (1959).

[4] I. M. Shmushkevich, JETP **36**, 645 (1959), Soviet Phys. JETP **9**, 449 (1959).

[5] É. I. Dolinskiĭ, Dissertation, Inst. Nuc. Phys. Moscow State Univ. 1959.

[6] H. Überall, Hyperfine Splitting Effects in the Capture of Polarized μ^- Mesons, preprint, Carnegie Inst. of Technol., 1959.

[7] Bernstein, Lee, Yang, and Primakoff, Phys. Rev. **111**, 313 (1958).

[8] Garwin, Lederman, and Weinrich, Phys. Rev. **105**, 1415 (1957).

[9] V. Telegdi, Proc. 1958 Ann. Intern. Conf. on High-energy Physics at CERN, p. 250.

[10] Ignatenko, Egorov, Khalupa, and Chultém, JETP **35**, 894 (1958), Soviet Phys. JETP **8**, 621 (1958).

[11] S. S. Gershteĭn, JETP **34**, 463 (1958), Soviet Phys. JETP **7**, 318 (1958).

Translated by J. G. Adashko
310

SOVIET PHYSICS JETP VOLUME 37(10), NUMBER 6 JUNE, 1960

FAST PHOTONEUTRONS FROM Be^9, C^{12}, *AND* Al^{27}

L. A. KUL'CHITSKIĬ and V. PRESPERIN

Leningrad Physico-technical Institute, Academy of Sciences, U.S.S.R.

Submitted to JETP editor July 2, 1959

J. Exptl. Theoret. Phys. (U.S.S.R.) **37**, 1524-1529 (December, 1959)

Be^9, C^{12}, and Al^{27} targets were irradiated by bremsstrahlung with 88 Mev peak energy and the angular distributions of photoneutrons with energies above 10 Mev were investigated. The energy spectrum of photoneutrons emitted by C^{12} at 75° was also investigated; the photoneutron and photoproton yields in the same energy interval were compared. The angular distributions are compared with calculations based on the quasi-deuteron model and direct photonuclear resonance. Qualitative agreement with the quasi-deuteron model is obtained.

1. INTRODUCTION

WHEN high-energy photons ($\gtrsim 150$ Mev) interact with nuclei a two-nucleon mechanism is basically responsible for the ejection of fast particles.[1-3] The direct production of high-energy particles is also possible above giant resonance and below ~ 150 Mev. The relative importance of these two mechanisms for different photon and particle energies is still not clear. Most work in this energy region has been concerned with the investigation of photoprotons.[4-6] Experimental studies of photoneutrons are also required in order to determine the interaction mechanism of photons and nuclei. However, such experiments by means of a ZnS scintillation detector of neutrons[7,8] do not lead to quantitative conclusions because of uncertainty regarding the efficiency with which neutrons of different energies are detected.

In the present work we investigated the angular distributions of photoneutrons ejected from Be^9, C^{12}, and Al^{27} with energies above 10 Mev, as well as the energy distribution of photoneutrons from C^{12} which were produced by bremsstrahlung with peak energy 88 Mev from the synchrotron of the Physico-technical Institute of the U.S.S.R. Academy of Sciences.

2. EXPERIMENTAL TECHNIQUE

The experimental setup is shown in Fig. 1. Neutrons with energies ≥ 10 Mev were registered by means of recoil protons from a paraffin converter. Recoil proton energies were measured by means of telescopes consisting of two scintillation counters serving as spectrometers.[9] The great advantage of such telescopes is their reliable ability to distin-

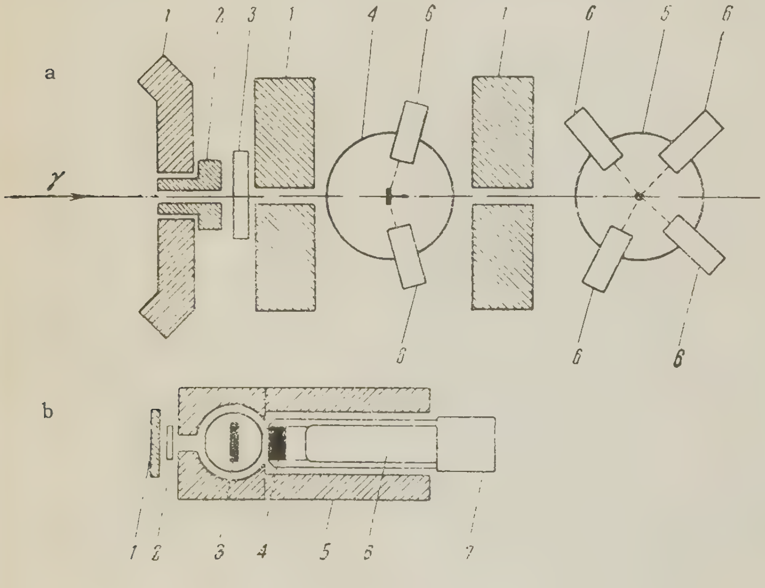

FIG. 1. Experimental setup. a) Overall arrangement: 1 – lead walls, 2 – lead collimator, 3 – monitor, 4 – table supporting telescopes and target for energy-distribution measurements, 5 – table supporting telescopes and target for angular distribution measurements, 6 – telescopes. b) Telescope: 1 – lead absorber in front of telescope, 2 – paraffin converter, 3 – NaI(Tl) crystal in hemispherical reflector of front telescope, 4 – NaI(Tl) crystal of back telescope, 5 – lead shield, 6 – photomultiplier, 7 – preamplifier.

guish recoil protons from the light-particle background which otherwise introduces a serious difficulty because of the very thick targets that were used. A lead plate placed in front of the converter absorbed the photoprotons and most of the electrons from the target. Energy distributions were measured by two independent telescopes positioned at 75°. Angular distributions were measured by four telescopes, each of which could be rotated around the target in the horizontal plane. The parameters of the combinations of converter and telescopes differed because of the different requirements for measurements of angular and energy distributions. The telescope geometry for energy-distribution measurements was as follows: diameter of the converter and of the diaphragm opening before the NaI(Tl) crystal of the back counter — 28 mm, converter thickness — 3 mm, front-counter NaI(Tl) crystal thickness — 0.6 mm, back-counter crystal thickness — 15 mm. The converter and first counter crystal were separated by 47 mm; the crystals of the first and second counters were separated by 40 mm. The distance between the target center and the converter was 170 mm. For the measurement of angular distributions the telescopes were used in conjunction with a thicker converter (5 mm), and to increase the effective scattering angle the converter was cemented directly to the thin crystal. The efficiency of neutron detection by this arrangement was four times greater than in the case of the energy-distribution measurements (with some reduction of the energy resolution). The two telescope counters were connected in coincidence. The electronic circuit used to select and register pulses was similar to that described in reference 9.

A flat target was used to study the energy distribution of photoneutrons from C^{12}, while cylindrical targets were used to study the angular distributions of photoneutrons from Be^9, C^{12}, and Al^{27}. The target thicknesses and diameters were such that the number of neutrons scattered inelastically in the targets themselves and in the lead shield before the telescope did not exceed 5% in the case of the energy distributions and 10% for the angular distributions.

The background was estimated by comparing measurements without a target and measurements in which the paraffin converter was replaced by an equivalent amount of carbon. The background amounted to less than 3% of the angular distributions and less than 5% of the energy distributions.

Relative measurements of the gamma radiation passing through the target were obtained by means of an aluminum ionization chamber, while absolute measurements were obtained with a thick-walled copper chamber that had been calibrated calorimetrically.[10,11]

3. TREATMENT OF MEASUREMENTS AND ESTIMATE OF ERRORS

Very thick converters were required to obtain a sufficiently high efficiency of neutron detection. A large (n, p)-scattering angle was selected for the angular-distribution telescopes. Suitable instrumental corrections were introduced when the experimental results were compared with theoretical calculations.

In the case of the angular-distribution telescopes it was necessary to determine the dependence of detection efficiency on neutron energy, since the measured and actual angular distributions disagreed over different energy distributions registered at different angles and with nonidentical efficiency. The relative efficiency $X(E)$ is proportional to

$$X(E) \sim \varepsilon_d(E)\,\varepsilon_p(E)\,\sigma(E),$$

where $\epsilon_d(E)$ is the effective converter thickness for neutrons with energy E, $\epsilon_p(E)$ is the fraction of recoil protons registered by the telescope and $\sigma(E)$ is the (n, p)-scattering cross section. Figure 2 shows the relative telescope efficiency as a function of neutron energy.

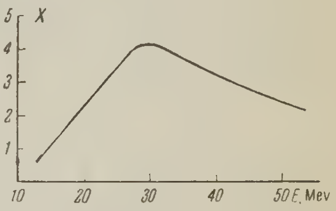

FIG. 2. Relative detection efficiency X(E) as a function of neutron energy for angular-distribution telescopes.

In energy-distribution measurements the neutron spectrum is determined from the recoil proton spectrum. Distortion of the neutron spectrum results from the fact that the (n, p)-scattering angle differs from 0° as a result of recoil proton energy losses in the converter and because the (n, p)-scattering cross section is a function of neutron energy. The mean scattering angle determined from the telescope geometry was 13°, corresponding to recoil protons with energy averaging 5% less than the neutron energy. This difference was neglected in calculating the effect of converter thickness; it was assumed that neutrons of a given energy produced a proton group of corresponding energy in the converter. The neutron spectrum was obtained as follows. A graphic method was used to determine the proton group that was produced in the converter by neutrons $N_0(E_i)$ in a 1-Mev energy interval with mean energy E_i. These graphs, plotted with 1-Mev intervals for all neutron energies, provided the basis for equations determining the separate proton groups $N(E_j)$:

$$N(E_j) = \sum_{i=j}^{i_{max}} k_i N_0(E_i). \qquad (1)$$

The cross section $\sigma(n, p)$ was taken into account in the coefficients k_i. The real neutron energy distribution $n(E)$ corresponds to the assigned distribution $N_0(E)$ in (1) that yields the experimental proton distribution $N(E)$.

The described method for computing the neutron energy spectrum introduces additional errors, principally as follows: 1) possible errors in determining the coefficients k_i in (1); 2) an error in determining the fraction of recoil protons registered by the telescope, in the calculation of absolute cross sections. The total error of the absolute cross sections is estimated at 40%, without including the statistical error.

4. EXPERIMENTAL RESULTS AND DISCUSSION

Figure 3 shows the energy distribution of neutrons from C^{12} at 75° for the 88-Mev bremsstrahlung. Only the statistical errors are indicated. In first approximation the spectrum falls off according to a power law $\sim E^{-n}$ with $n \approx 1.5$. In the range 15 — 45 Mev the total number of neutrons was found to equal, within the limits of error, the total number of protons in the same energy range.[12]

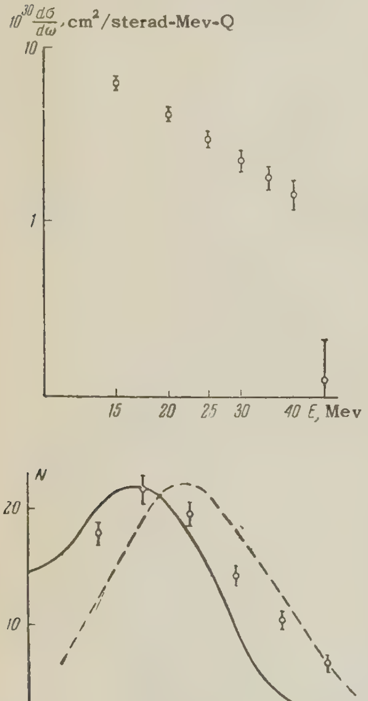

FIG. 3. Energy distribution of photoneutrons from C^{12} at laboratory angle 75°.

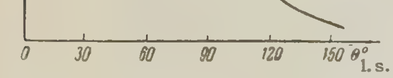

FIG. 4. Angular distribution of photoneutrons from C^{12}. Solid curve — converted data from reference 14; dashed curve — data calculated in reference 13.

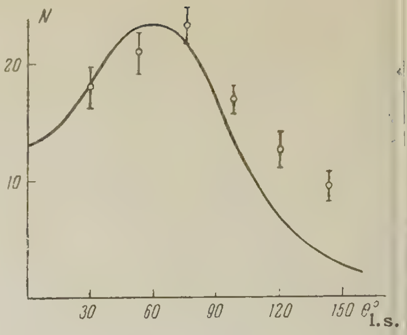

FIG. 5. Angular distribution of photoneutrons from Be^9. Solid curve — data calculated in reference 14.

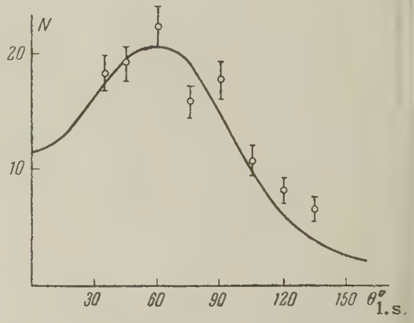

FIG. 6. Angular distribution of photoneutrons from Al^{27}. Solid curve — data calculated in reference 14.

Figures 4 to 6 show the angular distributions of photoneutrons from C^{12}, Be^9, and Al^{27} for the bremsstrahlung of peak energy $E_{\gamma max} = 88$ Mev, with indication of only the statistical errors. The vertical axis gives the number of neutrons N generated by a given radiation dose in relative units; the horizontal axis gives the laboratory angles of observation θ with respect to the photon beam direction. The peak of each angular distribution is strongly shifted toward small angles, being found at ~ 60°. Our results were compared with the angular distribution of neutrons from deuterium and with Dedrick's calculations[13] on the quasi-deuteron model. The solid curves represent the angular distributions of neutrons from deuterium, obtained by converting Allen's experimental results for protons.[14] I, which is proportional to the number of neutrons registered at a given angle, was obtained by numerical integration of

$$I \sim \int_{E_{\gamma_0}}^{E_{\gamma\,max}} N_\gamma(E_\gamma) \frac{d\sigma_d(E_\gamma)}{d\Omega} X(E_n)\, dE_\gamma,$$

where $N_\gamma(E_\gamma)$ is the number of photons with energy E_γ in the bremsstrahlung spectrum; $d\sigma_d(E_\gamma)/d\Omega$ is the differential cross section for the production of a photoneutron by the photodisintegration of a deuteron; $X(E_n)$ is a coefficient which is proportional to the telescope efficiency for neutrons with energy E_n (Fig. 2); $E_n = E'_n - \frac{1}{2} E_b$, where E'_n is the neutron energy prior to its ejection from the nucleus and E_b is the (γ, np)-reaction binding energy. E'_n for a given E_γ is determined from energy and momentum conservation in the photodisintegration of a deuteron. $E_{\gamma 0}$ is the energy of a photon which produces a neutron with the detection-threshold energy (9.7 Mev) and $E_{\gamma\,max}$ is the peak bremsstrahlung energy. The dashed line denotes the angular distribution of neutrons from C^{12} as calculated from Dedrick's paper.[13] All curves were normalized to yield the best agreement with experiment.

The shift of the neutron angular-distribution peak is similar to that of photoneutrons from deuterium although, especially for C^{12} and Be^9, the experimental result at small angles tends to fall below the deuteron curve. At large angles the situation is reversed. Better agreement would probably result if the momentum distribution of quasideuterons in the nucleus were taken into account, but the experimental results are in worse agreement with Dedrick's calculations for C^{12}. The observed angular distributions were also compared with the calculation of the direct resonance photoeffect in reference 15, which does not indicate a shift of the peak toward small angles.

Our results are in satisfactory qualitative agreement with the quasi-deuteron model. Calculations for the direct resonance photoeffect (neglecting magnetic interactions), which predict a forward shift for protons similar to that on the quasi-deuteron model, do not indicate a similar shift for neutrons and are consequently not in agreement with the observed angular distributions of photoneutrons. However, since the agreement with the quasi-deuteron mechanism is only approximate we cannot entirely exclude the direct resonance absorption of gamma rays.

[1] Odian, Stein, Wattenberg, Feld, and Weinstein, Phys. Rev. **102**, 837 (1956).

[2] M. Q. Barton and J. H. Smith, Phys. Rev. **110**, 1143 (1958).

[3] Baranov, Gol'danskiĭ, and Roganov, Phys. Rev. **109**, 1801 (1958).

[4] Bazhanov, Volkov, and Kul'chitskiĭ, JETP **35**, 322 (1958), Soviet Phys. JETP **8**, 224 (1959).

[5] Whitehead, McMurray, Aitken, Middlemas, and Collie, Phys. Rev. **110**, 931 (1958).

[6] N. V. Chuvilo and V. G. Shevchenko, Тр. Всесоюзн. конф. по ядерным реакциям при малых и средних энергиях (All-Union Conference on Nuclear Reactions at Low and Medium Energies), November, 1957, U.S.S.R. Acad. Sci., Moscow, 1958.

[7] S. A. E. Johansson, Phys. Rev. **97**, 434 (1955).

[8] W. R. Dixon, Can. J. Phys. **33**, 785 (1955).

[9] V. P. Chizhov and L. A. Kul'chitskiĭ, JETP **36**, 345 (1959), Soviet Phys. JETP **9**, 239 (1959).

[10] S. P. Kruglov, JETP **33**, 1060 (1957), Soviet Phys. JETP **6**, 817 (1958).

[11] S. P. Kruglov, J. Tech. Phys. (U.S.S.R.) **28**, 2310 (1958), Soviet Phys.-Tech. Phys. **3**, 2120 (1959).

[12] E. B. Bazhanov, JETP **37**, 374 (1959), Soviet Phys. JETP **10**, 267 (1960).

[13] K. G. Dedrick, Phys. Rev. **100**, 58 (1955).

[14] L. Allen, Phys. Rev. **98**, 705 (1955).

[15] G. M. Shklyarevskiĭ, JETP **36**, 1492 (1959), Soviet Phys. JETP **9**, 1057 (1959).

Translated by I. Emin
311

SOVIET PHYSICS JETP VOLUME 37(10), NUMBER 6 JUNE, 1960

COULOMB EXCITATION OF ODD-MASS NUCLEI BY MULTIPLY-CHARGED IONS

D. G. ALKHAZOV, A. P. GRINBERG, G. M. GUSINSKIĬ, K. I. EROKHINA, and I. Kh. LEMBERG

Leningrad Physico-technical Institute, Academy of Sciences, U.S.S.R.

Submitted to JETP editor July 2, 1959

J. Exptl. Theoret. Phys. (U.S.S.R.) 37, 1530-1542 (December, 1959)

High-lying levels in some light nuclei (Al^{27}, Sc^{45}, V^{51}, Nb^{93}), which previously could not be observed because of the large nuclear-reaction background when protons or alpha particles were used as bombarding particles, have now been excited by means of heavier ions. It has been established that some of the gamma lines observed previously when chromium was irradiated with protons or alpha particles do not result from Coulomb excitation of the corresponding levels in chromium. By using ions heavier than alpha particles it could be verified that other lines associated with nuclear levels that had been excited by alpha particles (Rb^{87}, Sn^{117}, Sn^{119}) are actually emitted as a result of Coulomb excitation. The partial lifetimes $\tau(E2)$ of excited levels have been determined for electric quadrupole transitions; measured values lie between 10^{-7} and 10^{-12} sec.

1. INTRODUCTION

THE Coulomb excitation of high-lying nuclear levels requires that the bombarding particles have fairly high energies. When protons or alpha particles are used for this purpose a considerable background resulting from nuclear reactions is often observed, especially in the cases of light and medium-weight elements. In some instances the large background prevents detection of the gamma line which is emitted following the Coulomb excitation of the target nucleus.

The use of high-energy alpha particles or protons may also distort the results (especially for light and medium-weight elements), due to the increased cross section for inelastic scattering that involves the formation of a compound nucleus and leads to excitation of the investigated level.

In many instances the excitation function is measured in order to confirm the Coulomb origin of the gamma line. The theoretical dependence of the Coulomb excitation cross section on bombarding energy is well known. However, when the Coulomb excitation of high-lying levels is investigated the excitation function can be investigated in only a small range of bombarding energies, since when the energy is reduced the Coulomb excitation cross section becomes small, while at higher energies the nuclear-reaction background is enhanced. On the other hand, it sometimes results from the competition of different processes for the breakdown of a compound nucleus, that the experimental excitation function for a given line, when it is emitted as the result of a nuclear reaction involving the formation of the compound nucleus, agrees very closely with the theoretical excitation function of the same line in the Coulomb process.* Thus even when the excitation function has been measured it is sometimes impossible to attain certainty that the given gamma line results from Coulomb excitation of a nuclear level rather than because of some nuclear reaction.

The above-mentioned difficulties can be overcome to a certain extent by using heavier bombarding ions, which produce a much smaller nuclear-reaction background than alpha particles or protons. The cross section for inelastic scattering involving the formation of a compound nucleus is considerably smaller for the heavy ions than for alpha particles or, even more so, for protons.

The low background level observed in gamma spectra produced by multiply-charged ions impinging on targets containing oxygen permits the use of such ions to investigate Coulomb excitation of nuclear levels even when the target is not made of pure metal. The use of the heavy ions is essential in order to establish the origin of the observed gamma line. The detection of identical gamma lines in gamma spectra produced by bombardment with either alpha particles or heavy ions, and especially the identical reduced probabilities of transitions from the ground state to the given excited states when different particles are used, provides strong evidence for the Coulomb origin of the gamma line under investigation.

---

*For example, see the remark about the excitation of Nb^{93} in reference 1.

The investigation of Coulomb excitation in odd-A nuclei encounters a number of difficulties which are not present in the case of even-even nuclei. In some instances the spins of excited states of odd-A nuclei are unknown. Calculation of the lifetime of a level requires knowledge of $B(E2)\downarrow$, the reduced probability of a transition from the excited to the ground level. Experimental studies of Coulomb excitation enable us to determine only $B(E2)\uparrow$, the reduced probability of the transition from the ground to the excited level. The spins of both the ground and excited levels must be known in order to calculate $B(E2)\downarrow$ from $B(E2)\uparrow$. The occurrence of Coulomb excitation signifies in the great majority of cases that the excited and ground levels have the same parity and that their spins do not differ by more than two units. This fact can be used in order to calculate the possible limits of $B(E2)\downarrow$. When the spin difference is only 1 either M1 or E2 radiation can be emitted. When the intensity ratio of M1 to E2 transitions is unknown the value of $B(E2)\uparrow$ enables us to calculate only the partial lifetime, $\tau(E2)$.

In odd-A nuclei it is frequently possible to excite several levels between which successive transitions are possible. The correct determination of $B(E2)\downarrow$ requires knowledge not only of the absolute gamma-ray yield from the direct transition to the ground state but also the gamma intensities of cascade transitions.

2. EXPERIMENTAL TECHNIQUE AND CALCULATION OF B(E2)

We used beams of the multiply-charged ions $N^{14;3+}$, $N^{14;4+}$, $O^{16;3+}$, $Ne^{20;4+}$, and $Ne^{22;4+}$ with energies from 16 to 36 Mev, which were produced by the cyclotron of the Physico-technical Institute (U.S.S.R. Academy of Sciences). A conventional deflector was used to extract the beam into an aluminum vacuum tube, and a system of two magnetic quadrupole lenses was used to focus the beam on the center of a target at the bottom of a Faraday cup. Exact focusing of the beam was achieved by replacing the Faraday-cup cylinder by another of the same length, provided with a ZnS-coated glass bottom. Such careful focusing was especially required in work with separated isotopes, which were available in very small quantities. The targets made of these isotopes were small (up to 5 mm in diameter) since sufficient target thickness was required for complete stopping of the ions. In order to prevent the projectiles from impinging (due to accidental defocusing of the beam, for example) on a ring of lead foil surrounding the target, the beam was collimated by a lead diaphragm (insulated from the Faraday cup) which was placed ~ 15 cm in front of the target. The diaphragm aperture was varied from 5 to 15 mm, depending on the target diameter.

It was established through special experiments that only a negligible amount of gamma radiation was produced by beam particles striking the edge of the diaphragm. The electric charge transferred to the target by ions was measured by an electronic current integrator which was calibrated separately for each experiment.

The gamma radiation resulting from ionic bombardment of the target was registered by a scintillation spectrometer. A NaI(Tl) crystal 40 mm thick and 40 mm in diameter was used in conjunction with a FEU-11 photomultiplier. The crystal, photomultiplier and preamplifier were shielded from stray magnetic fields. Excellent reproducibility of the "close" geometry was insured by the separation of only 2.7 mm between the target and the front plane of the crystal. The following absorbers separated the target from the crystal: 0.3 mm of copper, 1.3 mm of aluminum, 1 mm of magnesium oxide, 0.05 mm of lead and 0.05 mm of mica.

Amplified pulses from the preamplifier output were fed to a 50-channel pulse-height analyzer. The operation of the analyzer and the experimental technique are described in more detail in our earlier papers (references 2—4). Energy calibration of the gamma spectrometer was based on the following gamma lines: Hg^{203} (279.5 kev), Cs^{137} (661 kev), Zn^{65} (1120 kev), and Co^{60} (1170 and 1332 kev).

The reduced excitation probability was calculated by means of the formula

$$B(E2)\uparrow = 0.555\cdot 10^{-10}\,\frac{Z_i S_{ph}(1+\alpha_t)\,MZ_2^2 dE/d\rho x}{\eta\varepsilon_{ph}\omega A_\gamma \mu n}\times\left\{\int\limits_0^{E_{max}}(E-\Delta E)\,f_2(\xi)\,dE\right\}^{-1}. \qquad (1)$$

Here Z_i is the ionic charge in the extracted cyclotron beam; α_t is the total internal conversion coefficient; S_{ph} is the number of photons registered in the total energy peak for 1 microcoulomb of beam particles; M is the molecular weight of the target material in mass units; Z_2 is the nuclear charge of the investigated target atoms; $dE/d\rho x$ is the specific energy loss of ions in the target material in Mev/(mg/cm^2); η is the relative content of a given isotope in the investigated element; ϵ_{ph} is the ratio of the number of photons registered in the total energy peak to the total number of photons impinging on the crystal; ω is the relative solid angle; A_γ is the fraction of photons transmitted by the target and by the absorbers placed between the target and crystal; μ is the reduced mass in mass units; n is the number of atoms of the investigated element in a molecule of the target material; E is the collision energy in Mev; ΔE is the excited level energy; $f_2(\xi)$ is the Coulomb excitation function; ξ is a parameter defined by

$$\xi = 0.1575\, Z_1 Z_2 \sqrt{\mu}\,(1/\sqrt{E-\Delta E} - 1/\sqrt{E}); \qquad (2)$$

Z_1 is the nuclear charge of the bombarding particle.

The technique for determining S_{ph} from the experimental gamma spectra is described in detail in reference 2.

The coefficient $(1 + \alpha_t)$ was taken as unity, since α_t was very small in all the cases under consideration. The total spectrometer efficiency $\epsilon_{ph}\omega A_\gamma$ was determined in special experiments for a few values of E_γ by means of intensity-calibrated gamma-ray sources with the following energies: 279 kev (Hg^{203}), 661 kev (Cs^{137}) and 1332 kev (Co^{60}). Interpolation for other values of E_γ was based on a theoretical calculation of $\epsilon_{ph}\omega A_\gamma$ as a function of E_γ; this calculation was performed in reference 2 on the basis of data for ϵ_{ph} given in reference 5.

The literature contains very little information regarding the specific energy losses, in different materials, of heavy mulitply-charged ions with energies 10 – 40 Mev. In the present work the calculation of the specific energy loss of nitrogen ions with energies up to 25 Mev in different elements was based on the experimental range-energy relation for nitrogen ions in nickel which is given in reference 6. The conversion of $dE/d\rho x$ for a different element was based on the ratio between experimentally derived specific energy losses of protons with the same velocity as the nitrogen ions in nickel and in the given element.

The values of $dE/d\rho x$ for nitrogen ions of energy > 25 Mev and for oxygen ions in different elements were calculated in the same way, but the initial curves were the range-energy curves for these ions in nickel as plotted by the Longchamp method.[7] It should be noted that the Longchamp calculation of $dE/d\rho x$ for nitrogen ions in nickel is in good agreement with the calculation based on the data in reference 6.

The value of $dE/d\rho x$ for neon ions was calculated by means of the range-energy curve for neon ions in lead which was computed by Papino using the method described by him in reference 8.*

In reference 9 the values of $dE/d\rho x$ computed by different methods are compared with graphs of $dE/d\rho x$ as a function of Z_2, for C^{12}, N^{14} and O^{16} ions. The errors in the values of $dE/d\rho x$ calculated for heavy ions are estimated to be relatively large and may comprise 10 – 15%. On the other hand, the calculations indicated that $dE/d\rho x$ does not vary much with energy in the interval of present interest. (This is a relatively small energy range, because the cross section for Coulomb excitation falls off rapidly with diminishing bombarding energy.) In the calculations of B(E2) constant values were therefore assumed for $dE/d\rho x$.

Our results are given in the table. ΔE is the energy of observed gamma lines according to our data, ΔE^* is the value given in other investigations I_0 is the ground-state spin, I_f is the excited-state spin.* The table gives the reduced probability B(E2) for an electric quadrupole transition from the ground to the excited level according to our data (column 6)† and as given by other investigators (column 7). The last column shows the lifetime of the given state as calculated from our value of B(E2)↑.

We have estimated an error of 30 – 35% in the values of B(E2). In addition to the usual errors of ~ 20% incurred in investigations of Coulomb excitation we also took into account the error in B(E2) resulting from inaccurate determination of projectile energies, which in some instances may have amounted to 25%, and an error of ~ 15% in determining $dE/d\rho x$.

As a control we recorded the spectra of a number of gamma lines whose yield had been determined elsewhere. The discrepancy between our values of B(E2) and the values given in the literature was usually below 35%.

3. EXPERIMENTAL DATA FOR DIFFERENT ELEMENTS

Al^{27} ($Z = 13$). From data[11] on the beta decay of Mg^{27} it is known that the Al^{27} nucleus has two excited levels, 0.834 and 1.015 Mev, with spins $\frac{1}{2}^+$ and $\frac{3}{2}^+$ respectively. According to Mack[12] the ground-state spin of Al^{27} is $\frac{5}{2}^+$.

Heydenburg and Temmer[13] investigated the Coulomb excitation of nuclear levels in aluminum by means of 3-Mev alpha particles. Excitation was not observed because of the low alpha-particle energy, which could not be increased because of

---

*We are indebted to A. Papineau for his kindness in sending us a number of curves that he had computed.

*In cases where the spin of the excited level is unknown the possible limits of its value are indicated.

†Because of the improved experimental technique and the additional results obtained for $E_{N^{14}} = 40.9$ Mev the values of B(E2) given in the table are somewhat different from those in reference 10.

Nucleus	ΔE, Mev	ΔE^*, Mev	I_0	I_f	$\frac{B(E2)\uparrow}{e^2}\cdot 10^{48}$, cm^4	$\frac{B(E2)\uparrow^*}{e^2}\cdot 10^{48}$, cm^4	τ (E2), sec
1	2	3	4	5	6	7	8
Al^{27}	0.840	0.834	$^5/_2{}^+$	$^1/_2{}^+$	0.0021	—	$3.2\cdot 10^{-11}$ (c)
	1.010	1.015	$^5/_2{}^+$	$^3/_2{}^+$	0.0038	—	$1.3\cdot 10^{-11}$
Sc^{45}	0.375	0.377	$^7/_2{}^-$	$^3/_2{}^- — {}^{11}/_2{}^-$	0.0093	—	$(0.6—1.8)\cdot 10^{-9}$
	0.720	0.722	$^7/_2{}^-$	$^3/_2{}^- — {}^{11}/_2{}^-$	0.0045 (a)	—	—
V^{51}	0.930	0.928	$^7/_2{}^-$	$^3/_2{}^-$	0.011	—	$5.3\cdot 10^{-12}$ (d)
Cr^{53}	—	0.155	$^3/_2{}^-$	$(^5/_2{}^-)$	<0.0001	0.015	—
	—	0.370	$^3/_2{}^-$	$(^7/_2{}^-)$	<0.0001	—	—
Rb^{85}	0.150	0.148	$^5/_2{}^-$	$^3/_2{}^-$	0.0031	0.0032	$2.3\cdot 10^{-7}$
Rb^{87}	0.410	0.407	$^3/_2{}^-$	$^5/_2{}^-$	0.0073	0.0058	$1.4\cdot 10^{-9}$
Nb^{93}	0.760	0.764 0.759	$^9/_2{}^+$	$^5/_2{}^+ — {}^{13}/_2{}^+$	0.0023	—	$(8.6—20)\cdot 10^{-12}$
	0.985	0.977 0.971	$^9/_2{}^+$	$^5/_2{}^+ — {}^{13}/_2{}^+$	0.0044 (a)	—	$(1.2—2.7)\cdot 10^{-12}$
Sn^{117}	0.865	—	$^1/_2{}^+$	$^3/_2{}^+;\ {}^5/_2{}^+$	0.023 (b)	—	—
	1.030	—	$^1/_2{}^+$	$^3/_2{}^+;\ {}^5/_2{}^+$	0.083 (a)	—	$(1.2—2.6)\cdot 10^{-12}$ (e)
Sn^{119}	0.907	—	$^1/_2{}^+$	$^3/_2{}^+;\ {}^5/_2{}^+$	0.10	—	$(2.6—3.8)\cdot 10^{-12}$

---

a) In the calculation of B(E2)↑ it was assumed that no cascade transition occurs via a lower-lying level.

b) B(E2)↑ for ΔE = 0.865 Mev was calculated assuming, without confirmation, that a level with this energy is excited.

c) The true lifetime (τ) of the level.

d) The lifetime (τ) for the direct transition to the ground level.

e) In calculating limits for τ(E2) it was taken into account that photons with E = 0.865 Mev may be produced by a cascade transition from the 1.03-Mev level via a 0.165-Mev level.

the sharp rise of the gamma-ray background resulting from nuclear reactions.

In our investigation of Coulomb excitation in aluminum we used the following ions: $N^{14;3+}$ with E = 16.3 Mev, $O^{16;3+}$ with E = 18.2 Mev, $Ne^{20;4+}$ and $Ne^{22;4+}$ with 23.1 and 25.2 Mev respectively.* Figure 1 shows the gamma-ray spectra which were registered when 60 μ aluminum foil was bombarded with N^{14} and Ne^{20} ions. 0.51-Mev and 0.59-Mev gamma lines resulted from the nuclear reaction N + C. (More detailed information regarding the background lines resulting from reactions between nitrogen, carbon or oxygen ions and carbon or oxygen nuclei is given in reference 14.) The 1.63-Mev line is associated with the Coulomb excitation of the first Ne^{20} level.[15] 0.84-Mev and 1.01-Mev gamma lines corresponding to the above-mentioned excited levels of Al^{27} are observed as a result of bombardment with both nitrogen and neon ions. The fact that both lines result from the bombardment of aluminum with different ions and that the values of B(E2) calculated with data obtained by means of different ions are mutually consistent indicates that both lines result from Coulomb excitation in Al^{27}.

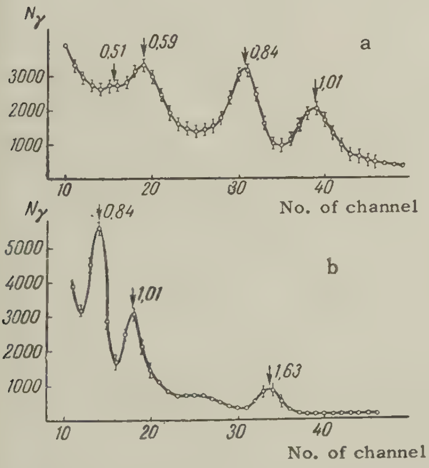

FIG. 1. Instrumental spectra of gamma rays from Coulomb excitation in aluminum: a – bombarded with 16.3-Mev N^{14} ions; b – bombarded with 23.1-Mev Ne^{20} ions. (Here and in the following figures the errors have only half of the magnitude represented by the vertical bars.)

To calculate the reduced probability of a transition from the ground level to excited levels of Al^{27} it is essential to know the branching ratio of direct and cascade transitions from the 1.01-Mev state. Since the cascade transition via the 840-kev level would involve the emission of 170-kev photons, for the purpose of determining the branching ratio we also studied the soft gamma-rays emitted by bombarded aluminum. It was found that the cascade-transition intensity comprised less than 4% of the direct-transition intensity. In references 11 and 16 this ratio is given as ~ 2%. In the calculations of B(E2) it was assumed that all radiation from the upper excited level of aluminum represents a direct transition to the ground level. The values of B(E2)↑ in the table are averages of data obtained in five experiments.

---

*Increase of nitrogen-ion energy to 25 Mev resulted in a sharp rise of the continuous gamma-ray background associated with nuclear reactions and in the appearance of background gamma lines. This prevented further investigation of Coulomb excitation in aluminum.

Using the known spins of the ground and first two excited levels of Al^{27}, we found that the partial lifetime $\tau(E2)$ of the 1.01-Mev level is 1.3×10^{-11} sec, while the lifetime of the 0.84-Mev level is 3.2×10^{-11} sec. In reference 17 an upper limit, $\tau < 10^{-10}$ sec, was indicated for each of these Al^{27} levels. Only the partial lifetime $\tau(E2)$ for the 1.01-Mev level can be calculated from the measurements, because the selection rules permit both E2 and M1 transitions from this level. $\tau(M1)$ can also be calculated from the ratio between E2 and M1 intensities.

Sc^{45} $(Z = 21)$. From inelastic neutron scattering data it is known that the Sc^{45} nucleus has excited levels at 377 and 722 kev.[18,19] The ground-state spin of Sc^{45} is $7/2^-$.[12] In studies of beta decay in Ca^{45} and Ti^{45} only transitions to the ground level of Sc^{45} were observed.

The Coulomb excitation of scandium was investigated earlier,[13,20] but no gamma lines were detected which could be assigned to the excitation of nuclear levels in Sc^{45}. The scandium oxide target which was used produced a high background from nuclear reactions of protons and alpha particles with oxygen.

We investigated the Coulomb excitation of Sc^{45} by means of triply-charged nitrogen and oxygen ions with 16.3 and 18.2 Mev, respectively, and quadruply-charged Ne^{20} and Ne^{22} ions with 23.1 and 25.2 Mev, respectively. These heavier ions permitted the use of scandium oxide targets.

Figure 2 shows the gamma-ray spectrum resulting from the bombardment of a ScO target with triply-charged nitrogen ions and quadruply-charged Ne^{20} ions. The 1.03-Mev and 1.37-Mev lines in Fig. 2b and the 0.65-Mev line in Fig. 2c are background lines which resulted from reactions of nitrogen ions with carbon (1.37 Mev) and oxygen (1.03 Mev), and of neon ions with oxygen (0.65 Mev). We assign the 375-kev and 720-kev lines to Coulomb excitation in Sc^{45}. Figure 2c shows the result obtained by subtracting the 0.65-Mev background line, the shape of which was determined separately by irradiating lead oxide with 23.1-Mev Ne^{20} ions. Following the subtraction the 750-kev line became distinct. The presence of 375-kev and 720-kev gamma lines in spectra obtained by irradiating scandium oxide with N^{14}, Ne^{20} and Ne^{22} ions and the agreement of the values of $B(E2)$ obtained with different ions indicate that these lines result from Coulomb excitation rather than from nuclear reactions.*

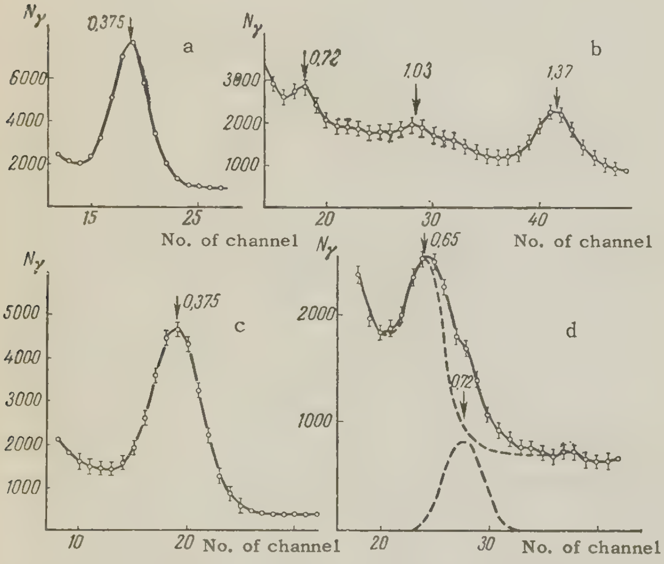

FIG. 2. Instrumental spectra of gamma rays from Coulomb excitation in scandium: a and b – bombarded with 16.3-Mev N^{14} ions; c and d – bombarded with 23.1-Mev Ne^{20} ions.

The mean values of $B(E2)\uparrow$ for the 0.375- and 0.720-Mev levels were calculated assuming that a cascade transition does not take place from the 0.72-Mev level and that the observed gamma lines have the energies of the levels for which $B(E2)$ was calculated. The spins of the excited Sc^{45} states are unknown. The partial lifetime $\tau(E2)$ of the 0.375-Mev Sc^{45} level lies within the range $(0.6 - 1.8) \times 10^{-9}$ sec, depending on the possible spin of this state ($3/2^-$, $5/2^-$, $7/2^-$, $9/2^-$, or $11/2^-$).

V^{51} $(Z = 23)$. From an investigation of the beta decay of Cr^{51} it is found that V^{51} has excited levels at 323 and 645 kev with spins and parities $5/2^-$ and $3/2^+$, respectively. From the beta decay of Ti^{51} it is known that V^{51} has excited levels at 323 and 928 kev with spins and parities $5/2^-$ and $3/2^-$. Alpha particles and protons have been used in a number of investigations of Coulomb excitation in vanadium[20–22], in which an excited level of V^{51} was found at 320 kev.

In the present work the vanadium metal target was bombarded with triply-charged 16.3-Mev and 19.7-Mev nitrogen ions and with quadruply-charged 26.0-Mev and 36.1-Mev nitrogen ions. Figure 3 shows the gamma spectra in the range 0.75 – 1.4 Mev which were produced by the ions with 16.3, 26.0 and 36.1 Mev. All spectra revealed a 930-kev gamma line, which is associated with excitation of a corresponding V^{51} level. It is noteworthy that the intensity of the 1.37-Mev background line in the case of vanadium, just as for other light elements, falls off compared with the continuous back-

---

*The 350-kev background line is always observed when any one of the targets is bombarded with nitrogen ions. However, the gamma line observed in experiments with scandium is so strong that the background line can be neglected in calculating the observed yield of the 375-kev line from Sc^{45}.

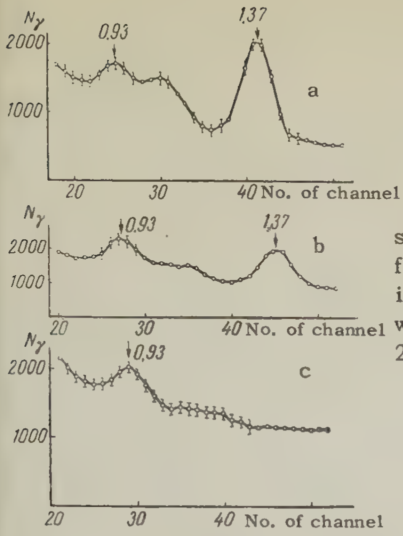

FIG. 3. Instrumental spectra of gamma rays from Coulomb excitation in vanadium by N^{14} ions with: (a) 16.3 Mev, (b) 26.0 Mev and (c) 36.1 Mev.

ground as the nitrogen ion energy is increased. For 36.1-Mev nitrogen ions this line is no longer observed. It is shown in the literature (references 23 and 24, for example) that in addition to the direct ground-state transition from the 0.93-Mev level a cascade occurs via the 0.323-Mev level. The 605-kev cascade line could not be observed in our work because of the 0.59-Mev background line resulting from a nuclear reaction between nitrogen ions and carbon. In calculating B(E2) for the excitation of the 0.93-Mev level we used data given in references 23 and 24 for the cascade branching ratio η from this level. In these sources η has the values 30% and 20%, respectively. We assumed $\eta = 25\%$, which was equivalent to assuming that the yield of excitations of the 0.93-Mev level is 1.25 times greater than the number of 0.93-Mev gamma rays. The tabular value of τ for $\Delta E = 0.93$ Mev was calculated for the transition from this level to the ground level assuming $3/2$ and $7/2$ as the respective spins of these levels.

Coulomb excitation at 320 kev was also observed when nitrogen ions were used. Our value for B(E2) agrees satisfactorily with the result obtained by Temmer and Heydenburg.[22]

Cr^{53} ($Z = 24$). Coulomb excitation in chromium has been studied by other investigators.[20,22] A 155-kev line was detected when a chromium oxide target enriched in Cr^{53} was bombarded with protons ($E_p \geq 1.3$ Mev).[20] This line was assigned to 155-kev excitation in Cr^{53}; the reduced excitation probability of this level was calculated to be $0.015 \times 10^{-48}\, e^2\, cm^4$.

Temmer and Hydenburg[22] bombarded a natural metallic chromium target with 6-Mev alpha particles. They detected among other gamma lines a 150-kev line which they assigned to radiation from an excited level in Fe^{53} following the reaction $Cr^{50}(\alpha, n\gamma)Fe^{53}$.

Gamma rays emitted by a target of natural metallic chromium bombarded with 3.4-Mev protons were studied in reference 25. The gamma spectrum included a 370-kev line with considerable intensity at proton energies below the $Cr^{53}(p, n\gamma)Mn^{53}$ threshold; this line was assigned to Cr^{53} excitation at this 370-kev level.

We have investigated the Coulomb excitation of chromium in order to verify the above data and hypotheses.

Experiments with Alpha Particles

A target made of pressed natural metallic chromium powder was irradiated with 6.6-Mev alpha particles. A 155-kev line was not observed, but a 130-kev line was observed and assigned to the reaction $Cr^{52}(\alpha, n\gamma)Mn^{55}$. From the 130-kev gamma-ray yield the value of $B(E2)\uparrow$ for $\Delta E = 155$ kev in Cr^{53} was calculated to be $0.0025 \times 10^{-48}\, e^2\, cm^4$, which is one-sixth of the result given in reference 20. The 370-kev line could not be detected because of the strong 420-kev background line resulting from $Cr^{52}(\alpha, n\gamma)Fe^{55}$.

Our chromium target enriched in Cr^{53} could not be used in experiments with alpha particles because the target material was Cr_2O_3, from which we could expect a strong gamma-ray background resulting from reactions between alpha particles and oxygen as well as a strong 350-kev line from the reaction $O^{18}(\alpha, n\gamma)Ne^{21}$. The amount of Cr_2O_3 was too small to permit the separation of metallic Cr^{53}.

Experiments with Multiply-charged Ions

In the experiments with multiply-charged ions three targets were used: 1) pressed natural metallic chromium powder, 2) electrolytic natural chromium, and 3) pressed chromium oxide with 95% enrichment in Cr^{53}. The projectiles were $N^{14;3+}$ with 16.3 and 19.7 Mev and $Ne^{20;4+}$ with 23.1 Mev.

A 155-kev line was not observed. Emission of a 123-kev line was observed from the first target but not from the electrolytic target. The first target apparently contained an iron impurity and the 123-kev line can be accounted for by 137-kev excitation in Fe^{57} followed by a cascade via a 14-kev level in Fe^{57}.

A 370-kev line was also not observed in the gamma spectra. The gamma spectra obtained by means of nitrogen ions always included a 350-kev background line produced by reactions between nitrogen ions and carbon. In these experiments $B(E2)\uparrow$ for the suggested 370-kev level in Cr^{53} was calculated from the total 350-kev gamma-ray yield. The value of $B(E2)\uparrow$ obtained in this manner is too high. No background gamma line in this energy region was observed in experiments with neon ions.

We have estimated the upper limits of the reduced excitation probabilities for 155- and 370-kev levels in Cr^{53}. For both levels the value of $B(E2)\uparrow_{\max}$ is 0.001×10^{-48} e^2 cm^4, which is considerably smaller than the estimate of $B(E2)$ for Cr^{53} that was based on single-particle considerations.

Since bombarding protons produce a very strong gamma-ray background it was impossible to observe gamma lines corresponding to chromium excitation with such values of $B(E2)\uparrow$.

Our experiments do not provide a basis for assuming the existence of 155- and 370-kev levels in Cr^{53}.

Rb^{85}, Rb^{87} ($Z = 37$). Thulin's investigation[26] of beta decay in Kr^{85}, Sr^{85} and Kr^{87} showed that Rb^{85} and Rb^{87} possess excited levels at 0.155 and 0.407 Mev, respectively, with spins $3/2^-$ and $5/2^-$. The spins of the ground states of Rb^{85} and Rb^{87} are $5/2^-$ and $3/2^-$ respectively.[12] Coulomb excitation in rubidium has also been studied by means of alpha particles.[27] The first levels of each of these isotopes were excited. Because of an oxygen impurity in the target the 407-kev line was observed against a very strong background.

We investigated Coulomb excitation in rubidium by means of $N^{14;3+}$ with 16.3 and 19.7 Mev, $N^{14;4+}$ with 26.0 Mev and $Ne^{20;4+}$ with 23.1 Mev. The targets were made of natural rubidium chloride and of rubidium chloride enriched in Rb^{87}. Figure 4 shows the gamma spectra obtained from RbCl and $Rb^{87}Cl$ targets bombarded with 16.3-Mev nitrogen ions. The table contains the mean values of $B(E2)$ based on two experiments in which the 150-kev level was excited and on six experiments in which the 0.41-Mev level was excited. The value of $B(E2)$ for the 155-kev level is in good agreement with the data in reference 27, but there is some discrepancy in the values for the 0.41-Mev level of Rb^{87}. The partial lifetimes $\tau(E2)$ of the first levels of Rb^{85} and Rb^{87} were calculated by us from the values obtained for $B(E2)\uparrow$.

Nb^{93} ($Z = 41$). From the study of beta decay in Zr^{93} we know[28] that Nb^{93} has a metastable 29-kev level with spin and parity $1/2^-$ and lifetime 3.65 years. The spin of the ground state is $9/2^+$.[12] Coulomb excitation of nuclear levels in niobium has been studied by Heydenburg and Temmer[13] and by McGowan and Stilson[1] using 3-Mev alpha particles and 2-Mev protons. The former investigators detected no excitation of Nb^{93} levels, but the latter, who used 3-Mev protons, observed 0.71- and 0.87-Mev gamma lines. Although measurements of the excitation function permitted the conclusion that both lines result from Coulomb excitation, a coincidence analysis showed that the two lines coincide with each other and with a still harder line. The association of these lines with Coulomb excitation in niobium is therefore entirely excluded.

Inelastic scattering of neutrons by niobium has been investigated in references 29 and 30. 736- and 957-kev lines were observed in the first of these studies, and 759- and 971-kev lines were observed in the second. In reference 29 measurements of (n, n′) reaction thresholds provided the basis for the suggestion that Nb^{93} has levels at 764 and 977 kev, with cascade transitions occurring via a metastable 29-kev level.

We studied Coulomb excitation in Nb^{93} by means of $N^{14;4+}$ ions with 26.0 and 36.1 Mev. Figure 5 shows the gamma spectrum which was observed when metallic niobium was bombarded with 36.1-Mev nitrogen ions. A 1.37-Mev background line was observed, as in preceding instances. 0.760- and 0.985-Mev lines were measured to within

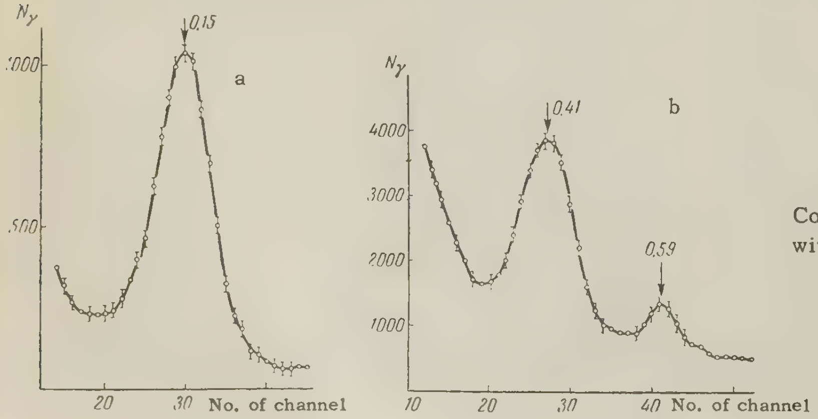

FIG. 4. Instrumental spectra of gamma rays from Coulomb excitation in Rb^{85} (a) and Rb^{87} (b) bombarded with 16.3-Mev N^{14} ions.

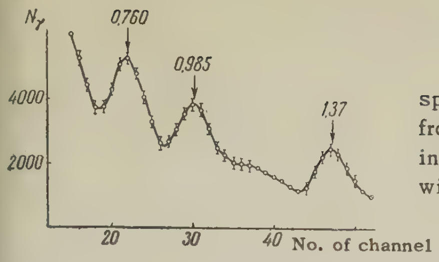

FIG. 5. Instrumental spectrum of gamma rays from Coulomb excitation in niobium bombarded with 36.1-Mev N^{14} ions.

±1%. Our measurements thus confirm Sinclair's results[30] but do not agree with the results given in reference 29. Since the observed excited levels of Nb^{93} (resulting from Coulomb excitation) must have positive parity, transitions from these levels to a metastable level with negative parity cannot occur. Therefore the gamma lines which we observed must represent a direct ground-level transition, in contradiction to the hypothesis advanced in reference 29. The table gives the mean values of $B(E2)\uparrow$ which were calculated assuming the absence of cascade transitions, with the gamma-ray energies thus equalling the energies of the levels. The limits of the partial lifetimes $\tau(E2)$ given in the table were calculated taking into account all possible values of spins for the excited Nb^{93} levels.

Sn^{117}, Sn^{119} $(Z = 50)$.* We had previously studied Coulomb excitation in Sn^{117} and Sn^{119} by means of 10- to 14.5-Mev alpha particles,[2] and had observed 0.865- and 1.03-Mev lines from Sn^{117} and a 0.907-Mev line from Sn^{119}. In this work the excitation function was measured in a relatively narrow bombarding energy range; for $E_\alpha < 10$ Mev the gamma-ray yield became small, while for $E_\alpha > 14.5$ Mev the nuclear-reaction background rose sharply. It was therefore desirable to verify whether the observed gamma rays resulted from reactions. We used 36.1-Mev nitrogen ions for the further investigation of Coulomb excitation in Sn^{117} and Sn^{119}. The targets were made of metallic tin enriched in Sn^{117} and Sn^{119}. The observed gamma spectra are shown in Fig. 6, where it is important to note that the ratios of the observed peaks to the background level are approximately four times as large as in the work with alpha particles. The calculated values of $B(E2)\uparrow$ based on the assumption that the gamma-ray energies equal the excited-level energies, are in good agreement with the results given in reference 2; differences do not exceed 10%. The fact that the same gamma lines were observed when the targets were bombarded with different particles and the good agreement of $B(E2)$ measured in experiments with alpha particles and with heavier ions provide confirmation that these lines result from Coulomb excitation.

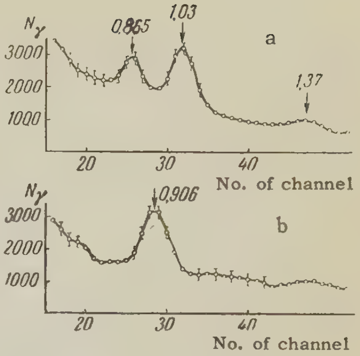

FIG. 6. Instrumental spectra of gamma rays from Coulomb excitation in Sn^{117} (a) and Sn^{119} (b) bombarded with 36.1-Mev N^{14} ions.

We were unable to determine whether 0.865-Mev gamma rays result from excitation of the corresponding level in Sn^{117} or from a cascade beginning at 1.03 Mev and proceeding to the ground level via a level at 0.16 Mev, which is known[31] from an investigation of beta decay in In^{117}. In our work with alpha particles and with heavier ions we obtained gamma spectra which included a 0.16-Mev line. The excitation function indicated that this line cannot be attributed to an excited level at 1.03 Mev, but this same measured excitation function does not agree very well with the assumption of a directly excited 0.16-Mev level. We intend to use a coincidence technique for further investigation of the origin of the 0.16- and 0.865-Mev lines resulting for Coulomb excitation in Sn^{117}.

The mean values of $B(E2)\uparrow$ given in the table were calculated on the assumption that the gamma-ray energies equal the excited-level energies. The indicated limits of the partial lifetimes take into account the possible spins of excited Sn^{117} and Sn^{119} levels.

We wish to thank A. B. Girshin, leader of the cyclotron team, for the assistance that we received.

---

*D. S. Andreev assisted us with the study of Coulomb excitation in Sn^{117} and Sn^{119}.

[1] F. K. McGowan and P. H. Stelson, Phys. Rev. **109**, 901 (1958).

[2] Alkhazov, Andreev, Erokhina, and Lemberg, JETP **33**, 1347 (1957), Soviet Phys. JETP **6**, 1036 (1958).

[3] Alkhazov, Grinberg, Gusinskiĭ, Erokhina, and Lemberg, JETP **35**, 1325 (1958), Soviet Phys. JETP **8**, 926 (1959).

[4] Alkhazov, Andreev, Grinberg, and Lemberg, Nuclear Phys. **2**, 65 (1956).

[5] Maeder, Muller, and Wintersteiger, Helv. Phys. Acta **27**, 3 (1954).

[6] Reynolds, Scott, and Zucker, Phys. Rev. **95**, 671 (1954).

[7] J. P. Longchamp, J. phys. radium **14**, 89 (1953).

[8] A. Papineau, Compt. rend. **242**, 2933 (1956).

[9] A. P. Grinberg and I. Kh. Lemberg, Izv. Akad. Nauk SSSR, Ser. Fiz. **23**, 887 (1959), Columbia Tech. Transl. in press.

[10] Alkhazov, Grinberg, Gusinskiĭ, and Lemberg, Программа и тезисы докладов IX ежегодного совещания по ядерной спектроскопии в Харькове (Program and Summaries of Papers, Ninth Annual Conference on Nuclear Spectroscopy at Kharkov), Acad. Sci. USSR 1959, p.41.

[11] W. S. Lyon and N. H. Lazar, Phys. Rev. **101**, 1524 (1956).

[12] I. E. Mack, Revs. Modern Phys. **22**, 64 (1950).

[13] N. P. Heydenburg and G. M. Temmer, Phys. Rev. **93**, 351 (1954).

[14] Alkhazov, Grinberg, Gusinskiĭ, and Lemberg, Izv. Akad. Nauk SSSR, Ser. Fiz. **23**, 1465 (1959), Columbia Tech. Transl. in press.

[15] Alkhazov, Grinberg, Lemberg, and Rozhdestvenskiĭ, JETP **36**, 322 (1959), Soviet Phys. JETP **9**, 222 (1959).

[16] Almqvist, Bromley, Gove, and Litherland, Bull. Am. Phys. Soc. **2**, 178 (1957).

[17] C. P. Swann and W. C. Porter, J. Franklin Inst. **261**, 371 (1956).

[18] Phillips, Gossett, Schiffer, and Windham, Phys. Rev. **99**, 655(A) (1955).

[19] Day, Johnsrud, and Lind, Bull. Am. Phys. Soc. **1**, 56 (1956).

[20] Mark, McClelland, and Goodman, Phys. Rev. **98**, 1245 (1955).

[21] G. M. Temmer and N. P. Heydenburg, Phys. Rev. **96**, 426 (1954).

[22] G. M. Temmer and N. P. Heydenburg, Phys. Rev. **104**, 967 (1956).

[23] M. Bunker and J. Starker, Phys. Rev. **97**, 1272 (1955).

[24] Burson, Jordan, and LeBlanc, Phys. Rev. **98**, 230 (1955).

[25] Val'ter, Zalyubovskiĭ, Klyucharev, and Lutsik, Ядерные реакции при малых и средних энергиях. (Nuclear Reactions at Low and Medium Energies), USSR Acad. Sci. 1958, p.279.

[26] S. Thulin, Phys. Rev. **87**, 684 (1952); Arkiv Fysik **9**, 137 (1955).

[27] Fagg, Geer, and Wolicki, Phys. Rev. **104**, 1073 (1956).

[28] L. Glendin and E. Steinberg; see Table of Isotopes by Hollander, Perlman, and Seaborg, Revs. Modern Phys. **25**, 469 (1953) (Russ. Transl., IIL, 1956).

[29] Rothman, Van Patter, Dubey, Porter, and Mandeville, Phys. Rev. **107**, 155 (1957).

[30] R. M. Sinclair, Phys. Rev. **107**, 1306 (1957).

[31] S. M. Kalebin, JETP **30**, 957 (1956), Soviet Phys. JETP **3**, 799 (1956).

Translated by I. Emin
312

SOVIET PHYSICS JETP VOLUME 37(10), NUMBER 6 JUNE, 1960

ELECTRIC CONDUCTIVITY OF THE EXPLOSION PRODUCTS OF CONDENSED EXPLOSIVES

A. A. BRISH, M. S. TARASOV, and V. A. TSUKERMAN

Submitted to JETP editor July 4, 1959

J. Exptl. Theoret. Phys. (U.S.S.R.) 37, 1544-1550 (December, 1959)

The electric conductivity of the explosion products of various condensed explosives was investigated by the electric-contact and the electromagnetic methods. The conductivity of the investigated explosives ranges from 0.1 and 6 mho/cm near the wave front and decreases with increasing distance from the front. The electric conductivity of the explosion products increases with increasing density of the explosive and with increasing intensity of the detonation wave. It is suggested that the high values of electric conductivity of the explosion products are due, in addition to thermal ionization, also to the high densities and pressures that occur on the front of the detonation wave.

INTRODUCTION

IN spite of considerable research in the field of explosions,[1-3] many physical processes that accompany the detonation of explosive substances have not yet been fully investigated. Among these phenomena is the high electric conductivity of the explosion products near the front of the detonation wave. The electric conductivity due to thermal ionization has been previously estimated from the experimentally-measured temperature of the explosion products[4] at $10^{-3} - 10^{-5}$ mho/cm. In 1947, however, the authors observed, in an investigation of the electric conductivity of the explosion products in the detonation of solid explosives [TNT, pentaerythritoltetranitrate (PETN), and others], that the experimental values of the electric conductivity near the front of the detonation wave may exceed by several orders of magnitude the calculated values given above.

In 1948/49 several methods were developed for the measurement of the electric conductivity of explosion products of various explosives. These have made it possible to ascertain the regular variation of the electric conductivity of the explosion products as a function of the charge density, pressure on the front of the detonation wave, and other characteristics.

This paper is a brief report on the features of the investigated recording method used, and of the experimental results obtained on the electric conductivity of explosion products near the front and behind the front of the detonation wave. We also discuss the possible causes of the high electric conductivity of the products of condensed explosives.

MEASUREMENT PROCEDURE

A resistance that varies rapidly with time is best measured with a cathode ray oscillograph with slaved sweep. The measurement of the electric phenomena in the explosion has many peculiarities that impose special requirements on the measuring circuit. The sizable electric charges and electromagnetic disturbances that arise during the explosion may serve as sources of electric noise, which distorts the oscillographic record and makes its unambiguous interpretation difficult. Such noise is particularly significant if the signals to the measuring circuits are small, when additional amplification must be used. Consequently the extensively used bridge circuits, whose outputs amount to hundredths and tenths of a volt, are of no use in the measurement of the conductivity of explosion products. Reliable results were made possible by the use of special measuring circuits, the outputs of which, for various values of explosion-product resistances, ranged from 10 to 150 volts and could be directly registered by the oscillograph without prior amplification. Only in relatively few experiments was intermediate amplification used.

The principal quantitative variations were determined by direct electric-contact measurement of the electric resistance of the explosion products. However, in view of the danger that the presence of metallic probes in the charge could distort the measurement results, an electromagnetic contactless registration method was developed for the high-conduction zone.

Let us describe the two methods briefly.

A. Electric-contact Measurements. The principal diagram of the method is shown in Fig. 1. Here C_a is an accumulating 4 μf capacitor, charged beforehand to 4 — 6 kv. During the explosion, special contacts apply a voltage to the triggering electrode of a T-409 thyratron. Capacitor C_a discharges through a high voltage-resistance R_h and two parallel resistances R_{sh} and R_x. The value of R_x prior to the explosion of the charge is close to infinity, but it becomes commensurate with R_{sh} at the instant when the detonation front reaches the tops of metallic electrodes E, imbedded in the investigated charge, in the end opposite to that where the explosion is initiated.

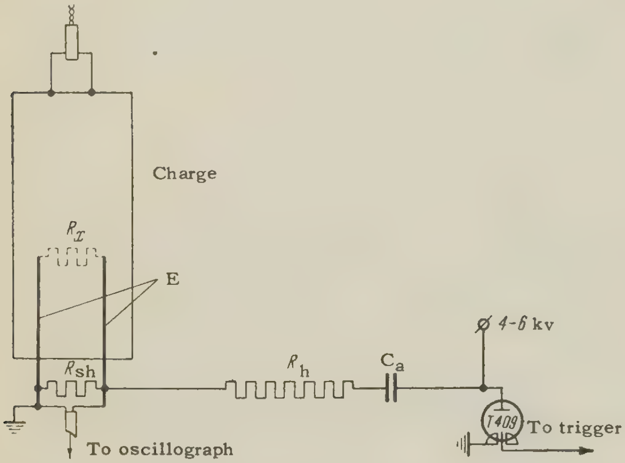

FIG. 1. Diagram of contact method for measuring electric conductivity of explosion products.

Connected in parallel with R_{sh} and R_x is a coaxial cable to transmit the voltage that develops across these resistances to the vertical plates of the oscillograph. If the high-voltage resistance R_x exceeds by many times the resistances R_{sh} and R_x, the discharge current in the capacitor C_a is practically independent of R_x, and the voltage registered across the electrodes E varies linearly with the total resistance $R_{sh}R_x/(R_{sh} + R_x)$. To determine the resistance R_x we can use, with sufficiently good approximation, the relation

$$R_x = U_x R_{sh}/(U_{sh} - U_x), \tag{1}$$

where U_{sh} and U_x are the respective voltages on the electrodes E prior to the instant when the detonation wave reaches the tops of the electrodes and after the production of the high-conductivity zone. The distinguishing feature of this method of measuring a rapidly-varying resistance is that there is no need for using the oscillograph to measure the absolute values of the voltages. The magnitude of the measured resistance R_x is determined here uniquely by the shunting resistance R_{sh} and the voltage-amplitude ratio $U_x/(U_{sh} - U_x)$. To measure the latter it is necessary only to insure a linear deflection of the electron beam with voltage; in most instruments this is satisfied with sufficient degree of accuracy at small amplitudes.

Figure 2 shows a typical oscillogram obtained with a circuit of Fig. 1. For the sake of clarity, the oscillogram shows the ordinates U_{sh} and U_x. In this experiment R_{sh} was 2 ohms, and the unknown resistance of the explosion products, calculated from (1), was found to be 0.47 ohms.

FIG. 2. Oscillogram of the variation in the electric conductivity measured with the circuit of Fig. 1; the frequency of the lower sine wave is 1 Mcs.

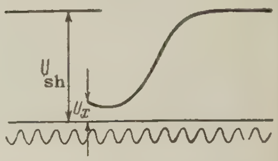

The measured resistance R_x is converted into specific electric conductivity of the explosion products by electrolytic simulation. For this purpose the electrodes, their mutual placements strictly preserved, are placed in an electrolytic bath. By measuring the interelectrode resistance at various electrolyte densities and various electrode depths, it is possible to estimate the specific electric conductivity corresponding to specified values of the resistance R_x.

An analysis of the circuit of Fig. 1 shows that the greatest accuracy of measurement (approximately 5%) can be reached when R_{sh} is close in value to R_x. Therefore, depending on the experimental conditions, the R_{sh} was varied from 1 to 100 ohms. The minimum measured value was approximately 10% of the value of the shunting resistance, 0.1 ohms at $R_{sh} = 1$ ohm. It was impossible to extend the measurement range on the low end, owing to the rise time of the current in the circuit comprising the inductance of the electrode system (approximately 5×10^{-8} henry) and the resistance R_{sh}. At $R_{sh} = 1$ ohm the rise time $\tau = 3L/R_{sh}$ amounts to 0.15 μsec. A further decrease in R_{sh} leads to an intolerably large increase in the rise time of the current in the measuring circuit.

B. The Electromagnetic Method. The idea of the method is gained from Fig. 3. The electromagnets produce a constant magnetic field (250 — 400 oe), the direction of which coincides with the horizontal axis of spherical charge 3. Measuring coil C is wound around the outer surface of the charge. The coil terminals are connected through

FIG. 3. Diagram of electromagnetic method of measuring the high-conductance zone.

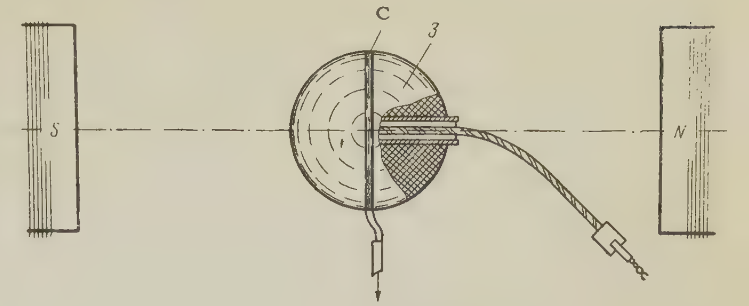

an amplifier to the vertical plates of the oscillograph.

Let us examine the phenomena that occur when the explosive charge is detonated at its center. In this case the detonation wave is a regular sphere, the diameter of which increases continuously with propagation of the detonation from the center of the charge to its periphery. This produces an annular current in the conducting layer of explosion products near the detonation front. The amplitude and the rise time of this current depend on the mass velocity of the explosion products (which determines the rate at which the magnetic flux builds up in the conducting ring) and on the electric conductivity of the explosion products in the front of the detonation wave. Owing to the inductive coupling between the annular current and the external measuring coil, a voltage will be produced at the terminals of the latter and is correspondingly registered on the oscillograph screen.

Figure 4 shows a characteristic measuring-coil voltage oscillogram obtained in the explosion of the charge. The measuring-coil voltage (upper curve) first rises relatively slowly and then rapidly.

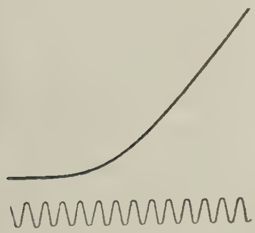

FIG. 4. Measuring-coil voltage oscillogram (circuit of Fig. 3); frequency of sine wave – 1 Mcs.

A quantitative determination of the specific electric conductivity of the explosion products under such experimental conditions entails certain difficulties. In addition to depending on the mass velocity and the resistance of the annular layer of conducting explosion products, the measuring-coil voltage depends also on the inductive coupling between the annular current and the coil. This coupling increases continuously as the wave front moves from the center to the outer boundary of the charge. However, as will be shown below, this electromagnetic method has yielded important qualitative information on the structure of the conducting region of the explosion products behind the front of the detonation wave.

EXPERIMENTAL RESULTS

Data on the electric conductivity of the explosion products of various explosives, obtained by the electric-contact method, are listed in the table.

The secondary-explosive charges were 60 mm in diameter and 140 mm long; they were initiated at one point on the end opposite the place where the electrodes were imbedded (divergent detonation wave). The gap between the electrodes was 10 mm, and the electrode diameter was 3 mm. The lead-azide charge was 15 mm in diameter and 30 mm long (electrodes 1 mm in cross section, 5 mm gap).

Experiments with molded charges had good reproducibility. Powdered charges as a rule

Electric conductivity of explosion products of various explosives

Explosive	Density δ_0, g/cm³	Detonation speed, D, km/sec	Average resistivity, ρ, ohm-cm	Average conductivity, $\gamma = 1/\rho$, mho/cm
Alloy of 50% TNT and 50% "hexogen" (molded)	1.64	7.7	0.2	5.0
50% TNT plus 50% "hexogen" (powdered charge)	0.8	5.7	1.0	1.0
Hexogen (powdered)	0.8	6.2	4.3	0.23
TNT (powdered)	0.8	4.5	0.25	4.0
PETN (powdered)	0.8	5.2	7.6	0.13
Tetryl (powdered)	0.8	5.0	6.3	0.16
Lead azide (powdered)	~0.9	2.7	0.16	6.2

gave a spread in the resistances of the explosion products within a factor 1.5. The data listed in the table for these charges are averages of 3 — 5 measurements. The specific resistivity of the explosion products of most investigated powdered charges ranged from 1 to 10 ohm-cm, with the exception of powdered TNT ($\rho = 0.25$ ohm-cm) and lead azide ($\rho = 0.16$ ohm-cm). The explosion products of a molded charge made of an alloy of TNT with "hexogen" have a considerably smaller resistivity than an analogous powdered charge (0.2 and 1 ohm-cm, respectively).

To determine the instant at which a high-conductivity zone occurs during the explosion of the charge, a special series of measurements was organized jointly with K. K. Krupnikov. One half of the end face of the charge was covered with a steel plate 2 mm thick. Contacts were installed on the outer surface of the plate to mark the instant when the shock wave emerged from the outer surface. The electrodes used to monitor the electric conductivity of the explosion products were in contact with the unprotected part of the charge end face. The time interval between the instant of occurrence of the high-conductivity zone and the instant of emergence of the shock wave to the free surface of the steel plate was measured on the oscillogram. Knowing the rate of propagation of the shock wave in steel for a given explosive charge (as determined in reference 5) it was possible to relate the position of the high-conductivity zone with the position of the detonation front.

Within the limits of time-measurement accuracy (± 0.01 μsec) it was found that the high conductivity region almost coincided with the front of the detonation wave.

To gain an idea of the variation of the electric conductivity of the explosion products behind the wave front, electromagnetic measurements of the conductivity were made for an explosion initiated at the center of a spherical charge made of an alloy of TNT with "hexogen."

At the authors' request, G. M. Gandel'man calculated the magnitude and variation of the voltage in the measuring coil, using the setup shown in Fig. 3. Since the thickness of the conducting layer is unknown, a quantity $\sigma = \rho/\Delta$ (ohms) was introduced into the computation (ρ — specific resistivity, Δ — thickness of conducting layer). Thus σ is the resistance (ohms) per square centimeter of the surface of the conducting layer.

The voltage E at the terminals of an n-turn coil of radius R is given for a spherical diverging detonation wave by

$$E = \frac{8\pi^2 n u^2 H}{\sigma R} r^2 \cdot 10^{-7} \text{ v}, \qquad (2)$$

where H is the intensity of the magnetic field, u the mass velocity of the explosion product behind the front of the wave, and r the running radius of the front of the detonation wave. It follows from (2) that if σ is constant, then the voltage in the measuring coil increases quadratically as the detonation wave propagates from the center to the periphery of the charge.

For self-similar propagation of a spherical detonation wave it is natural to assume that the effective thickness of the conducting layer increases linearly with the radius r of the wave. In this case the surface conductivity varies as the reciprocal of the radius r, and the voltage in the coil is directly proportional to r^3.

Figure 5 shows the time variation of the voltage, calculated from expression (2) for the cases $\sigma = \text{const}$ and $\sigma \sim 1/r$.

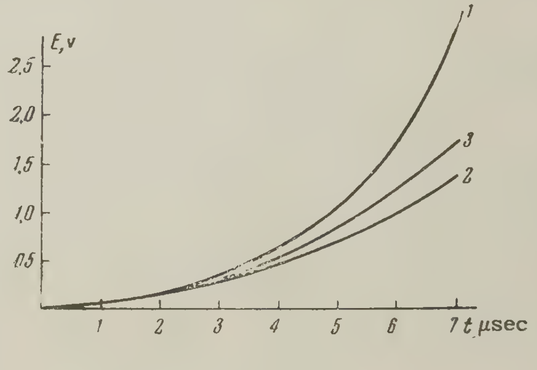

FIG. 5. Dependence of the measuring-coil voltage on the time, for a spherical diverging detonation wave; 1 — calculated curve for $\sigma = \text{const}$, 2 — calculated curve for $\sigma \approx 1/r$, 3 — experimental curve for a charge made up of an alloy of TNT with "hexogen."

The figure shows that the experimental curve 3 lies between the two calculated curves. This shows that the high-conductivity zone is located in a relatively narrow layer adjacent to the wave front, and corresponds to the high-pressure region. The value of σ calculated from the curve of Fig. 5 amounted to 0.26 or 0.27 ohms and was in good agreement with the conductivity as measured by the contact method.

The dependence of the conductivity of the explosion products on the pressure and density on the detonation wave front was investigated by the electric-contact method for an alloy of TNT and "hexogen." The results of these measurements, in the pressure range $10^5 - 10^6$ kg/cm², are shown in Figs. 6 and 7. It is clearly seen that the conductivity of the explosion products increases rapidly with increasing pressure, reaching values $\gamma > 100$ mho/cm at $p \approx 10^6$ kg/cm² and a relative density $\delta/\delta_0 \approx 2$.

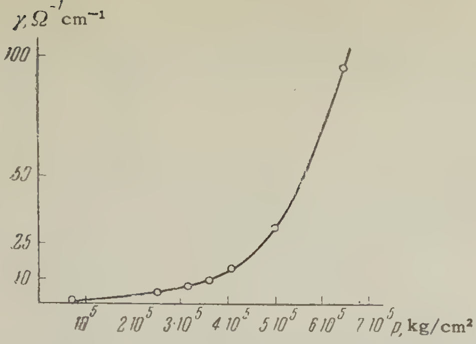

FIG. 6. Conductivity of explosion products (γ) vs. the pressure (p) on the front of the detonation wave.

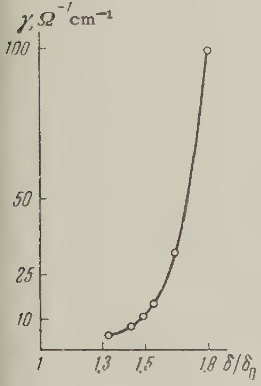

FIG. 7. Conductivity of explosion-products (γ) vs. relative density (δ/δ_0) on the front of the detonation wave.

DISCUSSION OF THE RESULTS

Two different causes are possible for the high conductivity on the front of the detonation wave: 1) thermal ionization, 2) chemical reaction in the front of the wave, and 3) increase in density of the substance under the influence of the high pressures.

The degree of thermal ionization can be calculated from the known Saha formula

$$x^2 = 1.337 T^{5/2} p^{-1} \exp\{-ev/kT\}. \tag{3}$$

Here x is the ratio of the number of ionized particles to their initial total number, p is the pressure, and ev is the ionization energy.

Equation (3) yields values of ρ which are four or five orders of magnitude greater than the experimentally observed specific resistivity of the explosion products. In addition, the degree of ionization in the Saha formula is inversely proportional to the pressure p. Experiment shows, on the other hand, that an increase in the pressure leads not to an increase but to sharp decrease in the resistivity of the conducting layer (see Fig. 6). Thermal ionization therefore does not explain the phenomenon described in the preceding section.

It has been suggested that the high conductivity in the chemical-reaction zone on the detonation wave front is due to the presence of certain impurities. In our experiments TNT, the explosion products of which contain a considerable amount of free carbon, has a conductivity one order of magnitude greater than other secondary explosive substances. High conductivity was observed also in the case of lead azide, the detonation products of which contain free lead. On the other hand, in specially performed experiments with charges of hexogen and PETN with 5% carbon dust or aluminum added, no increase was observed in the conductivity over the data obtained for the initial substances without conducting additives. Thus, the available experimental data do not lead to unequivocal conclusions regarding the influence of the chemical reaction on the high conductivity of the explosion products.

A careful examination of our experimental data makes it easy to disclose a common law — an increase of density and pressure within the wave front increases the conductivity of the explosion products. Thus, a change from a powdered TNT-hexogen charge to a molded charge of the same composition increases the conductivity five times. An increase in pressure on the wave front, to 6.5×10^5 kg/cm² and more, causes a further increase in the electric conductivity. These data show that the increase in pressure and density are reflected most noticeably in the conductivity of the explosion products. One can therefore propose the following pattern to explain the high conductivity in explosion of condensed media. High pressures, by increasing the density of the matter in the wave front, increase the interaction between the atoms. The simultaneous presence of a high temperature facilitates the creation of free electrons and ions. The combination of these phenomena leads to the formation of a high-conductivity zone.

The experimental data at our disposal do not allow us to separate the influence of high temperatures from that of the pressure. For charges of powder density, when the pressures in the wave front do not exceed 10^5 kg/cm², the formation of the high conductivity zone is apparently greatly influenced by the high temperature within the wave front. To the contrary, for dense gas charges at pressures above 6×10^5 kg/cm², for which the highest values of conductivity were obtained, the observed phenomena could be attributed essentially to the high pressures.

In conclusion, the authors express their deep gratitude to K. K. Krupnikov and G. M. Gandel'man for aid in the performance of the experiments and the reduction of the experimental data.

---

[1] Ya. B. Zel'dovich and A. S. Kompaneets, Теория детонации (Detonation Theory), Gostekhizdat, 1955.

[2] L. D. Landau and E. M. Lifshitz, Механика сплошных сред, (*Mechanics of Continuous Media*), 2d Ed., Gostekhizdat, 1954.

[3] K. P. Stanyukovich, Неустановившиеся движения сплошной среды (*Unsteady Motion of a Continuous Medium*), Gostekhizdat, 1955.

[4] Alintsev, Belyaev, Sobolev, and Stepanov, JETP **16**, 990 (1946).

[5] Al'tshuler, Krupnikov, Ledenev, Zhuchikhin, an Brazhnik, JETP **34**, 874 (1958), Soviet Phys. JETP **7**, 606 (1958).

Translated by J. G. Adashko
313

SOVIET PHYSICS JETP VOLUME 37 (10), NUMBER 6 JUNE, 1960

PARAMAGNETIC RESONANCE IN MAGNETICALLY DILUTE SYSTEMS

N. S. GARIF'YANOV

Physico-technical Institute, Kazan' Branch, Academy of Sciences, U.S.S.R.

Submitted to JETP editor July 4, 1959

J. Exptl. Theoret. Phys. (U.S.S.R.) **37**, 1551-1557 (December, 1959)

The dependence of the ratio b/c on the magnetic dipole-dipole interaction has been studied by the paramagnetic relaxation technique in parallel fields in the frequency range 1.6 — 300 Mcs at T = 90°K. Samples containing Cr^{+++}, Fe^{+++}, Mn^{++}, Cu^{++} and VO^{++} have been investigated.

INTRODUCTION

PARAMAGNETIC absorption $\chi''(H_{\|})$ in parallel fields (oscillating magnetic field H_ν parallel to the fixed magnetic field H) is due to spin-spin or spin-lattice relaxation, depending on the frequency and the temperature of the sample.

It has been shown experimentally by Gorter[1] and Kozyrev[2] that the absorption $\chi''_l(H_{\|})$ in undilute titrated salts of elements of the iron group in the frequency region near 10^7 cps in the temperature range 77 — 295°K is due primarily to spin-lattice relaxation. The experimental curves are in agreement with the thermodynamic theory of Casimir and Du Pre.[3] The absorption formula given by Casimir and Du Pre is

$$\chi''_l/\chi_0 = F\rho_l\nu/(1+\rho_l^2\nu^2). \tag{1}$$

Here χ_0 is the specific susceptibility for normal paramagnets, ν is the frequency of the oscillating field H_ν; ρ_l is the spin-lattice relaxation time

$$F = H_{\|}^2/(b/c + H_{\|}^2), \tag{2}$$

where b is the magnetic heat capacity and c is the Curie constant.

Gorter has shown[1] that the Casimir-Du Pre theory is not satisfactory at frequencies $\nu > 10^7$ cps because absorption due to spin-spin relaxation appears at these frequencies. Shaposhnikov[4] has formulated a thermodynamic theory which takes account of both lattice and spin-spin relaxation. The Shaposhnikov formula for spin-spin absorption in parallel fields is

$$\chi''_s/\chi_0 = (1-F)^2\rho_s\nu/\{1+(1-F)^2\rho_s^2\nu^2\}. \tag{3}$$

Experiments carried out by the author[5,6] indicate, however, that the absorption $\chi''_S(H_{\|})$ at frequencies 6×10^8 cps at T = 295°K in certain Mn^{++} and Gd^{+++} salts depends only on spin-spin relaxation. The experimental curves which were obtained are described approximately by the relation

$$\chi''_s/\chi_0 = (1-F)^2\rho_s\nu,. \tag{4}$$

where ρ_S is the spin-spin relaxation time. This expression is obtained from the Shaposhnikov formula (3) when $\rho_S^{-1} \gg \nu$. It is assumed that ρ_S is independent of $H_{\|}$. A relation has been obtained from Eq. (4) to find the quantity b/c experimentally:

$$b/c = (1+\sqrt{2}\ \Delta H_{\|})^2, \tag{5}$$

where $\Delta H_{\|}$ is the half-width of the spin-spin absorption curve.

Good agreement between the Shaposhnikov theory and experiment has also been obtained by Sitnikov[7] and Kurushin.[8]

The present work was undertaken to investigate the dependence of the ratio b/c on dilution for certain magnetic ions of the iron group.

EXPERIMENTAL METHOD AND SAMPLES

These paramagnetic absorption measurements were carried out in the range 1.6 — 300 Mcs using a technique which has been described earlier by the author.[9,10]

In order to investigate the detailed features of the complicated absorption curves, instead of using a fixed magnetic field H we used a field which was varied at a frequency of 50 cps with amplitudes up to 2500 oe. Hence the derivative of the absorption curve was obtained on the screen of the oscilloscope.

The magnetic field was calibrated by means of the resonance curve for $\chi''(H_\perp)$ in the free radical $\alpha\alpha$-diphenyl βpicril-hydrazine at frequencies of 560 and 280 Mcs. The salt $CuCl_2 \cdot 2H_2O$ was used to check that H_ν and H were parallel. Because of the strong exchange interaction in this salt[2] the absorption in parallel fields is independent of $H_{\|}$. Hence, in parallel fields only the resi-

TABLE I

Dilution	$\Delta H_{\parallel}$, oe	$10^6 \cdot b/c$, oe^2	Remarks
$CrK(SO_4)_2 \cdot 12H_2O$ (single crystal)			
1 : 0	400	~0.4	
1 : 5	70	0.01	
1 : 10	80	—	resonance peak
$CrCl_3$ (Supercooled solution)			
2 Molar	160	0.061	
1 »	92	0.021	
0.5 »	65	0.01	
0.25 »	80	—	resonance peak
$FeCl_3$ (Supercooled solution)			
1 Molar	85	0.017	
0.5 »	65	0.01	
0.25 »	50	0.008	
0.125 »	—	—	resonance peak

Dilution	$\Delta H_{\parallel}$, oe	$10^6 \cdot b/c$, oe^2	Remarks
$MnNH_4SO_4 \cdot 6H_2O$ (Polycrystalline powder)			
1 : 0	500	0.61	
1 : 1	480	0.56	
1 : 2	—	—	h.f.s.
1 : 5	—	—	h.f.s.
1 : 10	—	—	h.f.s.
$CuNH_4SO_4 \cdot 6H_2O$ (Polycrystalline powder)			
1 : 0	328	0.26	
1 : 1	200	0.1	
1 : 2	—	—	h.f.s.
1 : 5	—	—	h.f.s.
$CuCl_2$ (Supercooled solution)			
2 Molar	140	0.05	
1 »	—	—	h.f.s.

* $T = 90°$ K, $\nu = 295$ Mcs

dues of absorption due to the perpendicular components of H_ν are observed. The intensity of this absorption was found to be approximately 0.5% of the intensity of $\chi''(H_\perp)$.

The test samples were single crystals of $CrK(SO_4)_2 \cdot 12H_2O$ in $AlK(SO_4)_2 \cdot 12H_2O$ in the ratios 1 : 1, 1 : 5, 1 : 10, and 1 : 70; polycrystalline powders of $MnNH_4SO_4 \cdot 6H_2O$ and $CuNH_4SO_4 \cdot 6H_2O$ in $ZnNH_4SO_4 \cdot 6H_2O$ in the ratios 1 : 1, 1 : 2, 1 : 5, 1 : 10 and 1 : 100; and boron and silicate glasses, containing Cr^{+++} and Fe^{+++}. Most of the measurements were carried out in supercooled solutions[11] with a wide range of concentration. The supercooled state was realized by fast cooling to 90°K of glycerine solutions of the salts $CrCl_3$, $Cr(NO_3)_3$, $FeCl_3$, $CuCl_2$, $Cu(NO_3)_2$, and $VOCl_2$. The samples were placed in polystyrene ampules, since the glass ampules exhibit paramagnetic absorption lines due to the Fe^{+++} in the glass itself.

In the measurements with single crystals of $CrK(SO_4)_2 \cdot 12H_2O$ the magnetic field H was directed along one of the diagonals of the elementary cell.

RESULTS OF THE MEASUREMENTS

1. Spin-spin Relaxation at $\nu = 300$ Mcs.

The results of our experimental investigations in Cr^{+++}, Fe^{+++}, Mn^{++}, Cu^{++} and VO^{++} samples indicate that absorption in parallel fields at 300 Mcs at T = 90°K is due basically to spin-spin relaxation; there is no spin-lattice absorption. In dilute samples, however, in addition to the spin-spin relaxation, there is a resonance absorption peak for Cr^{+++} and Fe^{+++} and hyperfine structure lines (hfs) for Mn^{++}, Cu^{++}, and VO^{++}. Hence, in what follows our samples are divided into two groups.

I. Cr^{+++}, Fe^{+++}. In $CrK(SO_4)_2 \cdot 12H_2O$ single crystals diluted* in the ratio 1 : 5 and in supercooled glycerine solutions of $CrCl_3$, $Cr(NO_3)_3$, and $FeCl_3$ in the concentration range between 0.5 and 2 mole/l the $\chi''(H_\parallel)$ curves are due only to the spin-spin relaxation (cf. Fig. 1, A, B, and C). In this case the half-width $\Delta H_\parallel$ of the $\chi''_\parallel(H_\parallel)$ curves is narrowed as the concentration of the magnetic ions Cr^{+++} and Fe^{+++} is reduced. The experimental $\chi''_S(H_\parallel)$ curves are described by Eq. (4). The numerical values of b/c computed from Eq. (5) are given in Table I.

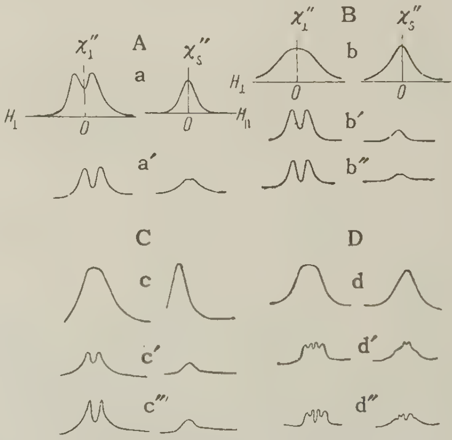

FIG. 1. Paramagnetic absorption curves in perpendicular and parallel fields at a frequency $\nu = 300$ Mcs at T = 90°K. A) $CrK(SO_4)_2 \cdot 12H_2O$, dilution: a) 1:5, a′) 1:10. B) glycerine supercooled solution of $CrCl_3$, dilution: b) 2, b′) 0.5, and b″) 0.25 M, C) glycerine supercooled solution of $FeCl_3$: c) 1, c′) 0.25, and c″) 0.06 M. D) glycerine supercooled solution of $CuCl_2$: d) 2, d′) 0.5, and d″) 0.06 M.

When the $CrK(SO_4)_2 \cdot 12H_2O$ single crystal is diluted further to the ratio 1 : 10 and in supercooled solutions containing Cr^{+++} and Fe^{+++}

---

*The spin-spin relaxation in undiluted $CrK(SO_4)_2 \cdot 12H_2O$ crystals has been investigated earlier by the author.[10]

TABLE II

Dilution	$\Delta H_{\parallel}$, oe	$10^6 \cdot b/c$, oe^2	Remarks
$CrK(SO_4)_2 \cdot 12H_2O$ (Single crystal)			
1 : 0	—	—	$\chi_l''(H_{\parallel})$
1 : 2	—	—	$\chi_l''(H_{\parallel})$
1 : 5	50	0.006	
1 : 10	20	0.001	
$CrCl_3$ (Supercooled solution)			
2 Molar	—	—	$\chi_l''(H_{\parallel})$
1 »	—	—	$\chi_l''(H_{\parallel})$
0.5 Molar	40	0.004	
0.25 »	20	0.001	
0.06 »	10	0.0002	
$FeCl_3$ (Supercooled solution)			
1 Molar	—	—	$\chi_l''(H_{\parallel})$
0.5 »	—	—	$\chi_l''(H_{\parallel})$
0.25 »	—	—	$\chi_l''(H_{\parallel})$
0.125 »	20	0.001	

* $T = 90°$ K, $\nu = 8.2$ Mcs

below 0.5 M, the $\chi_S''(H_{\parallel})$ curve exhibits a peak due to the resonance transition in the parallel fields; hence b/c cannot be found from Eq. (5). Furthermore, Eq. (4) no longer applies because $\rho_S^{-1} \sim \nu$. In highly dilute Cr^{+++} and Fe^{+++} samples (1 : 70 at approximately 0.03 M) only the absorption resonance peak is observed; absorption due to spin-spin relaxation is not found because in this case the "zero" absorption $\chi''(H = 0)$ vanishes.

Thus, in highly dilute Cr^{+++} and Fe^{+++} samples it is impossible to determine b/c from the $\chi_S''(H_{\parallel})$ curves at $\nu \geq 300$ Mcs. For this reason the further measurements of b/c in these samples were carried out at lower frequencies.

II. Mn^{++}, Cu^{++}, VO^{++}. In parallel fields at a frequency of 300 Mcs and T = 90°K, the $\chi_S''(H)$ curves fall off monotonically with increasing $H_{\parallel}$ in undiluted Mn^{++} and Cu^{++} Tutton salts and in concentrated supercooled solutions of Mn^{++}, Cu^{++}, and VO^{++}. Even at very small dilutions, the $\chi_S''(H_{\parallel})$ curves exhibit hfs lines at intermediate fields. In this case the intensity of the hfs lines in parallel fields is comparable with the intensity of the hfs lines in perpendicular fields but the absorption and number of hfs lines differ (cf. Fig. 1D). Thus, in dilute Mn^{++}, Cu^{++}, and VO^{++} solutions the presence of a strong hfs makes it impossible to determine b/c from Eq. (5).

2. Spin-spin Relaxation at 8.2 Mcs.

At frequencies of approximately 10^7 cps and T = 90°K, in Cr^{+++} and Fe^{+++} samples, depending on the concentration of magnetic ions one observes absorption due to spin-spin or spin-lattice relaxation or a combination of both (cf. Fig. 2A). Under these conditions, the lower the concentration of magnetic ions, the lower the frequencies of the oscillating field H_ν at which it is possible to observe absorption due to spin-spin relaxation. Furthermore, in dilute Cr^{+++} and Fe^{+++} samples the half-width of the $\chi_{\parallel}''(H_{\parallel})$ lines, due to the unresolved resonance maximum and the spin-spin absorption, is reduced when ν is reduced from 300 to 10 Mcs. The frequency dependence of the half-width of the $\chi_{\parallel}''(H_{\parallel})$ lines arises because the "fractional" resonance absorption is reduced, while the relative intensity of $\chi_S''(H_{\parallel})$ increases [because of the zero absorption $\chi''(H = 0)$] as the frequency is reduced.

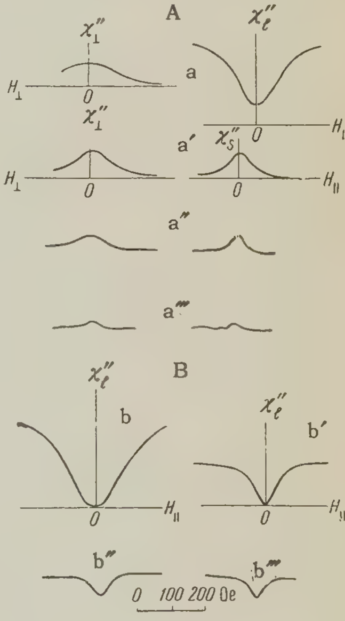

FIG. 2. Paramagnetic absorption curves $\chi''(H_{\parallel})$ (T = 90°K). A) supercooled $CrCl_3$ solution, $\nu = 8.2$ Mcs, dilution: a) 1, a') 0.5, a'') 0.25, and a''') 0.06 M; B) the same solution, $\nu = 1.6$ Mcs, dilution: b) 1, b') 0.5, b'') 0.25, and b''') 0.125.

The experimental $\chi_S''(H_{\parallel})$ curves obtained in dilute Cr^{+++} and Fe^{+++} samples at 8.2 Mcs and T = 90°K are described by Eq. (4). Hence, at this frequency b/c can be determined even in highly dilute Cr^{+++} and Fe^{+++} samples. The numerical values of b/c are shown in Table II. It is apparent from the table that b/c falls off to very small values as the concentration of Cr^{+++} and Fe^{+++} ions is reduced.

When the temperature of the sample is increased from 90 to 280°K the absorption due to spin-spin relaxation is replaced by absorption due to the spin-lattice relaxation. By changing the temperature of the sample it is possible to "equalize" these two relaxation modes; in this case the total absorption becomes independent of H.

In dilute Mn^{++}, Cu^{++} and VO^{++} samples, hfs lines are observed at weak fields.

3. Spin-Lattice Relaxation

It has been found that in Cr^{+++} and Fe^{+++} samples the mode of relaxation absorption in parallel fields in the neighborhood of 10^7 cps depends not only on the temperature of the sample, but also on the concentration of magnetic ions. The larger the concentration of magnetic ions, the higher the frequency of the oscillating magnetic field at which spin-lattice relaxation can be observed. The spin-lattice relaxation curves in the Fe^{+++} samples are observed at higher frequencies than in samples which contain Cr^{+++} at the same concentrations. The dependence of spin-spin relaxation on dilution has been discussed above.

At frequencies of approximately 10^6 cps and $T = 90°K$, over a wide range of concentrations of Cr^{+++}, Fe^{+++} and Mn^{++} the absorption is due basically to spin-lattice relaxation. The shape of the absorption curves also depends on the concentration of magnetic ions: the lower the concentration the smaller the values of H at which the dependence of χ''_l on H disappears (cf. Fig. 2B). Since the dependence of χ''_l on H in Eq. (1) is determined basically by the function $F = H_{||}^2/(b/c + H_{||}^2)$, the lower the values of b/c, the lower values of the field at which χ''_l becomes field independent, i.e., $\chi''_l(H_{||}) = \text{const}$.

In dilute Cr^{+++}, Fe^{+++} and Mn^{++} samples, even if one assumes a strong dependence of ρ_l on H, given by the Brons-Van Vleck formula, it is impossible to obtain this dependence of χ''_l on H if the value of b/c is not reduced. Thus, the investigation of spin-lattice relaxation curves in dilute Cr^{+++}, Fe^{+++}, and Mn^{++} samples also indicates a strong dependence of b/c on dilution.

4. Paramagnetic Resonance Absorption in Perpendicular Fields

In addition to measuring absorption in parallel fields, we investigated the $\chi''(H_\perp)$ resonance curves in perpendicular fields in the frequency range 5 — 300 Mcs in dilute solutions containing Cr^{+++}, Fe^{+++}, Cu^{++}, Mn^{++} and VO^{++}. The results of these measurements are given below for 300 Mcs and $T = 90°K$.

I. Cr^{+++}, Fe^{+++}. In dilute $CrK(SO_4)_2 \cdot 12H_2O$ single crystals we were able to observe a single resonance absorption line due to the $\frac{1}{2} - \frac{1}{2}$ transition with an effective g value of 2.5 (the value of the g factor depends on the orientation of the single crystal). However, resonance absorption maxima before and after the intersection of the $E_{-1/2}$, $E_{-3/2}$ levels could not be found.* In this case, a fixed magnetic field with intensities up to 6000 oe was superimposed on the 50-cycle alternating magnetic field. In the supercooled solutions of $CrCl_3$, $Cr(NO_3)_3$, and $FeCl_3$, and in the boride and silicate glasses containing Cr^{+++} and Fe^{+++} we were able to observe a single resonance absorption peak with $g = 2.5$ for Cr^{+++} and $g = 4$ for Fe^{+++}.

The half-width of the $\chi''(H_\perp)$ absorption curves in Cr^{+++} and Fe^{+++} samples is reduced with a reduction in the concentration of magnetic ions or in frequency. The magnitude of the zero absorption $\chi''(H = 0)$ is also reduced.

The departure of the g value from 2 is explained by the fact that the $E_{1/2}$ and $E_{-1/2}$ levels have a nonlinear dependence on H for arbitrary orientations in weak fields.

Thus, paramagnetic resonance spectra in these Cr^{+++} and Fe^{+++} samples can be described by a spin Hamiltonian with an effective spin $S' = \frac{1}{2}$ at low frequencies ($h\nu \ll \delta$).

II. Mn^{++}, Cu^{++}, VO^{++} hfs paramagnetic resonance lines have been observed at intermediate fields[12] in dilute samples containing these ions.

DISCUSSION OF THE RESULTS AND CONCLUSIONS

1. In samples containing Cr^{+++} ($S = \frac{3}{2}$), Fe^{++} and Mn^{++} ($S = \frac{5}{2}$), the heat capacity of the spin system depends on the level splitting in the electric field of the crystal and the dipole-dipole magnetic interactions. Hence, in the first approximation the total heat capacity can be given as a sum

$$b = b_{el} + b_{mag}.$$

However, in samples containing Cu^{++} and VO^{++}, in which case $S = \frac{1}{2}$, the heat capacity due to level splitting in the electric field vanishes:

$$b = b_{mag}, \qquad b_{el} = 0.$$

It is assumed that in magnetic dilution the electric field of the crystal lattice or the medium surrounding the magnetic ion is not changed but that the magnetic interactions depend on the dilution.

---

*This absorption maximum has been observed in undilute chrome potassium alums at $T = 300°K$.[10]

In the magnetically dilute systems containing Cr^{+++} and Fe^{+++} investigated by us there is a rather large initial splitting of the spin sub-levels in the electric field of the crystal $\delta \sim 0.2\ cm^{-1}$. Hence the fraction of the heat capacity due to b_{el} should be much larger than that due to b_{mag}. But, as has been shown above, b/c is reduced to very low values with a reduction in the magnetic interactions; consequently the fraction of the heat capacity due to the splitting of the levels in the electric field vanishes, that is to say, in the Cr^{+++} and Fe^{+++} samples which have been investigated it is necessary to assume the effective spin value $S' = \frac{1}{2}$. This same value $S' = \frac{1}{2}$ was obtained above in the interpretation of the resonance absorption spectra in perpendicular fields. Thus, in dilute Cr^{+++} and Fe^{+++} samples, when $h\nu \ll \delta$ we have

$$b = b_{\text{mag}}, \qquad b_{\text{el}} = 0.$$

2. The experimental curves for spin-spin absorption in dilute Cr^{+++} and Fe^{+++} samples are described by the Shaposhnikov theory.

3. From these investigations of the curves due to spin-spin or spin-lattice relaxation it may be concluded that in our highly dilute Cr^{+++} and Fe^{+++} samples (0.03 M) ρ_s remains smaller than ρ_l although the former increases directly with or as the square root of the concentration[2] in dilution. The inequality $\rho_s < \rho_l$ is confirmed by two facts: first, the spin-spin absorption curves are always observed at higher frequencies than the spin-lattice relaxation curves; second, the $\chi''_l(H_{||})$ curves are described by the Casimir-Du Pre formula (1), which applies only when $\rho_s \ll \rho_l$.

4. At approximately 10^7 cps, in dilute Cr^{+++} and Fe^{+++} samples $\chi''_s(H_{||})$ curves can be obtained T = 90° K whereas in the concentrated Cr^{+++} and Fe^{+++} samples at these same frequencies the curves are observed only at T ~ 20° K.[13] Thus, it may be concluded that the spin-lattice relaxation time is lengthened as the concentration of magnetic ions is reduced.

5. In dilute Cr^{+++} and Fe^{+++} compounds the relaxation time ρ_l depends on δ if $h\nu \ll \delta$. Under these conditions it is found that a higher value of δ means a larger value of ρ_l. A similar result has been obtained earlier by the author in studies of phase transitions in alums.[10]

6. It has been found that the $\chi''_s(H_{||})$ and $\chi''_l(H_{||})$ curves can compensate for each other, depending on the temperature of the sample, the frequency, and the concentration. In this case the total absorption curve is independent of $H_{||}$.

7. Fine-structure lines[14] and hfs lines are observed at intermediate and weak fields in parallel fields. In these cases the intensity of the fine-structure lines in perpendicular fields is comparable to the intensity of the hfs lines in parallel fields. At strong fields, however, the former are about 100 times weaker than the hfs lines in perpendicular fields.[15]

In conclusion the author wishes to thank S. A. Al'tshuler and B. M. Kozyrev for discussion of the results.

---

[1] C. J. Gorter, Paramagnetic Relaxation, Elsevier, New York, 1947, Russ. Transl. IIL, 1949.

[2] B. M. Kozyrev, Dissertation, Inst. Phys., U.S.S.R. Acad. Sci., Moscow, 1957.

[3] H. B. G. Casimir and F. K. Du Pre, Physica **5**, 507 (1938).

[4] I. G. Shaposhnikov, JETP **18**, 533 (1948).

[5] N. S. Garif'yanov, Dissertation, Kazan' State University 1953.

[6] N. S. Garif'yanov, JETP **25**, 359 (1953).

[7] K. P. Sitnikov, Dissertation, Kazan' State University, 1954.

[8] A. I. Kurushin, Izv. Akad. Nauk SSSR, Ser. Fiz. **20**, 1232 (1956), Columbia Tech. Transl. p. 1122.

[9] N. S. Garif'yanov and B. M. Kozyrev, JETP **30**, 272 (1956), Soviet Phys. JETP **3**, 255 (1956).

[10] N. S. Garif'yanov, JETP **35**, 612 (1958), Soviet Phys. JETP **8**, 426 (1959).

[11] N. S. Garif'yanov, Dokl. Akad. Nauk SSSR, **103**, 41 (1955).

[12] N. S. Garif'yanov, Izv. Akad. Nauk SSSR, Ser. Fiz. **21**, 824 (1957), Columbia Tech. Transl. p. 824.

[13] Smits, Derksen, Verstelle, and Gorter, Physica **22**, 773 (1956).

[14] N. S. Garif'yanov, JETP **36**, 1957 (1959), Soviet Phys. JETP **9**, 1393 (1959).

[15] W. A. Anderson and L. H. Piette, J. Chem. Phys. **30**, 591 (1959).

Translated by H. Lashinsky
314

SOVIET PHYSICS JETP VOLUME 37(10), NUMBER 6 JUNE, 1960

EXPERIMENTS IN THE PRODUCTION OF A NEW FERMIUM ISOTOPE

V. P. PERELYGIN, E. D. DONETS, and G. N. FLEROV

Submitted to JETP editor July 4, 1959

J. Exptl. Theoret. Phys. (U.S.S.R.) **37**, 1558-1563 (December, 1959)

A study has been made of the α-active products of the interaction between accelerated O^{16} ions and U^{238} nuclei. Evidence has been obtained of the formation of a new fermium isotope Fm^{249}, which has a half-life of about 150 sec and an α-particle energy of 7.9 ± 0.3 Mev. Excitation curves are presented for reactions involving the emission of four or five neutrons for oxygen ion energies between 84 and 98 Mev. A procedure is described for identifying transuranic elements by the registration of their successive α decays in nuclear photoemulsions.

THE hundredth element in the periodic table — fermium — was identified in 1952 by staff members of the University of California, Argonne National Laboratory, and Los Alamos Scientific Laboratory upon radiochemical analysis of the products from the first thermonuclear explosion.[1] Subsequently, different isotopes of fermium were obtained both by intensive thermal neutron irradiation[2-5] and by charged-particle bombardment.[6-8] The isotopes Fm^{250} to Fm^{256} had been produced by 1958. The identity of all these isotopes was established by radiochemical separation of the hundredth element with the aid of ion-exchange columns. In accordance with the systematics of Glass et al.,[9] fermium isotopes lighter than Fm^{250} must have such short lifetimes that it is apparently difficult or impossible to separate them chemically by the methods previously used. Such isotopes can only be obtained by charged-particle reactions, since the other production methods using successive neutron capture are excluded.

In 1958 Ghiorso[10] reported the formation of a new fermium isotope, the 36-second Fm^{248}, obtained by the reaction $Pu^{240}(C^{12}, 4n)$. The Fm^{248} was identified by an essentially new method, based on the physical effects of ejection of the compound nucleus from the target at the expense of the C^{12} momentum and on the establishment of the genetic relationship between the daughter and parent nuclei by means of the α-decay momentum of the latter. A total of eight fermium isotopes had been identified by 1959.

In the present work we present experimental results on the formation of light fermium isotopes by the interaction of accelerated O^{16} ions with U^{238} nuclei.

Oxygen ions with charge +5 were accelerated in the 1.5-meter cyclotron of the Atomic Energy Institute of the U.S.S.R. Academy of Sciences. The energy of the accelerated oxygen ions was found to be within 84 — 98 Mev. The beam was monochromatic.

The U^{238} target was prepared by vacuum evaporation or by deposition with tetraethylene glycol onto a nickel substrate. The number of target nuclei present was determined by their α activity. Targets of 200 to 800 $\mu g/cm^2$ of uranium were used.

We used a high-speed and highly sensitive method first employed by Flerov et al.,[11] for counting the α decay of the transuranic elements. The recoil nuclei ejected from the target were stopped in an aluminum foil, which was then quickly moved over to a photoplate which served as an α-decay detector. This counting method permits one to obtain the α-particle spectrum directly from the decay of the initial transuranic-element isotope, its half-life, and its excitation function.

Shortcomings of this method are the complexity and difficulty of systematic elimination of all probable sources of background.

The time cycle generally used in our experiments was as follows: exposure of the collector to the beam ~22 sec; movement of the collector a distance of 2 meters to the photoplate ~3 sec; exposure at the photoplate ~22 sec; returning the collector to the target ~3 sec. This irradiation cycle was generally carried on for 2 to 3 hours, using an ion current of 0.2 — 0.5 μa.

NIKFI T-1 photoplates were used as α-decay detectors in our experiments. The irradiated photoplates were developed in hydroquinone developer with NaOH. The developing process provided reliable discrimination between α particles and protons. The photoplates were examined on Zeiss Lumipan microscopes which used 20 × 1.5 × 15 magnification and which were equipped with goniometers and supplementary dial adjustment knobs for more accurate establishment of the track penetration depth. All tracks over 25 μ long were recorded; this length corresponds to a 5.75-Mev α particle.

On bombarding uranium with oxygen ions having energies up to 100 Mev, one should expect the formation of fermium isotopes Fm^{250}, Fm^{249}, and Fm^{248} by emission of four, five, and six neutrons respectively from the compound nucleus. The isotope Fm^{250} had been obtained earlier by the reaction $U^{238}(O^{16}, 4n)$.[6] Its half-life is 30 min, and its α-decay energy is 7.55 Mev.[8]

The isotope Fm^{249} has not been identified up to the present time. The systematics suggest a half-life of ~300 sec and decay energy of 7.8 Mev for Fm^{249}.

According to Ghiorso's data, Fm^{248} has a 36 sec half-life and a 7.8 Mev α particle.[12] Assuming the given O^{16} energies, it is predicted that no other transuranic nuclei of $Z = 100$ — products of the interaction — can have α-decay energies greater than 7.4 Mev.

Thus, if Fm^{248} or Fm^{249} are produced in our experiments, the first evidence obtained by the present method should be the appearance in the spectra of groups of α particles with energies above 7.6 Mev.

The α spectra we measured (Fig. 1) contained a line of about 7.4 Mev, which was definitely determined to be due to the α decay of Fm^{250}. When the O^{16} ion energy was increased to 89 Mev, a group of α particles with 7.9 ± 0.3 Mev energy appeared in the spectrum. This activity evidenced itself most sharply at 98 Mev.

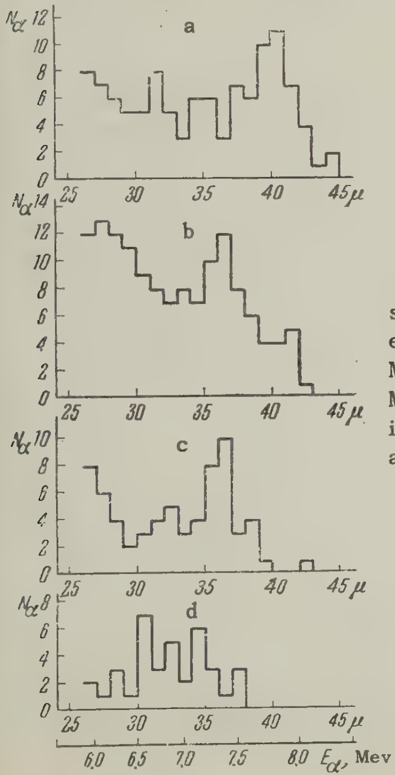

FIG. 1. The α-particle spectra for oxygen ion energies as follows: a – 98 Mev; b – 95 Mev; c – 89 Mev; d – 84 Mev. Identical irradiation cycles used in all four experiments.

Comparison of the measured spectra with those obtained by irradiating Pb, Bi, Hg, and Tl with oxygen ions showed that the 7.9 Mev activity cannot be ascribed to the presence of these impurities in the target.

Figure 2 shows the measured excitation curves for the 7.4- and 7.9-Mev α activities. With increasing oxygen ion energy (Fig. 2), the yield of the 7.9-Mev α activity rises when the Fm^{250} production cross section passes its maximum, and then drops sharply. It should be noted that the dependence on the O^{16} energy, which we found for the $U^{238}(O^{16}, 4n)$ reaction cross section, agrees within the limits of error with the results of Tarantin et al.[13] (for this reaction), obtained by a different method.

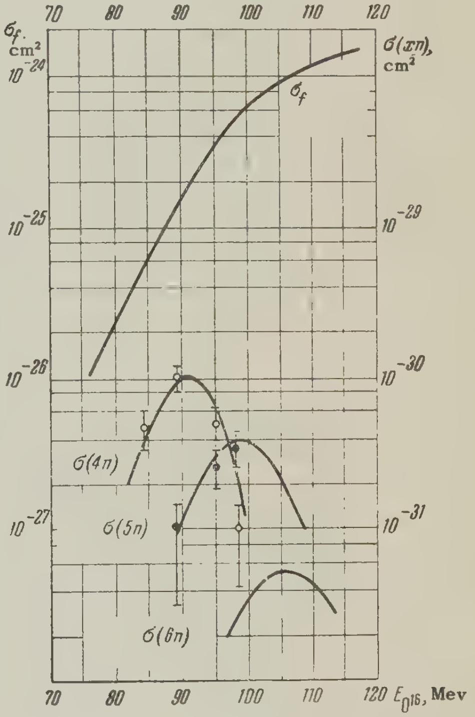

FIG. 2. Excitation curves; light and dark circles indicate excitation cross sections corresponding to 7.4 and 7.9 Mev α activities; the solid curves are the calculated excitation functions for reactions yielding 4n, 5n, and 6n; the upper curve is the U^{238} fission cross section.

Figure 2 also shows excitation curves for reactions yielding 4, 5, and 6 neutrons, calculated by Jackson's statistical model.[14] For these calculations, the temperature T was assumed to be equivalent to 1.60 Mev. For this temperature, the position of the maximum and the half-width value coincide in the experimental and calculated Fm^{250} excitation curves. The excitation curve for the 7.9-Mev α activity agrees well with the calculated curve for 5-neutron emission, and agrees poorly with the calculated curve for the 6-neutron reaction. The dependence of the U^{238} fission section σ_f on the O^{16} ion energy was taken from reference 15.

Experiments to determine the half-life of the 7.9-Mev α emitter were carried out at 98 Mev O^{16} energy. The same procedure was used as in finding the excitation curves. However, after the collector was exposed to the target, it was moved over to the photoplate not immediately, but after a certain fixed time interval. The irradiation was carried out in the following cycles: 22 — 3 — 22 — 3 sec; 50 — 50 — 50 — 3 sec; 100 — 100 — 100 — 3 sec; and 250 — 250 — 250 — 3 sec. From these experiments, the half-life of the 7.9 Mev α activity was found to be about 150 sec, accurate to about 40%. Therefore the 7.9-Mev α activity cannot be ascribed to the 36-sec decay of Fm^{248}.

In addition, the half-life of the 7.9-Mev activity was determined by the contact method, in which the stationary collector was irradiated at the target, removed from the vacuum system, and then moved into contact with the photoplate after 180, 300, 500, and 1000 sec. The 150 sec half-life thus obtained (Fig. 3) was in good agreement with the value obtained in the previous experiment. This experiment proves the absence of any significant contribution by long-lived α activities with ~ 7.9 Mev energy.

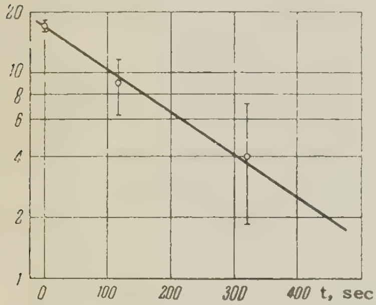

FIG. 3. Decay of the 7.9 Mev α emitter.

All of the above data indicate the formation of the isotope Fm^{249}. However, since no chemical identification was made of the 7.9-Mev 150-sec α activity, this set of experiments cannot be considered conclusive. In fact, the interaction of O^{16} nuclei with U^{238} may, for example, cause reactions involving major spallation and thus leading to the formation of neutron-deficient isotopes of Th and Ac having half-lives of the order of minutes. Ghiorso observed such reactions in the interaction of C^{12} and N^{14} with U^{238}.[10]

The decay products of the Th and Ac isotopes have energies of the order of 8 Mev; the presence of isomers possessing half-lives and energies close to those we have measured is not excluded. Experiments were therefore undertaken to detect α-particle pairs in photoemulsions from the successive decay series

$$Fm^{249} \xrightarrow{\alpha} Cf^{245} \xrightarrow{\alpha} Cm^{241}.$$

The recording of such associated successive α-decay events, together with the determination of the half-lives of parent and daughter nuclei, obviously permits the determination of the Z and A of the original nucleus, provided that the properties of the daughter nucleus are well known. Using our technique, it is possible to record α-particle pairs if the half-lives of both nuclei lie within the limits of several days to one or two seconds. If the 7.9 Mev α activity is explained by Fm^{249} decay, then, since the daughter nucleus Cf^{245} emits an α particle in 34% of decays, the number of α-particle pairs under these conditions is three-fold less than for the decay series

$$Fm^{248} \xrightarrow{\alpha} Cf^{244} \xrightarrow{\alpha} Cm^{240},$$

where the daughter nucleus Cf^{244} is β-stable.

In order to observe such α-particle pairs, special measures were adopted regarding the positioning of the collector and photoplate, insuring reproducibility of the collector position to within 10 μ. The accuracy of collector positioning was verified optically before and after irradiation. No deviation exceeding 10 μ was detected during the entire course of the work involving such positioning of the collector.

Since the probability of accidental coincidences, which could give a false reading, is directly proportional to the square of the distance from the photoplate to the collector, this distance was decreased to 100 — 150 μ. This distance was established within an accuracy of 30 μ. The irradiation was performed on a regular cycle of 22 — 3 — 22 — 3 sec. At the end of the irradiation, the collector was left next to the photoplate for another 60 to 90 min, in order to permit decay of the 45 min Cf^{245} daughter nuclei. Photoplate tracks with energies 7.9 ± 0.3 Mev and 7.1 ± 0.3 Mev were recorded, and then the dip angles θ_α and azimuth angles φ_α were determined for these tracks. In all, 95 α particles with energies of the order of 7.9 Mev were found in four photoplates. Four α-particle pairs were found.

The number of accidental coincidences was calculated with the aid of Poisson's distribution. This number was found to be equal to one for all four experiments. The probability of all four α-particle pairs having occurred by accidental coincidence is less than 2%.

Thus, after subtracting the background, we have three α pairs. For Fm^{249}, we would expect to find four occurrences of successive α decay among 95 α particles of 7.9 Mev. Therefore the observed α-particles pairs support our hypothesis concerning the formation of Fm^{249}.

The fortunate circumstance that the half-life of Fm^{249} is 150 sec, while the cross section can be as high as 4×10^{-31} cm^2, permitted us to perform the following experiment. The target and adjacent collector were irradiated for 10 min with a 0.5 – 0.7 μa beam of O^{16} ions of maximum energy. Then the collector was quickly removed from the vacuum chamber and quickly pressed between two layers of photoemulsion. The photoplates were exposed for three hours. A total of 17 α-particle tracks with about 7.9 Mev energy were found; in two of these cases, α particles of about 7.1 Mev energy were observed to start from the same point of the foil.

Here the probability of accidental coincidence is very small, since the distance between the layers did not exceed 15 μ. The number of α-particle pairs found in the close-contact experiment coincides with that expected for Fm^{249} decay.

Specific determination of the half-life of the 7.1 Mev α activity was not possible, but evaluation of the results of the previous experiments, in which the short-lived 7.9 Mev α activity was detected, places the 7.1 Mev α activity half-life within 20 – 60 min.

Thus, experiments on the detection of associated successive α-decay events have shown that the decay of Fm^{249} apparently does occur.

Other evidence for the occurrence of Fm^{249} decay is the α-particle spectrum found when using the cycle 22 – 3 – 22 – 3 sec for O^{16} of 98 Mev energy (Fig. 1, curve a), which shows that the 7.9-Mev line has 2 – 3 times more tracks than are found for the energy interval 7.1 ± 0.3 Mev.

The results of all the above experiments indicate the formation of the new fermium isotope Fm^{249}, having a 150 sec half-life and an α-particle energy of 7.9 ± 0.3 Mev.

In conclusion, the authors wish to express their deep thanks to V. V. Volkov, D. M. Parfanovich, S. M. Polikanov, A. M. Semchinova, and N. I. Tarantin for their help in the work and for profitable discussions.

[1] Ghiorso, Thompson, Higgins, Seaborg, Studier, Fields, Fried, Diamond, Mech, Pyle, Huizenga, Hirsch, Manning, Browne, Smith, and Spence, Phys. Rev. **99**, 1048 (1955).

[2] Harvey, Thompson, Ghiorso, and Choppin, Phys. Rev. **93**, 1129 (1954).

[3] Studier, Fields, Diamond, Mech, Friedman, Sellers, Pyle, Stevens, Magnusson, and Huizenga, Phys. Rev. **93**, 1428 (1954).

[4] Choppin, Thompson, Ghiorso, and Harvey, Phys. Rev. **94**, 1080 (1954).

[5] Choppin, Harvey, Thompson, and Ghiorso, Phys. Rev. **98**, 1519 (1955).

[6] Atterling, Forsling, Holm, Melander, and Astrõm, Phys. Rev. **95**, 585 (1954).

[7] Friedman, Gindler, Barnes, Sjoblom, and Fields, Phys. Rev. **102**, 585 (1956).

[8] Amiel, Chetam-Strode, Choppin, Ghiorso, Harvey, Holm, and Thompson, Phys. Rev. **106**, 553 (1957).

[9] Glass, Thompson, and Seaborg, J. Inorg. Nucl. Chem. **1**, 3 (1955).

[10] A. Ghiorso, Proc. Conf. on React. Betw. Complex Nucl., Gatlinburg, Tennessee, 1958, p. 34.

[11] Flerov, Polikanov, Karamyan, Pasyuk, Parfanovich, Tarantin, Karnaukhov, Druin, Volkov, Semchinova, Oganesyan, Khalizev, and Khlebnikov, Dokl. Akad. Nauk SSSR **120**, 73 (1958), Soviet Phys.-Doklady **3**, 546 (1958).

[12] A. Ghiorso, Proc. VIII Mendeleev Conf., M. 1959.

[13] Volkov, Guseva, Myasoedov, Tarantin, and Filippova, JETP **37**, 1207 (1959), Soviet Phys. JETP **10**, 859 (1960).

[14] T. D. Jackson, Can. J. Phys. **34**, 767 (1956).

[15] V. A. Druin and S. M. Polikanov, Ядерные реакции при малых и средних энергиях (Nuclear Reactions at Low and Medium Energies), U.S.S.R. Acad. Sci. M. 1958 p. 507.

Translated by D. A. Kellogg
315

SOVIET PHYSICS JETP VOLUME 37(10), NUMBER 6 JUNE, 1960

PARAMAGNETIC RESONANCE AND PARAMAGNETIC RELAXATION IN SALT SOLUTIONS OF THE IRON GROUP

V. I. AVVAKUMOV, N. S. GARIF'YANOV, B. M. KOZYREV, and P. G. TISHKOV

Physico-technical Institute, Kazan' Branch, Academy of Sciences, U.S.S.R.

Submitted to JETP editor July 6, 1959

J. Exptl. Theoret. Phys. (U.S.S.R.) 37, 1564-1569 (December, 1959)

Results of experiments on paramagnetic resonance and paramagnetic relaxation in liquid solutions of salts of the iron group are compared with the existing theories.

THE paramagnetic resonant absorption in solutions of salts of the iron group has been under investigation in our laboratory for several years. In the solutions investigated one can observe either a discrete line or a spectrum due to the hyperfine structure. No resolution of the fine structure of the lines is observed, but the fine structure may influence the line widths. The following quantities were measured: the position of the line (the effective g-factor), the line width or the width of the discrete components of the hyperfine structure, and the distance between the peaks of the hyperfine structure.

Measurements have also been carried out recently on the nonresonant paramagnetic absorption in solutions. This absorption is observed when the static magnetic field H_0 is parallel to the high-frequency field H_1. From these experiments we determined the spin-lattice relaxation time and the constant of magnetic specific heat b.

The main purpose of the present work was the verification of the theories of paramagnetic resonance and paramagnetic relaxation in solutions. Furthermore, some information was obtained on the structure of the solutions.

We assume that the lifetime of solvate complexes of paramagnetic ions is sufficient for them to be considered as solid formations in experiments on paramagnetic relaxation and paramagnetic resonance. The structure of the magnetic complex is connected with the spectrum of paramagnetic resonance and with the relaxation through the electric field created by the ligands on the magnetic ion. The spectral and relaxational characteristics are sensitive to the symmetry and strength of this field; these depend on the geometry and composition of the magnetic complex. Thus, from the spectrum of the paramagnetic resonance and from the data on relaxation measurements, several conclusions can be drawn regarding the structure of electrolytic solutions. In particular, the absence of a measurable resonance absorption in aqueous solutions of simple salts of Ti^{3+} and Co^{2+}, and the presence of this effect in aqueous solutions of Cr^{3+} and Cu^{2+}, show unequivocably that complexes of these four ions cannot have a tetrahedral structure — a conclusion which agrees with the results obtained by other methods of investigation (cf., e.g., reference 1).

Let us consider the structure of some hydrated ions in greater detail.

Cu^{2+}. Calculations in agreement with experiment enable us to assume that the complex $Cu^{2+}Y_6$ has the structure of a bipyramid, stretched as a result of the Jahn-Teller effect[2] along one of the fourfold symmetry axes. Kozyrev[3] has shown that in the case of six water complexes of copper in liquid solutions this effect has a dynamic character (as in the case of solid hydrated copper salts with trigonal symmetry). The essence of the dynamic effect is as follows. At a given orientation of ligands on the axes of a rectangular coordinate system, the bipyramidal complex may be stretched along any of the three coordinate axes, and all states of the complex will be energetically identical. For a transition from one state into another the system has to overcome a potential barrier which for the hydrated complex equals approximately 1000 cm^{-1}. It was calculated that this transition takes place with a frequency of $\sim 10^{11}$ sec^{-1}. The rebuilding of the electron density of the magnetic ion has the same frequency. The latter causes averaging of the g-factor, isotropy of the hyperfine structure constant, and a decrease in its value, which agrees with our experiments on the aqueous solutions of Cu^{2+} nitrate.[4] The stronger the complex, the greater its mass, and the lower its symmetry, the smaller is the transition frequency and, consequently, the lesser the extent to which the hyperfine structure should be averaged.[3] This explains the possibility of observing the hyperfine structure in the solutions of complex salts of copper, revealed for the first time by McGarvey.[5] The same is confirmed by the experiments of Rivkind and one of the authors[6] on paramagnetic resonance in solutions containing ethanolamine and diethanolamine complexes of Cu^{2+} in water and acetylacetonate and nitrate Cu^{2+} complexes in dioxane. The nitrate complex — as far as we know — was discovered by us for the first time. It is unstable because the hyperfine structure constant in it is very small.

Cr^{3+}. In the violet modification of Cr^{3+} salts, the octahedral complexes $[Cr(H_2O)_6]^{3+}$ are somewhat distorted. The electrical field on the ion has mainly a cubic symmetry with minor additions of fields of lower symmetry due to the action of particles of the second coordination sphere. The fields created by those particles, apparently, fluctuate rather slowly.* The presence of such fields is confirmed by comparison of the observed line width in solutions of chromium salts with data on spin-lattice relaxation time for the 0.1 M solution ($\Delta H = 200$ gauss, $\rho_l \sim 10^{-8}$ sec). These fields are weaker than the axial field in solid chrome alums because the full spectrum width in powder alums is much greater than the width of a discrete line observed in a solution. In the green modification of the Cr^{3+} salts the lines of paramagnetic resonance are much broader; this means that in this case the distortion of the octahedron is considerably greater; this is natural because the complex $[Cr(H_2O)_4X_2]^+$ as such is less symmetric.

Mn^{2+}. Magnetic complexes of manganese in dilute aqueous solutions have almost pure cubic symmetry. On the other hand, in nonaqueous solutions of manganese chloride, at a given relaxation time, very broad resonance lines are observed. This is explained by the presence of a strong axial component of the crystal field, caused apparently by the presence of ionic molecules, for example of the type $X^- - Mn - X^-$.

The measurements of paramagnetic relaxation in parallel fields $H_0 \parallel H_1$ at frequencies near 10^7 cps were conducted in solutions of Mn^{2+} salts at concentrations ranging from several moles per liter up to 0.25 mole/liter.[8] These experiments have shown that the effect of spin-lattice relaxation is well described by the phenomenological theory of Casimir and DuPre[9] with Shaposhnikov's[10] correction for the spin-spin absorption. The dependence of ρ_l on the field intensity H_0 agrees with the formula of Brons-Van Vleck.[11]

To explain the mechanism of spin-lattice relaxation, i.e., the nature of interactions between the magnetic complex and the surrounding liquid, two theories were put forward. Both are based on an assumed existence of stable solvate complexes. According to Al'tshuler and Valiev[12] the conversion of the energy of the magnetically excited particles into energy of thermal motion is due to the normal vibrations of the complex, which modulate the electric field that acts on the electron cloud of the paramagnetic ion. According to a second theory proposed by McConnell,[13] this energy conversion is due to the magnetic anisotropy of the complex, which rotates in the liquid relative to the field H_0.

The experimental values of ρ_l, for a given value of H_0, increase slowly with dilution: by approximately 50 — 60% as the concentration N is varied from several moles/liter to 0.25 M in the case of aqueous solutions of manganese chloride, manganese sulfate, and manganese nitrate. Neither does the anion have a substantial effect on the value of ρ_l.[8] This is not in contradiction with the theory of Al'tshuler and Valiev, although the dependence of ρ_l on concentration and on the nature of the anion is not explicitly accounted for in this theory. The same is true of McConnell's theory. The most important factor when deciding upon the choice of theory is the clarification of the dependence of ρ_l on the temperature. In Mn^{2+} salt solutions this dependence is in full agreement with the theory of Al'tshuler and Valiev, which predicts a maximum on the $\rho_l(T)$ curve. Measurements of $\rho_l(T)$ were carried out in a 2M solution of $Mn(NO_3)_2$. In this case ρ_l has practically no dependence on the concentration of Mn^{2+}, thus creating most favorable conditions for checking the theory. It appears that $\rho_l(T)$ actually passes through a maximum at 290 — 300°K (cf. Fig. 1). The position of the maximum corresponds to a natural frequency $\hbar\omega_0 \sim 200\ cm^{-1}$.

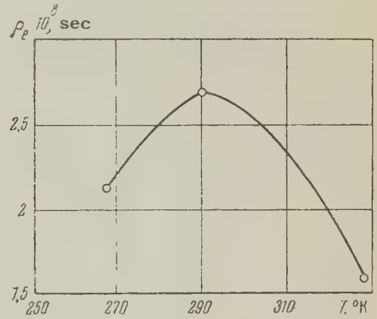

FIG. 1. Temperature dependence of the spin-lattice relaxation time ρ_l in a 2M aqueous solution of $Mn(NO_3)_2$.

In addition to relaxation times, the experiments in parallel fields yielded the values of magnetic specific heat constant b, or more accurately of their ratio to the Curie constant c. As shown by

---

*The presence of a rather stable second coordination sphere was recently proved by experiments on electron paramagnetic resonance in nonaqueous solutions of complex ions of divalent copper.[7]

Tishkov and Vishnevskaya[8] the magnetic specific heat constant depends substantially on the anion and greatly decreases with the dilution of the solution. The greater the dilution the closer are the values of b/c in different salts. The decrease of b/c with dilution depends on weakening of local magnetic fields, and also, apparently, on the gradual transition of the $Mn(H_2O)_4X_2$ type complexes into more symmetrical $Mn(H_2O)^{2+}$ complexes. To the latter complexes should correspond lower values of axial field constant D and consequently a smaller b/c. In our opinion, the presence of mixed complexes [e.g., of the $Mn(H_2O)_4Cl_2$ type] in concentrated solutions is also confirmed by the fact that the value of b/c for the solid salts $MnCl_2 \cdot 4H_2O$ and $MnSO_4 \cdot 4H_2O$ fits quite well on the curves of the corresponding solutions.

Solid manganese nitrate is surrounded by six molecules of water and for this reason the dependence of its b/c on the dilution is weakest and, apparently, determined mainly by the decrease in the magnetic dipole interactions.

Let us indicate the results of measurements of ρ_l in water-glycerine solutions of manganese chloride.[14] It is shown in reference 14 that $\rho_l(N)$ has a pronounced maximum, corresponding approximately to a content of 1 mole of glycerine per mole of manganese chloride in the solution. Such a dependence of b/c on concentration can be explained by the presence of mixed water-glycerine solvate shells in the ions of Mn^{2+}. These shells should decrease the symmetry of the electric field acting on Mn^{2+} and thus increase the value of b/c.

Besides the values of ρ_l, the experiments in parallel fields also yielded the values of ρ_s for different concentrations of Mn^{2+} salts in aqueous solutions. This enabled us to establish that the width of paramagnetic absorption curves in perpendicular fields at low frequencies ($\sim 10^7$ cps), within the errors of measurement, is equal to the sum of reciprocal values of ρ_l and ρ_s.

Measurements of the widths of the resonance lines in solutions of Mn^{2+}, Cr^{3+}, Cu^{2+} salts were carried out by Garif'yanov and Kozyrev at $\lambda = 3.2$ cm and temperatures from ~ 20° C to ~ 200° C, employing a specially developed method. The investigated solution of the paramagnet (cf. Fig. 2) was sealed in a barometric tube which was then inserted in the antinode of magnetic lines of a rectangular H_{103} cavity. The solution was heated by direct current flowing through platinum wire. The temperature was measured with a thermocouple in contact with the solution but not with the heater. As pointed out above, the widths of resonance lines are determined by the sum of reciprocal values of the spin-lattice and spin-spin relaxation times. The spin-spin relaxation due to the interactions between the magnetic ions should become longer with increasing solution temperature, owing to the averaging action of the Brownian motion in the liquid. The dependence of spin-lattice relaxation on T, on the other hand, may, according to the theory, vary for different ions.

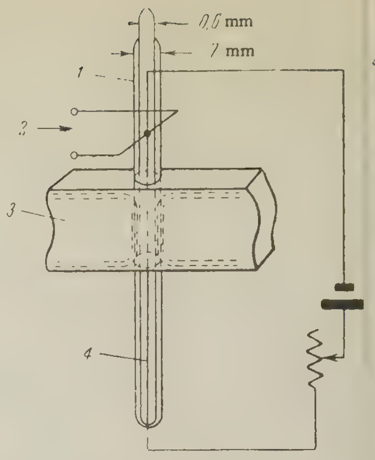

FIG. 2. Sketch of a device for the measurement of paramagnetic resonance in solutions at elevated temperatures: 1 – barometric tube, 2 – thermocouple, 3 – rectangular cavity resonator, 4 – platinum wire.

Experimental ΔH(T) curves for Mn^{2+} (where ΔH is the width of a discrete hyperfine component) show the presence of a minimum at $T \approx 340 - 350°K$ (cf. Fig. 3). The difference between this temperature and that of the maximum ρ_l ($T \approx 290 - 300°K$) corresponds to the expected value and can be attributed to the contribution of the spin-spin relaxation time to the line width. Thus, the resonance experiments on the Mn^{2+} solutions agree also qualitatively with the theory of Al'tshuler and Valiev.

The width of discrete hyperfine components in solutions of Mn^{2+} salts, as can be seen from Fig. 3, depends on the nuclear magnetic quantum number

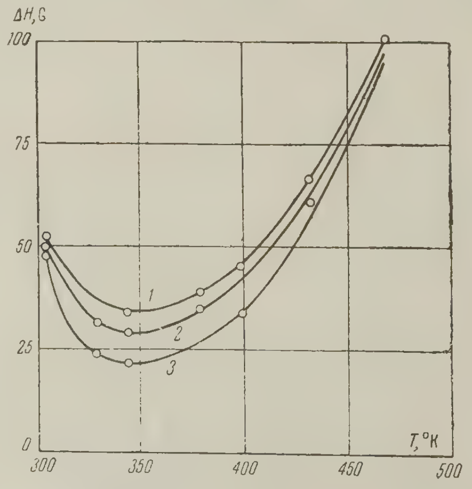

FIG. 3. Temperature dependence of the width ΔH of components of hyperfine structure absorption lines in 0.05M aqueous solution of $MnCl_2$ at 9400 Mcs: 1) m = ±5/2, 2) m = ±3/2, 3) m = ±1/2.

m: ΔH diminishes between the extreme peaks towards the center. This may easily be explained by taking into account the second-order terms in the Hamiltonian

$$\mathcal{H} = g\beta\overline{H}_0\hat{S} + A\hat{I}\hat{S}.$$

In the violet aqueous salt solutions of Cr^{3+} $[Cr(NO_3)_3 \cdot 6H_2O]$ a narrowing of the line is observed up to approximately $t \approx 150 - 180°C$; with further increase in temperature the width becomes constant and, at not too high concentrations (0.5 mole/liter), near 200° C, it starts to rise (Fig. 4). This also agrees qualitatively with the theory of Al'tshuler and Valiev. According to this theory the probability of relaxation transitions for Cr^{3+} is given by

$$A_{lk} \sim T^{-1/2}\coth(h\omega_0/2kT) \quad (\tau_l\omega_{lk} \ll 1),$$

where ω_0 is the natural frequency of the complex vibrations. With increasing temperature, this formula gives shortening of ρ_l for values of $h\omega_0/2kT$ sufficiently small compared with unity. Finally, the monotonic increase of ΔH with temperature for aqueous solutions of noncomplex salts Cu^{2+} (cf. Fig. 5) also agrees with the predictions of the above mentioned theory.

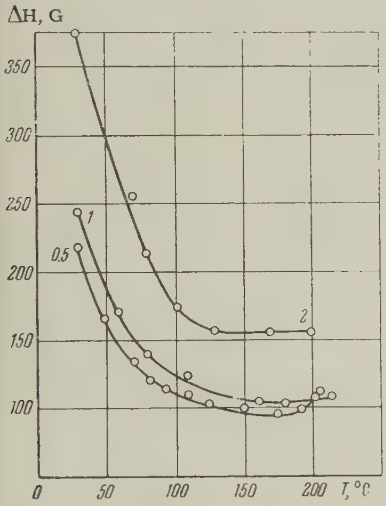

FIG. 4. Temperature dependence of absorption line width ΔH in aqueous chromium nitrate solutions at 9400 Mcs. 1) 2M $Cr(NO_3)_3$, 2) 1M $Cr(NO_3)_3$, 3) 0.5M $Cr(NO_3)_3$.

This is not the case for the above mentioned solutions of complex copper salts.[6] At $\nu \approx 10^{10}$ cps the width of a discrete component of hyperfine structure increases with increasing I_z. As the frequency is reduced to 10^9 cps the spectrum becomes more symmetrical and the line resolution improves. Both these facts agree qualitatively with the McConnell theory and are not explained by the other theory. The same apparently holds true for the solutions of vanadium salts.

Thus, the theory of Al'tshuler and Valiev describes the spin-lattice relaxation in those cases when we deal with magnetically isotropic ions (Mn^{2+}, Cr^{3+}, hydrated Cu^{2+} ion). For ions with strong magnetic anisotropy, however, the McConnell theory is more effective.

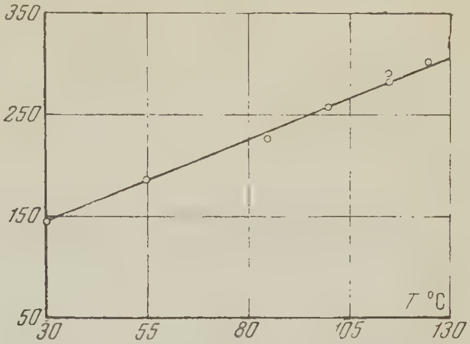

FIG. 5. Temperature dependence of absorption line width ΔH in 1M aqueous solution of $Cu(NO_3)_2$ at 9400 Mcs.

---

[1] U. Opik, M. H. L. Pryce. Proc. Roy. Soc. **A238**, 425 (1957).

[2] V. I. Avvakumov, JETP **37**, 1017 (1959), Soviet Phys. JETP **10**, 723 (1960).

[3] B. M. Kozyrev, Faraday Soc. Discussions **19**, 135 (1955).

[4] B. M. Kozyrev, doctoral dissertation, Physics Inst., Academy of Sciences, U.S.S.R. (1957).

[5] B. R. McGarvey, J. Phys. Chem. **61**, 1232 (1957).

[6] B. M. Kozyrev and A. I. Rivkind, Dokl. Akad. Nauk SSSR **127**, 1041 (1959).

[7] A. I. Rivkind, Тезисы докладов на совещании по парамагнитному резонансу, (Summaries of Reports of the Conference on Paramagnetic Resonance) Kazan', 1959, p. 10.

[8] P. G. Tishkov and G. P. Vishnevskaya, JETP **38**, 2 (1960), Soviet Physics JETP **11**, in press.

[9] H. B. G. Casimir, F. K. DuPré, Physica **5**, 507 (1938).

[10] I. G. Shaposhnikov, Doctoral dissertation, Physics Inst., Academy of Sciences, U.S.S.R. (1949).

[11] C. I. Gorter, Paramagnetic relaxation, Elsevier, New York, 1949, Russ. Transl. IIL, 1949.

[12] S. A. Al'tshuler and K. A. Valiev, JETP **35**, 947 (1958), Soviet Phys. JETP **8**, 661 (1959).

[13] H. J. McConnell, J. Chem. Phys. **25**, 709 (1956).

[14] P. G. Tishkov, JETP **36**, 1337 (1959), Soviet Phys. JETP **9**, 949 (1959).

Translated by Z. Scheidlinger

EFFECT OF PRESSURE ON THE RAMAN SPECTRUM OF OXYGEN

G. V. MIKHAĬLOV

P. N. Lebedev Institute, Academy of Sciences, U.S.S.R.

Submitted to JETP editor July 9, 1959

J. Exptl. Theoret. Phys. (U.S.S.R.) **37**, 1570-1574 (December, 1959)

The Raman spectrum of oxygen has been studied at pressures between 7 and 125 atmos. Broadening of lines in the rotational band of O_2 is of collision nature at these pressures, the effective collision broadening parameter being $\rho_\omega = 4.43$ A. The parameters that characterize the width of the Raman rotational lines are identical with those for O_2 measured on the basis of absorption in the microwave region. Unlike the lines of the rotational band, the Q branch of the vibrational transition of O_2 does not broaden with varying pressure. The observed width of the Q branch is explained by splitting of the Q branch with respect to J, owing to the interaction between vibrations and rotations.

THE pressure variation of the Raman scattering of a gas is directly connected with processes that occur during the molecule collisions. Specifically, the most important result of such an investigation is information on collision itself, gained by determining the connection between the spectrum and the phenomena that occur during impact.

Initially the investigation of Raman spectra of gases at various pressures was performed by the author on N_2;[1] the present work is a continuation of this study. .

The Raman spectrum of oxygen was investigated in the pressure range from 7 to 125 atmos at +27° C. At each point of the investigated pressure, 3 to 4 photographs were taken for the spectrum. The mean error is approximately 15% in the measurements of line width and 3 — 5% in the measurement of intensity. The apparatus and the experimental conditions were described in detail elsewhere.[1]

The Raman spectrum of oxygen consists of O and S branches of the rotational band, located on both sides of the excitation line, and of a vibrational band (O, Q, and S branches).

ROTATIONAL BAND OF THE OXYGEN RAMAN SPECTRUM

The rotational band, corresponding to the transitions $\Delta v = 0$, $\Delta J = \pm 2$, consists of individual equidistant lines spaced $\Delta\omega \approx 11.5\ \text{cm}^{-1}$ apart, with typical thermal distribution of intensity in the band. The rotation band lines were observed up to components corresponding to transitions with $J = 25$ in the O branch and $J = 35$ in the S branch.

At low pressures, the rotational band lines are sharp. As the pressure is increased, at 25 atmos, these lines broaden and start overlapping, and at higher pressures they merge into a continuous band with weak maxima (Fig. 1). The considerable separation of the oxygen rotational lines permitted a sufficiently detailed study of its variations. Quantitative measurements yielded the following results.

1. The frequencies of the rotational lines do not change over the entire pressure range investigated and coincide, within the measurement errors ($\pm 0.2\ \text{cm}^{-1}$), with the values calculated for O_2 with the nonrigid-rotator model.[2]

2. The rotational lines have a disperse form, and their width $2\gamma_\omega$ depends linearly on the pressure over the entire range from 7 to 125 atmos, while the relative broadening is $\gamma_\omega/p = 0.0555\ \text{cm}^{-1}\ \text{atmos}^{-1}$ (see table and Fig. 2). At all the investigated pressures, γ_ω is independent of J within the limits of experimental error (15 — 20%) ($3 < J < 15$).

The dispersed form of the lines, the linear variation of $\gamma_\omega(p)$, and the fact that the distance between the rotational levels is greater than the maximum observed line width indicate that the theory of impact broadening of spectral lines[3] can be applied to the rotational band. According to the impact theory, the line width 2γ is determined by the relation.

$$2\gamma = N v_{\text{rel}} \rho^2 / c,$$

where N is the number of molecules per unit volume, v_{rel} is the relative velocity of the colliding molecules, ρ is the effective collision radius, and c is the velocity of light. For oxygen at 300° K this relation leads to the following formula for the relative broadening:

$$2\gamma / p = (L v_{\text{rel}} / c) \rho^2 = 5.64\, \rho^2,$$

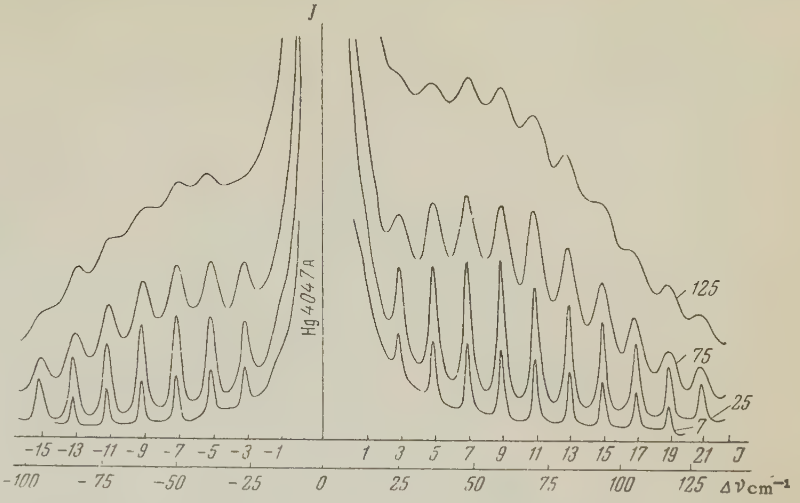

FIG. 1. Rotational band of the Raman spectrum of oxygen at pressures 7, 25, 75, and 125 atmos, temperature 27°C.

Width of the lines of the rotational band ($2\gamma_\omega$) and of the Q branch of the vibrational band ($2\gamma_Q$) of the Raman spectrum of oxygen at various pressures

p, atmos	$2\gamma_\omega^*$, cm^{-1}	$2\gamma_Q^{**}$, cm^{-1}
7	0.75±0.4	—
15	1.3 ±0.5	3.2
25	2.4 ±0.8	2.9
50	6.6 ±1.2	2.7
75	8.6 ±0.7	2.5
100	10.8 ±0.9	2.5
125	14.0 ±1.2	2.4
Average	—	2.65

*Average for all J.

**Observed width of the Q branch of Hg 4047 A, including the apparatus function.

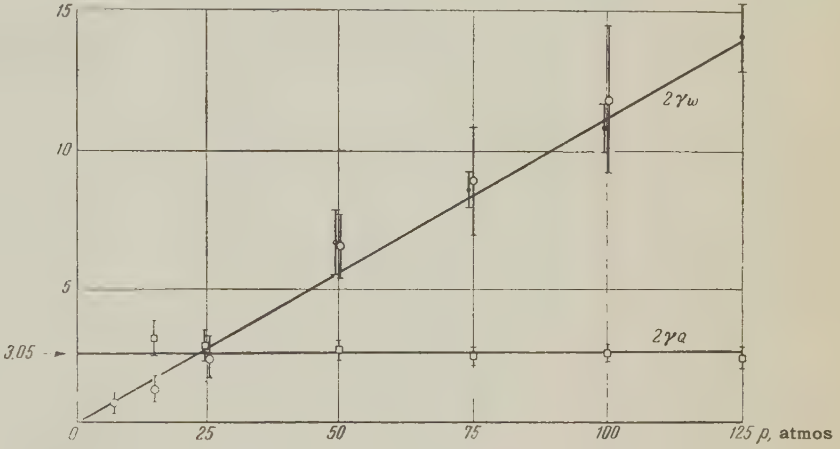

FIG. 2. Dependence of the line widths of the rotational band ($2\gamma_\omega$) and of the Q branch of the vibrational bands ($2\gamma_Q$) of Raman scattering of oxygen on the pressure. The two series of points for the widths of the rotational lines correspond to different data-reduction methods.

where 2γ is the total width of the line in cm^{-1}, p the pressure in atmospheres and ρ the effective radius of collision in Angstroms. Using the experimental value $\gamma_\omega/p = 0.0555$ cm^{-1} atmos^{-1}, we obtain for the effective collision radius, which determines the broadening of the O_2 rotational lines, a value $\rho_\omega = 4.43$ A. The measured value of ρ_ω is somewhat greater than the gas-kinetic diameter of O_2 ($d_0 = 3.61$ A), similar to what was found earlier for N_2: $\rho_\omega \approx 5.15 - 3.95$ A and $d_0 = 3.68$ A.[1,4] From ρ_ω we can determine the upper limit of the range of action of the impact broadening, determined by the condition $2\pi\rho^2 N \ll 1$. It follows hence that the impact theory is correct in the region $p \ll 70$ atmos, i.e., the investigated region is at the limit of applicability of the impact theory.

The results of this investigation of the broadening of rotational Raman lines of O_2 in the range from 7 to 125 atmos are in good agreement with analogous measurements in the range 3 – 10 atmos:[4] $\gamma_\omega/p = 0.0504$ (cm-atmos)$^{-1}$, $\rho_\omega = 4.35$ A, and $\gamma_\omega(J)$ remains constant within the limits of errors (~ 15%).

The results of the investigations of Raman scattering are in excellent agreement with the results of measurements of the width of rotational lines of O_2 based on absorption in the microwave band at pressures 1 – 8 mm Hg:[5] $\gamma_\omega/p = 0.0505$ (cm-atmos)$^{-1}$, $\rho_\omega = 4.35$ A, and the variation of $\gamma_\omega(J)$ does not exceed 15% of the total width.

The full agreement of the experimental data on the broadening of the rotational lines of O_2 in Raman scattering and in the microwave band allow us to assume that the nature of broadening is the same in both cases, and to apply to Raman scattering the same impact-broadening treatment of rotational lines as used for absorption in the microwave band. The quantum-mechanical theory of impact broadening in the microwave band was developed by Anderson[5] and was applied to microwave

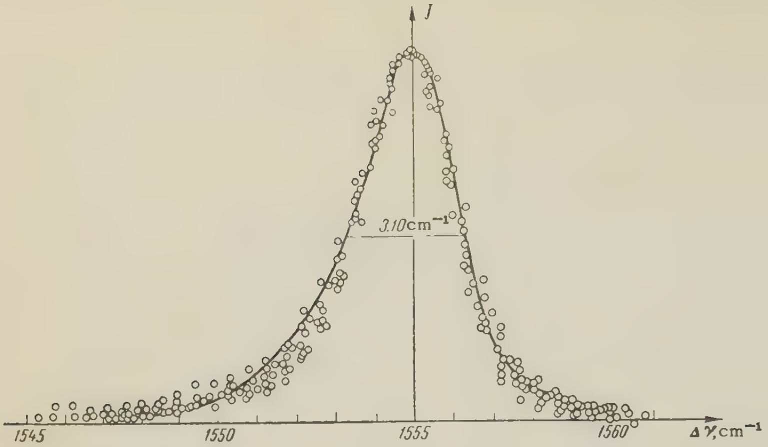

FIG. 3. Q branch of the vibrational band of Raman scattering of $O_2(\Delta\nu = 4358\ \text{A})$ at pressures from 15 to 125 atmos.

absorption of O_2 in reference 6, where the corresponding semi-empirical formula is given for the relative broadening of the rotational lines of O_2:

$$\gamma / p = C_1 + C_2 J^{-1/2} + C_3 [f(J+2) + f(J-2)].$$

Here the term $C_1 = 0.033\ (\text{cm-atmos})^{-1}$ is due to inelastic impacts that lead to quenching of the rotation. The second term is connected with the quadrupole and induced-polarization interaction of the colliding molecules, $C_2 = 0.011\ (\text{cm-atmos})^{-1}$. The last term is due to induced rotational transitions with $\Delta J = \pm 2$, $C_3 = 0.050\ (\text{cm-atmos})^{-1}$, and $f(J)$ is the number of molecules in the state J. This formula gives the correct value of γ/p, coinciding with experiment both for microwave absorption and for Raman scattering.

3. The distribution of the integrated intensity over individual lines in the rotational band obeys the thermal law and does not change over the entire investigated pressure range. The redistribution of the intensities in the band due to transfer to the central line can occur only once the levels overlap.[7] For the investigated region of pressures, the maximum observed broadening still does not lead to an overlap of levels, and this explains why the distribution of intensity in the band is retained.

VIBRATIONAL BAND OF THE RAMAN SPECTRUM OF OXYGEN

In the vibrational band of oxygen $(\Delta v = 1)$ one observes one sharp line with frequency $\Delta\nu = 1555$ cm^{-1}, corresponding to the Q branch $(\Delta J = 0)$; usually no O or S branches are observed, and only at considerable exposures and pressures does a weak and highly blurred skirt appear at the location of the S mode.

The Q branch of O_2 (Fig. 3) has an asymmetrical shape with a skirt in the violet side, and its true width remains constant at $1.8\ \text{cm}^{-1}$ in the investigated pressure range (see table and Fig.2). No frequency shift was observed for the Q branch.

The fact that the Q branch of O_2 is independent of pressure, as was also observed earlier for N_2, indicates that its impact broadening is small. Unlike the O and S branches of the rotational band (transitions $\Delta v = 0$, $\Delta J = \pm 2$), the Q branch consists of transitions without change in the state of rotation $(\Delta J = 0)$. It is therefore very probable that the width of the Q branch is influenced only by disturb-

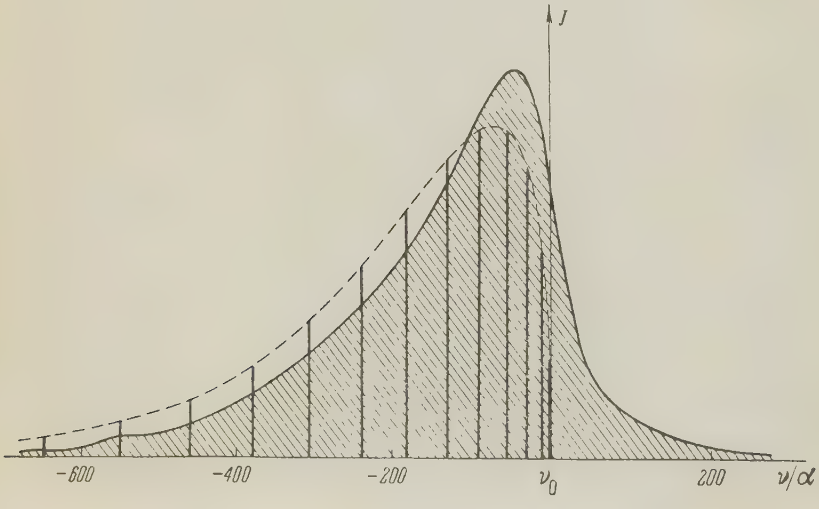

FIG. 4. Rotational structure and calculated form of the Q-branch contour for O_2.

ances in the oscillations upon impact and the rotation perturbation has no effect.

The observed width and shape of the contour of the Q branch for O_2, like that for N_2, is well explained by its rotational structure. The change in the moment of inertia of the molecule during vibration changes the distance between the rotational levels, and therefore the rotational components of the Q branch do not overlap exactly, but are split somewhat.[7] The resultant rotational structure of the Q branch is shown in Fig. 4 (individual lines). Starting from this structure, we have calculated the observed contour of the Q branch for which each component is broadened by a Gaussian apparatus function of width 1.6 cm^{-1} (shaded contour in Fig. 4). Comparison of the computed contour with the observed one (Fig. 3 solid curve — calculated, dots — experiment) shows that the width and shape of the Q branch are fully explained by its rotational structure.

The author expresses his gratitude to Prof. P. A. Bazhulin for attention and guidance of this investigation, to I. I. Sobel'man, whose valuable advice he used numerous times, to V. I. Malyshev and S. G. Rautian for discussions in the evaluation of the work.

---

[1] G. V. Mikhaĭlov, JETP **36**, 1368 (1959), Soviet Phys. JETP **9**, 974 (1959).

[2] G. Herzberg, Spectra and Structure of Diatomic Molecules, (Russ. Transl.) IIL, 1949, p. 78.

[3] S. Shen and M. Takeo, Revs. Modern Phys. **29**, 20-73 (1957), Russ. Transl. in Usp. Fiz. Nauk **66**, 391 (1958).

[4] Yu. A. Lazarev Оптика и спектроскопия (Optics and Spectroscopy), in press.

[5] P. V. Anderson, Phys. Rev. **78**, 647 (1949).

[6] Anderson, Smith, and Gordy, Phys. Rev. **87**, 561 (1952).

[7] I. I. Sobel'man, Izv. Akad. Nauk SSSR, Ser. Fiz. **17**, 554 (1953).

Translated by J. G. Adashko
317

SOVIET PHYSICS JETP VOLUME 37(10), NUMBER 6 JUNE, 1960

ELASTIC SCATTERING OF 8.7-Bev PROTONS BY PHOTOEMULSION NUCLEI[*]

B. P. BANNIK, V. G. GRISHIN, M. Ya. DANYSH, V. B. LYUBIMOV, and M. I. PODGORETSKIĬ

Joint Institute for Nuclear Research

Submitted to JETP editor June 9, 1959

J. Exptl. Theoret. Phys. (U.S.S.R.) **37**, 1575-1582 (December, 1959)

Elastic scattering of 8.7-Bev protons by photoemulsion nuclei was studied with a special method. The measured angular distribution of the scattering is in good agreement with that calculated from the optical model if the refraction in the nucleus is taken into account.

STUDY of the elastic scattering of high-energy particles is a convenient way of studying nuclear structure. Unfortunately, the relevant experiments require measurement of very small scattering angles. Thus, for example, in scattering of 9-Bev protons by photoemulsion nuclei, the range 0 — 1° includes a large part of the angular interval to be studied. In the present work a method was employed which made it possible to investigate the angular distribution right down to angles ~ 0.2°, in a way analogous to that employed in measuring multiple scattering.

The work was carried out with emulsion cameras, irradiated with the internal beam of 8.7-Bev protons of the proton synchrotron of the High-Energy Laboratory, Joint Institute for Nuclear Research. Camera No. 1 was composed of layers of photoemulsion NIKFI-R of thickness 450 μ. The intensity of radiation was about 10^4 particles/cm^2. The proton beam, which had an angular spread of about 0.2°, traversed the camera at an angle of 0.7° to the plane of the emulsion. The search for tracks and subsequent measurements were carried out with microscopes using a magnification of 60 × 10 × 1.5.

Because of large distortion in the photoemulsion, measurements of angles were relative. Pairs of tracks were chosen, and the distances between tracks were measured in the eyepiece scale at two points along the track, distant $l = 2$ mm from each other. The difference of the measured distances gave the projection of the angle θ between the tracks on the plane of the emulsion. Pairs of tracks satisfying the following conditions were chosen: 1) relativistic ionization, 2) the projection of the angle between the track and the axis of the beam should be less than 2°, 3) the distance between tracks should not be more than 50 — 60 μ in the plane of the emulsion, nor more than 25 — 30 μ in depth, 4) the track should have no visual inclination to the plane of the emulsion.[*]

By this means, 601 pairs of tracks at a distance R = 95 mm from the edge of the emulsion camera were measured. The angular distribution so obtained is shown in Fig. 1.[†] The root-mean-square error in the measurements was $\Delta\theta = 0.03°$.

In the same way, the angular distribution of 572 pairs of tracks (Fig. 2) was measured for R = 5 mm. Taking these as initial data, it is possible to calculate the form of the angular distribution at R = 95 mm, taking into account multiple Coulomb scattering and single and double nuclear elastic scattering. The contribution of triple nuclear scattering was small for R = 95 mm and was, therefore, not included.

The differential and total cross sections for elastic scattering $(d\sigma/d\Omega)_d$ and σ_d were calculated[‡] from the optical model[2]

$$\left(\frac{d\sigma}{d\Omega}\right)_d = \left| k_0 \int_0^\infty (1 - \exp\{-\bar{\sigma}\rho_0 S(b)\})\, J_0(k_0 b \sin\theta)\, b\, db \right|^2$$

$$\sigma_d = 2\pi \int_0^\infty (1 - \exp\{-\bar{\sigma}\rho_0 S(b)\})^2\, b db,$$

---

[*] A preliminary account was given at the Geneva High-Energy Conference.[1]

[*] In the selection it is desirable not to introduce discrimination connected with the angle of inclination of the track relative to the plane of the emulsion, since this can cause distortion in the measured distribution of horizontal angles. In fact, it turned out that some ambiguity inherent in condition 4 has no substantial effect.

[†] In order to exclude the background of secondary particles, the tracks of pairs with angle $\theta > 1°$ were followed backwards. Out of 19 cases with $\theta > 1°$, in 5 cases one of the tracks turned out to be a secondary particle. These cases were not included in the distribution shown in Fig. 1. The background for $\theta < 1°$ was evaluated from the angular distribution of secondary relativistic particles in nuclear interactions; the expected number of background particles was 17.

[‡] The calculations were carried out mainly by S. M. Bilen'kiĭ and R. M. Ryndin, to whom the authors would like to express their gratitude.

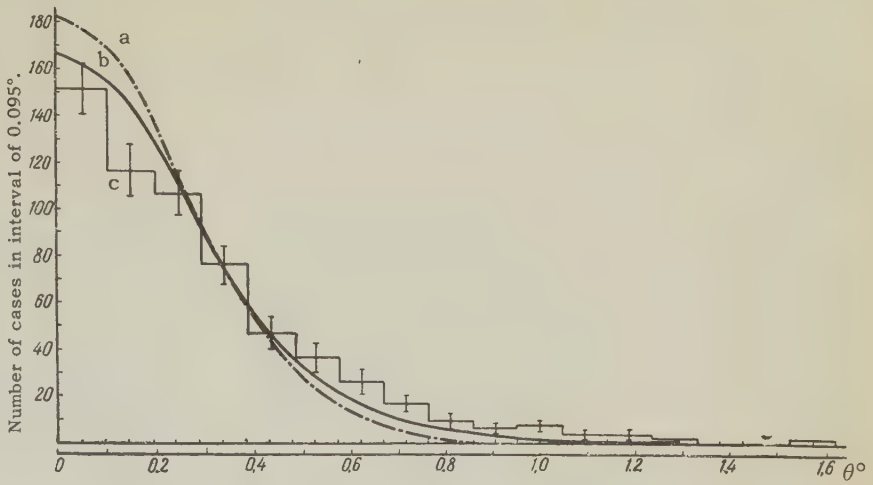

FIG. 1. Angular distribution at a distance R = 95 mm from the edge of the emulsion camera: a – calculated from the initial angular distribution at R = 5 mm taking multiple Coulomb scattering into account, b – calculated from the initial angular distribution taking multiple, Coulomb, and nuclear elastic scattering (for $k_1 = 0$) into account, c – measured.

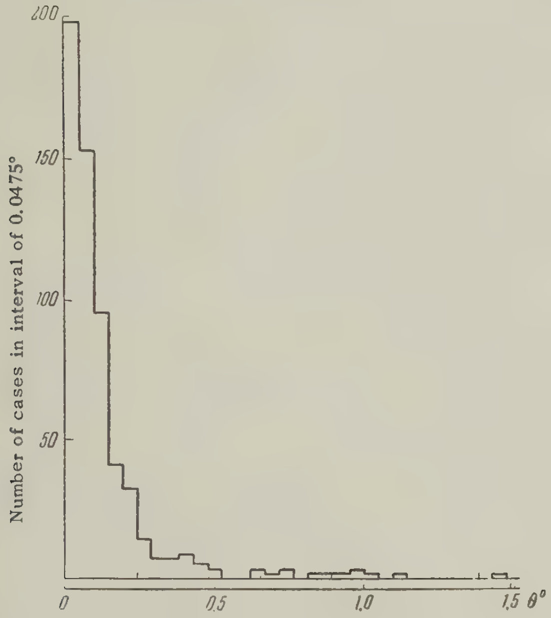

FIG. 2. Angular distribution measured at a distance R = 5 mm from the edge of the emulsion camera.

where the meaning of the various quantities is as in reference 2.

In these formulae, the real part of the index of refraction in nuclear matter was assumed to be unity. In other words, in the expression for the wave vector of the proton inside the nucleus

$$k = k_0 + k_1 + iK/2$$

where k_0 is the wave vector of the proton outside the nucleus and K is the absorption coefficient, k_1 was taken to be zero.

The quantity $\bar{\sigma}$ (total cross section for scattering of the proton by nucleons of the nucleus, averaged over protons and neutrons) was chosen so that the cross section for inelastic interactions

$$\sigma_a = 2\pi \int_0^\infty (1 - \exp\{-2\bar{\sigma}\rho_0 S(b)\})\, b\, db$$

corresponded to the mean free path $L_a = 34.7$ cm obtained from inelastic interactions of 8.7-Bev protons with photoemulsion nuclei.[3] The value obtained* $\bar{\sigma} = 34$ mb, is in agreement with results of the theoretical analysis of Grishin and Saitov[5] and with direct measurements of the cross sections for inelastic and elastic p-p interactions at 8.7 Bev, $\sigma_{in} = 21$ mb, $\sigma_{el} = 10 \pm 3$ mb;[6] $\sigma_{el} = 10 \pm 4$ mb;[7] $\sigma_{el} = 8.4 \pm 1.1$ mb.[8]

In carrying out all calculations, it was assumed for simplicity that the distribution of nucleon density in the nuclei was

$$\rho(r) = \begin{cases} \rho_0 & \text{for} \quad r \leqslant r_0 \\ \rho_0 (r_1 - r)/(r_1 - r_0) & \text{for} \quad r_0 \leqslant r \leqslant r_1, \\ 0 & \text{for} \quad r > r_1 \end{cases}$$

where $r_0 = (1.14\,A^{1/3} - 1.49) \times 10^{-13}$ cm, $r_1 = (1.14\,A^{1/3} + 1.49) \times 10^{-13}$ cm. These expressions obtained for ρ_0 and S(b) are practically the same as results of calculations using a more complicated form for the distribution.[2]

The angular distribution at R = 95 mm calculated from multiple Coulomb and nuclear scattering has the form

$$F(\theta) = \alpha_0 F_0(\theta) + \alpha_1 F_1(\theta) + \alpha_2 F_2(\theta).$$

where

$$\alpha_0 = e^{-t/L_d}, \qquad \alpha_1 = (t/L_d)\, e^{-t/L_d}, \qquad \alpha_2 = 1 - (\alpha_0 + \alpha_1)$$

denote the probabilities of traversing t = 90 mm without nuclear interaction and with one and two scatterings, respectively; L_d is the calculated value of the mean free path for elastic scattering of protons by photoemulsion nuclei, equal to 72 cm; $F_0(\theta)$, $F_1(\theta)$ and $F_2(\theta)$ are the angular distributions at R = 95 mm, calculated from the initial distribution at R = 5 mm under the assumption of: the absence of nuclear scattering (F_0), one scattering (F_1), and two scatterings (F_2).

---

*An analogous result was also obtained by Barashenkov and Huang Nen-Ning.[4]

The distribution $F(\theta)$ is given in Fig. 1, together with the curve of $F_0(\theta)$ for comparison. The agreement with experimental data is unsatisfactory.

An analogous result was obtained by another, more sensitive method. The plate was placed on the microscope stage so that the axis of the beam was parallel to the direction of motion of the stage. A pair of tracks was chosen, according to criteria more or less the same as those above, for measurement at $R = 10$ mm. The angle θ was measured twice for each pair, at distances $l = 2$ mm. The first measurement was carried out at $R = 10$ mm, the second at a distance $\mathscr{L} = 10$ mm from the first. In case one of the tracks went out of the field of view or out of the emulsion before $L = 10$ mm, then the second measurement was made at smaller $\mathscr{L}$. Measurement of the angle θ at distance $\mathscr{L}$ gave the value of the projection of the scattering angle φ. The accuracy of measurement was $\Delta\varphi = 0.09°$.

In all, 2276 pairs of tracks were measured, out of which all pairs with angle $\varphi > 0.2°$ (108 cases) were measured once again for $\mathscr{L} = l = 1$ mm with an MBI-8 microscope using magnification $90 \times 15 \times 1$. The error in the measurement was $\Delta\varphi = 0.03°$. As a result of the repeated measurements, it turned out that 31 pairs had angle $\varphi < 0.2°$ and one pair had angle $\varphi > 1.7°$.* Thus, 76 pairs had angles lying in the interval $0.2° < \varphi < 1.7°$.

Analogous measurements were carried out with another emulsion camera (No. 2) of better quality, also composed of layers of NIKFI-R emulsion of thickness $450\,\mu$ and irradiated under the same conditions.† As a result, 48 cases of scattering through angles between 0.2 and 1.7° were observed. Thus, a total of 124 cases of scattering in this angular interval were observed in the two cameras. Out of this number, it was necessary to discard cases connected with a) inelastic scattering inside the camera, b) inelastic scattering outside the camera, and c) distortion in the emulsion.

Cases of inelastic interaction inside the emulsion either accompanied by charged particles or without them, were excluded by visual scanning back along the path up to the point where it left the emulsion. Cases of rather slow secondary particles produced either inside or outside the camera, were excluded by measurement of the multiple Coulomb scattering.

Measurement of multiple scattering was carried out using a cell length of $2000\,\mu$, in the majority of cases by following the tracks into the neighboring layer of emulsion. In each case, the mean second difference D was found in units of divisions of the eyepiece micrometer (1 division equal to $0.0925\,\mu$). Results of the measurements are shown in Fig. 3. The mean value was $\bar{D} = 7.1 \pm 0.3$ divisions in all cases in which $D < 20$ divisions. The 11 cases with mean second difference $D > 20$ divisions ($p\beta c$ less than 2 Bev) were connected with secondary particles and inelastic collisions, and these were not included in the statistics.

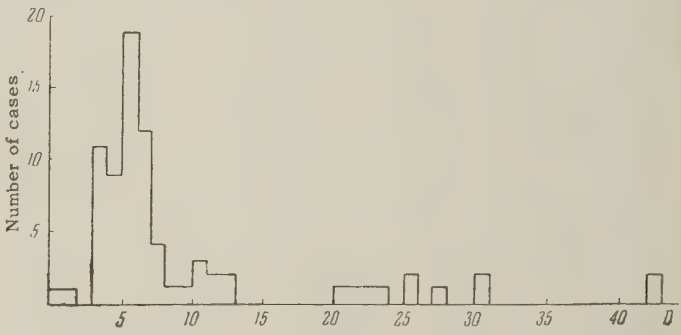

FIG. 3. Distribution of mean second differences.

Cases arising from distortion in the emulsion occurred, in spite of the relative measurements, in so far as the distance between the tracks of a pair could be rather large ($\sim 300\,\mu$). The effect of distortion was mainly excluded by secondary measurements on several neighboring tracks. The cases were connected with distortion and discarded if results of the secondary measurements differed from the first ones by more than 0.1°. There were 17 such cases in camera No. 1 and 19 in camera No. 2.

Final results are given in Tables I and II and on Fig. 4, where, for comparison, the curve calculated from the optical model is given. The experimental points lie higher than the calculated curve for angles $\varphi > 0.3°$. The number of cases of scattering through angles $\varphi > 0.3°$ was 62, whereas, according to the optical model it should be 31. This disagreement persists in the large-scale region. For angles $\varphi > 0.5°$, the numbers of measured and expected cases were 22 and 9, respectively.

It should be kept in mind that elastic scatterings through large angles by C, N, and O nuclei, were accompanied by nuclear recoils, which were observed. The corresponding cases (about five)

---

*Cases of scattering through angles $\varphi > 1.7°$ were not registered, since the efficiency of detection depended on the angle of scattering.

†In camera No. 2, 76 cases were observed in 2733 cm of track length. The value of the mean free path $L_a = 36.0 \pm 4.1$ cm agrees well with that obtained in ref. 3.

TABLE I. Results of measurements on MBI-8M microscopes

	Number of cases		
	Camera No. 1	Camera No. 2	Sum
$\varphi < 0.2°$	31	14	45
$\varphi > 1.7°$	1	1	2
Mean second difference D > 20 divisions ($p\beta c$ < 2 Bev)	8	3	11
Distortion	17	19	36
Elastic scattering through angles $0.2° < \varphi < 1.7°$	51	26	77
Total length of measured tracks, cm	4381	2873	7254

TABLE II

Angular interval, degrees	Number of cases				
	Camera No. 1	Camera No. 2	Sum	Calculated for a track length of 72.54 m	
				for $k_1=0$	for $k_1\neq0$
0.0—0.1	—	—	—	26.4	40.0
0.1—0.2	—	—	—	23.6	36.0
0.2—0.3	9	6	15	19.6	29.5
0.3—0.4	18	6	24	13.8	21.1
0.4—0.5	8	8	16	8.6	13.9
0.5—0.6	7	2	9	4.7	8.3
0.6—0.7	1	3	4	2.2	4.8
0.7—0.8	1	—	1	0.9	2.9
0.8—0.9	—	—	—	0.6	2.3
0.9—1.0	2	—	2	0.3	1.9
1.0—1.1	—	—	—	0.2	1.5
1.1—1.2	3	—	3	0.1	1.0
1.2—1.3	1	1	2	—	0.7
1.3—1.4	—	—	—	—	0.3
1.4—1.5	—	—	—	—	—
1.5—1.6	—	—	—	—	—
1.6—1.7	1	—	1	—	—

were discarded together with inelastic interactions.

In the angular region 0.2 – 0.3°, part of the cases of scattering might have been thrown out as a result of the selection system employed. Some cases may have been lost through exclusion of distortion. The contribution of these effects, according to a rough estimate, was 9 cases. If we take this correction into account, then the number of cases in the interval 0.2 – 0.3° was 24 ± 12. This correction was not introduced into the distribution shown on Fig. 4.

The effect of Coulomb scattering was considered in an approximate way. For angles $\varphi > 0.4°$ it was negligible. In the interval 0.2° – 0.3°, the cross sections for Coulomb and nuclear scattering were equal in magnitude. It is not excluded that in this angular region some interference between Coulomb and nuclear scattering exists. Clarification of this would demand substantially better statistics.

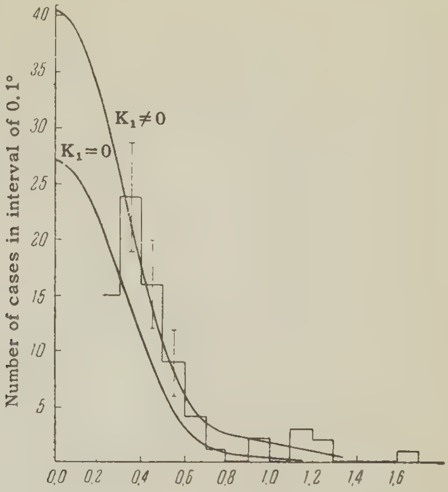

FIG. 4. Angular distribution of nuclear elastic scattering. The histogram gives the measured distribution. The smooth curves were calculated from the optical model with ($k_1 \neq 0$) and without refraction ($k_1 = 0$) in the nucleus.

The results of the measurements show that the cross sections for elastic scattering of 8.7-Bev protons on photoemulsion nuclei are in poor agreement with predictions of the optical mode, if the real part of the wave vector of the proton inside the nucleus is unchanged ($k_1 = 0$). Therefore, it is natural to assume that $k_1 \neq 0$. Then, because of the relation

$$k_1 = (2\pi\rho(r)/k_0)\,\mathrm{Re}\,f(0),$$

the real part of the amplitude for nucleon-nucleon scattering at zero angle, Re f(0), also differs from zero. This latter conclusion is in agreement with results of measurements of inelastic proton-proton scattering at 8.5 Bev,[8] from which one can obtain*

$$\mathrm{Re}\,f(0) = 15\cdot10^{-13}\,\mathrm{cm}.$$

This value was used in calculating k_1.

If the quantity k_1 differs from zero, then the expressions for the differential and total cross sections for elastic scattering take on the following form

$$\left(\frac{d\sigma}{d\Omega}\right)_d = \left|k_0\int_0^\infty (1-e^{-\bar{\sigma}\rho_0 S(b)}\cos\psi)\,J_0(k_0 b\sin\theta)\,b\,db\right|^2 + \left|k_0\int_0^\infty e^{-\bar{\sigma}\rho_0 S(b)}\sin\psi J_0(k_0 b\sin\theta)\,b\,db\right|^2,$$

$$\sigma_d = 2\pi\int_0^\infty (1-e^{-\bar{\sigma}\rho_0 S(b)}\cos\psi)^2\,b\,db + 2\pi\int_0^\infty e^{-2\bar{\sigma}\rho_0 S(b)}\sin^2\psi\,b\,db,$$

where

$$\psi = (4\pi/k_0)\,\rho_0 S(b)\,\mathrm{Re}\,f(0).$$

---

*In obtaining this result, possible effects of spin-dependent interactions were not considered. The value of Re f(0) is given in the laboratory system.

The angular distribution calculated taking k_1 into account is given in Fig. 4.* It is in satisfactory agreement with the measurements. The number of cases of scattering through angles $\varphi > 0.3°$ was equal to 58, with the experimental number 62. In the angular interval $\varphi > 0.5°$, the calculated and measured numbers of cases were equal to 23 and 22, respectively.

Below are given the values for the elastic and total cross sections for both light and heavy emulsion nuclei, calculated taking k_1 into account.

	σ_{tot}, mb	σ_{el}, mb
Heavy nuclei	1830	888
Light nuclei	407	156

The results of these measurements agree qualitatively with the data from measurements of scattering of 4.5 Bev neutrons by C, Cu and Pb[9].

The agreement between the measured angular distribution and the calculated one supports the choice of the value of k_1 and, consequently, the real part of the scattering amplitude $\mathrm{Re}\, f(0)$ differs from zero and is near to 15×10^{-13} cm. The quantity k_1 obtained from this value of $\mathrm{Re}\, f(0)$ under the assumption of a uniform distribution of nuclear matter, was $1.5 \times 10^{12}\ \mathrm{cm}^{-1}$. Using this number, one can calculate the effective potential for the nucleon-nucleus interaction

$$V = \hbar \beta c k_1 \approx 30\ \mathrm{Mev}.$$

For 1.4-Bev neutrons, a value V = 26 Mev was obtained for the potential.[10] Analogous results (V ~ 30 Mev) were obtained for protons with energy in the region of 1 Bev.[11,12] Thus, the effective interaction potential in the energy interval 1 to 9 Bev apparently remains constant.

The authors would like to take this opportunity to thank I. M. Gramenitskiĭ for valuable advice and help in the work, P. K. Markov and É. N. Tsygankov for useful discussions and V. M. Gorbunkov and A. I. Rodionov, who carried out part of the calculations. The measurements were carried out by L. I. Aver'yanova, Z. P. Golovina, T. A. Zhuravleva, N. V. Kirsanova, M. P. Koteneva, A. I. Maklachkova, G. A. Nurusheva, and G. P. Tyupikova, to whom the authors are deeply grateful.

---

*In the calculations, the following values were assumed: $r_0 = (1.08\ A^{1/3} - 1.49) \times 10^{-13}$ cm, $r_1\ A^{1/3} + 1.49) \times 10^{-13}$ cm.

---

[1] 1958 Ann. Int. Conf. on High-Energy Physics at CERN, p. 309.

[2] Cronin, Cool, and Abashian, Phys. Rev. **107**, 1121 (1957).

[3] Bogachev, Wang Shu-Feng, Gramenitskiĭ, Kirillova, Lebedev, Lyubimov, Markov, Merekov, Podgoretskiĭ, Sidorov, Tolstov, and Shafranova, Атомная энергия (Atomic Energy) **4**, 281 (1958).

[4] Barashenkov and Huang Nen-Ning, JETP **36**, 1319 (1959), Soviet Phys. JETP **9**, 935 (1959).

[5] V. G. Grishin and I. S. Saitov, JETP **33**, 1051 (1957), Soviet Phys. JETP **6**, 809 (1958).

[6] Bogachev, Bunyatov, Gramenitskiĭ, Lyubimov, Merekov, Podgoretskiĭ, Sidorov, and Tuvdendorzh, JETP **37**, 1225 (1959), Soviet Phys. JETP **10**, 872 (1960).

[7] Bogachev, Bunyatov, Merekov, and Sidorov, Dokl. Akad. Nauk SSSR **121**, 617 (1958), Soviet Phys.-Doklady **3**, 785 (1959).

[8] Lyubimov, Markov, Tsyganov, Cheng P'u-Ying and Shafranova, JETP **37**, 910 (1959), Soviet Phys. JETP **10**, 651 (1960).

[9] Atkinson, Hess, Perez-Mendez, and Wallace, Phys. Rev. Letters **2**, 168 (1959).

[10] Coor, Hill, Hornyak, Smith, and Snow, Phys. Rev. **98**, 1369 (1955).

[11] Booth, Ledley, Walker, and White, Proc. Phys. Soc. **A70**, 209 (1957).

[12] Chen, Leavith, and Shapiro, Phys. Rev. **99**, 857 (1955).

Translated by G. E. Brown
318

SOVIET PHYSICS JETP VOLUME 37 (10), NUMBER 6 JUNE, 1960

ELASTIC SCATTERING OF 390 Mev π^+ MESONS FROM PROTONS

E. L. GRIGOR'EV and N. A. MITIN

Joint Institute for Nuclear Studies

Submitted to JETP editor July 9, 1959

J. Exptl. Theoret. Phys. (U.S.S.R.) **37**, 1583-1586 (December, 1959)

Nuclear emulsions were used to study the angular distribution of (390 ± 25 Mev) π^+ mesons elastically scattered from hydrogen. The differential scattering cross section is given by formula (1). The phase shifts in the Fermi solution are $\alpha_3 = -34°$, $\alpha_{33} = 151°$ and $\alpha_{31} = -16°$, assuming that only S and P states are involved in the scattering.

EXPERIMENTS on the elastic scattering of positive π mesons from protons show that up to an energy of 300 Mev S and P states account for most of the cross section. Until recently, none of the experiments allowed conclusions to be drawn about the contributions of higher states, although phase analyses were carried out taking D waves into account.[1,2] That these attempts were unsuccessful seems to indicate that the D phase shifts are small compared to those in the S and P states. Presumably, the scattering of D waves would be more important at higher energies, and this lends interest to experiments with π mesons having energies in the range 300 – 400 Mev, a range which has not yet been studied in sufficient detail.

In the work being reported upon here, we studied the angular distribution of π^+ mesons having energy 390 ± 25 Mev scattered from hydrogen in nuclear emulsions. The measurements were made with emulsions NIKFI-R, 400 μ thick. The arrangements for irradiating the emulsions have been described previously.[1] The energy of the π^+ mesons was determined by a magnetic meson spectrometer and also by measurements of the energy possessed by those recoil protons from elastic π^+-p scattering events which stopped in the emulsion. These two complementary measurements of the meson energy gave results in good agreement with each other. Beryllium filters were placed in front of the emulsions to slow down protons in the π^+ meson beam.

The plates were scanned with a microscope of 630× magnification. A good fraction of the area of the emulsion was scanned a second time at the same magnification. The usual kinematic criteria were used to identify elastic scattering events of π^+ mesons on hydrogen: angular correlation between the scattered meson and the recoil proton and coplanarity. In those cases where the recoil proton stopped in the emulsion, we made the reasonable requirement that its energy had to agree with the calculated one. The results are shown in the table.

Differential cross section for the scattering of π^+ mesons of energy 390 ± 25 Mev by protons

Interval into which the mesons are scattered $\vartheta_{\text{c.m.}}$ degrees	Number of scattering events observed	Corrected number of scattering events	Differential cross section $10^{27} \cdot d\sigma/d\Omega$ cm²/sterad
10—30	32	40	9.35 ± 1.34
30—50	51	62	7.72 ± 0.91
50—70	48	48	4.53 ± 0.65
70—90	21	21	1.78 ± 0.38
90—110	5	7	0.57 ± 0.20
110—130	4	6	0.56 ± 0.21
130—150	5	6	0.82 ± 0.30
150—170	1	2	0.52 ± 0.33
Total	167	192	

Since the counting efficiency at different angles $\vartheta_{\text{c.m.}}$ depends differently on the aximuthal angle φ, corrections had to be made as shown in column 3. The differential cross sections were normalized to a value 34 mb for the total cross section.[3] The errors quoted are statistical.

Expanding the experimental results in powers of $\cos\vartheta$, we find that the differential cross section can be satisfactorily described by the formula

$$d\sigma / d\Omega = [(1.12 \pm 0.22) + (4.27 \pm 0.84)\cos\vartheta + (4.68 \pm 1.08) \times \cos^2\vartheta] \times 10^{-27} \text{ cm}^2/\text{sterad}, \qquad (1)$$

which is the solid line in the figure. Phase analysis of the scattering gives the following phase shifts, assuming that only S and P states need be considered:

I. $\alpha_3 = -34°, \quad \alpha_{33} = 151°, \quad \alpha_{31} = -16°,$

II. $\alpha_3 = -34°, \quad \alpha_{33} = 160°, \quad \alpha_{31} = -33°,$

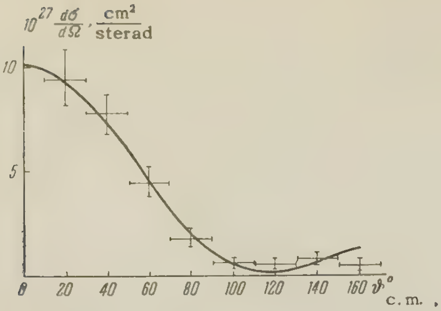

Angular distribution of 390-Mev π^+ mesons scattered from hydrogen.

One of these corresponds to the Fermi solution, the other to that of Yang. At high energies, these two solutions are quite close to each other. To decide which corresponds to the Fermi solution, of whose validity there is no doubt at the present time, it is necessary to make an analytic continuation of the phase shifts α_{33} and α_{31} from the low to the high energy region.

Approximate phase shifts α_{33} and α_{31} (for an SP analysis) over the energy interval 270 — 360 Mev[1,2] to 390 Mev show that the choice I corresponds to the Fermi solution.

The quantity

$$M = \sum_i \left[\frac{f(\alpha, \vartheta_i) - \sigma(\vartheta_i)}{\Delta\sigma(\vartheta_i)}\right]^2,$$

measures how much the cross section $f(\alpha, \vartheta_i)$ calculated from the phase shifts differs from the experimental one. Its value is 9.8, which is to be compared with the expected value $M = 5$, which is the difference between the number of experimental points and the number of free parameters. The observed value 9.8 is almost twice as big as the expected value 5. The observed value of M depends strongly on the last point, for the angles 150 — 170°, where the statistics are very poor; only one scattering event was actually observed to fall in this range of angles — the correction for counting efficiency brings this one event up to two. There can be no doubt that this point could be quite uncertain. If the interval 150 — 170° is excluded from the analysis, the observed value of M becomes 4.3, which is quite close to the expected value 4. Hence our data can be satisfactorily accounted for by S and P scattering only; i.e., from an objective point of view there is no need to introduce D waves. We noted the same situation earlier for π^+ mesons having an energy 360 Mev.[1]

It should be noted that when the angular distribution data has limited statistical accuracy, it is difficult to draw firm conclusions about the D-wave phase shifts, even though the data is fitted better when D waves are taken into account than when they are not. This is especially so when the D wave phase shifts are small; in addition, for large scattering angles ($\vartheta > 90°$), which are particularly sensitive to D waves, the statistics are poorest; the overwhelming proportion of mesons go into forward directions.

The most effective measure of how much D and higher states contribute is in the polarization of the recoil protons. Such measurements for π^+ meson energies of 307 Mev have shown[4] that the D phase shifts at 307 Mev are small, less than a few degrees. Taking both measurements of recoil proton polarization and the angular distribution of π^+ mesons scattered at 360 and 390 Mev into account, we can say that the D phase shifts are small up to ~400 Mev.

Our results on elastic π^+-p scattering at 390 Mev confirm a conclusion, drawn previously,[4] that for energies greater than 200 Mev, the phase shift α_3 as a function of meson momentum η in the center-of-mass system does not satisfy Orear's linear dependence $\alpha_3 = -6.3°\eta$,[5] although the phase shift does obey this rule at energies less than 200 Mev. The value $\alpha_3 = -34°$ at 390 Mev is considerably bigger, in absolute value, than the value $-16°$ computed from $\alpha_3 = -6.3°\eta$.

The above phase shifts can be used to calculate the real part of the forward scattering amplitude D_+, which turns out to be -1.29×10^{-13} cm. This can be compared with the value $D_+ = -1.35 \times 10^{-13}$ cm computed from the causality condition and the coupling constant $f^2 = 0.08$ for meson-nucleon scattering. The two amplitudes are in satisfactory agreement.

We should like to thank L. B. Parfenov for his help in irradiating the emulsions.

---

[1] E. L. Grigor'ev and N. A. Mitin, JETP **31**, 37 (1956); **32** 440 (1957). Soviet Phys. JETP **4**, 10 (1957); **5**, 378 (1957).

[2] A. I. Mukhin and B. M. Pontecorvo, JETP **31**, 550 (1956), Soviet Phys. JETP **4**, 373 (1957).

[3] Ignatenko, Mukhin, Ozerov, and Pontecorvo, Dokl. Akad. Nauk SSSR **103**, 209 (1955).

[4] E. L. Grigor'ev and N. A. Mitin, JETP **37**, 413 (1959); Soviet Phys. JETP **10**, 295 (1960).

[5] J. Orear, Phys. Rev. **96**, 176 (1954).

Translated by R. Krotkov
319

SOVIET PHYSICS JETP VOLUME 37(10), NUMBER 6 JUNE, 1960

ELASTIC SCATTERING OF 630 Mev NEUTRONS BY PROTONS

N. S. AMAGLOBELI and Yu. M. KAZARINOV

Joint Institute for Nuclear Research; Institute of Physics, Academy of Sciences, Georgian S.S.R.

Submitted to JETP editor July 9, 1959

J. Exptl. Theoret. Phys. (U.S.S.R.) 37, 1587-1593 (December, 1959)

The differential cross section $\sigma_{np}(\vartheta)$ for elastic n-p scattering was measured at angles $\vartheta = 11 - 180°$ in the c.m.s. for a mean neutron energy 630 Mev. Within the limits of error, the data thus obtained was identical with results of measurements carried out previously with neutrons of mean energy 580 Mev. The dependence of $\sigma_{np}(\vartheta)$ on angle in the neighborhood of $\vartheta = 180°$ was used to determine the pion-nucleon coupling constant by Chew's method.[4] A value $f^2 = 0.06 \pm 0.02$ was obtained.

ANALYSIS of data on the scattering of neutrons of energy ~ 600 Mev by protons[1-3] leads one to conclude that there is already a need for improving the accuracy of these data and continuing measurements at higher energies. For example, it would be possible to check Chew's method[4] of determining the renormalized pion-nucleon coupling constant from nucleon-nucleon scattering data only if the differential cross section is measured at more angles in the regions near 0° and 180° (c.m.s.). We meet the same needs in trying to determine from known angular distributions the maximum effective angular momentum l_{max} where, at given energy, the interaction effectively ceases. In addition, for future simultaneous analysis of n-p and p-p interactions it will be necessary to have data on elastic n-p scattering at 635 Mev, where the data of Golovin et al.[5] on polarization in n-p scattering already exist. It should be noted that it would also be very desirable to improve the existing data by employing either a more monoenergetic beam of neutrons or using a narrower part of the available spectrum of the neutron beam in the experiments.

The circumstances noted above necessitated a measurement of the differential cross section for n-p scattering for mean effective neutron energy of 630 Mev. The measurements were carried out on the synchrocyclotron of the Laboratory of Nuclear Problems of the Joint Institute for Nuclear Research.

EXPERIMENTAL ARRANGEMENT

The high-energy neutron beam used in the experiments was obtained by charge-exchange scattering of 680 Mev protons by a beryllium target. The energy distribution of neutrons in the beam was studied by Kiselev et al.[6] In the present experiments the part of the spectrum corresponding to neutrons of energies $E_n \geq 600$ Mev was used. The mean effective energy under these conditions and with the assumption of a constant total cross section for n-p scattering between 600 and 700 Mev turned out to be 630 ± 15 Mev.

Measurement of the differential cross section for the elastic scattering of neutrons by protons was carried out by two different methods for angles $\vartheta = 11 - 180°$ (c.m.s.).

1. In the angular region where the scattered neutron transfers a substantial part of its initial kinetic energy to the proton, the differential cross section was determined by detection of recoil protons. To do this, the differences in the number of charged particles from scatterers of polyethylene (CH_2) and graphite, placed alternatively in the beam, were measured for recoil angles of $\Phi = 0 - 70°$ (laboratory system). In order to obtain the total number of recoil protons for a given angle, corrections were introduced into the data so as to take into account the loss of recoil protons by nuclear absorption and multiple scattering in the filters that set the threshold of the detector, and also corrections for admixtures of charged mesons and electrons. The polyethylene and carbon scatterers were cylinders of equal stopping power for protons. The thickness of the scatterer was chosen so as to minimize the loss of protons through multiple scattering in the material of the scatterer. In the angular intervals $\Phi = 0 - 20°$ and 20° — 70°, the thicknesses of the polyethylene scatterers were 2.7 and 0.9 g/cm², respectively.

Scintillation counters connected in coincidence were used to detect the recoil protons. Their construction differed, depending on the angular interval studied. For angles $\Phi > 10°$, where the background of random coincidences did not exceed 1 or 2%, the detector was a telescope of three scintillation counters as shown in Fig. 1a. The energy threshold of the detector was determined by filters of tungsten or copper placed between the final two counters. The thicknesses of the filters for various angles were chosen so that the detector counted only those recoil protons corresponding to neutrons of energy greater than 600 Mev. The angular resolution of the detector was 2°.

In the angular interval $\Phi = 0 - 10°$, especially at 0° when the detector is in the primary neutron beam, the main sources of background are charged particles knocked out of the scintillator of the first counter, and also slow protons from the scatterers which overloaded the front counters and, in this way, increased the background of random coincidences. In order to decrease effects from the above sources of background, four scintillation counters (Fig. 1b) were used as detector in this angular interval. Here, the first counter was placed right at the scatterer, and filters determining the threshold of the detector were placed between the second, third and fourth counters. This decreased the solid angle which the last counters subtended at the scintillator of the first, and decreased the counts in the last three counters. The background from the scintillator of the first counter and the background of random coincidences then decreased substantially. The angular resolution in this case was determined by the dimensions of the scintillator of the second counter and constituted 1°.

Corrections for nuclear absorption and multiple scattering of the recoil protons in the filters were determined from the 660-Mev extracted beam of protons from the synchrocyclotron. For this, a polyethylene scatterer was placed in the proton beam and using two telescopes in coincidence (method of conjugate telescopes) elastic p-p scattering events were registered. The angle of the "defining" telescope relative to the beam axis was chosen so that the energies of the registered protons were the same as the mean energies of recoil protons in elastic n-p collisions at those angles Φ for which corrections for absorption were measured. Here the measurement of corrections reduced to a determination of the ratio of numbers of elastically scattered protons registered by the detector with and without filter.

A kinematic analysis of inelastic processes in the collisions of 630 Mev neutrons with protons showed that, because of the high threshold of the detector, corrections due to the admixture of charged π and μ mesons in the angular interval $\Phi = 0 - 25°$ were practically zero. For angles $\Phi = 30 - 70°$, determination of the proportion of mesons in the total number of charged particles registered by the detector was carried out by separating mesons from recoil protons either by velocity using a Cerenkov counter (angular interval $\Phi = 30 - 60°$) or from their ranges ($\Phi \geq 60°$).

II. For angles $\vartheta \leq 35°$, measurement of the differential cross section for elastic n-p scattering was carried out by direct determination of the number of neutrons scattered through the given angle. These experiments were carried out employing a neutron detector used earlier by the authors in studying n-p collisions at 580 Mev.[3] A cylindrical glass Dewar filled with liquid hydrogen was used as scatterer.[3]

The neutron detector consisted of five scintillation counters and a "converter" of polyethylene of thickness 5.6 g/cm^2 placed between the first two counters (Fig. 1c). Neutrons from elastic n-p collisions impinged on the converter and underwent charge-exchange scattering in it. The recoil protons coming out of the converter were detected

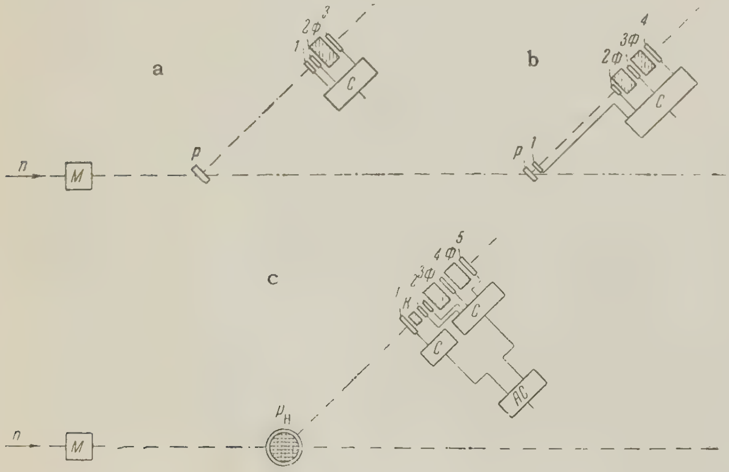

FIG. 1. Experimental arrangement: a,b – detectors for registering recoil protons, c – neutron detector. Notation: n – neutron beam, M – monitor, P – scatterer, P_H – Dewar with liquid hydrogen, 1,2,3,4,5 – scintillation counters, Φ – filter, K – converter, C – coincidence scheme, AC – anticoincidence scheme.

by the four final counters of the detector, connected in coincidence. The first counter was in anticoincidence with the remaining ones, so as to exclude charged particles from the target. The energy threshold of the detector was determined by copper filters placed between the third, fourth, and fifth counters.

In calculating the thicknesses of the filters for scattering angles $\theta = 15, 10, 5°$ (l.s.) it was assumed that the mean energy loss in charge exchange of the neutron in the light material comprised 15% of the initial energy. The angular resolution of the neutron detector was 2°.

Under working conditions, the background — i.e., the rate at which the neutron detector counted with the converter between the first and second counters, but without scatterer — was 50% of the counting rate with scatterer present for the angles $\theta = 15$ and $10°$, and was 70% for $\theta = 5°$. Investigations showed that neutrons undergoing diffraction scattering on the end of the steel collimator defining the neutron beam were the main source of background.

The angular distributions of scattered neutrons from elastic n-p collisions obtained by the two methods in the angular intervals $\vartheta = 180 - 35°$ and $35 - 11.5°$ (c.m.s.) were joined together at 35°. The absolute values of the differential cross section were determined by normalizing the angular distribution to the total cross section for elastic neutron-proton scattering σ_{np}^{el}. This cross section was found from the works of Dzhelepov et al.[7] and Prokoshkin and Tyapkin[8] by taking the difference between the total cross section $\sigma_{np} = (37 \pm 4) \times 10^{-27}$ cm^2 and the summed cross section for π meson production in collisions of 640-Mev neutrons with protons, $\sigma_{np}^{\pm,0} = (11.2 \pm 2) \times 10^{-27}$ cm^2. Here σ_{np}^{el} turned out to be $(25.8 \pm 4.5) \times 10^{-27}$ cm^2. It should be noted that the value of $\sigma_{np}^{\pm,0}$ employed was obtained by comparing cross sections for production of π mesons in p-d and p-p collisions and, possibly, differs somewhat from the true value of the cross section for inelastic n-p scattering. However, this difference does not, apparently, exceed the limits of error of the value given, since approximately the same value of σ_{np}^{el} is obtained if one uses the experiments carried out at 580 and 970 Mev.[1,9]

RESULTS OF MEASUREMENTS

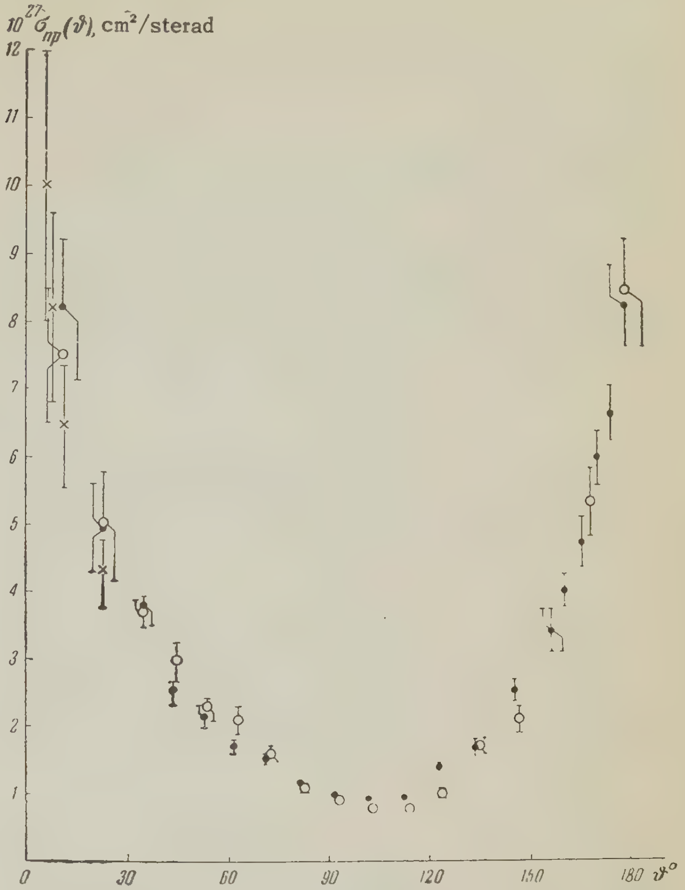

FIG. 2. Differential cross sections for elastic n-p scattering. ○ – data of references 2 and 3, $E_n = 580$ Mev; × – data of reference 4, $E_n = 590$ Mev; ● – data from the present work.

The measured dependence of cross section on scattering angle is shown in Fig. 2. The errors indicated in the figure are standard deviations. The error in measurement of the total elastic cross section (19%) from which the curve was normalized is not included in them. For comparison, $\sigma_{np}(\vartheta)$ for 580 Mev is shown on the same figure. From the figure it can be seen that the $\sigma_{np}(\vartheta)$ at 580 and 630 Mev are the same, within the limits of error.

The data obtained were used to determine the pion-nucleon coupling constant using the method proposed by Chew.[4] As is well known, Chew called attention to the fact that the real part of the amplitude for scattering of neutrons by protons, expressed in terms of the square of the momentum transfer Δ^2, has a pole in the nonphysical region at the point $\Delta^2 = -\mu^2$, where μ is the mass of the π meson. Thus, the renormalized pion-nucleon coupling constant f is determined by an extrapolation to this pole. Unfortunately, at present it is not possible to construct the n-p scattering amplitude from experimental data. Consequently, Chew proposed to use, instead of the scattering amplitude, the experimentally known dependence of the cross section for elastic n-p scattering $\sigma_{np}(\vartheta)$ in the angular region near

$\vartheta = 0°$ or $180°$, assuming that the presence of the pole at $\Delta^2 = -\mu^2$ will have a considerable effect on the character of the dependence of $\sigma_{np}(\vartheta)$ on angle near the limits of the physical region ($\vartheta = 0$ and $180°$). The procedure for determining f, which he recommended, leads in essence to an analytic continuation of the function $\sigma_{np}(\vartheta) \times (\Delta^2 + \mu^2)^2$ into the nonphysical region up to the point $\Delta^2 = -\mu^2$ and consists in practice of the following: the measured cross section $\sigma_{np}(\vartheta)$ is multiplied by the quantity

$$x^2 = \left(1 + \frac{\mu^2}{2k^2} + \cos\vartheta\right)^2 = \frac{(\Delta^2 + \mu^2)^2}{4k^4}$$

(k is the momentum of the particle in the c.m.s.), then the values of $\sigma_{np}(\vartheta)x^2$ so obtained are fitted to a power series of the form

$$A + Bx + Cx^2 + \ldots \qquad (1)$$

by the least squares method. The coefficient A obtained from this extrapolation of the function $\sigma_{np}(\vartheta)/4k^2$ to the point $\Delta^2 = -\mu^2$ is, according to meson theory, directly expressible[1] in terms of the constant f:

$$A = f^4 m^4/k^4 (m^2 + k^2),$$

where m is the nucleon mass. The interval of angles suitable for determining f^2 is given by the radius of convergence of the series Eq. (1) and is determined by the expression

$$-1 < \cos\vartheta < -1 + \mu^2/k^2.$$

In order to determine f^2 by the above method from the experimental values of $\sigma_{np}(\vartheta)x^2$, curves were constructed from several trial functions (from a linear function to a parabola of fourth order) by the least squares method. The results are given in the table where

$$M = \frac{1}{n-l}\sum_i \{[\sigma_{np}(\vartheta)x^2]_{0i} - [\sigma_{np}(\vartheta)x^2]_i\}^2 w_i$$

is a coefficient characterizing the goodness of a given solution, $(\sigma_{np}(\vartheta)x^2)_{0i}$ is the calculated value of the function at the i-th point, $(\sigma_{np}(\vartheta)x^2)_i$ is the measured value, w_i is the statistical weight of the given measurement, n is the number of points at which the scattering cross section was measured, l is the number of coefficients in the given trial function, and $x_0 = \mu^2/2k^2$ is the value of the quantity x at the edge of the physical region.

The values of f^2 so determined fluctuate between the limits 0.04 and 0.085. The mean value, found taking the goodness of fit into account, was $f^2 = 0.06 \pm 0.02$. Here the linear dependence was not included, since $A < 0$ for this function, and such a value is physically meaningless. It should be noted, however, that in order to improve the choice of the most suitable out of the functions given above, it would be very desirable to increase the number of experimental points in the interval of angles employed.

It is interesting to note that the curve for $f^2 = 0.85$, which must be analytically continued into the nonphysical region (Fig. 3, curve 2), is symmetrical about the edge of the physical region ($\Delta^2 = 0$). If one assumes that this property holds also at lower energies, and, without resorting to the procedure of analytical continuation, takes the relevant values of $\sigma_{np}(\vartheta)x^2$ from the branch of the curve in the physical region at $\Delta^2 = +\mu^2$, it turns out that the values of f^2 obtained fluctuate between 0.08 and 0.1 in a wide interval of neutron energies between 90 and 630 Mev.

The authors would like to take this opportunity

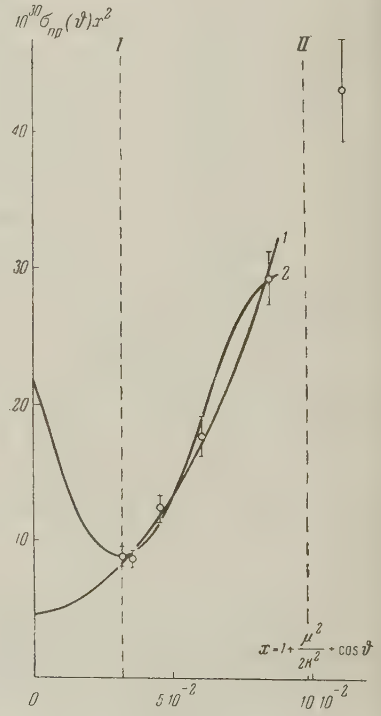

FIG. 3. Determination of the renormalized pion-nucleon coupling constant according to Chew's method. I – limit of the physical region. II – limit of applicability of the method. Curve 1 – $\sigma_{np}(\vartheta)x^2 = A + Bx^2$; 2 – $\sigma_{np}(\vartheta)x^2 = A + B(x - x_0)^2 + C(x - x_0)^4$.

Trial function	M	f^2	Trial function	M	f^2
$A + Bx$	2	—	$A + Bx + Cx^2$	3	0.07 ± 0.009
$A + Bx^2$	0.7	0.04 ± 0.006	$A + B(x - x_0)^2 + C(x - x_0)^4$	1.2	0.085 ± 0.01
$A + Bx^3$	1.8	0.05 ± 0.007			

to express their deep gratitude to Prof. V. P. Dzhelepov, their colleagues Yu. N. Simonov, V. A. Meshcheryakov and colleagues of the cryogenic laboratory V. N. Dmitrievskaya, Yu. A. Kuznetsov, A. V. Chekmenev for assistance in this work.

The authors are also very grateful to Prof. B. M. Pontecorvo, L. I. Lapidus, and A. A. Tyapkin for valuable remarks in discussion of the results.

---

[1] Yu. M. Kazarinov and Yu. N. Simonov, JETP **31**, 169 (1956), Soviet Phys. JETP **4**, 161 (1957).

[2] N. S. Amaglobeli and Yu. M. Kazarinov, JETP **33**, 53 (1958), Soviet Phys. JETP **7**, 37 (1958).

[3] Golovin, Dzhelepov, Katyshev, Konin, and Medved', JETP **36**, 735 (1959), Soviet Phys. JETP **9**, 516 (1959).

[4] G. F. Chew, Phys. Rev. **112**, 1380 (1958).

[5] Golovin, Dzhelepov, Nadezhdin, and Satarov, JETP **36**, 433 (1959), Soviet Phys. JETP **9**, 302 (1959).

[6] Kiselev, Oganesyan, Poze, and Flyagin, JETP **35**, 812 (1958), Soviet Phys. JETP **8**, 564 (1959).

[7] Dzhelepov, Satarov, and Golovin, Dokl. Akad. Nauk SSSR **104**, 717 (1959).

[8] Yu. D. Prokoshkin and A. A. Tyapkin, JETP **32**, 750 (1957), Soviet Phys. JETP **5**, 618 (1957).

[9] Batson, Culwick, Klepp, and Riddiford, Proc. Roy. Soc. **A251**, 233 (1959).

Translated by G. E. Brown
320

SOVIET PHYSICS JETP VOLUME 37(10), NUMBER 6 JUNE, 1960

ANGULAR DISTRIBUTION OF SHOWER PARTICLES IN EXPLOSION SHOWERS PRODUCED BY HIGH-ENERGY COSMIC-RAY PARTICLES

A. P. MISHAKOVA and B. A. NIKOL'SKIĬ

Submitted to JETP editor July 10, 1959

J. Exptl. Theoret. Phys. (U.S.S.R.) **37**, 1594-1603 (December, 1959)

The angular distribution of shower particles in showers with an energy of $10^{10}-10^{13}$ ev was investigated in the c.m.s. Experimental and theoretical results are presented for the variation of the number of shower particle pairs with the angle between the particles of the pair. It is concluded that a collision of the primary particle with a nucleus leads to a symmetric angular distribution of the shower particles in the c.m.s., and that there is no correlation between the angles of shower particle pairs.

1. INTRODUCTION

A large number of experiments have been devoted to the study of the angular distribution of shower particles in explosion showers produced by high-energy cosmic-ray particles. The main result of these investigations is in the conclusion concerning the anisotropy of the angular distribution of shower particles in c.m.s.: the greatest particle density corresponds to angles close to 0° and 180° in c.m.s., the velocity of the c.m.s. being determined by assuming the angular distribution of shower particles to be symmetrical with respect to the angle $\theta_{\text{c.m.s.}} = \pi/2$. This symmetry of the angular distribution should, in fact, occur in nucleon-nucleon collisions, in view of the symmetry of the system. A symmetrical distribution is, however, not evident if the collision is between a nucleon and a nucleus, which is usually the case for explosion showers observed in emulsions.

In our earlier investigation,[1] much experimental material on the angular distribution of shower particles in showers of $10^{10}-10^{13}$ ev was obtained. It was shown that, by a direct transformation from the laboratory system (l.s.) to c.m.s., asymmetrical angular distributions $F(\theta_{\text{c.m.s.}})$ with respect to the angle $\theta_{\text{c.m.s.}} = \pi/2$ are obtained, viz.: the number of shower particles at angles close to 180° in the c.m.s. is much greater than the number of particles traveling at angles close to 0°. It should be mentioned, however, that the observed effect of an asymmetrical angular distribution in the c.m.s. may follow from systematic errors that distort the function $F(\theta)$. The main reasons for a distortion of the angular distribution of shower particles are errors in the determination of the direction of the shower axis and the ensuing "smearing" of the function $F(\theta)$ in the region of small angles. The direction of the shower axis is usually defined as the direction of motion of the primary particle or as the direction of the center of gravity of all shower particles. It is clear that the direction of the center of gravity does not coincide exactly with the direction of the shower axis. It remains, however, the only method of shower-axis determination if the primary particle is a neutron. It is also impossible to determine in practice the angular distribution of shower particles with respect to the direction of the primary particle with a sufficient degree of accuracy in the case where the primary particle moves at a large angle to the surface of the emulsion. It should also be mentioned that if the shower develops in the plane of the emulsion, then the accuracy in the determination of angles between the primary and the secondary-particle paths in the c.m.s. is often insufficient to keep the smearing of the angular distribution in the region of small angles within the limits of $\Delta\theta \sim 5°$.

In the present article, as in reference 1, the angular distribution of shower particles is constructed with respect to the center of gravity, in order to use as large a number of showers as possible. The angular distribution obtained in this way is not good enough in the region $\theta \leq 10°$. The angular distributions of roughly half of all the showers were also analyzed taking the direction of the primary particle as the direction of the shower axis.

Another experimental quantity, which substantially supplements our information on the angular distribution of shower particles, is the angle between the shower particles. In the present experiment, the experimental variation of the number of

TABLE I. Principal characteristics of the showers

No. of shower	Primary particle	n_h+n_g*	n_s	$\vartheta_{1/2}$, degrees	$\gamma_c\ (\vartheta_{1/2})$	$\gamma_c\ (\bar{\lambda})$	$\bar{\gamma}_c$	γ, ev
1	n	5+8	35	1.05	54.5	25.1	39.8	$3.16\cdot10^{12}$
2	p	2+3	27	2.28	25.2	32.4	28.8	$1.65\cdot10^{12}$
3	α	1+2	35	10.7	5.3	4.73	5.01	$5.0\cdot10^{10}$
4	p	5+2	23	3.23	17.7	13.0	15.35	$4.7\cdot10^{11}$
5	p	0+0	10	1.03	55.5	48.3	51.9	$5.35\cdot10^{12}$
6	z	1+1	20	8.30	6.97	7.4	7.18	$1.03\cdot10^{11}$
7	p	3+4	15	3.28	17.9	14.1	16.0	$5.1\cdot10^{11}$
8	p	5+3	13	5.17	11.1	10.23	10.66	$2.26\cdot10^{11}$
9	p	3+2	17	5.92	9.68	13.95	11.81	$2.78\cdot10^{11}$
10	p	5+3	15	9.63	5.9	6.06	5.98	$7.12\cdot10^{10}$
11	p	12+7	24	8.26	6.97	6.41	6.69	$8.93\cdot10^{10}$
12	p	11+13	15	0.57	98.0	74.0	86.0	$1.47\cdot10^{13}$
13	p	5+3	27	2.37	24.0	16.6	20.3	$8.2\cdot10^{11}$
14	p	9+7	14	4.4	13.0	10.89	11.94	$2.82\cdot10^{11}$
15	α	12+3	42	8.95	6.35	6.41	6.38	$8.1\cdot10^{10}$
16	p	13+10	19	4.03	14.2	13.7	13.95	$3.88\cdot10^{11}$
17	p	1+2	29	7.45	7.67	6.19	6.93	$9.6\cdot10^{10}$
18	p	1+1	12	9.82	5.82	5.85	5.83	$6.77\cdot10^{10}$
19	p	2+2	27	1.42	40.5	41.6	41.05	$3.44\cdot10^{12}$
20	p	10+6	35	6.07	9.53	9.45	9.49	$1.8\cdot10^{11}$
21	α	7+3	33	2.33	24.0	20.9	22.45	$1.0\cdot10^{12}$
22	n	7+5	32	5.50	9.60	9.05	9.32	$1.74\cdot10^{11}$
23	p	1+1	20	2.03	28.2	20.4	24.3	$1.18\cdot10^{12}$
24	p	5+4	9	0.316	180	109.8	144.8	$4.18\cdot10^{13}$
25	p	6+4	20	1.92	30.0	17.6	23.8	$1.13\cdot10^{12}$
26	n	1+0	10	2.82	20.3	13.5	16.9	$5.7\cdot10^{11}$
27	p	1+2	19	5.43	10.5	8.27	9.68	$1.9\cdot10^{11}$
28	z	8+26	87	12.2	4.6	3.94	4.27	$3.64\cdot10^{10}$
29	p	14+6	23	11.5	4.9	4.77	4.83	$4.65\cdot10^{10}$
30	p	10+1	29	5.9	9.7	10.05	9.87	$1.94\cdot10^{11}$
31	p	1+2	43	1.37	42.0	38.4	40.2	$3.22\cdot10^{12}$
32	z	4+0	53	2.96	19.4	15.85	17.62	$6.2\cdot10^{11}$
33	p	7+3	37	13.0	4.37	6.25	5.31	$5.6\cdot10^{10}$
34	p	15+7	74	6.93	8.24	7.75	8.0	$1.27\cdot10^{11}$
35	p	13+6	29	4.68	12.2	9.15	10.62	$2.24\cdot10^{11}$
36	p	6+1	17	2.01	28.4	28.2	28.3	$1.6\cdot10^{12}$
37	α	6+8	31	4.78	12.0	10.1	11.05	$2.44\cdot10^{11}$
38	α	21+7	40	8.33	6.85	5.56	11.2	$2.5\cdot10^{11}$
39	z	1+2	70	5.55	10.3	10.24	10.27	$2.09\cdot10^{11}$

*$n_h + n_g$ – number of black and grey tracks in the shower.

pairs of shower particles with the angle between them has been obtained. The comparison of the results with the theoretical variation calculated assuming the absence of a systematical angular correlation between the shower particles enables us, for a given experimental accuracy, to obtain more reliable data on the angular distribution of shower particles in the region of small angles. This is due to the fact that from a change of the number of particle pairs with a given opening angle information is obtained on the angular distribution of particles irrespective of the direction of the shower axis, the measurement of which is subject to a large error. The experimental results on the angular correlation of shower particles may, in principle, indicate that a large energy fraction is concentrated in short-lived unstable particles.

In the present article, the conclusion is reached that the experimental data on the variation of the number of pairs of shower particles with the angle between the particles are in agreement with the assumption of a symmetrical angular distribution of shower particles in the c.m.s., and that a systematic correlation between the angles of shower particle pairs is absent.

2. EXPERIMENT

The results presented here are based on the analysis of 39 showers found in the scanning of emulsion chambers irradiated at 23 — 27 km altitude during 1956 — 1957. Data on the majority of these showers (32) have been published earlier.[1] The showers were found by surface scanning, and those events with a number of relativistic particles $n_s > 5$ and half-angle $\vartheta_{1/2} \leq 13°$ (the angle containing half of all shower particles) were selected.

The angular distribution of shower particles in the l.s. was measured by finding the coordinates x and y of the points of intersection of the tracks of shower particles with a plane perpendicular to the shower axis, as described in reference 1. The coordinates in the plane of the section of the shower axis were determined by the formulas

TABLE II. Experimental number of pairs of shower particles $N(\alpha)$ and the probabilities $\omega(\alpha)$ as a function of the opening angle α of the pair

E_0, ev	$\Sigma \frac{1}{2} n_s(n_s-1)$	N, ω	α				
			0—0.1	0.1—0.2	0.2—0.3	0.3—0.4	0.4—0.5
$< 5 \cdot 10^{10}$	9120	N	71	132	157	175	210
		ω	0.0078	0.0145	0.0172	0.0192	0.0230
$5 \cdot 10^{10} < E_0 < 2 \cdot 10^{11}$	6930	N	54	116	170	201	169
		ω	0.0078	0.0167	0.0245	0.0290	0.0244
$> 2 \cdot 10^{11}$	5422	N	46	76	126	121	113
		ω	0.0085	0.0140	0.0232	0.0223	0.0208
All showers	21472	N	171	324	453	497	492
		ω	0.0080	0.0151	0.0211	0.0231	0.0229
		ω_{corr}	0.0073 ± 0.00065	0.0150 ± 0.0009	0.0220 ± 0.0012	0.0240 ± 0.0012	0.0238 ± 0.001

$$x_0 = \sum x_i/n_s, \qquad y_0 = \sum y_i/n_s,$$

where n_s is the number of shower particles and x_i and y_i are their coordinates. In finding x_0 and y_0, it is reasonable to exclude particles traveling at large angles to the shower axis. The inclusion of such particles in showers with a relatively small number of particles ($n_s \approx 20$) would lead to a considerable spread of the directions of the center of gravity with respect to the direction of the shower axis. In the present experiment, therefore, only shower particles with angles $\vartheta_i < 1.4\vartheta_{1/2}$ were used in the final determination of coordinates x_0 and y_0. The distance L from the point of initiation of the shower to the section was chosen in such a way that the error in the determination of the angle of a shower particle $\delta\vartheta$ was smaller than $0.1\vartheta_{1/2}$ for a given shower ($\delta\vartheta = \Delta L$, where $\Delta \approx 1\mu$ is the experimental error in the determination of coordinates x_i and y_i). The mean value of the error in the measurement of the angle ϑ for the showers under consideration was equal to $\overline{\delta\vartheta/\vartheta_{1/2}} = 0.04$. For 16 showers it was possible to construct the angular distribution with respect to the direction of the primary particle.

The basic features of the showers studied are presented in Table I. The energy of a shower in the l.s. is $\gamma = 2\gamma_c^2 - 1$. The tabulated values of the energy of the showers in the c.m.s., $\gamma_c = 1/\sqrt{1-\beta_{\text{c.m.s.}}^2}$, were obtained assuming a symmetry of the angular distribution of the shower particles $F(\theta_{\text{c.m.s.}})$ with respect to the angle $\pi/2$, by means of the relations

$$\gamma_c(\vartheta_{1/2}) = \cot\vartheta_{1/2}, \qquad \ln\gamma_c(\bar{\lambda}) = -\overline{\ln\tan\vartheta} = \bar{\lambda}. \tag{1}$$

As mentioned above, the relative angles between shower particles were also measured. Evidently, the total number of all possible particle pairs in a shower with a number of shower particles n_s amounts to $n_s(n_s-1)/2$. However, in the present experiment, only pairs of particles with an opening angle $\eta \le 0.5\vartheta_{1/2}$ were considered. The summarized data on the distribution of these pairs as a function of the opening angle $\alpha = \eta/\vartheta_{1/2}$ are given in Table II. Table II also gives the values of the probability that a particle pair with the given opening angle α is observed, as given by

$$\omega(\alpha) = N(\alpha)/\sum \tfrac{1}{2} n_s(n_s-1), \tag{2}$$

where $N(\alpha)$ is the number of pairs with opening angle α, and $\sum n_s(n_s-1)/2$ represents the total number of pairs in all showers. The errors of the values of $\omega(\alpha)$ shown in the table represent statistical deviations.

From Table II it is clear that the experimental values of $\omega(\alpha)$ vary only little with E_0. This justifies the averaging of $\omega(\alpha)$ over all showers in the energy range under consideration. The accuracy of the determination of the angles $\alpha = \eta/\vartheta_{1/2}$ amounts to $\overline{\delta\alpha} = 0.02$ for $\alpha \le 0.2$, and was equal to $\overline{\delta\alpha} = 0.04$ for $\alpha > 0.2$. The errors $\delta\alpha$ lead to a distortion of the function $\omega(\alpha)$. Corrected values of $\omega(\alpha)$ from the data obtained for all showers are also presented in Table II as ω_{corr}. In determining ω_{corr}, the error in the determination of $\vartheta_{1/2}$ has also been taken into account. This error is due to the statistical fluctuations of the angular distribution of shower particles. The mean value of the error $\delta\vartheta_{1/2}$ has been found by the Monte-Carlo method, and is equal to $0.4\vartheta_{1/2}$, $0.3\vartheta_{1/2}$ and $0.2\vartheta_{1/2}$ for showers with $n_s = 10$, 20, and 40 respectively.

3. ANGULAR DISTRIBUTION OF SHOWER PARTICLES IN THE C.M.S.

The direction of motion of a particle in the l.s., ϑ, is related to the direction of motion in c.m.s., θ, by

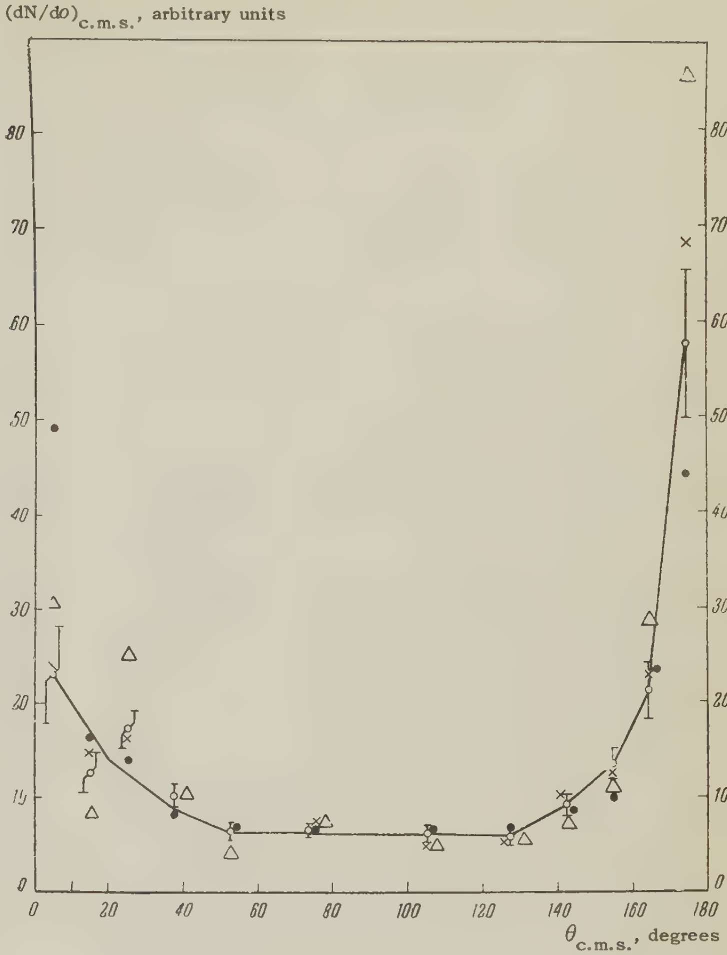

FIG. 1. Angular distribution of particles in the c.m.s. (dN/do – number of events per unit solid angle), constructed with respect to the direction of the center of gravity of shower particles: o – all showers; ×, Δ – nucleonic showers with $E_0 > 10^{11}$ ev and $E_0 > 10^{12}$ ev respectively. For a comparison, data of other authors (black points) on the measurements of F(θ) with respect to the primary particle for showers with small number of $n_h + n_g (E_0 > 10^{11}$ ev) are included.

$$\cot\vartheta = \gamma_c \frac{\cos\theta + \beta_{\text{c.m.s.}}/\beta}{\sin\theta}, \tag{3}$$

where β is the velocity of the particle in the c.m.s. For the particles under consideration, we can assume with a good degree of accuracy that $\beta_{\text{c.m.s.}} \approx \beta \approx 1$. Equation (3) then becomes

$$\cot\vartheta = \gamma_c \cot(\theta/2). \tag{3'}$$

The angular distribution F(θ) of shower particles in the c.m.s. obtained by means of this expression is shown in Fig. 1. It can be seen from Fig. 1 that the angular distribution obtained is asymmetrical for angles $\theta < 10°$ and $\theta > 170°$. As has been mentioned above, this asymmetry may follow from errors in the determination of the shower axis from the center of gravity. In fact, as has been shown in a calculation by the Monte-Carlo method, the mean value of the angle between the direction of the center of gravity and the shower axis Ω is equal to $\bar{\Omega} = 1.17\,\vartheta_{1/2}$ and $\bar{\Omega} = 0.13\,\vartheta_{1/2}$ for showers with $n_s = 20$ and $n_s = 40$ respectively. Such an error in the determination of the direction of shower axis (angle Ω) can substantially distort the angular distribution for angles $\theta < 10°$, if we assume that the real form of F(θ) for small angles is as different from the isotropic distribution as for angles close to $\theta \sim 180°$.

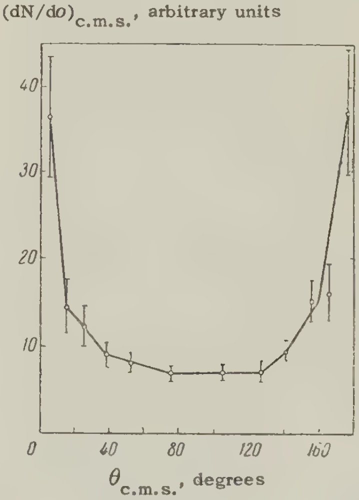

FIG. 2. Angular distribution of shower particles in c.m.s., constructed with respect to the direction of the primary particle.

Measurements of the angular distribution of shower particles with respect to the primary particle (see Fig. 2) confirm the assumption of a substantial distortion of the function F(θ) for small θ if the direction of the center of gravity of shower

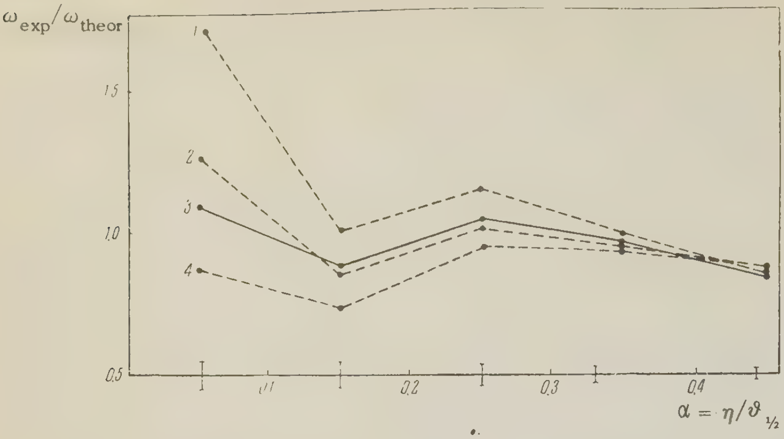

FIG. 3. Ratio of $\omega_{exp}/\omega_{theor}$ as a function of of the angle $\alpha = \eta/\vartheta_{1/2}$. Curves 1, 2, 3, and 4 correspond to different functions $F(\theta)$ shown in Fig. 4. Standard deviations, roughly similar for all curves, are shown.

particles is taken as the direction of the shower axis. As can be seen from Fig. 2, if the shower-particle angular distribution is constructed with respect to the direction of the primary particle, the number of particles in the region of small angles is greatly increased. Moreover, it can be seen that the angular distribution obtained in such a way is symmetrical within the limits of errors with respect to the angle $\theta = \pi/2$.

For comparison, Fig. 1 shows values of $F(\theta)$ obtained from the data of other authors* who measured the angular distribution of shower particles with respect to the direction of the primary particle. It should, however, be noted that these data have been obtained for showers with a small number of $n_h + n_g$, i.e., a large fraction of these showers originated in nucleon-nucleon collisions for which, from physical considerations, the distribution should be symmetrical with respect to $\theta = \pi/2$.

Additional information on the angular distribution of shower particles can be obtained from data on the number of pairs of shower particles with a given opening angle (see Table II). The probability that two shower particles will have an opening angle η is, obviously, given by the formula

$$\omega(\eta) = \int_{(A)} f(\vartheta_1)\, f(\vartheta_2)\, do_1 do_2, \qquad (4)$$

where $f(\vartheta)$ is the angular distribution of shower particles in the l.s., and the integration is over a region A, determined by the relation

$$\cos\eta = \cos\vartheta_1 \cos\vartheta_2 + \sin\vartheta_1 \sin\vartheta_2 \cos(\varphi_1 - \varphi_2).$$

It can be shown (see Appendix) that if $f(\vartheta)$ is given as a function of the relative angle $\vartheta/\vartheta_{1/2}$, then the expression for ω also depends only on the ratio $\alpha = \eta/\vartheta_{1/2}$. Thus, from a comparison of the calculated and the experimental functions $\omega(\alpha)$, one can draw conclusions about the function $f(\vartheta/\vartheta_{1/2})$. The quantity $\omega(\alpha)$ is especially sensitive to the form of the function $f(\vartheta/\vartheta_{1/2})$ for small angles $\vartheta/\vartheta_{1/2}$. The ratio $\omega_{exp}/\omega_{theor}$ is shown in Fig. 3 as a function of the angle α calculated for various functions $f(\vartheta/\vartheta_{1/2})$. The c.m.s. shower-particle angular distributions corresponding to these functions are shown in Fig. 4. These distributions are different only for small angles θ, first, because the function $F(\theta)$ is determined well enough experimentally for large angles, and second, because the function $\omega(\alpha)$ is sensitive to the shape of the angular distribution only in the region of small angles.

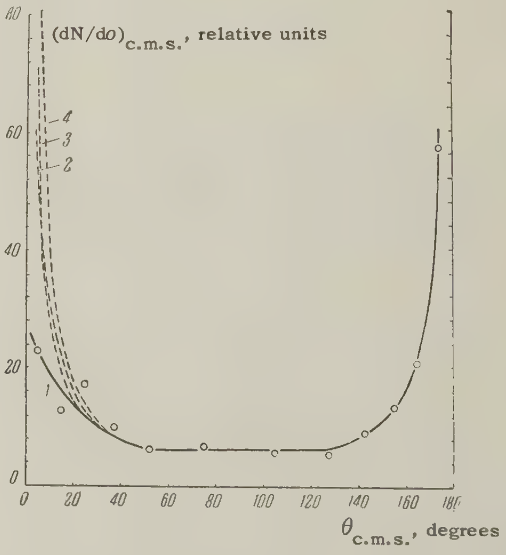

FIG. 4. Angular distribution $F(\theta)$ in c.m.s. used for calculating the theoretical values $\omega(\alpha)$ (see Fig. 3).

It can be seen from Fig. 3 that the best agreement between the calculated and the experimental values of $\omega(\alpha)$ is obtained for curves which correspond to a symmetrical c.m.s. distribution. The experimental curve of the angular distribution in the c.m.s., constructed by defining the direction of the shower axis as the center of gravity of the

---

*Data from the laboratories in Warsaw, Krakov, Budapest, Prague, and Berlin (private communications of M. Miesowicz, Petrzilka, Fenessy, Lanius, et al.).

TABLE III. Comparison of the experimental number of pairs N_{exp} with the calculated* N_{theor} for $\alpha < 0.1$

α	N_{exp}	N_{theor}	α	$N_{эксп}$	$N_{расч}$
0,00—0,01	2	1,7	0,05—0,06	13	18,8
0,01—0,02	6	5,1	0,06—0,07	28	22,2
0,02—0,03	8	8,6	0,07—0,08	15	25,6
0,03—0,04	10	12,0	0,08—0,09	28	29,1
0,04—0,05	17	15,4	0,09—0,10	44	32,5

*The calculated numbers are normalized so that $\Sigma N_{exp} = \Sigma N_{theor}$ for the range $\alpha = 0$–0.10.

shower particles, is in substantial disagreement with the value ω_{exp} in the region of small angles α. The values of ω_{theor} obtained for a symmetrical angular distribution in the c.m.s. are in good agreement with ω_{exp} also for considerably smaller opening angles α (see Table III).

The difference between ω_{exp} and ω_{theor} obtained for an asymmetrical c.m.s. angular distribution may also result from a systematical correlation between the angles of shower particle pairs. However, such an assumption is doubtful since, in that case, the correlation would not depend on the shower energy (see Table II), which is difficult to explain if one considers that the correlation is a result of the decay of short-lived particles. The assumption about the existence of a correlation also contradicts the variation of $\omega(\alpha)$ for small angles, which is characteristic for non-correlated particle pairs. Thus, from all that has been said above, one can conclude that the measurements of the angles between shower particles indicate a symmetrical c.m.s. angular distribution, but do not indicate an angular correlation of shower particle pairs. Experimental results on the measurements of the angular distribution of shower particles with respect to the primary particle direction also contradict asymmetry of $F(\theta)$ in the c.m.s.

CONCLUSION

Through an analysis of the experimental errors, the present experiment leads to the conclusion that a distortion of the angular distribution of shower particles takes place in the range of angles $\theta \lesssim 10°$. The distortion of $F(\theta)$ is the result of errors in the determination of the direction of the shower axis, which are especially large in constructing the angular distribution of shower particles with respect to the direction of their center of gravity, and amount to a quantity of the order of $\delta\vartheta_0 \sim (0.15$ to $0.20)\vartheta_{1/2}$. In the case where the direction of the primary particle is taken as a direction of the shower axis, the experimental errors $\delta\vartheta_0$ can be considerably smaller. This second method of constructing $F(\theta)$ is, however, only applicable for showers produced by charged particles, and which, in addition, are advantageously placed in the emulsion layer. The distortion of $F(\theta)$ leads to the lowering of the number of shower particles for small angles θ, which can be seen by comparing Fig. 1 and Fig. 2.

Additional information on the angular distribution of shower particles has been obtained through the study of the correlation between pairs of shower particles. It follows from the data obtained that the observed number of pairs of shower particles with a small opening angle corresponds to an angular distribution in the c.m.s. which is symmetrical with respect to the angle $\theta = \pi/2$. It should be mentioned that experimental data on the variation of the number of pairs of shower particles with the angle between them may be related to the angular distribution only in the absence of a systematic angular correlation of shower particles. The assumption about the existence of such a correlation is, however, not very probable, since the effect of an angular correlation would be independent of the shower energy, which is difficult to explain if one considers that the correlation would be a result of the decay of short-lived particles. The assumption of a correlation between shower particles is also contradicted by the experimental data on the dependence of the particle pairs on the opening angle of the pair. Thus, one can consider that the data presently available confirm an angular distribution of shower particles produced in the collision of fast particles with nuclei which is symmetrical in the c.m.s. No correlation between the angles of particle pairs is observed in the showers. The symmetry of $F(\theta)$ in nucleon-nucleus collisions, but at high energies of the incident particles, follows from the hydrodynamical theory of Landau and Belen'kiĭ.[2]

In conclusion, the authors express their deep gratitude to Prof. I. I. Gurevich, L. M. Barkov, and V. G. Vaks for helpful discussion in the course of the work, and to G. V. Ryzhova and V. B. Fedorov for their help.

APPENDIX

DETERMINATION OF THE FUNCTION $\omega(\alpha)$ ASSUMING THE ABSENCE OF ANGULAR CORRELATION OF SHOWER PARTICLES

As has been shown in Sec. 3, in the case where the angular distribution of shower particles is described by the function $f(\vartheta)$, the probability that two particles of the shower have an opening angle η is given by the relation $\omega(\eta) = \int_{(A)} f(\vartheta_1) f(\vartheta_2)\, do_1 do_2$, where the region of integration is given by the expression

$$\cos\eta = \cos\vartheta_1 \cos\vartheta_2 + \sin\vartheta_1 \sin\vartheta_2 \cos(\varphi_1 - \varphi_2).$$

We shall introduce an auxilliary function $g(\eta)$ which is defined in the following way:

$$g(\eta) = \int_0^{2\pi} d\varphi_1 \int_0^{2\pi} d\varphi_2 \int_0^{\pi} \sin\vartheta_1 f(\vartheta_1)\, d\vartheta_1 \int_0^{\pi} \sin\vartheta_2 f(\vartheta_2)\, d\vartheta_2 \cdot \delta[\cos\eta - \cos\vartheta_1 \cos\vartheta_2 - \sin\vartheta_1 \sin\vartheta_2 \cos(\varphi_1 - \varphi_2)].$$

This function is related to $\omega(\eta)$ by the obvious equation

$$\omega(\eta) = g(\eta) \sin\eta \approx g(\eta)\,\eta,$$

since, in the showers under consideration, $\eta \ll 1$.

Thus, the problem of finding the distribution $\omega(\eta)$ in the absence of a systematic correlation between shower particles is reduced to the determination of the function $g(\eta)$.

Introducing $\varphi = \varphi_1 - \varphi_2$, we can transform $g(\eta)$ to the form

$$g(\eta) = 4\pi \iint f(\vartheta_1) \sin\vartheta_1 f(\vartheta_2) \sin\vartheta_2 \frac{d\vartheta_1 d\vartheta_2}{\sin\vartheta_1 \sin\vartheta_2 \cos\varphi_0},$$

where

$$\cos\varphi_0 = \frac{\cos\eta - \cos\vartheta_1 \cos\vartheta_2}{\sin\vartheta_1 \sin\vartheta_2}, \qquad \left| \frac{\cos\eta - \cos\vartheta_1 \cos\vartheta_2}{\sin\vartheta_1 \sin\vartheta_2} \right| < 1.$$

We shall make the following substitution:

$$\vartheta_1 + \vartheta_2 = 2x, \quad \vartheta_1 - \vartheta_2 = 2y;$$

The integration region is then given by the expression

$$0 < x + y/2 < \pi, \quad 0 < x - y/2 < \pi, \qquad \left| \frac{2\cos\eta - \cos 2x - \cos y}{\cos y - \cos 2x} \right| < 1,$$

and the function $g(\eta)$ by the expression

$$g(\eta) = 4\pi \iint \frac{f(x + y/2) f(x - y/2)}{\sin\varphi_0}\, dx dy.$$

$$\left| \frac{2\cos\eta - \cos 2x - \cos y}{\cos y - \cos 2x} \right| \approx \left| \frac{2\sin^2 x + y^2/2 - \eta^2}{2\sin^2 x - y^2/2} \right| < 1.$$

Hence, it follows that $y < \eta$ and $2x > \eta$, since η is small ($\eta \ll 1$). Furthermore, we have

$$\sin^2\varphi_0 = 1 - \cos^2\varphi_0 = \frac{(4\sin^2 x - \eta^2)(\eta^2 - y^2)}{(2\sin^2 x - y^2/2)^2}.$$

Thus, $g(\eta)$ is transformed to the following form:

$$g(\eta) = 4\pi \int_{\eta/2}^{\pi} dx \int_{-\eta}^{\eta} f(x + y/2) f(x - y/2) \frac{(2\sin^2 x - y^2/2)\, dy}{\sqrt{(\eta^2 - y^2)(4\sin^2 x - \eta^2)}}.$$

Making the substitution $2x/\eta = \xi$ and $y/\eta = \kappa$, we obtain the following expression for $g(\eta)$:

$$g(\eta) = 8\pi \int_1^{\infty} d\xi \int_0^1 \Phi\left[\frac{\eta}{2}(\xi + \varkappa)\right] \Phi\left[\frac{\eta}{2}(\xi - \varkappa)\right] \frac{d\varkappa}{\sqrt{(\xi^2 - 1)(1 - \varkappa^2)}},$$

where $\Phi(x) = x f(x)$. From this expression, it is clear that, in the case where $\Phi(x)$ is given as a function of the relative angle $\vartheta/\vartheta_{1/2}$, $g(\eta)$ also is a homogeneous function of $\vartheta_{1/2}$, i.e., depends only on the ratio $\alpha = \eta/\vartheta_{1/2}$. However, for such a definition of the function $\Phi(x)$, the expression for $g(\eta)$ should be multiplied by a certain normalization factor. In fact, the determining function $g(\eta)$ of the angular distribution of shower particles $f(\vartheta)$ should be normalized to $\int f(\vartheta)\, 2\pi \sin\vartheta\, d\vartheta = 1$. Therefore, determining $\Phi(\vartheta/\vartheta_{1/2})$ from the experiment with the normalization $\int \Phi(\vartheta/\vartheta_{1/2})\, d(\vartheta/\vartheta_{1/2}) = 1$ $g(\eta)$ should be multiplied by $(\frac{1}{2}\pi\vartheta_{1/2})^2$. Hence

$$\omega(\eta)\, d\eta = g_1(\eta/\vartheta_{1/2})(\eta/\vartheta_{1/2})\, d(\eta/\vartheta_{1/2}),$$

where

$$g_1(\eta/\vartheta_{1/2}) \equiv g_1(\alpha) = \frac{2}{\pi} \int_1^{\infty} d\xi \int_0^1 \Phi\left[\frac{\alpha}{2}(\xi + \varkappa)\right] \times \Phi\left[\frac{\alpha}{2}(\xi - \varkappa)\right] \frac{d\varkappa}{\sqrt{(\xi^2 - 1)(1 - \varkappa^2)}}.$$

Thus, $\omega(\eta)\, d\eta$ is also a homogeneous function of $\vartheta_{1/2}$ and can be written as $\omega(\alpha)\, d\alpha$, where $\alpha = \eta/\vartheta_{1/2}$.

The given expression for $\omega(\alpha)$ can be represented in a simpler form by expanding the function Φ in a series of terms of a small parameter κ. However, such an expansion does not make it possible to obtain a good approximation for $\omega(\alpha)$ for an arbitrary function Φ. Therefore, in the present article, $\omega(\alpha)$ has been computed by numerical integration of the formulas given without any further simplification.

---

[1] Gurevich, Mishakova, Nikol'skiĭ, and Surkova, JETP **34**, 265 (1958), Soviet Phys. JETP **7**, 185 (1958).

[2] L. D. Landau and S. Z. Belen'kiĭ, Usp. Fiz. Nauk **56**, 309 (1955).

Translated by H. Kasha
321

SOVIET PHYSICS JETP VOLUME 37(10), NUMBER 6 JUNE, 1960

PRODUCTION OF MULTIPLY-CHARGED PARTICLES ON PHOTOGRAPHIC EMULSION NUCLEI BY 280-Mev POSITIVE PIONS

N. S. IVANOVA, V. I. OSTROUMOV, and Yu. V. PAVLOV

Radium Institute, Academy of Sciences, U.S.S.R.

Submitted to JETP editor July 21, 1959

J. Exptl. Theoret. Phys. (U.S.S.R.) **37**, 1604-1612 (December, 1959)

The production of fragments in nuclear disintegrations induced by 280-Mev π^+ mesons is studied with the aid of photographic emulsions. The angle, charge, and energy distributions of the emitted fragments are measured. An analysis of the experimental data and comparison with the results of theoretical calculations show that in the case under consideration the particles responsible for formation of the fragments are protons produced by absorption of π^+ mesons by quasi-deuteron pairs, and also recoil nucleons produced in scattering of pions by separate nucleons of the nucleus. Some suggestions are made concerning the mechanism of formation of such fragments, based on an analysis of the energy spectra of the fragments produced by particles of various energies.

INTRODUCTION

MANY hypotheses have been advanced to explain the process of production of multiply-charged particles (fragments) among the products of disintegration of complex nuclei, induced by high-energy particles. Not one of these, however, can explain fully the entire aggregate of experimental data. One hypothesis is that a substantial role is played in this process by the mesons produced in the nucleus when the incident particle is of sufficiently high energy.[1] A study of fragmentation induced by mesons is therefore of particular interest and can be quite important to the understanding of this process.

Recently certain data have been obtained on the production of multiply-charged particles induced by high-energy negative pions. Blau and Oliver[2] observed fragments in disintegrations of emulsion nuclei by 750-Mev π^- mesons, and a paper by one of the authors of the present article[3] contains preliminary data on the production of such fragments in interactions between 280-Mev π^+ mesons and emulsion nuclei. It is noted in that paper that absorption of a meson is not at all essential to the production of multiply-charged fragments, and that fragment production may be partially due also to fast nucleons produced in the scattering of a meson by individual nucleons of the nucleus.

It is the purpose of the present paper to study this process further, to investigate its principal characteristics (such as charge, energy, and angular distribution of the fragments produced by 280-Mev positive pions, and to compare the data obtained with the results of investigations of fragmentation by high-energy protons.

EXPERIMENTAL PROCEDURE

Two types of emulsions were used in the experiment: relativistic, type P-R, capable of registering charged particles with minimum ionization, and type P-9, which is less sensitive (proton sensitivity limit 35 — 40 Mev).* The first of these emulsions gives a more complete picture of the disintegration. However, it is difficult to obtain with it sufficiently large statistics of the events, since this emulsion can be exposed to only a small meson current. The principal characteristics of the fragments, such as their angular and charge distributions, the spectrum, etc., were obtained by observing stars in the P-9 emulsion, which was irradiated with a sufficiently larger (by approximately 10 — 15 times) meson current than the relativistic emulsion.

The plates were exposed in the extracted 300-Mev π^+-meson beam of the synchrocyclotron of the Joint Institute for Nuclear Research. Entering the emulsion were the 280-Mev mesons that passed through a copper absorber, which separated the protons of equal momentum from the beam.

The plates were scanned by area under a microscope and the stars with multiply-charged particles were counted. Fragments of charge $Z \geqslant 4$ were reliably identified visually. The angle of emission of each fragment was measured relative to the incident meson, and its charge and energy were determined (where possible).

---

*The P-R and P-9 emulsions were prepared in the laboratory of Professor N. A. Perfilov.

The charge was estimated by measuring the integral length of the track.[4] Calibration histograms were first prepared for each type of emulsion by using α-particle tracks and tracks of Li_3^8 and B_5^8, which are well separated, owing to decay into two α particles (hammer-like tracks). In addition, we used the tracks of the N_7^{14} ions, with which the type P-9 emulsions were specially irradiated. It follows from the resultant calibration histograms that the charge discrimination is sufficiently reliable for fragments with ranges greater than 20 μ at a fragment-track dip angle in the undeveloped emulsion not greater than 30°. The energy of the fragment whose charge was measured was estimated from the ranges and from the range vs. energy curves given by Papineau for multiply-charged particles.[5]

Disintegrations with fragments found in the relativistic emulsion were studied further to detect the entering fast pion ($E > 40$ Mev) and the emitted fast protons ($E > 50$ Mev), and the angular distributions of these particles were measured relative to the emitted fragment.

EXPERIMENTAL RESULTS

In all, 223 fragments were found in the stars produced by 280-Mev positive pions. Of these, 61 cases were observed in the P-R emulsion and 162 in the P-9 emulsion. About 60% of all observed fragments are attributed to pion interactions with heavy nuclei, and 40% to interactions with light nuclei (the separation criterion is analogous to that used in references 6 and 7). The charges of the track-producing particles were determined for 158 tracks. The charges of the remaining fragments were not determined, since their tracks either had too large a dip angle or passed outside the sensitive layer.

Charge Distribution

The charge distribution is shown in Fig. 1 separately for disintegrations of the heavy and light emulsion nuclei. For comparison, the same figure shows the results obtained with high-energy protons.[7,8] It is seen that in a case of heavy nuclei the relative yields of the fragments of different charges are almost independent of the bombarding-particle energy. There is a certain difference between our data on fragments from light nuclei and the results of the work by Lozhkin and Perfilov.[7]

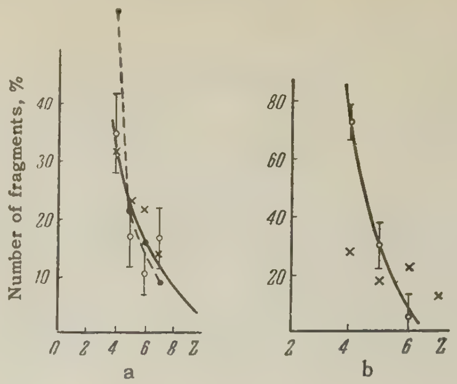

FIG. 1. Distribution of the fragments by charges: a – interaction with heavy emulsion nuclei, ○ – 280-Mev π^+ mesons (solid curve), × – 660-Mev protons,[7] ● – 6.2 Bev protons[8] (dotted curve); b – interaction with light emulsion nuclei (same symbols).

Energy Distribution

Figure 2 shows the individual energy spectra of fragments with charges 4, 5, 6, and 7, emitted from the heavy emulsion nuclei. The arrows indicate the heights of the potential barrier of the nucleus for emission of particles of the particular charge.* The same diagram shows the corresponding fragment energy distribution, obtained by Lozhkin and Perfilov[7] at bombarding-proton energies of 660

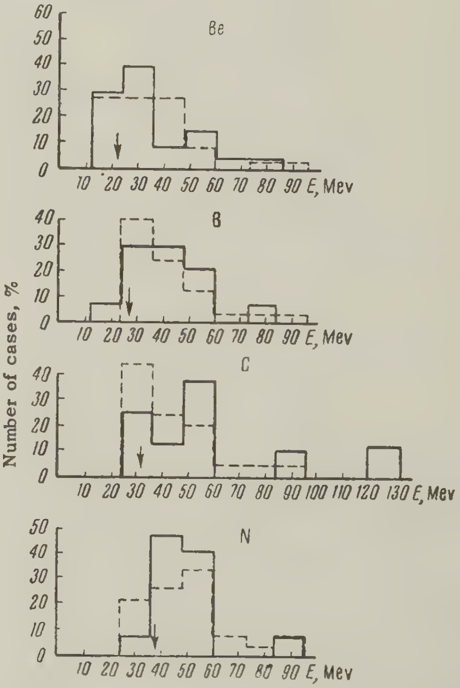

FIG. 2. Energy distributions of fragments with charges 4, 5, 6, and 7; solid line – fragments produced by 280-Mev π^+ mesons, dotted – by 660-Mev protons.[7]

---

*In the calculation of the barrier, account was taken of the fact that the nuclear cascades and α particles leave the nucleus earlier than the fragment, and the value of the charge and mass of the residual nucleus is correspondingly reduced.

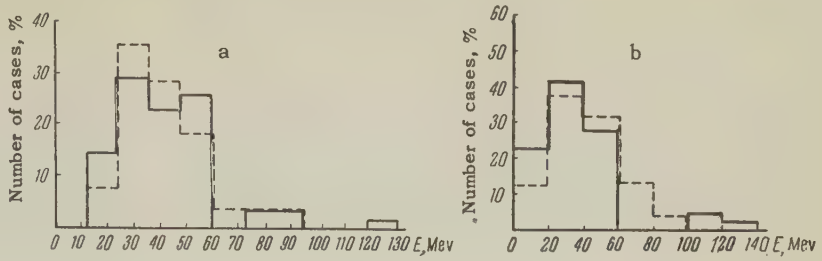

FIG. 3. Histogram of distribution of fragments by energies: a – for heavy emulsion nuclei, b – for light emulsion nuclei. Solid line – due to 280-Mev π^+ mesons, dotted – due to 660-Mev protons.[7]

Mev. All the histograms were normalized in area. It is seen from these histograms that the fragments produced by 280-Mev mesons have approximately the same energy distribution as fragments of corresponding charge produced by 660-Mev protons. Inasmuch as the statistic for each determination of charge is small, Fig. 3 shows histograms of the energy distributions of all multicharge particles with $Z \geq 4$, produced in the interaction between π^+ mesons (solid curve) or protons (dotted) and heavy (a) or light (b) emulsion nuclei.

In addition to the foregoing comparison with the data of Lozhkin and Perfilov,[7] the energy distribution of the fragments emitted from light emulsion nuclei under the influence of π^+ mesons can be compared with the data of Ostroumov and Yakovlev,[4] who measured the energy distributions of fragments emitted from carbon under the influence of 660-Mev protons. In this case, too, there is sufficiently good agreement between the energy distributions. Figure 4 shows the energy distributions calculated for one fragment nucleon, for interactions between 280-Mev mesons or 660-Mev protons[7] and the silver and bromine nuclei.

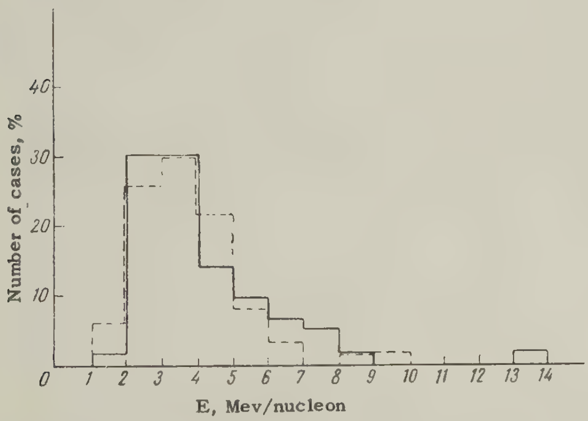

FIG. 4. Energy distribution per nucleon of multiply-charged fragment: solid line – interactions with 280-Mev π^+-mesons, dotted – with 660-Mev protons.[7]

From an examination of the foregoing data we conclude the following rather important fact: although the bombarding particles differ in nature and have different energies, the energy spectrum of the emitted fragments is the same.

Angular Distribution of Emitted Fragments

In an earlier paper by one of the authors[3] it is shown that the emitted fragments produced by 280-Mev π^+ mesons are highly directional. Figure 5 shows the angular distributions, separate for heavy and light nuclei, obtained in the present experiment for 223 fragments. As can be seen from the histogram, the directivity of the fragments emitted from light nuclei is somewhat more pronounced. In the case of heavy nuclei the number of fragments emitted in the forward hemisphere is 2.5 times that emitted in the backward one, while the corresponding factor for light nuclei is 3.4.

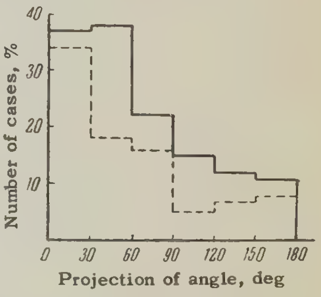

FIG. 5. Angular distribution of fragments relative to the direction of the incident π^+ mesons (projections of angles); solid line – interaction with the heavy emulsion nuclei, dotted – with the light nuclei.

Fast Protons and Pions Accompanying the Emission of Fragments

In the investigation of stars with fragments by means of relativistic emulsions, special attention was paid to the emitted scattered pions, fast protons (E > 50 Mev) and the correlation between the latter and the fragments. Figure 6 shows the distribution of angles of emission of multicharged fragments and the fast protons of the disintegration. It is seen from the curve that in most cases the

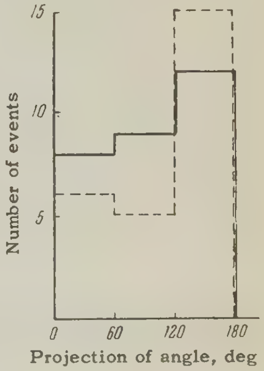

FIG. 6. Distribution of the number of events with respect to the angles of the fragment and of the fast proton (E > 50 Mev): solid line – events on heavy emulsion nuclei, dotted – on light emulsion nuclei.

fragment and the fast proton are emitted at angles 120 — 180°, and this correlation is more sharply pronounced on light nuclei.

In 18% of all the cases found in the relativistic emulsion, an emitted pion with energy > 40 Mev is observed. Consequently, as already indicated,[3] the process of fragment production is not necessarily due to the absorption of a pion.

Cross Section

The cross section for production, by 280-Mev π^+ mesons, of fragments with $Z \geq 4$ has been estimated for heavy and light emulsion nuclei from observations made in the relativistic P-R emulsion. The cross section for fragmentation was found to be $\sigma_h = (1.4 \pm 0.5)$ mb on heavy emulsion nuclei and $\sigma_l = (0.56 \pm 0.3)$ mb on light emulsion nuclei.

The value of σ_h obtained by us is somewhat higher than that given in reference 3, which, apparently, is undervalued because of insufficiently clear identification of the disintegration cases, since the fragment charges have not been determined in that investigation.

DISCUSSION OF THE RESULTS

In studying the process of fragment production induced by π^+ mesons in complex nuclei it is necessary first to attempt to ascertain whether in this case the production of the fragments is due to the mesons directly or to the fast nucleons produced in the nucleus as a result of scattering and absorption of the pions; in the latter case it is of interest to estimate the relative contribution of these two groups of nucleons to the fragmentation process. According to modern notions, fast mesons can interact with individual nucleons of a complex nucleus. Both elastic and inelastic scattering, scattering with charge exchange, and absorption of π^+ mesons, predominantly in the interaction with the (n, p) pair, are all possible. Of all the foregoing processes, the most probable are absorption and scattering, and consequently, the probability of appearance of fast nucleons in the nucleus is quite large. Let us therefore consider the possibility of production of fragments through such fast nucleons. Let us attempt to compare the angular distribution of the emitted fragments obtained in the present investigation with the distribution calculated on the basis of some model for their production.

We assume first that the emission of multiply-charged fragments in meson stars is due only to fast nucleons that arise when a meson is absorbed by a pair of nucleons (n, p):

$$\pi^+ + d \to p + p. \qquad (1)$$

In our case, when the energy of the incident meson is 280-Mev, the absorption results in two protons, each of 210-Mev energy. It is possible to calculate the angular distribution of the fragments if the distribution of the protons produced in reaction (1) is known, and also if the angular distribution of the fragments emitted in the disintegration of nuclei by protons of corresponding energies (~ 200 Mev) is known.

Data on the angular dependence of the cross section of reaction (1) at 280 Mev meson energies are taken from the paper by Neganov and Parfenov,[9] as the average results of experiments made with 316- and 260-Mev mesons. These values should be corrected for the motion of the quasi-deuteron in the nucleus. We assume its kinetic energy to be 10 Mev. We assume further that the variation of the differential cross section for fragmentation by protons produced in accordance with scheme (1) coincides with the differential cross section for the production of fragments on emulsion nuclei under the influence of a proton beam of approximately the same energy. The latter can be obtained by investigating stars with multiply-charged particles in an emulsion irradiated by a parallel beam of 200-Mev protons. A calculation of the differential cross section for the production of fragments under the influence of protons, which in turn have an angular distribution relative to a specified direction of the bombarding beam of positive pions, is carried out without segregating the disintegrations of heavy or light emulsion nuclei.

Figure 7 shows the experimental angular distribution of fragments from π^+ mesons (histogram) and the calculated angular distribution

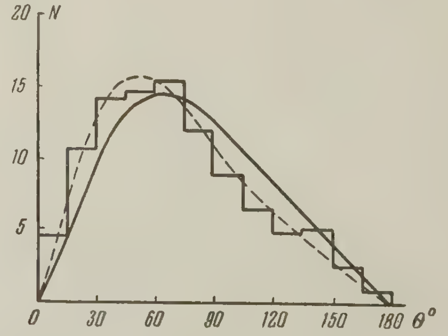

FIG. 7. Three-dimensional angular distribution of the emitted fragments produced by 280-Mev positive pions (for all emulsion nuclei). Histogram — experimental data; solid curve — calculated with allowance for only the absorption proton; dotted — calculated with allowance for absorption protons and recoil nuclei.

(solid curve). The discrepancy between the two is considerable. The choice of another value of quasi-deuteron energy in the nucleus (for example, 5 or 15 Mev) does not change this relationship significantly. We assume further that the emission of fragments is due to a considerable extent also to the recoil nuclei, produced during the scattering of mesons by large angles, in accordance with the reaction

$$\pi^+ + N \to \pi + N \qquad (2)$$

(N — nucleon). Such nucleons, with energies on the order of 100 — 200 Mev, are emitted with overwhelming probability into the forward hemisphere relative to the incident meson. Therefore the calculated curve should be shifted towards angles less than 90°. A χ^2 test has disclosed that the best agreement $[P(\chi^2) = 0.68]$ between the calculated and the experimental relationship is obtained if it is assumed that the contribution of the scattering nucleons from reaction (2) to the fragmentation process amounts to 70% of the contribution of the protons from reaction (1), i.e., ~ 60% of all the fragments are produced by absorption protons (1) and ~ 40% by recoil nucleons (2). A differential-cross section curve corrected with allowance for this effect is shown in Fig. 7 (dotted) and is in sufficiently good agreement with the experimental data.

A sufficiently convincing confirmation of the important role played in the fragmentation process both by absorption protons and recoil nuclei can be gained also from the analysis of our other experimental data. The correlation shown in Fig. 6 between the emitted fragment and a fast proton (E > 50 Mev), which indicates the preferred emission at an angle 120 — 180°, is more sharply pronounced for light nuclei. This should actually take place, if the fragments are formed to a considerable extent by one of the absorption protons, considering that the fragment travels preferably in the direction of motion of the proton that has led to its production. In addition, observation of simultaneous emission of a fragment and pion, which discloses that the emission of fragments need necessarily not be connected with the absorption of a meson, and the observed large angular directivity of the fragments emitted from the light nuclei, also indicate the significant role that recoil nuclei play in the fragment production process.

The probability of absorption of a meson by a nucleon pair (n, p) in the emulsion nuclei can be estimated from the values obtained for the relative participation of the absorption protons in the fragmentation process. The mean energy of the scattering nucleons [reaction (2)] is somewhat less than the energy of the protons produced in absorption [reaction (1)]. Unfortunately we do not know exactly the variation of the probability of fragment production with energy of incident particles in the 100 — 200 Mev region. Therefore our estimate of the probability of π^+-meson absorption is made under two extreme assumptions, when the ratio of the fragmentation cross sections for these two groups of nucleons (absorption and scattering) is taken to be 1 and 3. This yields a range of from 45 to 70% for the absorption probability. Consequently, it can be stated that the ratio $W_d/(W_d + W_p)$ for 280-Mev π^+ mesons on emulsion nuclei is 0.6 [W_d — probability of absorption by the pair in accordance with scheme (1), W_p — probability of scattering in accordance with scheme (2)]. Our estimates of the values of $W_d/(W_d + W_p)$ agree with the results of other investigations.[10,11]

On the basis of our experimental data we cannot deny emphatically the possibility of direct knock-out of fragments by mesons, but we consider the probability to be low. It is seen from Fig. 8 that there is no correlation whatever between the angle of emission of the fragment (relative to the incident meson) and its energy, and a complete lack of correspondence is observed with the curves cal-

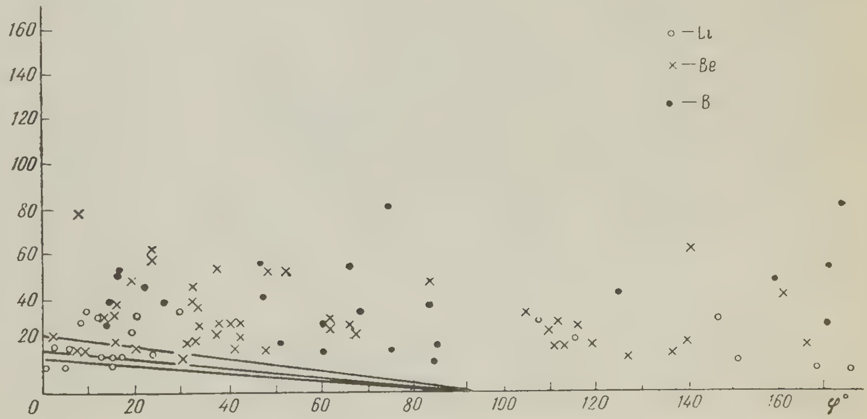

FIG. 8. Dependence of the fragment energy on the angle of emission relative to the incident π^+ mesons. Straight lines — calculated dependences for Li, Be, and B, under the assumption that they are elastically knocked out by the mesons.

culated under the assumption of elastic impact between the pion and a given substructure in the nucleus. It can be noted that if the complex of nucleons with which the meson collides has a momentum of its own, perhaps a considerable one, and if this process has been preceded by acts of meson scattering by single nucleons, the picture of the elastic (or quasi-elastic) impact may be greatly distorted and the unique correspondence between the angle of emission and the fragment energy may be disturbed. However, the form of the spectrum shown in Fig. 3 for the heavy emulsion nuclei does not agree with the assumption of the knock-out of a considerable fraction of the fragments by mesons, since the maximum energy transfer in the latter case is quite small (for example, it amounts to 37 Mev for Be$_4^9$).

An examination of Figs. 2, 3, and 4 leads to the conclusion that the energy spectrum of the fragments that arise in nuclear disintegrations is independent of the nature of the bombarding particles. From the foregoing analysis of fragmentation by pions it follows that in this case the fragment production is under the influence of neutrons with energy ~ 150 – 200 Mev.

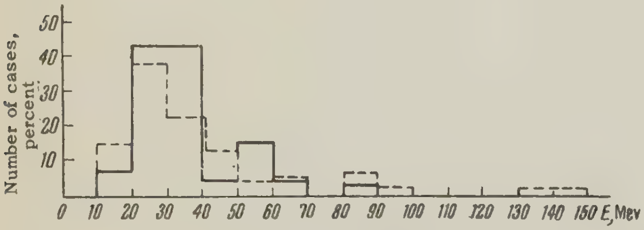

FIG. 9. Energy distribution of fragments with charge 4 (Be). Solid line – fragments produced by 280-Mev π^+ mesons, dotted – fragments produced by 6.2-Bev protons.[8]

Figure 9 shows the energy spectrum for Be atoms from heavy emulsion nuclei, produced by 280-Mev π^+ mesons and 6.2-Bev protons.[8] It is seen that in this case, too, as in the comparison with the energy spectrum due to 660-Mev protons, the distributions do not differ substantially. This signifies apparently that the fragments are not produced by direct knock out by primary nucleons, but are due to secondary nucleons which are produced in the nuclear cascade.* In all cases the most effective are nucleons of approximately the same energy (less than 150 – 200 Mev), which yields, in spite of the different energies of the primary particles, approximately the same fragment spectrum. The number of such secondary nucleons in each act of disintegration will indeed determine the cross section for fragmentation at a given energy of incident particle and increases with increasing energy of the particle. At primary nucleon energies, when the meson production in the nucleus becomes considerable, the absorption of this meson by a (n, p) nucleon pair increases the number of nucleons that contribute to fragment production, and thus influences the fragmentation cross section.

In conclusion, the authors consider it their duty to express gratitude to S. A. Tartakovskaya for help in scanning the photographic plates and to Professor N. A. Perfilov for continuous interest in this investigation.

---

*The conclusion that cascade nucleons play a substantial role in the fragmentation process was also made in references 6 and 12.

---

[1] Wolfgang, Baker, Caretto, Cummings, Friedlander, and Hudis, Phys. Rev. **103**, 394 (1956); R. Wolfgang and G. Friedlander, Phys. Rev. **96**, 190 (1954).

[2] M. Blau and A. Oliver, Phys. Rev. **102**, 489 (1956).

[3] N. S. Ivanova, JETP **34**, 1381 (1958), Soviet Phys. JETP **7**, 955 (1958).

[4] V. I. Ostroumov and Yu. P. Yakovlev, JETP **35**, 1358 (1958), Soviet Phys. JETP **8**, 949 (1959).

[5] A. Papineau, Compt. rend. **242**, 2933 (1956).

[6] Ostroumov, Perfilov, and Filov, JETP **36**, 367 (1959), Soviet Phys. JETP **9**, 254 (1959).

[7] O. V. Lozhkin and N. A. Perfilov, JETP **31**, 913 (1956), Soviet Phys. JETP **4**, 790 (1957); O. V. Lozhkin, Dissertation, Radium Inst. Acad. Sci., Leningrad, 1957.

[8] Nakagawa, Tamai, and Nomoto, Nuovo cimento **9**, 780 (1958).

[9] B. S. Neganov and L. B. Parfenov, JETP **34**, 767 (1958), Soviet Phys. JETP **7**, 528 (1958).

[10] Blinov, Lomanov, Shalamov, Shebanov, and Shchegolev, JETP **35**, 880 (1958), Soviet Phys. JETP **8**, 609 (1959).

[11] G. E. Belovitskiĭ, JETP **35**, 838 (1958), Soviet Phys. JETP **8**, 581 (1959).

[12] Lozhkin, Perfilov, Rimskiĭ-Korsakov, and Fremlin, JETP, in press.

Translated by J. G. Adashko
322

SOVIET PHYSICS JETP VOLUME 37(10), NUMBER 6 JUNE, 1960

SEARCH FOR PARTICLES WITH MASS BETWEEN 6 AND 25 ELECTRON MASSES

A. S. BELOUSOV, S. V. RUSAKOV, E. I. TAMM, and P. A. CERENKOV

Submitted to JETP editor July 29, 1959

J. Exptl. Theoret. Phys. (U.S.S.R.) **37**, 1613-1618 (December, 1959)

Experiments are described which have been undertaken in order to determine whether or not γ photons generate particles with mass (M) from 6 to 25 electron masses with production cross sections predicted by the electromagnetic theory of pair production. For this purpose fast coincidence circuits were used to measure the time of flight of particles between two scintillation counters. The particles were produced in a lead target located in the bremsstrahlung beam from a synchrotron. A comparison was made of the theoretical and experimental coincidence counting rates corresponding to detection of particles with the expected mass for the apparatus parameters. In each set of experiments the ratio of the electron counting rate to the background counting rate was also measured. The results indicate that the cross sections for the production of particles with unit charge, spin $\frac{1}{2}$, and mass ranging from 6 to 25 m_e by γ photons are not in accord with those predicted by electromagnetic theory.

1. INTRODUCTION

In electromagnetic theory there is no restriction on the existence of particles with mass between the mass of the electron and the μ meson.

In the first approximation the ratio of cross sections for the production of particle pairs with mass M and electron-positron pairs is equal to the square of the reciprocal of the mass ratio of the particles, i.e.,

$$\sigma_M / \sigma_{m_e} \approx (m_e / M)^2.$$

Hence, the observation of particles of mass M is difficult either because the cross section is small (for $M \gg m_e$) or because the mass of the proposed particles is very close to that of the electron (for $M = nm_e$, where n is a number of several times unity).

The problem of "heavy" electrons has been discussed in connection with the anomalous scattering of β-particles close to radioactive sources[1-3] and, more recently, in connection with the penetrating particles in wide atmospheric showers. There is available a large body of contradictory experimental data[4-7] which seems to favor the evidence against the existence of "heavy" electrons. In particular, the existence of particles with mass appreciably differing from the mass of the electron contradicts the picture of the development of cosmic showers obtained by cascade theory. Nevertheless, the analysis of earlier experimental cosmic-ray data does not give a definitive answer to the problem and the existence of these particles cannot be considered proved or disproved. In order to resolve this problem it is necessary to undertake special experiments with appropriate techniques. Using the possibilities offered by modern techniques it is possible to consider experiments which yield direct conclusions as to the existence of these particles within the framework of the present electromagnetic theory of pair production.

2. EXPERIMENTAL ARRANGEMENT

In order to determine the mass of a charged particle one must know any two of the following quantities: the momentum p, the energy E, or the velocity β. Usually one measures either the energy loss and the range in matter or the curvature of the trajectory in a magnetic field, or the range and the curvature. Then one of the measured parameters is used to compute the velocity β. Finally, the velocity and the second measured parameter can be used to determine the mass. It is also possible to use the scattering pattern of a particle and elastic collisions of a particle with electrons for this purpose. However, all these methods have a number of shortcomings;[8] the most important disadvantage is the inaccuracy due to the statistical nature of the quantities being measured.

In recent years coincidence circuits with very small resolution times ($\tau \approx 10^{-9}$ sec) have become available; thus it is possible to measure the velocity of relativistic particles directly, with good accuracy. We have used a method of this

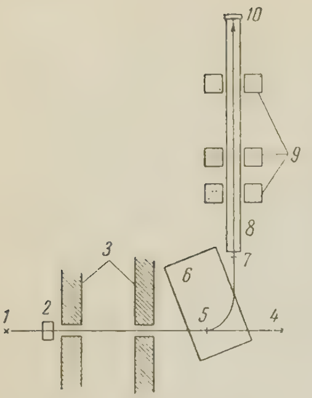

FIG. 1. Experimental geometry: 1) synchrotron target, 2) monitor chamber, 3) lead collimators, 4) direction of the bremsstrahlung beam, 5) lead target, 6) magnet, 7) scintillation counter, 8) vacuum tube, 9) focusing lenses, 10) scintillation counter.

kind to determine the velocity of a particle with a given momentum, i.e., to measure the momentum p and $\beta = v/c$.

The experimental arrangement is shown in Fig. 1. Particle pairs are produced in a lead target 5 which is bombarded by the bremsstrahlung beam from the synchrotron 4. To obtain particles with the desired momentum the target is located in a magnetic field 6. Further along the path of the particles there are two counters 7 and 10 which are separated by a distance S; if the time interval between the arrival of the particle in the first and second counters is measured (by the delay in an appropriate coincidence channel) data are obtained which can be used for determining the mass of the particle. The difference in the time of flight of a particle with mass M and an electron with the same momentum is given by the relation

$$\tau_0 = S(1 - \beta_m)/c\beta_M.$$

It is apparent that the basic disturbing factor in such an experiment is the electron background, which gives rise to spurious coincidences. Consequently, the possibilities of the experimental apparatus are limited by the ratio N_b/N_e, where N_b is the counting rate for spurious coincidences and N_e is the counting rate at the maximum of the electron delayed-coincidence curve. A particle of mass M can be identified if the following condition is satisfied:

$$N_b/N_e < N_M/N_e,$$

where N_M is the counting rate at the maximum of the delayed-coincidence curve for particles of mass M.

Using various values of M we can now estimate the ratio N_M/N_e; this quantity imposes definite requirements on the operation of the apparatus (in particular, the permissible level of the accidental coincidence background). If the system has the same detection efficiency for electrons and particles of mass M the ratio N_M/N_e is equal to the yield ratio for these particles and electrons. In the present case, as will be apparent below, this condition is satisfied; hence, we will refer to the ratio of the cross sections.

We are interested in the cross section for the production of particle pairs for which one member of the pair has a fixed momentum, say p_+. Since the apparatus detects particles over an angular range of ±5° with respect to the direction of the primary γ photons it is necessary to know the angular dependence of this cross section. It is also necessary to take account of the radiation spectrum of the synchrotron. A calculation of this kind is extremely difficult. However, at our request it was kindly undertaken by our colleagues of the theoretical division of the Institute of Physics, Academy of Sciences, V. I. Ritus and L. V. Pariĭskaya; these calculations are for particles with mass M of 1, 8, 10, 16, and 20 m_e.

The expression[9]

$$\frac{d\sigma}{d\Omega} = \int_{\varepsilon_+ + M}^{515 m_e} \frac{d\sigma}{d\varepsilon_+} \frac{dk}{k}$$

was integrated over the spectrum for a fixed value of the parameter p_+ and with respect to the angle φ on a "Ural" electronic computer. The angular dependence was approximated by a parabola; when this approximation is used the error is less than 10%.

In Fig. 2 are shown the angular distributions obtained for the quantity

$$F(\theta_+) = \int_{\varepsilon_+ + M}^{515 m_e} \frac{d\sigma}{d\varepsilon_+} \frac{dk}{k} (Z^2 \alpha r_0^2)^{-1} m_e c^2 \left(\frac{M}{m_e}\right)^3,$$

where ϵ_+ is the kinetic energy of the positively charged member of the pair, k is the momentum of the primary photon, r_0 is the classical radius of the electron, and the other quantities have the usual meanings. The area under a given curve is equal to the total cross section for the formation of particle pairs of a given mass with a fixed value of momentum.

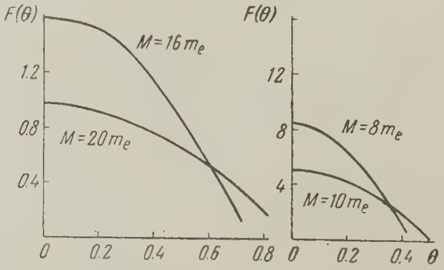

FIG. 2. The quantity $d\sigma/d\Omega$ as a function of the emission angle of the positively charged member of the pair θ_+ for particles with M = 8, 10, 16, and 20 m_e.

The true angular distribution of the detected particles differs from that which is obtained by this method because of scattering in the target. In converting from the angular distributions which have been obtained to the angular distribution in the plane we introduce a correction for scattering in the target.

The experiments were carried out with a lead target 0.5 mm thick for $M = 8$ and $12\,m_e$ and 0.25 mm thick for $M = 16$ and $20\,m_e$. The mean angle for multiple Coulomb scattering in this target is (cf. reference 10)

$$\bar{\theta}_c^2 = 16\pi N \frac{Z^2}{A} r_e^2 x \left(\frac{m_e c}{\beta p}\right)^2 \ln\left(\frac{137}{Z^{1/3} m_e c}\right),$$

where x is the thickness of the target in g/cm^2. The remaining quantities have the usual meanings. Calculations carried out with this formula give the following mean scattering angles:

M/m_e	1	1	8	10	16	20
Thickness of the Pb target, mm	0.5	0.25	0.5	0.5	0.25	0.25
$\bar{\theta}_c$, deg.	33	23.5	37.5	38	30.5	32

For electrons which leave the target the angular distribution is described by the Gaussian function

$$P(\theta)\,d\theta = \text{const}\cdot\exp\{-\theta^2/\overline{\theta_c^2}\}\,d\theta.$$

For the heavier particles, we can take in the first approximation a Gaussian distribution of the form

$$P(\theta)\,d\theta = \text{const}\cdot\exp\{-(\vartheta_m - \theta)^2/\overline{\theta^2}\}\,d\theta,$$

where $\overline{\theta^2} = \overline{\vartheta^2} + \overline{\theta_c^2}$, and ϑ_m is the angle corresponding to the maximum in the distribution and ϑ is the half width of the distribution.

The angular distributions for particles emitted from the target, corrected for scattering and normalized for the total cross section, are given in Fig. 3.

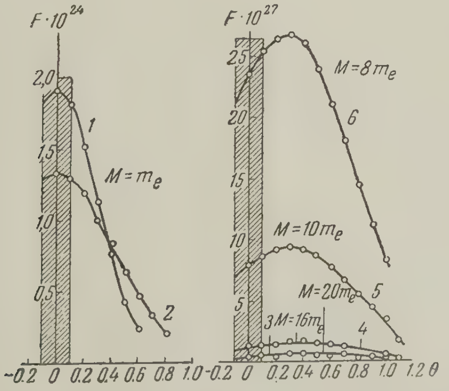

FIG. 3. Angular distributions of particles with M = 1, 8, 10, 16, and 20 m_e. The shaded areas indicate the operating angular regions ±5°. The thickness (b) for the curves: 1) b = 0.25 mm; 2) b = 0.5 mm; 3, 4) b = 0.25 mm; 5, 6) b = 0.5 mm.

From these curves we can estimate values for the ratio N_M/N_e for particles of different mass. The results of these calculations are:

M/m_e	8	10	16	20
N_M/N_e	$17\cdot10^{-3}$	$5.6\cdot10^{-3}$	$5.3\cdot10^{-4}$	$1.3\cdot10^{-4}$

We now estimate the accuracy in the measurement of the mass of the particles by this method. Differentiating the relation

$$Mc^2 = pc\sqrt{1-\beta^2}/\beta,$$

we have

$$d(Mc^2) = \frac{\sqrt{1-\beta^2}}{\beta}\,d(pc) + \frac{pc}{\beta^2\sqrt{1-\beta^2}}\,d\beta.$$

It is clear that the quantity d(pc) is determined by the width of the channel along which the particles move in the magnetic field from the target to the first counter and by the strength of this field. The value of $d\beta$ is determined by the resolution time of the apparatus. If S is the distance between the counters and t is the transit time between the counters, $dv = S\,dt/t^2$. Since $d\beta = (1/c)\,dv$, we have $d\beta = S\,dt/ct^2$ where dt is the inaccuracy in the determination of the transit time, i.e., the resolution time of the system $\tau = dt$.

For the apparatus parameters chosen by us [$pc = (10 \pm 1)$ Mev, $\tau = 3 \times 10^{-9}$ sec], $d(Mc^2)$ varies from 30% for $M = 12\,m_e$ to 19% for $M = 24\,m_e$.

3. APPARATUS

This work was carried out at the synchrotron of the Physics Institute of the Academy of Sciences, which yields a bremsstrahlung beam with a maximum energy of 265 Mev. The γ beam from the synchrotron passes through a monitoring ionization chamber 2 (cf. Fig. 1), two collimators 3, and strikes the target 5. The magnetic field is stabilized by an electronic system which stabilizes the excitation of the generator which supplies the magnet winding.

Particles with the desired momentum are extracted from the magnetic field along a channel in the lead shield and strike the first counter. The walls of the channel are made from aluminum in order to absorb electrons and low-energy photons produced as a result of showers in the lead shield. The channel is aligned by means of the current-carrying wire technique.[11]

The scintillator in the first counter is a thin (1 mm) plate of a solid solution of terphenyl-POPOP in polyvinyl toluene. The mean angle for multiple scattering of electrons in the scintillator is 4.5° and the mean energy loss is about 200 kev.

The space between the first and second counters

TABLE I

M, in units of m_e	$(N_M)_{\text{theor.}}$	$(N_M)_{\text{exp.}}$	N_b	$\frac{N_e}{N_b}$	$\frac{N_{\text{exp}}}{N_{\text{theor.}}}$
	per 10^5 monitor counts				
8 ± 2	570	3.6 ± 1.0	5.7 ± 1.5	3700	0.006
10 ± 2	82	2.6 ± 0.4	2.3 ± 0.4	7480	0.032
16 ± 4	55.5	10.5 ± 1.6	9.0 ± 1.6	5900	0.19
20 ± 5	14	2.9 ± 0.6	2.6 ± 0.6	13400	0.21

(15 m) is enclosed in a vacuum tube 8. The input window of the tube is a brass foil 100 μ thick while the output window is the plastic scintillator of the second counter, a disc 10 cm in diameter and 2 cm thick. FEU-33 photomultipliers are used in both counters; this tube has an improved resolution time. The first counter is covered with lead and aluminum and the second is placed inside the concrete wall in order to reduce the isotropic background.

In order to increase the solid angle of the apparatus particles passing through the first counter are focused in the desired direction by three magnetic lenses 9, mounted on the vacuum tube. Since the focusing effect of the electromagnetic lenses depends only on the momentum of particles, the efficiency of the system remains equal for electrons and particles of mass M.[12] Pulses from the counters are applied to a double coincidence circuit[13] with a variable delay in one of the channels.

4. MEASUREMENTS

The measurements were made alternately at a point at which an effect due to particles of the expected mass was to be expected, and at a point where only background was to be expected. In order to measure the background the delay was chosen to correspond to particles of such large mass that any effect due to these particles was smaller than the background. The efficiency of the apparatus was checked periodically by measuring the counting rate at the maximum of the electron delayed-coincidence curve.

The number of random coincidences, which determines the background of the system, is given by the expression

$$N_{\text{rand}} = 2\tau N_1 N_2 / f,$$

where τ is the resolving time of the system, N_1 and N_2 are the readings of the counters (the number of recorded counts per unit time) and f is the duty cycle of the accelerator. N_1 and N_2 can be reduced by shielding the counters with lead and by reducing the intensity of the accelerator beam; the quantity f can be increased by artificially stretching the synchrotron pulse to 3000 μsec. When these measures were taken the background was reduced to the values shown in the fifth column of Table I.

For the measurements in the region from 10 to 25 electron masses we used a germanium-diode coincidence system with a resolving time $\tau = 3 \times 10^{-9}$ sec. The resolving time sets the lower limit on the masses which can be measured. In turn, τ is limited by the duration of the pulses from the counters; hence, in searching for particles with mass $(8 \pm 2) m_e$ we used a differential coincidence scheme[14] with a resolution time $\tau = 1.5 \times 10^{-9}$ sec.

5. RESULTS

The results of the measurements for particles with mass from 6 to 25 m_e are shown in Table I. The theoretical values for different masses $(N_M)_{\text{theor}}$ obtained on the basis of the calculations and measurements of the electron counting rates normalized to the same accelerator beam intensity are shown (10^5 counts of the monitor chamber) together with the experimental values $(N_M)_{\text{exp}}$. The background in each set of measurements and the ratio of the electron counting rate to the background counting rate are also shown. These data characterize the system. The last column gives the ratio of the experimental counting rate to the calculated counting rate.

It is apparent from these results that γ photons do not produce particles with unit charge, spin ½, and masses from 6 to 25 m_e with cross sections predicted by electromagnetic theory. If the production of these particles is possible at all, the probability that the cross sections are smaller than those given in the last column of Table II is 99%.

In conclusion we wish to take this opportunity to express our gratitude to Academician V. I. Veksler for his interest in this work, to our colleagues Engineer P. N. Shareĭko, A. A. Rudenko, and A. D. Makov who helped in carrying out the experiment, and to the synchrotron operating crew, who were responsible for the operation of the accelerator.

TABLE II

M, in units of m_e	$\overset{*}{\sigma}_{\text{theor}}$	$\overset{**}{\sigma}_{\text{exp, lim}}$
8 ± 2	$3.1\cdot10^{-26}$	$2.9\cdot10^{-28}$
10 ± 2	$11.5\cdot10^{-26}$	$3.8\cdot10^{-27}$
16 ± 4	$1.45\cdot10^{-27}$	$2.9\cdot10^{-28}$
20 ± 5	$0.55\cdot10^{-27}$	$1.5\cdot10^{-28}$

*Computed from electromagnetic theory for $p_+ = 10$ Mev/c (with an accuracy of approximately 10%).

**The experimental value of the upper limit of σ for $p_+ = 10$ Mev/c.

---

[1] D. V. Skobel'tsin, Сб. Памяти С. Н. Вавилова, (Collection in Memory of S. N. Vavilov) U.S.S.R. Acad. Sci. 1952, p. 293.

[2] D. V. Skobel'tsin, Dokl. Akad. Nauk SSSR **21**, 435 (1938).

[3] W. Davies and D. F. Shaw, Proc. Phys. Soc. (London) **A64**, 1006 (1951).

[4] P. Auger and J. Dandin, Compt. rend. **226**, 169 (1948).

[5] U. Janossy and C. B. A. Melusner, Nature **63**, 181 (1949).

[6] E. W. Cowan, Science **108**, 534 (1948).

[7] D. Broadbent and U. Janossy, Proc. Roy. Soc. (London) **192**, 364 (1948).

[8] N. A. Dobrotin, Космические лучи. (Cosmic Rays) Gostekhizdat, 1954, p. 72.

[9] W. Heitler, The Quantum Theory of Radiation, Oxford, 1953, Russ. transl. IIL, M. 1956 Chap. V, §26.

[10] B. Rossi, High Energy Particles, Prentice Hall, New York, 1952, Russ. transl. Gostekhizdat 1955 p. 87.

[11] M. S. Kozodaev and A. A. Tyapkin, Приборы и техника эксперимента, (Instruments and Measurement Engg.) No. 1, 21 (1956).

[12] V. E. Cosslett, Introduction to Electron Optics, Oxford, 1946 Russ. transl. IIL, 1950.

[13] A. A. Rudenko, Приборы и техника эксперимента, (Instruments and Measurement Engg.) No. 6, 60 (1958).

[14] Yu. K. Akimov, ibid. No. 4, 98 (1957).

Translated by H. Lashinsky
323

SOVIET PHYSICS JETP VOLUME 37 (10), NUMBER 6 JUNE, 1960

QUASICLASSICAL SOLUTIONS OF THE RADIAL DIRAC EQUATIONS

N. I. ZHIRNOV

Moscow State Pedagogic Institute

Submitted to JETP editor March 16, 1959

J. Exptl. Theoret. Phys. (U.S.S.R.) **37**, 1619-1625 (December, 1959)

A new extension of the WKB method is proposed, which is applicable to the solution of the radial Dirac equations for bound states of electrons in atoms. Approximate solutions of the Dirac equations are expressed in terms of the exact solutions of the analogous equations for electrons in hydrogen-like atoms. A method for representing the approximate solutions analytically is indicated. The fine structure of the M-terms of mercury is calculated including screening of the nuclear Coulomb field.

1. INTRODUCTION

THE radial Dirac equations for a relativistic electron moving in a centrally-symmetric field U(r) can be written in the form

$$\begin{aligned} &\psi_2\Phi_1/\hbar c + d\Phi_2/dr - \varkappa\Phi_2/r = 0, \\ &\psi_1\Phi_2/\hbar c - d\Phi_1/dr - \varkappa\Phi_1/r = 0, \end{aligned} \qquad (1)$$

where

$$\psi_1 = W + mc^2 - U(r); \quad \psi_2 = W - mc^2 - U(r);$$

$$\Phi_1(r) = rg(r); \qquad \Phi_2(r) = rf(r);$$

g(r) and f(r) are the large and small components of the electron wave function; W is the relativistic energy of the electron (including its rest energy) and κ is a quantum number defined by the equations

$$\varkappa = -(l+1) \text{ for } j = l + {}^1/_2, \quad \varkappa = l \text{ for } j = l - {}^1/_2. \qquad (2)$$

A generalization of the WKB method which is applicable to the solution of equations (1) was given by Young and Uhlenbeck.[1] By analogy with the quasiclassical procedure for the radial Schrödinger problem in the one-dimensional case, they propose to look for approximate solutions of (1) in the form

$$\begin{aligned} \Phi_1(r) &= [A_0(r) + \hbar A_1(r) + \ldots]\exp[i\gamma(r)/\hbar]; \\ \Phi_2(r) &= [B_0(r) + \hbar B_1(r) + \ldots]\exp[i\gamma(r)/\hbar]. \end{aligned}$$

The Young-Uhlenbeck approximation describes the relativistic wave function of the electron quite accurately (especially at large distances from the nucleus).

However we should point out two difficulties associated with the Young-Uhlenbeck approximation. The first of these arises when we are looking for limiting states of an electron in a hydrogen-like field (i.e., states for which the principal quantum number n = |κ|). Another defect is the fact that, when we go to the limit c → ∞, the approximate solutions of (1) which are given by Young and Uhlenbeck do not go over into the quasiclassical solutions of the radial Schrödinger equation, despite the fact that there is such a limiting transition between the two sets of equations. In fact, if in Eqs. (1) we eliminate in turn the small and large components of the wave function, we get the equations:

$$\frac{d^2\Phi_1}{dr^2} - \frac{\psi_1'}{\psi_1}\frac{d\Phi_1}{dr} + \left[\frac{p^2(r)}{\hbar^2} - \frac{\varkappa(\varkappa+1)}{r^2} - \frac{\psi_1'}{\psi_1}\frac{\varkappa}{r}\right]\Phi_1 = 0, \qquad (3)$$

$$\frac{d^2\Phi_2}{dr^2} - \frac{\psi_2'}{\psi_2}\frac{d\Phi_2}{dr} + \left[\frac{p^2(r)}{\hbar^2} - \frac{\varkappa(\varkappa-1)}{r^2} + \frac{\psi_2'}{\psi_2}\frac{\varkappa}{r}\right]\Phi_2 = 0, \qquad (4)$$

where p(r) is the relativistic momentum of the electron, which is defined by

$$c^2p^2(r) = [W - U(r)]^2 - m^2c^4.$$

The nonrelativistic approximation, i.e., the radial Schrödinger equation, is then obtained by making the transiton to c → ∞ in (3). In doing this, we must set κ = l in (3) and drop Eq. (4), since the small component of the wave function vanishes in the limit.

In an attempt to overcome the intrinsic defects of the Young-Uhlenbeck approximation, Good[2] suggested that, in constructing approximate solutions of the Dirac equations, one should start from Eqs. (3) and (4), using Bessel functions of half-integral order, which are the exact solutions of the radial wave equations for a free particle. However this new methof of Good does not give good results when applied to the motion of an electron in a field of Coulomb type.

In addition, both the Young-Uhlenbeck method and Good's method lead to half-integral quantization rules in the nonrelativistic approximation. But half-integral quantization is not appropriate to the WKB method in all cases. The quantization rules for the WKB method, as was first pointed out by Petrashen',[3] depend essentially on the nature of the potential field in which the quasiclassical particle moves. In particular, for the motion of an electron in the self-consistent field of an atom, the most reasonable quantization rule is that given by Petrashen':

$$\int_{r_1}^{r_2} \sqrt{\hbar^{-2}r^2p^2(r) - l(l+1)}\,\frac{dr}{r} = \pi\left[n - \sqrt{l(l+1)}\right]. \quad (5)$$

In the present paper we propose, in constructing approximate solutions of the radial Dirac equations, to use functions which are the exact solutions of the radial Dirac problem for an electron in the Coulomb field of the nucleus. This assures agreement of the approximate and exact solutions for $U(r) \to -Ze^2/r$; for this reason we get good agreement between our solutions and the true one-electron functions near a point nucleus.

2. APPROXIMATE SOLUTIONS OF EQUATIONS (3) AND (4)

We look for approximate solutions of Eqs. (3), and in constructing the quasiclassical approximation we use the exact solutions of the analogous equations for a Coulomb field,

$$\frac{d^2G}{dS^2} - \frac{\varphi_1'}{\varphi_1}\frac{dG}{dS} + \left[\hbar^{-2}P^2(S) - \frac{\varkappa(\varkappa+1)}{S^2} - \frac{\varphi_1'}{\varphi_1}\frac{\varkappa}{S}\right]G = 0, \quad (6)$$

where

$$\varphi_1 = E + mc^2 + Ze^2/S;$$

$$c^2P^2(S) = (E + Ze^2/S)^2 - m^2c^4; \quad (6a)$$

S is the distance of the electron from the nucleus in a hydrogenlike atom (as distinguished from r, which is the analogous electron coordinate in the screened nuclear field) and G(S) is the large component of the relativistic wave function of an electron moving in the Coulomb field of a point nucleus, i.e.,

$$G(S) = A\left(\frac{1+\varepsilon^*}{N-\varkappa}\right)^{1/2}\exp\left\{-\frac{ZS}{Na_0}\right\}\left(\frac{2ZS}{Na_0}\right)^{\gamma}$$
$$\times\left\{-n'F\left(-n'+1;\ 2\gamma+1;\ \frac{2ZS}{Na_0}\right)\right.$$
$$\left.+(N-\varkappa)F\left(-n';\ 2\gamma+1;\ \frac{2ZS}{Na_0}\right)\right\}, \quad (6b)$$

where

$$N = \sqrt{n^2 - 2(n-k)(k-\gamma)}; \quad n' = n - k; \quad k = |\varkappa|;$$
$$\gamma = \sqrt{k^2 - \alpha^2Z^2}; \quad \varepsilon^* = E/mc^2 = \sqrt{1 - \alpha^2Z^2/N^2}; \quad (6c)$$

a_0 is the Bohr radius of the hydrogen atom, α is the fine structure constant, and F is the confluent hypergeometric function.

We try to find a solution of (3) of the form

$$\Phi_1(r) = T(r)\,G[S(r)]. \quad (7)$$

Substituting (7) in Eq. (3) and using Eq. (6), we find

$$\left(\frac{2T'}{T} + \frac{S''}{S'} + \frac{\varphi_1'}{\varphi_1}S' - \frac{\psi_1'}{\psi_1}\right)TS'\frac{dG}{dS} + \left\{\frac{T''}{T} - \frac{\varphi_1'}{\varphi_1}\frac{T'}{T}\right.$$
$$+\left[\hbar^{-2}p^2(r) - \frac{\varkappa(\varkappa+1)}{r^2} - \frac{\psi_1'}{\psi_1}\frac{\varkappa}{r}\right] - (S')^2$$
$$\left.\times\left[\hbar^{-2}P^2(S) - \frac{\varkappa(\varkappa+1)}{S^2} - \frac{\psi_1'}{\psi_1}\frac{\varkappa}{S}\right]\right\}TG = 0. \quad (8)$$

If we choose T in Eq. (8) to be

$$T(r) = (\psi_1/\varphi_1 S')^{1/2}, \quad (9)$$

the problem of integrating (3) is reduced to the integration of the equation

$$\frac{T''}{T} - \frac{\psi_1'}{\psi_1}\frac{T'}{T} + \left[\hbar^{-2}p^2(r) - \frac{\varkappa(\varkappa+1)}{r^2} - \frac{\psi_1'}{\psi_1}\frac{\varkappa}{r}\right]$$
$$-(S')^2\left[\hbar^{-2}P^2(S) - \varkappa(\varkappa+1)/S^2 - \frac{\varphi_1'}{\varphi_1}\frac{\varkappa}{S}\right] = 0. \quad (10)$$

Noting that $\kappa(\kappa+1)$ is of order $\hbar^{-2}$ and κ of order $\hbar^{-1}$ (in solving the radial Schrödinger problem by the WKB method, the corresponding step is the formal assignment of the order $\hbar^{-1}$ to the number $(l+\frac{1}{2})$, which is related to the replacement of $l(l+1)$ by $(l+\frac{1}{2})^2$ and the introduction of the effective momentum), keeping only terms of order $\hbar^{-2}$ and $\hbar^{-1}$ in (10) and dropping all terms which are small compared to these, we arrive at the following equation for determining the function S(r), which we shall call the screening function:

$$\hbar^{-2}p^2(r) - \frac{\varkappa(\varkappa+1)}{r^2} - \frac{\psi_1'}{\psi_1}\frac{\varkappa}{r} = (S')^2$$
$$\times\left[\hbar^{-2}P^2(S) - \frac{\varkappa(\varkappa+1)}{S^2} - \frac{\varphi_1'}{\varphi_1}\frac{\varkappa}{S}\right],$$

from which

$$\int_{r_1}^{r}\sqrt{\hbar^{-2}p^2(r) - \frac{\varkappa(\varkappa+1)}{r^2} - \frac{\psi_1'}{\psi_1}\frac{\varkappa}{r}}\,dr$$
$$= \int_{S_1}^{S}\sqrt{\hbar^{-2}P^2(S) - \frac{\varkappa(\varkappa+1)}{S^2} - \frac{\varphi_1'}{\varphi_1}\frac{\varkappa}{S}}\,dS, \quad (11)$$

where r_1 and S_1 are the first zeros of the integrands (i.e., the roots nearest to the nucleus). The introduction of the corresponding roots r_1 and S_1 in (11) assures that the screening function S(r) will be real over the whole range of r.

The integrands in (11) have either two positive roots (for bound states with $\kappa \neq -1$), or one root (for s-states and states of the continuous spectrum); in addition they have one simple pole at the points $r = 0$ and $S = 0$, respectively.

We note that, in the transition to the nonrelativistic approximation, the approximate solutions of equation (3) for the large component, which are given by formulas (6b, c), (7), (9) and (11), automatically go over into the quasiclassical solutions of the radial Schrödinger problem which were given by the author in reference 4.

Like the approximate solutions of (3), the approximate solutions of Eq. (4) for the small component can be represented in the form

$$\Phi_2(r) = Q(r)\, G_1[R(r)], \tag{12}$$

where

$$Q(r) = \left(\frac{\psi_2}{\varphi_2 R'}\right)^{1/2}; \quad \varphi_2 = E - mc^2 + Ze^2/R \tag{12a}$$

and $G_1(R)$ is the small component of the wave function of an electron moving in the Coulomb field of the nucleus, i.e.,

$$\begin{aligned} G_1(R) = &-A\left(\frac{1-\varepsilon^*}{N-\varkappa}\right)^{1/2} \exp\left\{-\frac{ZR}{Na_0}\right\}\left(\frac{2ZR}{Na_0}\right)^{\gamma} \\ &\times\left\{n'F\left(-n'+1;\, 2\gamma+1;\, \frac{2ZR}{Na_0}\right)\right. \\ &\left.+ (N-\varkappa)\, F\left(-n';\, 2\gamma+1;\, \frac{2ZR}{Na_0}\right)\right\}. \end{aligned} \tag{12b}$$

The screening function $R(r)$ for the small component is determined from the equation

$$\begin{aligned} &\int_{r_1}^{r} \sqrt{\hbar^{-2}p^2(r) - \frac{\varkappa(\varkappa-1)}{r^2} + \frac{\psi_2'}{\psi_2}\frac{\varkappa}{r}}\, dr \\ &= \int_{R_1}^{R} \sqrt{\hbar^{-2}P^2(R) - \frac{\varkappa(\varkappa-1)}{R^2} + \frac{\varphi_2'}{\varphi_2}\frac{\varkappa}{R}}\, dR, \end{aligned} \tag{13}$$

where, just as in (11), r_1 and R_1 are the zeros of the integrands which are closest to the nucleus; the integrands have either two positive roots (for bound states with $\kappa \neq 1$), or one root (for bound states with $\kappa = 1$ or for states of the continuous spectrum); in addition they have simple poles at the points $r = 0$ and $R = 0$ and a pole of order $\frac{1}{2}$ at a finite distance from the nucleus. The location of the poles of order $\frac{1}{2}$ is determined by the equations $r\psi_2(r) = 0$ and $R\varphi_2(R) = 0$, and computations show that they lie beyond the zeros of the integrands, i.e., outside the region where the electron wave function behaves quasiclassically.

3. EQUATIONS FOR THE ENERGY EIGENVALUES

The equations for making an approximate estimate of the eigenvalues of the electron energy arise in our version of the WKB method from the requirement that the screening functions determined from (11) and (13), should coincide with the screening functions determined from equations analogous to (11) and (13), but with the lower limits of integration taken to be either r_2 and S_2 (or R_2) or zero. Here r_2 and S_2 (or R_2) are the second zeros of the integrands of (11) and (13), i.e., the zeros which are further from the nucleus. As shown in references 3 and 4, this condition can be satisfied if:

a) the energy parameter W_1 which enters in $p^2(r)$ and $\psi_1(r)$ is chosen so that

$$\begin{aligned} &\int_{r_1}^{r_2} \sqrt{\hbar^{-2}p^2(r) - \frac{\varkappa(\varkappa+1)}{r^2} - \frac{\psi_1'}{\psi_1}\frac{\varkappa}{r}}\, dr \\ &= \int_{S_1}^{S_2} \sqrt{\hbar^{-2}P^2(S) - \frac{\varkappa(\varkappa+1)}{S^2} - \frac{\varphi_1'}{\varphi_1}\frac{\varkappa}{S}}\, dS \end{aligned} \tag{14a}$$

(for states with $\kappa \neq -1$) or

$$\int_0^{r_1} \sqrt{\hbar^{-2}p^2(r) + \frac{\psi_1'}{r\psi_1}}\, dr = \int_0^{S_1} \sqrt{\hbar^{-2}P^2(S) + \frac{\varphi_1'}{S\varphi_1}}\, dS \tag{14b}$$

(for s-states);

b) the energy parameter W_2 which appears in $p^2(r)$ and $\psi_2(r)$ is chosen so that

$$\begin{aligned} &\int_{r_1}^{r_2} \sqrt{\hbar^{-2}p^2(r) - \frac{\varkappa(\varkappa-1)}{r^2} + \frac{\psi_2'}{\psi_2}\frac{\varkappa}{r}}\, dr \\ &= \int_{R_1}^{R_2} \sqrt{\hbar^{-2}P^2(R) - \frac{\varkappa(\varkappa-1)}{R^2} + \frac{\varphi_2'}{\varphi_2}\frac{\varkappa}{R}}\, dR \end{aligned} \tag{15a}$$

(for states with $\kappa \neq 1$) or

$$\int_0^{r_1} \sqrt{\hbar^{-2}p^2(r) + \frac{\psi_2'}{r\psi_2}}\, dr = \int_0^{R_1} \sqrt{\hbar^{-2}P^2(R) + \frac{\varphi_2'}{R\varphi_2}}\, dR \tag{15b}$$

(for states with $\kappa = 1$).

Thus for each bound state of the electron in an atom, Eqs. (14) and (15) enable us to calculate two energy parameters W_1 and W_2, one of which (W_1) determines the large component of the wave function while the other (W_2) determines the small component. It should be noted that Eqs. (14), which determine the parameter W_1 of the large component, go over, in the limit $c \to \infty$, to the eigenvalue equations (5), which one gets for the quasiclassical solution of the radial Schrödinger problem, while Eqs. (15) have no nonrelativistic analogs. This fact compels us to choose the parameter W_1 for the eigenvalues of the electron energy. In any case this choice is an academic matter, since the difference between W_1 and W_2 is insignificant.

We have used the eigenvalue equation (14a) to compute the one-electron levels of the mercury atom for various states of the M-shell. The self-consistent field in which the radiating electron moves in a heavy atom was described using the statistical Thomas-Fermi potential, corrected at

TABLE I. One-electron levels of mercury

	Energy in Rydbergs				Fine structure of the level	
	$3P_{1/2}$	$3P_{3/2}$	$3D_{3/2}$	$3D_{5/2}$	$3P_{1/2}-3P_{3/2}$	$3D_{3/2}-3D_{5/2}$
Values computed from Eq. (14a)	249.4	217.2	184.9	178.1	32.2	6.8
Experimental values	241.7	209.8	176.0	169.3	31.9	6.7
Values computed from the fine structure formula	769.1	730.4	730.4	717.8	38.7	12.6

small and large distances from the nucleus,

$$U(r)=\begin{cases}-Ze^2(1-Ar)/r & \text{for } r\leqslant r_0=a_0/Z\\ -e^2/r-(Z-1)e^2\varphi_0(x)/r; & r_0\leqslant r<\infty\\ -e^2/r & \text{for } r\to\infty,\end{cases}\qquad(16)$$

where

$$x=r/\mu,\qquad \mu=0.8853\,a_0/(Z-1)^{1/3},$$

$$A=(Z-1)\,[1-\varphi_0(x_0)]/Zr_0;$$

and $\varphi_0(x)$ is the universal function which appears in the statistical theory of the atom (cf. reference 5).

The results of our computations and their comparison with the experimental data[6] and the results computed from the Sommerfeld-Dirac formula for the fine structure are given in Table I.

4. ADDITIONAL APPROXIMATION

The approximate radial functions for a relativistic electron which are given by our proposed method are continuous over the whole region of the field, which makes them suitable for estimating matrix elements for various processes of interaction of the matter with the radiation field. However, as Eqs. (11) and (13) show, the screening functions $S(r)$ and $R(r)$ cannot be represented exactly in analytic form, which makes it impossible to represent the approximate wave functions analytically. Computations show that the approximate analytic representation of the screening function which we found[3] for the solution of the radial Schrödinger problem can also be used for approximating the screening functions $S(r)$ and $R(r)$ of the relativistic one-electron wave functions.

The screening functions for both the large and small components can be represented approximately by analytic functions of the form

$$a\ln(1+br)+cr,\qquad(17)$$

where

$$c=[(1-\varepsilon^2)/(1-\varepsilon^{*2})]^{1/2};\ \varepsilon=W/mc^2,\qquad(17a)$$

while the constants a and b should be determined so that

$$a\ln(1+br_1)+cr_1=S_1,\qquad(17b)$$

$$a\ln(1+br_2)+cr_2=S_2.\qquad(17c)$$

In the case of s-states [for the screening function $S(r)$ of the large component] and states with $\kappa=1$ [for the screening function $R(r)$ of the small component] the value of S_2 (or R_2) should be computed from Eq. (11) or (13) for any point r_2 (preferably as close as possible to the nucleus, but satisfying $r_2>a_0/Z$). Condition (17a) is a consequence of Eqs. (11) and (13), which determine the screening functions.

For an electron in the mercury atom, in the $3P_{3/2}$ state, the screening function $S(r)$ for the large component, approximated by (17), has the form

$$S(r)=0.1224\ln(1+3.1928\,r/a_0)+0.5468\,r/a_0.\qquad(18)$$

In Table II the approximate screening function (18) is compared with the exact function $S(r)$ computed for this state from (11).

As the comparison shows, the approximation of the screening function by functions of the form (17) does not cause any significant distortion of the wave functions, since the approximate screening function differs (and then only insignificantly) from the exact function only at large distances, where the wave functions have practically gone to zero.

5. CONCLUSION

The approximate one-electron functions found by our proposed method are continuous over the whole region of the field, so that there is no necessity for developing special connection formulas, as for example one does in the Young-Uhlenbeck method. In our proposed approximation, there is also no difficulty in investigating limiting states; when we make the transition to the nonrelativistic approximation, the equations for the eigenvalues coincide with the Petrashen' quantization condition. A defect of the new approximation (which is shared by the Young-Uhlenbeck and Good approximations) is that the approximation introduces an unknown error

TABLE II. Screening function S(r) for the $3P_{3/2}$ state of Hg

$x = r/\mu$	r/a_0	Approximate function from (17)	Exact function computed from (11)	Relative error	$x = r/\mu$	r/a_0	Approximate function from (17)	Exact function computed from (11)	Relative error
0.03	0.0062	0.0056	0.0056	0.00	2.00	0.4126	0.3284	0.3294	0.30
0.10	0.0206	0.0191	0.0190	0.52	3.00	0.6190	0.4718	0.4732	0.30
0.20	0.0413	0.0377	0.0376	0.26	4.00	0.8253	0.6091	0.6109	0.30
0.40	0.0825	0.0737	0.0734	0.41	5.00	1.0316	0.7423	0.7445	0.30
0.60	0.1238	0.1084	0.1080	0.37	6.00	1.2379	0.8725	0.8752	0.31
0.80	0.1651	0.1420	0.1417	0.21	7.00	1.4443	1.0006	1.0036	0.30
1.00	0.2063	0.1747	0.1746	0.06	8.00	1.6506	1.1270	1.1304	0.30
1.60	0.3301	0.2685	0.2689	0.15					

into the wave function. Still we may state that the error introduced into the wave function by our approximation is considerably less than that introduced by the Young-Uhlenbeck and Good approximations.

---

[1] L. A. Young and G. E. Uhlenbeck, Phys. Rev. **36**, 1154 (1930).

[2] R. H. Good, Phys. Rev. **90**, 131 (1953).

[3] M. I. Petrashen', Dokl. Akad. Nauk SSSR **50**, 147 (1945); Уч. зап. ЛГУ, серия физ., (Sci. Papers, Leningrad State Univ., Physics series) **7**, 59 (1949).

[4] N. I. Zhirnov, JETP **32**, 1252 (1957), Soviet Phys. JETP **5**, 1021 (1957); Оптика и спектроскопия, (Optics and Spectroscopy) **4**, 125 (1958).

[5] P. Gombas, Die Statistische Theorie des Atoms und Ihre Anwendungen, Vienna, Springer, 1949.

[6] É. Vainshteĭn and M. Kakhana, Справочные таблицы по рентгеновской спектроскопии, (Reference Tables on X-ray Spectroscopy), Press of the Academy of Sciences, U.S.S.R., 1953.

Translated by M. Hamermesh

SOVIET PHYSICS JETP VOLUME 37 (10), NUMBER 6 JUNE, 1960

CONTRIBUTION TO THE THEORY OF RELATIVISTICALLY INVARIANT EQUATIONS

L. A. SHELEPIN

P. N. Lebedev Physics Institute, Academy of Sciences, U.S.S.R.

Submitted to JETP editor April 30, 1959

J. Exptl. Theoret. Phys. (U.S.S.R.) **37**, 1626-1638 (December, 1959)

A new method is proposed for investigating the group properties of the relativistically invariant equations $\alpha_\sigma \partial_\sigma \psi + \kappa\psi = 0$. The basis of the method is the study of the algebra of the α-matrices, the so-called U (α)-algebra. The commutation relations between the matrices, which completely determine the U (α)-algebra, can be directly deduced by the method. The structure of the U (α)-algebra and the associated infinitesimal group ring is studied in detail. The conditions for irreducibility are examined. Examples of commutation relations are given, in particular those which are satisfied by the Ginzburg and Pauli-Fierz equations. The proposed method substantially simplifies the calculations for particles of higher spin.

1. INTRODUCTION

WE investigate the relativistically invariant equations*

$$\alpha_\sigma \partial_\sigma \psi + \varkappa\psi = 0, \tag{1.1}$$

where the wave function ψ transforms according to a finite-dimensional representation S of the Lorentz group in the space R_1.

A general investigation of the relativistically invariant equations (1.1) is of value primarily from the point of view of finding the possibilities of the theory, the study of its symmetry properties, and the restriction of the possible variants of the theory. A clear understanding of the general properties of linear equations may also prove important for the construction of a nonlinear theory. It should also be noted that our investigations may also have an application to the phenomenological study of the interaction of various particles with nuclei having large spin values.

In order for (1.1) to be invariant under the Lorentz transformation

$$x_i' = l_{i\sigma} x_\sigma$$

the condition

$$l_{i\sigma}\alpha_\sigma = S\alpha_i S^{-1} \tag{1.2}$$

must be satisfied.

Condition (1.2) is satisfied if the infinitesimal matrices I_{ik}, defined by the equation

$$\psi' = \psi + \tfrac{1}{2}\varepsilon_{\rho\sigma} I_{\sigma\rho}\psi, \tag{1.3}$$

and the matrices α satisfy the relations

$$[I_{ik},\ I_{jl}] = -\delta_{ij}I_{kl} + \delta_{il}I_{kj} + \delta_{kj}I_{il} - \delta_{kl}I_{ij}, \tag{1.4}$$

$$[\alpha_i,\ I_{jk}] = \delta_{ij}\alpha_k - \delta_{ik}\alpha_j. \tag{1.5}$$

A consistent method for finding equations (1.1) which satisfy definite physical requirements was first developed in a paper of Gel'fand and Yaglom.[1] In their treatment they found the explicit form of the matrix α_0.

Another general method was considered by the author.[2] This investigation was carried out by using the direct product of generalized Dirac algebras. The matrices α_k were expressed in terms of known matrices, in particular the Dirac matrices. We might refer to this method as the parametric method.

There is still a third procedure. It consists in investigating the U (α)-algebra, i.e., the algebra of the α-matrices, consisting of quantities

$$G = c^\sigma\alpha_\sigma + c^{\rho\sigma}\alpha_\rho\alpha_\sigma + c^{\varkappa\rho\sigma}\alpha_\varkappa\alpha_\rho\alpha_\sigma + \ldots, \tag{1.6}$$

where the $c^{\cdots}$ are complex coefficients.

It is clear that studying relativistically invariant equations in the form of a U (α)-algebra has considerable advantages over the other methods. We do not have to consider the problem of equivalent transformations; it is much simpler to find irreducible equations and to find equations with particular physical properties (such as definiteness of charge or energy, definite spin or mass states); it becomes easier to compute various physical processes for particles with large spins, etc.

Earlier, Harish-Chandra[3] showed that the α_k must satisfy the commutation relations

---

*A summation over Greek indices is assumed throughout the paper. Both Greek and Latin indices take on the values 0, 1, 2, 3.

$$C_{k_1 k_2 \ldots k_n}(\alpha) = 0, \tag{1.7}$$

which completely determine the $U(\alpha)$-algebra. LeCouteur[4] found the transformation properties of quantities of the type $\bar{\psi}\eta G\psi$ (where η is the metric matrix), and pointed out some of the features of the $U(\alpha)$-algebra. However neither of these authors gave a procedure for finding the commutation relations. To find the commutation relations by using the explicit form of the matrices is an extremely difficult problem even for the simplest equations with maximum spin $^3/_2$, and is practically impossible for higher spins. In the present paper we examine the structure of the $U(\alpha)$-algebra and give a method for finding the commutation relations between the matrices α_k for any finite-dimensional ψ-function.

In Sec. 2 we consider the general scheme of the method and investigate the structure of the $U(\alpha)$-algebra. In Sec. 3 we analyze the structure of the infinitesimal group ring and give a method for investigating the irreducibility of the algebra. And finally, in the last section, the investigation is carried out using a convenient canonical representation. Examples of commutation relations are given, and the advantage of computing in the $U(\alpha)$-representation is demonstrated.

We plan in the future to formulate the physical requirements on the equations in algebraic form, and to enumerate the algebras of all irreducible equations through spin 2.

2. ESSENCE OF THE METHOD

We consider the $U(\alpha)$-algebra, whose elements are given in general by (1.6). Let $u_p(\alpha)$ be a linearly independent basis of the $U(\alpha)$-algebra. The basis $u_p(\alpha)$ transforms according to some representation of the Lorentz group:[3]

$$u_p(l\alpha) = \sum_q L_p^q u_q(\alpha). \tag{2.1}$$

Then, according to (1.2) and (1.6), the representations L and S are related by the equation

$$\sum_q L_p^q u_q(\alpha) = S(l)\, u_p(\alpha)\, S(l^{-1}). \tag{2.2}$$

This means that the operators $L(l)$ in a space R_2 form a representation of the Lorentz group which is equivalent to the direct product of the representation S and the adjoint representation $\tilde{S}$ (cf. references 4 and 5):

$$L = S \times \tilde{S} \tag{2.3}$$

The dimensionality of the space R_2 is the square of the dimensionality of the space R_1.

Thus all quantities of type (1.6) transform according to some representation of the Lorentz group. So, for example, the matrices of the Dirac algebra, for which S is the representation $D(0\,\frac{1}{2}) + D(\frac{1}{2}\,0)$, transform according to the representation

$$[D(0\,{}^1/_2) + D({}^1/_2\,0)] \times [D(0\,{}^1/_2) + D({}^1/_2\,0)] = [D(01) + D(10)] + 2D({}^1/_2\,{}^1/_2) + 2D(00). \tag{2.4}$$

In fact, of the 16 matrices of the Dirac algebra, $\gamma_i\gamma_k - \gamma_k\gamma_i$ transform according to the representation $D(1\,0) + D(0\,1)$; γ_i and $\gamma_i\gamma_5$ transform according to $D(\frac{1}{2}\,\frac{1}{2})$; the unit matrix E and γ_5 transform according to $D(0\,0)$. We also note that for essentially spinor representations S, for example $D(\frac{1}{2}\,\frac{1}{2}) + D(0\,1)$, because of (2.3), the matrices of the $U(\alpha)$-algebra transform according to a tensor representation

$$\begin{aligned}[D({}^1/_2\,{}^1/_2) + D(01)] \times [D({}^1/_2\,{}^1/_2) + D(10)] &= [D({}^3/_2\,{}^1/_2) + D({}^1/_2\,{}^3/_2)] + 2D(11)\\ &\quad + [D(10) + D(01)] + 2D({}^1/_2\,{}^1/_2) + D(00).\end{aligned} \tag{2.5}$$

Since from now on we shall consider only tensor representations, we introduce the following notation for $m \neq n$:

$$D(mn) + D(nm) = D(mnnm). \tag{2.6}$$

It is important to mention that, from equations of the type of (2.4) and (2.5), we can already state how many vectors, scalars, etc are contained in the $U(\alpha)$-algebra. We have been using the proper Lorentz group. An analogous argument could also be given for the full group and we could thus determine the number of pseudoscalars, scalars, pseudovectors, etc.

Relation (2.3) enables us to determine some of the properties of the $U(\alpha)$-algebra. To find these properties we must examine the structure of the algebra in somewhat more detail. The matrix α_i transforms according to the representation $D(\frac{1}{2}\,\frac{1}{2})$. The product of two matrices $\alpha_i\alpha_k$ transforms according to the representation $D(\frac{1}{2}\,\frac{1}{2}) \times D(\frac{1}{2}\,\frac{1}{2})$. This expression can be resolved into irreducible representations:

$$D({}^1/_2\,{}^1/_2) \times D({}^1/_2\,{}^1/_2) = D(11) + D(1001) + D(00). \tag{2.7}$$

From the products of three matrices $\alpha_i\alpha_k\alpha_l$ we can construct quantities (symmetrizers) which transform according to the irreducible representations into which we can resolve the product $D(\frac{1}{2}\,\frac{1}{2}) \times D(\frac{1}{2}\,\frac{1}{2}) \times D(\frac{1}{2}\,\frac{1}{2}) = [D(\frac{1}{2}\,\frac{1}{2})]^3$:

$$[D({}^1/_2\,{}^1/_2)]^3 = D({}^3/_2\,{}^3/_2) + 2D({}^3/_2\,{}^1/_2\,{}^1/_2\,{}^3/_2) + 4D({}^1/_2\,{}^1/_2). \tag{2.8}$$

Similarly,

$$D\,({}^1/_2\,{}^1/_2)]^4 = D\,(22) + 3D\,(2112) + 2D\,(2002) + 9D\,(11) + 6D\,(1001) + 4D\,(00), \qquad (2.9)$$

$$[D\,({}^1/_2\,{}^1/_2)]^5 = D\,({}^5/_2\,{}^5/_2) + 4D\,({}^5/_2\,{}^3/_2\,{}^3/_2\,{}^5/_2) + 5D\,({}^5/_2\,{}^1/_2\,{}^1/_2\,{}^5/_2) + 16D\,({}^3/_2\,{}^3/_2) + 20D\,({}^3/_2\,{}^1/_2\,{}^1/_2\,{}^3/_2) + 25D\,({}^1/_2\,{}^1/_2), \qquad (2.10)$$

etc.

We have already stated that the commutation relations completely determine the $U(\alpha)$-algebra. In addition they must be invariant under Lorentz transformations. But this means that the quantities $C_{k_1k_2\ldots k_n}(\alpha)$ which appear in (1.7) form the basis of some representation of the Lorentz group. Thus finding the commutation relations is related to the problem of finding all the irreducible tensor representations in the basis of the matrices α. But which representations of the Lorentz group, having as basis the symmetrizers of the matrices α, will give us the commutation relations (1.7)?

The answer to this question is given by comparing formulas (2.7) – (2.10) with the formula for the representation L, according to which the matrices of the $U(\alpha)$-algebra transform in the space R_2. We first write some formulas for the representation L, which we shall use later on.

If S corresponds to $D(\frac{1}{2}\ \frac{1}{2}) + D(0\ 0)$, L corresponds to

$$[D\,({}^1/_2\,{}^1/_2) + D\,(00)]^2 = D\,(11) + D\,(1001) + 2D\,({}^1/_2\,{}^1/_2) + 2D\,(00). \qquad (2.11)$$

Similarly, for $S \sim D(\frac{1}{2}\,\frac{1}{2}) + D(1001)$,

$$L \sim D\,(2002) + 2D\,({}^3/_2\,{}^1/_2\,{}^1/_2\,{}^3/_2) + 3D\,(11) + 2D\,(1001) + 4D\,({}^1/_2\,{}^1/_2) + 3D\,(00); \qquad (2.12)$$

for $S \sim D\,(1001) + D\,({}^1/_2\,{}^1/_2) + D\,(00)$,

$$L \sim D\,(2002) + 2D\,({}^3/_2\,{}^1/_2\,{}^1/_2\,{}^3/_2) + 3D\,(11) + 4D\,(1001) + 6D\,({}^1/_2\,{}^1/_2) + 4D\,(00); \qquad (2.13)$$

for $S \sim D(\frac{1}{2}\,0\,0\,\frac{1}{2}) + D(1\,\frac{1}{2}\,\frac{1}{2}\,1)$ (the representation S which occurs in the investigation of the Pauli-Fierz equation),

$$L \sim D\,(2112) + D\,(2002) + 2D\,({}^3/_2\,{}^3/_2) + 4D\,({}^3/_2\,{}^1/_2\,{}^1/_2\,{}^3/_2) + 6D\,(11) + 5D\,(1001) + 8D\,({}^1/_2\,{}^1/_2) + 4D\,(00); \qquad (2.14)$$

for $S \sim 2D(\frac{1}{2}\,0\,0\,\frac{1}{2}) + D(1\,\frac{1}{2}\,\frac{1}{2}\,1)$ (which is the representation of the equations of Ginzburg, Fradkin, Ulehla, cf. reference 2),

$$L \sim D\,(2112) + D\,(2002) + 2D\,({}^3/_2\,{}^3/_2) + 6D\,({}^3/_2\,{}^1/_2\,{}^1/_2\,{}^3/_2) + 10D\,(11) + 10D\,(1001) + 18D\,({}^1/_2\,{}^1/_2) + 10D\,(00). \qquad (2.15)$$

Comparing Eqs. (2.7) – (2.10) and (2.11) – (2.15), we see that for the existence of an algebra of matrices transforming according to the representation L, it is necessary that the particular symmetrizers which do not appear in (2.11) – (2.15) and which transform according to an irreducible representation of the Lorentz group, be equal to zero (or be expressed in terms of symmetrizers containing a smaller number of matrices α). So for (2.4) it is obvious that the symmetrizer corresponding to $D(1\,1)$ is equal to zero, etc. Thus we could enumerate all the commutation relations if we could, first, give all the irreducible representations of the Lorentz group in the basis of the symmetrizers of the matrices α; and second, if we could state which symmetrizers are independent (if, when the basis of one representation is equal to zero, we could say for which other representations it will also be zero), and thirdly, in case the basis is zero only for part of a set of identical representations, we could state which ones these are.

Let us proceed to the solution of these problems. For this purpose we first define the infinitesimal operator J_{ik} in the space R_2. Using (1.3) and (2.3):

$$J_{ik}\,G = [I_{ik},\, G]. \qquad (2.16)$$

Irreducible representations in the space R_2 must be invariant under the transformation (2.16).

In order to find the decomposition of the tensor space of matrix products $\alpha_{k_1}\alpha_{k_2}\ldots\alpha_{k_n}$ into irreducible spaces, we make use of the standard apparatus of the permutation group (cf. reference 5 and especially reference 6, Chapter IV). In doing this we must remember that we are resolving into invariant subspaces of products of matrices α, and their order plays an essential role because of the noncommutativity of the matrices. For this reason we must take account of the order of the cells in the Young patterns which enable us to determine the irreducible representations of the permutation group. This is the distinction between our problem and the case of symmetrization of commutative vectors, where representations with differing order of the cells are equivalent.

We make this clear on an example. Suppose we have a Young pattern consisting of four cells (cf. the figure). The numbers on the cells show where the corresponding matrix should stand. The symbols $ijkl$ are the indices of the matrices which are permuted according to this particular scheme.

Sometimes Young patterns are designated by abbreviated symbols like $[4^3, 2]$ (i.e., there are three rows of four cells and one row of two[5]). Young patterns with a fixed enumeration of the

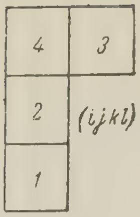

fields or with a definite arrangement of indices will be written starting with the top row, from left to right. The rows will be separated by commas. The numbers of the fields will be given in boldface type to distinguish them from the permuted indices. Thus the pattern shown in the figure can be written as

$$[43,2,\mathbf{1}], \quad [lk,j,i]. \tag{2.17}$$

We give the corresponding symmetrizer:

$$\begin{aligned}&\alpha_i\alpha_j\alpha_k\alpha_l - \alpha_i\alpha_k\alpha_l\alpha_j + \alpha_j\alpha_k\alpha_l\alpha_i - \alpha_j\alpha_i\alpha_l\alpha_k \\ &\quad + \alpha_k\alpha_i\alpha_l\alpha_j - \alpha_k\alpha_j\alpha_l\alpha_i + \alpha_i\alpha_j\alpha_l\alpha_k - \alpha_i\alpha_l\alpha_k\alpha_j \\ &\quad + \alpha_j\alpha_l\alpha_k\alpha_i - \alpha_j\alpha_i\alpha_k\alpha_l + \alpha_l\alpha_i\alpha_k\alpha_j - \alpha_l\alpha_j\alpha_k\alpha_i.\end{aligned} \tag{2.18}$$

However, not all the patterns with different enumeration of the fields are independent. If, as usual,[6] we define the symmetrizer associated with the Young diagram to be

$$c(\mathrm{s}) = \sum_{pq} \delta_q \mathrm{qp},$$

where $\mathbf{p}$ is a row-preserving permutation and $\mathbf{q}$ is a column-preserving permutation, then the equations

$$c(\mathrm{sp}) = c(\mathrm{s}), \qquad c(\mathrm{qs}) = \delta_q c(\mathrm{s}).$$

are valid for $c(\mathrm{s})$. This also means that only certain patterns are essential. For example, in the pattern of (2.17) the order of the cells 1 and 2 has no significance.

We now consider the Young symmetrizers $J(\alpha_{k_1}\alpha_{k_2}\cdots\alpha_{k_n})$, which are quantities analogous to (2.18). According to what we said above, the functions $J(\alpha_{k_1}\alpha_{k_2}\cdots\alpha_{k_n})$, corresponding to a definite Young pattern, occur in some one irreducible representation of the Lorentz group. Linear combinations of these functions constitute a basis of this representation.

Under transformations of the Lorentz group all the functions are transformed among themselves. In order to determine a basis of an irreducible representation, we must find those linear combinations of J-functions which are preserved under Lorentz transformations and transformed into one another. This can be done by using formula (2.16).

Below we shall enumerate all the irreducible representations of the Lorentz group in the basis of the symmetrizers of the α-matrices, up to and including products of four matrices. The basis elements are written in terms of J-functions. The number of basis elements is given in the slant brackets; the number of identical representations is given in curly brackets. The order of the cells is not given. The symbol $\sigma\sigma$ means $\alpha_\sigma\alpha_\sigma$, $i\sigma\sigma$ means $\alpha_i\alpha_\sigma\alpha_\sigma$, etc.

$$\text{Unit matrix E, } D(00),\ /1/. \tag{2.19}$$

$$\text{One matrix } \alpha_i,\ D(^1/_2\,^1/_2),\ /4/. \tag{2.20}$$

Products of two matrices:

$$D(11),\ [2],\ /9/; \quad D(1001),\ [1^2],\ /6/; \quad D(00),\ \sigma\sigma,\ /1/. \tag{2.21}$$

$$J(\alpha_i\alpha_k); \quad J(\alpha_i^2) - J(\alpha_k^2). \tag{2.22}$$

Products of three matrices:

$$\begin{gathered} D(^3/_2\,^3/_2),\ [3],\ /16/; \qquad \{2\},\ D(^3/_2\,^1/_2\,^1/_2\,^3/_2),\ [2,1],\ /16/; \\ D(^1/_2\,^1/_2),\ [1^3],\ /4/; \qquad \{3\},\ D(^1/_2\,^1/_2),\ i\sigma\sigma,\ /4/. \end{gathered} \tag{2.23}$$

$$J(\alpha_i\alpha_k\alpha_l); \qquad J(\alpha_i\alpha_l^2) - J(\alpha_i\alpha_k^2); \qquad J(\alpha_i^3) - J(\alpha_i\alpha_l^2). \tag{2.24}$$

Products of four matrices:

$$\begin{gathered} D(22),\ [4],\ /25/; \quad \{3\},\ D(2112),\ [3,1],\ /30/; \\ \{2\},\ D(2002),\ [2^2],\ /10/; \quad \{3\},\ D(11),\ [2,1^2],\ /9/; \\ D(00),\ [1^4],\ /1/; \quad \{6\},\ D(11),\ \sigma i\sigma k + \sigma k\sigma i,\ \sigma i\sigma i - \sigma k\sigma k,\ /9/; \\ \{6\},\ D(1001),\ \sigma\sigma ik - \sigma\sigma ki,\ /6/; \quad \{3\},\ D(00),\ \sigma\sigma\rho\rho,\ /1/. \end{gathered} \tag{2.25}$$

$$\begin{gathered} J(\alpha_i\alpha_k\alpha_l\alpha_m); \quad J(\alpha_i^2\alpha_l\alpha_m) - J(\alpha_k^2\alpha_l\alpha_m); \quad J(\alpha_i^2\alpha_l\alpha_m) - J(\alpha_l^3\alpha_m); \\ J(\alpha_k^2\alpha_i^2) - J(\alpha_k^2\alpha_q^2) - J(\alpha_i^2\alpha_r^2) + J(\alpha_q^2\alpha_r^2); \\ J(\alpha_i^4) - J(\alpha_i^2\alpha_k^2) + J(\alpha_k^4). \end{gathered} \tag{2.26}$$

The further process of recording symmetrizers and the corresponding relations between J-functions is analogous and presents no difficulties.

Thus we can write any symmetrizer using the rules formulated here. But this means that, for any matrix α_i, we can give the whole set of commutation relations corresponding to representations which are not contained in (2.3). The bases of such representations are equal to zero. In particular, it is easy to see that just the requirement of the occurrence of a maximum spin causes the basis of the completely symmetrized representation for the corresponding number of matrices to become equal to zero. For maximum spin $\frac{1}{2}$ – D(11); 1 – D($^3/_2$ $^3/_2$); $^3/_2$ – D(22), etc.

Thus we have given the complete answer to the first question. On the basis of what we have said, the answer to the second question also is clear. A symmetrizer of lower rank is equal to zero. This will be the case if and only if we can, in the Young pattern of the first symmetrizer, separate out a part corresponding to the symmetrizer of lower rank, with the cells numbered in the same sequence. So, for example, from the fact that the basis of the representation corresponding to **[23, 1]** is zero, it follows that the symmetrizers are zero for the Young patterns:

$$[234,1];\quad [34,21];\quad [3562,14]. \tag{2.27}$$

To determine which of the symmetrizers of identical representations enter in $U(\alpha)$, we must orthogonalize their bases. To do this it is necessary that they have no common basis elements, as, for example, for the patterns **[23, 1]**, [jk, i] and **[13, 2]**, [jk, i].

The necessary condition for orthogonalization is that when we reverse the order of the indices, the basis element is changed only by a constant factor. Thus the basis elements corresponding to the patterns

$$[23,1] - [21,3],\ [jk,\ i], \tag{2.28}$$

$$[23,1] + [21,3],\ [jk,\ i]. \tag{2.29}$$

are orthogonal. In these formulas the order of the indices ijk no longer matters.

In Sec. 4 we shall give a systematic procedure for obtaining commutation relations, using orthogonalization of bases in a suitable canonical representation. Here we mention only that, for the simplest equations, the separating out of identical representations can be done using the rules we have formulated for the Young patterns and the requirement that the commutation relations obtained in this way be free of contradictions. Thus, it is not hard to show that for (2.13), the basis vectors (2.29) are equal to zero while those in (2.28) are not. In resolving identical representations a direct check is also possible, but it is also important to use certain relations which come from the infinitesimal group ring, whose structure we shall now examine.

3. INFINITESIMAL GROUP RING. QUESTIONS OF IRREDUCIBILITY.

To investigate the structure of the infinitesimal group ring, we apply the method of Sec. 2. The linear closure of the infinitesimal operators of the Lie group form a subspace in the space R_2, which is invariant with respect to the representation $L = S \times \widetilde{S}$ (cf. reference 3). In our case this invariant subspace forms a basis of the representation D(1001). Any product of infinitesimal matrices is contained in $U(\alpha)$.[3] Consequently the space in which the infinitesimal group ring is defined is contained in R_2.

The direct product of two matrices $I_{ik} \times I_{rs}$ breaks up into symmetrizers according to the formula

$$D(1001) \times D(1001) = D(2002)$$
$$+ D(1001) + 2D(11) + 2D(00). \tag{3.1}$$

Analogous formulas can be written for three or more matrices. However, because of the commutation relations (1.4), only certain of the symmetrizers of type (3.1) are different from zero and independent.

Omitting the simple computations, we enumerate these symmetrizers by giving the corresponding Young patterns.

1 matrix:

$$D(1001),\ [1^2]. \tag{3.2}$$

2 matrices:

$$D(2002),\ [2^2];\quad D(11),\ [\,.\,.\,,\ \sigma\sigma];$$
$$D(00),\ [1^4];\quad D(00),\ [\nu\nu,\ \sigma\sigma]. \tag{3.3}$$

3 matrices:

$$D(3003),\ [3^2];\quad D(2112),\ [\,.\,.\,.\,,\ .\,\sigma\sigma];\quad D(1001),\ [\sigma\sigma,\ \nu\nu];$$
$$D(1001),\ [2^2,\ 1^2]. \tag{3.4}$$

4 matrices:

$$D(4004),\ [4^2];\quad D(2002),\ [\,.\,.\,\tau\tau,\ .\,.\,\sigma\sigma];$$
$$D(3113),\ [\,.\,.\,.\,.\,,\ .\,.\,\tau\tau];$$
$$D(11),\ [\,.\,.\,\sigma\sigma,\ \nu\nu\tau\tau];\quad D(22),\ [\,.\,.\,.\,.\,,\ \tau\tau\sigma\sigma];$$
$$D(00),\ [\sigma\sigma\tau\tau,\ \nu\nu\rho\rho];\quad D(2002),\ [3^2,\ 1^2];\quad D(00),\ [2^4];$$
$$D(11),\ [\,.\,.\,.\,,\ .\,\sigma\sigma,\ .\,,\,.\,];\ D(00),\ [\,.\,\sigma\sigma,\ .\,\nu\nu,\ .\,,\,.\,]\ \text{etc.} \tag{3.5}$$

It is not difficult to enumerate the patterns for larger numbers of matrices. In each of the cases there will be 6, 21, 55, 126 independent quantities, respectively [in agreement with (1.4)].

We know that the infintesimal operators for a given maximum spin satisfy the equations

$$I_{rs}^2 + {}^1\!/_4 = 0,\qquad I_{rs}(I_{rs}^2 + 1) = 0,$$
$$(I_{rs}^2 + {}^1\!/_4)(I_{rs}^2 + {}^9\!/_4) = 0\ \text{ etc.} \tag{3.6}$$

In order to satisfy these relations it is necessary, for the case of maximum spin $\frac{1}{2}$, that the independent symmetrizers contain one cell in each row; for spin 1 there must be two cells, etc. In the general case we have:

maximum spin $\frac{1}{2}$, independent symmetrizers:

$$E;\ [1^2];\ [1^4]; \tag{3.7}$$

maximum spin 1, independent symmetrizers:

$$E;\quad [2^2];\quad [\,.\,.\,,\sigma\sigma];\quad [\rho\rho,\sigma\sigma];$$

$$[2^2, 1^2];\quad [2^4];\quad [1^2];\quad [1^4]; \tag{3.8}$$

etc.

From the system of relations defining the infinitesimal group ring, we can obtain corresponding restrictions on the $U(\alpha)$-algebra, by using the operation (2.16). Thus, by using only (3.6), we find for maximum spin $\frac{1}{2}$,

$$[\alpha_r, I_{rs}^2 + {}^1/_4] = 2I_{rs}\alpha_s - \alpha_r = 0.$$

From this we find

$$\alpha_s\alpha_r + \alpha_r\alpha_s = 0, \qquad \alpha_r^2 - \alpha_s^2 = 0. \tag{3.9}$$

For maximum spin 1, we have

$$[\alpha_r, I_{rs}^3 + I_{rs}] = I_{rs}^2\alpha_s - I_{rs}\alpha_r = 0.$$

Multiplying the second equation on the right and left by α_r and α_s, and canceling terms in the highest power of I_{rs}, we get the equations

$$I_{rs}(\alpha_s^2 - \alpha_r^2) = \alpha_r\alpha_s + \alpha_s\alpha_r,$$

$$I_{rs}(\alpha_s\alpha_r + \alpha_r\alpha_s) = \alpha_r^2 - \alpha_s^2. \tag{3.10}$$

From this we find the relations between the matrices α_k corresponding to $D({}^3/_2\ {}^3/_2)$, [3].

Similarly, from the other minimal equations in (3.6), we find that the corresponding symmetric representation is equal to zero (cf. also Sec. 2). Equating the various symmetrizers to zero, we can find the corresponding $U(\alpha)$-algebra.

By means of the infinitesimal group ring, we obtain both reducible and irreducible equations. To find the irreducible equations, we make use of the following theorem.

If a matrix A commutes with all the elements of an algebra, and the algebra is irreducible, then the matrix is either a multiple of the unit matrix or is equal to zero.[6]

For an irreducible algebra, the center consists of the unit matrix. So, for example, for the algebra (3.9), α_r^2 commutes with all the matrices. Consequently $\alpha_r^2 = c$. Thus, for maximum spin $\frac{1}{2}$, for irreducible equations, we must have

$$\alpha_i\alpha_k + \alpha_k\alpha_i = 2c\delta_{ik}. \tag{3.11}$$

For the algebra corresponding to (2.13), as was shown in Sec. 2, the basis of the representations $D({}^3/_2\ {}^3/_2)$, [3] and (2.29) is equal to zero, which corresponds to the commutation relations

$$\alpha_s^3 = \alpha_r\alpha_s\alpha_r + \alpha_s\alpha_r^2 + \alpha_r^2\alpha_s, \qquad \alpha_q\alpha_s\alpha_q = \alpha_r\alpha_s\alpha_r,$$

$$\alpha_r\alpha_s\alpha_q + \alpha_q\alpha_s\alpha_r = 0 \tag{3.12}$$

We have two commutators

$$K_1 = \alpha_i\alpha_k\alpha_i\alpha_k, \qquad K_2 = (\alpha_i\alpha_q^2 + \alpha_q^2\alpha_i)\,\alpha_k\alpha_i\alpha_k. \tag{3.13}$$

For irreducible equations, they must be equal to constants c_1 and c_2. Then

$$\alpha_i\alpha_k\alpha_i\alpha_k\,(\alpha_i\alpha_q^2 + \alpha_q^2\alpha_i) = c_2\alpha_i$$

and, consequently,

$$\alpha_i\alpha_q^2 + \alpha_q^2\alpha_i = (c_2/c_1)\,\alpha_i.$$

Finally we obtain the relations determining the $U(\alpha)$-algebra:

$$\alpha_i\alpha_q^2 + \alpha_q^2\alpha_i = (c_2/c_1)\,\alpha_i, \qquad \alpha_s^3 - \alpha_r\alpha_s\alpha_r = (c_2/c_1)\,\alpha_s,$$

$$\alpha_s^4 - (c_2/c_1)\,\alpha_s^2 - c_1 = 0. \tag{3.14}$$

Thus we have as many commutators as there are arbitrary constants in the relativistically invariant equation. This technique can also be used to investigate the irreducibility of a given $U(\alpha)$-algebra.

4. THE CANONICAL REPRESENTATION. TRACES.

For the practical problem of finding the $U(\alpha)$-algebra, it is convenient to use a canonical basis formed from the matrices α. The connection between the natural basis, which was considered in Sec. 2, and the canonical basis is given by the formulas[5]

$$u^{{}^1/_2\,{}^1/_2}_{{}^1/_2\,{}^1/_2} = (1/\sqrt{2})\,(-i\alpha_1 + \alpha_2), \qquad u^{{}^1/_2\,{}^1/_2}_{{}^1/_2\,-{}^1/_2} = (1/\sqrt{2})\,(\alpha_0 + i\alpha_3),$$

$$u^{{}^1/_2\,{}^1/_2}_{-{}^1/_2\,{}^1/_2} = (1/\sqrt{2})\,(-\alpha_0 + i\alpha_3), \qquad u^{{}^1/_2\,{}^1/_2}_{-{}^1/_2\,-{}^1/_2} = (1/\sqrt{2})\,(i\alpha_1 + \alpha_2). \tag{4.1}$$

To construct symmetrizers containing products of the matrices α_k, we must use the Clebsch-Gordan formulas

$$v^{PQ}_{pq} = \sum_{\substack{p_1+p_2=p\\ q_1+q_2=q}} (P_1P_2p_1p_2\,|\,Pp)\,(Q_1Q_2q_1q_2\,|\,Qq)\,u^{P_1Q_1}_{p_1q_1}\,w^{P_2Q_2}_{p_2q_2}. \tag{4.2}$$

For example,

$$v^{11}_{11} = u^{{}^1/_2{}^1/_2}_{{}^1/_2{}^1/_2}\,u^{{}^1/_2{}^1/_2}_{{}^1/_2{}^1/_2}, \tag{4.3}$$

$$v^{11}_{10} = \frac{1}{\sqrt{2}}\,u^{{}^1/_2{}^1/_2}_{{}^1/_2{}^1/_2}\,u^{{}^1/_2{}^1/_2}_{{}^1/_2-{}^1/_2} + \frac{1}{\sqrt{2}}\,u^{{}^1/_2{}^1/_2}_{{}^1/_2-{}^1/_2}\,u^{{}^1/_2{}^1/_2}_{{}^1/_2{}^1/_2}. \tag{4.4}$$

Analogously, we can express the basis elements of any representation in terms of the quantities $u^{1/2\,1/2}_{pq}$, and go over to the natural basis by means of formulas (4.1). For a complete characterization of the representation, we need, in addition to the angular momenta and their projections, to state which and how many of the quantities $u^{1/2\,1/2}_{pq}$ form the representation. The basis elements will then be completely defined.

For example, the quantity (4.3) can be written symbolically as ${}_{[2]}u^{11}_{11}$; the quantities coresponding to (2.28) can be written as

$${}_{[3]}u^{{}^3/_2{}^1/_2}_{pq}\,[({}^1/_2{}^1/_2)\,(10) + (10)\,({}^1/_2{}^1/_2)],$$

$${}_{[3]}u^{{}^1/_2{}^3/_2}_{pq}\,[({}^1/_2{}^1/_2)\,(10) + (10)\,({}^1/_2{}^1/_2)]$$

[where the symbols in the square brackets on the right fix the order of construction of the quantities u_{pq}^{PQ} using (4.2)]. In this notation, the commutation relations of the Dirac algebra have the form

$$ {}_{[2]}u^{11}_{pq} = 0; \qquad {}_{[2]}u^{00}_{00} = 4\,{}_{[0]}u^{00}_{00} = 4E. \tag{4.5}$$

Here there is no longer any need to use the J-functions. Each component of the canonical basis is simply resolved into components with a smaller number of matrices [m] and the same symmetry. In the general case the commutation relations can be written in the form

$$ {}_{[m]}u^{PQ}_{pq} = \sum_{n<m} a_{n\,[n]}u^{PQ}_{pq}. \tag{4.6}$$

They are completely equivalent to the relations treated in Sec. 2.

Earlier we remarked that a necessary condition for orthogonality of the bases of identical representations is that, when the order of the matrices is reversed, each basis element is left unchanged except for a constant factor. The representations ${}_{[2]}u^{11}_{pq}$, ${}_{[3]}u^{3/2\,3/2}_{pq}$ and other completely symmetric representations, as well as ${}_{[2]}u^{10}_{pq}$, ${}_{[2]}u^{00}_{00}$ satisfy this condition. For the others we must perform a symmetrization. We thus orthogonalize the spaces corresponding to the identical representations.

For the product of three matrices, we can obtain the following relations:

$$\begin{aligned} &u^{3/2\,1/2}_{pq}[(1/2\,1/2)(11)+(11)(1/2\,1/2)] \\ &\qquad = u^{3/2\,1/2}_{pq}[(1/2\,1/2)(10)-(10)(1/2\,1/2)], \end{aligned}\tag{4.7}$$

$$\begin{aligned} &u^{3/2\,1/2}_{pq}[(1/2\,1/2)(11)-(11)(1/2\,1/2)] \\ &\qquad = u^{3/2\,1/2}_{pq}[(1/2\,1/2)(10)+(10)(1/2\,1/2)]. \end{aligned}\tag{4.8}$$

We thus have two orthogonal subspaces. Going over to the natural basis, we get formulas (2.28) and (2.29).

The products of three matrices also contain bases corresponding to the four representations $D(\frac{1}{2}\,\frac{1}{2})$. We give the result of the symmetrization directly in the natural basis for the individual basis elements. We have

$$\begin{gathered} 1)\ [1^3];\quad 2)\ \alpha_\sigma^2\alpha_i-\alpha_i\alpha_\sigma^2;\quad 3)\ \alpha_i\alpha_\sigma^2+\alpha_\sigma^2\alpha_i; \\ 4)\ \alpha_i\alpha_\sigma^2+\alpha_\sigma^2\alpha_i+4\alpha_\sigma\alpha_i\alpha_\sigma;\quad 5)\ \alpha_i\alpha_\sigma^2+\alpha_\sigma^2\alpha_i-2\alpha_\sigma\alpha_i\alpha_\sigma; \end{gathered}\tag{4.9}$$

but the elements 3, 4, and 5 are not independent. They can be expressed in terms of two independent orthogonal basis elements:

$$\begin{aligned} &1)\ a(\alpha_i\alpha_\sigma^2+\alpha_\sigma^2\alpha_i)+b\alpha_\sigma\alpha_i\alpha_\sigma, \\ &2)\ a'(\alpha_i\alpha_\sigma^2+\alpha_\sigma^2\alpha_i)+b'\alpha_\sigma\alpha_i\alpha_\sigma. \end{aligned}\tag{4.10}$$

The constants a, b, a′, b′ depend on the representation according to which ψ transforms, and on the constants in the equations. For the Duffin-Kemmer equation (spin 1), a = 0, b′ = 0.

Similarly we can get the formulas for products of four matrices. We shall give the orthogonal bases in natural form (for each of the vectors). First we introduce the notation

$$\begin{gathered} \alpha_0(\alpha_1^3-\alpha_1\alpha_2^2-\alpha_2\alpha_1\alpha_2-\alpha_2^2\alpha_1)=A_1; \\ \alpha_1\alpha_0\alpha_1^2-\alpha_1\alpha_0\alpha_2^2-\alpha_2\alpha_0\alpha_1\alpha_2-\alpha_2\alpha_0\alpha_2\alpha_1=A_2; \\ \alpha_1^2(\alpha_3\alpha_0\pm\alpha_0\alpha_3)-\alpha_2^2(\alpha_3\alpha_0\pm\alpha_0\alpha_3)=X_1^\pm; \\ (\alpha_1\alpha_3\alpha_1\alpha_0\pm\alpha_1\alpha_0\alpha_1\alpha_3)-(\alpha_2\alpha_3\alpha_2\alpha_0\pm\alpha_2\alpha_0\alpha_2\alpha_3)=Y_1^\pm; \\ \alpha_1(\alpha_3\alpha_0\pm\alpha_0\alpha_3)\alpha_1-\alpha_2(\alpha_3\alpha_0\pm\alpha_0\alpha_3)\alpha_2=Z_1^\pm; \\ (\alpha_3\alpha_1^2\alpha_0\pm\alpha_0\alpha_1^2\alpha_3)-(\alpha_3\alpha_2^2\alpha_0\pm\alpha_0\alpha_2^2\alpha_3)=V_1^\pm; \\ \alpha_\sigma^2(\alpha_3\alpha_0\pm\alpha_0\alpha_3)=X_2^\pm;\qquad \alpha_\sigma\alpha_3\alpha_\sigma\alpha_0\pm\alpha_\sigma\alpha_0\alpha_\sigma\alpha_3=Y_2^\pm; \\ \alpha_\sigma(\alpha_3\alpha_0\pm\alpha_0\alpha_3)\alpha_\sigma=Z_2^\pm;\quad \alpha_3\alpha_\sigma^2\alpha_0\pm\alpha_0\alpha_\sigma^2\alpha_3=V_2^\pm. \end{gathered}\tag{4.11}$$

We shall use the symbol ~ to denote reversal of the order of the matrices, e.g.

$$\widetilde{X}_2^+=(\alpha_3\alpha_0+\alpha_0\alpha_3)\,\alpha_\sigma^2.$$

We then have the following formulas for the bases of the representations:

$$D(22)\qquad A_1+\widetilde{A}_1+A_2+\widetilde{A}_2; \tag{4.12}$$

$$\begin{aligned} D(2112)\quad &\text{a) } (A_1+\widetilde{A}_1)-(A_2+\widetilde{A}_2), \\ &\text{b) } a_1(A_1-\widetilde{A}_1)+a_2(A_2-\widetilde{A}_2), \\ &\text{c) } a_3(A_1-\widetilde{A}_1)+a_4(A_2-\widetilde{A}_2); \end{aligned}\tag{4.13}$$

$$\begin{aligned} D(2002)\quad &\text{a) } (X_1^++\widetilde{X}_1^+)-Z_1^+-V_1^+, \\ &\text{b) } (X_1^++\widetilde{X}_1^+)+Z_1^++V_1^+-2(Y_1^++\widetilde{Y}_1^+); \end{aligned}\tag{4.14}$$

$$\begin{aligned} D(11)[2,1^2]\ &\text{a) } (X_1^-+\widetilde{X}_1^-)-(Y_1^-+\widetilde{Y}_1^-), \\ &\text{b) } a_5(X_1^--\widetilde{X}_1^-+Y_1^--\widetilde{Y}_1^-+2Z_1^-) \\ &\qquad +a_6(Y_1^--\widetilde{Y}_1^-+Z_1^--V_1^-), \\ &\text{c) } a_7(X_1^--\widetilde{X}_1^-+Y_1^--\widetilde{Y}_1^-+2Z_1^-) \\ &\qquad +a_8(Y_1^--\widetilde{Y}_1^-+Z_1^--V_1^-); \end{aligned}\tag{4.15}$$

$$\begin{aligned} D(11)\quad &\text{a) } a_9(X_2^+-\widetilde{X}_2^+)+a_{10}(Y_2^+-\widetilde{Y}_2^+), \\ &\text{b) } a_{11}(X_2^+-\widetilde{X}_2^+)+a_{12}(Y_2^+-\widetilde{Y}_2^+); \end{aligned}\tag{4.16}$$

$$\begin{aligned} D(11)\quad &\text{a) } a_{13}(X_2^++\widetilde{X}_2^+)+a_{14}(Y_2^++\widetilde{Y}_2^+) \\ &\qquad +a_{15}Z_2^++a_{16}V_2^+, \end{aligned}\tag{4.17}$$

and bases b), c), d), analogous to a), but with different constants;

$$\begin{aligned} D(1001)\quad &\text{a) } a_{17}(X_2^-+\widetilde{X}_2^-)+a_{18}(Y_2^-+\widetilde{Y}_2^-), \\ &\text{b) } a_{19}(X_2^-+\widetilde{X}_2^-)+a_{20}(Y_2^-+\widetilde{Y}_2^-); \end{aligned}\tag{4.18}$$

$$\begin{aligned} D(1001)\quad &\text{a) } a_{21}(X_2^--\widetilde{X}_2^-)+a_{22}(Y_2^-+\widetilde{Y}_2^-) \\ &\qquad +a_{23}Z_2^-+a_{24}V_2^-. \end{aligned}\tag{4.19}$$

and bases b), c), d), analogous to a), but with other constants;

$$D\ (00)\qquad \text{a)}\ [1^4],$$

$$\text{b)}\ \alpha_\sigma^2\alpha_\rho^2 - \alpha_\rho\alpha_\sigma^2\alpha_\rho,$$

$$\text{c)}\ a_{25}(\alpha_\rho^2\alpha_\sigma^2 + \alpha_\rho\alpha_\sigma^2\alpha_\rho) + a_{26}\alpha_\rho\alpha_\sigma\alpha_\rho\alpha_\sigma,$$

$$\text{d)}\ a_{27}(\alpha_\rho^2\alpha_\sigma^2 + \alpha_\rho\alpha_\sigma^2\alpha_\rho) + a_{28}\alpha_\rho\alpha_\sigma\alpha_\rho\alpha_\sigma. \qquad (4.20)$$

We can express the individual basis elements using the formulas of Sec. 2. Thus, for example, a) and b) of (4.14) and a) of (4.13) correspond to the patterns

$$[23,14]-[21,34],\ [jk,\ il];\ [23,14]+[21,34],\ [jk,\ il]:$$

$$[234,1]+[324,1]-[423,1],\ [jkl,\ i].$$

In constructing the commutation relations, it is important to know whether the U(α)-algebra contains the bases of representations which are identical with the one being considered, and which have the same symmetry and lower [m]. If such representations are not contained, the canonical basis vectors are equal to zero; if they are, the basis vectors are resolved according to formula (4.6). So for the Duffin-Kemmer equation (spin 1).

$$\alpha_\sigma\alpha_i\alpha_\sigma = a_1\alpha_i, \qquad \alpha_\sigma^2\alpha_i + \alpha_i\alpha_\sigma^2 = a_2\alpha_i. \qquad (4.21)$$

In separating out the repeated representations we can use the symmetry of the ψ-function under space reflection and charge conjugation.

If the U(α)-algebra can be represented as a direct product U(α′) × U(α″), then by multiplying term by term in the canonical basis we immediately obtain the independent basis elements. The fact that various commutation relations are satisfied can be checked using the simplest parametric representation. For example, for (2.15) $\alpha_i = \gamma_i + b\beta_i$; for (2.14) $\alpha_i = \gamma_i + b\gamma_l B^{li}$, etc.

Finding the independent basis vectors by using the direct product is not complicated, and the results can be gotten for spins 1, $^3\!/_2$, 2, $^5\!/_2$, 3 and even for higher spin values. As an example, we state that for the Ginzburg equation (2.14), those commutation relations are satisfied which are obtained by using formula (4.6) for the resolution of the bases of the representations (4.12); a) and b) of (4.13); b) of (4.14); a) and b) of (4.15); a) of (4.16); a) of (4.17); a) of (4.18); a) of (4.19); c) of (4.20). For the Pauli-Fierz equation (2.14), there is a further resolution of b) in (4.17); b) in (4.19); b) and d) in (4.20).

These are the complete commutation relations. The arbitrary constants in them are not independent. The constants can be related to the coefficients in the minimal equation for α_0, which has the form

$$(\alpha_0^2-\lambda_1^2)(\alpha_0^2-\lambda_2^2)(\alpha_0^2-\lambda_3^2)(\alpha_0^2-\lambda_4^2)=0$$

for (2.15), and

$$(\alpha_0^2-\lambda_1^2)(\alpha_0^2-\lambda_2^2)(\alpha_0^2-\lambda_3^2)=0,$$

for (2.14), or with the constants which appear in the expression for I_{ij} in terms of the matrices α. They depend on the representation according to which ψ transforms, and on the particular physical requirements imposed on the equations. It would therefore be useful to treat the problem by formulating the physical requirements on the equations in the form of the U(α)-algebra.

Here we remark only that the algebraic representation makes possible a basic simplification of the computations for particles with higher spin, which are extremely complicated by present methods, even for the simplest equations with maximum spin $^3\!/_2$.

We decomposed the tensor space of the products of matrices α_i into symmetrizers corresponding to irreducible representations of the Lorentz group. It is easy to see that only those matrices will have nonzero traces which are invariant under the full Lorentz group, i.e., those matrices whose bases are obtained by contraction of indices. Therefore we need consider only such matrices and find their traces.

From consideration of relativistic invariance, we can write the relation

$$\mathrm{Sp}\,\alpha_i\alpha_k\alpha_l\alpha_m = a_1\delta_{ik}\delta_{lm} + a_2\delta_{im}\delta_{kl} + a_3\delta_{il}\delta_{km}. \qquad (4.23)$$

Knowing the traces of the three invariants $\alpha_\rho\alpha_\rho\alpha_\sigma\alpha_\sigma$, $\alpha_\rho\alpha_\sigma\alpha_\sigma\alpha_\rho$, and $\alpha_\rho\alpha_\sigma\alpha_\rho\alpha_\sigma$, we can then determine the unknown coefficients. It is necessary to know only certain (basic) invariants, and to know how the others are expressed in terms of these basic invariants. This is all that we need to know in order to carry out the computations. It is entirely unnecessary to know all the commutation relations. The computation is then done by the standard method. It is no more complicated than for the Dirac algebra (provided that one has done the preliminary work).

We note that the computation of the basic traces can be done using the parametric representation which we treated in reference 2; we use the equation

$$\mathrm{Sp}\,(\chi_1\times\chi_2) = \mathrm{Sp}\,\chi_1\cdot\mathrm{Sp}\,\chi_2.$$

There is then no need to carry out the explicit multiplication of the matrices in the parametric representation (which may prove to be an irksome task). In particular, we can obtain from the formulas of reference 2 the traces for the equations of Ginzburg and of Pauli-Fierz, and also establish the relation between the representations which are treated here.

As we have seen, our investigation makes clear the structure of relativistically invariant equations, and enables us to find results which would be extremely difficult to get by other existing methods, and which would be practically impossible by such methods for higher spins of 2, $^5\!/_2$ and 3.

It is interesting to note that even for such a relatively simple equation as the Pauli-Fierz equation, Fradkin, in a paper specially devoted to this question,[7] succeeded in finding relations only between a set of five matrices, whereas we have seen that the basis relations involve only four matrices. Thus the relations found by Fradkin give only a very incomplete characterization of the algebra of the matrices of Pauli-Fierz.

The results we have obtained lead us to hope that it will be possible to give directly the general form of the $U(\alpha)$-algebra, and to determine the commutation relations completely without any essential calculation.

Here the method has been applied to the finite-dimensional representations, but the method described here may prove fruitful also for treating infinite-dimensional representations, which would be of definite interest for the theory of fields.

In conclusion I express my deep gratitude to Profs. V. L. Ginzburg, V. Ya. Faĭnberg and E. S. Fradkin for continued interest and valuable discussion.

---

[1] I. M. Gel'fand and A. M. Yaglom, JETP **18**, 703 (1948).

[2] L. A. Shelepin, JETP **34**, 1574 (1958), Soviet Phys. JETP **7**, 1085 (1958).

[3] Harish-Chandra, Phys. Rev. **71**, 793 (1947).

[4] K. J. LeCouteur, Proc. Roy. Soc. (London) A202, 284 (1950).

[5] G. Ya. Lyubarskiĭ, Теория групп и ее применение в физике, (Group Theory and its Application to Physics), GITTL, 1957.

[6] H. Weyl, The Classical Groups, Princeton University Press, 1946.

[7] É. E. Fradkin, Dokl. Akad. Nauk SSSR **115**, 907 (1957), Soviet Phys.-Doklady **2**, 399 (1957).

Translated by M. Hamermesh
325

A GENERALLY COVARIANT METHOD OF SUCCESSIVE APPROXIMATIONS IN GENERAL RELATIVITY

I. I. GUTMAN

Submitted to JETP editor May 5, 1959

J. Exptl. Theoret. Phys. (U.S.S.R.) 37, 1639-1648 (December, 1959)

A new mathematical approach to the problem of gravitational theory, which always ensures the uniqueness of a solution without using supplementary coordinate conditions, is proposed. To solve the problem, a generally covariant method of successive approximations is developed, in which the small expansion parameter is [illegible] ([illegible] is the Newtonian parameter). It is shown that the equations of successive approximation have, at all orders, the form of a covariant d'Alembertian with a right-hand side. There is introduced an energy-momentum tensor for the gravitational field (separated from the inertial force field) which satisfies a conservation law in inertial systems. In contrast to the Einstein-Infeld-Hoffmann and Fock methods, the method proposed is applicable to rapidly varying fields and for arbitrary velocities close to the speed of light.

1. GENERAL FORMULATION OF THE PROBLEM

The basic equations of general relativity are the ten Einstein equations:

$$G^{\mu\nu} = -\varkappa T^{\mu\nu} \quad (\mu, \nu = 1, 2, 3, 4), \qquad (1)$$

where

$$G^{\mu\nu} = R^{\mu\nu} - \tfrac{1}{2} g^{\mu\nu} R.$$

The mass tensor can be taken as known in the whole four-dimensional space if it is given in the whole three-dimensional space at some moment of time, and in addition, if the equations of motion of all volume elements of the system of the bodies considered are given.* But since we do not know the equations of motion if the metric of the space in which the bodies move is unknown, the left side of (1) remains unknown as long as these equations are unknown.

Therefore, Eqs. (1) contain, besides the ten unknown $g_{\mu\nu}$, additional unknown functions to be determined by the equations of motion. These equations of motion explicitly depend on the metric and therefore cannot be solved independently of (1) just as the latter equations cannot be solved independently of the equations of motion.

Let us determine how many equations of motion there should be. For this we write the most general expression for the mass tensor:

$$T^{\mu\nu} = \rho u^{\mu} u^{\nu} + p^{\mu\nu} + S^{\mu\nu}, \qquad (2)$$

where ρ is the density of rest mass, u^{μ} is the 4-vector velocity, $p^{\mu\nu}$ is the pressure tensor, going to $pg^{\mu\nu}$ in the isotropic case, $S^{\mu\nu}$ is the electromagnetic energy tensor divided by c^2. $S^{\mu\nu}$ is determined by the Maxwell equations, $p^{\mu\nu}$ can be expressed as a function of ρ by means of the equations of state of the matter, and u^{μ} has only three independent components, because of the identity

$$u^{\mu} u_{\mu} = 1.$$

In the result there remain four independent functions, which we can choose as ρ, u^1, u^2, and u^3.

The equation of motion is ordinarily expressed in the form

$$T^{\mu\nu}_{;\nu} = 0. \qquad (3)$$

It is considered that these equations follow from the field equations. This, however, is not exactly true. Equations (3) do not follow from (1), but simultaneously from (1) and from the identity

$$G^{\mu\nu}_{;\nu} = 0. \qquad (4)$$

In the method of Einstein, Infeld, and Hoffmann[1,2,3] in which the equations of motion are derived from the field equations, an essential use is made of the Bianchi identities, i.e., the equations of motion are in fact derived from (1) and (4).

Therefore, there are 14 independent equations (1) and (3). One can, however, go from this system of equations to another, fully equivalent, one:

$$G^{\mu\nu} = -\varkappa T^{\mu\nu}, \quad T^{\mu\nu}_{;\nu} = 0. \qquad (5)$$

---

*In general relativity it is impossible to consider the motion of an absolutely rigid body; we therefore consider the motion of each volume element of the body, and the equations of motion become partial differential equations.

$\epsilon_{\mu\nu}$. Just as with the Christoffel symbols $\Gamma^{\mu}_{\alpha\beta}$ for the fundamental metric $g_{\mu\nu}$, we introduce analogous symbols for the zeroth approximation metric:

$$\underset{0}{\Gamma}{}^{\mu}_{\alpha\beta} = \frac{1}{2}\varepsilon^{\mu\nu}(\varepsilon_{\nu\alpha,\beta} + \varepsilon_{\nu\beta,\alpha} - \varepsilon_{\alpha\beta,\nu}). \tag{9}$$

From the quantities $\Gamma^{\mu}_{\alpha\beta}$ and $\underset{0}{\Gamma}{}^{\mu}_{\alpha\beta}$, we can form the symbols used by Pugachev,[2] which can be represented as a third-rank tensor:

$$\Pi^{\mu}_{\alpha\beta} = \Gamma^{\mu}_{\alpha\beta} - \underset{0}{\Gamma}{}^{\mu}_{\alpha\beta}\,. \tag{10}$$

We introduce also the differential operator $\underset{0}{\nabla}_{\mu}$:

$$\underset{0}{\nabla}_{\mu}A^{\nu} = A^{\nu}_{,\mu} + \underset{0}{\Gamma}{}^{\nu}_{\mu\alpha}A^{\alpha}. \tag{11}$$

Using this operator, the expression for the covariant derivative can be written

$$\nabla_{\mu}A^{\nu} = \underset{0}{\nabla}_{\mu}A^{\nu} + \Pi^{\nu}_{\mu\alpha}A^{\alpha}. \tag{12}$$

The advantage of formula (12) over the ordinary description lies in the fact that both its terms are tensors.

Using the derivative $\underset{0}{\nabla}_{\mu}$ we can express the symbols $\Pi^{\mu}_{\alpha\beta}$ in terms of the tensor $g_{\mu\nu}$:

$$\Pi^{\mu}_{\alpha\beta} = \frac{1}{2}g^{\mu\nu}(\underset{0}{\nabla}_{\alpha}g_{\nu\beta} + \underset{0}{\nabla}_{\beta}g_{\nu\alpha} - \underset{0}{\nabla}_{\nu}g_{\alpha\beta}). \tag{13}$$

We write the expression for the Ricci tensor with these quantities:

$$R_{\mu\nu} = -\underset{0}{\nabla}_{\alpha}\Pi^{\alpha}_{\mu\nu} + \underset{0}{\nabla}_{\nu}\Pi^{\alpha}_{\mu\alpha} + \Pi^{\beta}_{\mu\alpha}\Pi^{\alpha}_{\nu\beta} - \Pi^{\alpha}_{\mu\nu}\Pi^{\beta}_{\alpha\beta}. \tag{14}$$

Substituting expansions (8) in (13), then (13) in (14), and finally (14) in (5) and also expansions (8) in (5), we get the following equations of successive approximations:

$$\underset{n}{B}_{\mu\nu} = -8\pi\underset{n-1}{T}_{\mu\nu} - \underset{n-1}{S}_{\mu\nu}, \tag{15}$$

$$\underset{0}{\nabla}_{\nu}\underset{n}{T}{}^{\mu\nu} = -\sum_{m=0}^{n-1}(\underset{n-m}{\Pi}{}^{\nu}_{\alpha\nu}\underset{m}{T}{}^{\mu\alpha} + \underset{n-m}{\Pi}{}^{\mu}_{\nu\alpha}\underset{m}{T}{}^{\nu\alpha}). \tag{16}$$

The tensor $\underset{n}{B}_{\mu\nu}$ has the form

$$\underset{n}{B}_{\mu\nu} = \frac{1}{2}(\underset{0}{\Box}\underset{n}{\gamma}_{\mu\nu} + \varepsilon_{\mu\nu}\underset{0}{\nabla}{}^{\alpha}\underset{0}{\nabla}{}^{\beta}\underset{n}{\gamma}_{\alpha\beta} - \underset{0}{\nabla}{}^{\alpha}\underset{0}{\nabla}_{\mu}\underset{n}{\gamma}_{\nu\alpha} - \underset{0}{\nabla}{}^{\alpha}\underset{0}{\nabla}_{\nu}\gamma_{\mu\alpha}), \tag{17}$$

where

$$\underset{n}{\gamma}_{\mu\nu} = \underset{n}{h}_{\mu\nu} - \frac{1}{2}\varepsilon_{\mu\nu}\varepsilon^{\alpha\beta}\underset{n}{h}_{\alpha\beta}. \tag{18}$$

The tensor $\underset{n-1}{S}_{\mu\nu}$ contains quantities of not greater than the $(n-1)$-th order of approximation, i.e., quantities already found previously.

A. Field Equations. Examine the method of solving (15). It is easy to see that they have the form of the identity

$$\underset{0}{\nabla}{}^{\nu}\underset{n}{B}_{\mu\nu} \equiv 0. \tag{19}$$

Introducing the notation $\underset{n-1}{D}_{\mu\nu} = 8\pi\underset{n-1}{T}_{\mu\nu} + \underset{n-1}{S}_{\mu\nu}$, we get, using (15) and (19),

$$\underset{0}{\nabla}{}^{\nu}\underset{n-1}{D}_{\mu\nu} = 0. \tag{20}$$

Rewriting (15) in the form

$$\hat{B}^{\alpha\beta}_{\mu\nu}\underset{n}{\gamma}_{\alpha\beta} = -\underset{n-1}{D}_{\mu\nu}, \tag{15a}$$

where the operator $\hat{B}^{\alpha\beta}_{\mu\nu}$ is

$$\hat{B}^{\alpha\beta}_{\mu\nu} = \frac{1}{2}(\underset{0}{\Box}\delta^{\alpha\beta}_{\mu\nu} + \varepsilon_{\mu\nu}\underset{0}{\nabla}{}^{\alpha}\underset{0}{\nabla}{}^{\beta} - \underset{0}{\nabla}{}^{\gamma}\underset{0}{\nabla}_{\mu}\delta^{\alpha\beta}_{\gamma\nu} - \underset{0}{\nabla}{}^{\gamma}\underset{0}{\nabla}_{\nu}\delta^{\alpha\beta}_{\gamma\mu}). \tag{21}$$

The Green's tensor $\hat{\Gamma}^{\alpha\beta}_{\gamma\delta}$ of equations (15a) should satisfy the symbolic equality

$$\hat{B}^{\gamma\delta}_{\mu\nu}\hat{\Gamma}^{\alpha\beta}_{\gamma\delta} = -\delta^{\alpha\beta}_{\mu\nu} + \hat{\Omega}^{\alpha\beta}_{\mu\nu}, \tag{22}$$

where

$$\delta^{\alpha\beta}_{\mu\nu} = \delta^{(\alpha}_{\mu}\delta^{\beta)}_{\nu} = \frac{1}{2}(\delta^{\alpha}_{\mu}\delta^{\beta}_{\nu} + \delta^{\beta}_{\mu}\delta^{\alpha}_{\nu})$$

and $\hat{\Omega}^{\alpha\beta}_{\mu\nu}$ identically satisfy the relations

$$\hat{\Omega}^{\alpha\beta}_{\mu\nu}\underset{n-1}{D}_{\alpha\beta} \equiv 0. \tag{23}$$

Using (20), it is easy to show that $\hat{\Gamma}^{\alpha\beta}_{\mu\nu}$ has the form

$$\hat{\Gamma}^{\alpha\beta}_{\gamma\delta} = 2\hat{U}\delta^{\alpha\beta}_{\gamma\delta}, \tag{24}$$

where $\hat{U}$ is an operator, an inverse d'Alembertian.

A further consequence of the relation (20) is the identity

$$\underset{0}{\nabla}{}^{\nu}\underset{n}{\gamma}_{\mu\nu} \equiv 0. \tag{25}$$

We note that a necessary condition for the existence of an operator inverse to the operator $\hat{B}^{\alpha\beta}_{\mu\nu}$ is condition (20), or equivalently, (25). Therefore only those coordinate conditions are compatible with the equations of successive approximations (15) which are compatible also with the identities (25).

B. Equations of Motion. In the Newtonian theory the velocities of bodies are zero-order quantities relative to the number γ/c^2. Therefore we put

$$\underset{0}{u}{}^{\mu} = \overset{0}{\underset{0}{u}}{}^{\mu} + \overset{1}{\underset{0}{u}}{}^{\mu}, \tag{26}$$

where $\overset{0}{\underset{0}{u}}{}^{\mu}$ is the velocity of the volume element relative to the center of mass of the body, determined from the zero-order equations, and $\overset{1}{\underset{0}{u}}{}^{\mu}$ is the velocity of the center of mass, determined from the first-order equations. From (26), we represent $\underset{0}{T}{}^{\mu\nu}$ as

where

$$\underset{0}{\nabla}_{\nu}\overset{0}{\underset{0}{T}}{}^{\mu\nu} = 0, \tag{16a}$$

$$\underset{0}{\nabla}_{\nu}\overset{1}{\underset{0}{T}}{}^{\mu\nu} + \underset{1}{\Pi}{}^{\nu}_{\alpha\nu}\overset{1}{\underset{0}{T}}{}^{\alpha\mu} + \underset{1}{\Pi}{}^{\mu}_{\alpha\nu}\overset{1}{\underset{0}{T}}{}^{\alpha\nu} = 0; \tag{16b}$$

from here we get the equations for $\underset{1}{T}{}^{\mu\nu}$

$$\underset{0}{\nabla}_{\nu}\underset{1}{T}{}^{\mu\nu} + \underset{1}{\Pi}{}^{\nu}_{\alpha\nu}\overset{0}{\underset{0}{T}}{}^{\alpha\mu} + \underset{1}{\Pi}{}^{\mu}_{\alpha\nu}\overset{0}{\underset{0}{T}}{}^{\alpha\nu} = 0. \tag{16c}$$

The higher-order approximations for the energy tensor are calculated by the general formula (16). If (16b) are multiplied by g and integrated over the volume, while throwing away the terms of higher order in smallness relative to v/c, we get the equations of motion in integral form, coinciding with the Fock equations.[3] Therefore the generally-covariant method gives more in the first approximation than the E.I.H. or Fock methods in the second approximation.

4. CONSERVATION LAWS

Formulas (20) and (25) can be interpreted as generalizations of the conservation laws. $\underset{n-1}{D}{}_{\mu\nu}$ can be pictured as the energy tensor of the field sources, consisting of two parts: the energy tensor of the matter and of the electromagnetic field $\underset{n-1}{T}{}_{\mu\nu}$ and the energy tensor of the gravitational field $\underset{n-1}{S}{}_{\mu\nu}$, entering as the field source. The tensor $\underset{n}{\gamma}{}_{\mu\nu}$ can be interpreted as the energy-momentum of the gravitational field realizing the interaction.

The conservation law (20) is different from the ordinary one. In the first place, the energy and momentum in the new law form a tensor, in distinction to the pseudotensor $t^{\mu\nu}$; and second, the conservation in the old law takes place in all coordinate systems, while, in the new law, conservation in the ordinary sense takes place only in inertial systems, when

$$\underset{0}{\Gamma}{}^{\mu}_{\alpha\beta} = 0.$$

In order to reconcile the two laws, one must suppose that the $t^{\mu\nu}$ represent the energy-momentum, not of a pure gravitational field, but of a gravitational field and a field of inertial forces. Actually, although the 4-momentum of a pure gravitational field $S_{\mu\nu}$ is conserved only in inertial systems, one can try to generalize this law by introducing fictitious inertial forces. Insofar as the 4-momentum of the latter do not form a tensor, the general expression for the 4-momentum of the field $t^{\mu\nu}$ does not form a tensor either. However, in the inertial reference system, when on the one hand the 4-momentum of the inertial forces goes to zero, and on the other the derivative $\underset{0}{\nabla}_{\nu}$ goes to $\partial/\partial x^{\nu}$, both conservation laws must coincide.

CONCLUSION

The proposed method has many features in common with the E.I.H. and Fock methods. For example, as in the E.I.H. method,[4] no coordinate conditions are set down beforehand; and, as in the Fock method, the Einstein equations with the right hand side and the equations $\nabla_{\nu}T^{\mu\nu} = 0$ are used. However, there are a great many differences, too.

As is well known, the E.I.H. method considers the metric of the space to zero order to be

$$\eta_{\mu\nu} = \begin{pmatrix} 1 & & & \\ & -1 & & \\ & & -1 & \\ & & & -1 \end{pmatrix}. \tag{27}$$

The coordinate system is not fixed, but the class of possible coordinates is limited by the requirement that the metric be quasi-Galilean, i.e., that it differ little from $\eta_{\mu\nu}$. Afterwards, when the first order corrections $\underset{1}{h}{}_{\mu\nu}$ are found, the class of possible coordinate systems becomes even more restricted, since the difference can be only in quantities of the second order $\underset{2}{h}{}_{\mu\nu}$. Continuing this process to infinity, one can uniquely fix the coordinate system.

In contrast to this, though the space in the zero order of the theory proposed is supposed Galilean, nevertheless its metric $\epsilon_{\mu\nu}$ does not, generally speaking, have the form (27). The system of coordinates is picked all at once and is not defined more and more from approximation to approximation, so that to pick one or the other coordinate system for the tensor $g_{\mu\nu}$, one must only give $\epsilon_{\mu\nu}$ in the corresponding system. If we pick, for example, Galilean coordinates in the zero approximation, we get the same coordinates as in the E. I. H. method.

Concerning the Fock method, the essential difference between it and the method proposed is its use of the harmonic conditions:

$$\partial\sqrt{-g}\, g^{\mu\nu}/\partial x^{\nu} = 0. \tag{28}$$

However, to first order in γ/c^2 the conditions (28) coincide with the identities

$$\underset{0}{\nabla}_{\nu}\underset{1}{\gamma}{}^{\mu\nu} = 0, \tag{25a}$$

obtained from (25) by raising the index μ with the aid of the tensor $\epsilon^{\mu\nu}$ and by writing it in Galilean (inertial) coordinates. According to this, the results obtained by the Fock method coincide with those got by the E.I.H. method.

The general difference between the present method and the preceeding ones is the choice of the small parameter λ. Previously, c^{-2} served as the expansion parameter, where it was supposed that the velocities of the bodies were small in comparison to c and that differentiation with respect to time led to a higher-order quantity. The choice of γ/c^2 as λ makes the generally-covariant method suitable for arbitrary velocities and arbitrary time variations of the fields.

Finally, the method proposed above makes it possible to pick uniquely an inertial reference system in which fictitious inertial forces exist. This coordinate system coincides with that fixed by the E.I.H. method and, approximately, with the harmonic system.

The author expresses his deep gratitude to Prof. M. G. Kreĭn and V. V. Malyarov for their interest in the work and for valuable discussions on questions arising from it.

---

[1] Einstein, Infeld, and Hoffman, Ann. Math. **39**, 65 (1938).

[2] Ya. I. Pugachev, Dissertation, Moscow State University, 1956.

[3] V. A. Fock, Теория пространства, времени и тяготения, (Theory of Space, Time and Gravitation), Gostekhizdat, 1955.

[4] A. Einstein and L. Infeld, Ann. Math. **41**, 455 (1940).

Translated by W. Ramsay
326

SOVIET PHYSICS JETP VOLUME 37 (10), NUMBER 6 JUNE, 1960

ON THE STABILITY OF A LOW PRESSURE PLASMA

B. B. KADOMTSEV

Submitted to JETP editor July 29, 1959

J. Exptl. Theoret. Phys. (U.S.S.R.) **37**, 1646-1651 (December, 1959)

A local stability condition for an arbitrary toroidal system is derived. The problem of the stability of a low pressure plasma in such systems is discussed.

1. In this paper the stability of a plasma in toroidal systems is investigated. In such systems the surfaces of constant pressure $p = \text{const}$ represent a family of surfaces of toroidal type enveloping each other, on which the lines of force of the magnetic field and the current lines lie in their entirety. Following Kruskal and Kulsrud[1] we introduce the following functions of p:

$$\psi = \int \mathbf{H} d\mathbf{S}_2, \qquad \chi = \int \mathbf{H}\, d\mathbf{S}_1;$$

$$I = \int \mathbf{j}\, d\mathbf{S}_2, \qquad J = \frac{c}{4\pi}\int \mathbf{H}\, d\mathbf{l}_1 - \frac{c}{4\pi}\int \mathbf{H}\, d\mathbf{l}_0 - \int \mathbf{j}\, d\mathbf{S}_1.$$

Here ψ is the longitudinal magnetic flux through the cross section S_2 of the surface of $p = \text{const}$; χ is the azimuthal flux through the surface S_1 passing through an arbitrary closed contour l_1 (which makes not a single turn about the small perimeter) along the toroid $p = \text{const}$, and the magnetic axis l_0, which is a limiting surface of constant pressure as its transverse dimension tends to zero; I is the longitudinal current, J is the azimuthal current including the current of the external winding; Ω is the volume of the toroid $p = \text{const}$.

For the investigation of stability it turns out to be more convenient to introduce a special curvilinear system of coordinates. We introduce on the surfaces $p = \text{const}$ or, what is the same thing, $\psi = \text{const}$, arbitrary longitudinal ζ' and transverse θ' coordinates which vary over the range from 0 to 1 as we go completely around the toroid. θ', ζ' together with ψ form a certain curvilinear coordinate system. As was shown in reference 1 the magnetic field may be represented in the geometry under consideration in the form

$$\mathbf{H} = \nabla\psi \times \nabla\vartheta, \tag{1}$$

where

$$\vartheta = \theta' - \mu\zeta' + \lambda, \qquad \mu = \mu(\psi) = d\chi/d\psi,$$

while λ is a certain single-valued function of the coordinates. As may be seen from (1), $\mathbf{H}\nabla\vartheta = 0$, i.e., the relation $\vartheta = \text{const}$ defines the position of the line of force on the surface $\psi = \text{const}$ and, consequently, the quantity μ represents the number of turns of the line of force along the small perimeter in one revolution along the toroid.

We now introduce new coordinates θ, ζ such that $\vartheta = \theta - \mu\zeta$. In terms of these coordinates as we move along ζ all the lines of force rotate with respect to θ with the same constant velocity μ. The choice of the coordinates θ, ζ is, of course, quite arbitrary, and this will be partially made use of in subsequent developments.

Since ϑ is defined up to an arbitrary function of ψ, then it is possible by choosing it, i.e., by displacing the origin of θ, ζ to insure that $G_{12} = G_{13} = 0$, where $G_{ik} = \int (g_{ik}/\sqrt{g})\, d\theta\, d\zeta$, g_{ik} is the metric tensor, $g = \operatorname{Det} g_{ik}$. We shall assume in future that this condition is satisfied.

In terms of the coordinates ψ, θ, ζ the contravariant components of the magnetic field are equal to $H^i = (1/\sqrt{g})\{0, \mu, 1\}$, while the covariant components are given by $H_i = \mu g_{i2}/\sqrt{g} + g_{i3}\sqrt{g}$. From this we obtain

$$I = \frac{c}{4\pi}\int\limits_{\zeta=\text{const}} H_2 d\theta = \frac{c}{4\pi}(\mu G_{22} + G_{23}),$$

$$J = \frac{c}{4\pi}\int\limits_{\theta=\text{const}} H_3 d\zeta = \frac{c}{4\pi}(\mu G_{23} + G_{33}). \tag{2}$$

As Kruskal and Kulsrud have shown the equation for plasma equilibrium may be written in the form

$$\frac{dp}{d\psi}\frac{d\Omega}{d\psi} = -\frac{1}{c}\left(\mu\frac{dI}{d\psi} + \frac{dJ}{d\psi}\right). \tag{3}$$

2. If the usual assumption of perfect conductivity is made it is convenient to utilize the energy principle[2,3] for the investigation of plasma stability. We assume that the plasma fills the whole volume up to the perfectly conducting walls. Then the normal component of the displacement of the plasma from the position of equilibrium reduces to zero at the walls and the total energy E of small vibrations is given in the hydrodynamic approximation by

$$E = T + V = \frac{\omega^2}{2}\int \rho\boldsymbol{\eta}^2 d\mathbf{r} + \frac{1}{2}\int \gamma p\,(\operatorname{div}\boldsymbol{\eta})^2\,d\mathbf{r}$$

$$+ \frac{1}{8\pi}\int (\operatorname{curl}\,[\boldsymbol{\eta}\times\mathbf{H}])^2\,d\mathbf{r} - \frac{1}{8\pi}\int [\boldsymbol{\eta}\times\operatorname{curl}\,\mathbf{H}]\operatorname{curl}[\boldsymbol{\eta}\times\mathbf{H}]d\mathbf{r}$$

$$+ \frac{1}{2}\int \boldsymbol{\eta}\nabla p\,\operatorname{div}\boldsymbol{\eta}\,d\mathbf{r}, \tag{4}$$

where ρ is the plasma density, ω is the increment (it is assumed that the displacement of the plasma from the position of equilibrium η varies with time in accordance with $e^{\omega t}$).

The equation for the small vibrations of the plasma may be obtained from the variational principle $\delta E = 0$, with the energy E of these oscillations itself being equal to zero. This means that instability may occur only in the case when the potential energy is negative. Therefore in investigating stability we could restrict ourselves only to the potential energy V. Nevertheless, we shall also investigate the kinetic energy T, which will enable us not only to obtain estimates for the increment ω but also to discuss correctly the behavior of a perturbation near a singular point.*

In this discussion we can restrict ourselves to the case of small increments $\omega \to 0$, since we are interested first of all in the stability criterion, i.e., in the condition under which a solution with $\omega > 0$ appears. By assuming the increment ω to be small, we shall temporarily neglect the kinetic energy. We shall decompose the displacement η into two terms $\eta = \eta_{tr} + \eta_{\|}$, where $\eta_{\|}$ is parallel to the vector $\mathbf{h} = \mathbf{H}/H$, while the third component η^3_{tr} vanishes. It may be easily shown that the component of the displacement $\eta_{\|}$ along the field does not appear in the last three terms of (4) and is contained only in the first two terms. If the perturbation is not constant along the lines of force then by means of an appropriate choice of $\eta_{\|}$ one may obtain the result that the second term in (4) vanishes, and then the potential energy will be equal to the sum of the last three terms, which we shall denote by V_{tr}.

The advantage of the variational principle consists of the fact that by utilizing different types of trial functions for η one can obtain certain necessary conditions for stability. We shall here investigate perturbations of the form

$$\eta^1 = \xi(\psi)\exp\{2\pi i\,(m\theta + n\zeta)\},$$

$$\eta^2 = -(i/2\pi)\,\alpha(\psi)\exp\{2\pi i\,(m\theta + n\zeta)\},$$

where, without restricting generality, ξ, α may be regarded as real functions. For such perturbations the potential energy V_{tr} takes on the following form

$$V_{tr} = \frac{1}{8\pi}\int\Big\{4\pi^2 G_{11}(\mu m + n)^2\xi^2 + G_{22}\Big(\frac{d}{d\psi}\mu\xi - n\alpha\Big)^2$$

$$+ 2G_{23}\Big(\frac{d}{d\psi}\mu\xi - n\alpha\Big)\Big(\frac{d\xi}{d\psi} + m\alpha\Big) + G_{33}\Big(\frac{d\xi}{d\psi} + m\alpha\Big)^2\Big\}\,d\psi$$

$$+ \frac{1}{2c}\int\Big\{c\frac{dp}{d\psi}\,\frac{d^2\Omega}{d\psi^2}\,\xi^2 + 2\alpha\xi\,(\mu m + n)\frac{dI}{d\psi} - \xi^2\frac{d\mu}{d\psi}\frac{dI}{d\psi}$$

$$- 2\xi\Big(\frac{d\xi}{d\psi} + m\alpha\Big)\Big(\mu\frac{dI}{d\psi} + \frac{dJ}{d\psi}\Big)\Big\}d\psi. \tag{5}$$

Here the first integral is always positive, and instability may arise only as a result of the second integral. Therefore, the neighborhood of the points $\psi = \psi_0$, where $\mu m + n = 0$ and the integrand of the first integral is a minimum, represents the greatest danger from the point of view of stability. As has been shown by Suydam[4] for the case of a straight filament with cylindrical symmetry, in the neighborhood of these points, where the displacement η is almost along the lines of force, an instability of local type may arise. A similar result was obtained by Johnson et al.[5] for a straight filament slightly inhomogeneous along its axis. It is of interest to generalize this discussion to the case of an arbitrary toroidal system.

In investigating an instability of local type we may in (5) set

$$\mu m + n = m\frac{d\mu}{d\psi}(\psi - \psi_0) \equiv m\mu' x$$

and assume that all the coefficients are constant. On minimizing the expression obtained above with respect to α we obtain after additional integration by parts

$$V_{tr} = \frac{1}{8\pi}\int\Big\{4\pi^2 G_{11} m^2\mu'^2 x^2\xi^2 + R\mu'^2\Big(\frac{d}{dx}x\xi\Big)^2\Big\}\,dx + \frac{1}{2}\int Q\xi^2 dx, \tag{6}$$

where

$$Q = \frac{dp}{d\psi}\Big\{\frac{d^2\Omega}{d\psi^2} - \frac{I\mu'}{\mu I + J}\frac{d\Omega}{d\psi} + \frac{1}{\mu I + J}\Big(\mu\frac{dI}{d\psi} + \frac{dJ}{d\psi}\Big)\frac{d\Omega}{d\psi}\Big\},$$

$$R = G_{22} - 4\pi I^2/c\,(\mu I + J) > 0.$$

We now take into account inertia which we had neglected earlier. It finds its expression not only in the existence of kinetic energy, but also in the fact that for small values of x the plasma does not have time to smooth out the pressure along the lines of force, and therefore it is necessary to take its compressibility into account. In order not to make the discussion too complicated, we simplify somewhat the expression for the kinetic energy T, viz. we shall replace it by a smaller quadratic form T′, which represents a sum of squares:

$$T' = \frac{\omega^2}{2}\int\Big\{A\Big(\frac{d\xi}{dx}\Big)^2 + B\eta_{\|}^2\Big\}\,d\mathbf{r}, \tag{7}$$

where $B \sim \rho$, $A \sim \rho a^2/m^2$, a is the small radius of the toroid $\psi = \text{const}$. Here we have completely neglected the kinetic energy of motion in the direction ψ, and have taken into account the fact that $m\alpha \sim d\xi/d\psi$. The replacement of T by T′ leads only to an overestimate of the increment ω, and has no effect at all on the condition of stability.

---

*The last consideration was pointed out by A. A. Vedenov.

By finding the minimum of $E = T' + V$ with respect to $\eta_{\|}$ we obtain

$$\omega^2 B\eta_{\|} - \gamma p\,(\mathbf{h}\nabla)\operatorname{div}\boldsymbol{\eta} = 0. \qquad (8)$$

Here $(\mathbf{h}\nabla) = (1/H\sqrt{g})\,d/d\zeta$, where $d/d\zeta$ is the total derivative along $\mathbf{h}$. Let

$$\eta_{\|} = f(\mathbf{r})\exp\{2\pi i\,(m\theta + n\zeta)\},$$

where $f(\mathbf{r})$ is some arbitrary real function. We multiply (8) by $H\sqrt{g}$ and integrate with respect to ζ along a line of force. On taking into account the fact that for small x the exponential $\exp\{2\pi i\,(m\theta + n\zeta)\}$ is a slowly varying function along a line of force, we obtain

$$(\omega^2/2\pi i m\mu' x)\langle BH\sqrt{g}\,f\rangle \times \exp\{2\pi i\,(m\theta+n\zeta)\} - \gamma p\operatorname{div}\boldsymbol{\eta} = 0, \qquad (9)$$

where the angular brackets indicate averaging along the line of force. We now multiply (9) by $\sqrt{g}\,\exp\{-2\pi i\,(m\theta + n\zeta)\}$ and integrate with respect to θ, ζ. On taking into account the fact that $\operatorname{div}\boldsymbol{\eta} = \operatorname{div}\boldsymbol{\eta}_{\mathrm{tr}} + (\mathbf{H}\nabla)\,\eta_{\|}/H$, we obtain

$$\frac{\omega^2}{2\pi i m\mu' x}\langle BH\sqrt{g}\,f\rangle\frac{d\Omega}{d\psi} - \gamma p\left\{\xi\frac{d^2\Omega}{d\psi^2} + 2\pi i m\mu' x\int\frac{f}{H}\,d\zeta\, d\theta\right\} = 0. \qquad (10)$$

From (9) and (10) we obtain

$$\operatorname{div}\eta = \frac{\omega^2}{\omega^2+\varkappa^2 x^2}\frac{d^2\Omega}{d\psi^2}\left(\frac{d\Omega}{d\psi}\right)^{-1}\xi\exp\{2\pi i\,(m\theta+n\zeta)\}, \qquad (11)$$

where

$$\varkappa^2 = 4\gamma p\pi^2 m^2\mu'^2\int\frac{f}{H}\,d\theta\, d\zeta\Big/\frac{d\Omega}{d\psi} \times\langle BH\sqrt{g}\,f\rangle \approx \gamma p\,\frac{4\pi^2 m^2\mu'^2}{\rho\,\langle H^2\rangle}\left(\frac{d\Omega}{d\psi}\right)^{-2}. \qquad (12)$$

On substituting (11) into the expression for the energy E and on neglecting the kinetic energy of longitudinal motion we finally obtain

$$E = \frac{1}{2}\int\left\{\omega^2 A\frac{d\Omega}{d\psi}\left(\frac{d\xi}{dx}\right)^2 + \frac{R}{4\pi}\mu'^2\left(\frac{d}{dx}x\xi\right)^2 + \gamma p\frac{\omega^4}{(\omega^2+\varkappa^2x^2)^2} \times\left(\frac{d^2\Omega}{d\psi^2}\right)^2\left(\frac{d\Omega}{d\psi}\right)^{-1}\xi^2 + \pi G_{11}m^2\mu'^2x^2\xi^2 + Q\xi^2\right\}dx. \qquad (13)$$

Variation of (13) with respect to ξ leads to a differential equation of the second order which may be brought into the following form

$$\frac{d^2u}{ds^2} - \left\{\frac{1}{(1+s^2)^2} + \frac{q}{1+s^2} + \frac{q'}{(1+s^2)(1+k^2s^2)^2} + \omega^2 b\frac{s^2}{1+s^2}\right\}u = 0, \qquad (14)$$

where

$$s^2 = \frac{R\mu'^2}{4\pi A\omega^2 d\Omega/d\psi}x^2,\quad u = \xi\sqrt{1+s^2},\quad b = \frac{16\pi^3 G_{11}Am^2 d\Omega/d\psi}{(R\mu')^2},$$
$$k^2 = \frac{4\pi A\varkappa^2 d\Omega/d\psi}{R\mu'^2} \sim \frac{8\pi p}{H^2},\quad q = \frac{4\pi Q}{R\mu'^2},\quad q' = \frac{4\pi\gamma p}{R\mu'^2}\left(\frac{d^2\Omega}{d\psi^2}\right)^2\left(\frac{d\Omega}{d\psi}\right)^{-1}.$$

Equation (14) is analogous to the Schrödinger equation for a particle whose potential energy is given by the expression in the figure brackets, while the existence of bound states with $\omega^2 > 0$ yields instability, while the absence of bound states corresponds to stability. In the region $s^2 \gg 1$ it simplifies considerably:

$$d^2u/ds^2 - qs^{-2}u = \omega^2 bu. \qquad (15)$$

As $\omega \to 0$ this equation has the solution $u = s^{\nu}$, where

$$\nu = \tfrac{1}{2} \pm \tfrac{1}{2}\sqrt{1+4q}.$$

Thus, if $q < -\frac{1}{4}$, then u is an oscillating function, and, consequently, instability occurs. On the other hand, by utilizing the comparison theorem it may be shown that equation (14) in the case $q > -\frac{1}{4}$ does not have any bound states, i.e., locally the plasma is stable. In expanded form this condition is represented by the following inequality:

$$\frac{dp}{d\psi}\left\{\frac{d^2\Omega}{d\psi^2} - \frac{I\mu'}{\mu I + J}\frac{d\Omega}{d\psi} + \frac{1}{\mu I+J}\left(\mu\frac{dI}{d\psi} + \frac{dJ}{d\psi}\right)\frac{d\Omega}{d\psi}\right\} > -\frac{R}{16\pi}\left(\frac{d\mu}{d\psi}\right)^2. \qquad (16)$$

An estimate shows that perturbations are local with respect to ψ only in the case $m^2 \gg 1$. Therefore condition (16) is only necessary: it refers only to perturbations with large values of m, i.e., which are local also with respect to the azimuth θ.

3. We now consider the case of a low-pressure plasma, when $\epsilon = 8\pi p/H^2 \ll 1$. In this case, as follows from the equation of equilibrium (3), $\mu dI/d\psi$ and $dJ/d\psi$ are small quantities together with $dp/d\psi$. We assume that the field is inhomogeneous along the torus (as is the case in the stellarator with a helical winding[6] and in traps with a corrugated field[7]), and we also assume that the magnitude of the field modulation is sufficiently large so that $d^2\Omega/d\psi^2$ is not a small quantity. Since the longitudinal current $I \sim \epsilon J \ll J$, then on the left hand side of the inequality (16) we may neglect all the terms with the exception of the first one, and we may set $R \approx G_{22}$.

By making use of the arbitrariness in the choice of the coordinates θ, ζ, we can make R a minimum. In order of magnitude we have

$$g_{22} \sim (2\pi r)^2, \qquad \sqrt{g} \sim \pi r^2\,(d\zeta/dz)^{-1},$$

where $r = r(z)$ is the average radius of the section $\zeta = \mathrm{const}$ of the toroid $\psi = \mathrm{const}$; z is a certain longitudinal coordinate $0 < z < L$, where L is the length of the toroid. It may be easily verified that G_{22} is a minimum at $\sqrt{g} \sim r$, i.e.,

$$G_{22}=4\pi^2a^2\left(\frac{d\Omega}{d\psi}\right)^{-1}=4\pi^2\left(\frac{d\Omega}{d\psi}\right)^{-1}\int\limits_0^L r^2\frac{dz}{L},$$

where a is the rms value of the small radius r.

On taking into account the fact that along a line of force $d\theta = \mu\, d\zeta$, and consequently, $dl = \sqrt{g}\, H\, d\zeta$, we obtain

$$\frac{d\Omega}{d\psi}=\iint\sqrt{g}\,d\theta d\zeta=\iint\frac{hdl}{H}\,d\theta=-U,$$

where U is the value of the integral along the line of force $\int dl/H$ averaged over θ. Thus, for systems with a sufficiently strongly modulated field the condition of stability (16) may be written in the form

$$\nabla p\nabla U<(\pi a^2/4\,|\,U\,|)\,(\nabla\mu)^2. \tag{17}$$

In a low pressure plasma $k^2 \sim \epsilon \ll 1$, therefore equation (14) may be reduced to the form (15) only when $s^2 \gg 1/\epsilon$, and the increment ω of the corresponding perturbations is of order $\sqrt{\epsilon/b}$. In the range $1 \ll s^2 \ll 1/\epsilon$ we should set $q + q'$ instead of q in equation (15), and the corresponding condition of stability then has the form $q + q' > -\frac{1}{4}$, or

$$\nabla p\nabla U<(\pi a^2/4\,|\,U\,|)\,(\nabla\mu)^2+\gamma p\,(\nabla U)^2/\,|\,U\,|. \tag{18}$$

This condition corresponds to more rapid compressible perturbations with $\omega \sim 1/\sqrt{b}$. In the case $\mu \to 0$ it goes over into the condition of stability for systems with closed lines of force,[7] while the increment of slower incompressible perturbations, for which the plasma has time to smooth out the pressure along the lines of force, tends to zero, so that condition (17) no longer applies for such a transition.

The condition (17) may be interpreted as the tendency of the plasma to occupy the space with the minimum "potential energy" U, with such a displacement being prevented by the effect of the cross over of the lines of force. Both in the stellarator with the helical winding, and in the trap with the corrugated field the "potential energy" U is minimal at the chamber walls, and this is where the plasma tends to migrate. In this respect they differ essentially from the system with guard rings,[7] where U is minimum inside the chamber and increases towards the outer conductors. Therefore, it would be desirable to carry out an experimental investigation of the stability of plasma in such systems.

---

[1] M. Kruskal and R. Kulsrud, Second United Nations Intern. Conf. on the Peaceful Uses of Atomic Energy, Geneva, 1958, P/1876.

[2] Hain, Lüst, and Schlüter, Z. Naturforsch. **12A**, 833 (1957).

[3] Bernstein, Frieman, Kruskal, and Kulsrud, Proc. Roy. Soc. (London) **A224**, 19 (1958).

[4] B. Suydam, Second United Nations Intern. Conf. on the Peaceful Uses of Atomic Energy, Geneva, 1958, P/354.

[5] Johnson, Oberman, Kulsrud, and Freiman, ibid. P/1875.

[6] L. Spitzer, ibid., P/2170.

[7] B. B. Kadomtsev and S. I. Braginskiĭ, ibid. P/2212.

Translated by G. Volkoff
327

SOVIET PHYSICS JETP VOLUME 37(10), NUMBER 6 JUNE, 1960

μ^--MESIC MOLECULAR PROCESSES IN HYDROGEN

V. B. BELYAEV, S. S. GERSHTEĬN, B. N. ZAKHAR' EV, and S. P. LOMNEV

Joint Institute of Nuclear Research

Submitted to JETP editor June 7, 1959

J. Exptl. Theoret. Phys. (U.S.S.R.) **37**, 1652-1662 (December, 1959)

A number of mesic atomic and mesic molecular processes are discussed that occur in a medium composed of hydrogen isotopes (formation of mesic molecules, $H_\mu^{(1)} + H^{(2)} \rightarrow (H^{(1)}H^{(2)})_\mu$; elastic collisions and charge transfer of mesic atoms, $H_\mu^{(1)} + H^{(2)} \rightarrow H_\mu^{(1)} + H^{(2)}$, $H_\mu^{(1)} + H^{(2)} \rightarrow H^{(1)} + H_\mu^{(2)}$). The levels of the mesic molecules are determined. The calculations were performed on the BÉSM electronic computer, with corrections for the motion of the nuclei taken into account to order m_μ/M.

A special feature of mesic hydrogen atoms is their neutral behavior, since at distances larger than the Bohr orbit of the mesic atom (2.57×10^{-11} cm) the charge of the nucleus is almost completely screened by that of the meson. This causes a number of mesic molecular processes that occur with μ^- mesons in hydrogen (or in a mixture of the hydrogen isotopes), such as the transfer of the μ^- meson between different nuclei (charge transfer), the formation of mesic hydrogen molecules, and so on. These processes play a large part in the catalysis of reactions in hydrogen which was predicted by Frank,[1] Zel'dovich,[2] and Sakharov[3] and has been studied experimentally in papers by Alvarez and others[4] and by Ashmore and others.[5] On the other hand, as has already been pointed out,[6-8] mesic molecular processes in hydrogen offer very important possibilities for the experimental determination of the law of the interaction $\mu^- + p \rightarrow n + \nu$ (in particular, for an experimental distinction between the $V-A$ and $V+A$ interaction types[8]).

Earlier papers have given the cross section for transfer of mesons from protons to deuterons,[9-12] and also calculations of the probability for the formation of the mesic molecules $(pp)_\mu$ and $(pd)_\mu$.[11,13] In the present paper we calculate the cross section for charge transfer and the probabilities of formation of mesic molecules for all the hydrogen isotopes.

Let us consider a system consisting of nuclei of hydrogen isotopes with the masses M_1 and M_2 and a μ^- meson. Let $\mathbf{r}$, $\mathbf{R}_1$, $\mathbf{R}_2$ be the coordinates of the meson and the nuclei.* With neglect of the spin interaction, the Hamiltonian of the system is

$$\hat{H} = -\frac{1}{2}\Delta_{\mathbf{r}} - \frac{1}{2M_1}\Delta_{\mathbf{R}_1} - \frac{1}{2M_2}\Delta_{\mathbf{R}_2} - \frac{1}{r_1} - \frac{1}{r_2} + \frac{1}{R}, \quad (1)$$

where

$$r_1 = |\mathbf{r} - \mathbf{R}_1|, \ r_2 = |\mathbf{r} - \mathbf{R}_2|; \ R = |\mathbf{R}_2 - \mathbf{R}_1|.$$

Assuming that the μ^- meson is in a K orbit, we shall try to find the wave function of the system in the form

$$\Psi = G(\mathbf{R})\Sigma_g(R; \mathbf{r}) + H(\mathbf{R})\Sigma_u(R; \mathbf{r}), \quad (2)$$

where $G(\mathbf{R})$ and $H(\mathbf{R})$ describe the relative motion of the nuclei,* and Σ_g and Σ_u represent wave functions of the μ^- meson in the field of stationary nuclei separated by the distance R. For $R \rightarrow \infty$

$$\Sigma_g \rightarrow (e^{-r_1} + e^{-r_2})/\sqrt{2\pi}; \quad \Sigma_u \rightarrow (e^{-r_1} - e^{-r_2})/\sqrt{2\pi}, \quad (3)$$

and for $R \rightarrow 0$ the wave functions Σ_g and Σ_u respectively go over into the wave functions of the 1s and 2p states of the He ion.

Substituting Eq. (2) in the Schrödinger equation

$$\hat{H}\Psi = E\Psi \quad (4)$$

and using the fact that the wave functions Σ_g and Σ_u satisfy the equation

$$\left(-\frac{1}{2}\Delta_r - \frac{1}{r_1} - \frac{1}{r_2} + \frac{1}{R}\right)\Sigma_i = E_i(R)\Sigma_i(\mathbf{r}, R) \quad (i = g, u), \quad (5)$$

after multiplication by Σ_g and Σ_u and integrating over the coordinates of the meson we get a system of equations for $G(\mathbf{R})$ and $H(\mathbf{R})$:

---

*In what follows we shall use mesic atomic units ($\hbar = 1$, $e = 1$, $m_\mu = 207 m_e = 1$; the mesic atomic unit of length is $\hbar/m_\mu e^2 = 2.57 \times 10^{-11}$ cm, and the mesic atomic unit of energy is $m_\mu e^4/\hbar^2 = 5.6 \times 10^3$ ev.

*We note that since the wave function (2) depends only on the difference of the coordinates in the coordinate system we have chosen, the center of mass of the system is at rest.

$$-\frac{1}{2M_{12}}\Delta_R G+\left(E_g+\frac{1}{2M_{12}}K_{gg}\right)G$$
$$+\frac{1}{2M_{12}}K_{gu}H-\frac{1}{M_{12}}\mathbf{Q}_{gu}\nabla_R H=EG,$$
$$-\frac{1}{2M_{12}}\Delta_R H+\left(E_u+\frac{1}{2M_{12}}K_{uu}\right)H$$
$$+\frac{1}{2M_{12}}K_{ug}G-\frac{1}{M_{12}}\mathbf{Q}_{ug}\nabla_R G=EH, \tag{6}$$

where $1/M_{12} = 1/M_1 + 1/M_2$ and the quantities $K_{ij}/2M_{12}$ and Q_{ij}/M_{12} are the matrix elements between the functions Σ_g and Σ_u of the operators

$$\frac{1}{2M_{12}}\hat{K}=-\frac{1}{2}\left(\frac{1}{M_1}\Delta_{\mathbf{R}_1}+\frac{1}{M_2}\Delta_{\mathbf{R}_2}\right),$$
$$\frac{1}{2M_{12}}\hat{\mathbf{Q}}=\left(-\frac{1}{M_1}\nabla_{\mathbf{R}_1}+\frac{1}{M_2}\nabla_{\mathbf{R}_2}\right). \tag{7}$$

It is easy to show that in virtue of the normalization conditions for Σ_g and Σ_u the diagonal matrix elements of the operator $\hat{\mathbf{Q}}$ are zero, and because of the orthogonality of Σ_g and Σ_u the off-diagonal elements are opposite in sign:

$$\mathbf{Q}_{gu}=-\mathbf{Q}_{ug}=\mathbf{Q}. \tag{8}$$

If we use the symmetry properties of Σ_g and Σ_u under interchange of the nuclei, we can separate out the dependence of the matrix elements on the masses:

$$K_{ii}=\int\Sigma_i(-\Delta_{R_1})\Sigma_i d\tau \quad (i=g,\ u),$$
$$K_{ij}=\frac{M_2-M_1}{M_2+M_1}\int\Sigma_i(-\Delta_{\mathbf{R}_1})\Sigma_j d\tau \quad (i\neq j),$$
$$\mathbf{Q}=\frac{M_2-M_1}{M_2+M_1}\int\Sigma_g(-\nabla_{\mathbf{R}_1})\Sigma_u\,d\tau=Q\frac{\mathbf{R}}{R}. \tag{9}$$

Thus in the case of identical nuclei, $M_1 = M_2$, the system of equations (6) falls apart into two independent equations. This result is quite understandable, since because of symmetry in the case of identical nuclei the wave function (2) can contain only one term (either Σ_g or Σ_u). The terms $K_{ij}(R)/2M_{12}$ and $Q(R)/M_{12}$ are corrections to the adiabatic potentials which take into account the motion of the nuclei to first order in m_μ/M_{12}. Since for the meson the ratio m_μ/M_{12} is not as small as it is for the electron, these terms make an important contribution. For $R \to \infty$, $Q \to 0$, and the terms $K_{ij}(\infty)/2M_{12}$ give to accuracy $(m_\mu/M_1)^2$, $(m_\mu/M_2)^2$, the corrections that come from the reduced masses in the isolated mesic atoms. In fact, if we note that the energy of the isolated mesic atoms (in mesic atomic units) is

$$E_1^0=-M_1/2(M_1+1)\approx-{}^1/_2+1/2M_1;$$
$$E_2^0=-M_2/2(M_2+1)\approx-{}^1/_2+1/2M_2 \tag{10}$$

and use the fact that for $R \to \infty$ the matrix elements of the operator $(-\Delta_{\mathbf{R}_1})$ are equal to $\frac{1}{2}$ (Appendix), we can write

$$\{E_g(\infty)+K_{gg}(\infty)/2M_{12}\}$$
$$=\{E_u(\infty)+K_{uu}(\infty)/2M_{12}\}=(E_1^0+E_2^0)/2,$$
$$K_{gu}(\infty)/2M_{12}=K_{ug}(\infty)2M_{12}=(E_1^0-E_2^0)/2=\Delta E/2. \tag{11}$$

Removing from the quantities $E_g(R)$, $E_u(R)$, and $K_{ij}(R)/2M_{12}$ their values for $R = \infty$,

$$E_{gu}(R)=E_{gu}(\infty)+E'_{gu}(R),\quad K_{ij}(R)=K_{ij}(\infty)+K'_{ij}(R),$$

we rewrite the system of equations (6) in the form

$$-\frac{1}{2M_{12}}\Delta_R G+\left(E'_g+\frac{1}{2M_{12}}K'_{gg}\right)G$$
$$+\left(\frac{1}{2}\Delta E+\frac{1}{2M_{12}}K'_{gu}\right)H-\frac{1}{M_{12}}Q\frac{dH}{dR}=E'G,$$
$$-\frac{1}{2M_{12}}\Delta_R H+\left(E'_u+\frac{1}{2M_{12}}K'_{uu}\right)H$$
$$+\left(\frac{1}{2}\Delta E+\frac{1}{2M_{12}}K'_{ug}\right)G+\frac{1}{M_{12}}Q\frac{dG}{dR}=E'H, \tag{12}$$

where the energy E' is the energy relative to the half sum of the levels of the isolated mesic atoms:

$$E'=E-(E_1^0+E_2^0)/2$$

(in the case of identical nuclei E' is measured simply from the level of the isolated mesic atom).

Separating the angular dependence of $G(\mathbf{R})$ and $H(\mathbf{R})$,

$$G_L(\mathbf{R})=R^{-1}g_L(R)Y_{L,\,M_L}(\theta,\ \varphi),$$
$$H_L(\mathbf{R})=R^{-1}h_L(R)Y_{L,\,M_L}(\theta,\ \varphi) \tag{13}$$

[where $Y_{L,M_L}(\theta, \varphi)$ is a spherical harmonic], we get for $g(R)$ and $h(R)$ the equations

$$-\frac{1}{2M_{12}}\frac{d^2g_L}{dR^2}+\left(E'_g+\frac{1}{2M_{12}}K'_{gg}+\frac{L(L+1)}{2M_{12}R^2}\right)g_L$$
$$+\left(\frac{1}{2}\Delta E+\frac{1}{2M_{12}}K'_{gu}\right)h_L-\frac{1}{2M_{12}}QR\frac{d}{dR}\left(\frac{h_L}{R}\right)=E'g_L,$$
$$-\frac{1}{2M_{12}}\frac{d^2h_L}{dR^2}+\left(E'_u+\frac{1}{2M_{12}}K'_{uu}+\frac{L(L+1)}{2M_{12}R^2}\right)h_L$$
$$+\left(\frac{1}{2}\Delta E+\frac{1}{2M_{12}}K'_{ug}\right)g_L+\frac{1}{M_{12}}QR\frac{d}{dR}\left(\frac{g_L}{R}\right)=E'h_L.$$

The potentials $E'_g(R)$ and $E'_u(R)$ have been determined from the equations (5) by many authors, beginning with a paper by Teller.[14] In the present work we have used values of $E'_g(R)$ and $E'_u(R)$ taken from a paper by Bates et al.[15] Values of the functions $K'_{gg}(R)$ and $K'_{uu}(R)$ can be obtained by a slight recalculation from a paper by Dalgarno and McCarroll,[16] and the values of $Q(R)$, $K'_{ug}(R)$, $K'_{gu}(R)$ have been calculated in the "united atom" (UA) and "linear combination of atomic orbitals" (LCAO)[15] approximations for small and large values of R, respectively (for further details see

Appendix). In studying the asymptotic behavior of the solution for R → ∞ it is convenient to introduce the functions

$$a_L(R)=\{g_L(R)+h_L(R)\}/\sqrt{2},$$
$$b_L(R)=\{g_L(R)-h_L(R)\}/\sqrt{2}. \qquad (14)$$

Comparing them with Eqs. (2) and (3), it is easy to see that for R → ∞ the functions a(R) and b(R) respectively describe the radial motion of the nucleus of mass M_2 relative to the mesic atom with mass M_1 and that of the nucleus of mass M_1 relative to the mesic atom of mass M_2.

The functions (14) satisfy the equations

$$-\frac{1}{2M_{12}}\frac{d^2a_L}{dR^2}+\left\{\frac{1}{2}\left[\left(E'_g+\frac{K'_{gg}}{2M_{12}}\right)+\left(E'_u+\frac{K'_{uu}}{2M_{12}}\right)\right]\right.$$
$$\left.+\frac{1}{4M_{12}}(K'_{gu}+K'_{ug})+\frac{L(L+1)}{2M_{12}R^2}+\frac{\Delta E}{2}\right\}a_L$$
$$+\left\{\frac{1}{2}\left[\left(E'_g+\frac{K'_{gg}}{2M_{12}}\right)-\left(E'_u+\frac{K'_{uu}}{2M_{12}}\right)\right]\right.$$
$$\left.-\frac{1}{4M_{12}}(K'_{gu}-K'_{ug})\right\}b_L+\frac{Q}{M_{12}}R\frac{d}{dR}\left(\frac{b_L}{R}\right)=E'a_L,$$

$$-\frac{1}{2M_{12}}\frac{d^2b_L}{dR^2}+\left\{\frac{1}{2}\left[\left(E'_g+\frac{K'_{gg}}{2M_{12}}\right)+\left(E'_u+\frac{K_{uu}}{2M_{12}}\right)\right]\right.$$
$$\left.-\frac{1}{4M_{12}}(K_{gu}-K_{ug})+\frac{L(L+1)}{2M_{12}R^2}-\frac{\Delta E}{2}\right\}b_L$$
$$+\left\{\frac{1}{2}\left[\left(E'_g+\frac{K'_{gg}}{2M_{12}}\right)-\left(E'_u+\frac{K'_{uu}}{2M_{12}}\right)\right]\right.$$
$$\left.+\frac{1}{4M_{12}}(K'_{gu}-K'_{ug})\right\}a_L-\frac{Q}{M_{12}}R\frac{d}{dr}\left(\frac{a_L}{R}\right)=E'b_L \qquad (15)$$

and the boundary condition at R = 0

$$a(0)=b(0)=0. \qquad (16)$$

For R → ∞, Eqs. (15) have the form

$$-\frac{1}{2M_{12}}\frac{d^2a}{dR^2}=\left(E'-\frac{\Delta E}{2}\right)a,$$
$$-\frac{1}{2M_{12}}\frac{d^2b}{dR^2}=\left(E'+\frac{\Delta E}{2}\right)b. \qquad (17)$$

For definiteness let $M_1 < M_2$, so that $\Delta E > 0$. Then three types of motion are possible, depending on the value of E′.

a) $E' > \frac{1}{2}\Delta E$, i.e., the energy lies above the K level of the lighter mesic atom. The meson can be either on the nucleus M_1 or on the nucleus M_2. If the meson was originally on the nucleus M_1 and charge transfer occurs to the nucleus M_2, we must impose on the wave functions the condition that for R → ∞ the function b(R) must contain only a diverging wave:

$$a(R)\approx C_1e^{ik_1R}+C_2e^{-ik_1R}, \quad b(R)\approx C_3e^{ik_2R};$$
$$k_1^2=2M_{12}\left(E'-\tfrac{1}{2}\Delta E\right), \quad k_2^2=2M_{12}\left(E'+\tfrac{1}{2}\Delta E\right). \qquad (18)$$

b) $-\frac{1}{2}\Delta E < E' < \frac{1}{2}\Delta E$, i.e., the energy lies between the levels of the isolated mesic atoms. At R → ∞ the meson cannot be on the lighter nucleus for energetic reasons. This case corresponds to scattering of a mesic atom with nucleus M_2 by the nucleus M_1, without the possibility of charge transfer. We must impose on the wave functions the condition that for R → ∞ the function a(R) must not contain an exponentially increasing term:

$$a(R)\approx D_1e^{-\varkappa_1R}, \ b(R)\approx D_3e^{-ik_2R}+D_4e^{ik_2R};$$
$$\varkappa_1^2=-k_2^2=-2M_{12}\left(E'-\tfrac{1}{2}\Delta E\right). \qquad (19)$$

It is obvious that the conditions (16) and (19) [and also the conditions (16) and (18)] can be satisfied for any energy in the range in question, and that apart from normalization they determine the solution of the system of equations (15).

c) $E' < -\frac{1}{2}\Delta E$ is the region of the discrete spectrum, corresponding to bound states of the mesic molecule. For R → ∞ two conditions are to be imposed on the solution — the absence of increasing exponentials in both of the functions a(R) and b(R):

$$a(R)\approx F_1e^{-\varkappa_1R}, \quad b(R)\approx F_2e^{-\varkappa_2R};$$
$$\varkappa_1^2=2M_{12}\left(|E'|+\tfrac{1}{2}\Delta E\right), \quad \varkappa_2^2=2M_{12}\left(|E'|\tfrac{1}{2}\Delta E\right). \qquad (20)$$

The conditions (20) and (16) can be satisfied only for definite values of E′, which are the energy levels of the mesic molecule. To find solutions that satisfy the conditions (16) at R = 0 and asymptotic conditions of the type (18), (19), or (20) for R → ∞, we can proceed as follows: find two linearly independent solutions satisfying the conditions (16), and construct from them a linear combination satisfying the asymptotic conditions for R → ∞. We note that between any two solutions of the system of two second-order linear equations (12) there exists a relation, which we can find easily if we note that

$$K'_{gu}-K'_{ug}=-2\,\mathrm{div}\,\mathbf{Q}.$$

In fact, if $\{G_1; H_1\}$ and $\{G_2; H_2\}$ are solutions of the system (12), then

$$\mathrm{div}\,\{(G_2\nabla G_1-G_1\nabla G_2)+(H_2\nabla H_1-H_1\nabla H_2)$$
$$+2\mathbf{Q}(H_1G_2-H_2G_1)\}=0. \qquad (21)$$

For the functions (14), which satisfy the conditions (16), the identity (21) takes the form

$$(a_2da_1/dR-a_1da_2/dR)+(b_2db_1/dR-b_1db_2/dR)$$
$$+2Q(a_1b_2-a_2b_1)=0. \qquad (22)$$

The relation (22) can be used to check the accuracy of numerical integrations. As our linearly independent solutions of the equations (15) we can take, for example, the solutions given at $R = 0$ by the conditions*

$$a(0) = b(0) = 0,\ a'(0) = b'(0) = 1 \quad \text{or}\ g(0) = h(0) = h'(0),\ g'(0) = \sqrt{2}; \tag{23}$$

$$a(0) = b(0) = 0,\ a'(0) = -b'(0) = 1 \ \text{or}\ g(0) = h(0) = g'(0),\ h'(0) = \sqrt{2}. \tag{24}$$

The charge-exchange cross section. In the energy range $E' \geq \Delta E/2$ we can form from the independent solutions (15) fixed at $R = 0$ by the conditions (23) and (24) a linear combination that satisfies Eq. (18). The effective cross section for charge exchange is determined from the asymptotic form of the solutions for $R \to \infty$ by a procedure analogous to that in reference 10. The effective charge-exchange cross section can be represented in the form

$$\sigma_{\text{ce}} = 4\pi f a_\mu^2 v_0 / v$$

(where v is the speed before the collision, $v_0 = (2\Delta E/M_{12})^{1/2}$, and $a_\mu = \hbar^2/m_\mu e^2$). Values of the coefficient f determined by numerical computation are shown in Table I, which also shows values of the quantity $\sigma_{\text{ce}} v$.

TABLE I

Process	f	$\sigma_{\text{ce}}v$, cm³/sec
$p_\mu + d \to d_\mu + p$	2.11	$3.42 \cdot 10^{-13}$
$p_\mu + t \to t_\mu + p$	0.84	$1.49 \cdot 10^{-13}$
$d_\mu + t \to t_\mu + d$	0.0067	$1.15 \cdot 10^{-15}$

Cross section for scattering of a heavy mesic atom by nuclei of a lighter isotope.† In the energy range $-\Delta E/2 < E' < \Delta E/2$, for the case of small concentration of the heavy hydrogen isotope, the most important process is the elastic scattering of the heavy mesic atoms by the nuclei of the light isotope, and thereafter, after slowing down of the mesic atom, the formation of mesic molecules. By forming from the linearly independent solutions fixed by the conditions (23) and (24) a linear combination satisfying Eq. (19), one can easily express the effective cross section for elastic scattering in terms of the parameters of the solutions for $R \to \infty$. For mesic atoms with small kinetic energy the wave functions in the region $r_0 \ll R \ll 1/k_2$ are of the form

$$b \approx R - \lambda,\quad a \approx D \exp\{-\varkappa_1^0 R\},\quad \varkappa_1^0 = \sqrt{2M_{12}\Delta E}. \tag{25}$$

TABLE II

Process	λ	$10^{20}\sigma_{el}$, cm²
$d_\mu + p \to d_\mu + p$	2.03	3.39
$t_\mu + p \to t_\mu + p$	2.66*	5.84*
$t_\mu + d \to t_\mu + d$	6.7	36.9

*Value obtained with $K_{gg} = 0$. The calculations with the correct K_{gg} give a value $\lambda \sim 10$, which is dubious.

The normalization in Eq. (25) is chosen so that for $R \to \infty$ we have a plane wave with coefficient 1. The effective scattering cross section is given by $\sigma_{el} = 4\pi\lambda^2 a_\mu^2$. Values of λ and σ_{el} for various cases are shown in Table II. We note that the value of σ_{el} for the case $d_\mu + p \to d_\mu + p$ is not anomalously small, as was stated by Cohen, Judd, and Riddell.[11] The range l of a d_μ atom formed by charge transfer can be found from the formula

$$l = (1/kN\bar{\sigma}_{\text{el}}) \ln(E_1/E_2), \tag{26}$$

where $k = 2M_{12}/(M_1 + M_2) = 4/9$ is the average fraction of the energy transferred in a $d_\mu + p$ collision; $N = 4 \times 10^{22}$; $E_1 = 45$ ev is the energy received by the mesic atom d_μ in the charge transfer; and $E_2 \sim 2 \times 10^{-4}$ ev is the final (thermal) energy (furthermore it is assumed as a rough approximation that the d_μ moves in a straight line, since in the laboratory coordinate system the deflection of the d_μ in a collision with a proton cannot exceed 30°). According to Eq. (26) the value of the range is $l \sim 0.1$ mm (the displacement on account of diffusion of the d_μ at thermal energy is also of the order of 0.1 mm); this is clearly smaller than the experimentally observed "gap" of ~1 mm.

The energy levels of mesic molecules. For the energy range $E' < -\frac{1}{2}\Delta E$ let the solutions of the equations (15) with the respective initial conditions (23) and (24) have the forms

$$a_i(R) \approx F_1^{(i)}(E')\, e^{-\varkappa_1 R} + F_2^{(i)}(E')\, e^{\varkappa_1 R},$$
$$b_i(R) \approx F_3^{(i)}(E')\, e^{-\varkappa_2 R} + F_4^{(i)}(E')\, e^{\varkappa_2 R} \qquad (i = 1.2). \tag{27}$$

Then when we form a linear combination of these solutions we can secure elimination of the increasing exponentials only provided

$$\begin{vmatrix} F_2^{(1)}(E') & F_2^{(2)}(E') \\ F_4^{(1)}(E') & F_4^{(2)}(E') \end{vmatrix} = 0. \tag{28}$$

The condition (28) determines the energy levels of

---

*Since the functions $a(R)$ and $b(R)$ fall off exponentially inside the potential barriers for $R \to 0$, in the numerical integration we can, without appreciable error, prescribe the conditions (23) and (24) for some small value $R_0 \neq 0$ ($R_0 = 0.2$). This corresponds to replacement of the potentials $E_g + K_{gg}/2M_{12}$ and $E_u + K_{uu}/2M_{12}$ by infinite walls at $R = R_0$.

†The wave functions of the continuous spectrum, and also those for the energy levels, are given in a preprint by V. B. Belyaev, S. S. Gershteĭn, B. I. Zakhar'ev, and S. P. Lomnev, issued at the Joint Institute of Nuclear Research.

TABLE III. Levels of mesic molecules*

	$L=0$		$L=1$		$L=2$	$L=3$
	$n=0$	$n=1$	$n=0$	$n=1$	$n=0$	$n=0$
$(pp)_\mu$	252	—	109	—	—	—
$(dd)_\mu$	330	40	226	7?	88	—
$(tt)_\mu$	367	86	288	45	170	55
$(pd)_\mu$	220	—	90	—	—	—
$(pt)_\mu$	213	—	98	—	—	—
$(dt)_\mu$	319	32	232	—	102	—

*The levels are given in electron volts; for mesic molecules with unlike nuclei the energy levels are measured from the level of the heavier isotope.

the mesic molecules. By carrying out numerical integrations of the system (15) for various values of E' one can pick out the values that satisfy the condition (28). Energy levels of the mesic molecules obtained in this way are shown in Table III.

Energy levels of mesic molecules with identical nuclei. As has already been noted, for mesic molecules with identical nuclei the system falls apart into two independent equations. The effective interaction potentials with corrections allowing for the motion of the nuclei, $E'_g + K'_{gg}/2M_{12}$, are approximated to good accuracy by the well known Morse function

$$U = A\left[e^{-2\alpha(R-R_0)} - 2e^{-\alpha(R-R_0)}\right].$$

Values of the effective interaction potentials have been given in a dissertation* by Gershteĭn; it also gives parameters for the Morse function which give good approximations.† The deviations of the Morse functions from the true values of the effective interaction potentials cannot cause much change in the values of the levels, since these deviations are appreciable only in the regions (of very large and very small R) where the wave functions fall off exponentially. The values of the levels are shown in Table III.

Formation of mesic molecular ions. Moving through the medium, mesic hydrogen atoms can pass freely through the electron shells of the hydrogen molecules because of their neutrality and small size; approaching the nuclei, they can form mesic molecules, or more exactly mesic molecular ions, $(pp)^+_\mu$, $(pd)^+_\mu$, and so on (in analogy with the well known molecular ions H_2^+, HD^+, and so on). In principle the binding energy of the mesic molecule can be released as radiation or transferred to one of the electrons of the shell, or also to the nucleus that had been chemically bound to the one with which the mesic molecule (H_2) is formed. This latter sort of transition, however, can contribute appreciably only in a case in which the mesic molecule is formed with a very small binding energy (of the order of the binding energy of the ordinary molecule). As can be seen from Table III, this condition is not satisfied for any of the mesic molecules [with the possible exception of $(dd)_\mu$]. Since the dimensions of mesic molecules are much smaller than atomic dimensions, the ratios between the probabilities of formation of mesic molecules by radiative processes and by transfer of energy to an electron of the shell can be found by using the standard theory of internal conversion by electrons in nuclear transitions. For the range of energy transfers in question (tens and hundreds of ev) the internal conversion coefficients are extremely large; therefore the probabilities of radiative formation of mesic molecules are very much smaller than that for conversion formation of these molecules. Since the formation of mesic molecules occurs at small relative energies of the mesic atoms, the most important process will be the electric dipole transition from the s wave of the continuous spectrum, with internal conversion to an electron.

Let ρ_1, ρ_2, and ρ_μ be the respective distances from the nuclei M_1 and M_2 and the μ^- meson to an arbitrary point; then at large distances the Coulomb field of the system is of the form

$$e/\rho_1 + e/\rho_2 - e/\rho_\mu \approx e/\rho + \mathbf{d}\rho/\rho^3,$$

where ρ is the distance from the center of mass of the nuclei and $\mathbf{d}$ is the dipole moment of the system:

$$\mathbf{d} = e\mathbf{R}\,(M_2 - M_1)/2\,(M_2 + M_1) - e\,(\mathbf{r}_1 + \mathbf{r}_2)/2, \tag{29}$$

where

$$\mathbf{R} = \mathbf{R}_2 - \mathbf{R}_1,\ \mathbf{r}_1 = \mathbf{r} - \mathbf{R},\ \mathbf{r}_2 = \mathbf{r} - \mathbf{R}_2.$$

---

*Defended at the Institute of Physical Problems, Academy of Sciences, U.S.S.R.

†Compare with reference 17, where the approximations were made without including corrections for the motion of the nuclei.

If we take as the wave functions of the electron the exact Coulomb functions of the hydrogen atom, then in analogy with the conversion probability for a nuclear transtion we get for the probability of formation of a mesic molecule by dipole conversion

$$W = \frac{16}{3}\,\frac{1}{\hbar a_e^3}\,\frac{2\pi\eta^2 \exp(-4\eta \tan^{-1}\eta)\,N}{(1+\eta^2)(1-\exp\{-2\pi\eta\})}\sum_{M_L}|\langle \mathrm{d}\rangle|^2, \qquad (30)$$

where $a_e = \hbar^2/m_e e^2$, $\eta = e^2/\hbar v_e$ (m_e and v_e are the mass and speed of the electron), $N = 4 \times 10^{22}$ cm^{-3} is the number of nuclei in 1 cm^3, and $\langle \mathrm{d} \rangle$ is the matrix element of the dipole moment taken between wave functions of the mesic molecule belonging to the continuous and discrete spectra, respectively,

$$\langle \mathrm{d}\rangle = \int \Psi_{mol}^{f*}\,\mathrm{d}\Psi_{mol}^{i}\,d\mathrm{R}\,d\mathrm{r}_\mu \qquad (31)$$

[the integration in Eq. (31) is taken over the coordinates of the μ^- meson and the nuclei]. Integration over the meson coordinates in Eq. (31) leads to the integral

$$\mathrm{d}_{gu} = \int \Sigma_g \frac{1}{2}(\mathrm{r}_1 + \mathrm{r}_2)\,\Sigma_u d\mathrm{r}_\mu.$$

From considerations of symmetry it is clear that $\mathbf{d}_{gu}$ is directed along $\mathbf{R}$: $\mathbf{d}_{gu} = \gamma(R)\,\mathbf{R}$, where $\gamma(R)$ is some function of R. In the LCAO approximation we have

$$\gamma(R) = 1/2\sqrt{1 - e^{-2R}(1 + R + R^2/3)^2} \approx -{}^1/_2 \text{ for } R > 3.$$

The LCAO approximation is not valid for small R, but it is clear that since the nuclear function H(R) that corresponds to the repulsive state Σ_u falls off exponentially at small R, small values of R make a negligible contribution to the matrix element $\langle \mathrm{d} \rangle$. We note that the approximation $\gamma = -{}^1/_2$ holds well even for small R, if the calculation of d_{gu} is made with the exact functions Σ_g and Σ_u.[18] The summation in Eq. (30) is taken over all possible final states of the mesic molecule. In the calculation of $\langle \mathrm{d} \rangle$ it is assumed that the normalization of the continuous-spectrum wave function is chosen so that at infinity there is a plane wave with the coefficient 1, and the discrete-spectrum wave function is of course normalized to unity. The matrix element $\langle \mathrm{d} \rangle$ then has the dimensions $^{5/2}_{\mu}$, where $a_\mu = \hbar^2/m_\mu e^2$. Separating out the dimensional factor, we can conveniently rewrite the formula (30) in the form

$$W = \frac{16}{3}(Na_e^3)\left(\frac{m_e}{m_\mu}\right)^5 \frac{e^2}{\hbar a_e}\,\frac{2\pi\eta^2 \exp\{-4\eta \tan^{-1}\eta\}}{(1+\eta^2)(1-\exp\{-2\pi\eta\})}\left\{\sum_{M_L}|\langle \mathrm{d}\rangle|^2\right\}, \qquad (32)$$

where the matrix element $\langle \mathrm{d} \rangle$ is calculated in dimensionless ("mesic-atomic") units. It is easy to see that the first term in the dipole moment (29) has nonvanishing matrix elements only for transitions with meson functions of the same parity ($\Sigma_g \rightarrow \Sigma_g$; $\Sigma_u \rightarrow \Sigma_u$), whereas the second term in Eq. (29) gives transitions only between meson functions of different parities ($\Sigma_u \rightarrow \Sigma_g$; $\Sigma_g \rightarrow \Sigma_u$). Dipole transitions from the s wave of the continuous spectrum can occur only to the rotational state with L = 1. It can be seen from Table III that for all the mesic molecules [except $(tt)_\mu$] the transition goes into the lowest such rotational level (L = 1; n = 0). For the mesic molecule $(tt)_\mu$ the transition into a vibration-rotation level (L = 1; n = 1) is also possible. The probabilities for the formation of the mesic molecules $(dd)_\mu$ and $(tt)_\mu$ with identical nuclei can be calculated in the same way as has been done for the mesic molecule $(pp)_\mu$.[13] In units of 10^6 sec^{-1}, the probabilities for formation of these mesic molecules are

$(pp)_\mu$	$(dd)_\mu$	$(tt)_\mu$
1.53	0.0057	0.38

For mesic molecules with unlike nuclei the calculations of greatest interest are those that give the probabilities for formation of mesic molecules in collisions of a mesic atom of the heavier isotope with a lighter nucleus, for example $d_\mu + p \rightarrow (dp)_\mu$ (in the $p_\mu + d$ collision a much more probable process is the charge exchange $p_\mu + d \rightarrow d_\mu + p$). The wave function of the initial state is of the form

$$\Psi_{mol}^{(i)} = G_0(R)\,\Sigma_g + H_0(R)\,\Sigma_u,$$

where the functions G_0, H_0 are connected with the functions $a_0(R)$, $b_0(R)$ by the relations (13) and (14). The wave function of the final state, corresponding to a rotational level of the mesic molecule with L = 1, is of the form

$$\Psi_{mol}^{(f)} = \{g_1(R)\,\Sigma_g + h_1(R)\,\Sigma_u\}\,Y_{1,M}(\theta,\varphi)/R.$$

Carrying out the integration over the angles and the summation over M_L, we get in mesic atomic units:

$$\sum_M |\langle \mathrm{d}\rangle|^2 = \frac{4\pi}{(M_1 + M_2)^2}$$

$$\times\left|\int_{-\infty}^{\infty}\{M_1 a_0(R)\,a_1(R) - M_2 b_0(R)\,b_1(R)\}\,R\,dR\right|^2. \qquad (33)$$

The integrals in Eq. (33) have been calculated numerically. The probabilities for formation of the mesic molecules $(pd)_\mu$, $(pt)_\mu$, and $(dt)_\mu$ found from Eqs. (32) and (33) are (in units 10^6 sec^{-1})

$(pd)_\mu$	$(dt)_\mu$	$(pt)_\mu$
0.68	0.001	0.25

The values found for the probabilities of formation of the mesic molecules $(pp)_\mu$, $(pd)_\mu$, and $(dd)_\mu$

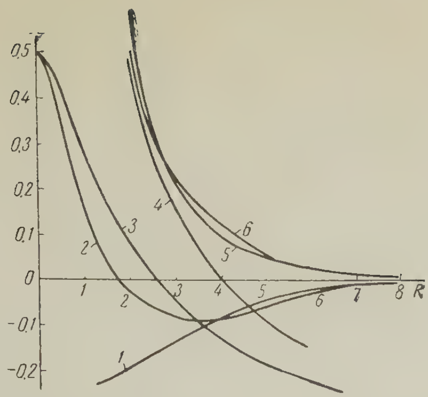

Curve 1 – K_{gg} (LCAO); 2 – K_{gg} (exact); 3 – K_{gg} (UA); 4 – K_{uu} (UA); 5 – K_{uu} (LCAO); 6 – K_{uu} (exact).

agree well in order of magnitude with the values necessary for the interpretation of the experimental data.[4,5] The fact that for the heavy isotopes the probability of molecule formation is smaller than for $(pp)_\mu$ is quite understandable, since when the reduced mass is large the values of the wave function in the classically forbidden region, which make the main contribution to the dipole moment, are much smaller than they are for $(pp)_\mu$. [The probability for formation of $(tt)_\mu$ is comparatively large because of a resonance,[2] cf. Table III.] Because of the small probability for formation of the mesic molecules $(dd)_\mu$, etc., from the repulsive state the contribution from 0-0 transitions becomes important; these transitions have been considered by Zel'dovich.[2]

The writers consider it their pleasant duty to express their gratitude to Ya. B. Zel'dovich, at whose suggestion this work was done, for a discussion and valuable comments, and also to A. D. Sakharov and Ya. Smorodinskiĭ.

APPENDIX

The functions $K_{gg}(R)$ and $K_{uu}(R)$ have been calculated by Dalgarno and McCarroll[16] by means of the accurate Σ_g and Σ_u wave functions given in the paper by Bates and others.[15] We give for comparison values of $K_{gg}(R)$ and $K_{uu}(R)$ calculated in the LCAO approximation, which holds for large values of R,

$$\Sigma_g = \{2\pi(1+s)\}^{-1/2}(e^{-r_1}+e^{-r_2}),$$
$$\Sigma_u = \{2\pi(1-s)\}^{-1/2}(e^{-r_1}-e^{-r_2}),$$

where $s = (1 + R + R^2/3)\,e^{-R}$, and in the UA approximation, which holds for small R, when Σ_g and Σ_u go over respectively into the 1s and 2p levels of He:

$$\Sigma_g = e^{-(r_1+r_2)}/N_g,\quad \Sigma_u = -e^{-(r_1+r_2)}(r_1\cos\theta_1 - r_2\cos\theta_2)/N_u,$$
$$N_g^2 = \frac{1}{8}\pi e^{-2R}\left(1+2R+\frac{4}{3}R^2\right),$$
$$N_u^2 = 4\pi\left(1+R+\frac{9}{20}R^2+\frac{9}{60}R^3+\frac{1}{60}R^4\right)e^R.$$

In the LCAO approximation:

$$K_{gg} = \frac{1}{2} - \frac{s}{2(1+s)} - \frac{1}{36}\,\frac{R^2(1+R)^2}{(1+s)^2}\,e^{-2R}.$$

In the UA approximation:

$$K_{gg} = 1 - (N_g'/N_g)^2_{R\to 0} \approx 1 - 16R^2/9;$$
$$K_{uu} = 2/R^2 + 1/4 - (N_u'/N_u)^2_{R\to 0} \approx 2/R^2 + 1/4.$$

For comparison, the diagram shows the values of K_{gg} and K_{uu} calculated by Dalgarno and McCarroll,[16] and their values according to the LCAO and UA approximations. For the quantity Q(R) the calculations give

$$LCAO:\qquad Q = -\frac{M_2-M_1}{M_2+M_1}\,\frac{R(R+1)\,e^{-R}}{6\sqrt{1-s^2}}.$$
$$UA:\quad Q = -\frac{M_2-M_1}{M_2-M_1}\,\frac{16\pi}{81}\,\frac{e^{-3R/2}}{N_gN_u}\left(1+\frac{3}{2}R+\frac{3}{4}R^2\right).$$

We note that for $R \to 0$ the value of Q calculated according to the LCAO approximation agrees rather well with the value calculated by the UA approximation for $R \to 0$:

$$Q_{LCAO} \to -\left(\frac{M_2-M_1}{M_2+M_1}\right)\frac{1}{2\sqrt{3}} = -0.289\,\frac{M_2-M_1}{M_2+M_1},$$
$$Q_{UA} \to -\frac{M_2-M_1}{M_2+M_1}\,\frac{16\sqrt{2}}{81} = -0.28\,\frac{M_2-M_1}{M_2+M_1}.$$

Thus over the entire range of R we can adopt the approximation $Q = Q_{LCAO}$. The values of $K_{gu}(R)$ and $K_{ug}(R)$ in the LCAO and UA approximations are

$$LCAO: K_{gu} = \frac{1}{2\sqrt{1-s^2}}$$
$$\times\left\{1+e^{-R}\left(1+R-\frac{R^2}{3}\right)-\frac{R^2(1+R)^2}{9(1-s)}\,e^{-2R}\right\}\frac{M_2-M_1}{M_2+M_1},$$
$$LCAO: K_{ug} = \frac{1}{2\sqrt{1-s^2}}$$
$$\times\left\{1-e^{-R}\left(1+R-\frac{R^2}{3}\right)-\frac{R^2(1+R)^2}{9(1+s)}\,e^{-2R}\right\}\frac{M_2-M_1}{M_2+M_1};$$
$$UA: K_{gu} = \frac{M_2-M_1}{M_2+M_1}\,\frac{64\pi}{81}\,\frac{e^{-3R/2}}{N_gN_u}$$
$$\times\left(1+\frac{3}{2}R+\frac{3}{4}R^2\right)\left(1-\frac{R}{2}\,\frac{N_u'}{N_u}\right)\frac{1}{R},$$
$$K_{ug} = \frac{M_2-M_1}{M_2+M_1}\,\frac{64\pi}{81}\,\frac{e^{-3R/2}}{N_gN_u}$$
$$\times\left[\frac{1}{2}\,\frac{N_g'}{N_g}\left(1+\frac{3}{2}R+\frac{3}{4}R^2\right)+\frac{3}{8}R+\frac{9}{16}R^2\right].$$

The behavior of these functions for $R \to 0$ is given by:

$$LCAO: K_{gu} \to \frac{M_2-M_1}{M_2+M_1}\,\frac{2}{\sqrt{3}R} \approx 1.15\,\frac{1}{R}\,\frac{M_2-M_1}{M_2+M_1},$$
$$K_{ug} \to \frac{M_2-M_1}{M_2+M_1}\,\frac{7\sqrt{3}}{18}\,R \approx 0.67R\,\frac{M_2-M_1}{M_2+M_1};$$
$$UA: K_{gu} \to \frac{M_2-M_1}{M_2+M_1}\,\frac{64\sqrt{2}}{81R} \approx 1.12\,\frac{1}{R}\,\frac{M_2-M_1}{M_2+M_1},$$
$$K_{ug} \to \frac{M_2-M_1}{M_2+M_1}\,\frac{8\sqrt{2}}{35}\,R \approx 0.32R\,\frac{M_2-M_1}{M_2+M_1}.$$

[1] F. C. Frank, Nature **160**, 525 (1947).

[2] Ya. B. Zel'dovich, Dokl. Akad. Nauk SSSR **95**, 493 (1954).

[3] A. D. Sakharov, Report of Physical Institute, Academy of Sciences (FIAN), 1948.

[4] Alvarez, Bradner, Crawford, Crawford, Falk-Vairant, Good, Gow, Rosenfeld, Solmitz, Stevenson, Ticho, and Tripp, Phys. Rev. **105**, 1127 (1957).

[5] Ashmore, Nordhagen, Strauch, and Townes, Proc. Phys. Soc. **71**, 161 (1958).

[6] S. S. Gershteĭn, JETP **34**, 463 (1958); **34**, 993 (1958). Soviet Phys. JETP **7**, 318, 685 (1958).

[7] V. B. Belyaev and B. N. Zakhar'ev, JETP **35**, 996 (1958), Soviet Phys. JETP **8**, 696 (1959).

[8] Ya. B. Zel'dovich and S. S. Gershteĭn, JETP **35**, 821 (1958), Soviet Phys. JETP **8**, 570 (1959).

[9] Ya. B. Zel'dovich and A. D. Sakharov, JETP **32**, 947 (1957), Soviet Phys. JETP **5**, 775 (1957).

[10] S. S. Gershteĭn, Dokl. Akad. Nauk SSSR **117**, 956 (1957), Soviet Phys.-Doklady **2**, 559 (1958).

[11] Cohen, Judd, and Riddell, Phys. Rev. **110**, 1471 (1958).

[12] Shimizu, Mizuno, and Izuyama, Progr. Theoret. Phys. **20**, 777 (1958).

[13] Ya. B. Zel'dovich and S. S. Gershteĭn, JETP **35**, 649 (1958), Soviet Phys. JETP **8**, 451 (1959).

[14] E. Teller, Z. Physik **61**, 458 (1930).

[15] Bates, Ledsham, and Stewart, Phil. Trans. Roy. Soc. London **246**, No. 911, 215 (1953).

[16] A. Dalgarno and R. McCarroll, Proc. Roy. Soc. **A237**, 383 (1956).

[17] Gallone, Prosperi, and Scotti, Nuovo cimento **6**, 168 (1957).

[18] A. Dalgarno and V. Poots, Proc. Phys. Soc. **A67**, 343 (1954).

Translated by W. H. Furry
328

SOVIET PHYSICS JETP VOLUME 37 (10), NUMBER 6 JUNE, 1960

ON THE COLLISIONS OF NUCLEONS WITH LARGE ORBITAL ANGULAR MOMENTUM

A. D. GALANIN, A. F. GRASHIN, B. L. IOFFE, and I. Ya. POMERANCHUK

Submitted to JETP editor July 12, 1959

J. Exptl. Theoret. Phys. (U.S.S.R.) 37, 1663-1679 (December, 1959)

The two-meson exchange contribution to the nucleon-nucleon scattering amplitude is calculated for large orbital angular momenta $l \gg 1$. The connection between this amplitude and the scattering of real mesons by nucleons is established with the aid of dispersion relations. The method is valid when the inequality $l \gg 1$ is satisfied as well as the condition $l\mu/p \gg 1$ (μ is the meson mass and p the nucleon momentum in the c.m. system).

1. INTRODUCTION

OKUN' and Pomeranchuk[1] have shown that only interactions occurring through the exchange of one meson play a part in collisions of nucleons with large orbital angular momentum, and it follows that the phases of the corresponding amplitudes can be calculated theoretically.* In such a general form this assertion holds as a consequence only of the general physical consideration, that for increasing orbital angular momenta larger and larger impact parameters become important. However, for this assertion to be more than purely academic and to acquire practical significance, it is necessary to show that already for comparatively small values of the angular momentum one can obtain the scattering phase shifts to good accuracy from the one-meson approximation.

An estimate of the accuracy of the one-meson approximation can be obtained by calculating the next approximation in powers of the "peripheralness of the collision" — the two-meson approximation, when the colliding nucleons exchange two mesons. In the present paper these calculations are carried out with the following restrictions.

1. The values of the orbital angular momenta, for which we calculate the phase shifts, are large: $l \gg 1$.

2. For given l the nucleon energy is bounded from above by the inequality $l\xi \gg 1$, where $\xi = \mu/p$, μ is the π-meson mass, and p is the momentum of the nucleon in the c.m. system.

The second assumption has a simple physical interpretation: the quasi-classical impact parameter $r_0 = l\xi/\mu \gg 1/\mu$, i.e., this assumption is the condition that the collision should be a peripheral one. In other words, only when this condition is satisfied is it meaningful to classify the interactions in powers of "peripherality" with a small expansion parameter.

The method discussed enables us to obtain the major part of the asymptotic expansion of the two-meson phase shift in terms of the small parameter $1/L(l\xi)$ which equals $1/l$ for small energy ($\xi^2 \gtrsim 1$) and as the energy increases ($\xi^2 \ll 1$) grows to $1/l\xi$. The calculation is based on the idea that, under the stated conditions, the important contribution from the virtual mesons exchanged by the nucleons comes from those with the physical energy-momentum relation, $\omega^2 - k^2 = \mu^2$ not from those with the physical energy $\omega = 0$ and momentum transfer $q^2 = 4\mu^2$.

The nucleon-nucleon scattering amplitude is expressed in terms of the amplitude for scattering such mesons by the nucleons, and can subsequently be calculated exactly with the help of the dispersion relations for pion-nucleon scattering at fixed momentum transfer. Apart from these amplitudes we consider separately terms corresponding to lowest order perturbation theory (with renormalized coupling constant g^2) for meson-nucleon scattering. Although these terms tend to zero for $\omega = 0$, their contribution, due to the pole, at the small value of $\omega = \mu^2/2m$ is comparable in magnitude with, but opposite in sign to, the contribution from the dispersion-relation terms.

2. SCATTERING PHASE SHIFTS FOR LARGE ORBITAL ANGULAR MOMENTA

The scattering matrix and the scattering phase shift for nucleon-nucleon scattering can be expressed as integrals of the amplitudes $M(E, \cos\theta)$, corresponding to different spin states ($E = \sqrt{m^2 + p^2}$ is the total energy, θ is the scattering angle in the center of mass system; the spin and charge indices are not written out):

---

*References to previous work are given in reference 1.

$$I_{l,m}(E) = \int_{-1}^{+1} P_l^{(m)}(\cos\theta)\, M(E, \cos\theta)\, d\cos\theta, \qquad (2.1)$$

where $P_l^{(m)}$ is the associated Legendre polynomial. We restrict ourselves to a discussion of the integral (2.1) with $m = 0$ (the cases $m = 1$, $m = 2$ can be treated analogously).

To calculate the integral (2.1) for large l, it is convenient to use the analytic properties of the scattering amplitude as a function of $\cos\theta$ (or, equivalently, the square of the momentum transfer) for fixed energy in the center of mass system; which have been discussed by Mandelstam[2] for the case of pion-nucleon scattering. For nucleon-nucleon scattering the validity of this method is less certain than for pion-nucleon scattering and, apart from intuitive considerations, is only supported by the analysis of lowest-order perturbation theory. It should be remarked, however, that (as will be made clear below) for our conclusions the complete dispersion formula is not necessary, but only the position of the first (nearest) singularity is important, and this is hardly to be doubted.

Proceeding just as in reference 2, we express the nucleon-nucleon scattering amplitude in the form[3]

$$(2\pi)^4 T(p_1, p_1'; p_2, p_2')\, \delta(p_1 + p_2 - p_1' - p_2')$$
$$= i\frac{m^2}{4\pi E}\int d^4x d^4y e^{i(p_1'x + p_2'y)}\, \bar{u}_\mu(p_1')\, \bar{u}_\nu(p_2')$$
$$\times \langle -p_1 | T(\eta_\mu(x), \eta_\nu(y)) | p_2\rangle$$

or

$$T(p_1, p_1'; p_2, p_2') = i\frac{m^2}{4\pi E}\int d^4x e^{i(p_1'-p_2')x/2}\, \bar{u}_\mu(p_1')\, \bar{u}_\nu(p_2')$$
$$\times \left\langle -p_1 \left| T\left(\eta_\mu\left(\frac{x}{2}\right), \eta_\nu\left(-\frac{x}{2}\right)\right)\right| p_2\right\rangle. \qquad (2.2)$$

Here p_1, p_2, p_1', p_2' are the 4-momenta of the nucleons before and after the collision, $u(p_1')$, $u(p_2')$ are final-state spinors, $\eta(x)$ is the right hand part of the Dirac equation for the nucleons [the metric is $(+1, -1, -1, -1)$].

As usual[4,5] in place of the scattering amplitude we introduce the function $M(p_1, p_1'; p_2, p_2')$ defined by the retarded commutator

$$M(p_1, p_1'; p_2, p_2') = i\frac{m^2}{4\pi E}\int d^4x\, e^{i(p_1'-p_2')x/2}\, \theta(x_0)\, \bar{u}_\mu(p_1')\, \bar{u}_\nu(p_2')$$
$$\times \left\langle -p_1 \left| \left\{\eta_\mu\left(\frac{x}{2}\right), \eta_\nu\left(-\frac{x}{2}\right)\right\}\right| p_2\right\rangle. \qquad (2.3)$$

The function M is divided into a dispersive part $D(p_1, p_1'; p_2, p_2')$ and absorptive part $A(p_1, p_1'; p_2, p_2')$

$$M(p_1, p_1'; p_2, p_2') = D(p_1, p_1'; p_2, p_2') + iA(p_1, p_1'; p_2, p_2'), \qquad (2.4)$$

coming from setting $\theta(x_0)$ in the form $\theta(x_0) = \frac{1}{2}(\epsilon(x_0) + 1)$. The absorptive part is expressed as

$$A(p_1, p_1'; p_2, p_2') = A_1(p_1, p_1'; p_2, p_2') + A_2(p_1, p_1'; p_2, p_2'); \qquad (2.5)$$

$$A_1(p_1, p_1'; p_2, p_2')$$
$$= 2\pi^3(m^2/E)\sum_n \bar{u}_\mu(p_1')\, \bar{u}_\nu(p_2')\langle -p_1 | \eta_\mu(0) | n\rangle$$
$$\times \langle n | \eta_\nu(0) | p_2\rangle\, \delta(p_n - p_1' + p_1),$$
$$A_2(p_1, p_1'; p_2, p_2')$$
$$= 2\pi^3(m^2/E)\sum_n \bar{u}_\mu(p_1')\, \bar{u}_\nu(p_2')\langle -p_1 | \eta_\nu(0) | n\rangle$$
$$\times \langle n | \eta_\mu(0) | p_2\rangle\, \delta(p_n - p_2' + p_1), \qquad (2.6)$$

where $|n\rangle$ is a physical state with 4-momentum p_n and the summation is taken over the complete set of states with given 4-momentum and baryon number (equal to zero).

The expression for the scattering amplitude $T(p_1, p_1'; p_2, p_2')$ in terms of dispersive and absorptive parts has the same form as (2.4), except that A_2 occurs with the opposite sign. For real nucleon-nucleon scattering in the center-of-mass system $E_1' - E_1 = 0$, $E_2' - E_2 = 0$, so that $E_n = 0$. Hence it follows that for real processes the absorptive part vanishes and the function $M(p_1, p_1'; p_2, p_2')$ coincides with the scattering amplitude. Note that A_2 differs from A_1 by interchange of the variables describing the first and second nucleon after scattering. Apart from spin and charge variables, $M(p_1, p_1'; p_2, p_2')$ is a function of the two invariants $(p_1 + p_2)^2 = 4E^2$ and $q^2 = (p_1' - p_1)^2 = 2p^2(1 - \cos\theta)$.

The dispersion relation in q^2 at constant E^2 can be obtained using the method of Goldberger[4] and integrating with respect to q^2 the expression for the absorptive part, coming from (2.3) we obtain*

$$M(E, q^2) = \frac{1}{\pi}\int_{-\infty}^{\infty} \frac{A(E, q'^2)}{q'^2 - q^2 - i\varepsilon}\, dq'^2, \qquad (2.7)$$

if $\operatorname{Im} q^2 \geq 0$. The relation (2.7) has been written in symbolic form; in actual fact (2.7) must hold for each independent charge and spin amplitude.

In the sum over intermediate states it is convenient to separate the one-meson states. Then there are left in the summation terms beginning with the two-meson state which only occur for $p_n^2 > 4\mu^2$. Bearing this in mind, (2.7) can be expressed in the form

---

*The dispersion relations are written without additional subtractions. The subtraction terms do not affect our case because for $l > 0$ they vanish after substituting (2.7) into (2.1) and integrating with respect to $\cos\theta$.

$$M(E, q^2) = -\frac{g^2}{4E} v_1'^{*} v_2'^{*} \left[\frac{q^2}{q^2 - \mu^2} \tau_\alpha^{(1)} \tau_\alpha^{(2)} + \frac{r^2}{r^2 - \mu^2} \frac{3 - \tau_\alpha^{(1)} \tau_\alpha^{(2)}}{2} \right] v_1 v_2$$

$$+ \frac{1}{\pi} \int\limits_{4\mu^2}^{\infty} \frac{A_1(E, q'^2)}{q'^2 - q^2 - i\varepsilon} dq'^2 - \frac{1}{\pi} \int\limits_{4\mu^2}^{\infty} \frac{A_2(E, r'^2)}{r'^2 - r^2 + i\varepsilon} dr'^2, \quad (2.8)$$

where $r^2 = (p_2' - p_1)^2 = -2p^2(1 + \cos\theta)$, $\tau_\alpha^{(1)}$ and $\tau_\alpha^{(2)}$ are the isotopic-spin matrices for the nucleons 1 and 2, g^2 is the renormalized pion-nucleon coupling constant ($g^2 = 14.5$), and v_1, v_2 are two component spinors. The functions $A_1(E, q'^2)$ and $A_2(E, q'^2)$ are determined by the relation (2.6) in which the summation over intermediate states starts from the two-meson states. In the integration of $A_2(E, q'^2)$ we express q^2 in terms of $r^2 = 4m^2 - 4E^2 - q^2$; this way of writing makes clear the antisymmetry of the scattering amplitude.

The quantity $2iA_1(E, q^2)$ [and similarly $2iA_2(E, q^2)$] can be obtained as the discontinuity in the scattering amplitude occurring when q^2 crosses the real axis from above at a point lying to right (left) of the point $q^2 = 4\mu^2$ ($q^2 = -4(\mu^2 + p^2)$). This assertion follows directly from (2.8), if we take into account that (2.8) [or (2.7)] determines the scattering amplitude in the upper half of the complex q^2 plane. The analytic continuation into the lower half plane has to be carried out, crossing the segment of the real axis $-4(\mu^2 + p^2) < q^2 < 4\mu^2$, where the amplitude has no singularities (other than poles).

To calculate the scattering phase shift, we substitute (2.8) into (2.1). In this the integration of the pole term in (2.8) gives the contribution to the scattering phase shift of the one-meson approximation calculation. For the singlet amplitude the one-meson approximation gives (the index m = 0 is dropped)

$$I_l^{(1)} = (g^2\xi^2 / 2E)\lambda_T Q_l\left(1 + \frac{1}{2}\xi^2\right), \quad (2.9)$$

where $\lambda_T = 1$ for even l (the isotopic spin T = 1), $\lambda_T = -3$ for odd l (T = 0) and $Q_l(t)$ is the Legendre function of the second kind

$$Q_l(t) = \frac{1}{2} \int\limits_{-1}^{1} \frac{P_l(t')}{t - t'} dt'. \quad (2.10)$$

The correction to the approximation is obtained from the calculation of (2.1) with the two last terms of (2.8) substituted, and bearing in mind the relation $Q_l(t) = (-1)^{l+1} Q_l(-t)$, this turns out to be equal to

$$I_l^{(2)} = \frac{1}{\pi p^2} \int\limits_{4\mu^2}^{\infty} dq'^2 Q_l(1 + q'^2 / 2p^2) [A_1(E, q'^2)$$

$$+ (-1)^{l+1} A_2(E, q'^2)]. \quad (2.11)$$

The calculation of the integrals $I_{l,m}(E)$ for m = 1 and m = 2 leads to expressions analogous to (2.9) and (2.11); the only difference being that instead of the function $Q_l(t)$, the functions $(t^2 - 1)^{1/2} Q_l^{(1)}$ and $(t^2 - 1) Q_l^{(2)}$ are obtained. In order to be convinced of this it is sufficient to substitute (2.8) into (2.1) and take into account the equations (remember that $l > 1$)

$$-\frac{1}{2} \int\limits_{-1}^{1} \frac{(1 - t'^2)^{1/2}}{t - t'} P_l^{(1)}(t')\, dt' = (t^2 - 1)^{1/2} Q_l^{(1)}(t);$$

$$\frac{1}{2} \int\limits_{1}^{1} \frac{1 - t'^2}{t - t'} P_l^{(2)}(t')\, dt' = (t^2 - 1)\, Q_l^{(2)}(t).$$

The contribution of the term A_2 in (2.11) is equal to the contribution from the term A_1. This conclusion follows directly from the fact that, in the singlet state, for T = 0, $A_2 = A_1$ and the amplitude contains only odd l, and for T = 1, $A_2 = -A_1$ and the amplitude contains only even l. Therefore

$$I_l^{(2)} = \frac{2}{\pi p^2} \int\limits_{4\mu^2}^{\infty} dq'^2 Q_l(1 + q'^2 / 2p^2) A_1(E, q'^2). \quad (2.12)$$

We now make use of the condition $l \gg 1$. For large l, the function $Q_l(1 + z^2/2)$ decreases rapidly with increasing z: if $z \gg 1$, then $Q_l(1 + z^2/2) \sim Z^{-2(l+1)}$, while if $z \ll 1$, but $lz \gg 1$, then $Q_l(1 + z^2/2) \sim e^{-lz}$. It should be considered that besides the condition $l \gg 1$, the condition $l\xi \gg 1$ is also satisfied, where $\xi = \mu/p$ (for $\xi < 1$). Hence in the integral (2.12) a small region of integration, near the lower limit, contributes. We make use of the following expression for the function $Q_l(t)$ [see reference 6, formula (6.777)]

$$Q_l(t) = \sqrt{\pi} \frac{\Gamma(l + 1)}{\Gamma(l + 3/2)} \exp\left\{-(l + 1) \ln |t + \sqrt{t^2 - 1}|\right\}$$

$$\times F\left(\frac{1}{2}, l + 1, l + \frac{3}{2}, (t + \sqrt{t^2 - 1})^{-2}\right) \quad (2.13)$$

and make a power series expansion of the exponent in the hypergeometric function in the neighborhood of $t_0 = 1 + 2\xi^2$ ($\Delta t = t - t_0$):

$$Q_l(t) = Q_l(t_0) \exp\{-\Delta t\,(l + 1) / \sqrt{t_0^2 - 1}\}$$

$$\times \left[1 + \frac{(l + 1)\, t_0}{(t_0^2 - 1)^{3/2}} \frac{(\Delta t)^2}{2}\right] \left[1 - \frac{\Delta t}{2(t_0^2 - 1)(t_0 + \sqrt{t_0^2 - 1})}\right]. \quad (2.14)$$

After substituting (2.14) in (2.12) the integral $I_l^{(2)}$

becomes

$$I_l^{(2)} = \frac{8}{\pi}\xi^2 Q_l(t_0)\int_0^{\infty} d\left(\frac{q'^2-4\mu^2}{4\mu^2}\right)$$

$$\times\exp\{-L(q'^2-4\mu^2)/4\mu^2\}\,A_1(E, q'^2),$$

$$A_1(E, q^2) = \frac{1}{2i}[M(E, q^2+i0) - M(E, q^2-i0)], \quad \textbf{(2.15)}$$

where

$$L = (l+1)\frac{\xi}{\sqrt{1+\xi^2}} \approx \begin{cases} l\xi & \text{for } \xi \ll 1, \\ l+1 & \text{for } \xi \gg 1. \end{cases} \qquad (2.16)$$

It is not difficult to verify that terms from the expansion of the square brackets in (2.14) for large L make a small contribution (of order 1/L) to the integral (2.15), so that our expansion is justified and (2.15) is accurate to order 1/L.

Now we show that if L is large it is not necessary to use the complete dispersion relation (2.7) to obtain (2.15). We only need use the interior of an ellipse in the complex q^2 plane passing through the point $q^2 = 4\mu^2 + \kappa^2$ (the constant $\kappa^2 \gg 4\mu^2/L$) and having foci at the points $q^2 = 0$ and $q^2 = -4\mu^2/\xi^2$, there being no singularities other than the poles and the cuts on the real axis for $q^2 \geq 4\mu^2$ and $q^2 \leq -4\mu^2(1+\xi^{-2})$. To prove this we transform the integral (2.1) making use of the relation

$$I_l = \frac{1}{2p^2}\int_{-4p^2}^{0} P_l(1+q^2/2p^2)\,M(E, q^2)\,dq^2$$

$$= \frac{1}{2p^2\pi i}\oint_C Q_l(1+q^2/2p^2)\,M(E, q^2)\,dq^2, \qquad (2.1')$$

and deforming the contour C (shown dotted in Fig. 1) into the contour $C_1 + C_1' + C_2$. The boundary of the complex region swept out is of the form of the above-mentioned ellipse, and we expand the ellipse to the point where it is far from the nearest singular points in the complex region. If we include with the ellipse the points on the real semi-axis $q^2 = 4\mu^2 + \kappa^2$, then (2.1′) can be written in the form

$$I_l = -\frac{1}{p^2}Q_l\left(1+\frac{1}{2}\xi^2\right)\mathrm{Res}\,[M(E, \mu^2)$$

$$+ (-1)^l M(E, -\mu^2-4p^2)] + \frac{1}{2p^2\pi i}$$

$$\times\int_{4\mu^2}^{\infty} Q_l(1+q^2/2p^2)\,[\Delta M(E, q^2)$$

$$-(-1)^l\,\Delta M(E, -q^2-4p^2)]\,dq^2 + fQ_l\left(1+\frac{4\mu^2+\kappa^2}{2p^2}\right),$$

$$\Delta M(E, q^2) = M(E, q^2+i\varepsilon) - M(E, q^2-i\varepsilon) = 2iA(E, q^2), \qquad (2.11')$$

which is equivalent to (2.9) and (2.11), except for the last term (f is some smoothly varying function of p^2 and l). Comparing with the integral along the cut ($q^2 \geq 4\mu^2$) this contribution involves the additional small factor

$$Q_l\left(1+\frac{4\mu^2+\kappa^2}{2p^2}\right) \Big/ Q_l\left(1+\frac{4\mu^2}{2p^2}\right) \ll 1$$

and for large l it can be ignored.

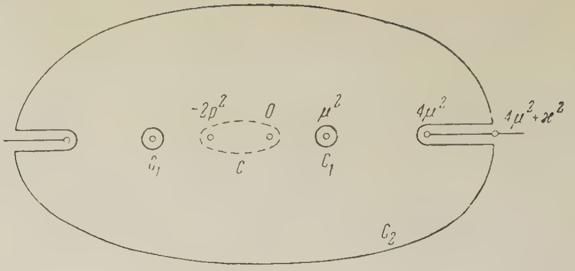

FIG. 1

It follows from (2.15) that we must be interested in values of the amplitude $A_1(E, q^2)$ for $q^2 - 4\mu^2 \sim 4\mu^2/L \leq 4\mu^2$. In this case, in the sum over intermediate states (2.6) only the two-meson states remain, because the next state (three π mesons) corresponds to a value of q^2 of at least $9\mu^2$, and states with nucleon-antinucleon pairs lie even higher. Thus the expression for $A_1(E, q^2)$ takes the form

$$A_1(E, q^2) = \frac{m^2}{4E(2\pi)^3}\sum_{\alpha,\beta}\int d\mathbf{k}_1\,d\mathbf{k}_2\,\bar{u}_\mu(p_1')\,\bar{u}_\nu(p_2')$$

$$\times\langle -p_1|\eta_\mu(0)|k_1, \alpha; k_2, \beta\rangle\langle k_1, \alpha; k_2, \beta|\eta_\nu(0)|p_2\rangle$$

$$\times\delta(k_1+k_2-q), \qquad (2.17)$$

where k_1 and k_2 are the four-momenta of two π mesons propagating in charge states α and β, and $q = p_2' - p_1'$.

The matrix elements occurring in (2.17) are simply related to the invariant matrix element $f_{\alpha,\beta}(p, p'; k, k')$ for meson-nucleon scattering (ω is the meson energy)

$$\bar{u}_\mu(p_1')\langle -p_1|\eta_\mu(0)|k_1, \alpha; k_2, \beta\rangle = \frac{2\pi}{\sqrt{\omega_1\omega_2}}f_{\alpha\beta}(p_1, p_1'; k_1, -k_2),$$

$$\bar{u}_\nu(p_2')\langle k_1, \alpha; k_2, \beta|\eta_\nu(0)|p_2\rangle = \frac{2\pi}{\sqrt{\omega_1\omega_2}}f_{\alpha\beta}(p_2, p_2'; -k_1, k_2), \qquad (2.18)$$

for which[7-10]

$$f_{\alpha\beta}(p, p'; -k_1, k_2) = f^*_{\alpha\beta}(p', p; k_1, -k_2). \qquad (2.19)$$

Substituting (2.18) in (2.17) we obtain

$$A_1(E, q^2) = \frac{m^2}{8\pi E}\sum_{\alpha,\beta}\int\frac{d\mathbf{k}_1\,d\mathbf{k}_2}{\omega_1\omega_2}f_{\alpha\beta}(p_1, p_1'; k_1, -k_2)$$

$$f_{\alpha\beta}(p_2, p_2'; -k_1, k_2)\;\delta(k_1+k_2-q). \qquad (2.20)$$

The integral in (2.20) is written in a manifestly invariant form (since dk/ω is an invariant). It is convenient to analyze it in the coordinate system in which the 4-vector q has only a time component. In this system $\omega_1 = \omega_2 = q/2$, $\mathbf{k}_1 = -\mathbf{k}_2 \equiv \mathbf{k}$, $k = \sqrt{q^2/4 - \mu^2} \sim \mu/L^{1/2}$, so that the components of the vector **k** are small. It is easy to see that if we set $k_1 = q/2 + k$, $k_2 = q/2 - k$ then also in the other coordinate systems in which we are interested, for example in the center of mass system of the nucleons, the components of the vector k turn out to be of order $\mu/L^{1/2}$. Therefore to calculate to lowest approximation in $1/L$ we can neglect k* and simply set $k_1 = k_2 = q/2$. This approximation is invalid only for those terms in $f_{\alpha\beta}$ which change rapidly in the region $0 < k \lesssim \mu/L^{1/2}$.

The matrix element $f_{\alpha\beta}(p_1, p_1'; k+q/2, k-q/2)$ can be expressed as a function of the two invariants $\nu = (p_1+p_1')(k+q/2)/2$, q^2, and is written as

$$f_{\alpha\beta}(p_1, p_1'; k+q/2, k-q/2) = \bar{u}(p_1')[L_{\alpha\beta}(\nu, q^2) + (\hat{k}+\hat{q}/2) M_{\alpha\beta}(\nu, q^2)]u(p_1'), \tag{2.21}$$

where $L_{\alpha\beta}$ and $M_{\alpha\beta}$ are scalar functions of their arguments. (For $f_{\alpha\beta}[p_2, p_2'; -(k+q/2), -(k-q/2)]$ there is an analogous expression.) The term proportional to $\hat{q}$ can be discarded on account of the equation

$$\bar{u}(p_1')\hat{q}u(p_1) = \bar{u}(p_1')(\hat{p}_1' - \hat{p}_1)u(p_1) = 0. \tag{2.22}$$

We assume first that $f_{\alpha\beta}$ is a sufficiently slowly varying function of k, so that we can neglect k and set $k_1 = k_2 = q/2$. Hence $\nu = \nu_0 \equiv (2p_1+q)(q/2)/2 = 0$, $q^2 = 4\mu^2$, whence

$$f_{\alpha\beta}(p_1, p_1'; q/2, -q/2) = \bar{u}(p_1') L_{\alpha\beta}(0, 4\mu^2) u(p_1), \tag{2.23}$$

and, as follows from (2.19), $L_{\alpha\beta}(0, 4\mu^2)$ is real. Substituting (2.23) in (2.20) and integrating over $\mathbf{k}_1$ and $\mathbf{k}_2$ (in the coordinate system in which $\mathbf{q} = 0$), we find

$$A_1(E, q^2) = (m^2/2E)\sqrt{q^2/4\mu^2 - 1}\,\bar{u}(p_1') \times L_{\alpha\beta}(0, 4\mu^2)u(p_1)\bar{u}(p_2')L_{\alpha\beta}(0, 4\mu^2)u(p_2). \tag{2.24}$$

We obtain the well-known result,[11] that at the branch point, the absorptive part of the amplitude, which in the given case coincides with the imaginary part,† is proportional to $\sqrt{q^2 - 4\mu^2}$.

Apart from terms sufficiently slowly varying near the point $\nu = 0$, $q^2 = 4\mu^2$, there is also a term in $f_{\alpha\beta}$ in which we can only set $\nu = 0$, $q^2 = 4\mu^2$ for very large, in practice uninteresting, values of L. This pole term corresponds to the single nucleon intermediate state in the meson-nucleon scattering amplitude, and is given by lowest order perturbation theory with renormalized coupling constant g^2. The pole term in $f_{\alpha\beta}$ takes the form*

$$f_{p\alpha\beta}(p_1, p_1'; k_1, -k_2) = g^2\bar{u}(p_1')[\gamma_5(\hat{p}_1 + \hat{k}_1 - m)^{-1}\gamma_5\tau_\alpha\tau_\beta + \gamma_5(\hat{p}_1 + \hat{k}_2 - m)^{-1}\gamma_5\tau_\beta\tau_\alpha]u(p_1) = -g^2\bar{u}(p_1') \times[(2p_1k_1 + \mu^2)^{-1}\tau_\alpha\tau_\beta - (2p_1k_2 + \mu^2)^{-1}\tau_\beta\tau_\alpha]\hat{k}u(p_1). \tag{2.25}$$

Since $f_{p\alpha\beta}$ contains the small factor $\hat{k}$, one would expect that this term could generally be neglected. However, (2.25) has a pole situated extremely close to the point $k = 0$ [at a distance $\mu^2/2m$ from it; see (2.27)]. Therefore the integral with the pole term must be calculated correctly. In order to be convinced of this, consider the interference term, in which for one amplitude we take the pole term and for the other, the constant (2.23). In this case both terms in the square brackets in (2.25) contribute equally and, for example, for one of the interference terms we find

$$-\frac{m^2g^2}{8\pi E}\int\frac{d\mathbf{k}_1 d\mathbf{k}_2}{\omega_1\omega_2}\bar{u}(p_1')\hat{k}u(p_1)\frac{1}{2p_1k_1+\mu^2}\bar{u}(p_2')L_{\alpha\alpha}(0, 4\mu^2)u(p_2) \times\delta(k_1 + k_2 - q). \tag{2.26}$$

In the coordinate system in which $\mathbf{q} = 0$, the singlet part (2.26) can be expressed as

$$\frac{mg^2}{8\pi E}\int\frac{d\mathbf{k}}{\omega^2}\,\frac{\mathbf{k}\mathbf{p}_1}{\mu^2 - q^2/2 - 2\mathbf{k}\mathbf{p}_1}\,\delta(q - 2\omega)\,\bar{u}(p'_2)L_{\alpha\alpha}(0, 4\mu^2)u(p_2). \tag{2.27}$$

(the spinor normalization is $\bar{u}u = 1$, and we neglect terms of order $\sim q^2/4m^2$). In getting from (2.26) to (2.27), we take into account the fact that the energy of nucleon 1, in the coordinate system we have chosen, is given before the collision by $E_1 = -q/2$ and afterwards by $E_1' = q/2$. The component of the momentum $\mathbf{p}_1$, occurring in the integral (2.27) is purely imaginary for $q/2 < m$. Therefore if we choose the z axis along the direction of the purely imaginary vector $\mathbf{p}_1$, the scalar product $\mathbf{k}\cdot\mathbf{p}_1$ is equal to

$$\mathbf{k}\mathbf{p}_1 = k_z p_1 = i\sqrt{m^2 - q^2/4}\sqrt{q^2/4 - \mu^2} \times\cos\vartheta \approx im\sqrt{q^2/4 - \mu^2}\cos\vartheta$$

and, after integrating the δ-function, the integral (2.27) takes the form

---

*Although the components of the vector k are small, of order $\sim 1/L^{1/2}$, nevertheless the error we make in neglecting them is of order $\sim 1/L$ since the terms linear in k vanish on integration over angles.

†The absorptive part stops to coincide with the imaginary part when in changing the arguments E, q^2 we cross a branch line (not counting the line $q^2 = 4\mu^2$). The first such line to appear is the line $q^2 = 4\mu^2 + \mu^4/p^2$ which corresponds to the vanishing of all four denominators in the simple four-vertex diagram.

*Our notation follows reference 13: $\gamma_5^2 = 1$.

$$\int \frac{d\mathbf{k}}{\omega^2} \frac{\mathbf{kp}_1}{\mu^2 - q^2/2 - 2\mathbf{kp}_1} \delta(q - 2\omega)$$

$$= \frac{4\pi}{q} \sqrt{\frac{q^2}{4} - \mu^2} \int_{-1}^{1} dx \frac{imx\sqrt{q^2/4 - \mu^2}}{\mu^2 - q^2/2 - 2imx\sqrt{q^2/4 - \mu^2}}$$

$$\approx -\frac{4\pi}{q} \sqrt{\frac{q^2}{4} - \mu^2} \left\{ 1 - \frac{\mu^2}{2m\sqrt{q^2/4 - \mu^2}} \right.$$

$$\left. \times \tan^{-1} \frac{2m\sqrt{q^2/4 - \mu^2}}{\mu^2} \right\}. \qquad (2.28)$$

From (2.28) it is clear that, for extremely small $q^2/4 - \mu^2 \ll (\mu/2m)^2\mu^2$, the contribution of the pole term is proportional to $(q^2/4 - \mu^2)^{3/2}$ and, as expected, after substitution in (2.15) gives a contribution L times smaller than the more basic term (2.24). But in (2.15) such small values of $q^2/4 - \mu^2$ play a fundamental part only for very large orbital angular momenta when $L \gtrsim (2m/\mu)^2$. This never occurs, of course, for any practical case. On the contrary, the interesting case is $L \ll (2m/\mu)^2$. Then for most of the range of integration in (2.15) $(q^2/4 - \mu^2) \gg (\mu/2m)^2\mu^2$, and (2.28) reduces to $-(4\pi/q)\sqrt{q^2/4 - \mu^2}$. Using (2.27) and (2.28), we arrive at the result that for $L \ll (2m/\mu)^2$ the interference term (2.26), when substituted into (2.15), gives a contribution of the same order in 1/L as the main term (2.24) and differs from it only by a factor of order $f^2(\mu/m) \sim 1$ [remembering that $L_{\alpha\alpha}(0, 4\mu^2) \sim 1/\mu$].

Thus, to calculate $A_1(E, q^2)$, the matrix element $f_{\alpha\beta}$ must be introduced as the sum of the pole term (2.25) and the remaining part of the matrix element $\tilde{f}_{\alpha\beta} = f_{\alpha\beta} - f_{p\alpha\beta}$, which need only be evaluated at the point $\nu = 0$, $q^2 = 4\mu^2$. For more precise results, we must take into account the first terms in the expansion* of $\tilde{f}_{\alpha\beta}$ in terms of ν and k. We shall carry out the calculation in four-dimensional form, directly calculating the discontinuity in the scattering amplitude, $\Delta M(E, q^2) = 2iA_1(E, q^2)$, and substituting it into (2.15). Therefore we translate our analysis into the usual diagram language.

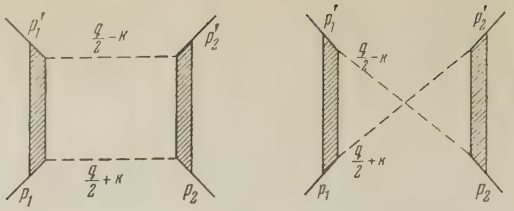

a b

FIG. 2

The two-meson approximation to the nucleon-nucleon scattering amplitude is computed with the aid of the diagrams shown in Figs. 2a and 2b. The shaded portions of these drawings represent the combination of all diagrams with two external nucleons and two meson lines. The scattering amplitude, corresponding to the diagram of Fig. 1 up to the terms with no discontinuity for $q^2 \geq 4\mu^2$ (i.e., nonsingular in the neighborhood of $q^2 = 4\mu^2$), can be expressed as

$$M(E, \cos\theta) = (m/2\pi i) \int d^4k f_{\alpha\beta}(p_1, p_1 + q; k + q/2, k - q/2)$$

$$\times f_{\alpha\beta}(p_2, p_2 - q; -k - q/2,$$

$$-k + q/2) [(k + q/2)^2$$

$$-\mu^2]^{-1} [(k - q/2)^2 - \mu^2]^{-1}, \qquad (2.29)$$

where the meson-nucleon scattering amplitude $f_{\alpha\beta}$ must be calculated as discussed above. The coefficient ½ occurs in (2.29) because the meson-nucleon scattering amplitude $f_{\alpha\beta}$ includes both diagrams in which first a meson of momentum k + q/2 is absorbed in the state α and then a meson of momentum k − q/2 emitted in the state β, and also diagrams with the absorption and emission in the opposite order, which leads to the duplication of all diagrams for nucleon-nucleon scattering. It follows from (2.20) and (2.29) that the meson Green's function must be evaluated on the mass shell $(k_1^2 = k_2^2 = \mu^2)$. Therefore we replace the meson Green's function by its free value.

We now consider the role of meson-meson scattering. As (2.20) indicates, $f_{\alpha\beta}$ is the exact meson-nucleon scattering amplitude, with the meson-meson scattering into account, so that, for example, diagrams of the type illustrated in Fig. 3 contribute to $f_{\alpha\beta}$. At first glance, it would seem that by inserting this diagram into the right and left hand parts of Fig. 2, we make the mistake of counting the diagram of Fig. 4 twice. But as a matter of fact the diagram of Fig. 4 is actually doubled in the neighborhood of the singularity at $q^2 = 4\mu^2$ since the singularity can arise (i.e., the meson lines can become real) both on the left and right hand sides of the meson-meson scattering vertex.*

---

*The result of integrating the product of this term and the pole can be small of order $\sim\mu/m$, but not L^{-1}, and its contribution may turn out to be essential.

*The meson-nucleon scattering amplitude arising from meson-meson scattering has a singularity for $q^2 = 4\mu^2$ and near this point (for $\hat{k} = 0$) is proportional to $a + ib\sqrt{q^2 - 4\mu^2}$. One might expect such a singularity to give rise to correction terms of order $L^{-1/2}$. In perturbation theory it can be seen that such corrections do not in fact arise. This result can be obtained from (2.20) if we take account of (2.19) and the reality of the coefficients a and b.

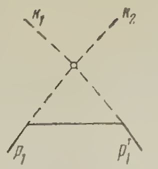

FIG. 3

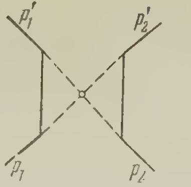

FIG. 4

3. APPLICATION OF THE DISPERSION RELATIONS FOR MESON-NUCLEON SCATTERING

In this section we calculate the meson-nucleon scattering amplitude $f_{\alpha\beta}(p_1, p_1+q; k+q/2, k-q/2)$, for small $\hat{k}$ and $q^2 = 4\mu^2$, as the analytic continuation of the scattering amplitude in the physical region. We consider the difference between the scattering amplitude and the pole term $\tilde{f}_{\alpha\beta} = f_{\alpha\beta} - f_{p\alpha\beta}$. We express $\tilde{f}_{\alpha\beta}$ in the form (2.21) and expand in powers of k, restricting ourselves to terms linear in k:

$$\tilde{f}_{\alpha\beta}(p_1, p_1+q; k+q/2, k-q/2) = \tilde{L}_{\alpha\beta}(0, 4\mu^2) + (\partial\tilde{L}_{\alpha\beta}(\nu, 4\mu^2)/\partial\nu)_{\nu=0}\left[p_1k + \frac{kq}{2}\right] + \hat{k}\tilde{M}_{\alpha\beta}(0, 4\mu^2). \quad (3.1)$$

The terms proportional to kq vanish when integrated over k, since in the coordinate system where $q = 0$, the invariant $kq = 0$. Therefore (3.1) acquires the form

$$\tilde{f}_{\alpha\beta} = \tilde{L}_{\alpha\beta}(0, 4\mu^2) + p_1k(\partial\tilde{L}_{\alpha\beta}(\nu, 4\mu^2)/\partial\nu)_{\nu=0} + \hat{k}\tilde{M}_{\alpha\beta}(0, 4\mu^2). \quad (3.2)$$

The squares of all external 4-momenta appearing in (3.1) are equal to their free-particle values: $p_1^2 = p_1'^2 = m^2$, $k_1^2 = k_2^2 = \mu^2$. In this sense $f_{\alpha\beta}$ is the matrix element for the scattering of real mesons by nucleons. However, the values of the energies of these mesons and the momentum transfer are unphysical in a physical coordinate system. In fact, from the equation $\nu_0 = 0$, it follows that in the Breit coordinate system, in which the sum of the nucleon momenta before and after scattering is equal to zero $(\mathbf{p}_1 + \mathbf{p}_1' = 0)$, the meson total energy $\omega = 0$. On the other hand, the square of the momentum transfer $q^2 = q_0^2 - \mathbf{q}^2 = 4\mu^2$ is positive, while for real scattering processes it is always negative. This means that the meson-nucleon scattering amplitude in which we are interested cannot be obtained directly with the help of experimental data on meson-nucleon scattering and we have to make use of analytic continuation of the amplitude to the values $\omega = 0$, $q^2 = 4\mu^2$.

We first examine the dependence of (3.2) on the isotopic variables. The functions $L_{\alpha\beta}(\nu, q^2)$ and $M_{\alpha\beta}(\nu, q^2)$ can be expressed in the following form

$$L_{\alpha\beta}(\nu, q^2) = \delta_{\alpha\beta}L^{(1)}(\nu, q^2) - i\varepsilon_{\alpha\beta\gamma}\tau_\gamma L^{(2)}(\nu, q^2),$$

$$M_{\alpha\beta}(\nu, q^2) = \delta_{\alpha\beta}M^{(1)}(\nu, q^2) - i\varepsilon_{\alpha\beta\gamma}\tau_\gamma M^{(2)}(\nu, q^2), \quad (3.3)$$

where

$$L^{(1)} = \tfrac{1}{2}(L_+ + L_-) = \tfrac{1}{3}(L_1 + 2L_3),$$

$$L^{(2)} = \tfrac{1}{2}(L_+ - L_-) = \tfrac{1}{3}(L_3 - L_1),$$

$$M^{(1)} = \tfrac{1}{2}(M_+ + M_-) = \tfrac{1}{3}(M_1 + 2M_3),$$

$$M^{(2)} = \tfrac{1}{2}(M_+ - M_-) = \tfrac{1}{3}(M_3 - M_1) \quad (3.4)$$

and L_+, $M_+(L_-, M_-)$ are the matrix elements for the scattering of $\pi^+(\pi^-)$-mesons by protons: L_1, M_1 and L_3, M_3 are the matrix elements for meson-nucleon scattering associated with states of total isotopic spin ½ and 3/2.

It follows from (2.19) that $L^{(1)}$, $L^{(2)}$, $M^{(1)}$, $M^{(2)}$ have simple symmetries when ν is replaced by $-\nu$:

$$L^{(1)}(\nu, q^2) = L^{(1)*}(-\nu, q^2), \quad L^{(2)}(\nu, q^2) = -L^{(2)*}(-\nu, q^2),$$

$$M^{(1)}(\nu, q^2) = -M^{(1)*}(-\nu, q^2), \quad M^{(2)}(\nu, q^2) = M^{(2)*}(-\nu, q^2). \quad (3.5)$$

From the general relations for the imaginary part of the scattering amplitude, it is not difficult to see that for $\nu = 0$ and $q^2 \leq 4\mu^2$, the imaginary parts of the quantities $L^{(i)}$ and $M^{(i)}$ must vanish.* It therefore follows also from (3.5) that

$$\tilde{f}_{\alpha\beta} = \delta_{\alpha\beta}\tilde{L}^{(1)}(0, 4\mu^2) - i\varepsilon_{\alpha\beta\gamma}\tau_\gamma\{p_1k(\partial\tilde{L}^{(2)}(\nu, 4\mu^2)/\partial\nu)_{\nu=0} + \hat{k}\tilde{M}^{(2)}(0, 4\mu^2)\}. \quad (3.6)$$

The quantities on the right-hand side of (3.6) can be expressed in terms of their values for physical energies with the aid of the dispersion relations in energy for fixed momentum transfer squared, q^2. The question of for which values of q^2 such dispersion relations are valid has been studied in a series of papers.[14-16] The authors of these papers, however, were only interested in negative q^2 corresponding to real processes. The validity of the dispersion relations for $q^2 > 0$ and, in particular, at the point $q^2 = 4\mu^2$ in which we are interested, can be verified without difficulty. We express the meson-nucleon scattering matrix element in the Breit coordinate system as a function of ω (the meson energy in this system) and q^2 (the momentum transfer) in the following form:

---

*The imaginary part of the meson-nucleon scattering amplitude turns out to be non-zero only for meson energies for which real states of the meson-nucleon system can appear [in the Breit coordinate system this corresponds to energies $\omega > \omega_1 = (m\mu + q^2/4)/(m^2 - q^2/4)^{1/2}$] or else real states of the two-meson system. As is easily seen, the latter circumstance leads to the appearance of an imaginary part for the scattering amplitude for $q^2 > 4\mu^2$, while for $q^2 \to 4\mu^2$ the imaginary part tends to zero proportional to $\sqrt{q^2 - 4\mu^2}$.

$$f_{\alpha\beta}(\omega, q^2) = i\int d^4x \exp\{i[\omega t - \mathbf{nr}\sqrt{\omega^2 - \mu^2 + q^2/4}]\}\,\theta(x_0)$$
$$\times\langle p_1'|[j_\beta(x/2), j_\alpha(-x/2)]|p_1\rangle. \qquad (3.7)$$

Here $j_\alpha(x)$ is the nucleon current, $\mathbf{n}$ is some unit vector. The components of the nucleon and meson momenta in the Breit coordinate system in the general case have the form

$$\mathbf{p}_1 = \{0, 0, \sqrt{\mathbf{q}^2}/2\}, \qquad \mathbf{p}_1' = \{0, 0, -\sqrt{\mathbf{q}^2}/2\},$$
$$\mathbf{k}_1 = \{k_x, k_y, -\sqrt{\mathbf{q}^2}/2\}, \quad \mathbf{k}_1' = \{k_x, k_y, \sqrt{\mathbf{q}^2}/2\}$$

or, if we introduce a unit vector $\mathbf{n}$ in the x, y plane:

$$\mathbf{n} = \{k_x, k_y\}(k_x^2 + k_y^2)^{-1/2},$$

then

$$\mathbf{k}_1 = \{\mathbf{n}\sqrt{\omega^2 - \mu^2 - \mathbf{q}^2/4}, -\sqrt{\mathbf{q}^2}/2\},$$
$$\mathbf{k}_1' = \{\mathbf{n}\sqrt{\omega^2 - \mu^2 - \mathbf{q}^2/4}, \sqrt{\mathbf{q}^2}/2\}$$

($\mathbf{k}_1$ is the momentum of the incident meson, $\mathbf{k}_1'$ that of the scattered one; $\mathbf{k}_1' = -\mathbf{k}_2$). The quantity $\nu = k_1(p+p')/2$ is related to the energy ω by the relation $\nu = \omega\sqrt{m^2 + \mathbf{q}^2/4}$.

As is well known, the difficulty in establishing the dispersion relations on the basis of formula (3.7) lies in the fact that in analytically continuing $f_{\alpha\beta}(\omega, q^2)$ in the complex ω plane for values of $\omega^2 < \mu^2 - q^2/4$, the root in the exponent in (3.7) becomes purely imaginary and the whole expression diverges when integrated with respect to $\mathbf{r}$. It is obvious that for $q^2 > 0$ (equivalent to a decreased meson mass) the proof becomes even easier than for the case of forward scattering. In particular, for $q^2 = 4\mu^2$, the exponential in (3.7) takes the quite simple form $\exp[i\omega(t - \mathbf{n}\cdot\mathbf{r})]$ and the analyticity of $f_{\alpha\beta}(\omega, q^2)$ in the upper half of the ω plane and, consequently, the existence of dispersion relations, follows directly from the vanishing of the retarded current commutator for $t^2 - r^2 < 0$ and $t < 0$.

It is convenient to write the dispersion relations not for the quantities L and M, but for the meson-nucleon scattering-matrix elements, without spin flip $[f(\omega, q^2)]$ and with spin flip $[\varphi(\omega, q^2)]$. The relationship between the quantities f and φ, and L and M is given by the relation

$$\bar{u}(p')[L^{(i)}(\omega, q^2) + \hat{k}_1 M^{(i)}(\omega, q^2)]u(p) \equiv v'^*[f^{(i)}(\omega, q^2)$$
$$+ i\sigma[\mathbf{k}_1\mathbf{k}_1']\varphi^{(i)}(\omega, q^2)]v,$$
$$i = 1, 2, \qquad (3.8)$$

where v' and v are two-component spinors describing the spin states of the initial and final nucleons in their rest system, and σ are the 2×2 Pauli matrices. Expressing $u(p)$ and $u(p')$ in terms of the two-component spinors v, we obtain the relation between L, M and f, φ in the Breit system:

$$f^{(i)}(\omega, q^2) = \frac{E}{m}L^{(i)}(\omega, q^2) + \omega M^{(i)}(\omega, q^2),$$
$$\varphi^{(i)} = -\frac{1}{2m}M^{(i)}(\omega, q^2), \qquad (3.9)$$

where E is the nucleon energy in the Breit system: $E = \sqrt{m^2 + \mathbf{q}^2/4}$, $\mathbf{q}^2 = -q^2$.

The matrix elements $f^{(i)}(\omega, q^2)$, $\varphi^{(i)}(\omega, q^2)$ can be expressed in terms of the scattering amplitudes (with and without spin flip) in the center of mass system of the meson and nucleon. If the invariant matrix element (3.8) is written in the center of mass system as*

$$\bar{u}_c(p_c')[L^{(i)}(\omega_c, q^2) + \hat{k}_{1c}M^{(i)}(\omega_c, q^2)]u_c(p_c)$$
$$= \frac{E_c + \omega_c}{m}v'^*[f_c^{(i)}(\omega_c, q^2) + i\sigma[\mathbf{k}_{1c}\mathbf{k}_{1c}']\varphi_c^{(i)}(\omega_c, q^2)]v \quad (3.10)$$

(the index c labels the center of mass system) and we take into account that $L^{(i)}$ and $M^{(i)}$ are invariant, then the relation between f_c, φ_c and f, φ is easily found after we express f_c and φ_c in terms of L and M and make use of (3.9). We obtain the result[10]

$$f^{(i)}(\omega, q^2) = \frac{E_c + \omega_c}{m}\left\{\frac{E^2 + mE_c}{E(E_c + m)}f_c^{(i)}(\omega_c, q^2)\right.$$
$$\left.- \frac{1}{2}\mathbf{q}^2\frac{E^2 - E_c^2}{E(E_c + m)}\varphi_c^{(i)}(\omega_c, q^2)\right\},$$

$$\varphi^{(i)}(\omega, q^2) = -\frac{1}{2m}\frac{1}{E_c + m}f_c^{(i)}(\omega_c, q^2)$$
$$+ \left[1 + \frac{\mathbf{q}^2}{4m(E_c + m)}\right]\varphi_c^{(i)}(\omega_c, q^2), \qquad (3.11)$$

in which the meson energy in the center of mass system, E_c, is related to the energy in the Breit system by†

$$E\omega = (E_c + \omega_c)\,\omega_c - \mu^2 - \mathbf{q}^2/4. \qquad (3.12)$$

For meson energies in the center of mass system of the order of $2 - 3\mu$ which contribute to the dispersion relations, we can, to good accuracy ($\sim(\mu/m)^2$), replace (3.11) by the approximate expression

---

*The factor $(E_c + \omega_c)/m$ on the right-hand side of (3.10) is introduced so that the quantities f_c and φ_c should be exactly equal to the scattering amplitudes.

†Note that, as (3.12) indicates, in the case in which we are interested, (the point $\omega = 0$ and $q^2 = 4\mu^2$), ω_c also equals zero, i.e., the Breit system coincides with the center-of-mass system. This can, in fact, also be seen directly from the explicit expressions for the components of the nucleon and meson momenta in the Breit system.

$$f^{(i)}(\omega, q^2) = \frac{E_c+\omega_c}{m} f_c^{(i)}(\omega_c, q^2), \qquad \varphi^{(i)}(\omega, q^2) = \varphi_c^{(i)}(\omega_c, q^2). \tag{3.13}$$

The amplitudes $f_{c,T}(\omega_c, q^2)$, $\varphi_{c,T}(\omega_c, q^2)$ corresponding to given values of the total isotopic spin $T = \frac{1}{2}, \frac{3}{2}$, have the following known expansion in Legendre polynomials[10]

$$\begin{aligned} f_{c,T}(\omega_c, q^2) &= \frac{1}{2ik_c}\sum_l [(l+1)\exp\{2i\delta_{l+}^T(\omega_c)\} \\ &+ l\exp\{2i\delta_{l-}^T(\omega_c)\} - (2l+1)]\, P_l(1-\mathbf{q}^2/2k_c^2), \\ \varphi_{c,T}(\omega_c, q^2) &= \frac{1}{2ik_c^3}\sum_l [\exp\{2i\delta_{l+}^T(\omega_c)\} \\ &- \exp\{2i\delta_{l-}^T(\omega_c)\}]\, \dot{P}_l(1-\mathbf{q}^2/2k_c^2), \end{aligned} \tag{3.14}$$

where $\delta_{l+}^T(\omega_c)$ and $\delta_{l-}^T(\omega_c)$ are the scattering phase shifts for isotopic spin T and total angular momentum $j = l + \frac{1}{2}$ and $j = l - \frac{1}{2}$, and $\dot{P}_l(x) = dP_l(x)/dx$.

The dispersion relations for the functions $\tilde{f}^{(i)}(\omega, q^2)$ and $\tilde{\varphi}^{(i)}(\omega, q^2)$ have the form

$$\begin{aligned} &\mathrm{Re}\,[f^{(1)}(\omega, q^2)] - \mathrm{Re}[f^{(1)}(\omega_0, q^2) - f_p^{(1)}(\omega_0, q^2)] \\ &\quad = \frac{2}{\pi}(\omega^2-\omega_0^2)\int_{\omega_1}^{\infty} \omega'\,d\omega' \frac{\mathrm{Im}\, f^{(1)}(\omega', q^2)}{(\omega'^2-\omega^2)(\omega'^2-\omega_0^2)}, \\ &\mathrm{Re}\,[\tilde{f}^{(2)}(\omega, q^2)] - \frac{\omega}{\omega_0}\mathrm{Re}\,[f^{(2)}(\omega_0, q^2) - f_p^{(2)}(\omega_0, q^2)] \\ &\quad = \frac{2}{\pi}\omega(\omega^2-\omega_0^2)\int_{\omega_1}^{\infty} d\omega' \frac{\mathrm{Im}\, f^{(2)}(\omega', q^2)}{(\omega'^2-\omega^2)(\omega'^2-\omega_0^2)}, \\ &\mathrm{Re}\,[\tilde{\varphi}^{(1)}(\omega, q^2)] = \frac{2\omega}{\pi}\int_{\omega_1}^{\infty} d\omega' \frac{\mathrm{Im}\,\varphi^{(1)}(\omega', q^2)}{\omega'^2-\omega^2}, \\ &\mathrm{Re}\,[\tilde{\varphi}^{(2)}(\omega, q^2)] = \frac{2}{\pi}\int_{\omega_1}^{\infty} \omega'\,d\omega' \frac{\mathrm{Im}\,\varphi^{(2)}(\omega', q^2)}{\omega'^2-\omega^2}, \end{aligned} \tag{3.15}$$

where ω_1 is the lowest energy for which meson + nucleon states are possible $[\omega_1 = (m\mu - q^2/4)/(m^2+q^2/4)^{1/2}$: the energy corresponding to ω_1, in the center of mass system of the meson and nucleon is equal to μ], ω_0 is some fixed energy. In the last two relations in (3.15) it is not necessary to make a subtraction, since the spinflip scattering amplitude must decrease with energy as also must the amplitude for any inelastic process.[18] Hence it follows that for large energies φ_c must fall off rapidly and the integral will converge without the aid of additional subtractions.

The values of $f_p^{(1)}$ and $f_p^{(2)}$ occurring can easily be calculated, if the expression (2.25) for the pole term is written in the form

$$\begin{aligned} &g^2 v'^{*}\Big\{-\omega\Big[\frac{1}{2E\omega+\mu^2+\mathbf{q}^2/2} + \frac{1}{2E\omega-\mu^2-\mathbf{q}^2/2}\Big]\delta_{\alpha\beta} \\ &\quad - i\varepsilon_{\alpha\beta\gamma}\tau_\gamma\Big[-\frac{\omega}{2E\omega-\mu^2-\mathbf{q}^2/2} + \frac{\omega}{2E\omega+\mu^2+\mathbf{q}^2/2}\Big] \\ &\quad + \frac{i}{2m}\boldsymbol{\sigma}[\mathbf{k}_1\times\mathbf{k}_1']\Big[\Big(\frac{1}{2E\omega+\mu^2+\mathbf{q}^2/2} + \frac{1}{2E\omega-\mu^2-\mathbf{q}^2/2}\Big)\delta_{\alpha\beta} \\ &\quad - i\varepsilon_{\alpha\beta\gamma}\tau_\gamma\Big(\frac{1}{2E\omega-\mu^2-\mathbf{q}^2/2} - \frac{1}{2E\omega+\mu^2+\mathbf{q}^2/2}\Big)\Big]\Big\} v \\ &\quad \equiv v'^{*}\{f_p^{(1)}(\omega, q^2)\delta_{\alpha\beta} - i\varepsilon_{\alpha\beta\gamma}\tau_\gamma f_p^{(2)}(\omega, q^2) + i\boldsymbol{\sigma}[\mathbf{k}_1\times\mathbf{k}_1'] \\ &\quad \times [\varphi_p^{(1)}(\omega, q^2)\delta_{\alpha\beta} - i\varepsilon_{\alpha\beta\gamma}\tau_\gamma\varphi_p^{(2)}(\omega, q^2)]\} v. \end{aligned} \tag{3.16}$$

We express f and φ in the subtraction and integral terms in (3.15) in terms of the scattering amplitude in the center of mass system, and for ω_0 we take the threshold energy μ in this system (i.e., $\omega_0 = \omega_1$ in the Breit system). Then, after substituting $f_p^{(1)}$ and $f_p^{(2)}$ from (3.16) the dispersion relations for the quantities $f^{(1)}$, $f^{(2)}$ and $\varphi^{(2)}$ in which we are interested, take the form

$$\begin{aligned} \tilde{f}^{(1)}(\omega, q^2) &= \frac{m+\mu}{m} f_c^{(1)}(\mu, q^2) + \frac{g^2}{m} + \frac{2}{\pi}(\omega^2-\omega_1^2)\int_{\mu}^{\infty} d\omega_c'\frac{d\omega'}{d\omega_c'}\,\omega'\,\frac{E_c'+\omega_c'}{m}\,\frac{\mathrm{Im}\, f_c^{(1)}(\omega', q^2)}{(\omega'^2-\omega^2)(\omega'^2-\omega_1^2)}, \\ \tilde{f}^{(2)}(\omega, q^2) &= \frac{\omega}{\omega_1}\frac{m+\mu}{m} f_c^{(2)}(\mu, q^2) + \frac{g^2}{2m}\frac{\mu^2+\mathbf{q}^2/2}{m\mu-\mathbf{q}^2/4}\frac{\omega}{\omega_1} + \frac{2\omega}{\pi}(\omega^2-\omega_1^2)\int_{\mu}^{\infty} d\omega_c'\frac{d\omega'}{d\omega_c'}\,\frac{E_c'+\omega_c'}{m}\,\frac{\mathrm{Im}\, f_c^{(2)}(\omega', q^2)}{(\omega'^2-\omega^2)(\omega'^2-\omega_1^2)}, \\ \tilde{\varphi}^{(2)}(\omega, q^2) &= \frac{2}{\pi}\int_{\mu}^{\infty} d\omega'\,\frac{d\omega'}{d\omega_c'}\,\omega'\,\frac{\mathrm{Im}\varphi_c^{(2)}(\omega', q^2)}{\omega'^2-\omega^2}. \end{aligned} \tag{3.17}$$

In the pole term on the right hand side of (3.17) we have neglected small corrections of order $(\mu/m)^2$ and omitted Re on the left hand side, since we shall be interested in values of ω in the neighborhood of zero, and $q^2 = 4\mu^2$, where the amplitude is real. In the integral term in (3.17) we have changed to integration with respect to the meson energy in the center of mass system, ω_c', so that the lower limit of the integral becomes equal to μ.

The calculation of the right hand side of (3.17) and, in particular, of the value of the scattering amplitude in the unphysical region, can be carried out based on the following considerations.[19,10] For fixed q^2, physically realizable states begin at $\omega_{c\,\min} = \sqrt{\mu^2 + q^2/4}$, so that the region from

$\omega_c' = \mu$ to $\omega_c' = \omega_{c\,\min}$ is unphysical. However, if we make use of the expansion of the scattering amplitude in Legendre polynomials (3.14), then it is easy to see that the value of the scattering phase shift $\delta_l(\omega_c)$ is always taken for physical values of $k_c > 0$ and the unphysical behavior comes about entirely from unphysical values of $\cos\theta$: $|\cos\theta_c| > 1$. The analytic continuation of the Legendre polynomials $P_l(\cos\theta_c)$ for values of $|\cos\theta_c| > 1$ is known and, consequently, the calculation of the integrals on the right hand side of (3.17) will be quite correct, provided that in analytically continuing $f_c(\omega_c, q^2)$ and $\varphi_c(\omega_c, q^2)$ in q^2 we do not go outside the limits of the region in which this analytic continuation is legitimate.

In the example of meson-nucleon scattering in perturbation theory, it has been shown[20] that the nearest singularity to the point $q^2 = 0$, from which we begin our analytic continuation of $f(\omega, q^2)$ and $\varphi(\omega, q^2)$, comes at $q^2 = 4\mu^2$, so that we can expect the analytic continuation to be permissible for $q^2 < 4\mu^2$. This singularity corresponds to meson-nucleon scattering through a two-meson intermediate state and is of the nature of a branch point of the type $\sqrt{4\mu^2 - q^2}$. But, as is well known, the power series in x for a function like $(1-x)^{1/2}$ is absolutely convergent at the point $x = 1$ and gives the correct value of the function (equal to zero). This allows us to extend our analytic continuation to the point $q^2 = 4\mu^2$ also, and, consequently, the values of $f_c(\omega_c, 4\mu^2)$ and $\varphi_c(\omega_c, 4\mu^2)$ can be obtained by analytic continuation of $f_c(\omega_c, q^2)$, $\varphi_c(\omega_c, q^2)$ from small values of q^2. The singular terms of such an analytic continuation must vanish. This last conclusion is in agreement with the remark in the last footnote of Sec. 2, where it was shown that terms proportional to $\sqrt{4\mu^2 - q^2}$, give small contributions of order $1/L$, which in the zero-order approximation can be neglected.*

From all the above, it follows that we can calculate the right hand side of (3.17), if we write the scattering amplitude in the form (3.14), take the scattering phase shifts from experiment, and analytically continue the Legendre polynomials $P_l(\cos\theta_c)$ to the value $\cos\theta_c = 1 + 2\mu^2/k_c^2$.

For practical purposes it is sufficient to consider only the three phase shifts δ_1, δ_3, and δ_{33} in the expansion (3.14). We choose the energy dependence of the phase shifts in agreement with Orear's phase-shift analysis:[21]

$$\delta_1 = 0.16\ k_c/\mu, \qquad \delta_3 = -0.11\, k_c/\mu,$$

$$\cot\delta_{33} = (\mu/k_c)^3(8.05 - 3.8\,\omega^*)\,\omega^*, \qquad \omega^* = E_c + \omega_c - m.$$

The calculation gives

$$\frac{m+\mu}{m} f_c^{(1)}(\mu, 4\mu^2) = 0.70/\mu, \qquad \frac{m+\mu}{m\omega_1} f_c^{(2)}(\mu, 4\mu^2) = 0.23/\mu^2,$$

$$-\frac{2}{\pi}\omega_1^2 \int_\mu^\infty \frac{d\omega'}{d\omega_c'} d\omega_c' \frac{E_c' + \omega_c'}{m\omega'} \frac{\operatorname{Im} f_c^{(1)}(\omega_c', 4\mu^2)}{\omega'^2 - \omega_1^2} = -0.23/\mu,$$

$$-\frac{2}{\pi}\omega_1^2 \int_\mu^\infty \frac{d\omega'}{d\omega_c'} d\omega_c' \frac{E_c' + \omega_c'}{m\omega'^2} \frac{\operatorname{Im} f_c^{(2)}(\omega', 4\mu^2)}{\omega'^2 - \omega_1^2} = -0.047/\mu^2,$$

$$\frac{2}{\pi} \int_\mu^\infty \frac{d\omega'}{d\omega_c'} d\omega_c' \frac{1}{\omega'} \operatorname{Im} \varphi_c^{(2)}(\omega', 4\mu^2) = 0.028/\mu^2. \qquad (3.18)$$

Combining (3.18) with the value of the pole term ($g^2 = 14.5$), we have:

$$\widetilde{f}^{(1)}(0, 4\mu^2) = \frac{g^2}{\mu}\left(\frac{\mu}{m} + \frac{0{,}70}{g^2} - \frac{0{,}23}{g^2}\right) = 0.18\,\frac{g^2}{\mu},$$

$$\frac{\partial}{\partial\omega}\widetilde{f}^{(2)}(\omega, 4\mu^2)\big|_{\omega=0} = \frac{g^2}{\mu^2}\left(-0.0085 + \frac{0{,}23}{g^2} - \frac{0{,}047}{g^2}\right)$$

$$= 0.0041\,\frac{g^2}{\mu^2};$$

$$\widetilde{\varphi}^{(2)}(0, 4\mu^2) = 0.0126\, g^2/m\mu^2. \qquad (3.19)$$

Hence, using (3.9), we obtain for the quantities entering into (3.6)

$$\widetilde{L}^{(1)}(0, 4\mu^2) = 1.2\, g^2/m, \quad (\partial\widetilde{L}(\nu, 4\mu^2)/\partial\nu)_{\nu=0} = 0.029\, g^2/m\mu^2,$$

$$\widetilde{M}^{(2)}(0, 4\mu^2) = -0.025\, g^2/\mu^2. \qquad (3.20)$$

Let us consider the accuracy of the results we have obtained. It follows from (3.19) and (3.17) that in calculating the principal term $\widetilde{L}^{(1)}(0, 4\mu^2)$, the main contribution (more than 80%) is given by the subtracted pole term $f_p^{(1)}(\omega_0, 4\mu^2)$, which is calculated exactly. The contribution of the integral in (3.17) to $f^{(1)}$ is less than 10%; therefore the uncertainty which can arise due to inaccuracies in the high energy part of its calculation (in fact the integral already converges for energies $\omega_c \sim 2.5\mu$ and the uncertainty in it, apparently, does not exceed 10%) does not exceed 1% of $\widetilde{L}^{(1)}$. The contribution of the subtraction term $f_c^{(1)}(\mu, 4\mu^2)$ to $\widetilde{L}^{(1)}$ is about 25%. The P phase shift plays a fundamental part in this calculation, since for fixed q^2 and $k_c \to 0$, the terms due to the P phase shift do not tend to zero. Taking the D phases given by Mukhin and Pontecorvo[22] into account in the most unfavorable case

$$\delta_{3,j=5/2} = -0{,}2\,\frac{\pi}{180}\left(\frac{k_c}{\mu}\right)^5, \qquad \delta_{3,j=3/2} = 0$$

reduces $f_c^{(1)}(\mu, 4\mu^2)$ by 7%. The inaccuracy in $f_c^{(1)}(\mu, 4\mu^2)$ arises mainly from the fact that the function $f_c^{(1)}(\mu, q^2)$ has a singularity of the type $\sqrt{4\mu^2 - q^2}$ (see footnote at the end of Sec. 2), and the calculation of $f_c^{(1)}(\mu, 4\mu^2)$ as an analytic continuation in q^2 of only the S, P and D amplitudes is not good enough. It may be thought that $f_c^{(1)}(\mu, 4\mu^2)$ might contain errors of ~ 25% and, consequently, that the quantity $\tilde{L}^{(1)}(0, 4\mu^2)$ is determined to within an accuracy ~ 5 – 7%. For this to be so, it is assumed that meson-meson scattering is not anomalously large and that the singular part of $f_c^{(1)}(\mu, 4\mu^2)$ does not contain a large coefficient. Such an assumption is not feasible, if the meson-meson scattering has a low energy resonance. In that case, for an accurate estimate of $f_c^{(1)}(\mu, 4\mu^2)$ one must take into account higher phase shifts. The estimate obtained from the main D phase shifts in view of the absence of data on higher phase shifts, and possible experimental errors,[22] may turn out to be not quite accurate.

---

*Note that, since the contributions to the imaginary part of the scattering amplitude from the branch point $q^2 = 4\mu^2$ are strictly zero for $q^2 < 4\mu^2$, these terms generally do not affect the analytic continuation of $\operatorname{Im} f_c(\omega_c', q^2)$ [or $\operatorname{Im}\varphi_c(\omega_c', q^2)$] up to $q^2 = 4\mu^2$. The discussion in the text is only important for the term $\operatorname{Re} f_c^{(1)}(\omega_0, q^2)$ in (3.15).

The terms $\partial L^{(2)}/\partial\nu$ and $M^{(2)}$ are much less important than $L^{(1)}$ and therefore errors in their calculation do not affect later results. The main errors here come about from inaccuracies in the calculation of the integral from the imaginary part of $\varphi_c^{(2)}(\omega_c', q^2)$ for large energies and apparently go up to 15 – 20%.

Substituting $f_{\alpha\beta}$ in the form $f_{p\alpha\beta} + \tilde{f}_{\alpha\beta}$ into (2.28) leads to a sum of several terms, between which there are strong cancellations, as further calculation shows (see reference 23); in other words, if we replace $f_{\alpha\beta}$ by the lowest perturbation approximation, the accuracy of the results is poor. Such compensation of $f_{p\alpha\beta}$ and $\tilde{f}_{\alpha\beta}$ strongly increases the effect of errors in the determination of the quantity $\tilde{L}^{(1)}(0, 4\mu^2)$. The actual calculation of the two-meson phase shift and its comparison with the one-meson term will be carried out in a subsequent paper.[23]

---

[1] L. B. Okun' and I. Ya. Pomeranchuk, JETP **36**, 300 (1959), Soviet Phys. JETP **9**, 207 (1959).

[2] S. Mandelstam, Phys. Rev. **112**, 1344 (1959).

[3] Lehmann, Symanzik, and Zimmerman, Nuovo cimento **1**, 205 (1955).

[4] M. Goldberger, Phys. Rev. **99**, 979 (1955).

[5] V. Ya. Faĭnberg and E. S. Fradkin, Dokl. Akad. Nauk SSSR **109**, 507 (1956), Soviet Phys.-Doklady **1**, 455 (1957).

[6] I. M. Ryzhik, I. S. Gradshteĭn, Таблица интегралов, (Tables of Integrals), Gostekhizdat, 1951.

[7] A. Salam, Nuovo cimento **3**, 424 (1956); A. Salam and W. Gilbert, Nuovo cimento **3**, 607 (1956).

[8] B. L. Ioffe, JETP **31**, 583 (1956), Soviet Phys. JETP **4**, 534 (1957).

[9] E. S. Fradkin, JETP **31**, 515 (1956), Soviet Phys. JETP **4**, 450 (1957).

[10] R. H. Capps and G. Takeda, Phys. Rev. **103**, 1877 (1956).

[11] R. J. Eden, Proc. Roy. Soc. **A210**, 388 (1952).

[12] Karplus, Sommerfield, and Wichman, Phys. Rev. **114**, 376 (1959); L. D. Landau, JETP **37**, 62 (1959), Soviet Phys. JETP **10**, 45 (1960).

[13] R. P. Feyman, Phys. Rev. **76**, 749, 769 (1949).

[14] Bogolyubov, Medvedev, and Polivanov, Вопросы теории дисперсионных соотношений, (Problems in the Theory of Dispersion Relations), Fizmatgiz, 1958.

[15] Bremermann, Oehme, and Taylor, Phys. Rev. **109**, 2178 (1958).

[16] H. Lehmann, Nuovo cimento **10**, 579 (1958).

[17] N. N. Bogolyubov and D. V. Shirkov, Введение в теорию квантованных полей, (Introduction to the Theory of Quantized Fields), Gostekhizdat, 1957, p. 404.

[18] I. Ya. Pomeranchuk, JETP **30**, 423 (1956), Soviet Phys. JETP **3**, 306 (1956). L. B. Okun' and I. Ya. Pomeranchuk, JETP **30**, 424 (1956), Soviet Phys. JETP **3**, 307 (1956).

[19] M. L. Goldberger, Proc. of the Sixth Annual Rochester Conference, N.Y., 1956.

[20] K. Symanzik, Progr. Theoret. Phys. **20**, 690 (1958).

[21] J. Orear, Phys. Rev. **100**, 288 (1955).

[22] A. I. Mukhin and B. M. Pontecorvo, JETP **31**, 550 (1956), Soviet Phys. JETP **4**, 373 (1957).

[23] Galanin, Grashin, Ioffe, and Pomeranchuk, JETP, in press.

Translated by R. F. Peierls
329

SOVIET PHYSICS JETP VOLUME 37(10), NUMBER 6 JUNE, 1960

ULTRASONIC ABSORPTION IN METALS IN A MAGNETIC FIELD. II

V. L. GUREVICH

Institute of Semiconductors, Academy of Sciences, U.S.S.R.

Submitted to JETP editor June 16, 1959

J. Exptl. Theoret. Phys. (U.S.S.R.) **37**, 1680-1691 (December, 1959)

Ultrasonic absorption in a metal located in a strong magnetic field H is considered, the Larmor radius of the conduction electrons being much smaller than the wavelength of the sound. Various limiting cases corresponding to different relationships between these two lengths and the mean free path are investigated. The absorption coefficient is computed by solving simultaneously the kinetic equation and the Maxwell equations. It has been found that there are two absorption mechanisms in the magnetic field. One of these, a deformation mechanism, determines the absorption even in the absence of the magnetic field. The coefficient of this absorption can be expressed in terms of the deformation potential, that is, in terms of functions which determine the change in the electron energy caused by the deformation. At experimentally obtainable ultrasonic frequencies and in a strong magnetic field, this relation is found to be quite simple in a number of cases. The magnitude of the deformation potential can be estimated with satisfactory accuracy on the basis of the absorption data.

Induction absorption is due to electric fields which arise when the conductor, deformed by the sound wave, crosses the magnetic lines of force. Absorption is determined by the Joule heat generated by the currents created by these fields. The coefficient of induction absorption can be expressed in terms of certain combinations of the components of the conductivity tensor, account being generally made of their time and spatial dispersion and dependence on H. The asymptotic value of the conductivity tensor in a strong magnetic field has been determined with account of spatial dispersion.

IN a previous work[1]* the ultrasonic absorption in metals in a magnetic field was studied theoretically under the condition $l \gtrsim r \gtrsim \lambdabar$, where l is the mean free path of the conduction electrons, $r/2\pi$ the Larmor radius, and $2\pi\lambdabar$ the sound wavelength. In the present research, the ultrasonic absorption is studied in a strong magnetic field H, for which the condition $r/\lambdabar \lesssim 1$ is satisfied. All limiting cases of relations between these two lengths and l have been considered.

There are two sound absorption mechanisms in a strong magnetic field. The first of these, the deformation mechanism, leads to absorption even in the absence of a magnetic field. It is connected with the fact that the energy of the electron increases in the deformed metal, in first approximation proportional to the deformation tensor. Because of the finite velocity of the deformation in the sound wave, the contribution depends on time; the distribution function of the conduction electrons departs from equilibrium, and this leads to the dissipation of sound energy.

In addition to the strictly deformation effect, it is necessary in general to take into account the electric fields which arise in the metal as a result of the inhomogeneity of the deformation in the sound field and the finite velocity of its change. These fields are determined by the Maxwell equations in which appear the charge density and the currents computed with account both of the strictly deformation effect and of these same electric fields.

Induction absorption is brought about by electric fields which arise in a system of coordinates attached to the moving lattice, when the conductor deformed by the sound wave crosses the magnetic lines of force. These magnetic fields are also determined by means of Maxwell's equations. The energy absorbed is equal to the Joule heat which is generated by the currents created by these electric fields. Depending on the conditions of the experiment (the ultrasonic frequency ω, the relative orientation of the vectors **k**, **H**, and **u**, the value of the magnetic field)* the absorption coefficient is determined by one of the two mechanisms described. In the different cases, measurement of the absorption coefficient Γ gives information on the properties of the metal.

---

*We shall henceforth denote this paper by I and add this numeral to references to the corresponding equations.

*The notation in this paper coincides with that used in I.

If $l/\lambdabar \gg 1$ and the absorption is determined directly by the deformation effect, the coefficient Γ has a very simple relation with the deformation potential, i.e., with the functions $\Lambda_{ik}(\mathbf{p})$ that determine the change of the electron energy under the deformation. The connection between the coefficient Γ and the functions $\Lambda_{ik}(\mathbf{p})$ is by no means so simple, and the analysis of the experimental data is much more complicated if there also exist electric fields brought about by reason of the inhomogeneity of the deformation in the sound field in addition to this effect in the case of absorption. This is precisely the case, for example, in the absence of a magnetic field at experimentally obtainable frequencies. It is shown that in certain cases a strong magnetic field changes the situation: the role of the electric fields in sound absorption becomes negligibly small while the connection between the coefficient Γ and the functions $\Lambda_{ik}(\mathbf{p})$ is very simple. Therefore, the investigation of the deformation sound absorption in a strong magnetic field permits us to estimate the magnitude of the deformation potential with great accuracy.

The induction absorption coefficient is rather simply expressed in terms of the components of the conductivity tensor, in general with consideration of its temporal and spatial dispersion and their dependence on the magnetic field. Measurement of Γ permits us to determine certain combinations of these components which make it possible to estimate the qualitative peculiarities of the spectrum of the conduction electrons.

We shall now proceed to a quantitative solution of this problem.

1. To each of the absorption mechanisms mentioned, there correspond definite terms in the part of the kinetic equation that contains the inhomogeneity. The meaning of these terms is especially clear if we write the equation not in the system of coordinates K′, connected with the deformed lattice, as was done in I, but in a fixed (laboratory) system K.

The coordinates of the electron in these systems are related by the equation

$$\mathbf{r} = \mathbf{r}' + \mathbf{u}. \tag{1.1}$$

The energy of the electron in the system K′, in first approximation in the small quantity $\mathbf{u}$,

$$\varepsilon'(\mathbf{p}') = \varepsilon_0(\mathbf{p}') + \lambda_{ik} u_{ik}. \tag{1.2}$$

In (1.2) there should still enter a term connected with the Stewart-Tolman effect. But it is shown in reference 3 that it is small in comparison with other components which determine the change in the energy of the electron in the sound field; therefore we shall neglect it.

The corresponding Hamilton-Jacobi equation is

$$\left(\frac{\partial S}{\partial t}\right)_{\mathbf{r}'} + \varepsilon\left(\frac{\partial S}{\partial \mathbf{r}'}\right) = 0. \tag{1.3}$$

but

$$\left(\frac{\partial S}{\partial t}\right)_{\mathbf{r}'} = \left(\frac{\partial S}{\partial t}\right)_{\mathbf{r}} + \left(\frac{\partial S}{\partial \mathbf{r}}\right)\dot{\mathbf{u}} = -\varepsilon(\mathbf{p}) + \mathbf{p}\dot{\mathbf{u}}, \tag{1.4}$$

$$p_i' = \frac{\partial S}{\partial x_i'} = \sum_k \frac{\partial S}{\partial x_k}\frac{\partial x_k}{\partial x_i'} = p_i + \sum_k p_k \frac{\partial u_k}{\partial x_i}. \tag{1.5}$$

Then the energy of the electron in the system K is given by

$$\varepsilon(\mathbf{p}) = \varepsilon'(\mathbf{p}) + \mathbf{p}\dot{\mathbf{u}} + \sum_{i,k} v_i p_k \, \partial u_k/\partial x_i. \tag{1.6}$$

The equilibrium distribution function in K′ is

$$F_0' = F^0(\varepsilon') = [e^{(\varepsilon'-\mu)/T} + 1]^{-1}.$$

It is clear that $F_0' d^3\mathbf{p}' d^3\mathbf{r}' = F_0 d^3\mathbf{p} d^3\mathbf{r}$, as follows from the meaning of the quantities entering into this equality, which are proportional to the mean number of occupied states in the given element of phase space. But the product $d^3\mathbf{p} d^3\mathbf{r}$ is itself invariant relative to canonical transformations. Hence it is easy to conclude that the equilibrium distribution function in the K system is equal to $F_0 = F^0(\epsilon - \mathbf{p}\cdot\dot{\mathbf{u}})$.

In this system the kinetic equation has the form

$$\frac{\partial F}{\partial t} + \frac{\partial \varepsilon}{\partial \mathbf{p}}\frac{\partial F}{\partial \mathbf{r}} - \frac{\partial \varepsilon}{\partial \mathbf{r}}\frac{\partial F}{\partial \mathbf{p}} - \frac{e}{c}[\mathbf{v}\times\mathbf{H}]\frac{\partial F}{\partial \mathbf{p}} + \frac{f}{t_0} = \frac{\partial F^0(\varepsilon)}{\partial \varepsilon} e\mathbf{E}\mathbf{v}. \tag{1.7}$$

On the right hand side there appears the electric field **E** which is determined by solution of Maxwell's equations.

It is very important to note that, inasmuch as the equilibrium distribution function depends not only on the energy, the component is given by

$$-(e/c)[\mathbf{v}\times\mathbf{H}]\,\partial F_0/\partial\mathbf{p} = -(e/c)[\dot{\mathbf{u}}\times\mathbf{H}]\,\mathbf{v}\partial F^0(\varepsilon)/\partial\varepsilon.$$

This has the same structure as the term containing the electric field; therefore, in order to take it into account, it suffices to replace **E** by $\mathbf{E} + [\dot{\mathbf{u}} \times \mathbf{H}/c]$ on the right hand of (1.7).

Expanding $F = F_0 - \chi \partial F^0(\epsilon)/\partial\epsilon$, we obtain the equation (4.3, I) for the function χ, where $\Lambda_{ik} = \lambda_{ik} - \overline{\lambda}_{ik}$ [the last component in (4.2, I) is written incorrectly and is in fact missing]. It follows from the form of this equation that in the absence of a constant magnetic field only the symmetric part of the tensor $\partial u_i/\partial x_k$ enters into the expression for the dissipative function. If the constant magnetic field is sufficiently large and the induction absorption is appreciable, then the dissipation can be determined both for the symmetric and for the antisymmetric parts of this tensor.

The electric current is composed of the equilibrium current, equal to $N_0 e\dot{\mathbf{u}}$, and the nonequilibrium current (determined by the function χ). The former is completely compensated by the lattice current. Thus the total current is determined only by the function χ.

Simultaneous solution of the kinetic equation and Maxwell's equations is given in general form in I. We need to analyze it in a number of limiting cases. Perhaps the simplest of these is the case of the induction absorption of sound. We shall begin with it.

2. The rate of dissipation of the energy density in this case is equal to

$$T\dot{S} = {}^1/_2 \operatorname{Re} \sum_{\mu\nu} \sigma^{-1}_{\mu\nu} \; j_\mu j^*_\nu = {}^1/_2 \operatorname{Re} \sum_{\mu\nu} \sigma_{\mu\nu} \mathscr{E}_\mu \mathscr{E}^*_\nu. \quad (2.1)$$

Here $\sigma_{\mu\nu}$ is the conductivity tensor, which, generally speaking, takes account of time and spatial dispersion.

The quantities $\mathscr{E}_\mu$ enter in the part of the kinetic equation that contains the inhomogeneity. They represent the components of the electric field in the system of coordinates connected to the moving lattice. They are determined from Maxwell's equations and the condition

$$j_\xi = 0, \quad (2.2)$$

which, as is easily shown, is equivalent to the vanishing of the volume charge density. We shall assume that this system xyz is connected with the magnetic field (the axis z is directed along **H**); in the system $\xi\eta\zeta$ the axis ξ is directed along **k** at an angle θ with the z axis, while the axes η and y coincide. The symbol β designates either η or ζ.

Taking the condition (2.2) into account, we obtain

$$T\dot{S} = {}^1/_2 \operatorname{Re} \sum_{\beta\beta'} s_{\beta\beta'} \mathscr{E}_\beta \mathscr{E}^*_{\beta'}, \quad (2.3)$$

where

$$s_{\beta\beta'} = \sigma_{\beta\beta'} - \sigma_{\beta\xi}\sigma_{\xi\beta'}/\sigma_{\xi\xi}. \quad (2.4)$$

According to I,

$$\mathscr{E}_\beta = \sum_{\beta'} (1-d)^{-1}_{\beta\beta'} G_{\beta'}, \quad (2.5)$$

where

$$d_{\beta\beta'} = -(4\pi i\omega/k^2c^2)\, s_{\beta\beta'}, \quad (2.6)$$

It is seen from these equations that the induction absorption is different from zero only if the induction field **G** has components perpendicular to the direction of propagation of sound.

In the present work, we shall distinguish two limiting cases: a) $|d_{\beta\beta'}| \ll 1$ and b) $|d_{\beta\beta'}| \gg 1$. The physical meaning of these inequalities are the following: $|d_{\beta\beta'}| \sim \lambda\!\!\!^{-2}/\delta^2$, where $\delta = \sqrt{c/2\pi\omega s}$ is the skin depth computed with account of the dispersion of the conductivity tensor and its dependence on the magnetic field. In case a) the skin depth is much greater than the wavelength. This means that the electric fields associated with the eddy currents are small in comparison with the induction fields, so that the total field $\mathscr{E}_\beta = G_\beta$.

In case b) the skin depth is much less than the wavelength, the eddy currents almost exactly compensate the induction, so that the total current

$$\mathscr{E}_\beta = -\sum_{\beta'} d^{-1}_{\beta\beta'} G_{\beta'} \quad (2.7)$$

is of the order of $G\lambda\!\!\!^{-2}/\delta^2$.

Corresponding to the above, the coefficient of absorption in the first case is

$$\Gamma = (H^2/2\rho c^2 w) \operatorname{Re} \sum_{\beta\beta'} s_{\beta\beta'} \nu_\beta \nu_{\beta'}, \quad (2.8a)$$

where w is the group sound velocity, while in the second case

$$\Gamma = (c^2H^2k^4/32\pi^2\rho w\omega^2) \operatorname{Re} \sum_{\beta\beta'} s^{-1}_{\beta\beta'} \nu_\beta \nu_{\beta'}. \quad (2.8b)$$

Here $\boldsymbol{\nu} = \mathbf{u} \times \mathbf{H}/uH$.

These equations immediately determine the dependence of Γ on ω and **H** under the conditions $r/l \gg 1$, $l/\lambda\!\!\!^- \ll 1$, while the components of the tensor $s_{\beta\beta'}$ depend weakly on **H** and **k**.

In order to find out when the induction absorption mechanism plays the principal role, we must compare (1.5) with the equation

$$\Gamma \sim N_0\mu_0\omega^2 t_0/\rho w^3, \quad (2.9)$$

which determines the coefficient of deformation absorption under these conditions (it was obtained in the works of Akhiezer[2] and Akhiezer, Kaganov, and Lyubarskiĭ[3]). Comparison shows that the induction absorption dominates over the deformation absorption if the vectors **k**, **H** and **u** are appropriately oriented with respect to each other and

$$r/\lambda\!\!\!^- \ll 1 \quad (2.10a)$$

in case a) or

$$r\lambda\!\!\!^-/\delta^2 \ll 1 \quad (2.10b)$$

in case b). Thus the absorption coefficient can depend strongly on the magnetic field and on the condition $r/l \gg 1$.

The estimates (2.10) are in fact always accurate, and not merely in the range of fields and frequencies defined by the inequalities $r \gg l$, $l \ll \lambdabar$. One must understand them only as the necessary conditions which need always be satisfied in order that the induction absorption be much greater than the deformation. They are obtained from the equating of the quantities

$$\sum_{ik} \Lambda_{ik} u_{ik} \text{ and } \sum_{\beta\beta'} v_\beta (1-d)^{-1}_{\beta\beta'} G_{\beta'},$$

which appear on the right side of the kinetic equation (4.3, I).

If $r/l \ll 1$ and $l/\lambdabar \ll 1$, then spatial dispersion is absent and the dependence of the conductivity tensor on **H** is substantial; measurements of the coefficient Γ furnish information on this dependence. Theoretically it was determined in the researches of I. Lifshitz, Azbel' and Kaganov[4] and I. Lifshitz and Peschanskiĭ[5]. For closed trajectories in quasimomentum space — and only such interest us in this research — it has the form:

$$\sigma_{ik}(\mathbf{H}) = \begin{pmatrix} \gamma_0^2 a_{xx} & \gamma_0 a_{xy} & \gamma_0 a_{xz} \\ \gamma_0 a_{yx} & \gamma_0^2 a_{yy} & \gamma_0 a_{yz} \\ \gamma_0 a_{zx} & \gamma_0 a_{zy} & a_{zz} \end{pmatrix}, \qquad (2.10)$$

where $\gamma_0 = 2\pi/\Omega_0 t_0 = 2\pi m_0 c/eHt_0$. Here Ω_0 is the Larmor frequency, m_0 = characteristic mass (of the order of the average effective mass of the electron over the trajectories). The quantities a_{ik}, generally speaking, are of the order of σ_0 — the conductivity of the metal in the absence of a magnetic field. The different components of the tensor depend differently on the field; therefore quite different formulas are obtained for the coefficient of absorption, depending on the relative orientations of the vectors **k** and **H** and the direction of the polarization of the sound. We shall carry this through below.

1) The vectors **k** and **H** are parallel (more accurately, $\vartheta \ll \gamma_0$). In case a) the induction absorption is insignificant. In case b)

$$\Gamma \sim (c^2 H^2 \omega^2 / 32\pi^2 \rho w^5 \sigma_0) \nu_\perp^2 \quad (\nu_\perp = \nu_\eta^2 + \nu_\zeta^2). \qquad (2.11)$$

2) The vectors **k** and **H** are mutually perpendicular (more accurately $\cos\vartheta \ll \gamma_0$). In case a),

$$\Gamma \sim (\sigma_0 H^2/\rho c^2 w) \nu_\perp^2, \qquad (2.12a)$$

In case b),

$$\Gamma \sim (c^2 H^2 \omega^2 / 32\pi^2 \rho w^5 \sigma_0) \nu_\perp^2. \qquad (2.12b)$$

3) The angle ϑ differs appreciably from either zero or $\pi/2$. Then in case a),

$$\Gamma \sim (\sigma_0 H^2/\rho c^2 w) \nu_\zeta^2, \qquad (2.13)$$

if $|\nu_\xi/\nu_\eta| \gg \gamma_0$ and the induction absorption is small in comparison with the deformation if $|\nu_\xi/\nu_\eta| \ll \gamma_0$. In case b)

$$\Gamma \sim (v_0^2 t_0 H^4 \omega^2 / 32\pi^2 \rho N_0 \mu_0 w^5) \nu_\eta^2, \qquad (2.14)$$

if $|\nu_\eta/\nu_\xi| \gg \gamma_0$, and

$$\Gamma \sim (c^2 H^2 \omega^2 / 32\pi^2 \rho w^5 \sigma_0) \nu_\zeta^2, \qquad (2.15)$$

if $|\nu_\eta/\nu_\xi| \ll \gamma_0$. Here v_0 is of the order of the mean velocity on the Fermi surface.

It is equally simple to analyze the case in which the density of electrons N_- is equal to the density of holes N_+ (then the expansion of the components σ_{xy} and σ_{yx} begins with a term proportional to γ_0^2). We shall not compute the corresponding formulas. Making use of the results of the researches of I. Lifshitz et al.,[4,5] it is also easy to consider the case of open trajectories in quasimomentum space.

There is now left one final possibility:* $r \ll \lambdabar \ll l$. Here both the dependence on the field **H** and the spatial dispersion of the conductivity tensor

$$\sigma_{\mu\nu} = (2e^2/h^3) \int dp_z m^* \int_0^{2\pi} d\tau\, v_\mu \int_{-\infty}^{\tau} d\tau'\, v_\nu \exp\left[\int_\tau^{\tau'} (-i\alpha + \gamma)\, d\tau''\right], \qquad (2.16)$$

are both significant; in this last equation m^* is the effective mass of the electron on the given trajectory.

Expanding in powers of the small quantities γ_0 and $\alpha_0 = 2\pi k v_0/\Omega_0$, we find the asymptotic value of the conductivity tensor in a strong magnetic field:

$$\sigma_{\mu\nu}(\mathbf{k}, \mathbf{H}) = \begin{pmatrix} (\gamma_0/\alpha_0)^2 a_{\xi\xi} & (\gamma_0^2/\alpha_0)\, a_{\xi\eta} & (\gamma_0/\alpha_0)^2 \sin\vartheta\, a'_{\xi\zeta} + (\gamma_0^2/\alpha_0) a''_{\xi\zeta} \\ (\gamma_0^2/\alpha_0)\, a_{\eta\xi} & \alpha_0\gamma_0 a_{\eta\eta} & \gamma_0 a_{\eta\zeta} \\ (\gamma_0/\alpha_0)^2 \sin\vartheta\, a'_{\zeta\xi} + (\gamma_0^2/\alpha_0) a''_{\zeta\xi} & \gamma_0 a_{\zeta\eta} & (\gamma_0/\alpha_0)^2 \sin^2\vartheta\, a'_{\zeta\zeta} + \alpha_0\gamma_0 a''_{\zeta\zeta} \end{pmatrix}, \qquad (2.17)$$

if $\cos\vartheta \gg \gamma_0/\alpha_0$ and

$$\sigma_{\mu\nu}(\mathbf{k}, \mathbf{H}) = \begin{pmatrix} \gamma_0^2 a_{\xi\xi} & \gamma_0 a_{\xi\eta} & \gamma_0 a_{\xi\zeta} \\ \gamma_0 a_{\eta\xi} & \alpha_0^2 a_{\eta\eta} & \gamma_0 a_{\eta\zeta} \\ \gamma_0 \varkappa_{\zeta\xi} & \gamma_0 a_{\zeta\eta} & a_{\zeta\zeta} \end{pmatrix}, \qquad (2.18)$$

if $\cos\vartheta \lesssim \gamma_0/\alpha_0$.

In both cases it is assumed that $N_+ \neq N_-$ and that the time dispersion of the tensor $\sigma_{\mu\nu}$ is unimportant (the frequency of the ultrasound is ω

---

*If the spatial dispersion is substantial ($l \gg \lambdabar$), while the dependence on the magnetic field is insignificant ($r \gg l$), then $r \gg \lambdabar$ and the induction absorption is small.

$\ll t_0^{-1}$). It is easy to prove that under the latter condition the components of the tensor $\sigma_{\mu\nu}$ are real and satisfy the condition $\sigma_{\mu\nu}(\mathbf{k}, \mathbf{H}) = \sigma_{\mu\nu}(-\mathbf{k}, \mathbf{H})$. If $N_+ = N_-$, then the only difference is that when the vectors **k** and **H** are parallel the expansion of components $\sigma_{\xi\eta}$ and $\sigma_{\eta\xi}$ begins with a term proportional to $\alpha_0\gamma_0$; if $\mathbf{k} \perp \mathbf{H}$, the expansion of the components $\sigma_{\xi\eta}$ and $\sigma_{\eta\xi}$ begins with a term proportional to γ_0^2.

In general, the quantities $a_{\mu\nu}$ are of the order σ_0, although some of them can vanish for reasons of symmetry. Thus, if the vectors **k** and **H** are directed along the axis of a crystal of third, fourth, or sixth order, then

$$a_{\xi\eta} = a_{\eta\xi} = a_{\xi\zeta} = a_{\zeta\xi} = 0. \tag{2.19}$$

Using (2.17) and (2.18) to compute the tensor $s_{\beta\beta'}$, we obtain the following estimate for the asymptotic value of the coefficient of absorption in a strong magnetic field ($N_+ \neq N_-$):

1) The vectors **k** and **H** are parallel (more precisely, $\vartheta \ll \gamma_0$): in case a),

$$\Gamma \sim (N_0\mu_0\omega / \rho v_0 w^2)\, \nu_\perp^2; \tag{2.20a}$$

In case b),

$$\Gamma \sim (\mu_0 c^2 H^2 \omega^3 / 32\pi^2 N_0 e^2 \rho v_0 w^6)\, \nu_\perp^2. \tag{2.20b}$$

2) The vectors **k** and **H** are mutually perpendicular (more precisely, $\cos\vartheta \lesssim \gamma_0/\alpha_0$) $s_{\beta\beta'} \sim \sigma_0$; the estimates in both cases follow directly from Eqs. (2.8).

We shall not compute the intermediate orientations of the vectors **k** and **H** in the case $N_+ = N_-$. It is very simple to obtain them since the asymptotic value of the tensor $\sigma_{\mu\nu}$ is known.

In order to make clear what absorption mechanism dominates, it is necessary to compare the formulas obtained here with those which determine the deformation sound absorption.* We shall undertake this comparison in the next section.

3. We must first explain to what extent the electric fields that arise because of inhomogeneities of deformation in the sound field are significant for the absorption. It is evident that they are small and do not affect the absorption in the case of a sufficiently large inequality $l \ll \lambdabar$. In fact, in such a case, the deformation at a distance of the order l is almost homogeneous, the electric fields are comparatively small, and their contribution to the absorption is of higher order in $l/\lambdabar$. The coefficient Γ for the condition $r \ll l$ has the same order as that for $\mathbf{H} = 0$, and

$$\Gamma \sim N_0\mu_0\omega^2 t_0 / \rho w^3. \tag{3.1}$$

This estimate can easily be obtained by solving the kinetic equation directly and then computing the dissipative function.

If $l \gg \lambdabar$, the electric fields can play a significant role in the absorption. In this case, a longitudinal electric field (parallel to **k**) will generally lead to some effect, while the transverse field can lead to significant effects only for definite relations between the quantities $\lambdabar$ and δ.

The components of the field are determined by a set of three equations. One of these is the condition of the vanishing of the volume charge density. It is easy to put this in the form

$$j_\xi = \sum_\nu \sigma_{\xi\nu} E'_\nu + j_{\xi 0} = 0. \tag{3.2}$$

The other two are Maxwell equations (4.5, I). With the aid of (3.2) we get from these equations

$$E_\beta = \sum_{\beta_1\beta_2} \left(\frac{d}{1-d}\right)_{\beta\beta_1} s^{-1}_{\beta_1\beta_2} J_{\beta_2}. \tag{3.3}$$

Here the transverse "deformation current" is

$$J_\beta = j_{\beta 0} - \sigma_{\beta\xi} j_{\xi 0} / \sigma_{\xi\xi}, \tag{3.4}$$

$$j_{\nu 0} = -(2e/h^3) \int \hat{R}\Lambda\dot{u}\, d\Sigma \Big/ v. \tag{3.5}$$

If $|\delta| \sim \lambdabar^2/\delta^2 \gg 1$ [case b)], the eddy currents

$$j'_\beta = \sum_{\beta'} s_{\beta\beta'} E_{\beta'}$$

almost exactly compensate the deformation currents, and with considerable accuracy,

$$E_\beta = -\sum_{\beta'} s^{-1}_{\beta\beta'} J_{\beta'}.$$

The transverse electric field is shown to be rather large and in a number of cases, in addition to the usual deformation mechanism, plays a significant role in sound absorption.

In the opposite limiting case a), $E_\beta \sim (\lambdabar/\delta)^2 \times (J_\beta/s)$. That is, if the inequality $\delta \gg \lambdabar$ is sufficiently strong, the transverse field is small and does not have a significant effect on the absorption. In the work of Akhiezer et al.,[3] the absorption of ultrasound was investigated for $\mathbf{H} = 0$. It was shown there that if the transverse field is small, the effect from the longitudinal field is of higher order in $\lambdabar/l \ll 1$, and the absorption coefficient is

---

*The dissipative function is quadratic in the velocities $\dot{u}$. Therefore, those interference terms must enter into the formula for Γ which are brought about by the interaction of the two sound absorption mechanisms. However, we have here considered only the limiting case in which one of the mechanisms of the absorption is much less significant than the other. For such conditions, the interference terms are small.

$$\Gamma = \frac{2\pi}{h^3 \rho w \omega^2 u_0^2} \int |\Lambda \dot{u}|^2 \delta(\mathbf{kv})\, \delta(\varepsilon_0 - \mu_0)\, d^3\mathbf{p} \sim N_0\mu_0\omega / \rho v_0 w^2. \tag{3.6}$$

The absorption is chiefly determined by the electrons whose velocities are perpendicular to the vector **k**. Therefore the connection between the functions $\Lambda_{ik}(\mathbf{p})$ and the absorption coefficient is obtained very simply and, if the electron conductivity spectrum is known, the value of these functions can be determined with great accuracy.

If we compute the absorption coefficient under such conditions for a strong magnetic field ($\gamma_0 \ll |\tilde{\alpha}| \ll 1$) we obtain the similar expression

$$\Gamma = \frac{2\pi}{h^3 \rho w \omega^2 u_0^2} \int |\Lambda \dot{u}|^2 \delta(\mathbf{k}\tilde{\mathbf{v}})\, \delta(\varepsilon_0 - \mu_0)\, d^3\mathbf{p} \sim N_0\mu_0\omega / \rho v_0 w^2. \tag{3.7}$$

In this case the absorption is chiefly determined by the electrons whose velocities in the **k** direction vanish when averaged over one period.

The case in which $\alpha_0 \gg \gamma_0$, but $|\tilde{\alpha}| \lesssim \gamma$, i.e., when $\mathbf{k} \perp \mathbf{H}$, we shall consider in the next section.

We now treat the sound absorption for the condition $\delta \ll \bar{\lambda}$. We begin with investigation of the case in which the magnetic field is absent. Then it is not difficult to obtain the estimates: $s_{\beta\beta'} \sim \sigma_0\bar{\lambda}/l$, $J_\beta \sim j_0\bar{\lambda}/l$, where j_0 is some characteristic value of the current density of the order of $N_0 e v_0 t_0 \dot{u}_{ik}$. Thence

$$ev_\beta E_\beta \sim \Lambda \dot{u}, \tag{3.8}$$

i.e., these terms, which enter on the right side of the kinetic equation (4.3,I) are of the same order. The transverse field leads to an expression for the absorption coefficient:

$$\Gamma = \frac{2\pi}{h^3 \rho w \omega^2 u_0^2} \int \left(|\Lambda \dot{u}|^2 + e^2 \left| \sum_\beta v_\beta E_\beta \right|^2 \right) \delta(\mathbf{kv})\, \delta(\varepsilon_0 - \mu_0)\, d^3\mathbf{p}. \tag{3.9}$$

The longitudinal field is once again insignificant.

In both limiting cases a) and b), the order of magnitude and the frequency dependence of Γ are the same; however, the value of the absorption coefficient in the second case is the larger. The graph of the dependence $\Gamma(\omega)$ for the case $l \gg \bar{\lambda}$ consists of two straight lines, the one corresponding to lower frequencies being the steeper. The lines are joined in the transition region and the frequency ω_0, where $|d_{\beta\beta'}| \sim 1$. This frequency is of the order of $(4\pi N_0 e^2 v_0 w^3/\mu_0 c^2)^{1/2}$, which amounts to about 10^{10} sec^{-1} for typical metals.

The graph consists of only a single line if for any reason — let us say, as the consequence of the symmetry of the problem — the transverse field is equal to zero. This is the case, for example, if longitudinal sound is propagated along the axis of a crystal of third, fourth, or sixth order.

Thus for ultrasonic waves that are experimentally obtainable, the absorption coefficient is determined by Eq. (3.9), in which enters the transverse electric field. Here as before, the fundamental role in the sound absorption is played by the electrons moving in planes of equal phase of the sound wave (their velocities are directed almost perpendicularly to the wave vector **k**). However, in the creation of the current determining this field, all electrons close to the Fermi surface take part in equal measure. The components E_β are connected in complicated fashion with the functions $\Lambda_{ik}(\mathbf{p})$. Further, it appears that the connection between these functions and the coefficient Γ is not as simple as in Eq. (3.6).* Therefore, it is of interest to find out whether or not a magnetic field would change the state of affairs.

However, before undertaking the solution of this problem, it is useful to note another possibility in the behavior of the sound absorption coefficient for the case when $\mathbf{H} = 0$. To be precise, we assume that the Fermi surface consists of several non-connecting sheets, topologically equivalent to parallel planes (although it is not known whether such planes are actually found in metals). Then for certain directions of the vector **k**, there are no electrons with velocities parallel to the wave front. In this case the coefficient Γ is completely independent of the frequency and has the order of magnitude

$$\Gamma \sim N_0\mu_0 / \rho v_0^2 t_0 w. \tag{3.10}$$

In such a case a sharp anisotropy of the coefficient Γ for change in the direction **k** should be observed.

4. We now proceed to the study of sound absorption in a strong magnetic field under the condition $\delta \ll \bar{\lambda}$. In all cases we shall be interested only in the principal terms of the expansion in powers of $1/H$. In order to determine the components of the electric field, we shall write down the asymptotic tensor $s_{\beta\beta'}^{-1}$, which is easily obtained with the aid of Eqs. (2.17) and (2.18). Let $N_+ \neq N_-$. We shall distinguish the following cases:

A. $\mathbf{H} \parallel \mathbf{k}$ (more precisely, $\vartheta \lesssim \gamma_0$),

$$s^{-1} = \begin{pmatrix} \alpha_0 b_{\eta\eta}/\gamma_0 & b_{\eta\zeta}/\gamma_0 \\ b_{\zeta\eta}/\gamma_0 & \alpha_0 b_{\zeta\zeta}/\gamma_0 \end{pmatrix}.$$

B. The angle $\vartheta \gtrsim \sqrt{\alpha_0^3/\gamma_0}$, and is not equal to $\pi/2$.

$$s^{-1} = \begin{pmatrix} \alpha_0^{-2} b_{\eta\eta} & b_{\eta\zeta}/\gamma_0 \\ b_{\zeta\eta}/\gamma_0 & \alpha_0 b_{\zeta\zeta}/\gamma_0 \end{pmatrix}.$$

---

*V. P. Silin has come to the same conclusion, as has been made known to the author.

Here the quantities $b_{\beta\beta'}$ are the order of $1/\sigma_0$.

C. $\mathbf{H} \perp \mathbf{k}$ (more precisely, $\cos\vartheta \lesssim \gamma_0/\alpha_0$). All the components $s^{-1}_{\beta\beta'} \sim 1/\sigma_0$.

It is very simple to obtain estimates of the components of the "deformation current," and with their help to estimate the components of the transverse field. The results are given in the following table:

Case	Component	Order of the current density	Order of the field intensity ($E_0 \sim \Lambda\dot{u}/ev_0$)
A	η ζ	$\gamma_0 j_0$ $\gamma_0 j_0$	E_0 E_0
B	η ζ	$\gamma_0 j_0$ $(\gamma_0/\alpha_0)^2 j_0$	$(\gamma_0/\alpha_0^2) E_0$ E_0
C	η ζ	$(\gamma_0/\alpha_0) j_0$ $(\gamma_0/\alpha_0) j_0$	$(\gamma_0/\alpha_0) E_0$ $(\gamma_0/\alpha_0) E_0$

From this it is seen that in case A the role of the transverse field in sound absorption is exceedingly small. In fact, solution of the kinetic equation (4.3, I) yields

$$\chi(\tau) = \hat{R}\Lambda\dot{u} + e\sum_{\nu} E'_{\nu}\hat{R}v_{\nu}$$

$$= \left(\hat{r}\Lambda\dot{u} + e\sum_{\nu} E'_{\nu}\hat{r}v_{\nu}\right) \Big/ [e^{2\pi(-i\tilde{\alpha}+\tilde{\gamma})} - 1]. \qquad (4.1)$$

In the computation of $\hat{r}\Lambda\dot{u}$ we have limited ourselves to the zeroth term in the expansion in terms of the small quantity α:

$$\hat{r}\Lambda\dot{u} = \int\limits_{\tau}^{\tau+2\pi} \exp\left[\int\limits_{\tau}^{\tau'} (-i\alpha + \gamma)\, d\tau''\right] \Lambda\dot{u}\, d\tau' \approx 2\pi\tilde{\Lambda}\dot{u}, \qquad (4.2)$$

inasmuch as $\tilde{\Lambda} \neq 0$, in general. On the other hand, $\hat{r}v_\beta$ is determined by the first term in the expansion in powers of α (the zeroth term vanishes since $\tilde{v}_\beta = 0$). Therefore, the transverse field is insignificant in the absorption. It can be shown that the longitudinal field also plays no role. The coefficient Γ is determined by the simple expression

$$\Gamma = \frac{2\pi}{h^3 \rho w \omega^2 u_0^2} \int |\Lambda\dot{u}|^2 \,\delta(\mathbf{k}\tilde{\mathbf{v}})\, \delta(\varepsilon_0 - \mu_0)\, d^3\mathbf{p}. \qquad (4.3)$$

Carrying out the same investigation in case B, we find that the result for (4.3) is also valid here.

As has already been remarked, if $\bar{\lambda} \ll \delta$, the absorption coefficient in cases A and B is also determined by Eq. (4.3). This inequality is realized in magnetic fields at much lower frequencies than for $\mathbf{H} = 0$. The frequency ω_0 for which $\bar{\lambda} \sim \delta$ is of the order $(N_0 e^2 w^4/\mu_0 c^2 t_0)^{1/3}$, which for $t_0 \sim 10^{-10}$ sec amounts to about 10^9 sec^{-1}.

We now return to case C. It is easily shown that

$$\Gamma \sim N_0 \mu_0 \omega^2 t_0 / \rho w^3, \qquad (4.4)$$

independently of the relation between $\bar{\lambda}$ and δ.

A comparison of Eqs. (4.3) and (4.4) shows that the absorption coefficient is a highly anisotropic function of the angle between the vectors $\mathbf{k}$ and $\mathbf{H}$. The coefficient Γ increases rapidly when these vectors are mutually perpendicular.

The case $N_+ = N_-$ is investigated just as easily. We shall not compute the corresponding formulas, but only note that if $\bar{\lambda} \gg d$ and case A occurs, the transverse field can make a significant contribution to the sound absorption. In case B, the expression (4.3) remains valid, only $\Gamma = \Gamma_+ + \Gamma_-$, where the first component is determined by hole, and the second by electron, quantities.

5. Thus, we have found that the sound absorption in metals in a magnetic field can be determined by two mechanisms — induction and deformation. The first of these possesses the following distinguishing characteristics.

1) A strong dependence of the coefficient Γ on the direction of sound polarization for a given relative orientation of the vectors $\mathbf{k}$ and $\mathbf{H}$. Induction absorption is generally absent if the directions of the vectors $\mathbf{u}$ and $\mathbf{H}$ coincide, or if the field $\mathbf{G} = \dot{\mathbf{u}} \times \mathbf{H}/c$ is directed along $\mathbf{k}$.

2) The absorption coefficient increases with the magnetic field, being proportional mostly to the second, and sometimes to the fourth, power of H.

The peculiarities of the deformation mechanism of absorption are these.

1) Weak dependence of the coefficient Γ on the direction of sound polarization.

2) The absorption coefficient reaches saturation in a strong magnetic field.

3) The absorption coefficient is proportional to either the second or the first power of the frequency, and in the latter case does not depend on the temperature. (The case of such an electron spectrum which was considered at the end of Sec. 3 is an exception.)

Unfortunately, present-day experimental data on sound absorption in a strong magnetic field are rather sketchy. A brief review of them is given by Rodriguez.[6] In addition to the data tabulated there, the papers of Galkin and Korolyuk[7] and Reneker[8] should also be mentioned.

In a comparison of theory and experimental data, the following comes to the fore. It follows from theory that the coefficient Γ must be proportional to the fourth power of the magnetic field. Actually, the solution of Eq. (4.3, I) — the function χ — is proportional in a strong field to an integral power of H. But the absorption coefficient is determined by the dissipation function $T\dot{S}$, which is quadratic in χ. Further, in reference 6, the proportionality of Γ to odd (and even to negative) powers of H was observed. Here the dependence on the field was different for different directions of the sound polarization, which evidently testifies to the predominance of induction absorption for certain directions of polarization. In this connection, the following observations can be made.

In the first place, determining the coefficient Γ, we compute the principal term in the expansion in powers of 1/H. As a rule, this means that not only the condition $\gamma_0 \ll \alpha_0 \ll 1$ is considered satisfied, but also the inequality $\alpha_0^2 \ll \gamma_0$. Also, there must exist a transition region of values of H, where the two first inequalities hold while the third is replaced by its reciprocal. It is possible that the path of the function $\Gamma(H)$ in this region duplicates the power dependence with odd negative exponents.

In the second place, only closed trajectories of the electron in quasimomentum space have been considered in I and in the present paper. The electrical conductivity in a magnetic field in the case of open trajectories was computed in the researches of I. Lifshitz et al.[4,5] It has been shown that if the specimen possesses even a comparatively weakly defined polycrystalline structure, the diagonal components of the conductivity tensor can be inversely proportional to the first power of H, thanks to averaging over the orientations of the crystals. If the sound wavelength is much greater than the dimensions of the crystallites, then direct use can be made of the results of Ĭ. Lifshitz and Peschanskiĭ[5] in the calculation of the coefficient of induction absorption. These results yield a coefficient Γ which is proportional to an odd positive power of H. Generally, the entire question of sound absorption in the case of open trajectories, and of averaging over the orientations of the crystallites, is of great interest and deserves special attention.

In the third place, one must remark that in this research we have considered the spectrum of electron conductivities and a deformation potential of general form. In particular, we assumed that $\tilde{\Lambda}_{ik}u_{ik} \neq 0$. In some cases, for example, if the materials are isotropic and the sound vibrations are transverse, $\tilde{\Lambda}_{ik}u_{ik} = 0$, and the dependence of the absorption coefficient on the field must be different from that represented by the general theory. In particular, Γ can be a decreasing function of H.

Finally, we observe that the expression for the coefficient Γ can be generalized without difficulty to the case in which $\omega t_0 \gg 1$ by means of methods used in the present work. Ultrasonic frequencies satisfying these conditions are not attainable experimentally at the present time. However, the corresponding formulas give estimates of the length of the free path of the phonons in the metal which is of interest for the study of the drag of electrons by phonons.

In conclusion to the paper, the author wishes to express his gratitude to L. D. Landau for discussion of the work and for a number of useful remarks.

---

[1] V. L. Gurevich, JETP **37**, 71 (1959); Soviet Phys. JETP **10**, 51 (1960).

[2] A. I. Akhiezer, JETP **8**, 1330 (1938).

[3] Akhiezer, Kaganov, and Lyubarskiĭ, JETP **32**, 837 (1957); Soviet Phys. JETP **5**, 685 (1957).

[4] Lifshitz, Azbel', and Kaganov, JETP **31**, 63 (1956); Soviet Phys. JETP **4**, 41 (1957).

[5] I. M. Lifshitz and V. G. Peschanskiĭ, JETP **35**, 1251 (1958), Soviet Phys. JETP **8**, 875 (1959).

[6] S. Rodriguez, Phys. Rev. **112**, 80 (1958).

[7] A. A. Galkin and A. P. Korolyuk, JETP **36**, 1307 (1959); Soviet Phys. JETP **9**, 925 (1959).

[8] D. H. Reneker, Phys. Rev. Lett. **1**, 441 (1958).

Translated by R. T. Beyer
330

SOVIET PHYSICS JETP VOLUME 37(10), NUMBER 6 JUNE, 1960

OSCILLATIONS OF AN ELECTRON-ION PLASMA

L. M. KOVRIZHNYKH

P. N. Lebedev Physics Institute, Academy of Sciences, U.S.S.R.

Submitted to JETP editor June 19, 1959

J. Exptl. Theoret. Phys. (U.S.S.R.) **37**, 1692-1696 (December, 1959)

The spectrum of longitudinal oscillations of an electron-ion plasma is considered for the high temperature case (Maxwell distribution) and the low temperature case (Fermi distribution). It is shown that at low values of the wave vector **k** the dispersion equation is characterized by two branches, which have different properties: an optical branch, for which the ion motion is not important, and an acoustic branch. At high values of **k**, however, only the acoustic branch exists; the properties of this branch are determined by the parameters of the ion component of the plasma.

In the present work we investigate the oscillation spectrum of an electron-ion plasma produced as a result of a small initial departure from the equilibrium distribution. Detailed investigations of plasma oscillations have been carried out by Landau[1] for the high temperature case (Maxwell distribution), and Gol'man[2] for the low-temperature case (Fermi distribution). In that work the motion of the ions was neglected; it will be shown, however, that this motion has an important effect on the nature of the spectrum which is obtained. A dispersion equation which takes account of ion motion has been obtained by Silin.[3,4] However the expressions found by this author for the dependence of frequency ω and damping γ on wave vector **k** are incorrect. For example, the statement that there are two branches applies only at low values of k; at high values of k these two branches degenerate into one branch whose properties are determined by the parameters of the ion component of the plasma.

1. DISPERSION EQUATION

For a uniform plasma the asymptotic form of the potential as a function of time is, as is well known,[1,3] determined by the roots of the equation

$$D(p, k) = 0 \qquad (p = i\omega - \gamma), \tag{1.1}$$

where

$$D(p, k) = 1 - ik\frac{\omega_e^2}{k^2}\int_L \frac{\partial f_0^{(e)}}{\partial \zeta}\, d\zeta \frac{1}{p + ik\zeta} - ik\frac{\omega_i^2}{k^2}\int_L \frac{\partial f_0^{(i)}}{\partial \zeta}\frac{d\zeta}{p + ik\zeta},$$

$$f_0^{(e,\, i)}(\zeta) = \frac{1}{\eta_{e,\, i}}\iint_{-\infty}^{\infty} F^{(e,\, i)}(\mathbf{v})\, d\xi\, d\eta \qquad (d\mathbf{v} = d\xi\, d\eta\, d\zeta),$$

$$\omega_e^2 = 4\pi e^2 n_e / m_e, \qquad \omega_i^2 = 4\pi e^2 Z^2 n_i / m_i; \tag{1.2}$$

$F^{(t)}(\mathbf{v})$ and $F^{(e)}(\mathbf{v})$ are the equilibrium distribution functions for the ions and electrons, n_i and $n_e = Zn_i$ are the corresponding densities, Z is the charge of the ion, k is the wave number, ω is the frequency, γ is the damping factor and the contour L is taken in such a way that the point $\zeta = ip/k$ always lies above the path of integration.

2. OSCILLATION SPECTRUM FOR A HIGH-TEMPERATURE PLASMA

We first consider the case in which the electron temperature is much higher than the degeneracy temperature. We use classical statistics and assume that the electron and ion equilibrium distribution functions are Maxwellian, i.e.

$$f_0^{(e)}(\zeta) = \left(\frac{m_e}{2\pi\varkappa T_e}\right)^{1/2} \exp\left\{-\frac{m_e\zeta^2}{2\varkappa T_e}\right\},$$

$$f_0^{(i)}(\zeta) = \left(\frac{m_i}{2\pi\varkappa T_i}\right)^{1/2} \exp\left\{-\frac{m_i\zeta^2}{2\varkappa T_i}\right\}, \tag{2.1}$$

where κ is the Boltzmann constant and T_e and T_i are the electron and ion temperatures respectively.

Substituting Eq. (2.1) in Eq. (1.2) and taking account of the fact that

$$\int_L \frac{e^{t^2}}{s + t}\, dt = i\pi e^{-s^2}\left[1 - \frac{2i}{\sqrt{\pi}}\int_0^s e^{t^2}\, dt\right],$$

after integration with respect to ζ, we obtain

$$D(p, k) = 1 + \frac{2}{x^2}\Big\{1 + \alpha^2 - i\sqrt{\pi}\, s\,[2e^{-s^2} - w(s)]$$

$$- i\sqrt{\pi}\,\alpha^2\beta s\,[2e^{-\beta^2 s^2} - w(\beta s)]\Big\} = 0, \tag{2.2}$$

where we have introduced the dimensionless variables

$$x^2 = 2\,(ka_e)^2 = 2\alpha^2\,(ka_i)^2, \quad a_e^2 = \varkappa T_e / m_e\omega_e^2, \quad a_i^2 = \varkappa T_\iota / m_i\omega_i^2,$$

$$\alpha^2 = ZT_e / T_i, \quad \beta^2 = m_i T_e / m_e T_i,$$

$$s = p / i\sqrt{2}ka_e\omega_e = p / i\sqrt{2}ka_i\omega_i\beta,$$

and the function[*]

$$w\,(s) = e^{-s^2}\left[1 + (2i / \sqrt{\pi}) \int\limits_0^s e^{t^2}\,dt\right]. \tag{2.3}$$

First of all we may note that Eq. (2.2) has n-roots in the lower half plane of s (including the real axis). For this reason, only damped solutions are possible for the potential $(\gamma > 0)$. Furthermore, as follows from the definition [cf. Eq. (2.3)], when $\operatorname{Im} s \geq 0$ the function $w(s)$ is bounded. Consequently when $x^2 \to \infty$ Eq. (2) can only have roots characterized by $\operatorname{Im} s > \operatorname{Re} s$. Thus, in studying the dispersion equation one must distinguish two cases, depending on whether the mean-square velocity of the electrons is smaller $(\beta^2 < 1)$ or greater $(\beta^2 > 1)$ than the mean-square velocities of the ions. In the first case, when $x^2 \to \infty$ the last term (associated with the ion component) in Eq. (2.2) for $D(p, k)$ is unimportant, whereas in the second case it is decisive. In the work of Silin cited above, however, the ionic motion is not considered in the short wave region and for this reason the result is incorrect.

We now investigate the solutions of the dispersion equation (2.2), limiting ourselves to the case in which the mean-square velocity of the electrons is much higher than the mean-square velocity of the ions, i. e., $T_i \ll m_i T_e / m_e$.

When $ka_e \ll 1$ the dispersion equation always yields two oscillation branches: an optical branch, for which $\omega(0) \neq 0$, and an acoustic branch, for which $\omega(0) = 0$. In the region $ka_e \sim 1$ these two branches degenerate into a single branch which, when $ka_e \gg 1$ and $ka_e \gg \alpha$, corresponds to highly damped oscillations. The behavior of the optical branch $(ka_e \ll 1)$ is independent of the parameters of the ion component of the plasma; for it[1,3][†]

$$\omega^2 = \omega_e^2\,[1 + 3\,(ka_e)^2] \qquad (ka_e \ll 1),$$

$$\gamma = \sqrt{\frac{\pi}{8}}\,\frac{\omega_e}{(ka_e)^3}\exp\left\{-\left[\frac{1}{2\,(ka_e)^2} + \frac{3}{2}\right]\right\}. \tag{2.4}$$

The behavior of the acoustic branch, however, depends on the parameter α^2. If $\alpha^2 \gg 1$, when $ka_e \ll \alpha$ we have

$$\omega^2 = \omega_i^2\left[\frac{(ka_e)^2}{(ka_e)^2 + 1} + 3\,(ka_i)^2\right],$$

$$\gamma = \sqrt{\frac{\pi}{8}}\,\frac{\omega_i ka_e}{[(ka_e)^2 + 1]^2}\left[\frac{\alpha}{\beta} + \alpha^3\exp\left\{-\left(\frac{\alpha^2}{2\,(ka_e)^2 + 2} + \frac{3}{2}\right)\right\}\right], \tag{2.5}$$

that is to say, when $T_e \gg T_i$ the plasma can exhibit weakly damped acoustic oscillations. If in this case, however, $ka_e \gg 1$, the frequency of these oscillations is a weak function of wave length and actually coincides with the ion Langmuir frequency ω_i.

When $\alpha \lesssim 1$ and $ka_e \ll \alpha$ we have

$$\omega^2 = 2\omega_i^2\,(ka_i)^2\,(\operatorname{Re} s')^2,$$

$$\gamma = \sqrt{2}\omega_i\,(ka_i)\operatorname{Im} s', \tag{2.6}$$

where s' is a root of the equation[*]

$$(1 + \alpha^2) / \alpha^2 = i\sqrt{\pi}\,s'\,[2e^{-s'^2} - w\,(s')]. \tag{2.7}$$

When $\alpha^2 \ll 1$ this equation has the solution

$$\operatorname{Re} s' = \pi / \sqrt{2}\,\xi, \quad \operatorname{Im} s' = \xi / \sqrt{2}, \quad \alpha^2\xi\sqrt{2\pi}\exp(\xi^2 / 2) = 1.$$

If $\alpha \sim 1$, however, Eq. (2.7) must be solved numerically. In order-of-magnitude terms $\operatorname{Re} s' \sim \operatorname{Im} s' \sim 1$. Thus, when $\alpha \lesssim 1$ the acoustic waves are strongly attenuated.

For short waves $(ka_e)^2 \gg \alpha^2$, as has already been noted, and the ratio of the damping factor to the frequency must be greater than unity. Consequently the important term in the dispersion equation is the last term and Eq. (2.2) assumes the form

$$1 = 2\sqrt{\pi}\,i\beta s\,(ka_i)^{-2}\exp(-\beta^2 s^2).$$

The solution corresponding to minimum damping is obviously

$$\omega^2 = \pi^2\omega_i^2\,(ka_i)^2 / \xi, \qquad \gamma = \omega_i ka_i\xi \qquad (ka_i \gg 1), \tag{2.8}$$

where ξ is determined from the equation

$$\sqrt{2\pi}\xi\exp(\xi^2 / 2) = (ka_i)^2.$$

It is interesting to note that in the limiting case $T_i \to 0$ the frequency of the short wave oscillations $(ka_e \gg 1)$ is independent of wave length, being equal to ω_i; under these conditions the relative magnitude of the damping factor is very small and it falls off as the reciprocal of the cube of the wave number [cf. Eq. (2.5)], that is to say, the oscillations are essentially undamped. When $m_i \to \infty$ the acoustic branch vanishes and when $ka_e \gg 1$, in general the dispersion equation does not have nontrivial solutions, i.e., in the short wave region there are no solutions of the type $\exp[(i\omega - \gamma)t]$ for the potential (cf. references 1 and 3).

---

[*] Detailed tables of the function $w(s)$ are given in reference 6.

[†] Here and in what follows we neglect quantities of order Zm_e/m_i compared with unity.

[*] We may note that there is an error in the analagous equation for the acoustic branch given in reference 4.

Thus, for short waves ($ka_e \gg 1$ and $ka_e \gg \alpha$) both the frequency and damping of the oscillations are determined by the parameters of the ion component of the plasma.

3. OSCILLATIONS OF A LOW-TEMPERATURE PLASMA

We now consider the oscillation spectrum of a low-temperature plasma, in which case the electron gas is highly degenerate. Assuming a Fermi distribution, with a temperature T_e for the electrons and, as before, a Maxwellian distribution for the ions, in place of Eq. (2.2) we have

$$1+\frac{2\alpha_1^2}{x_1^2}\left\{1-i\sqrt{\pi}\beta_1 s_1\left[2e^{-\beta_1^2 s_1^2}-w(\beta_1 s_1)\right]\right\}$$
$$+\frac{3}{2x_1^2}\{2-\psi(s_1)-i\pi s_1 f_0(s_1)[1+\mathrm{Sg}\,\mathrm{Im}\,s_1]\}=0. \quad (3.1)$$

Here

$$x_1^2=2(kd)^2=2\alpha_1^2(ka_i)^2, \qquad d^2=\zeta_0/m_e\omega_e^2, \qquad \alpha_1^2=Z\zeta_0/\varkappa T_i,$$
$$s_1=p/i\sqrt{2}kd\omega_e=p/i\sqrt{2}ka_i\omega_i\beta_1, \qquad \beta_1^2=m_i\zeta_0/m_e\varkappa T_i,$$

$\zeta_0 = p_0^2/2m_e$ is the limiting Fermi energy

$$f_0(s_1)=\left[1+\exp\frac{s_1^2-1}{\varepsilon}\right]^{-1}, \qquad \varepsilon=\varkappa T_e/\zeta_0\ll 1,$$

and the function

$$\psi(s_1)=\begin{cases} s_1\ln\dfrac{s_1+1}{s_1-1}+\dfrac{\pi^2\varepsilon^2}{6}\left[s_1^2-1\right]^{-2} & \text{for } \left|s_1^2-1\right|\gg\pi\varepsilon \\ \sim\pm\ln\pi\varepsilon & \text{for } \left|s_1^2-1\right|\ll\pi\varepsilon \end{cases}, \quad (3.2)$$

where the principal value of the logarithm is taken ($-\pi < \arg \ln \leq \pi$).

We investigate the roots of Eq. (3.1), limiting ourselves to the case in which the ion temperature is not excessively high $\kappa T_i \ll m_i\zeta_0/m_e$. Then, as in the classical case, it can be shown that Eq. (3.1) has damped solutions only ($\gamma > 0$). Furthermore, as follows from Eq. (3.2), the function $\psi(s_1)$ is bounded; consequently, for $(kd)^2 \gg \ln(1/\pi\epsilon)$ the dispersion equation can have only solutions with $\gamma > \omega$. In this case, obviously the important term is the one which takes account of the ion motion.

As in the high-temperature case, at small values of k we again have two branches. When $kd \ll 1$, for the optical branch

$$\omega^2=\omega_e^2\left[1+\tfrac{6}{5}(kd)^2\left(1+\tfrac{5}{12}\pi^2\varepsilon^2\right)\right],$$

$$\gamma=\frac{\omega_e}{(kd)^3}\left\{\frac{3\pi}{4\sqrt{2}}\exp\left[-\frac{5+6(kd)^2}{10\varepsilon(kd)^2}\right]\right.$$
$$\left.+\sqrt{\frac{\pi}{8}}\alpha_1^2\beta_1\exp\left[-\frac{\beta_1^2[5+6(kd)^2]}{10(kd)^2}\right]\right\}. \quad (3.3)$$

Whence it follows that with complete degeneracy ($\epsilon \to 0$) the damping factor remains finite and is determined by the ion temperature.

For shorter waves $1 \ll (kd)^2 \ll \ln(1/\pi\epsilon)$

$$\omega^2=2\omega_e^2(kd)^2\left\{1+4\exp\left[-\tfrac{2}{3}(2(kd)^2+3)\right]\right\},$$

$$\gamma=4\sqrt{2}\omega_e(kd)\exp\left\{-\frac{2}{3}[2(kd)^2+3]\right\}\left\{\frac{2\sqrt{\pi}}{3}\alpha_1^2\beta_1 e^{-\beta_1^2}\right.$$
$$\left.+\pi\exp\left\{-\frac{4}{\varepsilon}\exp\left[-\frac{2}{3}(2(kd)^2+3)\right]\right\}\right\}. \quad (3.4)$$

With $\alpha_1^2 \lesssim 1$ the acoustic branch is determined from the following equation when $kd \ll \alpha_1$:

$$(3+2\alpha_1^2)/2\alpha_1^2=i\sqrt{\pi}\beta_1 s_1\left[2e^{-\beta_1^2 s_1^2}-w(\beta_1 s_1)\right].$$

In this case the relative magnitude of the damping factor is of the order of unity and the acoustic waves are highly damped. However, if $(kd) \ll \alpha_1$, as is generally the case, when $\kappa T_i \ll Z\zeta_0$ we have [cf. Eq. (2.5)]:

$$\omega^2=\omega_i^2\left[\frac{2(kd)^2}{2(kd)^2+3}+3(ka_i)^2\right],$$

$$\gamma=\frac{\sqrt{2}\,\omega_i kd}{[2(kd)^2+3]^2}\left\{\frac{3\pi\alpha_1}{2\beta_1}+\sqrt{\pi}\,\alpha_1^3\exp\left[-\left(\frac{\alpha_1^2}{2(kd)^2+3}+\frac{3}{2}\right)\right]\right\}, \quad (3.5)$$

i.e., it is possible to have weakly damped acoustic waves.

Finally, for very short waves $(kd)^2 \gg \alpha_1^2$, at any values of the parameter α_1 there is a branch which corresponds to highly damped oscillations. The corresponding expressions for frequency and damping coincide with those found in the classical case and are determined by Eq. (2.8).

We wish to emphasize that if $T_e \neq 0$, in the short wave region $[(kd)^2 \gg \ln(1/\pi\epsilon)]$, as before, there is only the acoustic branch; this is given by Eqs. (2.8) and (3.5) if $\alpha_1^2 \gg \ln(1/\pi\epsilon)$ and by Eq. (2.8) if $\alpha_1^2 \ll \ln(1/\pi\epsilon)$. In the limiting case of total degeneracy, however, as follows from Eqs. (2.8) and (3.4) the dispersion equation has two branches for any values of the wave vector **k**.

We may summarize the results which have been obtained.

In the long-wave region the longitudinal oscillation spectrum of a plasma exhibits two branches: one optical and the other acoustic. The relative damping of the optical waves is very small. At low temperatures the acoustic oscillations are also essentially undamped. At high temperatures, however, weak damping of the acoustic waves is possible only at high values of the ratio T_e/T_i. In general, in the short-wave region there is only the acoustic branch, which is highly damped. The frequency and damping in this case are determined completely by the parameters of the ion component of the plasma.

The author is indebted to V. L. Ginzburg, M. S. Rabinovich, V. P. Silin and A. A. Rukhadze for valuable discussions.

---

[1] L. D. Landau, JETP **16**, 574 (1946).

[2] I. I. Gol'dman, JETP **17**, 681 (1947).

[3] V. P. Silin, JETP **23**, 649 (1952).

[4] V. P. Silin, Тр. ФИАН, (Trans. Inst. Phys., Acad. Sci. U.S.S.R.) **6**, 201 (1954).

[5] A. A. Vlasov, Теория многих частиц, (Theory of Many Particles) Gostekhizdat, 1950.

[6] V. N. Fadeeva and N. M. Terent'ev, Таблицы значений интеграла вероятностей, (Tables of Values of the Probability Integral) Gostekhizdat, 1954.

Translated by H. Lashinsky
331

SOVIET PHYSICS JETP VOLUME 37(10), NUMBER 6 JUNE, 1960

*RELATIVISTIC SPHERICAL FUNCTIONS. III**

A. Z. DOLGINOV and A. N. MOSKALEV

Leningrad Physico-technical Institute, Academy of Sciences, U.S.S.R.

Submitted to JETP editor June 25, 1959

J. Exptl. Theoret. Phys. (U.S.S.R.) **37**, 1697-1707 (December, 1959)

An expansion of the wave function of a particle has been obtained in terms of the irreducible representations of the Lorentz group. This gives a relativistically-invariant classification of states. The connection between different methods of constructing irreducible representations has been established.

1. INTRODUCTION

THE infinite-dimensional representations of the Lorentz group were utilized for the first time by I. S. Shapiro[1,2] for a relativistically-invariant classification of particle states. He utilized the method of constructing irreducible representations which was proposed by Gel'fand and Naĭmark.[3,4] Although this method[1-4] has been developed in detail and is convenient from a mathematical point of view, nevertheless as yet it has not received widespread acceptance among physicists. Apparently, the method to which the physicists are more accustomed is the one proposed by one of the present authors.[5,6] It represents a direct relativistic generalization of the method of the theory of representations of the three-dimensional rotation group. In particular, the possibility arises of utilizing the techniques of Clebsch-Gordan, Racah,[7] and Fano,[8,9] which are widely used in physics. It was thus of interest to establish the correspondence between the above two methods of constructing representations in order that the results obtained by one method could be transferred to the other method. In the course of this investigation we succeeded in obtaining a number of useful relationships, among them an integral representation for the Fano functions.

We shall show that by means of the methods of references 5 and 6 one can obtain an expansion of the wave function of a particle in terms of the irreducible representations of the Lorentz group. (The proposed form of this expansion may turn out to be useful for a relativistically-invariant classification of particles.) It holds for particles of arbitrary spin. The expansion of the wave function for a system of particles also presents no difficulties.

2. UNITARY REPRESENTATIONS OF THE LORENTZ GROUP

1. We recapitulate briefly those results from the papers of Gel'fand and Naĭmark[3,4] which we shall need for the subsequent presentation.

Each proper Lorentz transformation (i.e., a transformation without an inversion) may be made to correspond to a complex matrix of the second rank a with a determinant equal to unity. A purely spatial rotation corresponds to a unitary matrix which we shall denote by u. The matrix u is determined by three independent parameters which may be chosen, for example, in the form of the angles ϑ, θ, θ':

$$u=\begin{pmatrix} \cos\frac{\vartheta}{2}e^{i\theta} & \sin\frac{\vartheta}{2}e^{i\theta'} \\ -\sin\frac{\vartheta}{2}e^{-i\theta'} & \cos\frac{\vartheta}{2}e^{-i\theta} \end{pmatrix}, \qquad (1)$$

where

$$\theta=(\varphi_1+\varphi_2)/2, \qquad \theta'=(\varphi_1-\varphi_2+\pi)/2,$$
$$0\leqslant\vartheta\leqslant\pi, \qquad 0\leqslant\theta\leqslant 2\pi, \qquad 0\leqslant\theta'\leqslant 2\pi;$$

φ_2, ϑ, φ_1 are the Eulerian angles of the rotation.

An irreducible representation of the Lorentz group may be characterized by two numbers:[3,4] k_0 and c. The number k_0 determines the lowest dimension of representations of the three-dimensional subgroup contained in the given representation of the Lorentz group. It may assume only integral or half-integral positive values. The number c may be an arbitrary complex number. We shall investigate only the principal series of representations of the Lorentz group, which contains a three-dimensional scalar as one of the basis functions. Moreover, $k_0 = 0$, $c = in$, where n is real. The representations of the principal series are unitary.

Each Lorentz transformation which is described by the matrix a may be made to correspond to an operator V_a, which operates on the totality of functions $f(u) \equiv f(\vartheta, \theta, \theta')$. The scalar product of the functions $f(u)$ is defined by the formula

---

*This paper is a continuation of references 5 and 6.

$$(f_1, f_2) = \int f_1^*(u) f_2(u)\, du, \qquad (2)$$

where $du = (\frac{1}{8}\pi^2) \sin\vartheta\, d\vartheta\, d\theta\, d\theta'$, while the integration is taken over the whole range of variation of the variables ϑ, θ, θ'. The functions $f(u)$ are assumed to be quadratically integrable:

$$\int |f(u)|^2 du < \infty.$$

Each matrix a may be uniquely represented in the form

$$a = k\bar{a}, \qquad k = \begin{pmatrix} 1/\lambda & \mu \\ 0 & \lambda \end{pmatrix}; \qquad (3)$$

$\bar{a}$ is a unitary matrix of the form (1). λ may be assumed to be real: $\lambda^2 = |a_{21}|^2 + |a_{22}|^2$;

$$\bar{a}_{22} = \bar{a}_{11}^* = a_{22}/\lambda, \qquad \bar{a}_{21} = -\bar{a}_{12}^* = a_{21}/\lambda. \qquad (4)$$

The result of the operation of the operators V_a on the functions $f(u)$ is defined by the following formula

$$V_a f(u) = (\alpha(ua)/\alpha(\overline{ua}))\, f(\overline{ua}), \qquad (5)$$

where

$$\alpha(a) = |a_{22}|^{-2-m+i\rho} a_{22}^m \quad \text{and } ua = k(\overline{ua}).$$

The numbers m and ρ are related to k_0 and c in the following manner:

$$k_0 = |m/2|, \qquad c = i\rho/2.$$

In the case which is of interest to us we have $m = 0$, $\rho = 2n$. The operators V_a provide a linear representation of the Lorentz group:

$$V_{a_1}V_{a_2} = V_{a_1a_2} \text{ and } V_a = 1 \text{ when } a = 1.$$

2. In a different method of constructing the representations of the Lorentz group which was discussed in detail in the papers by one of the authors[5,6] the basis functions are chosen to be functions which are analytic continuations of the four-dimensional spherical harmonics in Euclidean space.[10] The basis functions have for their arguments the angles specifying the orientation of the radius vector in four-dimensional space-time. They are different for time-like and space-like arguments. In the first case we set $t = \rho \times \cosh\alpha$, $|\mathbf{r}| = \rho \sinh\alpha$, where ρ is the interval; in the second case we set $t = \rho\sinh\alpha$, $|\mathbf{r}| = \rho\cosh\alpha$. We denote by ϑ and φ the angles specifying the three-dimensional radius vector $\mathbf{r}(r, \vartheta, \varphi)$.

For the principal series of representations in the case $t^2 - r^2 > 0$ the basis functions have the form

$$\Psi_{nlm}(\omega) \equiv \Psi_{nlm}(\alpha, \vartheta, \varphi) = \Pi_l(n, \alpha) Y_{lm}(\vartheta, \varphi), \qquad (6)$$

where

$$\Pi_l(n, \alpha) = \frac{\sinh^l\alpha}{M_l} \cdot \frac{d^{l+1}\cos n\alpha}{d(\cosh\alpha)^{l+1}},$$

$$M_l = \sqrt{n^2(n^2+1^2)\ldots(n^2+l^2)}. \qquad (7)$$

In order to go over to the case $t^2 - r^2 < 0$ we must replace α by $\alpha + i\pi/2$.

The functions Ψ are orthogonal and normalized:

$$\int \Psi_{nlm}(\omega) \Psi_{n'l'm'}^*(\omega)\, d\omega = \frac{\pi}{2}\delta(n-n')\,\delta_{ll'}\delta_{mm'}, \qquad (8)$$

where

$$d\omega = \sinh^2\alpha \sin\vartheta\, d\alpha\, d\vartheta\, d\varphi.$$

The result of the operation of the infinitesimal rotation operator on the functions Ψ may be written with the help of the Clebsch-Gordan coefficients in the following form

$$H_\mu\Psi_{nlm} = (-)^\mu \sqrt{l(l+1)}\, C_{lm\,1\mu}^{l\Lambda} \Psi_{nl\Lambda},$$
$$F_\mu\Psi_{nlm} = i\sum_L C_L^{nl} C_{l0\,10}^{L0} C_{L\Lambda\,1-\mu}^{lm} \Psi_{nL\Lambda}, \qquad (9)$$

where H_μ and F_μ are the cyclic components of the operators **H** and **F** which are respectively the spatial and the time parts of the infinitesimal rotation operator:

$$H_{\pm1} = \pm(H_x \pm iH_y)/\sqrt{2}, \quad H_0 = H_z$$

and similarly in the case of F_μ;

$$C_{l+1}^{nl} = \sqrt{n^2 + (l+1)^2}, \qquad C_{l-1}^{nl} = -\sqrt{n^2 + l^2}.$$

The transformation of the functions Ψ_{nlm} under finite rotations has been defined in reference 6.

We shall henceforth refer to this representation of the Lorentz group as representation II to distinguish it from the representation by means of the operators V_a, to which we shall refer as representation I.

3. CONNECTION BETWEEN DIFFERENT SPECIFIC FORMS OF THE REPRESENTATIONS OF THE LORENTZ GROUP

It is of interest to find the basis functions of representation I and to establish their connection with the basis functions of representation II. The basis functions may be obtained by utilizing the condition that the result of operating on them with the infinitesimal rotation operator is given by formula (9). The form of the operators H_μ and F_μ, which correspond to this representation of the Lorentz group may be found by the method indicated by Naĭmark.[4]* Straightforward calculations yield

$$H_{\pm 1}f = \pm \frac{1}{\sqrt{2}} e^{\pm i(\theta' - \theta)}$$
$$\left\{ \pm \frac{\partial f}{\partial \vartheta} + \frac{i}{2} \tan \frac{\vartheta}{2} \frac{\partial f}{\partial \theta} + \frac{i}{2} \cot \frac{\vartheta}{2} \frac{\partial f}{\partial \theta'} \right\},$$
$$H_0 f = \frac{i}{2} \left\{ \frac{\partial f}{\partial \theta} - \frac{\partial f}{\partial \theta'} \right\},$$
$$F_{\pm 1} f = \pm \frac{1}{\sqrt{2}} e^{\pm i(\theta' - \theta)} \Big\{ (i + n) \sin \vartheta f$$
$$- i \cos \vartheta \frac{\partial f}{\partial \vartheta} \mp \frac{1}{2} \tan \frac{\vartheta}{2} \frac{\partial f}{\partial \theta} \pm \frac{1}{2} \cot \frac{\vartheta}{2} \frac{\partial f}{\partial \theta'} \Big\},$$
$$F_0 f = (i + n) \cos \vartheta f + i \sin \vartheta \, \partial f / \partial \vartheta. \tag{10}$$

By utilizing this result in formulas (9) we obtain a system of equations for the determination of the basis functions $f_{nlm}(u)$ of representation I. On solving this system of equations we obtain

$$f_{nlm}(u) = (-)^l \sqrt{4\pi} A_l(n) Y_{lm}(\vartheta, \varphi), \tag{11}$$

where $\varphi = \theta' - \theta$,

$$A_l(n) = [\Gamma(l + 1 - in)$$
$$\times \Gamma(1 + in)]^{1/2} [\Gamma(l + 1 + in) \Gamma(1 - in)]^{-1/2}.$$

The functions f are orthonormal:

$$\int f_{nlm}(u) f^*_{nl'm'}(u) \, du = \delta_{ll'} \delta_{mm'} . \tag{12}$$

In representation II the basis functions of the representation are at the same time also matrix elements of the rotation operator. A similar situation exists in the case of the spherical harmonics Y_{lm}, which, in addition to being the basis functions of the representation of the three-dimensional rotation group, are at the same time related to the matrix elements of the rotation operator by the following relation

$$Y_{lm}(\vartheta, \varphi) = \sqrt{(2l + 1)/4\pi} \, D^l_{m0}(\vartheta, \varphi).$$

However, there is no similar relation in the case of representation I. As we shall now show, the matrix elements of the operator V_a calculated by means of the basis functions f_{nlm} of representation I coincide with the basis functions Ψ_{nlm} of representation II. In this way we establish the connection between the two representations.

First of all we note that the following relation holds†

$$\Pi_l(n, \alpha) = -\frac{n}{\sqrt{2l + 1}} (f_{n00}, V_\varepsilon f_{nl0}), \tag{13}$$

where

$$\varepsilon = \begin{pmatrix} e^{-\alpha/2} & 0 \\ 0 & e^{\alpha/2} \end{pmatrix}. \tag{14}$$

It follows from formula (5) that

$$V_a f(u) = [\lambda(ua)]^{2in - 2} f(\overline{ua}), \tag{15}$$

where $[\lambda(a)]^2$ is given by formula (4). Therefore, relation (13) may be written in the following explicit form:

$$\Pi_l(n, \alpha) = (-)^{l+1} \frac{n}{2} A_l(n)$$
$$\times \int_0^\pi \left[\cos^2 \frac{\vartheta}{2} e^\alpha + \sin^2 \frac{\vartheta}{2} e^{-\alpha} \right]^{in - 1} P_l(\cos \vartheta') \sin \vartheta \, d\vartheta, \tag{16}$$
$$\cos \vartheta' = \left(\cos^2 \frac{\vartheta}{2} e^\alpha - \sin^2 \frac{\vartheta}{2} e^{-\alpha} \right) \Big/ \left(\cos^2 \frac{\vartheta}{2} e^\alpha + \sin^2 \frac{\vartheta}{2} e^{-\alpha} \right). \tag{17}$$

We can verify the validity of this by checking that the right hand side of (16) satisfies the same recurrence relations which are satisfied by $\Pi_l(n, \alpha)$, for example:

$$\frac{d\Pi_l}{d\alpha} = \sqrt{n^2 + (l + 1)^2} \frac{l + 1}{2l + 1} \Pi_{l+1} - \sqrt{n^2 + l^2} \frac{l}{2l + 1} \Pi_{l-1}. \tag{18}$$

In virtue of the fact that the representation is unitary, we have

$$(V_a f_1, V_a f_2) = (f_1, f_2). \tag{19}$$

Therefore formula (13) may be written in a different form:

$$\Pi_l(n, \alpha) = -\frac{n}{\sqrt{2l + 1}} (V_{\varepsilon^{-1}} f_{n00}, f_{nl0}), \tag{20}$$

or in expanded form:

$$\Pi_l(n, \alpha) = (-)^{l+1} \frac{n}{2} A_l(n)$$
$$\times \int_0^\pi \left[\cos^2 \frac{\vartheta}{2} e^{-\alpha} + \sin^2 \frac{\vartheta}{2} e^\alpha \right]^{-in - 1} P_l(\cos \vartheta) \sin \vartheta \, d\vartheta. \tag{21}$$

This may also be seen directly by means of the substitution (17).

It follows from formula (21) that

$$\left[\cos^2 \frac{\vartheta}{2} e^{-\alpha} + \sin^2 \frac{\vartheta}{2} e^\alpha \right]^{-in - 1} \equiv [\lambda(u\varepsilon^{-1})]^{-2in - 2}$$
$$= \frac{1}{n} \sum_l (-)^{l+1} (2l + 1) A^*_l(n) \Pi_l(n, \alpha) P_l(\cos \vartheta). \tag{22}$$

By utilizing these results it may be shown that

$$\Psi_{nlm}(\alpha, \vartheta, \varphi) = -(n/\sqrt{4\pi}) (f_{n00}, V_{\varepsilon u} f_{nlm}), \tag{23}$$

where ϵ is given by formula (14), and u is given by formula (1). Indeed, in virtue of the fact that the representation is unitary

$$(f_{n00}, V_{\varepsilon u} f_{nlm}) = (V_{u^{-1}\varepsilon^{-1}} f_{n00}, f_{nlm}), \tag{24}$$

$$V_{u^{-1}\varepsilon^{-1}} f_{n00}(u_1) = [\lambda(u_1 u^{-1} \varepsilon^{-1})]^{2in - 2}$$
$$= \left[\cos^2 \frac{\Omega}{2} e^{-\alpha} + \sin^2 \frac{\Omega}{2} e^\alpha \right]^{in - 1}, \tag{25}$$

---

*The operators introduced in that paper are related to H_μ and F_μ in the following manner: $H_\pm = \pm\sqrt{2} H_{\pm 1}$, $H_3 = H_0$ (similarly in the case of F_μ).

†A proof of this for the case $l = 0$ is given in Naĭmark's paper.[4]

where $\cos\Omega = \cos\vartheta\cos\vartheta_1 + \sin\vartheta\sin\vartheta_1\cos(\varphi-\varphi_1)$ On making use of (22), we obtain

$$[V_{u^{-1}\varepsilon^{-1}}f_{n00}(u_1)]^* = -\frac{\sqrt{4\pi}}{n}\sum_{lm}\Pi_l(n,\ \alpha)\,Y_{lm}(\vartheta,\ \varphi)\,f^*_{nlm}(u_1), \tag{26}$$

from which (23) follows.

Thus, the matrix elements of the operators in representations I and II coincide. The transition from one system of basis functions to the other is realized by means of the following unitary transformation

$$\int F_n(\omega,\ u)\,f_{nlm}(u)\,du = \Psi_{nlm}(\omega),$$
$$\int F^*_{n'}(\omega,\ u)\,\Psi_{nlm}(\omega)\,d\omega = \frac{\pi}{2}\,\delta(n-n')\,f_{nlm}(u), \tag{27}$$

where

$$F_n(\omega,\ u_1) = \sum_{lm}\Psi_{nlm}(\omega)\,f^*_{nlm}(u_1)$$
$$= -\frac{n}{\sqrt{4\pi}}\left[\cos^2\frac{\Omega}{2}e^{-\alpha} + \sin^2\frac{\Omega}{2}e^{\alpha}\right]^{-in-1}. \tag{28}$$

4. THE CLEBSCH-GORDAN EXPANSION. INTEGRAL REPRESENTATION OF THE FANO FUNCTION

As an example of the application of the results of the preceding section we discuss the Clebsch-Gordan expansion. The Clebsch-Gordan expansion for the infinite-dimensional representations of the Lorentz group was obtained independently and simultaneously by Toptygin and one of the present authors[11] and by Naĭmark.[12] The expansion carried out in reference 11 referred to the Ψ_{nlm} functions, while the one carried out in reference 12 referred to the functions f(u). Let us establish the connection between the results of these papers. This will enable us at the same time to obtain a number of useful relationships for the Fano functions. Naĭmark[12] gave an expansion of the product of two functions of representation I characterized by the numbers (m_1, ρ_1) and (m_2, ρ_2) in terms of functions which are characterized by the numbers (m_3, ρ_3). Also the inverse expansion has been obtained. This expansion is carried out with the aid of a unitary operator in accordance with a formula which, in the case that is of interest to us $(m_1 = m_2 = m_3 = 0)$, has the following form

$$f_{n_3}(u_3) = \int du_1\int du_2 f_{n_1}(u_1)\,f_{n_2}(u_2)\,b_{n_1n_2n_3}(u_1,\ u_2,\ u_3),$$
$$f_{n_1}(u_1)\,f_{n_2}(u_2) = \frac{1}{4\pi^4}\int_0^\infty n_3^2dn_3\int du_3 f_{n_3}(u_3)\,b^*_{n_1n_2n_3}(u_1,\ u_2,\ u_3). \tag{29}$$

If the matrices u_i are specified by means of the angles ϑ_i, θ_i, θ'_i in accordance with formula (1), the expression for $b_{n_1n_2n_3}$ may be written in the form

$$b_{n_1n_2n_3}(u_1,\ u_2,\ u_3) = \pi^{3/2}\left(\sin\frac{\Omega_{12}}{2}\right)^{-i(n_1+n_2+n_3)-1}\left(\sin\frac{\Omega_{13}}{2}\right)^{i(-n_1+n_2+n_3)-1}$$
$$\times\left(\sin\frac{\Omega_{23}}{2}\right)^{i(n_1-n_2+n_3)-1}, \tag{30}$$

where

$$\cos\Omega_{ik} = \cos\vartheta_i\cos\vartheta_k + \sin\vartheta_i\sin\vartheta_k\cos(\varphi_i-\varphi_k),\ \varphi_i = \theta'_i - \theta_i.$$

By utilizing the expansion

$$\left[\sin\frac{\vartheta}{2}\right]^{2a-2} = \sum_l F_l(a)\,(2l+1)\,P_l(\cos\vartheta),$$
$$F_l(a) = \Gamma(a)\,\Gamma(l+1-a)\,[\Gamma(1-a)\,\Gamma(l+1+a)]^{-1}, \tag{31}$$

we may represent $b_{n_1n_2n_3}$ in the following form

$$b_{n_1n_2n_3} = \sum i^{l_1+l_2-l_3}\sqrt{(2l_1+1)(2l_2+1)}$$
$$\times B_{l_1l_2l_3}C^{l_3m_3}_{l_1m_1l_2m_2}f^*_{n_1l_1m_1}f^*_{n_2l_2m_2}f_{n_3l_3m_3}. \tag{32}$$

Here we have

$$B_{l_1l_2l_3} = \pi^{3/2}i^{l_1+l_2-l_3}A_{l_1}(n_1)\,A_{l_2}(n_2)\,A^*_{l_3}(n_3)$$
$$\times\sum(-)^{L_1}(2L_1+1)(2L_2+1)$$
$$\times(2L_3+1)\,[(2l_1+1)(2l_2+1)(2l_3+1)]^{-1/2}$$
$$\times F_{L_1}(a)\,F_{L_2}(b)\,F_{L_3}(c)\,C^{l_10}_{L_10L_20}C^{l_20}_{L_30L_10}C^{l_30}_{L_20L_30}$$
$$\times W(L_1L_2l_2l_3;\ l_1L_3),$$
$$a = \tfrac{1}{2} - \tfrac{1}{2}i(n_1+n_2+n_3),\ b = \tfrac{1}{2} + \tfrac{1}{2}i(-n_1+n_2+n_3),$$
$$c = \tfrac{1}{2} + \tfrac{1}{2}i(n_1-n_2+n_3), \tag{33}$$

W(abcd; ef) is a Racah function, $C^{a\alpha}_{b\beta c\gamma}$ are the Clebsch-Gordan coefficients. In the course of obtaining this formula the following expansion was utilized

$$Y_{l_1m_1}Y_{l_2m_2} = \sum_{l_3}\sqrt{(2l_1+1)(2l_2+1)/4\pi(2l_3+1)}$$
$$\times C^{l_3m_3}_{l_1m_1l_2m_2}C^{l_30}_{l_10l_20}Y_{l_3m_3}$$

and also the Racah formula summed over the magnetic quantum numbers.[7] On taking in formula (29) for the functions $f_{n_i}(u_i)$ $(i = 1, 2)$ the basis functions $f_{n_il_im_i}(u_i)$ [in this case $f_{n_3}(u_3)$ will not be a basis function] and on utilizing the relationship between the functions $\Psi_{n_il_im_i}$ and the functions $f_{n_il_im_i}$ which is given by formula (27), we obtain the following Clebsch-Gordan expansion (see Appendix):

$$\Psi_{n_1l_1m_1}(\omega)\,\Psi_{n_2l_2m_2}(\omega)$$
$$= \frac{1}{8\pi^{3/2}}\int_0^\infty dn_3 \sum_{l_3} i^{l_1+l_2-l_3+2}\sqrt{(2l_1+1)(2l_2+1)}$$
$$\times C^{l_3m_3}_{l_1m_1l_2m_2}\, n_1n_2n_3 B_{l_1l_2l_3} B^*_{000}\,\Psi_{n_3l_3m_3}(\omega). \tag{34}$$

By utilizing the representation of $B_{l_1l_2l_3}$ in the form of the integral

$$B_{l_1l_2l_3}C^{l_30}_{l_10\,l_20} = i^{l_1+l_2-l_3}\sqrt{2l_3+1}\,A_{l_1}(n_1)\,A_{l_2}(n_2)\,A^*_{l_3}(n_3)$$
$$\times\int b_{n_1n_2n_3}P_{l_1}(u_1)\,P_{l_2}(u_2)\,P_{l_3}(u_3)\,du_1\,du_2\,du_3, \tag{35}$$

it is possible to obtain relations which connect functions $B_{l_1l_2l_3}(n_1n_2n_3)$ with different values of l. These relations* turn out to be the same as in the case of the Fano functions $X(j_1j_1l_1;\ j_2j_2l_2;\ j_3j_3l_3)$ with $2j_i + 1 = in_i$. Therefore we have

$$B_{l_1l_2l_3}(n_1n_2n_3) = \Phi(n_1n_2n_3)\,X(j_1j_1l_1;\ j_2j_2l_2;\ j_3j_3l_3), \tag{36}$$

where $\Phi(n_1n_2n_3)$ no longer depends on l_i. For the evaluation of $\Phi(n_1n_2n_3)$ it is convenient to utilize formula (33) in which we set $l_1 = l_2 = l_3 = 0$. From this we obtain the following expression:

$$\Phi(n_1n_2n_3) = \pi^{3/2}\sqrt{n_1n_2n_3}\sum_L(2L+1)\,F_L(a)\,F_L(b)\,F_L(c)$$
$$= \pi^{3/2}\frac{\sqrt{n_1n_2n_3}}{abc}\,{}_5F_4\left(1,\ \frac{3}{2},\ 1-a,\ 1-b,\ 1-c;\right.$$
$$\left.\frac{1}{2},\ 1+a,\ 1+b,\ 1+c;\ 1\right), \tag{37}$$

${}_5F_4$ is the generalized hypergeometric function.[13] For these values of its arguments ${}_5F_4$ may be simply expressed in terms of Γ functions.[13] Finally we obtain

$$\Phi(n_1n_2n_3) = \pi^{3/2}\sqrt{n_1n_2n_3}\,\Gamma(a)\,\Gamma(b)\,\Gamma(c)\,\Gamma(a+b+c-1)$$
$$\times[\Gamma(a+b)\,\Gamma(a+c)\,\Gamma(b+c)]^{-1}. \tag{38}$$

The final form of the Clebsch-Gordan expansion for the functions Ψ is given by:

$$\Psi_{n_1l_1m_1}(\omega)\,\Psi_{n_2l_2m_2}(\omega)$$
$$= \frac{1}{\sqrt{4\pi}}\int_0^\infty dn_3\sum_{l_3} i^{l_1+l_2-l_3+2}\sqrt{(2l_1+1)(2l_2+1)}$$
$$\times n_1n_2n_3\,B(n_1n_2n_3)\,C^{l_3m_3}_{l_1m_1l_2m_2}\,X(j_1j_1l_1;\ j_2j_2l_2;\ j_3j_3l_3)$$
$$\times(j_1j_10;\ j_2j_20;\ j_3j_30)\,\Psi_{n_3l_3m_3}(\omega). \tag{39}$$

Here we have

$$B(n_1n_2n_3) = (1/4\pi^4)\,|\Phi(n_1n_2n_3)|^2$$
$$= \sinh\pi n_1\sinh\pi n_2\sinh\pi n_3\left[4\cosh\frac{\pi}{2}(n_1+n_2+n_3)\right.$$
$$\times\cosh\frac{\pi}{2}(n_1+n_2-n_3)$$
$$\left.\times\cosh\frac{\pi}{2}(n_1-n_2+n_3)\cosh\frac{\pi}{2}(-n_1+n_2+n_3)\right]^{-1}. \tag{40}$$

The result obtained above agrees with the results of reference 11.

Formulas (33) and (35) which give an analytic expression for the Fano function $X(j_1j_1l_1;\ j_2j_2l_2;\ j_3j_3l_3)$ for the case of purely imaginary values of $2j_i + 1 = in_i$, turn out to be particularly useful since they remain valid for the case of real j_i. These formulas give a new representation of the Fano function which differs from those known previously. The integral representation of the Fano functions allows us to investigate their analytic properties for complex values of their arguments. By applying analogous methods to the representations with $k_0 \neq 0$ we can obtain integral representations of the Fano functions of a more general form $X(j_1j_1'l_1;\ j_2j_2'l_2;\ j_3j_3'l_3)$.

With the aid of expansion (32) we can obtain orthogonality relations for the Fano functions with complex values of their arguments. From formulas (29) it follows that:

$$\int b_{n_1n_2n_3}(u_1,u_2,u_3)\,b^*_{n_1n_2n_3'}(u_1,u_2,u_3')\,du_1du_2$$
$$= 4\pi^4n_3^{-2}\,\delta(n_3-n_3')\,\delta(u_3-u_3'), \tag{41}$$

$$\int b_{n_1n_2n_3}(u_1,u_2,u_3)\,b^*_{n_1n_2n_3}(u_1',u_2',u_3)\,n_3^2\,dn_3\,du_3$$
$$= 4\pi^4\delta(u_1-u_1')\,\delta(u_2-u_2'). \tag{42}$$

By utilizing (32) we may easily obtain from the preceding formulas

$$n_3^2\,B(n_1,n_2,n_3)\sum_{l_1l_2}(2l_1+1)(2l_2+1)\,X(j_1j_1l_1;\ j_2j_2l_2;\ j_3j_3l_3)$$
$$\times X^*(j_1j_1l_1;\ j_2j_2l_2;\ j_3'j_3'l_3) = \delta(n_3-n_3'), \tag{43}$$

$$\sum_{l_3}\int n_3^2\,B(n_1n_2n_3)(2l_1+1)(2l_2+1)\,X(j_1j_1l_1;\ j_2j_2l_2;\ j_3j_3l_3)$$
$$\times X^*(j_1j_1l_1';\ j_2j_2l_2';\ j_3j_3l_3)\,C^{l_3m_3}_{l_1m_1l_2m_2}\,C^{l_3m_3}_{l_1'm_1'l_2'm_2'}\,dn_3$$
$$= \delta_{l_1l_1'}\,\delta_{l_2l_2'}\,\delta_{m_1m_1'}\,\delta_{m_2m_2'}. \tag{44}$$

From this, in particular, the following normalization condition for the Fano functions may be obtained

$$(2l_1+1)(2l_2+1)$$
$$\times\int B(n_1n_2n_3)\,|X(j_1j_1l_1;\ j_2j_2l_2;\ j_3j_3l_3)|^2\,n_3^2\,dn_3 = 1.$$

5. EXPANSION OF THE WAVE FUNCTION OF A PARTICLE IN TERMS OF THE IRREDUCIBLE REPRESENTATIONS OF THE LORENTZ GROUP

We now proceed to utilize the results obtained earlier for a relativistically-invariant classification of particle states. First of all we consider a free scalar particle of mass M. We introduce the notation

$$\sinh\alpha = |\mathbf{p}|/M,\ \cosh\alpha = E_p/M,\ \omega\to(\alpha,\ \vartheta,\ \varphi),$$

---

*One method of obtaining such relations is, for example, the replacement of the variables in (35) by means of formula (17) and the utilization of the condition $\partial B_{l_1l_2l_3}(n_1n_2n_3)/\partial\alpha = 0$.

$d\omega = d^3\mathbf{p}/E_pM^2$, $\Psi(\mathbf{p})$ is the particle wavefunction. Shapiro[1] has proposed to define the state of a particle by means of the basis functions of the irreducible representation I. These functions $f_n(\nu)$ are related to $\Psi(\mathbf{p})$ by the following relations

$$\Psi(\mathbf{p}) = 2\int_0^\infty dn \int d\Omega(\boldsymbol{\nu}) \left[\frac{E_p - \mathbf{p}\boldsymbol{\nu}}{M}\right]^{-1-in} f_n(\boldsymbol{\nu}),$$

$$f_n(\boldsymbol{\nu}) = \frac{n^2}{16\pi^3}\int \frac{d^3\mathbf{p}}{E_p}\left[\frac{E_p - \mathbf{p}\boldsymbol{\nu}}{M}\right]^{-1+in} \Psi(\mathbf{p}). \qquad (45)$$

If in place of $f_n(\nu)$ we utilize the basis functions of representation II we will obtain

$$\Psi_M(\omega) = \int_0^\infty dn\, \Phi_n(\omega), \quad \Phi_n(\omega) = \frac{2M^2}{\pi}\int d\omega_1 \frac{\sin n\gamma}{\sinh \gamma} \Psi_M(\omega_1),$$

$$\cosh\gamma = (EE_1 + \mathbf{p}\mathbf{p}_1)/M^2. \qquad (46)$$

From (22) we can obtain the following expansion

$$\left[\frac{E - \mathbf{p}\boldsymbol{\nu}}{M}\right]^{-1-in} = \frac{4\pi}{n}\sum_l (-)^{l+1} A_l^*(n)\,\Pi_l(n,\alpha)\, Y_{lm}^*(\boldsymbol{\nu})\, Y_{lm}\left(\frac{\mathbf{p}}{|\mathbf{p}|}\right). \qquad (47)$$

By utilizing (47) we can obtain (45) from (46). The expansion of the wave function for a particle with spin was obtained by Zastavenko and Chou Kuang-Chao[14] on the basis of the transformation (45). In representation II the analogous expansion has a simpler appearance. The wavefunction of a particle with spin s may be represented in the form $\Psi_\sigma(\mathbf{p}) = u_\sigma(\mathbf{p})f(\mathbf{p})$, where $u_\sigma(\mathbf{p})$ is a column of two components $u^{s0}_{\sigma 0}$ and $u^{0s}_{0\sigma}$ which under four-dimensional rotations transform according to equivalent representations, and under reflections go over into one another. In the case of spin $\frac{1}{2}$ they correspond to two components of a bispinor. $u^{s0}_{\sigma 0}$ transforms according to a finite-dimensional representation (cf. reference 5), while $f(\mathbf{p})$ is a scalar.

In order to obtain an expansion of the wavefunction $\Psi_\sigma(\mathbf{p})$ in terms of irreducible representations we write $f(\mathbf{p})$ in the following form

$$f(\omega) = \sum_{lm}\int_0^\infty dn\, a_{lm}(n)\, \Psi_{nlm}(\omega).$$

By utilizing results obtained earlier,[6] we can easily write the following equation

$$u^{s0}_{\sigma 0}(\eta,\lambda).\,\Psi_{nlm}(\omega) = \sum_{k_0 j}(-)^{j-l-k_0}(2J + 2k_0 + 1)$$
$$\times[(2l+1)/(2s+1)(2J+1)]^{1/2}$$
$$\times C^{j\mu}_{lms\lambda} W(JJsj;\ lJ + k_0)\, T^{nk_0}_{j\mu s\sigma}(\eta), \qquad (48)$$

where $\eta \equiv (\omega, \Omega_2) \equiv (\Omega_1, \alpha, \Omega_2)$ and

$$T^{nk_0}_{j\mu s\sigma}(\eta) = \sum_\varkappa D^j_{\mu\varkappa}(\Omega_1)\, D^s_{\varkappa\sigma}(\Omega_2)\, Q^{js}_{nk_0\varkappa}(\alpha), \qquad (49)$$

$$Q^{js}_{nk_0\varkappa}(\alpha)$$
$$= \sum_{f=|j-s|}^{j+s} (2f+1)[(2j+1)/(2J+1)]^{1/2} W(JJ + k_0 fs;\ jJ)$$
$$\times C^{s\varkappa}_{f0j\varkappa}\, e^{\varkappa\alpha}\, \Pi_f(n,\alpha). \qquad (50)$$

Here σ is the spin variable, while λ is the component of the particle spin. The angles $\Omega_2 \equiv (\varphi_2, \vartheta_2, \chi_2)$ define the direction of the particle spin in the rest system with $OZ \parallel \mathbf{p}$, while the angles $\Omega_1 \equiv (\varphi_1, \vartheta_1, \chi_1)$. define the direction of the momentum $\mathbf{p}$ in the reference system chosen by us; $\tanh\alpha = v/c$.

The quantities $T^{nk_0}_{j\mu s\sigma}(\eta)$ are matrix elements of the rotation operator in four-dimensional space. They transform according to the irreducible infinite-dimensional unitary representation of the Lorentz group which corresponds to a definite value of $n \equiv -i(2J+1)$ and k_0. The following orthogonality condition holds for these quantities

$$\int T^{nk_0^*}_{j\mu s\sigma}(\eta)\, T^{n'k_0'}_{j'\mu's'\sigma'}(\eta)\, d\eta = N\delta(n - n')\,\delta_{k_0k_0'}\,\delta_{jj'}\,\delta_{ss'}\,\delta_{\mu\mu'}\,\delta_{\sigma\sigma'},$$

$$d\eta \equiv \sinh^2\alpha\, d\alpha\, d\Omega_1 d\Omega_2,$$

$$N^{-1} = (2\pi)^{-5}|(2J+1)(2J + 2k_0 + 1)|. \qquad (51)$$

On substituting (48) and (51) into $\Psi_\sigma(\eta)$ we shall obtain the desired expansion

$$\Psi_\sigma(\eta) = \sum_{k_0=-s}^{s}\int dn\, \Phi^{nk_0}_{s\sigma}(\eta), \qquad (52)$$

$$\Phi^{nk_0}_{s\sigma}(\eta) = N^{-1}\int d\eta_1\, T^{nk_0}_{s\sigma s\sigma}(\widehat{\eta\eta_1})\, \Psi_\sigma(\eta_1);$$

$$T^{nk_0}_{s\sigma s\sigma}(\widehat{\eta\eta_1}) = \sum_{j\mu} T^{nk_0^*}_{j\mu s\sigma}(\eta_1)\, T^{nk_0}_{j\mu s\sigma}(\eta); \qquad (53)$$

$\widehat{\eta\eta_1}$ is the angle between the directions which are defined by the angles η and η_1 in four-dimensional space.

For the wave function of a system of particles one can obtain formulas analogous to (52). In obtaining these formulas it is necessary to utilize the Clebsch-Gordan expansion for the product of two $T^{nk_0}_{j\mu s\sigma}(\eta)$. This expansion will be analogous to the expansion (50) of reference 6, if in that expansion we take for $C(N_1l_1N_2l_2Nl)$ and $C(N_1l_1'N_2l_2'Nl)$ functions which differ from their definition in reference 6 by replacing $X(J_1J_1l_1;\ J_2J_2l_2;\ JJl)$ by $X(J_1J_1 + k_0l_1;\ J_2J_2 + k_0l_2;\ JJ + k_0l)$.

APPENDIX

According to (27) we have

$$\Psi_{n_1l_1m_1}(\omega)\,\Psi_{n_2l_2m_2}(\omega)$$
$$= \int du_1du_2\, F_{n_1}(\omega, u_1)\, F_{n_2}(\omega, u_2)\, f_{n_1l_1m_1}(u_1)\, f_{n_2l_2m_2}(u_2).$$

By utilizing the expansion (29) we obtain

$$\Psi_{n_1 l_1 m_1}(\omega) = \Psi_{n_2 l_2 m_2}(\omega) = \frac{1}{4\pi^4}\int_0^\infty n_3^2\, dn_3 \int du_1 du_2 du_3\, F_{n_1}(\omega,\ u_1)$$

$$\times F_{n_2}(\omega,\ u_2)\, \overset{*}{b}_{n_1 n_2 n_3}(u_1,\ u_2,\ u_3)\, f_{n_3}(u_3), \qquad \text{(A.1)}$$

where, according to the first of equations (29) and expansion (32), we have

$$f_{n_3}(u_3) = \sum_{l_3} i^{l_1+l_2-l_3}\sqrt{(2l_1+1)(2l_2+1)}$$

$$\times B_{l_1 l_2 l_3}(n_1 n_2 n_3)\, C^{l_3 m_3}_{l_1 m_1 l_2 m_2}\, f_{n_3 l_3 m_3}(u_3).$$

Let us discuss the integral occurring in (A.1)

$$I = \int du_1 du_2 du_3\, F_{n_1}(\omega,\ u_1)\, F_{n_2}(\omega,\ u_2)$$

$$\times \overset{*}{b}_{n_1 n_2 n_3}(u_1,\ u_2,\ u_3)\, f_{n_3 l_3 m_3}(u_3).$$

We introduce into this integral new variables in accordance with the following formula

$$u_i' = \overline{u_i u^{-1}\varepsilon^{-1}}, \qquad u_i = \overline{u_i'\varepsilon u}.$$

We also have

$$F_{n_i}(\omega.\ u_i) = -(n_i/\sqrt{4\pi})\,[\lambda(u_i u^{-1}\varepsilon^{-1})]^{-2in_i-2}$$

$$= -(n_i/\sqrt{4\pi})\,[\lambda(u_i'\varepsilon u)]^{2in_i+2},$$

$$\overset{*}{b}_{n_1 n_2 n_3}(u_i) = \overset{*}{b}_{n_1 n_2 n_3}(u_i')\,[\lambda(u_1'\varepsilon u)]^{-2in_1+2}[\lambda(u_2'\varepsilon u)]^{-2in_2+2}$$

$$\times[\lambda(u_3'\varepsilon u)]^{-2in_3+2},$$

$$du_i = du_i'/[\lambda(u_i'\varepsilon u)]^4.$$

Therefore

$$I = \frac{n_1 n_2}{4\pi}\int du_1'\, du_2'\, du_3'\, \overset{*}{b}_{n_1 n_2 n_3}$$

$$\times(u_1',\ u_2',\ u_3')\,[\lambda(u_3'\varepsilon u)]^{2in_3-2}\, f_{n_3 l_3 m_3}(\overline{u_3'\varepsilon u}).$$

Since

$$\int \overset{*}{b}_{n_1 n_2 n_3}(u_1' u_2' u_3')\, du_1'\, du_2' = \overset{*}{B}_{000},$$

we obtain

$$I = -\frac{n_1 n_2}{n_3\sqrt{4\pi}}\,\overset{*}{B}_{000}\,\Psi_{n_3 l_3 m_3}(\omega).$$

From this formula (34) follows.

---

[1] I. S. Shapiro, Dokl. Akad. Nauk SSSR **106**, 647 (1956), Soviet Phys.-Doklady **1**, 91 (1956).

[2] I. S. Shapiro, Thesis, Physics Institute, Acad. Sci. U.S.S.R., 1955.

[3] I. M. Gel'fand and M. A. Naĭmark, Izv. Akad. Nauk SSSR, Ser. Mat. **11**, 411 (1947).

[4] M. A. Naĭmark, Usp. mat. nauk **9**, 19 (1954).

[5] A. Z. Dolginov, JETP **30**, 746 (1956), Soviet Phys. JETP **3**, 589 (1956).

[6] A. Z. Dolginov and I. N. Toptygin, JETP **37**, 1441 (1959), Soviet Phys. JETP **10**, 1022 (1960).

[7] G. Racah, Phys. Rev. **62**, 438 (1942).

[8] Arima, Horie, and Tanabe, Progr. Theoret. Phys. (Kyoto) **11**, 143 (1954).

[9] H. Matsunobo and H. Takebe, Progr. Theoret. Phys. (Kyoto), **14**, 589 (1955).

[10] V. A. Fock, Z. Phys. **98**, 145 (1935).

[11] A. Z. Dolginov and I. N. Toptygin, JETP **35**, 794 (1958); Soviet Phys. JETP **8**, 550 (1959).

[12] M. A. Naĭmark, Dokl. Akad. Nauk SSSR **119**, 872 (1958).

[13] H. Bateman, Higher Transcendental Functions, New York, 1953.

[14] Chou Kuang-Chao and L. G. Zastavenko, JETP **35**, 1417 (1958); Soviet Phys. JETP **8**, 990 (1959).

Translated by G. Volkoff

ON THE STABILITY OF PLANE POISEUILLE FLOW OF A PLASMA OF FINITE CONDUCTIVITY IN A MAGNETIC FIELD

Yu. A. TARASOV

Submitted to JETP editor, July 4, 1959

J. Exptl. Theoret. Phys. (U.S.S.R.) **37**, 1708-1713 (December, 1959)

The stability of flow of a plasma in a longitudinal magnetic field with respect to infinitesimal perturbations is considered for magnetic Reynolds numbers $R_m \lesssim 1$.

1. STATEMENT OF THE PROBLEM

THE motion of an incompressible conducting fluid in a magnetic field is described by the equations of magnetohydrodynamics:

$$\frac{\partial U_i}{\partial t} + U_j \frac{\partial U_i}{\partial x_j} - \frac{\mu}{4\pi\rho} H_j \frac{\partial H_i}{\partial x_j} = -\frac{\partial W}{\partial x_i} + \nu \nabla^2 U_i,$$

$$\frac{\partial H_i}{\partial t} + U_j \frac{\partial H_i}{\partial x_j} - H_j \frac{\partial U_i}{\partial x_j} = \lambda \nabla^2 H_i \qquad \mu = 1,$$

$$\frac{\partial U_i}{\partial x_i} = 0, \qquad \frac{\partial H_i}{\partial x_i} = 0, \qquad W = \frac{1}{\rho}\left(p + \frac{\mu H^2}{8\pi}\right), \qquad \lambda = \frac{1}{4\pi\mu\sigma}. \tag{1}$$

Here ν is the kinematic viscosity and σ is the conductivity of the fluid. The character of the flow is determined by the values of three dimensionless parameters R_g, R_m, and A, where $R_g = U_c L/\nu$ is the hydrodynamic Reynolds number, $R_m = U_c L/\lambda$, the magnetic Reynolds number, and $A = B_0/U_c\sqrt{4\pi\rho}$ the Alfvén number.

The values U_c, B_0, and L represent the velocity, magnetic field induction, and size characterizing the flow. For certain values of these dimensionless parameters, infinitesimal perturbations begin to increase with time, i.e., the flow becomes unstable. To find these critical values, we can express the unknown as the sum of a stationary term and a small perturbation:

$$\mathbf{U} = \mathbf{U}_0 + \mathbf{u}, \qquad \mathbf{B} = \mathbf{B}_0 + \mathbf{b}, \qquad P = P_0 + p. \tag{2}$$

Substituting (2) in (1), we obtain a system of equations for the perturbations. We shall assume that the stationary velocity and magnetic field are directed along the x axis, while the z axis is perpendicular to the parallel boundary planes. Consequently, we are interested in solutions of the form:[1]

$$f(\mathbf{r}, t) = f(z)\, e^{i(kx - \omega t)}.$$

Eliminating the velocity from system (1), we obtain a sixth order differential equation for the z component of magnetic field perturbation, b_z:

$$\left\{\left(W - \frac{\omega}{k}\right)^2 - A^2 - \frac{iW''}{kR_m}\right\} b_z'' + 2W'\left(W - \frac{\omega}{k}\right) b_z'$$
$$- k^2\left\{\left(W - \frac{\omega}{k}\right)^2 - A^2 - \frac{iW''}{kR_m}\right\} b_z = -\frac{i}{k}\left\{\frac{L^2(W - \omega/k)}{R_g} b_z\right.$$
$$\left. + \frac{(W - \omega/k)}{R_m} L^2 b_z\right\} + \frac{L^3 b_z}{k^2 R_g R_m}. \tag{3}$$

Here

$$W \equiv U_0/U_c, \qquad L \equiv d^2/dz^2 - k^2.$$

The z component of the velocity, u_z, is connected with b_z by the relation

$$u_z = \left(W - \frac{\omega}{k}\right) b_z + \frac{i}{kR_m}(b_z'' - k^2 b_z). \tag{4}$$

The boundary conditions at the walls require that

$$\mathbf{u} = 0, \qquad \mathbf{bn} = 0.$$

Hence we obtain six boundary conditions for the complex quantity b_z:

$$b_z = 0, \qquad b_z'' = 0,$$
$$\left(W - \frac{\omega}{k}\right) b_z' + \frac{i}{kR_m}(b_z''' - k^2 b_z') = 0. \tag{5}$$

If we substitute the six linearly independent solutions of (3) into (5), equate the determinant of the resulting system of six homogeneous equations (i.e., the secular determinant) to zero, and solve for the imaginary part of ω_i, we obtain the relation

$$\omega_i = f(R_g, R_m, k, A).$$

The stability boundary, i.e., the neutral stability curve, is found by setting $\omega_i = 0$. This yields the relation $R_g = R_g(k, R_m, A)$. Since Eq. (3) is invariant under the substitution $z \to -z$, its solutions can be divided into symmetrical and asymmetrical groups. We shall limit our consideration to symmetrical perturbations only, since these are the most unstable in hydrodynamics.

The problem of the stability of a fluid with ideal conductivity has been solved by Velikhov.[2] In this connection the critical Alfvén number for a Poiseuille flow proved to be 0.1. Stuart[3] has investigated the problem of the stability of a fluid with poor conductivity. In his treatment the first term on the right-hand side of Eq. (4) is neglected in comparison to the second term, i.e., it is assumed that $kR_m \ll 1$. Stuart obtained a fourth order differential equation in the velocity perturbation. The magnetic field enters into this equation in the form of the combination $q = kA^2R_m$. Stuart found that the critical number q was equal to 0.1. However, no unique conclusion was derived by Stuart as to the closure of the neutral stability curves.

The present paper deals with the case where $kR_m \lesssim 1$, which is of particular interest since it includes a high-velocity region and temperatures on the order of 5,000 – 10,000°. In this case the starting point must be the differential equation of the sixth order, Eq. (3).

2. SOLUTION OF THE PERTURBATION EQUATION

Since large values for R_g entail a loss of stability, we shall seek an asymptotic solution of Eq. (3) in powers of $1/kR_g$;

$$b_z = b_z^{(0)} + \frac{1}{kR_g} b_z^{(1)} + \ldots .$$

The zero approximation $b_z^{(0)}$ is the solution of the fourth-order equation

$$[kR_m (W - \omega/k)^2 - q - iW''] b_z^{(0)''} + kR_m \cdot 2W' (W - \omega/k) b_z^{(0)'}$$
$$- k^2 [kR_m (W - \omega/k)^2 - q - iW''] b_z^{(0)}$$
$$= -i \{(W - \omega/k) [b_z^{(0)\mathrm{IV}} - 2k^2 b_z^{(0)''} + k^4 b_z^{(0)}]\}, \tag{6}$$

where $q = kR_mA^2$. Once we have solved this equation, we can find two symmetrical solutions. We shall seek a solution of Eq. (6) in the form of a power series in k^2:

$$b_z^{(0)} = b_0 + k^2 b_1 + k^4 b_2 + \ldots$$

The first term, b_0, is obtained from the equation:

$$[(W - \omega/k) b_0^{\mathrm{IV}} - W'' b_0''] = 0. \tag{7}$$

The two symmetrical solutions of this equation are

$$b_{0,1} = 1, \qquad b_{0,2}'' = W - \omega/k = z_0^2 - z^2,$$
$$\text{i.e. } b_{0,2} = z_0^2 z^2/2 - z^4/12,$$

where

$$z_0^2 = 1 - \omega/k.$$

The second term, b_1, is obtained from the equation:

$$\left[\left(W - \frac{\omega}{k}\right) b_1^{\mathrm{IV}} - W'' b_1''\right] = \left[\frac{ikR_m (W - \omega/k)^2}{k^2} b_0'\right]' - \frac{iq}{k^2} b$$
$$+ \left[iq - ikR_m \left(W - \frac{\omega}{k}\right)^2 + 2\right] b_0 + 2\left(W - \frac{\omega}{k}\right) b_0''. \tag{8}$$

Equations for b_2, b_3, etc. can be obtained in an analogous manner. From Eq. (8) one obtains an expression for the second derivative of the first symmetrical solution:

$$b_{1,1}'' = (iq + 2) \frac{z^2}{2z_0^2} - ikR_m \left[\frac{4}{15} z_0^2 z^2 - \frac{2}{15} z_0^2 \ln \frac{z_0^2 - z^2}{z_0^2} (z_0^2 - z^2)\right.$$
$$\left. + (z_0^2 - z^2) \frac{z^2}{10}\right]. \tag{9}$$

From this expression we obtain the quantities $b_{1,1}$, $b_{1,1}'$, $b_{1,1}'''$.

For the next or $b_{2,1}$ approximation we omit terms not containing k^4, qk^2, etc. Thus, the first symmetrical solution will have the form:

$$b_{z,1}^{(0)} = b_{0,1} + k^2 b_{1,1} + k^4 b_{2,1} + \ldots$$

The expression for the second derivative of the second symmetrical solution has the form:

$$b_{1,2}'' = (z_0^2 - z^2) \frac{ikR_m}{k^2} b_{0,2} - \frac{iq}{3k^2} z^2 + \frac{iq}{6k^2} (z_0^2 - z^2) \ln \frac{z_0^2 - z^2}{z_0^2}$$
$$+ iq \left[\frac{3}{40} z_0^2 z^2 + \frac{1}{15} (z_0^2 - z^2) z_0^2 \ln \frac{z_0^2 - z^2}{z_0^2} - \frac{1}{120} (z_0^2 - z^2) z^2\right]$$
$$+ \frac{41}{60} z_0^2 z^2 - \frac{2}{15} z_0^2 (z_0^2 - z^2) \ln \frac{z_0^2 - z^2}{z_0^2} + \frac{11}{60} (z_0^2 - z^2) z^2$$
$$- ikR_m \left[\frac{19}{840} z_0^6 z^2 + \frac{1}{105} z_0^6 (z_0^2 - z^2) \ln \frac{z_0^2 - z^2}{z_0^2} + (z_0^2 - z^2)\right.$$
$$\left. \times \left(\frac{1}{42} z_0^2 z^4 - \frac{11}{840} z^2 z_0^4\right)\right]. \tag{10}$$

From which we can find $b_{1,2}$; $b_{1,2}'$, and $b_{1,2}'''$. In like fashion we can find the next approximation. These series converge rapidly, even for $k^2 \sim 1$ and $kR_m \sim 1$. The quantity q approaches the value $\lesssim 0.1$.

The third solution of Eq. (3) is assumed to have the form

$$b_z = \exp\left\{\int g(z)\, dz\right\}, \tag{11}$$

where

$$g(z) = \sqrt{kR_g}\, g_0 + g_1 + g_2/\sqrt{kR_g} + O(1/kR_g).$$

For g_0 we obtain the expression

$$g_{0;\,1,2} = \pm\sqrt{i(W - \omega/k)}. \tag{12}$$

However, these three solutions cannot be considered correct near the point z_0, which is a branch point.

Approximate solutions near the point z_0 can be found, once the coefficients of Eq. (3) have been expanded in a series about the z_0 point. Let us change scale and introduce a new variable η:

$$z - z_0 = \varepsilon\eta, \text{ where } \varepsilon = i\,(-W_0' kR_g)^{-1/3}.$$

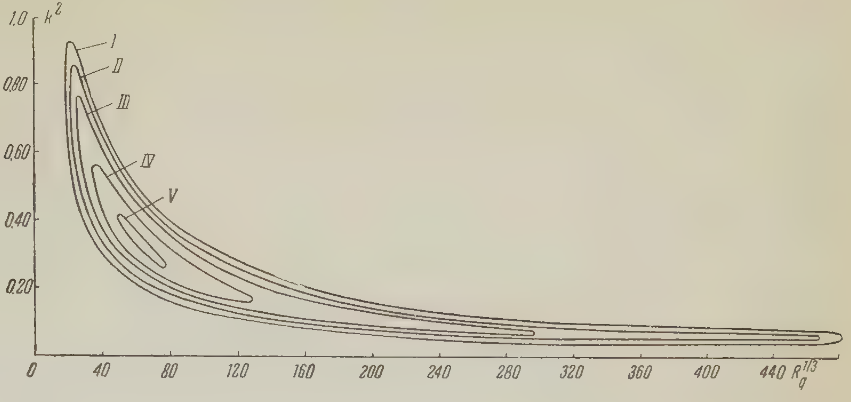

FIG. 1. Neutral curves for $R_m = 1$; curves designated I, II, III, IV, and V correspond to the values $A^2 = 0.063$, 0.07, 0.09, 0.11, and 0.12, respectively.

We now write b_z as $b_z = b_{z,0} + \epsilon b_{z,1} + \epsilon^2 b_{z,2} + \ldots$ and substitute it in Eq. (3). For $b_{z,0}$ we get the equation $b_{z,0}^{VI} + \eta b_{z,0}^{IV} = 0$. There are two solutions of this equation which are of the form

$$b_5 = \iiiint h_1 d\eta, \qquad b_6 = \iiiint h_2 d\eta, \tag{13}$$

where*

$$h_i(z) = \left(\tfrac{2}{3} z^{3/2}\right)^{1/3} H_{1/3}^{(i)}\left(\tfrac{2}{3} z^{3/2}\right)$$

These must be combined with the solutions given by (11), which are correct far from the resonance point. One of these solutions increases exponentially from the wall toward the center of the flow. So that the asymptotic solutions given by (13) coincide with the solutions given by (12) it is necessary to impose the condition:

$$-\tfrac{1}{6}\pi < \arg\zeta < \tfrac{7}{6}\pi \qquad (\zeta = i\eta).$$

This enables us to find the correct path around the branch point. Upon passage through a branch point, the imaginary part of the logarithm in Eq. (10) is increased by $(-i\pi)$.

For the third solution one must form a symmetrical combination of expressions like (11). However, the term containing $g_{0,2}$ increases exponentially from the wall toward the center of the flow and therefore contributes but little near the wall. Consequently one can use the exponential form with $g_{0,1}$, which near the point z_0 passes over into b_5 of (13).

Thus three symmetrical solutions are found which must be substituted in the boundary conditions, Eq. (5), at $z = 1$. The flow is found to be unstable for those perturbations for which the z_0 point is near the wall, i.e., the expression for b_5 from (13) must be used as the third solution.

Finally the approximate expression for the secular determinant is given by

$$F_1(\zeta_1) = F_2(k, R_m, A^2, z_0), \tag{14}$$

where

$$\zeta_1 = \frac{i(1 - z_0)}{\varepsilon} = (1 - z_0)(-W_0' k R_g)^{1/3},$$

$$F_1 = \iint\limits_{-\infty}^{\zeta} h_1 d\zeta \Big/ \zeta \int\limits_{-\infty}^{\zeta} h_1 d\zeta,$$

$$F_2 = \frac{b_{z,2}^{(0)} b_{z,2}^{(0)''} - b_{z,1}^{(0)''} b_{z,1}^{(0)}}{(1 - z_0)\left(b_{z,2}^{(0)'''} b_{z,1}^{(0)} - b_{z,1}^{(0)'''} b_{z,2}^{(0)} + k^2 b_{z,1}^{(0)'} b_{z,2}^{(0)} - k^2 b_{z,2}^{(0)'} b_{z,1}^{(0)}\right)}.$$

By fixing R_m and A^2 and eliminating z_0 it is possible to obtain the neutral curves $k^2 = f(R_g)$.

To solve Eq. (14), the graphical method given by Tollmein[4] was used. Plotting the imaginary part of F_1 against the real part, we obtain a curve with ζ_1 as the parameter. Next we fix the values of R_m and A^2 and for various values of z_0 plot the imaginary part of F_2 as a function of the real part in the same diagram with F_1. The quantity k is the variable parameter along the F_2 curve. The intersection of the F_1 and F_2 curves gives the required values for k and R_g.

3. RESULTS

The present analysis provides a series of neutral curves for several values of R_m. Figure 1 shows a series of neutral curves for $R_m = 1$. The curves are closed for large values of R_g for the values of A^2 selected here. As A^2 increases, the curves enclose a progressively narrower area, and when the critical value A^2_{crit} is reached, they shrink to a point, i.e., any further increase of the Alfvén number would result in an absence of instability. When $R_m = 1$, the value of A^2_{crit} lies between 0.12 and 0.13, which is to say that this value of A_{crit} is about 3.5 times greater than the A_{crit} for a plasma with ideal conductivity. Figure 2 indicates the dependence of A_{crit} on R_m. It is apparent from Fig. 2 that when R_m is increased from $R_m \sim 3$ or 4 to $R_m = \infty$, the magnitude of A_{crit} varies only slightly. For example, when $R_m = 3$, $A_{crit} \simeq 0.17$, and when

---

*Here $H_{1/3}^{(i)}$ denotes the Hankel functions of order 1/3.

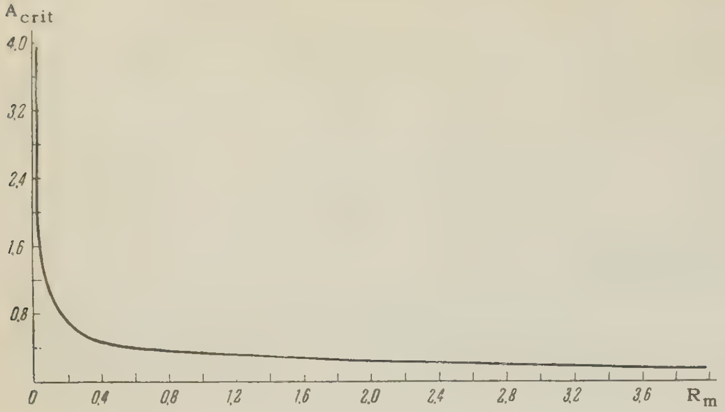

FIG. 2. Dependence of A_{crit} on R_m.

$R_m = \infty$, $A_{crit} = 0.1$. For a flow with a velocity $U_c = 10^5$ cm/sec and a density $\rho = 10^{-3}$ g/cm, the magnetic field H_{crit} necessary to stabilize a fluid with ideal conductivity will be ~ 1,100 gauss, while when $R_m = 3$, $H_{crit} \sim 1{,}850$ gauss.

The mechanism of the development and decay of perturbations resembles in many ways the same mechanism in conventional hydrodynamics. Without going into this analogy in detail, we observe that there is a definite connection between the neutral curves in Fig. 1 and Shen's curves with constant ω_i (reference 1, p. 42), which as ω_i increases become closed. As the magnetic field is increased only those perturbations cause instability which increase at a rather fast rate.

In conclusion I wish to thank E. P. Velikhov for discussions on the questions dealt with here.

---

[1] C. C. Lin, The Theory of Hydrodynamic Stability, Cambridge, 1955 (Russ. Transl., M. IIL, 1958).

[2] E. P. Velikhov, JETP **36**, 1192 (1959), Soviet Phys. JETP **9**, 848 (1959).

[3] J. T. Stuart, Proc. Roy. Soc. **A221**, 189 (1954).

Translated by A. Skumanich
333

SOVIET PHYSICS JETP VOLUME 37 (10), NUMBER 6 JUNE, 1960

DISPERSION RELATIONS FOR THE SCATTERING OF γ QUANTA BY NUCLEONS

L. I. LAPIDUS and CHOU KUANG-CHAO

Joint Institute of Nuclear Research

Submitted to JETP editor July 1, 1959

J. Exptl. Theoret. Phys. (U.S.S.R.) **37**, 1714-1721 (December, 1959)

Dispersion relations for the scattering of γ quanta by nucleons with one subtraction are considered. For forward scattering six relations have been obtained which do not contain unknown constants or infrared divergencies.

1. Dispersion relations for the scattering of γ quanta by nucleons have been considered by a number of authors.[1-6] The presence of infrared divergencies, however, limits the applicability of these relations for the analysis of the experimental data.

In the present paper we derive dispersion relations in a form which is convenient for practical application. In a forthcoming paper[7] we shall use these relations in the discussion of the scattering of γ quanta near the threshold for meson production.

Before discussing the dispersion relations for the scattering of γ quanta by nucleons, we consider in somewhat more detail the kinematics of the process. Let k and k′ be the momentum four-vectors of the incident and the scattered photon, and p and p′, those of the incident and scattered nucleons. These quantities are related by the conservation law

$$k + p = k' + p'. \tag{1}$$

We introduce the notation

$$P = \tfrac{1}{2}(p + p').$$

Following Prange,[8] we choose the following four orthogonal vectors as basis vectors:

$$P' = P - (PK)\,K/K^2,\quad K = \tfrac{1}{2}(k + k'),$$
$$Q = \tfrac{1}{2}(k - k'),\quad N_\mu = i\varepsilon_{\mu\nu\lambda\sigma}P'_\lambda K_\nu Q_\sigma. \tag{2}$$

The scattering amplitude can be written in the form

$$\mathscr{M} = \bar{u}(p')\, e'_\mu N_{\mu\nu} e_\nu\, u(p), \tag{3}$$

$N_{\mu\nu}$ can be expressed in terms of invariant functions,

$$N_{\mu\nu} = \sum_{\sigma\sigma'} \eta^\sigma_\mu C_{\sigma\sigma'} \eta^{\sigma'}_\nu, \tag{4}$$

where η^σ are the four basis vectors of (2).

Gauge invariance requires that $e'k' = ek = 0$, $k'_\mu N_{\mu\nu} = 0$, and $N_{\mu\nu}k_\nu = 0$. As a consequence, $N_{\mu\nu}$ consists of a sum of eight invariant functions, $\mathscr{M}_1, \ldots, \mathscr{M}_8$, of the two invariants $M\nu = -PK$ and Q^2:

$$\begin{aligned} e'_\mu N_{\mu\nu} e_\nu = {} & \frac{Q^2}{M^2\nu^2 - Q^2(Q^2+M^2)}(e'P')(eP')[\mathscr{M}_1 + i\hat{k}\mathscr{M}_2] \\ & + \frac{1}{Q^2[M^2\nu^2 - Q^2(Q^2+M^2)]}(e'N)(eN)[\mathscr{M}_3 + i\hat{k}\mathscr{M}_4] \\ & - \frac{i}{M^2\nu^2 - Q^2(Q^2+M^2)}[(e'P')(eN) \\ & - (e'N)(eP')]\gamma_5[\mathscr{M}_5 + i\hat{k}\mathscr{M}_7] - \frac{i}{M^2\nu^2 - Q^2(Q^2+M^2)} \\ & \times [(e'P')(eN) + (e'N)(eP')]\gamma_5[\mathscr{M}_8 + i\hat{k}\mathscr{M}_6]. \end{aligned} \tag{5}$$

The normalization factors $Q^2/[M^2\nu^2 - Q^2(Q^2 + M^2)]$ have been introduced for convenience.

It can be shown that the following relations hold in an arbitrary system (thus, in particular, in the Breit system and in the center of mass system):

$$\frac{Q^2(e'P')(eP')}{M^2\nu^2 - Q^2(M^2+Q^2)} = \frac{(\mathbf{e}'\boldsymbol{\varkappa})(\mathbf{e}\boldsymbol{\varkappa}')}{|\boldsymbol{\varkappa}||\boldsymbol{\varkappa}'|\sin^2\theta} = \frac{(\mathbf{e}'\mathbf{k})(\mathbf{e}\mathbf{k}')}{\sin^2\theta},$$
$$\frac{(e'N)(eN)}{M^2\nu^2 - Q^2(M^2+Q^2)} = \frac{(\mathbf{e}'[\mathbf{k}\times\mathbf{k}'])(\mathbf{e}[\mathbf{k}\times\mathbf{k}'])}{\sin^2\theta} = \frac{(\mathbf{e}'\boldsymbol{\rho})(\mathbf{e}\boldsymbol{\rho})}{\sin^2\theta},$$
$$\frac{-[(e'P')(eN) \mp (e'N)(eP')]}{M^2\nu^2 - Q^2(Q^2+M^2)} = \frac{(\mathbf{e}'\mathbf{k})(\mathbf{e}\boldsymbol{\rho}) \mp (\mathbf{e}'\boldsymbol{\rho})(\mathbf{e}\mathbf{k}')}{\sin^2\theta}, \tag{6}$$

where $\boldsymbol{\kappa} = |\kappa|\mathbf{k}$; θ is the angle between $\mathbf{k}$ and $\mathbf{k}'$; $\mathbf{k}$ and $\mathbf{k}'$ are unit vectors along $\boldsymbol{\kappa}$ and $\boldsymbol{\kappa}'$: $\boldsymbol{\rho} = \mathbf{k} \times \mathbf{k}'$. We prove (6) in the Breit system, where

$$\mathbf{P} = 0, \qquad \mathbf{P}' = -(PK)\,\mathbf{K}/K^2 = -M\nu\mathbf{K}/Q^2. \tag{7}$$

The following formulas are easily seen to be correct:

$$|\varkappa| = k_0 = M\nu/\sqrt{Q^2 + M^2}, \tag{8}$$

$$2Q^2 = k_0^2(1 - \cos\theta), \tag{9}$$

$$k_0^2 - Q^2 = \frac{M^2\nu^2 - Q^2(Q^2+M^2)}{Q^2 + M^2} = \frac{k_0^2}{2}(1 + \cos\theta). \tag{10}$$

Multiplying (9) and (10), we obtain

$$\frac{k_0^4}{4}\sin^2\theta = \frac{Q^2[M^2\nu^2 - Q^2(Q^2+M^2)]}{Q^2 + M^2}. \tag{11}$$

With the help of (8) we write (11) in the form

$$k_0^2 \sin^2\theta = 4Q^2[M^2\nu^2 - Q^2(Q^2+M^2)]/M^2\nu^2. \qquad (12)$$

From (5) and (7) we obtain, finally,

$$\frac{Q^2}{M^2\nu^2 - Q^2(Q^2+M^2)}\,\frac{M^2\nu^2}{Q^4}\,\frac{1}{4}(\mathbf{e}'\boldsymbol{\varkappa})(\mathbf{e}\boldsymbol{\varkappa}') = \frac{(\mathbf{e}'\boldsymbol{\varkappa})(\mathbf{e}\boldsymbol{\varkappa}')}{k_0^2\sin^2\theta} = \frac{(\mathbf{e}'\mathbf{k})(\mathbf{e}\mathbf{k}')}{\sin^2\theta}. \qquad (13)$$

Using the formula

$$N = -\sqrt{Q^2+M^2}\,\frac{1}{2}[\mathbf{k}\times\mathbf{k}'], \qquad (14)$$

the remaining equations of (6) can be proved in an analogous fashion. As is known, the requirement of invariance under time reversal (or, as will be shown below, the requirement of "crossing symmetry") reduces the number of independent invariant functions to six ($\mathcal{M}_7 = \mathcal{M}_8 = 0$).

The general expression for the amplitude for the scattering of γ quanta by particles with spin $\frac{1}{2}$ can be written in the form[9-11]

$$\begin{aligned}\mathcal{M} &= R_{1c}(\mathbf{e}\mathbf{e}') + R_{2c}(\mathbf{s}_c\mathbf{s}_c') + iR_{3c}(\boldsymbol{\sigma}[\mathbf{e}'\times\mathbf{e}]) + iR_{4c}(\boldsymbol{\sigma}[\mathbf{s}_c'\times\mathbf{s}_c])\\ &\quad + iR_{5c}[(\boldsymbol{\sigma}\mathbf{k}_c)(\mathbf{s}_c'\mathbf{e}) - (\boldsymbol{\sigma}\mathbf{k}_c')(\mathbf{s}_c\mathbf{e}')]\\ &\quad + iR_{6c}[(\boldsymbol{\sigma}\mathbf{k}_c')(\mathbf{s}_c'\mathbf{e}) - (\boldsymbol{\sigma}\mathbf{k}_c)(\mathbf{e}'\mathbf{s}_c)], \qquad (15)\end{aligned}$$

where R_1, R_3, and R_5 describe the electric, and R_2, R_4, and R_6 describe the magnetic transitions; $\mathbf{e}$ and $\mathbf{e}'$ are the polarization vectors before and after the collision; $\mathbf{s} = \mathbf{k}\times\mathbf{e}$, $\mathbf{s}' = \mathbf{k}'\times\mathbf{e}'$, where $\mathbf{k}$ and $\mathbf{k}'$ are unit vectors in the direction of the momentum of the γ quantum before and after the scattering; the label "c" refers to the center-of-mass system.

The expression for $\mathcal{M}$ containing the terms not higher than those linear in the energy of the γ quanta[12,13] can be written in the form

$$\begin{aligned}\mathcal{M} &= -e^2M^{-1}(\mathbf{e}\mathbf{e}') + ieM^{-1}(2\mu - e/2M)\nu_c(\boldsymbol{\sigma}[\mathbf{e}'\times\mathbf{e}])\\ &\quad + 2\mu^2\nu_c(\boldsymbol{\sigma}[\mathbf{s}_c\times\mathbf{s}_c']) + ieM^{-1}\mu\nu_c[(\mathbf{e}\mathbf{k}_c')(\boldsymbol{\sigma}\mathbf{s}_c') - (\mathbf{e}'\mathbf{k}_c)(\boldsymbol{\sigma}\mathbf{s}_c)]. \qquad (16)\end{aligned}$$

With the help of the relation

$$\begin{aligned}&(\boldsymbol{\sigma}\mathbf{s}')(\mathbf{e}\mathbf{k}') - (\boldsymbol{\sigma}\mathbf{s})(\mathbf{e}'\mathbf{k})\\ &\quad = -2(\boldsymbol{\sigma}[\mathbf{e}'\times\mathbf{e}]) + (\boldsymbol{\sigma}\mathbf{k}')(\mathbf{e}\mathbf{s}') - (\boldsymbol{\sigma}\mathbf{k})(\mathbf{e}'\mathbf{s}), \qquad (17)\end{aligned}$$

we can bring (16) into the form (15). Here

$$R_1^0 = -e^2/M,\ R_2^0 = 0,\ R_3^0 = -2(e/2M)^2\nu_c,\ R_4^0 = -2\mu^2\nu_c,$$
$$R_5^0 = 0,\ R_6^0 = (e/M)\mu\nu_c. \qquad (18)$$

We write the scattering amplitude in the Breit system in the form (15), and obtain from a comparison of (15) and (5) the relations

$$\begin{aligned}R_1\sin^2\theta &= E(\mathcal{M}_1\cos\theta + \mathcal{M}_3)/M - k_0(\mathcal{M}_2\cos\theta + \mathcal{M}_4),\\ R_2\sin^2\theta &= -E(\mathcal{M}_3\cos\theta + \mathcal{M}_1)/M + k_0(\mathcal{M}_2 + \mathcal{M}_4\cos\theta),\\ R_3 &= k_0^2\mathcal{M}_2/2M,\quad R_4 = -k_0^2\mathcal{M}_4/2M,\\ R_5\sin^2\theta &= \frac{k_0^2}{2M}(\mathcal{M}_2\cos\theta + \mathcal{M}_4)\\ &\quad - \frac{k_0}{2M}(1+\cos\theta)\mathcal{M}_5 - \frac{k_0E}{2M}(1-\cos\theta)\mathcal{M}_6,\\ R_6\sin^2\theta &= -\frac{k_0^2}{2M}(\mathcal{M}_2 + \mathcal{M}_4\cos\theta) + \frac{k_0}{2M}(1+\cos\theta)\\ &\quad \times\mathcal{M}_5 - \frac{k_0E}{2M}(1-\cos\theta)\mathcal{M}_6. \qquad (19)\end{aligned}$$

It is easily seen that for $\theta\to 0$ we obtain ($E = M$, $k_0 = \nu$)

$$\begin{aligned}R_1 + R_2|_{\theta=0} &= \tfrac{1}{2}[\mathcal{M}_1 - \mathcal{M}_3 - \nu(\mathcal{M}_2 - \mathcal{M}_4)],\\ R_3|_{\theta=0} &= \nu^2\mathcal{M}_2/2M,\\ R_4|_{\theta=0} &= -\nu^2\mathcal{M}_4/2M,\\ R_5 + R_6|_{\theta=0} &= [\nu^2(\mathcal{M}_2 - \mathcal{M}_4) + M\nu\mathcal{M}_6]/4M. \qquad (20)\end{aligned}$$

It can be shown[1-4] from the general principles of quantum field theory that the $\mathcal{M}_i$, as functions of ν, are analytic for $\theta = 0$ ($Q^2 = 0$) and for

$$Q^2 < Q_{\max}^2 = \frac{(2M+m_\pi)(6M^2+9Mm_\pi+4m_\pi^2)}{4M(M+m_\pi)^2}\,m_\pi^2 \approx 3m_\pi^2,$$

where m_π is the mass of the π meson.

Regarding the forward scattering amplitude, one usually restricts oneself to two dispersion relations for the functions $R_1 + R_2$ and $R_3 + R_4 + 2R_5 + 2R_6$. It is seen from formulas (20) that for $\theta = 0$ we actually have four dispersion relations for $R_1 + R_2$, R_3, R_4, and $R_5 + R_6$ separately.

2. The retarded causal amplitude for the scattering of photons can be written in the form

$$\begin{aligned}\bar{u}(p')N_{\mu\nu}^{ret}u(p) &= -2\pi^2 i(p_0p_0'/M^2)^{1/2}\\ &\quad\times\int d^4z e^{-ikz}\left\langle p'\left|\theta(z_0)\left[j_\mu\left(\frac{z}{2}\right),\left[j_\nu\left(-\frac{z}{2}\right)\right]\right|p\right\rangle\right.. \qquad (21)\end{aligned}$$

Analogously, we can write for the advanced causal amplitude

$$\begin{aligned}\bar{u}(p')N_{\mu\nu}^{adv}u(p) &= -(2\pi^2)i(p_0p_0'/M^2)^{1/2}\\ &\quad\times\int d^4z e^{-ikz}\left\langle p'\left|\theta(-z_0)\left[j_\mu\left(\frac{z}{2}\right),\ j_\nu\left(-\frac{z}{2}\right)\right]\right|p\right\rangle. \qquad (22)\end{aligned}$$

We define the quantities $D_{\mu\nu}$ and $A_{\mu\nu}$ by

$$D_{\mu\nu} = (N_{\mu\nu}^{ret} + N_{\mu\nu}^{adv})/2,\quad A_{\mu\nu} = (N_{\mu\nu}^{ret} - N_{\mu\nu}^{adv})/2i. \qquad (23)$$

Taking the complex conjugate on both sides of (21) and recalling that j_μ is a Hermitian operator, we get

$$\beta N_{\mu\nu}^{+ret}(p'k'pk)\beta = N_{\mu\nu}^{ret}(p - k'p' - k). \qquad (24)$$

Changing the order of j_μ and j_ν in the commutator in (21) and replacing the integration variable z by $-z$, we obtain

$$N_{\mu\nu}^{ret}(p'k'pk) = N_{\mu\nu}^{adv}(p' - kp - k'). \qquad (25)$$

Substituting (5) in (24) and (25), we have

$$\begin{aligned}\mathcal{M}_{1,3}^*(\nu, Q^2) &= \mathcal{M}_{1,3}(-\nu, Q^2),\quad \mathcal{M}_{2,4}^*(\nu, Q^2) = -\mathcal{M}_{2,4}(-\nu, Q^2),\\ \mathcal{M}_{5,6}^*(\nu, Q^2) &= \mathcal{M}_{5,6}(-\nu, Q^2),\quad \mathcal{M}_7 = \mathcal{M}_8 = 0. \qquad (26)\end{aligned}$$

With the help of (26) the dispersion relations can be easily written in the form

$$D_{1,3,5,6}(\nu, Q^2) = \frac{2}{\pi}\,\mathrm{P}\int_0^\infty \frac{\nu' A_{1,3,5,6}(\nu', Q^2)}{\nu'^2 - \nu^2}\,d\nu',$$

$$D_{2,4}(\nu, Q^2) = \frac{2\nu}{\pi}\,\mathrm{P}\int_0^\infty \frac{A_{2,4}(\nu', Q^2)}{\nu'^2 - \nu^2}\,d\nu'. \qquad (27)$$

Let us consider the dispersion relations for $Q^2 = 0$, when the Breit system coincides with the laboratory system and ν becomes the energy of the γ quantum in the laboratory system (l.s.). We obtain two dispersion relations by simply setting $Q^2 = 0$ in (27). Four more relations follow if we first differentiate with respect to Q^2 and then set $Q^2 = 0$. Since the dispersion relations for $\mathscr{M}_{2,4}$ in the e^2 approximation contain infrared divergencies of the type $1/\nu - 1/\nu_0$, we find that for $Q^2 = 0$ the only dispersion relations of practical use are those for the combinations

$$R_1 + R_2 \equiv L_1, \quad R_5 + R_6 \equiv L_2,$$

and for the quantities

$$R_3 \equiv L_3, \quad R_4 \equiv L_4,$$

which do not contain terms which become infinite for $\nu \rightarrow 0$. For $Q^2 = 0$ we have $L = L(\nu)$, and it can be shown by comparing (20) and (26) that

$$L_1(-\nu) = L_1(\nu), \quad L_{2,3,4}(-\nu) = -L_{2,3,4}(\nu). \tag{28}$$

We can therefore write down the following dispersion relations for these quantities

$$\operatorname{Re} L_1(\nu) - \operatorname{Re} L_1(0) = \frac{2\nu^2}{\pi} \mathrm{P} \int_{\nu_0}^{\infty} \frac{\operatorname{Im} L_1(\nu')}{\nu'(\nu'^2 - \nu^2)} d\nu',$$

$$\operatorname{Re} L_{2,3,4}(\nu) - \nu \operatorname{Re} L'_{2,3,4}(0) = \frac{2\nu^3}{\pi} \mathrm{P} \int_{0}^{\infty} \frac{\operatorname{Im} L_{2,3,4}(\nu')}{\nu'^2(\nu'^2 - \nu^2)} d\nu',$$

$$\nu_0 = m_\pi(1 + m_\pi / 2M). \tag{29}$$

We shall derive two more dispersion relations in the following section.

From (18) we find

$$\operatorname{Re} L_1(0) = -e^2 / M, \quad \nu \operatorname{Re} L'_2(0) = \frac{e}{M}\mu\nu = \frac{e^2}{M}\frac{1}{2}\frac{\nu_0}{M}\lambda\frac{\nu}{\nu_0},$$

$$\mu = \frac{e}{2M}\lambda, \qquad \nu \operatorname{Re} L'_3(0) = -2\left(\frac{e}{2M}\right)^2 \nu = -\frac{1}{2}\frac{e^2}{M}\frac{\nu_0}{M}\frac{\nu}{\nu_0},$$

$$\nu \operatorname{Re} L'_4(0) = -2\mu^2\nu = -\frac{1}{2}\frac{e^2}{M}\lambda^2\frac{\nu_0}{M}\frac{\nu}{\nu_0}. \tag{30}$$

The first of the relations (29) is brought into the usual form by using the optical theorem:

$$\operatorname{Re}[R_1(\nu) + R_2(\nu)] = -\frac{e^2}{M} + \frac{\nu^2}{2\pi^2} \mathrm{P} \int_{\nu_0}^{\infty} \frac{\sigma(\nu')\, d\nu'}{\nu'^2 - \nu^2}; \tag{29'}$$

it then coincides with the relation obtained by Gell-Mann, Goldberger, and Thirring.[1]

3. In the center-of-mass system the quantities $R_{1c}, \ldots, R_{6c}$ can be expressed in terms of the scattering amplitudes in states with definite angular momentum and parity.

Let us denote the amplitudes for the electric dipole transitions with total angular momentum $1/2$ and $3/2$ by $\mathscr{E}_1$ and $\mathscr{E}_3$, respectively; let $\mathscr{E}_2$ be the amplitude for the electric quadrupole transition with total angular momentum $3/2$, and likewise $\mathfrak{M}_1$, $\mathfrak{M}_3$, and $\mathfrak{M}_2$ the amplitudes for the magnetic dipole and quadrupole transitions. We must further introduce the amplitudes $C'(\mathfrak{M}_3, \mathscr{E}_2)$, $C'(\mathscr{E}_2, \mathfrak{M}_3)$, $C'(\mathscr{E}_3, \mathfrak{M}_2)$, and $C'(\mathfrak{M}_2, \mathscr{E}_3)$ corresponding to the transitions from the states $\mathfrak{M}_i$ into $\mathscr{E}_k$. Invariance under time reversal requires that

$$C'(\mathfrak{M}_3, \mathscr{E}_2) = C'(\mathscr{E}_2, \mathfrak{M}_3), \quad C'(\mathscr{E}_3, \mathfrak{M}_2) = C'(\mathfrak{M}_2, \mathscr{E}_3). \tag{31}$$

Finally, using the technique of projection operators, we find for states with $j \leq 3/2$

$$R_{1c} = \mathscr{E}_1 + 2\mathscr{E}_3 + 2\mathscr{E}_2 \cos\theta - \mathfrak{M}_2,$$

$$R_{2c} = \mathfrak{M}_1 + 2\mathfrak{M}_3 + 2\mathfrak{M}_2 \cos\theta - \mathscr{E}_2,$$

$$R_{3c} = \mathscr{E}_1 - \mathscr{E}_3 + 2\mathscr{E}_2 \cos\theta + \tfrac{1}{2}\mathfrak{M}_2 + \sqrt{6}\, C'(\mathscr{E}_3, \mathfrak{M}_2),$$

$$R_{4c} = \mathfrak{M}_1 - \mathfrak{M}_3 + 2\mathfrak{M}_2 \cos\theta + \tfrac{1}{2}\mathscr{E}_2 + \sqrt{6}\, C'(\mathfrak{M}_3, \mathscr{E}_2),$$

$$R_{5c} = -\mathscr{E}_2 - \sqrt{6}\, C'(\mathfrak{M}_3 \mathscr{E}_2) \equiv -\mathscr{E}_2 - C(\mathfrak{M}_3, \mathscr{E}_2),$$

$$R_{6c} = -\mathfrak{M}_2 - \sqrt{6}\, C'(\mathscr{E}_3, \mathfrak{M}_2) \equiv -\mathfrak{M}_2 - C(\mathscr{E}_3, \mathfrak{M}_2). \tag{32}$$

Using the relations (16) and (18), we can separate out the energy dependence of these quantities for $\nu_c \rightarrow 0$ in the form

$$\mathscr{E}_1^0 + 2\mathscr{E}_3^0 = -e^2 / M, \quad \mathscr{E}_1^0 - \mathscr{E}_3^0 = -[2(e/2M)^2 - e\mu / M]\nu_c,$$

$$\mathscr{E}_2^0 = 0, \quad \mathfrak{M}_1^0 = -4\mu^2\nu_c / 3, \quad \mathfrak{M}_3^0 = 2\mu^2\nu_c / 3, \mathfrak{M}_2^0 = 0,$$

$$C^0(\mathscr{E}_2, \mathfrak{M}_3) = 0, \quad C^0(\mathscr{E}_3, \mathfrak{M}_2) = -e\mu\nu_c / M. \tag{33}$$

In addition to (29) we can derive two more dispersion relations by differentiating

$$R_3 = k_0^2 \mathscr{M}_2 / 2M \text{ and } R_4 = k_0^2 \mathscr{M}_4 / 2M$$

with respect to Q^2 and then setting $Q^2 = 0$. The factor k_0^2 in R_3 and R_4 goes to ν^2 for $Q^2 \rightarrow 0$ and thus compensates for the possible infrared divergency in $\mathscr{M}_2$ and $\mathscr{M}_4$.

Let us now consider the quantity

$$R_3 = \frac{k_0^2}{2M}\mathscr{M}_2 = \frac{M\nu^2}{2}\frac{\mathscr{M}_2(\nu, Q^2)}{\sqrt{Q^2 + M^2}}.$$

If $M_2(\nu, Q^2)$ is an analytic function of ν for $Q^2 < Q^2_{\mathrm{max}}$, then R_3 and $\partial R_3 / \partial Q^2$ will also be analytic functions of ν. Since the contribution of the one-nucleon state to R_3 has the form

$$D\nu\nu_b^2 / (\nu_b^2 - \nu^2),$$

where D is some constant and $\nu_b = Q^2/M$, it is at once clear that

$$D \frac{\partial}{\partial Q^2} \frac{\nu\nu_b^2}{\nu_b^2 - \nu^2}\bigg|_{Q^2=0} = 0,$$

i.e., the contribution of the one-nucleon state to the dispersion relation for $\partial R_3 / \partial Q^2$ for $Q^2 = 0$ reduces to zero. If we restrict ourselves to the states included in formulas (32), we have

$$\partial R_3 / \partial Q^2 = -2\mathscr{E}_2(\nu) / \nu^2. \tag{34}$$

For these same states $\mathscr{E}_2(\nu)/\nu^2$ will be an analytic function of ν whose crossing symmetry agrees with the symmetry of R_3. Then the dispersion relations for $\mathscr{E}_2(\nu)/\nu^2$ can be written in the form

$$\operatorname{Re}\frac{\mathscr{E}_2(\nu)}{\nu^2}=\frac{2\nu}{\pi}\int_0^\infty\frac{\operatorname{Im}\mathscr{E}_2(\nu')\,d\nu'}{\nu'^2(\nu'^2-\nu^2)}=\frac{2\nu}{\pi}\int_{\nu_0}^\infty\frac{\operatorname{Im}\mathscr{E}_2(\nu')\,d\nu'}{\nu'^2(\nu'^2-\nu^2)}$$

or, finally,

$$\operatorname{Re}\mathscr{E}_2(\nu)=\frac{2\nu^3}{\pi}\int_{\nu_0}^\infty\frac{\operatorname{Im}\mathscr{E}_2(\nu')\,d\nu'}{\nu'^2(\nu'^2-\nu^2)}. \tag{35}$$

Combining (33) with the dispersion relation for R_5+R_6, we see that $\mathscr{E}_2(\nu)$ and $C(\mathscr{E}_2, \mathfrak{M}_3)$ obey separately the dispersion relation (35).

Analogously, by considering the derivative of R_4, we can show that $\mathfrak{M}_2$ also satisfies the dispersion relation (35). For the states included in formulas (32) it was possible, in the final result, to obtain six dispersion relations for the eight quantities characterizing the scattering of γ quanta. We did not succeed in removing the difficulties connected with the presence of infrared divergencies in the other relations. The repeated differentiation with respect to Q^2 gives rise to the appearance of unknown constants, which have been calculated by some authors with the help of perturbation theory and which can be determined experimentally if sufficient experimental data are available, in analogy to the procedure used in the scattering of mesons and nucleons. In the present paper we shall not employ this method.

To carry out calculations with the help of the dispersion relations for the scattering of γ quanta by nucleons, we require rather detailed data on the amplitude for photoproduction. From the available data we may conclude that $\operatorname{Im}\mathfrak{M}_2=0$. If we further use $\mathfrak{M}_2^0=0$, we find

$$\mathfrak{M}_2=0. \tag{36}$$

With the assumptions

$$C(\mathfrak{M}_2, \mathscr{E}_3)=C(\mathscr{E}_3, \mathfrak{M}_2)=C^0(\mathscr{E}_3, \mathfrak{M}_2)=-e\mu\nu/M,$$

$$\mathfrak{M}_1=\mathfrak{M}_1^0=-4\mu^2\nu/3,$$

which do not contradict the available experimental data on photoproduction, the number of dispersion relations will agree with the number of functions introduced.

To calculate the imaginary parts of the amplitude we make use of the unitarity of the S matrix. For γ quantum energies below the threshold of π meson production the imaginary parts of the quantities $R_1, \ldots, R_6$ are small. Above the threshold the imaginary parts of $R_1, \ldots, R_6$ are determined by the unitarity requirement on the S matrix. Neglecting the terms which are quadratic in the electromagnetic interaction, we obtain the relation

$$\begin{aligned}i[\mathscr{M}^+(-\mathbf{k}', -\mathbf{e}', -\mathbf{k}, -\mathbf{e}, -\boldsymbol{\sigma})-\mathscr{M}(\mathbf{k}', \mathbf{e}', \mathbf{k}, \mathbf{e}, \boldsymbol{\sigma})]\\ =\frac{\nu_c}{2\pi}\int d\Omega(\mathbf{q}_+)\,[T^+_{\gamma\to\pi^+}(\mathbf{q}_+, \mathbf{k}', \mathbf{e}', \boldsymbol{\sigma})\,T_{\gamma\to\pi^+}(\mathbf{q}_+, \mathbf{k}, \mathbf{e}, \boldsymbol{\sigma})]\\ +\frac{\nu_c}{2\pi}\int d\Omega(\mathbf{q}_0)\,[T^+_{\gamma\to\pi^0}(\mathbf{q}_0, \mathbf{k}', \mathbf{e}', \boldsymbol{\sigma})\,T_{\gamma\to\pi^0}(\mathbf{q}_0, \mathbf{k}, \mathbf{e}, \boldsymbol{\sigma})],\end{aligned} \tag{38}$$

where

$$\begin{aligned}T_{\gamma\to\pi}(\mathbf{q}, \mathbf{k}, \mathbf{e}, \boldsymbol{\sigma})&=iE_1(\boldsymbol{\sigma}\mathbf{e})-M_1\{([\mathbf{k}\times\mathbf{e}]\,\mathbf{q})-i(\boldsymbol{\sigma}[[\mathbf{k}\times\mathbf{e}]\,\mathbf{q}])\}\\ &-M_3\{2([\mathbf{k}\times\mathbf{e}]\,\mathbf{q})+i(\boldsymbol{\sigma}[[\mathbf{k}\times\mathbf{e}]\,\mathbf{q}])\}\\ &+\frac{i}{2}E_2\{(\boldsymbol{\sigma}\mathbf{k})(\mathbf{e}\mathbf{q})+(\boldsymbol{\sigma}\mathbf{e})(\mathbf{k}\mathbf{q})\}\end{aligned} \tag{39}$$

is the amplitude for the photoproduction of pions on a proton. For the lowest states E_1 corresponds, as is known, to a transition from a state with angular momentum $J=\frac{1}{2}$ and negative parity accompanied by the creation of a meson in the $s_{1/2}$ state; M_1 corresponds to a transition from $J=\frac{1}{2}$ with creation of a meson in the $p_{1/2}$ state; M_3 and and E_2 correspond to a transition from $J=\frac{3}{2}^+$ with creation of a meson in the $p_{3/2}$ state. It follows from (38) that above the threshold

$$\begin{aligned}\operatorname{Im}R_{1c}&=\nu_c\left\{|E_1|^2+\frac{1}{3}|E_2|^2\cos\theta\right\}=\nu_cA_1,\\ \operatorname{Im}R_{2c}&=\nu_c\{|M_1|^2+2|M_3|^2-|E_2|^2/6\}=\nu_cA_2,\\ \operatorname{Im}R_{3c}&=\operatorname{Im}R_{1c},\\ \operatorname{Im}R_{4c}&=\nu_c\{|M_1|^2+|M_3|^2+|E_2|^2/12+(E_2^*M_3\\ &+E_2M_3^*)/2\}=\nu_cA_4,\\ \operatorname{Im}R_{5c}&=-y_c\{|E_2|^2/6\\ &+(E_2^*M_3+E_2M_3^*)/2\}=\nu_cA_5,\quad \operatorname{Im}R_{6c}=0.\end{aligned} \tag{40}$$

It is easily seen with the help of (40) that the total interaction cross section for the γ quanta is

$$\begin{aligned}\sigma_t&=(4\pi/\nu_c)\operatorname{Im}[R_{1c}(0°)+R_{2c}(0°)]\\ &=4\pi[|E_1|^2+|M_1|^2+2|M_3|^2-|E_2|^2/6],\end{aligned} \tag{41}$$

this agrees, as it should, with the total cross section for the photoproduction of π mesons.[14] Using (40) we obtain

$$\begin{aligned}\operatorname{Re}\mathscr{E}_2(\nu)&=\frac{1}{6}\frac{2\nu^3}{\pi}\int_{\nu_0}^\infty\frac{d\nu'}{\nu'}\frac{|E_2^+|^2+|E_2^0|^2}{\nu'^2-\nu^2},\\ \operatorname{Re}\mathfrak{M}_3(\nu)&=\frac{2}{3}\mu^2\nu+\frac{2\nu^3}{\pi}\int_{\nu_0}^\infty\frac{d\nu'}{\nu'}\frac{|M_3^+|^2+|M_3^0|^2}{\nu'^2-\nu^2},\\ \operatorname{Re}[\mathscr{E}_1(\nu)+2\mathscr{E}_3(\nu)]&=-\frac{e^2}{M}\\ &+\frac{\nu^2}{2\pi^2}\int_{\nu_0}^\infty\frac{d\nu'(\sigma^0+\sigma^+)}{\nu'^2-\nu^2}-\operatorname{Re}\mathscr{E}_2(\nu)-2\operatorname{Re}[\mathfrak{M}_3(\nu)-\mathfrak{M}_3^0],\\ \operatorname{Re}[\mathscr{E}_1(\nu)-\mathscr{E}_3(\nu)]&\\ =-\left[2\left(\frac{e}{2M}\right)^2-\frac{e}{M}\mu\right]\nu&+\frac{2\nu^3}{\pi}\int_{\nu_0}^\infty\frac{d\nu'}{\nu'}\frac{|E_1^+|^2+|E_1^0|^2}{\nu'^2-\nu^2},\\ \operatorname{Re}C(\mathfrak{M}_3, \mathscr{E}_2)=\operatorname{Re}C(\mathscr{E}_2, \mathfrak{M}_3)&=\frac{2\nu^3}{\pi}\int_{\nu_0}^\infty\frac{d\nu'}{\nu'}\frac{(\operatorname{Re}E_2^*M_3)^++(\operatorname{Re}E_2^*M_3)^0}{\nu'^2-\nu^2}.\end{aligned} \tag{42}$$

The contribution from multiple π meson production and from the production of other particles is neglected. If it is shown by further analysis that Im $\mathfrak{M}_2 \neq 0$, it is not difficult to take this into account.

---

[1] Gell-Mann, Goldberger, and Thirring, Phys. Rev. **95**, 1612 (1954).

[2] N. N. Bogolyubov and D. V. Shirkov, Dokl. Akad. Nauk SSSR **113**, 529 (1957).

[3] A. A. Logunov and A. R. Frenklin, Nucl. Phys. **7**, 573 (1958).

[4] A. A. Logunov and P. Ş. Isaev, Nuovo cimento **10**, 917 (1958).

[5] T. Akiba and J. Sato, Progr. Theoret. Phys. **19**, 93 (1958).

[6] R. H. Capps, Phys. Rev. **106**, 1031 (1957) and **108**, 1032 (1957).

[7] L. I. Lapidus and Chou Kuang-Chao, JETP, in press.

[8] R. E. Prange, Phys. Rev. **110**, 240 (1958).

[9] V. I. Ritus, JETP **33**, 1264 (1957), Soviet Phys. JETP **6**, 972 (1957).

[10] L. I. Lapidus, JETP **34**, 922 (1958), Soviet Phys. JETP **7**, 638 (1958).

[11] M. Kawaguchi and S. Minami, Progr. Theoret. Phys. **12**, 789 (1954). A. A. Logunov and A. N. Tavkhelidze, JETP **32**, 1393 (1957), Soviet Phys. JETP **5**, 1134 (1957).

[12] F. E. Low, Phys. Rev. **96**, 1428 (1954).

[13] M. Gell-Mann and M. L. Goldberger, Phys. Rev. **96**, 1433 (1954).

[14] M. Gell-Mann and K. M. Watson, Ann. Rev. Nucl. Science **4**, 219 (1954).

Translated by R. Lipperheide
334

SOVIET PHYSICS JETP VOLUME 37(10), NUMBER 6 JUNE, 1960

PROPAGATION OF A STRONG ELECTROMAGNETIC-GRAVITATIONAL WAVE IN VACUO

A. S. KOMPANEETS

Institute of Chemical Physics, Academy of Sciences, U.S.S.R.

Submitted to JETP editor, July 1, 1959

J. Exptl. Theoret. Phys. (U.S.S.R.) **37**, 1722-1726 (December, 1959)

It is shown that a strong electromagnetic-gravitational wave possesses a system of rectilinear and parallel characteristics so that the velocity of propagation of any small additional disturbance will always be equal to that of light. Therefore, it cannot be expected that there should exist solutions with a Euclidean metric at infinity which would be qualitatively different from ordinary electromagnetic waves in finite spatial regions.

As is well known, there exist two points of view with respect to the present situation in classical field theory. For many years the point of view was held, and is still held by many now, that a unified classical field theory has not yet been developed, and that one may hope that such a world geometry might be constructed from which certain new unified field equations of gravitation and electromagnetism will be obtained in a manner similar to that in which the gravitational equations are obtained from the Riemann geometry. Moreover, the unified form of writing Maxwell's and Einstein's equations[1] which has been achieved already is considered to be of no consequence as it introduces no new physical ideas into the theory.

The other point of view consists of supposing that the existing classical field theory has received its final formulation, and that no further improvement of electrodynamics through its geometrization (in essence, and not in form) is required.[2]

Of course, in such a case, one has in mind a field not containing any particles, since particles are quantum and not classical objects. The energy-momentum tensor T_{ik} for matter refers already to a macroscopic, phenomenological theory. Therefore, the problem of the existence of a unified classical field theory may be solved only for a field not containing any particles.

It is difficult to imagine an actual experiment which might decide this question. Therefore, one has to seek confirmation of the theory in its internal consistency.

At the basis of contemporary gravitation theory lies the assumption of the Riemann character of space in which only continuous and single valued groups of transformations are admitted. All consequences of the equations of gravitation and electrodynamics must not contradict this assumption and, naturally, must also not be contrary to the well known properties of continuity of the electromagnetic field.

The equations of Maxwell and of Einstein belong to the hyperbolic type, with the coefficients of the derivatives being themselves functions of the unknown quantities, i.e., of the components of the metric tensor. Equations of such type do not always have continuous solutions. For example, in gasdynamics continuous solutions obtained from smooth initial conditions sometimes lead to the necessity for the appearance of discontinuities, i.e., of shock waves.[3] A similar situation would be completely inadmissible in classical field theory, since it would contradict the basic assumption of the Riemann nature of space or of the continuity of the electromagnetic field. It would be desirable to show that such discontinuities never arise by starting from the equations in their most general form. However, so far we have succeeded only in considering the metric of a more special form, which was adopted by us earlier.[4] It generalizes to a certain extent the Einstein-Rosen metric.[5] The present work differs from that of references 4 and 5 by the fact that in it the electromagnetic field is treated on the same basis as the gravitational field.

The principal result of the present work consists of the fact that for the chosen type of metric there always exists a coordinate system in which each family of characteristics consists of parallel straight lines. The velocity of any additional small disturbance, gravitational or electromagnetic, in this system of coordinates is always equal to the fundamental constant c. Disturbances do not overtake each other, therefore discontinuities can never arise, in contrast to the equations of gas dynamics. Thus, the results which we have obtained provide evidence in favor of the position that the contemporary classical field theory requires no further improvement.

We now consider the propagation of a wave. We start by assuming a metric of the following form[4]

$$-ds^2 = Adx_1^2 + Cdx_2^2 + 2Bdx_2\,dx_3 + Ddx_3^2 - Adx_4^2, \qquad (1)$$

where the coefficients A, B, C, D, are regarded to be functions only of x_1 and x_4 (it is sufficient to assume this for the investigation of the characteristics). Maxwell's equations for the contravariant components of the electromagnetic field have the following form

$$\frac{\partial}{\partial x_4}(F^{14}\sqrt{-g}) = 0, \qquad (2a)$$

$$\frac{\partial}{\partial x_1}(F^{21}\sqrt{-g}) + \frac{\partial}{\partial x_4}(F^{24}\sqrt{-g}) = 0, \qquad (2b)$$

$$\frac{\partial}{\partial x_1}(F^{31}\sqrt{-g}) + \frac{\partial}{\partial x_4}(F^{34}\sqrt{-g}) = 0, \qquad (2c)$$

$$\frac{\partial}{\partial x_1}(F^{41}\sqrt{-g}) = 0. \qquad (2d)$$

From equations (2a) and (2c) we see that $F^{14} = 0$, so that the field may be regarded as purely transverse. Therefore for the components of the energy-momentum tensor we obtain the following expression

$$T_{11} = T_{44} = {}^1\!/_2\,(F_{12}F_1^2 + F_{13}F_1^3 + F_{42}F_4^2 + F_{43}F_4^3). \qquad (3)$$

Therefore

$$T_1^1 = -T_4^4, \qquad (4)$$

from which it follows also that

$$T_2^2 = -T_3^3, \qquad (5)$$

since $T_i^i = 0$.

We now write down Einstein's equations for the components of the contracted curvature tensor R_{22}, R_{23}, R_{33} (cf. reference 4). We choose the units for measuring the electromagnetic field in such a way that the gravitational equations should have the following form $R_{ik} = T_{ik}$ (the subscript on the symbols C, D, B, α denotes differentiation with respect to x_1, x_4):

$$\begin{aligned} &C_{44} - C_{11} + (2\alpha)^{-1}[C_1\alpha_1 - C_4\alpha_4 \\ &\quad + 2C(B_1^2 - C_1D_1 + C_4D_4 - B_4^2)] = 2AT_{22}, \\ &D_{44} - D_{11} + (2\alpha)^{-1}[D_1\alpha_1 - D_4\alpha_4 \\ &\quad + 2D(B_1^2 - C_1D_1 + C_4D_4 - B_4^2)] = 2AT_{33}, \\ &B_{44} - B_{11} + (2\alpha)^{-1}[B_1\alpha_1 - B_4\alpha_4 \\ &\quad + 2B(B_1^2 - C_1D_1 + C_4D_4 - B_4^2)] = 2AT_{23} \\ &\qquad (\alpha \equiv CD - B^2). \end{aligned} \qquad (6)$$

We multiply the first of these equations by D, the second by C, the third by $-2B$, and add. On taking into account the fact that $g^{22} = D\alpha^{-1}$, $g^{33} = C\alpha^{-1}$, $g^{23} = -B\alpha^{-1}$, we obtain on the right hand side $T_2^2 + T_3^3 = 0$, in accordance with (5). On the left hand side, as was shown in reference 4, we shall have

$$\alpha_{11}^{1/2} - \alpha_{44}^{1/2} = 0. \qquad (7)$$

It is particularly convenient to choose for the solution (cf. reference 5):

$$\alpha^{1/2} = (CD - B^2)^{1/2} = x_1. \qquad (8)$$

From the equations for the components R_{44}, R_{11} and R_{14} we obtain[4]

$$L_1 - (4x_1)^{-1}(B_1^2 + B_4^2 - C_1D_1 - C_4D_4) = x_1T_{44}, \qquad (9)$$

$$L_4 - (2x_1)^{-1}(2B_1B_4 - C_1D_4 - C_4D_1) = x_1T_{14}. \qquad (10)$$

Here $L \equiv \ln A^{1/2}$. The indices 44 and 14 on T are tensor indices.

We now prove the compatibility of (9) and (10). In order to do this we first of all calculate the difference

$$\frac{\partial}{\partial x_4}(x_1T_{44}) - \frac{\partial}{\partial x_1}(x_1T_{14}) = -\left(\frac{\partial}{\partial x_4}(x_1AT_4^4) + \frac{\partial}{\partial x_1}(x_1AT_4^1)\right)$$

$$= -\left(\frac{\partial}{\partial x_4}(\sqrt{-g}\,T_4^4) + \frac{\partial}{\partial x_1}(\sqrt{-g}\,T_4^1)\right). \qquad (11)$$

In accordance with the equation $T_{4,i}^i = 0$, expression (11) is equal to $\sqrt{-g}\,\Gamma_{4i}^n T_n^i$. By utilizing the values of the Christoffel symbols and (4) we obtain

$$\frac{\partial}{\partial x_4}(x_1T_{44}) - \frac{\partial}{\partial x_1}(x_1T_{14})$$

$$= \sqrt{-g}\,(\Gamma_{24}^2T_2^2 + \Gamma_{42}^3T_3^2 + \Gamma_{43}^2T_2^3 + \Gamma_{43}^3T_3^3), \qquad (12)$$

which in turn can be reduced to the following form

$$(2x_1)^{-1}(T_{22}C_4 + T_{33}D_4 - 2T_{23}B_4). \qquad (13)$$

On substituting the second derivatives of B, C, D from (6) we see that (9) and (10) do not contradict one another. Thus, the metric (1) chosen by us is compatible with the assumption that the electromagnetic field is transverse.

We now obtain the characteristics of the wave equations of the electromagnetic field. In order to do this we write Maxwell's equations in mixed components F_k^i. To the equations (2b, c) we must also add the first pair which follows from the fact that $F_{i,k} = A_{i,k} - A_{k,i}$:

$$\frac{1}{x_1}\frac{\partial}{\partial x_1}x_1F_1^2 - \frac{\partial F_4^2}{\partial x_4} = 0, \qquad \frac{1}{x_1}\frac{\partial}{\partial x_1}x_1F_1^3 - \frac{\partial F_4^3}{\partial x_4} = 0;$$

$$\frac{\partial}{\partial x_4}CF_1^2 + \frac{\partial}{\partial x_4}BF_1^3 - \frac{\partial}{\partial x_1}CF_4^2 - \frac{\partial}{\partial x_1}BF_4^3 = 0,$$

$$\frac{\partial}{\partial x_1}BF_1^2 + \frac{\partial}{\partial x_1}DF_1^3 - \frac{\partial}{\partial x_1}BF_4^2 - \frac{\partial}{\partial x_1}DF_4^3 = 0. \qquad (14)$$

On constructing in accordance with the general rule the characteristic determinant (cf. reference 6), we obtain

$$\begin{vmatrix} 1 & -\lambda & 0 & 0 \\ 0 & 0 & 1 & -\lambda \\ C\lambda & -C & B\lambda & -B \\ B\lambda & -B & D\lambda & -D \end{vmatrix} = \varkappa (1-\lambda^2)^2 = 0. \qquad (15)$$

Consequently, it has the double roots $\lambda = \pm 1$, i.e., small additional electromagnetic disturbances are propagated with the fundamental velocity also in curved space. The same was proved in reference 4 for gravitational disturbances propagating in a space with the metric (1). Here we have shown the compatibility of the two assertions. Thus, the propagation of an arbitrarily strong electromagnetic wave through space cannot lead in classical theory to a violation of the Riemann nature of the metric.

We can also make a remark with respect to solutions which have a Euclidean metric at infinity. In regions where the metric is Euclidean, the electromagnetic field can only be of the type which is obtained from the ordinary Maxwell equations without taking into account the general theory of relativity. But this field is connected by fixed rectilinear characteristics with regions of space having a non-Euclidean metric. Therefore, the field in curved regions of space cannot differ qualitatively from the result which would be obtained in Euclidean space. In other words, there is no basis for asserting that in the general theory of relativity there arise such new solutions of the equations of electrodynamics which do not have Euclidean analogs.

Therefore, it is doubtful that there exist so-called "geons" postulated by Wheeler[7] as exact nonsingular solutions of the equations of gravitation and electromagnetism in which the electromagnetic field contains itself within a finite volume by gravitational forces (the field in a finite volume which is in thermal equilibrium perhaps could contain itself, but this would correspond to approximate solutions).

For the same reasons one can doubt another prediction by Wheeler,[2] that the presence or absence of charges may be explained by the topological connectivity of space. On continuing the rectilinear characteristics from infinity into the non-Euclidean region, we cannot expect that this will be accompanied by a change in the topological connectivity. Both conclusions stated above concerning "geons" and "topological charges" are also reached in the course of an analytic investigation of the equations.*

Naturally, this refers only to the case of the solutions discussed above which depend on two variables (x_1 and x_4, or x_1 and x_2, which is algebraically very similar, although it leads to elliptic equations). It still remains to investigate what happens when the solutions depend on more than two variables. The following consideration may be used as an argument against the existence of three-dimensional "geons." As is well known, a two-dimensional potential well is always capable of retaining a bound particle in quantum mechanics, while a three-dimensional potential well is not always able to do so. In other words, the wave equation with variable coefficients has a solution which decays exponentially at infinity in two dimensions, while the analogous equation in three dimensions does not have such a solution. But we see that a similar equation in gravitational theory does not have decaying solutions even in two dimensions. Therefore, there is reason for supposing that a fortiori it does not have a three-dimensional solution of such a type.

---

[1] W. Pauli, Ann. Physik **18**, 305 (1933). L. D. Landau and E. M. Lifshitz, Теория поля, (Field Theory), 1st ed., 1941, §100. [Transl., Addison Wesley, 1951].

[2] J. A. Wheeler, Ann. Phys. **2**, 525 (1957).

[3] L. D. Landau and E. M. Lifshitz, Механика сплошных сред, (Mechanics of Continuous Media), 1953, p. 453.

[4] A. S. Kompaneets, JETP **34**, 953 (1958), Soviet Phys. JETP **7**, 659 (1958).

[5] A. Einstein and N. Rosen, J. Franklin Inst. **223**, 43 (1937).

[6] R. Courant and K. Friedrichs, Shock Waves and Supersonic Flow, Interscience, N.Y. 1948 (Russ. transl. IIL, 1950).

[7] J. A. Wheeler, Phys. Rev. **97**, 1511 (1955).

Translated by G. Volkoff
335

---

*For example, the potential of a cylindrical wave is equal to $\varphi = \sqrt{2}\tanh[\frac{1}{2}J_0(kx_1)\cos(kx_4)]$ in agreement with the usual expression for it $\varphi_0 = J_0(kx_1)\cos(kx_4)$.

SOVIET PHYSICS JETP VOLUME 37 (10), NUMBER 6 JUNE, 1960

POLARIZATION PHENOMENA IN RADIATIVE COLLISIONS OF TWO ELECTRONS

V. L. LYUBOSHITZ

Voronezh State University

Submitted to JETP editor July 7, 1959

J. Exptl. Theoret. Phys. (U.S.S.R.) **37**, 1727-1740 (December, 1959)

Two-row matrix formalism is used for the description of polarization phenomena in the collision of two Dirac particles of arbitrary energy. Radiative collisions of two polarized electrons are considered. The structure of the general formulas for the polarization parameters after the collision is investigated, and concrete calculations are carried out in the ultra-relativistic and nonrelativistic limits taking into consideration polarization of the target electrons.

A considerable number of papers[1-6] has been devoted to radiative collisions of two electrons or of an electron and a positron. However, polarization phenomena are not discussed in these papers. The present paper has two aims. The principal aim of the paper is the general investigation of polarization effects in radiative collisions of two electrons, and the calculation of the polarization parameters in the ultra-relativistic and the nonrelativistic limits. Our second aim is the application of the formalism of two-row matrices to the description of polarization phenomena in the collision of Dirac particles of arbitrary energies; in our opinion this leads to a certain simplification of awkward calculations since it avoids the necessity of introducing projection operators into the formulas.

1. DESCRIPTION OF THE POLARIZATION OF DIRAC PARTICLES BY MEANS OF TWO-ROW MATRICES

In the first nonvanishing (Born) approximation the use of a covariant four-row density matrix[7-9] for the description of polarization phenomena in the collision of Dirac particles is not unavoidable. Indeed, the wavefunction of a free particle, normalized per unit volume, may be represented in the following form (we everywhere set $\hbar = c = 1$)

$$u^{(i)} = \begin{pmatrix} \varphi^{(i)} \\ \chi^{(i)} \end{pmatrix} \left(\frac{E+\mu}{2E} \right)^{1/2}, \tag{1a}$$

where

$$\varphi^{(i)} = \begin{pmatrix} C_1^{(i)} \\ C_2^{(i)} \end{pmatrix}, \quad |C_1^{(i)}|^2 + |C_2^{(i)}|^2 = 1; \quad \chi^{(i)} = \frac{\boldsymbol{\sigma}\mathbf{p}}{E+\mu}\varphi^{(i)}. \tag{1b}$$

We define the elements of the density matrix in the following manner:

$$\rho_{\alpha\beta} = \sum_i w^{(i)} C_\alpha^{(i)} C_\beta^{(i)*} \quad (\alpha, \beta = 1, 2),$$

where $w^{(i)}$ is the probability of the pure state $u^{(i)}$ occurring in the mixed ensemble. Then

$$\rho = (1 + \boldsymbol{\zeta}\boldsymbol{\sigma}) / 2. \tag{2}$$

Here $\boldsymbol{\sigma} = (\sigma_1, \sigma_2, \sigma_3)$ is the Pauli vector operator;

$$\boldsymbol{\zeta} = \mathrm{Sp}\, \rho\boldsymbol{\sigma} = \sum_i w^{(i)} \varphi^{(i)*} \boldsymbol{\sigma} \varphi^{(i)}$$

is the average spin of the particle in its proper coordinate system (in units of $\hbar/2$), or the polarization vector. Expression (2) which is ordinarily used only in the nonrelativistic limit completely describes the polarization of a free Dirac particle in the general case.

The four-row density matrix[7-9] with elements $\widetilde{P}_{lk} = u_l \bar{u}_k$ ($l, k = 1, 2, 3, 4$, normalized to the volume E/μ) is related to ρ by the following simple expression

$$\widetilde{P} = \begin{pmatrix} \rho & -\rho \dfrac{\boldsymbol{\sigma}\mathbf{p}}{E+\mu} \\ \dfrac{\boldsymbol{\sigma}\mathbf{p}}{E+\mu} & -\dfrac{(\boldsymbol{\sigma}\mathbf{p})\,\rho\,(\boldsymbol{\sigma}\mathbf{p})}{(E+\mu)^2} \end{pmatrix} \left(\frac{E+\mu}{2\mu} \right). \tag{3}$$

We now go over to a system consisting of two Dirac particles with four-momenta $p_1 = \{\mathbf{p}_1, iE_1\}$, $p_2 = \{\mathbf{p}_2, iE_2\}$. If for the description of polarization we utilize parameters taken in the proper coordinate systems of each of the particles, we may carry over the nonrelativistic formalism developed by Wolfenstein and Ashkin[10] and by Dalitz[11] without any changes directly to the case of arbitrary $\mathbf{p}_1$ and $\mathbf{p}_2$. In this case the density matrix of two Dirac particles is given by

$$\rho^{(1,2)} = \frac{1}{4} \Big\{ 1^{(1)} \times 1^{(2)} + 1^{(1)} \times (\boldsymbol{\zeta}^{(2)}\boldsymbol{\sigma}) + (\boldsymbol{\zeta}^{(1)}\boldsymbol{\sigma}) \times 1^{(2)} + \sum_{i,k} T_{ik}\, \sigma_i^{(1)} \times \sigma_k^{(2)} \Big\}, \quad (i, k = 1, 2, 3) \tag{4}$$

where × denotes the direct matrix product; $\boldsymbol{\zeta}^{(1)} = (\zeta_1^{(1)}, \zeta_2^{(1)}, \zeta_3^{(1)})$, $\boldsymbol{\zeta}^{(2)} = (\zeta_1^{(2)}, \zeta_2^{(2)}, \zeta_3^{(2)})$ are the average spins in the states p_1 and p_2 (after reduction to the rest system); T_{ik} is the polarization correlation tensor.

For independent particles we have

$$\rho^{(1,2)} = \rho^{(1)} \times \rho^{(2)}, T_{ik} = \zeta_i^{(1)} \zeta_k^{(2)} \quad (i, k = 1, 2, 3). \tag{4a}$$

We consider the collision of Dirac particles in which a transition occurs from the states p_1 and p_2 into the states $q_1 = \{\mathbf{q}_1, iW_1\}$, $q_2 = \{\mathbf{q}_2, iW_2\}$. We denote the polarization vectors for the particles before collision by $\boldsymbol{\zeta}_0^{(1)}$ and $\boldsymbol{\zeta}_0^{(2)}$, and after collision by $\boldsymbol{\zeta}^{(1)}$ and $\boldsymbol{\zeta}^{(2)}$. We note that an expression of the type $(u'^* Cu)$, where $C = \begin{pmatrix} C_{11} & C_{12} \\ C_{21} & C_{22} \end{pmatrix}$, may be brought, in virtue of relations (1a) and (1b), into the form $(\varphi'^* D\varphi)$, where

$$D = \left\{C_{11} + \frac{\boldsymbol{\sigma}\mathbf{p}}{E' + \mu} C_{21} + C_{12} \frac{\boldsymbol{\sigma}\mathbf{p}}{E + \mu} + \frac{(\boldsymbol{\sigma}\mathbf{p}') C_{22} (\boldsymbol{\sigma}\mathbf{p})}{(E + \mu)^2}\right\} \times \left(\frac{E' + \mu}{2E'}\right)^{1/2} \left(\frac{E + \mu}{2E}\right)^{1/2}. \tag{5}$$

From this it follows that in the Born approximation the element of the scattering matrix S between states of complete polarization for each of the particles may be written with the aid of the first components of the Dirac wave functions.

Let $\varphi^{(1)}, \varphi^{(2)}, \varphi_0^{(1)}, \varphi_0^{(2)}$ be the first components of the wave functions in the states corresponding to $\{q_1\boldsymbol{\zeta}^{(1)}\}$, $\{q_2\boldsymbol{\zeta}^{(2)}\}$, $\{p_1\boldsymbol{\zeta}_0^{(1)}\}$, $\{p_2\boldsymbol{\zeta}_0^{(2)}\}$. Then for identical particles we have

$$(\{q_1\zeta^{(1)}\}, \{q_2, \zeta^{(2)}\} | S | \{p_1\zeta_0^{(1)}\}, \{p_2\zeta_0^{(2)}\}) = \sum_{\alpha,\beta=1}^{n} \{\varphi^{(1)*} A_{(\alpha)} \varphi_0^{(1)}\} \{\varphi^{(2)*} B_{(\alpha)} \varphi_0^{(2)}\} - \sum_{\alpha,\beta=1}^{n} \{\varphi^{(2)*} A'_{(\alpha)} \varphi_0^{(1)}\} \{\varphi^{(1)*} B'_{(\alpha)} \varphi_0^{(2)}\}. \tag{6}$$

$A_{(\alpha)}$ and $B_{(\alpha)}$ are two-row matrices, $A'_{(\alpha)}$ and $B'_{(\alpha)}$ are obtained from $A_{(\alpha)}$ and $B_{(\alpha)}$ by means of the replacement $q_1 \rightleftarrows q_2$, n is the number of matrices $A_{(\alpha)}$. If a photon is emitted in the collision, then one of the matrices $A_{(\alpha)}$ and $B_{(\alpha)}$ is a linear function of the polarization vector $\mathbf{e}$.

The density matrix after the collision is related to the density matrix before the collision by the well known expression

$$\rho^{(1,2)} = S\rho_0^{(1,2)} S^+ / \mathrm{Sp}_{1,2}\, S\rho_0^{(1,2)} S^+.$$

By regarding the particles before the collision as independent, and by going over to the two-row matrices $A_{(\alpha)}$, $B_{(\alpha)}$, $A'_{(\alpha)}$, $B'_{(\alpha)}$, we obtain for the case of elastic scattering

$$\Phi = \mathrm{Sp}_{1,2}\, S\rho_0^{(1,2)} S^+ = \sum_{\alpha,\beta=1}^{n} \{(\mathrm{Sp}\, A_{(\alpha)} \rho_0^{(1)} A^+_{(\beta)}) (\mathrm{Sp}\, B_{(\alpha)} \rho_0^{(2)} B^+_{(\beta)}) + (\mathrm{Sp}\, A'_{(\alpha)} \rho_0^{(1)} A'^+_{(\beta)}) (\mathrm{Sp}\, B'_{(\alpha)} \rho_0^{(2)} B'^+_{(\beta)}) - 2\mathrm{Re}\, (\mathrm{Sp}\, A_{(\alpha)} \rho_0^{(1)} A'^+_{(\beta)} B_{(\alpha)} \rho_0^{(2)} B'^+_{(\beta)})\}, \tag{7}$$

$$\zeta^{(1)} = \frac{1}{\Phi} \mathrm{Sp}_{1,2} \boldsymbol{\sigma}^{(1)} S\rho_0^{(1,2)} S^+ = \frac{1}{\Phi} \sum_{\alpha,\beta}^{n} \{(\mathrm{Sp}\, \boldsymbol{\sigma} A_{(\alpha)} \rho_0^{(1)} A^+_{(\beta)}) (\mathrm{Sp}\, B_{(\alpha)} \rho_0^{(2)} B^+_{(\beta)}) + (\mathrm{Sp}\, A'_{(\alpha)} \rho_0^{(1)} A'^+_{(\beta)})(\mathrm{Sp}\, \boldsymbol{\sigma} B'_{(\alpha)} \rho_0^{(2)} B'^+_{(\beta)}) - 2\mathrm{Re}(\mathrm{Sp}\, \boldsymbol{\sigma} A_{(\alpha)}\rho_0^{(1)} A'^+_{(\beta)} B_{(\alpha)} \rho_0^{(2)} B'^+_{(\beta)})\}, \tag{8}$$

$$\zeta^{(2)} = \frac{1}{\Phi} \mathrm{Sp}_{1,2} \boldsymbol{\sigma}^{(2)} S\rho_0^{(1,2)} S^+ = \frac{1}{\Phi} \sum_{\alpha,\beta}^{n} \{(\mathrm{Sp}\, A_{(\alpha)} \rho_0^{(1)} A^+_{(\beta)}) (\mathrm{Sp}\, \boldsymbol{\sigma} B_{(\alpha)} \rho_0^{(2)} B^+_{(\beta)}) + (\mathrm{Sp}\, \boldsymbol{\sigma} A'_{(\alpha)} \rho_0^{(1)} A'^{(+}_{(\beta)}) (\mathrm{Sp}\, B'_{(\alpha)} \rho_0^{(2)} B'^+_{(\beta)}) - 2\mathrm{Re}\, (\mathrm{Sp}\, \boldsymbol{\sigma} B_{(\alpha)} \rho_0^{(2)} B'^+_{(\beta)} A_{(\alpha)} \rho_0^{(1)} A'^+_{(\beta)})\}, \tag{9}$$

$$T_{ik} = \frac{1}{\Phi} \mathrm{Sp}_{1,2}\, \sigma_i^{(1)} \times \sigma_k^{(2)} S\rho_0^{(1,2)} S^+ = \frac{1}{\Phi} \sum_{\alpha,\beta}^{n} \{(\mathrm{Sp}\, \sigma_i A_{(\alpha)} \rho_0^{(1)} A^+_{(\beta)}) (\mathrm{Sp}\, \sigma_k B_{(\alpha)} \rho_0^{(2)} B^+_{(\beta)}) + (\mathrm{Sp}\, \sigma_k A'_{(\alpha)} \rho_0^{(1)} A'^+_{(\beta)}) (\mathrm{Sp}\, \sigma_i B'_{(\alpha)} \rho_0^{(2)} B'^+_{(\beta)}) - 2\mathrm{Re}\, (\mathrm{Sp}\, \sigma_i A_{(\alpha)} \rho_0^{(1)} A'^+_{(\beta)} \sigma_k B_{(\alpha)} \rho_0^{(2)} B'^+_{(\beta)})\}, \tag{10}$$

where

$$\rho_0^{(1)} = \tfrac{1}{2} (1 + \zeta_0^{(1)} \boldsymbol{\sigma}), \quad \rho_0^{(2)} = \tfrac{1}{2} (1 + \zeta_0^{(2)} \boldsymbol{\sigma}).$$

In the case of radiative scattering formulas (7 — 10) continue to hold, only they must be summed over the two opposite polarizations of the photon $\mathbf{e}_1$ and $\mathbf{e}_2 \perp \mathbf{e}_1$.

In the next section we shall consider in greater detail the radiative collision of two charged Dirac particles.

2. THE CONNECTION BETWEEN THE MATRICES FOR ELASTIC AND INELASTIC SCATTERING

As is well known, the polarization of electromagnetic radiation is characterized by the three components of the Stokes vector-parameter[12-14] with $\epsilon_1^2 + \epsilon_2^2 + \epsilon_3^2 \leq 1$. In such a case the density matrix is given by

$$\rho^{(3)} = \tfrac{1}{2} (1 + \varepsilon_1\omega_1 + \varepsilon_2\omega_2 + \varepsilon_3\omega_3) = \tfrac{1}{2} (1 + \boldsymbol{\varepsilon}\boldsymbol{\omega}), \tag{11}$$

where $\boldsymbol{\epsilon}$ is a vector in Poincare space,[13] while

$$\omega_1 = \begin{pmatrix} 1 & 0 \\ 0 & -1 \end{pmatrix}, \quad \omega_2 = \begin{pmatrix} 0 & 1 \\ 1 & 0 \end{pmatrix}, \quad \omega_3 = \begin{pmatrix} 0 & -i \\ i & 0 \end{pmatrix}.$$

For a system consisting of a photon and two Dirac particles the density matrix may be written in the following form:

$$\rho^{(1,\,2,\,3)} = \tfrac{1}{8}\{1^{(1)} \times 1^{(2)} \times 1^{(3)} + (\zeta_0^{(1)}\,\sigma^{(1)}) \times 1^{(2)} \times 1^{(3)}$$

$$+ 1^{(1)} \times (\zeta_0^{(2)}\,\sigma^{(2)}) \times 1^{(3)} + \sum_{i,\,k=1}^{3} T_{ik}^{(1,2)}\,\sigma_i^{(1)} \times \sigma_k^{(2)} \times 1^{(3)}$$

$$+ 1^{(1)} \times 1^{(2)} \times (\varepsilon\omega^{(3)}) + \sum_{i,\,\mu=1}^{3} T_{i\mu}^{(1,3)}\,\sigma_i^{(1)} \times 1^{(2)} \times \omega_\mu^{(3)}$$

$$+ \sum_{i,\,\mu=1}^{3} T_{i\mu}^{(2,3)}\,1^{(1)} \times \sigma_i^{(2)} \times \omega_\mu^{(3)}$$

$$+ \sum_{i,k,\mu=1}^{3} T_{ik\mu}^{(1,2,3)}\,\sigma_i^{(1)} \times \sigma_k^{(2)} \times \omega_\mu^{(3)}\Big\}, \qquad (12)$$

where $Sp_{1,2}\,\rho^{(1,2,3)} = \rho^{(3)}$ (formula 11), $Sp_3\,\rho^{(1,2,3)} = \rho^{(1,2)}$ (formula 4).

By definition,[12–14] if the effective cross section for the emission of a photon of polarization **e** summed over the spins of the Dirac particles in the final state is equal to $\Phi(\mathbf{e})$, then we have

$$\varepsilon_1 = \frac{\Phi(\mathbf{e}_1) - \Phi(\mathbf{e}_2)}{\Phi(\mathbf{e}_1) + \Phi(\mathbf{e}_2)}$$

$$= \frac{Sp_{1,2}\,\mathscr{E}(\mathbf{e}_1)\,\rho_0^{(1,2)}\,\mathscr{E}(\mathbf{e}_1)^+ - Sp_{1,2}\,\mathscr{E}(\mathbf{e}_1)\,\rho_0^{(1,2)}\,\mathscr{E}(\mathbf{e}_2)^+}{\sum\limits_{\mathbf{e}_1\mathbf{e}_2} S\ p_{1,2}\,\mathscr{E}(\mathbf{e})\,\rho_0\quad \mathscr{E}(\mathbf{e})^+},$$

$$\varepsilon_2 = \frac{\Phi[(\mathbf{e}_1 + \mathbf{e}_2)/\sqrt{2}] - \Phi[(\mathbf{e}_1 - \mathbf{e}_2)/\sqrt{2}]}{\Phi(\mathbf{e}_1) + \Phi(\mathbf{e}_2)}$$

$$= \frac{Sp_{1,2}\,\mathscr{E}(\mathbf{e}_1)\,\rho_0^{(1,2)}\,\mathscr{E}(\mathbf{e}_2)^+ + Sp_{1,2}\,\mathscr{E}\quad {}_2)\,\rho_0^{(1,2)}\,\mathscr{E}(\mathbf{e}_1)^+}{\sum\limits_{\mathbf{e}_1\mathbf{e}_2} Sp_{1,2}\,\mathscr{E}(\mathbf{e})\,\rho_0^{(1,2)}\,\mathscr{E}(\mathbf{e})^+},$$

$$\varepsilon_3 = \frac{\Phi[(\mathbf{e}_1 + i\mathbf{e}_2)/\sqrt{2}] - \Phi[(\mathbf{e}_1 - i\mathbf{e}_2)/\sqrt{2}]}{\Phi(\mathbf{e}_1) + \Phi(\mathbf{e}_2)}$$

$$= i\,\frac{Sp_{1,2}\,\mathscr{E}(\mathbf{e}_1)\,\rho_0^{(1,2)}\,\mathscr{E}(\mathbf{e}_2)^+ - Sp_{1,2}\,\mathscr{E}(\mathbf{e}_2)\,\rho_0\quad \mathscr{E}(\mathbf{e}_1)^+}{\sum\limits_{\mathbf{e}_1\mathbf{e}_2} Sp_{1,2}\,\mathscr{E}(\mathbf{e})\,\rho_0^{(1,2)}\,\mathscr{E}(\mathbf{e})^+},$$

$$\Phi = \Phi(\mathbf{e}_1) + \Phi(\mathbf{e}_2) = \sum_{\mathbf{e}_1\mathbf{e}_2} Sp_{1,2}\,\mathscr{E}(\mathbf{e})\,\rho_0^{(1,2)}\,\mathscr{E}(\mathbf{e})^+ = Sp_{1,2,3}\,\rho^{(1,2,3)}, \qquad (13)$$

where $\mathscr{E} = \begin{pmatrix}\mathscr{E}(\mathbf{e}_1)\\ \mathscr{E}(\mathbf{e}_2)\end{pmatrix}$ is the radiative collision matrix. Evidently formulas (13), as well as formulas (7) – (10) for the polarization parameters of the Dirac particles (summed over both photon polarizations), are a consequence of the following relation for $\rho^{(1,2,3)}$:

$$\rho^{(1,2,3)} = \frac{1}{\Phi}\begin{pmatrix}\mathscr{E}(\mathbf{e}_1)\,\rho_0^{(1,2)}\,\mathscr{E}(\mathbf{e}_1)^+ & \mathscr{E}(\mathbf{e}_1)\,\rho_0^{(1,2)}\,\mathscr{E}(\mathbf{e}_2)^+\\ \mathscr{E}(\mathbf{e}_2)\,\rho_0^{(1,2)}\,\mathscr{E}(\mathbf{e}_1)^+ & \mathscr{E}(\mathbf{e}_2)\,\rho_0^{(1,2)}\,\mathscr{E}(\mathbf{e}_2)^+\end{pmatrix}. \qquad (14)$$

For the parameters characterizing the correlation of the polarizations of the photon and the particles we obtain

$$T_{i1}^{(1,3)} = Sp_{1,\,2,3}\,\sigma_i^{(1)} \times \omega_1^{(3)}\,\rho^{(1,2,3)}/Sp\rho^{(1,2,3)}$$

$$= \frac{Sp_{1,2}\,\sigma_i^{(1)}\,\mathscr{E}(\mathbf{e}_1)\,\rho_0^{(1,2)}\,\mathscr{E}(\mathbf{e}_1)^+ - Sp_{1,2}\,\sigma_i^{(1)}\,\mathscr{E}(\mathbf{e}_2)\,\rho_0^{(1,2)}\,\mathscr{E}(\mathbf{e}_2)^+}{\sum\limits_{\mathbf{e}_1,\,\mathbf{e}_2} Sp_{1,2}\,\mathscr{E}(\mathbf{e})\,\rho_0^{(1,2)}\,\mathscr{E}(\mathbf{e})^+} \qquad (15)$$

etc., in analogy with (13), with the unit matrix being replaced by σ_i, where $i = 1, 2, 3$.

The expressions for $T_{i\mu}^{(2,3)}$, $T_{ik\mu}^{(1,2,3)}$ can be obtained from (15) if the following replacements are carried out: $\sigma_i^{(1)} \to \sigma_i^{(2)}$ and $\sigma_i^{(1)} \to \sigma_i^{(1)} \times \sigma_k^{(2)}$.

We now obtain the relation of the matrix $\mathscr{E}$ to the matrix S which describes elastic scattering. Let

$$(\{q_1\zeta^{(1)}\}, \{q_2\zeta^{(2)}\}\,|\,S\,|\,\{p_1\zeta_0^{(1)}\}\{p_2\zeta_0^{(2)}\})$$

$$= \sum_{\alpha=1}^{n} \{u(q_1\zeta^{(1)})L_{(\alpha)}^{(q_1p_1)}u(p_1\zeta_0^{(1)})\}\{u(q_2\zeta^{(2)})M_{(\alpha)}^{(q_2p_2)}u(p_2\zeta_0^{(2)})\}$$

$$- \sum_{\alpha=1}^{n} \{u(q_2\zeta^{(2)})\,L_{(\alpha)}^{\prime(q_2p_1)}u(p_1\zeta_0^{(1)})\}\{u(q_1\zeta^{(1)})\,M_{(\alpha)}^{\prime(q_1p_2)}u(p_2\zeta_0^{(2)})\};$$

$$S = \sum_{\alpha}^{n} L_{(\alpha)}^{(q_1p_1)} \times M_{(\alpha)}^{(q_2p_2)} - L_{(\alpha)}^{\prime(q_2p_1)} \times M_{(\alpha)}^{\prime(q_1p_2)}$$

$$= C(\{q_1p_1\}, \{q_2, p_2\}, \gamma^{(q_1p_1)}, \gamma^{(q_2p_2)})$$

$$- C(\{q_2p_1\}, \{q_1p_2\}, \gamma^{(q_2p_1)}, \gamma^{(q_1p_2)}),$$

where in the notation $L^{(q_1p_1)}$, $M^{(q_1p_2)}$ etc. introduced above the upper index refers to the states of the particles which correspond to the matrix element.

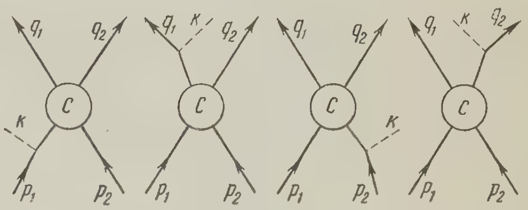

Feynman diagrams for the radiative collision of two particles.

Feynman diagrams for the radiative collision of two particles are shown in the figure. Diagrams corresponding to exchange are obtained by means of interchanging the lines q_1 and q_2.

From this we obtain for $\mathscr{E}(\mathbf{e})$ in first order perturbation theory

$$\mathscr{E}(\mathbf{e}) \sim \frac{e}{\sqrt{\omega}}\Big[\Big\{\hat{e}\,\frac{i(\hat{q}_1 + \hat{k}) - \mu}{(q_1 + k)^2 + \mu^2}\Big\}$$

$$\times C(\{q_1 + k, p_1\}, \{q_2, p_2\}, \gamma^{(q_1p_1)}, \gamma^{(q_2p_2)})$$

$$+ C(\{q_1, p_1 - k\}, \{q_2, p_2\}, \gamma^{(q_1p_1)}, \gamma^{(q_2p_2)})\Big\{\frac{i(\hat{p}_1 - \hat{k}) - \mu}{(p_1 - k)^2 + \mu^2}\,\hat{e}\Big\}$$

$$+ \Big\{\hat{e}\,\frac{(\hat{q}_2 + \hat{k}) - \mu}{(q_2 + k)^2 + \mu^2}\Big\}C(\{q_1p_1\}, \{q_2 + k, p_2\}, \gamma^{(q_1p_1)}, \gamma^{(q_2p_2)})$$

$$+ C(\{q_1p_1\}, \{q_2, p_2 - k\}, \gamma^{(q_1p_1)}, \gamma^{(q_2p_2)})\Big\{\frac{i(\hat{p}_2 - \hat{k}) - \mu}{(p_2 - k)^2 + \mu^2}\,\hat{e}\Big\}$$

$$- \Big\{\hat{e}\,\frac{i(\hat{q}_2 + \hat{k}) - \mu}{(q_2 + k)^2 + \mu^2}\Big\}C(\{q_2 + k, p_1\}, \{q_1, p_2\}, \gamma^{(q_2p_1)}, \gamma^{(q_1p_2)}\})$$

$$- C(\{q_2, p_1 - k\}, \{q_1, p_2\}, \gamma^{(q_2p_1)}, \gamma^{(q_1p_2)})\Big\{\frac{i(\hat{p}_1 - \hat{k}) - \mu}{(p_1 - k)^2 + \mu^2}\,\hat{e}\Big\}$$

$$- \Big\{\hat{e}\,\frac{i(\hat{q}_1 + \hat{k}) - \mu}{(q_1 + k)^2 + \mu^2}\Big\}C(\{q_2, p_1), \{q_1 + k, p_2\}, \gamma^{(q_1p_2)}, \gamma^{(q_2p_1)})$$

$$- C(\{q_2p_1\}, \{q_1, p_2 - k\}, \gamma^{(q_2p_1)}, \gamma^{(q_1p_2)})\Big\{\frac{i(\hat{p}_2 - \hat{k}) - \mu}{(p_2 - k)^2 + \mu^2}\,\hat{e}\Big\}. \qquad (16)$$

e is the charge of the particle, ω is the frequency of the radiation, $\mathbf{e}$ is the photon polarization vector.

3. CHARACTERISTIC FEATURES OF POLARIZATION PHENOMENA IN THE RADIATIVE COLLISION OF TWO ELECTRONS

We express the third-order scattering matrix element for the radiative collision of two electrons in the form (6) with the aid of two-row matrices (cf. Appendix). We note that each of the two-row matrices may be written in the form $M + i\sigma\mathbf{N}$, where for real $\mathbf{e}$ we have

$$\operatorname{Im} M = 0, \qquad \operatorname{Im} \mathbf{N} = 0. \tag{17}$$

If we do not take radiation corrections into account condition (17) leads to a number of consequences.

a) The effective cross section for the radiative collision of two electrons may be written in the general case in the following form

$$\Phi = \Phi_0 + (\boldsymbol{\alpha}^{(1)}\boldsymbol{\zeta}_0^{(1)}) + (\boldsymbol{\alpha}^{(2)}\boldsymbol{\zeta}_0^{(2)}) + \sum_{i,k=1}^{3} \gamma_{ik}\zeta_{0i}^{(1)}\zeta_{0k}^{(2)}.$$

From condition (17) and formula (10) it follows that $\boldsymbol{\alpha}^{(1)} = 0$, $\boldsymbol{\alpha}^{(2)} = 0$, $\gamma_{ik} = \Phi_0 T_{ik}^{(\mathrm{unp})}$, where Φ_0 is the effective cross section for the radiative collision of unpolarized electrons, while $T_{ik}^{(\mathrm{unp})}$ is the polarization correlation tensor after the collision of unpolarized electrons. From this it follows

$$\Phi = \Phi_0\Big(1 + \sum_{i,k} T_{ik}^{(\mathrm{unp})}\zeta_{0i}^{(1)}\zeta_{0k}^{(2)}\Big) \quad (i, k = 1, 2, 3). \tag{18}$$

b) The components of the polarization vector for the particle after the collision may be written in the following manner:

$$\zeta_i = \frac{1}{\Phi}\Big\{c_i + \sum_{k=1}^{3} a_{ik}^{(1)}\zeta_{0k}^{(1)} + \sum_{k=1}^{3} a_{ik}^{(2)}\zeta_{0k}^{(2)} + \sum_{k,l=1}^{3} b_{ikl}^{(1,2)}\zeta_{0k}^{(1)}\zeta_{0l}^{(2)}\Big\}.$$

For electrons condition (18) leads to the result that $c_i = 0$ and the tensor $b_{ikl}^{(1,2)} = 0$ for all $i, k, l = 1, 2, 3$. Consequently we have

$$\zeta_i = \frac{1}{\Phi}\Big\{\sum_{k=1}^{3} \alpha_{ik}^{(1)}\zeta_{0k}^{(1)} + \sum_{k=1}^{3} \alpha_{ik}^{(2)}\zeta_{0k}^{(2)}\Big\}. \tag{19}$$

If the electrons are unpolarized before the collision, we have $\boldsymbol{\zeta}^{(1)} = \boldsymbol{\zeta}^{(2)} = 0$.

c) The polarization correlation tensor for Dirac particles is given by

$$T_{ik} = \frac{1}{\Phi}\Big\{l_{ik} + \sum_{m=1}^{3} v_{ikm}^{(1)}\zeta_{0m}^{(1)} + \sum_{m=1}^{3} v_{ikm}^{(2)}\zeta_{0m}^{(2)} + \sum_{m,n=1}^{3} \omega_{ikmn}\zeta_{0m}^{(1)}\zeta_{0n}^{(2)}\Big\}.$$

For two electrons we have $v_{ikm}^{(1)} = v_{ikm}^{(2)} = 0$, so that

$$T_{ik} = \frac{1}{\Phi}\Big\{l_{ik} + \sum_{m,n=1}^{3} \omega_{ikmn}\zeta_{0m}^{(1)}\zeta_{0n}^{(2)}\Big\}. \tag{20}$$

Here l_{ik}, ω_{ikmn} are tensors of the second and of the fourth rank which do not depend on the spins. The linear polarization parameters may be represented in the form $\epsilon_1 = \Phi_{\epsilon_1}/\Phi$, $\epsilon_2 = \Phi_{\epsilon_2}/\Phi$, where Φ_{ϵ_1} and Φ_{ϵ_2} have the same structure as Φ in (19). The degree of linear polarization consequently does not depend on the polarization of one of the electrons if the second one is unpolarized.

d) In the case of circular polarization we have

$$\varepsilon_3 = \frac{1}{\Phi}\Big\{g + (\mathbf{f}\boldsymbol{\zeta}_0^{(1)}) + (\mathbf{d}\boldsymbol{\zeta}_0^{(2)}) + \sum_{i,k} h_{ik}^{(1,2)}\zeta_{0i}^{(1)}\zeta_{0k}^{(2)}\Big\}.$$

In the case of a radiative collision of electrons $g = 0$, $h_{ik} = 0$ and

$$\varepsilon_3 = \frac{1}{\Phi}\{(\mathbf{f}\boldsymbol{\zeta}_0^{(1)}) + (\mathbf{d}\boldsymbol{\zeta}_0^{(2)})\}. \tag{21}$$

If the electrons are unpolarized the circular polarization of bremsstrahlung is equal to zero.

e) We consider the polarization parameters which refer simultaneously to the electrons and to the photon. From formulas (15) and condition (17) it follows that

$$T_{i\alpha}^{(1,3)} = \frac{1}{\Phi}\Big\{\sum_{k=1}^{3} A_{ik\alpha}^{(1)}\zeta_{0k}^{(1)} + \sum_{k=1}^{3} A_{ik\alpha}^{(2)}\zeta_{0k}^{(2)}\Big\} \quad (\alpha = 1, 2),$$

$$T_{i3}^{(1,3)} = \frac{1}{\Phi}\Big\{B_{i3} + \sum_{k,l=1}^{3} c_{ikl3}\zeta_{0k}^{(1)}\zeta_{0l}^{(2)}\Big\} \quad (\alpha = 3,\ i = 1, 2, 3); \tag{22}$$

$$T_{ik\alpha}^{(1,2,3)} = \frac{1}{\Phi}\Big\{D_{ik\alpha} + \sum_{l,m=1}^{3} H_{iklm\alpha}\zeta_{0l}^{(1)}\zeta_{0m}^{(2)}\Big\} \quad (\alpha = 1, 2),$$

$$T_{ik3}^{(1,2,3)} = \frac{1}{\Phi}\Big\{\sum_{l=1}^{3} F_{ikl3}^{(1)}\zeta_{0l}^{(1)} + \sum_{l=1}^{3} F_{ikl3}^{(2)}\zeta_{0l}^{(2)}\Big\} \ (\alpha = 3,\ i = 1, 2, 3). \tag{23}$$

Later we shall evaluate the circular polarization of "forward" and "backward" bremsstrahlung and the polarization of the electron scattered forward in the ultra-relativistic limit; in making this calculation we shall consider the incident electron to be longitudinally polarized, while the target has arbitrary polarization. In addition, we shall consider polarization phenomena in the nonrelativistic limit.

We note that if there exists no coupling between the apparatus recording the electrons and the photons, then the polarization parameters for the bremsstrahlung must be averaged over all possible values of the momenta of one of the electrons consistent with the laws of conservation of energy and momentum. For example,

$$\hat{\varepsilon}_3 = \int \varepsilon_3\rho_f\Phi d\Omega_{\mathbf{q}_1} \Big/ \int \rho_f\Phi d\Omega_{\mathbf{q}_1}, \tag{24}$$

where ρ_f is the density of states;[3]

$$\rho_f = \frac{\omega^2|\mathbf{q}_1|^2 d\Omega_{\mathbf{k}} d\Omega_{\mathbf{q}_1} d\omega}{|\mathbf{q}_1|/W_1 + (|\mathbf{q}_2|/W_2)\partial|\mathbf{q}_2|/\partial|\mathbf{q}_1|}.$$

In exactly the same way the polarization parameters for the electrons must be averaged over all possible values of the photon momenta.

4. THE ULTRA-RELATIVISTIC LIMIT

We use the system of units in which $\hbar = c = \mu = 1$.

In the laboratory coordinate system the momentum of the incident electron $E_l \gg 1$. In the center of mass system we have two electrons with momenta $\mathbf{p}_1 = -\mathbf{p}_2 = \mathbf{p}$, with $|\mathbf{p}| \gg 1$ and

$$|\mathbf{p}_1| = |\mathbf{p}_2| = E_1 = E_2 = E.$$

The laws of conservation of energy and momentum in the center of mass system take on the following form:

$$2E = W_1 + W_2 + \omega, \quad \mathbf{q}_2 = -\mathbf{q}_1 - \mathbf{k} = \mathbf{q}. \tag{25}$$

If after the radiative collision $W_1 \gg 1$, then it follows from (25) that

$$W_1 = (E - \omega) E / (E - \omega \sin^2 \phi / 2),$$

where ϕ is the angle between $\mathbf{k}$ and $\mathbf{q}$, while $\omega = |\mathbf{k}|$.

We consider the emission of the photon "forward" and "backward." In this case the degree of linear polarization integrated over the scattering angles for the electron is equal to zero. We shall carry out the calculation of the circular polarization in the center of mass system. We can then go over to the laboratory system of coordinates by means of the well known formulas of the theory of relativity which in the ultra-relativistic limit have the following form

$$E_l = 2E^2; \quad \omega_l = 2\omega E. \tag{26}$$

We shall integrate the result over the scattering angle of one of the electrons. We shall consider such large energies that $\ln E_l \gg 1$ ($E_l \sim 1000$ Mev). Then for the interval $(E - \omega)/E \sim 1$ we may simplify the calculation considerably if we restrict ourselves to integration over the small angles $\theta_0 \approx \sin \theta_0$ and neglect the values of the initial function at the upper limit. In carrying out this calculation we consider the state density to be constant. If the target is unpolarized we obtain

$$\varepsilon_3 = P_1 \frac{A}{B}, \qquad A = 3\,\frac{2E-\omega}{\omega} \ln 2E^2 \frac{E-\omega}{\omega},$$

$$B = \left\{ \left| \frac{2E-\omega}{\omega} \right|^2 + 1 + \frac{7E-\omega}{8E} + \frac{3}{32}\,\frac{E-\omega}{E} \right\} \ln\left(2E^2 \frac{E-\omega}{\omega}\right)$$

$$+ \frac{5}{16} \ln\left(2E^2 \frac{(E-\omega)^2}{\omega}\right), \tag{27}$$

P_1 is the degree of longitudinal polarization of the incident electron.

For the central part of the spectrum we may take $\ln E_l = \ln 2E^2 \gg \ln (E - \omega)/\omega$. Then on denoting $\omega_l/E_l \approx \omega/E = \gamma$, we obtain

$$\hat{\varepsilon}_3 = P_1 \frac{3\,(2/\gamma - 1)}{{}^{47}\!/_{32} + (2/\gamma - 1)^2 + 3\,(1-\gamma)/32 + (7+\gamma)/8}. \tag{28}$$

At the lower limit of the spectrum we have $\epsilon_3 = \omega_l/E_l$, as can be seen from (27). Moreover, the relation $\lim\limits_{\omega \to 0} \widetilde{\epsilon}_3 = 0$ which follows from the above discussion transcends the limitation of the approximation $\ln E_l \gg 1$ ($E_l \gg 1$), and is of a more general nature.

The magnitude of $\widetilde{\epsilon}_3$ increases as γ is increased. It should be noted that the transverse polarization of the incident electron does not affect the circular polarization of the "forward" bremsstrahlung.

We now examine the influence of the polarization of the target on $\widetilde{\epsilon}_3$. It is due exclusively to the recoil of the target electrons (momentum and energy of recoil are given by $p_l \sim 1$, $E_l \sim 1$). We obtain

$$\widetilde{\varepsilon}_3 = P_1 \frac{A}{B + P_1 P_2 C} + P_2 \frac{D}{B + P_1 P_2 C}.$$

Here A and B are the same as in (27),

$$P_2 = \frac{(\boldsymbol{\zeta}_0^{(2)} \mathbf{p})}{|\mathbf{p}|}, \quad C = \frac{1}{2}\left(\frac{2E-\omega}{\omega}\right) \ln\left(2E^2 \frac{E-\omega}{\omega}\right),$$

$$D = \frac{1}{2} \ln\left(2E^2 \frac{E-\omega}{\omega}\right) + \frac{1}{4} \ln\left(2E^2 \frac{(E-\omega)^2}{\omega}\right). \tag{29}$$

For the middle part of the spectrum we have

$$\widetilde{\varepsilon}_3 = \frac{3P_1\,(2/\gamma - 1) + {}^{7}\!/_{8} P_2}{{}^{47}\!/_{32} + (2/\gamma - 1)^2 + {}^{3}\!/_{32}\,(1-\gamma) + (7+\gamma)/8 + {}^{1}\!/_{2} P_1 P_2\,(2/\gamma - 1)}. \tag{30}$$

Formulas (28) and (30) become exact in the limit $E_l \to \infty$ ($\gamma \neq 0$, $\gamma \neq 1$).

The circular polarization at the upper limit of the spectrum, where the intensity of bremsstrahlung increases sharply, has to be discussed separately, since formulas (28) and (30) do not hold for $\omega \approx E$. Let the electron have the momentum $|\mathbf{q}_1| \ll 1$ after scattering. Then $\omega \approx E - \frac{1}{2}$. In the first approximation the matrix element in this case has the form

$$(q|\mathscr{E}|p) \sim \frac{1}{(W_2 - E_2)^2 - (\mathbf{q}_2 - \mathbf{p}_2)^2} \left(\varphi^{(1)*} i\,(\boldsymbol{\sigma}\,[\mathbf{n} \times \mathbf{e}])\,\varphi_0^{(1)}\right) \left(\varphi^{(2)*} \varphi_0^{(2)}\right).$$

Then, independently of the target polarization, we shall obtain for the circular polarization $\widetilde{\epsilon}_3 = P_1$ up to terms of order $1/E_l$. We note that the same formula holds also at the upper limit of the "forward" bremsstrahlung spectrum in the field of a nucleus.[15]

In order to obtain the circular polarization of the photon emitted backward in the center of mass system we must in formula (30) replace $P_1 \rightleftarrows -P_2$. In the laboratory system of coordinates the photon energy in this case is equal to $\omega_l \approx \frac{1}{2}\omega/E = \frac{1}{2}\gamma$.

If the target is polarized, while the incident electron is unpolarized, then in the case $\omega_l \sim 1$, $(\frac{1}{2} - \omega_l)/\omega_l \sim 1$ we have

$$\tilde{\varepsilon}_3 = -P_2 \frac{3\,(1/\omega_l - 1)}{{}^{47}/_{32} + (1/\omega_l - 1)^2 + (7 + 2\omega_l)/8 + 3\,(1 - 2\omega_l)/32}. \tag{31}$$

In the case $\omega_l = \frac{1}{2}$ we have

$$\tilde{\varepsilon}_3 = -(\zeta_0^{(2)}\mathbf{p})/|\mathbf{p}| = (\zeta_0^{(2)}\mathbf{k})/\omega \qquad (|\mathbf{k}| = \omega) \tag{32}$$

independently of the polarization of the incident electron.

Thus, the circular polarization of the "forward" bremsstrahlung is mainly affected by the polarization of the incident electron, with $\tilde{\epsilon}_3$ being independent of target polarization at the upper limit of the spectrum, while the circular polarization of the "backward" bremsstrahlung, on the other hand, depends primarily on the target polarization.

We now consider the longitudinal polarization of the electron scattered forward averaged over all the directions of photon emission, assuming that $W_1 \gg 1$. After carrying out the integration in the approximation $\ln E_l \gg 1$, $\ln W_1 \gg 1$ we obtain (for an unpolarized target)

$$P_{q_1} = P_1\,(M - N - L)/(M + N),$$

$$M = W_1^2\left\{16\,(E + W_1)^2 + \frac{1}{16}\frac{(13E - W_1)^2(E - W_1)^2}{E^2}\right\}\ln 2E^2$$
$$+ E^2\left\{16\,(E + W_1)^2 + \frac{19}{4}\frac{(E - W_1)^4}{4E^2}\right\}\ln 2EW_1$$
$$- \left\{32\,(E + W_1)^2 + \frac{3\,(E - W_1)^2\,(5E + W_1)^2}{4E^2}\right\}$$
$$\times \frac{EW_1}{E^2 + W_1^2}\{W_1^2 \ln 2E^2 + E^2 \ln 2EW_1\},$$

$$N = 32\,(E - W_1)^2\left\{\frac{W_1^4}{E^2 + W_1^2}\ln\frac{4E^4W_1}{E - W_1} + \frac{E^4}{E^2 + W_1^2}\ln\frac{4E^3W_1^2}{E - W_1}\right.$$
$$\left. - W_1^2 \ln 2E^2 - E^2 \ln 2EW_1\right\},$$

$$L = 6\,(E + W_1)\frac{(E - W_1)^2}{2E}\left\{W_1^2 \ln 2E^2 + E^2 \ln 2EW_1\right.$$
$$\left. - \frac{EW_1^3 \ln 2E^2 + E^3W_1 \ln 2EW_1}{E^2 + W_1^2}\right\}. \tag{33}$$

As $E_l \to \infty$ the accuracy of formula (33) improves. If $\ln E/(E - W_1) \ll \ln 2E^2 = E_l$, then for $\lambda = W_1/E$ we obtain

$$P_{q_1} = P_1\{16\,(1 + \lambda)^2 + \tfrac{1}{16}(13 - \lambda)^2 - \tfrac{3}{2}(1 - \lambda)(5 + \lambda)$$
$$- 32\,(1 - \lambda^2)^2/(1 + \lambda^2) - 3\,(1 + \lambda)(1 - \lambda^2)\}\{16\,(1 + \lambda)^2$$
$$+ \tfrac{1}{16}(13 - \lambda)^2 + \tfrac{19}{16}(1 - \lambda)^2 - \tfrac{3}{2}(1 - \lambda)(5 + \lambda)$$
$$+ 32\,(1 - \lambda^2)^2/(1 + \lambda^2)\}^{-1}. \tag{34}$$

In the case $W_1 \approx E$ we have $P_{q_1} = P$, as may be seen from (33). Such a result holds for Møller scattering. Since a circularly polarized photon carries away angular momentum, we shall have $P_{q_1} \neq P_1$ in the case $W_1 < E$, while for $\lambda < 0.28$ the longitudinal polarization changes sign. For small values of q the direct and the exchange terms make equal contributions to the result.

For the polarization of an electron with $|\mathbf{q}_1| \ll 1$ (in the laboratory system $|\mathbf{q}_{1l}| \sim \sqrt{E_l}$) we obtain

$$\zeta^{(1)} = -\tfrac{1}{2}(\zeta_0^{(1)} + \zeta_0^{(2)}), \tag{35}$$

where $\zeta_0^{(1)}$ and $\zeta_0^{(2)}$ are respectively the polarization vectors for the incident electron and the target.

5. THE NONRELATIVISTIC LIMIT

In the nonrelativistic limit we may, as before, utilize the Born approximation, provided ${}^1/_{137} \ll |\mathbf{p}| \ll 1$. In the center-of-mass system the law of conservation of energy has the following form $p^2 = \frac{1}{2}(q_1^2 + q_2^2) + \omega$. From this it follows that $\omega \sim |\mathbf{p}|^2$; $\omega \ll |\mathbf{p}|$, with $\mathbf{q}_1 \approx -\mathbf{q}_2 = \mathbf{q}$.

The formula for the element of the scattering matrix is simplified considerably in the nonrelativistic limit (cf. Appendix).

As a result of summing $|(\mathbf{q}|\mathscr{E}|\mathbf{p})|^2$ over the electron spins and the polarizations of the photon in the final state we obtain

$$\Phi = \mathrm{const}\,\frac{1}{\omega^3}\left\{\frac{1}{(\mathbf{p} - \mathbf{q})^4}\alpha + \frac{1}{(\mathbf{p} + \mathbf{q})^4}\beta\right.$$
$$\left. - \frac{1}{(\mathbf{p}^2 - \mathbf{q}^2)^2}\gamma\,(1 + \zeta_0^{(1)}\zeta_0^{(2)})\right\},$$

$$\alpha = (\mathbf{pn})\{\mathbf{p}^2 - (\mathbf{pn})^2\} + (\mathbf{qn})\{\mathbf{q}^2 - (\mathbf{qn})^2\}$$
$$- 2\,(\mathbf{pn})(\mathbf{qn})\{(\mathbf{pq}) - (\mathbf{pn})(\mathbf{qn})\} + \frac{\omega^2\,(\mathbf{p} - \mathbf{q}, \mathbf{n})}{(\mathbf{p} - \mathbf{q})^4}\{(\mathbf{p} - \mathbf{q})^2$$
$$- (\mathbf{p} - \mathbf{q}, \mathbf{n})^2\} + 2\omega\frac{(\mathbf{p} - \mathbf{q}, \mathbf{n})}{(\mathbf{p} - \mathbf{q})^2}(\mathbf{pn})\{(\mathbf{p} - \mathbf{q}, \mathbf{p})$$
$$- (\mathbf{p} - \mathbf{q}, \mathbf{n})(\mathbf{pn})\} - 2\omega\frac{(\mathbf{p} - \mathbf{q}, \mathbf{n})}{(\mathbf{p} - \mathbf{q})^2}(\mathbf{qn})\{(\mathbf{p} - \mathbf{q}, \mathbf{q})$$
$$- (\mathbf{p} - \mathbf{q}, \mathbf{n})(\mathbf{qn})\}, \qquad \beta = \alpha(-\mathbf{q}),$$

$$\gamma = (\mathbf{pn})^2\{\mathbf{p}^2 - (\mathbf{pn})^2\} + (\mathbf{qn})^2\{\mathbf{q}^2 - (\mathbf{qn})^2\} - 2\,(\mathbf{qn})(\mathbf{pn})\{(\mathbf{pq})$$
$$- (\mathbf{pn})(\mathbf{qn})\} + \frac{\omega^2\,(\mathbf{p} - \mathbf{q}, \mathbf{n})(\mathbf{p} + \mathbf{q}, \mathbf{n})}{(\mathbf{p}^2 - \mathbf{q}^2)^2}\{(\mathbf{p}^2 - \mathbf{q}^2)$$
$$- (\mathbf{p} - \mathbf{q}, \mathbf{n})(\mathbf{p} + \mathbf{q}, \mathbf{n})\} + \frac{\omega\,(\mathbf{p} - \mathbf{q}, \mathbf{n})}{(\mathbf{p} - \mathbf{q})^2}(\mathbf{pn})\{(\mathbf{p} - \mathbf{q}, \mathbf{p})$$
$$- (\mathbf{p} - \mathbf{q}, \mathbf{n})(\mathbf{pn})\} - \omega\frac{(\mathbf{p} - \mathbf{q}, \mathbf{n})}{(\mathbf{p} - \mathbf{q})^2}(\mathbf{qn})\{(\mathbf{p} - \mathbf{q}, \mathbf{q})$$
$$- (\mathbf{p} - \mathbf{q}, \mathbf{n})(\mathbf{qn})\} + \omega\frac{(\mathbf{p} + \mathbf{q}, \mathbf{n})}{(\mathbf{p} + \mathbf{q})^2}(\mathbf{pn})\{(\mathbf{p} + \mathbf{q}, \mathbf{p})$$
$$- \omega\frac{(\mathbf{p} + \mathbf{q}, \mathbf{n})}{(\mathbf{p} + \mathbf{q})^2}(\mathbf{qn})\{(\mathbf{p} + \mathbf{q}, \mathbf{p}) - (\mathbf{p} + \mathbf{q}, \mathbf{n})(\mathbf{qn})\}. \tag{36}$$

If we carry out the integration over all the directions of photon emission **n** for a given **q** and assume that[2] $\rho_f = \mathbf{q}^2\omega^2/2\,(2\pi)^6$, then we shall obtain for the differential cross section the following expression

$$d\Phi = \frac{8}{15} r_0^2 \frac{1}{137} \frac{|\mathbf{q}|^2 d|\mathbf{q}| \sin\theta_0 \, d\theta_0}{|\mathbf{p}|(\mathbf{p}^2-\mathbf{q}^2)} \left\{\left(\frac{1}{(\mathbf{p}-\mathbf{q})^4} + \frac{1}{(\mathbf{p}+\mathbf{q})^4}\right)\right.$$

$$\times (4(\mathbf{p}^2-\mathbf{q}^2)^2 + 3\mathbf{p}^2\mathbf{q}^2\sin^2\theta_0) - (1+\zeta_0^{(1)}\zeta_0^{(2)})$$

$$\left.\times\left(\frac{4(\mathbf{p}^2-\mathbf{q}^2)^2 + 3\mathbf{p}^2\mathbf{q}^2\sin^2\theta_0}{(\mathbf{p}^2-\mathbf{q}^2)^2} + \frac{6\mathbf{p}^4\mathbf{q}^4\sin^2\theta_0}{(\mathbf{p}^2-\mathbf{q}^2)^4}\right)\right\}, \qquad (37)$$

r_0 is the classical electron radius. Formula (37) for unpolarized electrons agrees with the corresponding formula due to Garibyan.[4] The spin correction arises exclusively due to exchange (the term which is proportional to $\zeta_0^{(1)}\zeta_0^{(2)}$ is given by the interference between the direct and the exchange terms). There is no azimuthal asymmetry, just as in the case of Møller scattering. The change in the electron polarization after a radiative collision is also a pure exchange effect.

For a fixed **k**

$$\zeta_q = \frac{\zeta_0^{(1)}\alpha(\mathbf{p}+\mathbf{q})^4 + \zeta_0^{(2)}\beta(\mathbf{p}-\mathbf{q})^4 - (\mathbf{p}^2-\mathbf{q}^2)\gamma(\zeta_0^{(1)}+\zeta_0^{(2)})}{\alpha(\mathbf{p}+\mathbf{q})^4 + \beta(\mathbf{p}-\mathbf{q})^4 - (\mathbf{p}^2-\mathbf{q}^2)\gamma(1+\zeta_0^{(1)}\zeta_0^{(2)})}, \qquad (38)$$

α and γ are found from (36).

After averaging over all **n** we obtain

$$\zeta_q = \left\{\zeta_0^{(1)}\frac{(\mathbf{p}+\mathbf{q})^4}{(\mathbf{p}+\mathbf{q})^4+(\mathbf{p}-\mathbf{q})^4} + \zeta_0^{(2)}\frac{(\mathbf{p}-\mathbf{q})^4}{(\mathbf{p}+\mathbf{q})^4+(\mathbf{p}-\mathbf{q})^4}\right.$$

$$\left. - M(\zeta_0^{(1)}+\zeta_0^{(2)})\right\}[1-M(1+\zeta_0^{(1)}\zeta_0^{(2)})]^{-1},$$

where

$$M = \left\{\frac{4(\mathbf{p}^2-\mathbf{q}^2)^2 + 3\mathbf{p}^2\mathbf{q}^2\sin^2\theta_0}{(\mathbf{p}^2-\mathbf{q}^2)^2} + \frac{6\mathbf{p}^4\mathbf{q}^4\sin^2\theta_0}{(\mathbf{p}^2-\mathbf{q}^2)^4}\right\}$$

$$\times\left(\frac{1}{(\mathbf{p}-\mathbf{q})^4}+\frac{1}{(\mathbf{p}+\mathbf{q})^4}\right)^{-1}\{4(\mathbf{p}^2-\mathbf{q}^2)^2 + 3\mathbf{p}^2\mathbf{q}^2\sin^2\theta_0\}^{-1}. \qquad (39)$$

An unpolarized electron acquires as a result of scattering by a polarized target an average spin which is equal to

$$\zeta_q = \zeta_0^{(2)}\left\{\frac{(\mathbf{p}-\mathbf{q})^4}{(\mathbf{p}+\mathbf{q})^4+(\mathbf{p}-\mathbf{q})^4} - M\right\}\Big/(1-M). \qquad (40)$$

For the polarization correlation tensor of the electrons we obtain

$$T_{ik} = \frac{\{\alpha(\mathbf{p}+\mathbf{q})^4+\beta(\mathbf{p}-\mathbf{q})^4\}\zeta_{0i}^{(1)}\zeta_{0k}^{(2)} - (\mathbf{p}^2-\mathbf{q}^2)\gamma(\zeta_{01}^{(1)}\zeta_{0k}^{(2)}+\delta_{ik})}{\alpha(\mathbf{p}+\mathbf{q})^4+\beta(\mathbf{p}-\mathbf{q})^4-(\mathbf{p}^2-\mathbf{q}^2)\gamma(1+\zeta_0^{(1)}\zeta_0^{(2)})}. \qquad (41)$$

In the case $\zeta_0^{(1)} = \zeta_0^{(2)} = 0$ we obtain $T_{ik}^{(\mathrm{unp})} = 0$, if $i \neq k$, while in the case $i = k$ we have

$$T_{ii} = -\frac{\gamma(\mathbf{p}^2-\mathbf{q}^2)}{\alpha(\mathbf{p}+\mathbf{q})^4+\beta(\mathbf{p}-\mathbf{q})^4-\gamma(\mathbf{p}^2-\mathbf{q}^2)^2}. \qquad (41a)$$

We now consider the linear polarization of bremsstrahlung for a photon momentum **k**. For the basic polarization unit vectors we shall take the unit vectors $\mathbf{e}_1$ and $\mathbf{e}_2$, which are directed respectively along $[\mathbf{p}\times\mathbf{n}]\times\mathbf{n}$ and $\mathbf{p}\times\mathbf{n}$.

In the case $\widetilde{\epsilon}_1 = \int \epsilon_1 \rho_f \Phi d\Omega_q / \int \rho_f \Phi d\Omega_q$ we obtain an awkward expression containing logarithms which we shall not reproduce here. In this case $0 < \widetilde{\epsilon}_1 < 1$; $\epsilon_1 = 1$ for $k = p^2/2$. Calculation shows that $\widetilde{\epsilon}_2 = 0$.

With regard to the circular polarization we have in the first approximation $\epsilon_3 = 0$. In the second approximation we shall obtain for ϵ_3 and $\widetilde{\epsilon}_3$ a quantity of order of magnitude $|\mathbf{p}| \ll 1$.

In conclusion we will note that polarization phenomena in radiative collisions of electrons with positrons in the ultra-relativistic limit do not differ qualitatively from polarization phenomena in the collision of two electrons. In the nonrelativistic limit all the polarization effects are of order $|\mathbf{p}|^2$, and may be neglected. Linear polarization of bremsstrahlung exists in the direction of the vector $[[\mathbf{p}-\mathbf{q}]\times\mathbf{n}]\times\mathbf{n}$.

All the results of Sec. 3 for radiative collisions of two electrons hold also for radiative collisions of an electron and a positron.

The author expresses his deep gratitude to Professor Ya. A. Smorodinskiĭ for guiding this work.

APPENDIX

We write the elements of the scattering matrix for radiative collisions of electrons with the aid of two-row matrices in the following form

$$(q|\mathscr{E}|p) \sim \frac{e^3}{\overline{\omega V}}\{(\varphi^{(1)*}C^{(q_1p_1)}\varphi_0^{(1)})(\varphi^{(2)*}D^{(q_2p_2)}\varphi_0^{(2)})$$

$$-\sum_{\mathbf{m}_1\mathbf{m}_2\mathbf{m}_3}(\varphi^{(1)*}C_{\mathbf{m}}^{'(q_1p_1)}\varphi_0^{(1)})(\varphi^{(2)*}D_{\mathbf{m}}^{'(q_2p_2)}\varphi_0^{(2)})$$

$$+(\varphi^{(2)*}C^{(q_2p_2)}\varphi_0^{(2)})(\varphi^{(1)*}D^{(q_1p_1)}\varphi_0^{(1)})$$

$$-\sum_{\mathbf{m}_1\mathbf{m}_2\mathbf{m}_3}(\varphi^{(2)*}C_{\mathbf{m}}^{'(q_2p_2)}\varphi_0^{(2)})(\varphi^{(1)*}D_{\mathbf{m}}^{'(q_1p_1)}\varphi_0^{(1)})\}$$

$-\{$ the same, with the following replacement:

$$\varphi^{(1)} \rightleftarrows \varphi^{(2)}, \ q_1 \rightleftarrows q_2\}.$$

Here $\mathbf{m}_1$, $\mathbf{m}_2$ and $\mathbf{m}_3$ is a set of three mutually perpendicular unit vectors

$$\mathbf{m}_1 = \frac{\mathbf{q}_1+\mathbf{p}_1}{|\mathbf{q}_1+\mathbf{p}_1|}, \quad \mathbf{m}_2 = \frac{\mathbf{q}_1-\mathbf{p}_1}{|\mathbf{q}_1-\mathbf{p}_1|}, \quad \mathbf{m}_3 = \frac{[\mathbf{q}_1\times\mathbf{p}_1]}{|[\mathbf{q}_1\times\mathbf{p}_1]|};$$

$$\begin{aligned}
C^{(q_1p_1)} = {} & \frac{(W_1+\mu)^{1/2}(E_1+\mu)^{1/2}}{2(E_1W_1)^{1/2}(q_2-p_2)^2}\left\{\frac{1}{q_1k}\left[\omega\frac{(\mathbf{q}_1\mathbf{e})}{W_1+\mu}+\omega\frac{(\mathbf{p}_1\mathbf{e})}{E_1+\mu}+2(\mathbf{e}\mathbf{q}_1)\left(1+\frac{q_1p_1}{(E_1+\mu)(W_1+\mu)}\right)+\omega\frac{(\mathbf{q}_1\mathbf{e})(\mathbf{p}_1\mathbf{n})-(\mathbf{p}_1\mathbf{e})(\mathbf{q}_1\mathbf{n})}{(W_1+\mu)(E+\mu)}\right.\right.\\
& \left.+i\left(\boldsymbol{\sigma},\omega\frac{[\mathbf{q}_1\times\mathbf{e}]}{W_1+\mu}-\omega\frac{[\mathbf{p}_1\times\mathbf{e}]}{E_1+\mu}+2(\mathbf{e}\mathbf{q}_1)\frac{[\mathbf{q}_1\times\mathbf{p}_1]}{(W_1+\mu)(E_1+\mu)}-\omega[\mathbf{n}\times\mathbf{e}]-\omega\frac{\mathbf{q}_1(\mathbf{p}_1[\mathbf{n}\times\mathbf{e}])}{(W_1+\mu)(E_1+\mu)}+\omega\frac{[\mathbf{q}_1\times\mathbf{e}](\mathbf{p}_1\mathbf{n})-[\mathbf{q}_1\times\mathbf{n}](\mathbf{p}_1\mathbf{e})}{(W_1+\mu)(E_1+\mu)}\right)\right]\\
& +\frac{1}{p_1k}\left[\omega\frac{(\mathbf{q}_1\mathbf{e})}{W_1+\mu}+\omega\frac{(\mathbf{p}_1\mathbf{e})}{E_1+\mu}-2(\mathbf{e}\mathbf{p}_1)\left(1+\frac{q_1p_1}{(W_1+\mu)(E_1+\mu)}\right)-\omega\frac{(\mathbf{q}_1\mathbf{e})(\mathbf{p}_1\mathbf{n})-(\mathbf{p}_1\mathbf{e})(\mathbf{q}_1\mathbf{n})}{(W_1+\mu)(E_1+\mu)}+i\left(\boldsymbol{\sigma},\omega\frac{[\mathbf{q}_1\times\mathbf{e}]}{W_1+\mu}-\omega\frac{[\mathbf{p}_1\times\mathbf{e}]}{E_1+\mu}\right.\right.\\
& \left.\left.\left.-2(\mathbf{e}\mathbf{p}_1)\frac{[\mathbf{q}_1\times\mathbf{p}_1]}{(E_1+\mu)(W_1+\mu)}+\omega[\mathbf{n}\times\mathbf{e}]+\omega\frac{\mathbf{q}_1(\mathbf{p}_1[\mathbf{n}\times\mathbf{e}])}{(W_1+\mu)(E_1+\mu)}-\omega\frac{[\mathbf{q}_1\times\mathbf{e}](\mathbf{p}_1\mathbf{n})-[\mathbf{q}_1\times\mathbf{n}](\mathbf{p}_1\mathbf{e})}{(W_1+\mu)(E_1+\mu)}\right)\right]\right\},
\end{aligned}$$

$$\begin{aligned}
C_{\mathbf{m}}^{(q_1p_1)} = {} & \frac{(W_1+\mu)^{1/2}(E_1+\mu)^{1/2}}{2(E_1W_1)^{1/2}(q_2-p_2)^2}\left\{\frac{1}{q_1k}\left[k(\mathbf{m}\mathbf{e})\left(1+\frac{q_1p_1}{(W_1+\mu)(E_1+\mu)}\right)+2(\mathbf{q}_1\mathbf{e})\left(\frac{\mathbf{q}_1\mathbf{m}}{W_1+\mu}+\frac{\mathbf{p}_1\mathbf{m}}{E_1+\mu}\right)+\omega\frac{(\mathbf{q}_1\mathbf{e})(\mathbf{p}_1\mathbf{m})-(\mathbf{m}\mathbf{q}_1)(\mathbf{p}_1\mathbf{e})}{(W_1+\mu)(E_1+\mu)}\right.\right.\\
& +\omega\frac{(\mathbf{p}_1\mathbf{e})(\mathbf{n}\mathbf{m})-(\mathbf{n}\mathbf{p}_1)(\mathbf{m}\mathbf{e})}{E_1+\mu}+i\left(\boldsymbol{\sigma},\omega(\mathbf{m}\mathbf{e})\frac{[\mathbf{q}_1\times\mathbf{p}_1]}{(W_1+\mu)(E_1+\mu)}+2(\mathbf{q}_1\mathbf{e})\left(\frac{[\mathbf{q}_1\times\mathbf{m}]}{W_1+\mu}-\frac{[\mathbf{p}_1\times\mathbf{m}]}{E_1+\mu}\right)+\omega\frac{(\mathbf{q}_1\mathbf{e})[\mathbf{p}_1\times\mathbf{m}]-[\mathbf{q}_1\times\mathbf{m}](\mathbf{p}_1\mathbf{e})}{(W_1+\mu)(E_1+\mu)}\right.\\
& -\omega\frac{[\mathbf{p}_1\times\mathbf{e}](\mathbf{n}\mathbf{m})-[\mathbf{p}_1\times\mathbf{n}](\mathbf{m}\mathbf{e})}{E_1+\mu}+\omega\frac{[\mathbf{q}_1\times\mathbf{e}](\mathbf{n}\mathbf{m})-[\mathbf{q}_1\times\mathbf{n}](\mathbf{m}\mathbf{e})}{W_1+\mu}+\omega\frac{\mathbf{q}_1(\mathbf{p}_1[\mathbf{e}\times\mathbf{m}])}{(W_1+\mu)(E_1+\mu)}-\omega\frac{\mathbf{q}_1([\mathbf{n}\times\mathbf{e}]\mathbf{m})}{W_1+\mu}-\omega\frac{\mathbf{p}_1([\mathbf{n}\times\mathbf{e}]\mathbf{m})}{E_1+\mu}\\
& \left.\left.+\omega[\mathbf{e}\times\mathbf{m}]\right)\right]+\frac{1}{p_1k}\left[\omega(\mathbf{m}\mathbf{e})\left(1+\frac{q_1p_1}{(W_1+\mu)(E_1+\mu)}\right)-2(\mathbf{p}_1\mathbf{e})\left(\frac{\mathbf{p}_1\mathbf{m}}{E_1+\mu}+\frac{\mathbf{q}_1\mathbf{m}}{W_1+\mu}\right)-\omega\frac{(\mathbf{q}_1\mathbf{e})(\mathbf{p}_1\mathbf{m})-(\mathbf{q}_1\mathbf{m})(\mathbf{p}_1\mathbf{e})}{(W_1+\mu)(E_1+\mu)}\right.\\
& +\omega\frac{(\mathbf{p}_1\mathbf{e})(\mathbf{n}\mathbf{m})-(\mathbf{n}\mathbf{p}_1)(\mathbf{m}\mathbf{e})}{E_1+\mu}+\omega\frac{(\mathbf{q}_1\mathbf{e})(\mathbf{n}\mathbf{m})-(\mathbf{q}_1\mathbf{n})(\mathbf{m}\mathbf{e})}{W_1+\mu}+i\left(\boldsymbol{\sigma},\omega(\mathbf{m}\mathbf{e})\frac{[\mathbf{q}_1\times\mathbf{p}_1]}{(W_1+\mu)(E_1+\mu)}-2(\mathbf{p}_1\mathbf{e})\left(\frac{[\mathbf{q}_1\times\mathbf{m}]}{W_1+\mu}-\frac{[\mathbf{p}_1\times\mathbf{m}]}{E_1+\mu}\right)\right.\\
& -\omega\frac{[\mathbf{q}_1\times\mathbf{e}](\mathbf{p}_1\mathbf{m})-[\mathbf{q}_1\times\mathbf{m}](\mathbf{p}_1\mathbf{e})}{(W_1+\mu)(E_1+\mu)}-\omega\frac{[\mathbf{p}_1\times\mathbf{e}](\mathbf{n}\mathbf{m})-[\mathbf{p}_1\times\mathbf{n}](\mathbf{m}\mathbf{e})}{E_1+\mu}+\omega\frac{[\mathbf{q}_1\times\mathbf{n}](\mathbf{n}\mathbf{m})-[\mathbf{q}_1\times\mathbf{n}](\mathbf{m}\mathbf{e})}{W_1+\mu}\\
& \left.\left.\left.-\omega\frac{\mathbf{q}_1(\mathbf{p}_1[\mathbf{e}\times\mathbf{m}])}{(W_1+\mu)(E_1+\mu)}-\omega\frac{\mathbf{q}_1([\mathbf{n}\times\mathbf{e}]\mathbf{m})}{W_1+\mu}-\omega\frac{\mathbf{p}_1([\mathbf{n}\times\mathbf{e}]\mathbf{m})}{E_1+\mu}+\omega[\mathbf{m}\times\mathbf{e}]\right)\right]\right\},
\end{aligned}$$

$$D^{(p_1q_1)} = 1+\frac{p_1q_1}{(W_1+\mu)(E_1+\mu)}+i\left(\boldsymbol{\sigma},\frac{[\mathbf{q}_1\times\mathbf{p}_1]}{(W_1+\mu)(E_1+\mu)}\right),$$

$$D_{\mathbf{m}}^{(p_1q_1)} = \frac{\mathbf{p}_1\mathbf{m}}{E_1+\mu}+\frac{\mathbf{q}_1\mathbf{m}}{W_1+\mu}+i\left(\boldsymbol{\sigma},\frac{[\mathbf{q}\times\mathbf{m}]}{W_1+\mu}-\frac{[\mathbf{p}_1\times\mathbf{m}]}{E_1+\mu}\right),$$

$$pq \doteq (\mathbf{p}\mathbf{q})-EW, \qquad (p-q)^2 \doteq (\mathbf{p}-\mathbf{q})^2-(E-W)^2.$$

$C^{(p_2q_2)}$, $D^{(p_2q_2)}$, $C^{(p_1q_2)}$ etc. are obtained from the above by means of replacing the appropriate indices, $\mathbf{n}$ is a unit vector in the direction of photon propagation. In the nonrelativistic limit in the center of mass the quantities $C_{\mathbf{m}}^{(p_1q_1)}$, $D_{\mathbf{m}}^{(p_1q_1)}$ etc. are equal to zero.

$$C^{(q_1p_1)} = \frac{4\omega(\mathbf{p}-\mathbf{q},\mathbf{n})}{(\mathbf{p}-\mathbf{q})^2}(\mathbf{p}-\mathbf{q},\mathbf{e})+2\{\mathbf{p}\mathbf{e})(\mathbf{p}\mathbf{n})-(\mathbf{q}\mathbf{e})(\mathbf{q}\mathbf{n})\},$$

$$C^{(q_1p_2)} = \frac{4\omega(\mathbf{p}+\mathbf{q},\mathbf{n})}{(\mathbf{p}+\mathbf{q})^2}(\mathbf{p}+\mathbf{q},\mathbf{e})+2\{(\mathbf{p}\mathbf{e})(\mathbf{p}\mathbf{n})-(\mathbf{q}\mathbf{e})(\mathbf{q}\mathbf{n})\},$$

$$C^{(q_2p_2)} = C^{(q_2p_1)} = 2\{(\mathbf{p}\mathbf{e})(\mathbf{p}\mathbf{n})-(\mathbf{q}\mathbf{e})(\mathbf{q}\mathbf{n})\},$$

$$D^{(q_1p_1)} = D^{(q_2p_2)} = D^{(q_1p_2)} = D^{(q_2p_1)} = I, \text{ where } I = \begin{pmatrix}1&0\\0&1\end{pmatrix}.$$

---

[1] A. I. Akhiezer and V. B. Berestetskiĭ, Квантовая электродинамика, (Quantum Electrodynamics), GITTL, 1953.

[2] J. Katzenstein, Phys. Rev. **78**, 160 (1950).

[3] P. É. Nemirovskiĭ, JETP **18**, 893 (1948).

[4] G. M. Garibyan, JETP **24**, 617 (1953).

[5] G. M. Garibyan, Izv. Akad. Nauk Arm. S.S.R. **3**, 1 (1952).

[6] J. Joseph and F. Rohrlich, Revs. Modern Phys. **30**, 354 (1958).

[7] H. A. Tolhoek, Revs. Modern Phys. **28**, 277 (1956).

[8] L. Michel and A. S. Wightman, Phys. Rev. **98**, 1190 (1955).

[9] G. Bobel, Nuovo cimento **6**, 1241 (1957).

[10] L. Wolfenstein and J. Ashkin, Phys. Rev. **85**, 947 (1952).

[11] R. H. Dalitz, Proc. Roy. Soc. (London) **A65**, 175 (1952).

[12] U. Fano, Phys. Rev. **93**, 121 (1954).

[13] G. V. Rozenberg, Usp. Fiz. Nauk **55**, 81 (1955).

[14] H. Banerjee, Phys. Rev. **111**, 532 (1958).

[15] K. W. McVoy, Phys. Rev. **111**, 1933 (1958).

Translated by G. Volkoff

SOVIET PHYSICS JETP VOLUME 37(10), NUMBER 6 JUNE, 1960

CONDENSATION OF A CLOUD OF VAPORIZED MATTER EXPANDING IN VACUUM

Yu. P. RAĬZER

Submitted to JETP editor May 18, 1959

J. Exptl. Theoret. Phys. (U.S.S.R.) 37, 1741-1750 (December, 1959)

We consider the kinetics of condensation of a cloud of vaporized matter expanding in vacuo. It is shown that, under a variety of initial conditions, the matter expands at infinity partly as a gas and partly in the form of very small particles of a condensate, and the number and size of these particles depends on the evaporated mass and on its initial temperature. It is suggested that when a large meteorite strikes the surface of a planet without an atmosphere the substance of the planet and the body of the meteorite may evaporate and consequently condense; this process may be one of the sources of cosmic dust. The feasibility of laboratory investigations of the condensation of metallic vapors and of the properties or small particles involved are discussed.

WHEN a high velocity meteorite strikes a surface of a planet or satellite that has no atmosphere (such as the moon), a cloud of evaporated matter is formed and expands in vacuo. To a certain degree, a similar phenomenon is encountered under laboratory conditions, for example, when wires are exploded by electric currents in vacuo, in high-intensity pulsed x-ray tubes,[1] etc.

What is the state of a substance undergoing very large expansion? The point is that the expanding and cooling gas (more accurately, the vapor) must become saturated at a certain instant of time, after which condensation should begin.[2] According to the laws of thermodynamics, a vapor adiabatically expanded to infinity and cooled to zero temperature should become fully condensed. On the other hand, it is clear that in the limit of very rapid expansion, a pure gas is scattered to infinity, since there is not enough time for condensation to take effect. The degree of condensation during the stage of large expansion and, what is most interesting, the number and sizes of the condensate particles, are determined by the kinetics of condensation during the expansion process, an examination of which is indeed the topic of the present paper.

It is found that when tremendous meteorites strike the surface of a small planet (having a low critical velocity) without atmosphere, a considerable mass of the initally evaporated ground and meteorite body are scattered in space in the form of minute solid particles. A hypothesis can be advanced that this process is one of the sources of cosmic dust.

A study of the kinetics of condensation in an expanding cloud and a clarification of the conditions under which the condensate particles become noticeable may bring about new ways of experimental investigation of condensation of vapors of usually solid substances, and also of the optical properties of minute particles.

1. QUALITATIVE ASPECT OF THE CONDENSATION PROCESS

We shall examine condensation by using a simple model of a gas sphere expanding adiabatically in vacuo, without touching upon the hydrodynamics of the process that has resulted in the gas cloud. By suitable choice of sphere parameters — mass M and energy E — such a model can always be reconciled more or less correctly with the specific conditions of interest. For the sake of being definite, let us assume that in the initial instant of time the gas was stationary and its density equaled the normal density of the solid state ρ_0. The condensation begins during the stage of large expansion and strong cooling (it is assumed that the initial internal energy $\epsilon_0 = E/M$ exceeds slightly the heat of evaporation U). Here almost all the energy is already kinetic and the gas is scattered almost inertially with a mean velocity $u = \sqrt{2\epsilon_0}$. Accurate to a factor on the order of unity, the radius of the boundary of the sphere is $r = ut$ and the mean density is*

$$\rho = 3M / 4\pi r^3 = \rho_0 (t_0 / t)^3, \tag{1}$$

where $t_0 = r_0/u$ is the time scale, and r_0 is the initial radius. The law of cooling is given by the adiabatic equation

$$T = [Ae^{S/R}\rho]^{\gamma-1} \sim t^{-3(\gamma-1)}. \tag{2}$$

---

*We shall be interested only in quantities averaged over the mass.

Here S is the specific entropy, γ the adiabatic exponent, and A a constant determined by the well-known formulas of statistical mechanics. Saturation takes place when the Poisson adiabat (1) intersects the vapor-tension curve, which can be represented approximately as

$$\rho = Be^{-U/RT}, \quad B \approx \text{const.} \tag{3}$$

After passing through the saturation stage, the vapor continues to cool "by inertia," following the Poisson adiabat, and becomes supersaturated (see diagram). The speed of formation of the nuclei of the liquid phase depends to a very high degree on the degree of supersaturation, and therefore the number of produced condensation centers increases very rapidly with increasing supersaturation. Even a short time after passing through the saturation state, which is considerably shorter than the saturation time t_1 itself, the speed of condensation becomes such that the liberation of latent heat stops the increase in supersaturation (supercooling).

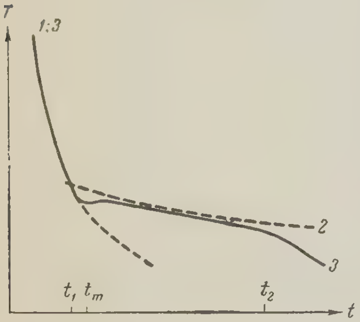

Schematic time dependence of the temperature of the substance. 1 – Poisson adiabat, 2 – equilibrium curve for a two-phase system with specified entropy (initially, at a small degree of condensation, the curve almost coincides with the vapor-tension curve), 3 – true adiabat of the substance.

Moreover, the condensation accelerates even if the number of centers is constant, owing to the increase in the surface of the drops to which the vapor molecules adhere. Therefore the accelerating condensation not only stops the rise in supercooling, but slows it down. The formation of new nuclei, which is exceedingly sensitive to the magnitude of supersaturation, immediately ceases and condensation from now on proceeds via adhesion of vapor molecules to the drops already present. Thus, all the condensation centers are generated at the very beginning of the process, directly after saturated state is reached. Their number, which at that time equals the number of particles of condensate scattering to infinity, depends on the maximum supersaturation attained, which in turn is determined by the interplay between two opposite influences: cooling of the vapor due to the work of expansion, and heating of the vapor due to the latent heat liberated during condensation.

After passing through the maximum, the degree of supersaturation does not fall to zero; by regulating the balance between the adhesion of molecules to the drops and evaporation of the drops, it is automatically set at a level where a small excess of adhesion over evaporation exists: the speed of condensation has "followed" the expansion and a state close to saturation has been maintained in the system. In this case the adiabat creeps along the equilibrium curve of the two-phase system (of fixed entropy) and almost coincides with it.

At large expansion the acts of adhesion become too rare; the rate of adhesion, which is proportional to the density, i.e., $\sim t^{-3}$, is no longer capable of "following" the expansion, and the thermodynamic "equilibrium" in the system is disturbed, leading to so-called quenching. Soon the condensation ceases completely, and the residue of the gas (together with the drops) is again cooled rapidly along the Poisson adiabat (see diagram).

The degree of condensation in the final state (or, at a known number of drops — the dimensions of the condensate particles) is determined by the instant when the thermodynamic "equilibrium" is disturbed and quenching occurs. All the numerical calculations will henceforth pertain to the evaporation and condensation of iron meteorites. The table lists the calculated temperature and number of atoms of iron per cm^3, T_1 and n_1, at the instant when saturation is reached, for certain values of the initial energy ϵ_0. The same table lists the entropy S, on which the parameters of the saturated state depend directly, and the initial temperature T_0 (as well as the scattering velocity u).* For iron vapor in the region of condensation, $\gamma = 5/3$, $A = 6.65 \times 10^{-4}\ \text{cm}^3\,\text{g}^{-1}\,\text{deg}^{3/2}$, and $B = 3.3 \times 10^4\ \text{g/cm}^3$.

2. EQUATIONS FOR THE KINETICS OF THE CONDENSATION

Let us write down the adiabatic equation in the condensation region

---

*In the calculation of the thermodynamic functions of a gas at the density of solid iron, $\rho_0 = 7.87\ \text{g/cm}^3$, the nuclear specific heat was represented by the formula $c_{\text{nuc}} = 3R$ at $T < T'$ and $c_{\text{nuc}} = {}^3\!/_2 R$ at $T > T'$, where T' is the temperature at which the kinetic energy of thermal motion of the nuclei, ${}^3\!/_2 RT'$, is equalized with the height of the potential barrier for the free displacement of the atoms in the body, i.e., with a magnitude on the order of the self-diffusion activation energy. We used $T' = 19{,}000°$. The electronic portion of the specific heat is found from Latter's data,[3] based on calculations by the Thomas-Fermi method. In the temperature interval $T \approx 2$–30 ev and at a density ρ_0 the electron energy is fairly well approximated by the formula $\varepsilon_e = 0.865\,T^{1.8}$ ev/atom. The Debye temperature of iron is $\Theta = 420°$.

ε_0, ev/atom	T_0, ev	S, cal/mole-deg	u, km/sec	T_1, deg	n_1, cm^{-3}
25.6	5	48.3	9.2	3100	$8.01\cdot10^{19}$
71.9	10	60.8	15.5	2130	$7.15\cdot10^{16}$
138	15	71.5	21.4	1700	$2.86\cdot10^{14}$
222	20	81.3	27.2	1430	$1.43\cdot10^{12}$

$$[c_1(1-x)+c_2x]\,dT + RT(1-x)\,dV/V$$
$$-[U-(c_2-c_1)T]\,dx = 0. \qquad (4)$$

Here c_1 and c_2 are the specific heats of the vapor (at constant volume) and the liquid, $V = 1/\rho$ is the specific volume, and x is the degree of condensation $[(c_2-c_1)T \ll U$ in the third term].

If $I(t)$ is the speed of formation of condensation centers, i.e., the number of surviving nuclei per molecule per second, and $g(t, t')$ is the number of molecules contained at the instant t in a drop that has grown from a nucleus produced at the instant t', then the degree of condensation at the instant t is

$$x = \int_{t_1}^{t} I(t')\,g(t, t')\,dt'. \qquad (5)$$

We make the following basic assumption: let the expansion be so slow that the process of production of the nuclei is quasi-stationary, i.e., the rate of production at each instant coincides with the rate under stationary conditions, in which the supersaturation is maintained constant (equal to the actual value at a given instant), and the supercritical nuclei are eliminated from the system and are replaced by an equivalent amount of vapor (the limits of applicability of this assumption will be explained below).*

Under stationary conditions and in the absence of ions, the speed of production of nuclei is known to be[5,6]

$$I_n = Ce^{-\beta} = n\bar{v}2\omega\sqrt{\sigma/kT}\,e^{-\beta}, \qquad (6)$$
$$\beta = \Delta\Phi_{max}/kT = 16\pi\sigma^3\omega^2/3k^3q^2T\theta = b/\theta^2. \qquad (7)$$

Here n is the number of molecules of vapor per cm^3, $\bar{v}$ their thermal velocity, σ the surface tension, ω the volume per molecule in the liquid, $q = U/R$, and b is an arbitrary symbol. θ is the degree of supercooling, which is connected with the radius r^* of a critical nucleus containing $g^* = 4\pi r^{*3}/3\omega$ molecules by the condition for maximum thermodynamic potential $\Delta\Phi(r)$:

$$\theta = (T_{eq} - T)/T_{eq} = 2\sigma\omega/kqr^*, \qquad (8)$$

where T_{eq} is the temperature of vapor saturated at a given density, expressed by (3).

It is known that the electric charge facilitates greatly the formation of condensation centers. When a gas expands in vacuo, the ionization during the stage of strong cooling is always much greater than the thermodynamic-equilibrium value, as a result of the quenching effect,[7] so that the number of ions is quite considerable. Unlike the process in a cloud chamber, where so-called critical supersaturation is produced artificially and all ions simply become condensation centers, in the case of "slow" expansion saturation does not reach a critical value and the condensation is produced by far from all ions. Bearing this in mind, we must generalize the formula for the rate of production of nuclei to include the case of charged nuclei.

After finding the maximum value of the known expression[6] for the increase in thermodynamic potential of the system upon production of a charged drop of radius r in the vapor, and transforming $[\Delta\Phi_e(r)]_{max}$ with the aid of (7), we can represent the activation energy in the following form

$$\beta_e = \Delta\Phi_{e\,max}/kT = \beta(\theta)\,[1 + 8a^3/r_e^{*3} - 6a^3/dr_e^{*2}], \qquad (9)$$

where d is the effective radius of the ion in the drop, which must be defined as a radius of the molecular cell in the liquid, $d = (3\omega/4\pi)^{1/3}$, r_e^* is the critical radius of the charged nucleus [connected with the supercooling* θ by the condition that $\Delta\Phi_e(r)$ be a maximum], and $a = (e^2/16\pi\sigma)^{1/3}$.

In the limit as $\theta \to 0$ the difference between the charged and uncharged nuclei disappears: $r_e^* \approx r^*$ and $\Delta\Phi_{e\,max} \approx \Delta\Phi_{max}$. Calculations show that when the supercooling is only slightly less than the critical value θ_k both radii are almost the same. To the contrary, the activation energy $\Delta\Phi_{e\,max}$ is considerably less than $\Delta\Phi_{max}$ down to very small values of supersaturation, which indeed corresponds to a sharp predominance of production of charged nuclei.

---

*An analogous assumption was used by Tunitskiĭ,[4] who considered the condensation of a homogenous vapor at constant volume and specified initial supersaturation.

*$\theta = (2\sigma\omega/kqr_e^*)(1-a^3/r_e^{*3})$; the maximum (critical) value of supercooling corresponds to the radius $r_e^* = 4^{1/3}a$ and is equal to $\theta_k = (3\sigma\omega/2)\times4^{1/3}kqa$. For $\theta \geqslant \theta_k$ the maximum of the function $\Delta\Phi_e(r)$ vanishes and the charged complexes of all sizes exhibit a tendency to grow without limit. The nuclei usually contain one ion each so that e is the electron charge; the dielectric constant of the drop is assumed to be infinite.

Deriving successively the formula for the rate of formation of charged nuclei (per ion), it is possible to show that when the supercooling is not too close to critical the factor preceding the exponent is quite close to C in (6)

Thus, at $\theta < \theta_k$ the total rate of formation of condensation centers (per molecule) is

$$I = I_n + yI_e = C\,(e^{-\beta} + ye^{-\beta_e}), \qquad (10)$$

where y is the number of ions per molecule.

The rate of growth of a supercritical drop equals the difference between the rates of adhesion and evaporation of the molecules. We neglect as an approximation the difference between the evaporation from a drop and the evaporation from a flat liquid surface (this, as shown by calculation, does not exaggerate the rate of growth greatly). In addition, we assume that the temperature of the drop coincides with the temperature of the vapor (the heat of condensation liberated by the drop is dissipated sufficiently rapidly). Assuming furthermore a coefficient of accommodation equal to unity, we can write[5,6]

$$dg\,/\,dt = 4\pi d^2\, g^{2/3}\, n\bar{v}\,[1 - e^{-q\theta/T}]. \qquad (11)$$

The system comprising (4), (5), and (1) should be solved with initial conditions $T = T_1$ and $x = 0$ at $t = t_1$.

3. NUMBER OF CONDENSATION CENTERS

All the condensation centers are generated during a very short time interval, when the supercooling is close to the maximum value $\theta_{\max}$. The total number of centers (per molecule) is

$$\nu = \int\limits_{t_1}^{\infty} I\,[\theta\,(t')]\,dt' = I\,(\theta_{max})\,\Delta t_m, \qquad (12)$$

where Δt_m is the effective duration of the saturation maximum.

Relegating the approximate calculation of $\theta_{\max}$ and ν to the appendix, we give here only the final results. The maximum supercooling, as a function of the parameters of the saturated state and of the constants of the substance, is determined from the transcendental equation

$$\frac{1}{I\,(\theta_{max})\,t_1} = 5.3\cdot 10^{-5}\,\frac{q}{T_1}\left\{\frac{\bar{c}_1\theta_{max}^3}{b}\left[1 - \exp\left(-\frac{q}{T_1}\,\theta_{max}\right)\right]\frac{t_1}{\tau_1}\right\}^3, \qquad (13)$$

where the function $I(\theta)$ is given by (6) – (10), $\bar{c}_1 = c_1/R$, and the reciprocal time, $1/t_1 = 4\pi d^2 n_1\bar{v}_1$, is a quantity of the order of the probability of the gas-kinetical collisions of the vapor molecule during the instant of saturation, since d, by definition, is of the order of the radius of the molecule. The number of condensation centers is

$$\nu = I\,(\theta_{max})\,\frac{\pi}{2}\,\bar{c}_1\,\frac{\theta_{max}^3}{b}\,t_1 = 5\cdot 10^3\,\frac{T_1}{q}\left(\frac{b}{\bar{c}_1\theta_{max}^3}\right)^2\left(\frac{\tau_1}{t_1}\right)^3\left[1 - \exp\left(-\frac{q}{T_1}\,\theta_{max}\right)\right]^{-3}. \qquad (14)$$

In the derivation of (13) and (14) we used the condition that the nuclei were produced by a quasi-stationary process; this defined the concept of "slowness" of expansion, which was assumed at the very outset. This condition states that the relaxation time for the establishment of a stationary rate of production of nuclei during the instant when they are produced most intensely (i.e., at the maximum supercooling) is small compared with the effective duration Δt_m of maximum supercooling. The relaxation time, as shown by Zel'dovich,[5] is on the order of the time necessary to grow from a small subcritical complex to a nucleus of critical dimensions, with allowance for the random character of the adhesion and evaporation of the molecules: $\tau_{rel} = g^{*2}/4D$, where $D = n\bar{v}4\pi r^{*2}$ is the coefficient of "diffusion along the g axis." Determining Δt_m by comparing (14) and (12) and performing simple transformations we obtain the condition for "slow" expansion in the following form

$$\delta = \frac{\Delta t_{max}}{\tau_{\mathbf{rel}}} = \frac{\pi}{2^{1/3}}\,\bar{c}_1\left(\frac{q}{T_1}\right)^{4/3}\left(\frac{\theta_{max}}{b^{1/3}}\right)^7\frac{t_1}{\tau_1} \geqslant 1. \qquad (15)$$

Let us examine a specific example: say, that of an iron meteorite of mass $M = 33 \times 10^3$ tons striking the moon.* Without going into an analysis of the hydrodynamics of the impact, we assume for the initial heating of the equivalent body of the meteoritic sphere a value $\epsilon_0 = 71.9$ ev/atom ($T_0 = 10$ ev $= 116{,}000°$). The speed of scattering is $u = 15.5$ km/sec (it is greater than the critical velocity for the moon, which equals 2.4 km/sec). Obviously, the meteorite would fall with the same velocity were all its kinetic energy converted upon impact instantaneously and without condensation into heat concentrated in the body of the meteorite itself. In fact, the heating chosen corresponds to a large rate of fall.

Iron vapor becomes saturated at an instant $t_1 = 6.8 \times 10^{-2}$ sec if scattered to 1050 m with $T_1 = 2130°$ and $n_1 = 7.15 \times 10^{16}$ cm^{-3}. An estimate based on the previously described method[7] shows that at the instant of saturation the degree of ionization is $y = 2.1 \times 10^{-4}$ (while the equilibrium ionization should be $y_{eq} = 4 \times 10^{-8}$). We assume for the calculation a surface tension* $\sigma = 1100$ erg/cm^2 and $q = 47{,}500°$. Solution of (13) yields $\theta_{max} = 0.0765$, which is less than the critical supercooling $\theta_k = 0.119$. Here $g^* = 46$, $\beta_e = 24.4$, and $\beta = 43.1$. The number of condensation centers, based on (14), is $\nu = 4 \times 10^{-11}$ per atom. Of these, only a negligible fraction, $\sim 10^{-5}$, are uncharged. The criterion for the "slowness" of the process (15) is fulfilled with great margin, $\delta = 98$.

---

*For comparison we recall that the mass of the Tunguska (iron) meteorite is estimated to be 40×10^3 tons.

Because of the exponential character of $I(\theta)$, the value of θ_{max}, as can be seen from (13), depends only logarithmically on the right half of the equation. It is found to be exceedingly stable, almost insensitive to the initial parameters of the sphere and to the approximations made in the derivation of the formulas. Thus, when the right half of (13) is changed by a factor of 10^{10}, θ_{max} changes by merely 20 – 40%. In particular, θ_{max} and ν depend little on the concentration of the ions: a solution of (13) on the assumption that there are no ions, $y = 0$, yields $\theta_{max} = 0.09$, hence $\nu = 1.5 \times 10^{-11}$.

The very weak dependence of the value of the maximum supercooling on the initial conditions makes it possible to establish approximate similarity laws for the transition from one set of initial conditions to another set upon condensation of a given substance. Noting that the saturation temperature also depends very weakly, logarithmically, on the initial conditions, owing to the exponential character of the vapor-tension curve, we obtain approximately from (14) and (15)

$$\nu \approx \text{const} \cdot (t_1/\tau_1)^{-3}, \qquad \delta \approx \text{const} \cdot (t_1/\tau_1). \tag{16}$$

The quantity t_1/τ_1 has a simple physical meaning: this is of the order of magnitude of the number of collisions experienced by a vapor molecule during the entire time from the instant of saturation to infinity. In fact, if the expansion law $n \sim t^{-3}$ and the definition of τ_1 [see (13)] are taken into account, we find for the number of collisions an order of magnitude

$$\int_{t_1}^{\infty} n\bar{v}\pi d^2 dt \sim n_1 \bar{v}_1 \pi d^2 t_1 \sim t_1/\tau_1.$$

In our example the "number of collisions" is $t_1/\tau_1 = 1.1 \times 10^6$. Thus, the criterion of "slowness" of the expansion process, $\delta \gg 1$, necessitates that the "number of collisions" be $t_1/\tau_1 \gg 10^4$.

4. DEGREE OF CONDENSATION AND DIMENSIONS OF PARTICLES IN THE FINAL STATE

Let us consider the stage of thermodynamic "equilibrium." By definition, the temperature at this stage is at all times close to the temperature of saturated vapor in a system with constant entropy, and therefore the degree of condensation $x(t)$ which "follows" the expansion can in first approximation be determined simply from the adiabatic equation (4), in which we put $T \approx T_{eq}$.

Considering that the temperature of the saturated vapor depends very weakly, logarithmically, on the density and that calculations show that it changes little during the entire quasi-equilibrium stage, we assume approximately that $T \approx T_{eq} \approx T_1 \approx$ const. We then obtain from (4), subject to the initial condition $t = t_1$ and $x = 0$

$$dx/dt = (3T_1/q)(1 - x)/t, \qquad x = 1 - (t_1/t)^{3T_1/q}. \tag{17}$$

The degree of supercooling θ is obtained in the next approximation from the kinetic equation, which is now equivalent to the equation of drop growth, since $x = \nu g$ and $\nu =$ const. Noting that $n = n_1(1 - x)(t_1/t)^3$ and assuming approximately $T = T_{eq} = T_1$, we write the equation of drop growth (11) in the form

$$dx/dt = \frac{\nu^{1/3}}{\tau_1} x^{2/3}(1 - x)\left(\frac{t_1}{t}\right)^3 \varphi(\theta), \quad \varphi(\theta) = 1 - \exp\left(-\frac{q}{T_1}\theta\right). \tag{18}$$

With the aid of (17) we obtain the function $\varphi(t)$, and consequently also $\theta(t)$:

$$\varphi = \frac{3T_1}{q}\frac{\tau_1}{t_1}\frac{1}{\nu^{1/3}}\left(\frac{t}{t_1}\right)^2\left[1 - \left(\frac{t_1}{t}\right)^{3T_1/q}\right]^{-2/3}. \tag{19}$$

The function $\varphi(t)$ goes through a minimum at $t = \frac{4}{3}t_1$ ($T_1/q \ll 1$) (for which it can be shown that $\varphi_{min} \ll 1$ and $\theta_{min} \ll \theta_{max}$) and then increases; the supercooling increases simultaneously.

The thermodynamic "equilibrium" is maintained as long as the adhesion and evaporation of drops cancel each other out to a considerable degree and the excess of adhesion over evaporation is small compared with the rates of these processes themselves (the quantity φ, which characterizes the difference in these rates, is much less than unity). A growth in the difference in the rates to a value on the order of the rates themselves [i.e., a growth in φ to ~ 1, and in θ to $\sim T_1/q$; see (18)] signifies that the thermodynamic equilibrium in the system is disturbed and that quenching begins. The instant of occurrence of quenching t_2 can be found from (19) by putting $\varphi = 1$ and calculating the degree of condensation $x_2 = x(t_2)$ with the aid of (17).

---

*According to reference 8, $\sigma = 1220–950$ erg/cm^2 at $T = 1570$°K; we were unable to find other data for conditions closer to ours.

A decrease in the rate of drop evaporation below the rate of adhesion at $t > t_2$ signifies that the heat of condensation is now carried away from the drops slowly, and that the temperature of the drop becomes higher than the temperature of the surrounding vapor.

There is no longer need, however, for further examination of the kinetics with allowance for the temperature difference. It is easy to show that even under extreme assumptions the degree of condensation after the instant t_2 remains almost constant, and upon scattering to "infinity" and cooling to "zero" temperature the resultant degree of condensation is $x_\infty \approx x_2$.*

In the numerical example considered in the preceding section, $t_2 = 2.65$ sec and $x_\infty = 0.44$, i.e., approximately half the iron vapor escapes into space in the form of a gas and the other half in the form of solid particles which contain on the average $g_\infty = x_\infty/\nu = 10^{10}$ atoms each and have a radius $r_\infty = 3.1 \times 10^{-5}$ cm (a total of approximately 3×10^{21} particles; the coagulation of the particles is estimated to be negligible). The equation for the final degree of condensation also obeys an approximate similarity law. Namely, it is seen from (19) that $t_2/t_1 \approx \text{const}$, since $\tau_1/t_1\nu^{1/3} \approx \text{const}$. Consequently, the degree of condensation, according to (17), is also $x_2 \approx \text{const}$, i.e., in the final state $x_\infty \approx \text{const} = 0.44$. The size of the iron particles in scattering to infinity (substituting the numerical value for the constant based on our example) is $r_\infty = 2.8 \times 10^{-11}(t_1/\tau_1)$ cm.

The solution obtained in this paper is correct up to the case when very small particles are produced. Thus, at the limit of applicability of the approximations, i.e., at $\delta \approx 1$, we have $t_1/\tau_1 = 10^4$ and $r_\infty \approx 2.8 \times 10^{-7}$ cm ($g_\infty = 8 \times 10^4$ atoms). In "fast" processes, when $\delta < 1$, the complexes formed are still smaller, and when the number of collisions t_1/τ_1 becomes not too large, there is no "condensation" at all.

The number of collisions, from the definitions of the quantities t_1 and τ_1, is

$$t_1/\tau_1 = t_0 (n_0/n_1)^{1/3} 4\pi d^2 n_1 \bar{v}_1 \sim M^{1/3} \varepsilon_0^{-1/2} [n_1(\varepsilon_0)]^{2/3},$$

i.e., the dimensions of the condensate particles, r_∞, are proportional to the linear dimensions of the evaporated body and decrease very rapidly with increasing initial heating.

In conclusion, let us carry out the estimate for conditions close to those in the laboratory. Thus, for example, when 1 g of iron with initial heat $\epsilon_0 = 13$ ev/atom (corresponding to $T_0 \approx 35{,}000°$) is evaporated, the condensation of the vapor expanding in vacuo terminates at $t_2 \approx 5 \times 10^{-5}$ sec when scattered by approximately 30 cm, and the dimensions of the condensate particles are $r_\infty \approx 10^{-4}$ cm. It is not particularly difficult to generalize the kinetic computations to include the case of scattering not in a vacuum, but in a gas with finite pressure. By suitable choice of evaporation conditions it is possible to obtain particles of desired size in the laboratory.

I take this opportunity to thank Ya. B. Zel'dovich for interest in the work and for valuable discussions.

APPENDIX

APPROXIMATE CALCULATION OF THE NUMBER OF CONDENSATION CENTERS

Maximum supersaturation is reached within a time $t_m - t_1 \ll t_1$ after the instant of saturation, when the temperature and the volume differ little from the values at the instant of saturation T_1, V_1, and $x \ll 1$. Introducing θ instead of T into the adiabatic equation (4) and putting approximately $t \approx t_1$ and $T = T_{eq} \approx T_1$, we obtain

$$\frac{\bar{c}_1}{3} t_1 \frac{d\theta}{\partial t} = 1 - \frac{qt_1}{3T_1}\frac{dx}{dt}; \qquad \theta,\ x,\ \frac{dx}{dt} = 0 \quad \text{for} \quad t = t_1. \tag{20}$$

As long as the right half is close to unity the supercooling increases linearly with time; it slows down only in the region of the maximum.

Differentiating (5), we write down the condition for the maximum of θ $(d\theta/dt = 0)$:

$$\left(\frac{dx}{dt}\right)_m = I(\theta_{max})\, g^*(\theta_{max}) + \int_{t_1}^{t_m} I(t') \frac{dg\,(t_m t')}{dt}\, dt' = \frac{3T_1}{qt_1}. \tag{21}$$

Since the function $I(\theta)$ is highly peaked and the principal contribution to the integral in (21) is made by time values very close to the upper limit, when θ is close to θ_{max}, we extend the expansion near the maximum

$$\theta' \equiv \theta(t') = \theta_{max} - \alpha(t_m - t')^2,$$
$$\alpha = -\tfrac{1}{2}(d^2\theta/dt^2)_m > 0 \tag{22}$$

to the entire interval of integration. We put also $\theta = \theta_{max}$, $n = n_1$, and $T = T_1$ in (11). Integrating (11), we can write approximately

---

*If it is assumed that at $t > t_2$ the drops merely join together the vapor molecules but are not evaporated, we obtain $x_\infty = x_2 + (3/2)(1 - x_2)T_1/q$. To the contrary, by assuming that the drops are only evaporated as a result of the stored thermal energy, and there is no adhesion, we find $x_\infty = x_2 - 3T_1/q$. Both values are quite close to x_2, since $T_1/q \ll 1$. We note that cooling of the drops by radiation causes their evaporation to cease and accelerates the solidification.

$$\frac{dg}{dt}=\left(\frac{t-t'}{\tau_1}\right)^2\frac{[1-\exp(-q\theta_{max}/T_1)]^3}{9\tau_1}+\left(\frac{dg}{dt}\right)_0. \tag{23}$$

Let us insert (23) and (10) in (21) and break up the interval into two, corresponding to charged and uncharged drops.

Going from the integration variable t' to θ', in accordance with (22), and then to β' and β_e, we evaluate the integrals by using expansions of the following type

$$\beta'\equiv\beta(\theta')=\beta+(d\beta/d\theta)_m(\theta'-\theta_{max}),\qquad \beta=\beta(\theta_{max}) \tag{24}$$

for the transformation of the slow factors in front of the exponentials. (An estimate shows that $d\beta_e/d\theta \approx d\beta/d\theta = -2\beta/\theta$.)

To find the unknown curvature of the maximum of α, we differentiate (20) with respect to time, differentiate (5) twice, and calculate $(d^2x/dt^2)_m$ by the foregoing method. This yields the lacking equation for α.

It can be shown that when the "slowness" condition is satisfied by the process (15) the first term in (21) is much smaller than the integral and, furthermore, the term containing the initial rate of drop growth $(dg/dt)_0$ is also small.

Physically this means that the principal role in the rate of condensation is played by the rate of growth of the drops, which accelerates because of the increasing surface, and not by the production of the critical nuclei themselves, a process which in itself is not in position to suppress the growth in supersaturation when $\theta = \theta_{max}$ (the drops have time to grow strongly for the duration Δt_m of the maximum).

Neglecting the foregoing terms, we can readily eliminate α from the system of equations for the unknowns θ_{max} and α, and to obtain the principal equation (13). Calculating integral (12) by this method, we find the number of centers of condensation (14).

The time to reach maximum supersaturation can be obtained by extrapolating the linear law of $\theta(t)$ up to θ_{max}, which is justified, since the duration of the maximum Δt_m is much shorter than $t_m - t_1$. We obtain

$$t_m-t_1={}^1/_3\bar{c}_1t_1\theta_{max}. \tag{25}$$

The degree of the condensation at the instant of maximum is

$$x_m=0.166\,\bar{c}_1T_1\theta^3_{max}/qb\ll 1. \tag{26}$$

Note added in proof (October 29, 1959). As was graciously reported to us by I. S. Shklovskiĭ, the question of interplanetary matter was investigated in detail by V. G. Fesenkov.[9] Fesenkov suggests that the dust in the solar system is formed as a result of purely mechanical pulverization of matter upon collision between meteoritic bodies and asteroids and planets without atmospheres, and does not dwell on the physical process occurring during the impact. This effect pertains to the later stage of propagation of the shock wave, when its amplitude is no longer sufficient for complete evaporation of the substance, and exists along with the phenomenon noted in the article.

---

[1] V. A. Tsukerman and M. A. Manakova, J. Tech. Phys. (U.S.S.R.) **27**, 391 (1957), Soviet Phys.-Tech. Phys. **2**, 353 (1957).

[2] Ya. B. Zel'dovich and Yu. P. Raĭzer, JETP **35**, 1402 (1958), Soviet Phys. JETP **8**, 980 (1959).

[3] R. Latter, Phys. Rev. **99**, 1854 (1955).

[4] N. Tunitskiĭ, J. Phys. Chem. (U.S.S.R.) **15**, 1061 (1941).

[5] Ya. B. Zel'dovich, JETP **12**, 525 (1942).

[6] Ya. I. Frenkel', Кинетическая теория жидкостей (Kinetic Theory of Liquids), U.S.S.R. Acad. Sci., 1945.

[7] Yu. P. Raĭzer, JETP **37**, 580 (1959), Soviet Phys. JETP **10**, 411 (1960).

[8] N. K. Adam, The Physics and Chemistry of Surfaces, Oxford, 1941 (Russ. Transl., Gostekhizdat, 1947).

[9] V. G. Fesenkov, Метеорная материя в межпланетном пространстве. (Meteoritic Matter in Interplanetary Space), U.S.S.R. Acad. Sci., 1947.

Translated by J. G. Adashko
337

SOVIET PHYSICS JETP VOLUME 37(10), NUMBER 6 JUNE, 1960

ELECTRON AND MUON NEUTRINOS

B. PONTECORVO

Joint Institute for Nuclear Research

Submitted to JETP editor July 9, 1959

J. Exptl. Theoret. Phys. (U.S.S.R.) **37**, 1751-1757 (December, 1959)

Some processes due to free neutrinos, not heretofore considered, are discussed. Particular attention is paid to those processes which, in principle, could help decide whether two neutral lepton pairs [electron pair (ν_e and $\bar{\nu}_e$) and muon pair (ν_μ and $\bar{\nu}_\mu$)] exist.

To answer the fundamental question about the identity of ν_μ and ν_e a method is proposed which in essence is analogous to the method used to distinguish neutrinos from antineutrinos or K^0 mesons from $\bar{K}^0$ mesons. In principle the problem is solved when an experiment is carried out showing whether a beam of $\bar{\nu}_\mu$ is capable of initiating transitions which can without any doubt be initiated by $\bar{\nu}_e$ (for example the reaction $\bar{\nu}_\mu + p \rightarrow e^+ + n$).

The suggested experiment, although difficult, should be feasible with accelerators capable of producing more intense beams then those produced by present-day accelerators.

INTRODUCTION

Bethe and Peierls[1] in 1934 were the first to estimate the cross section for production of β particles in the collisions of free neutrinos with nuclei at energies of the order of 1 Mev. As is well known the cross section turned out to be of the order of 10^{-44} cm^2 and for this reason effects due to free neutrinos were for a long time considered to be unobservable. Subsequently it was shown by the author and by Alvarez[2,3] that such experiments are quite feasible and only recently Reines and Cowan, and also Davis, successfully performed experiments in which free antineutrinos from reactors were used. These experiments proved that neutrinos can be observed and are therefore "real," that they are two-component neutrinos[4] and also that the neutrino and antineutrino are different particles.[5]

The aim of the present work is to emphasize the possibility of solving certain physical problems by studying effects due to free neutrinos not heretofore discussed. The corresponding experiments may turn out to be not feasible today, however it seems to us a discussion of them is no more premature than the discussion in its time of the antineutrino experiments from reactors.

The question discussed is the possibility of deciding, in principle, whether the neutrino emitted in the $\pi \rightarrow \mu$ decay (ν_μ) and the neutrino emitted in β decay (ν_e) are identical particles or not.

REACTIONS DUE TO NEUTRINOS

All slow processes known to us are apparently due to the interactions of the following fermion pairs:

$$(e^+\nu_e),\quad (\mu^+\nu_\mu),\quad (p\bar{n}),\quad (p\bar{\Lambda}),$$
$$(e^-\bar{\nu}_e),\quad (\mu^-\bar{\nu}_\mu),\quad (\bar{p}n),\quad (\bar{p}\Lambda). \qquad (1)$$

Any pair of particles may interact with itself or with another pair and, according to the Markov-Sakata-Okun' scheme, of all the strange particles only the Λ hyperon is included in the "strange" pair. In the language of the universal interactions theory[7,8] this scheme implies that the current J^+ entering into the weak interactions Lagrangian consists of four terms

$$J^+ = J(e^+\nu_e) + J(\mu^+\nu_\mu) + J(p\bar{n}) + J(p\bar{\Lambda}), \qquad (2)$$

each of which corresponds to one of the abovementioned pairs.

Some of the processes that may be induced by free neutrinos are listed below using the assumption that the Markov-Sakata-Okun' scheme and the universal interactions theory are valid.

The identity of ν_e and ν_μ is an open question and is discussed in the next section. Neither theoretical nor experimental arguments exist for the assertion that ν_e and ν_μ are identical particles. Therefore below, as well as in the above expression for the current, we use the notation $(e^+\nu_e)$, $(\mu^+\nu_\mu)$ instead of the conventional $(e^+\nu)$, $(\mu^+\nu)$.

We consider here collision of neutrinos with real targets, i.e., with negative electrons, protons and nuclei (A). Among the processes listed only 1, 2, 3 and 10 have been prěviously discussed in the literature. In the present work we restrict ourselves for the majority of the processes to brief comments inserted in the Table. Below we discuss in more detail only those processes that have a bearing on the question of the distinguishability of the ν_e and ν_μ particles.

ARE ν_e AND ν_μ IDENTICAL PARTICLES?

The upper limit on the mass of the neutral leptons emitted in μ decay, the magnitude of the Michel parameter ρ and theoretical considerations permit one to conclude that the neutral leptons in μ decay have either vanishing or very small mass and are not identical. On this basis the decay of μ mesons is usually described by the scheme $\mu \rightarrow e + \nu + \bar{\nu}$. However it is easy

Some reactions induced by free neutrinos on real targets

Process No.	Reaction	Remarks
1	$\bar{\nu}_e + p \rightarrow e^+ + n$	In the study of this process[4] free neutral leptons were observed for the first time. The experiment confirmed the two-component nature of the neutrino.
2	$\bar{\nu}_e + Cl^{37} \rightarrow Ar^{37} + e^-$ [2,3,5]	The absence of this process[5] proved that ν_e and $\bar{\nu}_e$ are distinct.
3	$\nu_e + Cl^{37} \rightarrow Ar^{37} + e^-$	A study of this process could be of interest for astrophysics, in particular for measuring the neutrino flux from the sun.[9]
4	$\nu_e + A \rightarrow \pi^+ + e^- + A,$ $\bar{\nu} + A \rightarrow \pi^- + e^+ + A$	Inverse $\pi - e$ decay in the field of a nucleus. π^+ mesons are produced by ν_e, π^- mesons are produced by $\bar{\nu}_e$.
5	$\bar{\nu}_e + e^- \rightarrow \pi^- + \pi^0$	
6	$\bar{\nu}_e + p \rightarrow \Lambda + e^+,$ $\bar{\nu}_e + A \rightarrow$ hyperfragment $+ e^+$	Only $\bar{\nu}$ (and not ν) can produce strange particles.
7	$\bar{\nu}_e + n \rightarrow \Sigma^- + e^+$	This process is possible only in nuclear matter.
8	$\nu_e + A \rightarrow K^+ + e^- + A,$ $\bar{\nu}_e + A \rightarrow K^- + e^+ + A$	See process 4.
9	$\bar{\nu}_e + e^- \rightarrow K^- + K^0$	See process 5.
10	$\bar{\nu}_e + e^- \rightarrow \bar{\nu}_e + e^-,$ $\nu_e + e^- \rightarrow \nu_e + e^-$	Neutrino scattering by electrons is predicted by the universal theiry of weak interactions.[8]
11	$\nu_e + A \rightarrow \nu_e + e^+ + e^- + A$ $\bar{\nu}_e + A \rightarrow \bar{\nu}_e + e^+ + e^- + A$	e^+e^- pair production in the field of a nucleus.* This process is the inverse of the lepton electron bremsstrahlung described in reference 10.
12	$\bar{\nu}_e + e^- \rightarrow \bar{\nu}_\mu + \mu^-,$ $\nu_e + e^- \rightarrow \nu_\mu + \mu^-$	Inverse μ decay Forbidden if $\nu_e \neq \nu_\mu$.
13	$\bar{\nu}_e + A \rightarrow \bar{\nu}_\mu + e^+ + \mu^- + A,$ $\nu_e + A \rightarrow \nu_\mu + e^- + \mu^+ + A$	$\mu - e$ pair creation in the field of a nucleus.
14	$\bar{\nu}_e + p \rightarrow \mu^+ + n,$ $\bar{\nu}_\mu + p \rightarrow e^+ + n$	Inverse μ capture. Forbidden if $\nu_e \neq \nu_\mu$.
15	$\nu_\mu + A \rightarrow \pi^+ + \mu^- + A,$ $\bar{\nu}_\mu + A \rightarrow \pi^- + \mu^+ + A$	Inverse $\pi - \mu$ decay in the field of a nucleus.
16	$\bar{\nu}_\mu + p \rightarrow \Lambda + \mu^+,$ $\bar{\nu}_\mu + p \rightarrow \Lambda + e^+,$ $\bar{\nu}_\mu + A \rightarrow$ hyperfragment $+ \mu^+$	Forbidden if $\nu_e \neq \nu_\mu$.

*This process was recently studied theoretically by Ya. B. Smorodinskiĭ and Chou Kuang Chao.

Process No.	Reaction	Remarks
17	$\nu_\mu + A \to \mu^- + K^+ + A,$	
	$\bar{\nu}_\mu + A \to \mu^+ + K^- + A,$	
18	$\nu_\mu + A \to \nu_\mu + \mu^+ + \mu^- + A,$	Neutrino scattering by μ meson in the field of a nucleus.
	$\bar{\nu}_\mu + A \to \bar{\nu}_\mu + \mu^+ + \mu^- + A$	
19	$\nu_\mu + e^- \to \nu_e + \mu^-,$	Inverse μ decay.
	$\bar{\nu}_\mu + e^- \to \bar{\nu}_e + \mu^-$	Forbidden if $\nu_e \neq \nu_\mu$.
20	$\nu_\mu + A \to A + \mu^- + e^+ + \nu_e,$	$\mu-e$ pair creation in the field of a nucleus.
	$\bar{\nu}_\mu + A \to A + \mu^+ + e^- + \bar{\nu}_e$	
21	$\nu_\mu + e^- \to \nu_\mu + e^-$	If $\nu_e \neq \nu_\mu$ this reaction is possible only as a second order process.

to see that the totality of experimental and theoretical information only implies that the two neutral leptons in μ decay must not be identical, and does not necessarily require that they be particle and antiparticle. The possible existence of two pairs of neutrinos was already considered by Oneda and Pati.[11] At first sight the hypothesis of two types of neutrinos — electron neutrino (ν_e, $\bar{\nu}_e$) and muon neutrino (ν_μ, $\bar{\nu}_\mu$) — may seem an unnecessary complication. However there are arguments that make the hypothesis of distinct electron and muon neutrinos attractive.

The absence in nature of a number of processes of the type $\mu + p \to e + p$, $\mu \to e + e + e$, etc. shows that in each of the currents in the weak interactions Lagrangian apparently only pairs consisting of one charged and one neutral particle are permitted [see Eqs. (1) and (2)]. The existence of only a "charged" current, as was pointed out by Gell-Mann and Feynman,[8] could be very naturally explained if there existed in nature a charged vector boson B, coupled to various fermions with "intermediate" strength; then all weak interaction processes known to us would be due to an interaction of second order in the "intermediate" coupling constant. As was shown by Feinberg, and also by Gell-Mann and Feynman,[12] the nonlocality in the μ-e decay process corresponding to an intermediate vector boson would imply a probability for decay through the channel $\mu \to e + \gamma$ in contradiction with experimental data.[13]

However it is not difficult to see that even if the B meson existed the probability in question would be zero* (as is fully consistent with experiment) if the electron and muon neutrinos are different. Thus, the fact that the weak interactions current in the Lagrangian is "charged" could be very well explained on the hypothesis of an intermediate boson only provided ν_e and ν_μ are different. Besides this argument it seems to us the hypothesis of two different types of neutrinos, unable to annihilate each other,* is attractive from the point of view of symmetry and systematics of particles and also could help us understand the difference in the nature of the muon and electron.

It follows from the above that experimental information on the identity of ν_e and ν_μ is of paramount importance. One possibility consists in measuring the helicity of the μ meson. If only one kind of neutrino-antineutrino pair exists in nature then the V-A interaction requires that the helicity of the μ^- meson be positive. Should this helicity be found experimentally to be negative it would serve as a strong argument in favor of the existence of two kinds of neutrinos; the μ^+ decay could be described according to the scheme $\mu^+ \to e^+ + \nu_e + \nu_\mu$.

The experiments of Love et al.[15] however show that the helicity of the μ^- meson is apparently positive. Therefore the question on the existence of two kinds of neutrinos in nature remains open. The positive helicity of the μ^- meson indicates however that if two kinds of neutrino-antineutrino pairs do exist in nature then the weak interactions should be described as in (1) and the decay of the μ^+ meson should proceed according to the scheme $\mu^+ \to e^+ + \nu_e + \bar{\nu}_\mu$. Here, as usual, the electron neutrino is defined as the particle emitted with the positron in β decay. Its helicity has been determined experimentally and was found to be negative[16] (the helicity of $\bar{\nu}_e$ is, of course, the opposite). As regards ν_μ and $\bar{\nu}_\mu$: these particles are defined as having respectively negative and positive helicities. The decay of the π^+ meson is thus described by $\pi^+ \to \mu^+ + \nu_\mu$. This notation was used in the preceding section.

---

*The $\mu \to e + \gamma$ process is also possible in the absence of the B meson in higher order of perturbation theory as long as there is only one kind of neutrino-antineutrino pair, whereas it is absolutely forbidden if $\nu_e \neq \nu_\mu$.

*We note, in particular, that if ν_e, $\bar{\nu}_e$ and ν_μ, $\bar{\nu}_\mu$ are different the muonium system ($\mu^+ e^-$) cannot make transitions[14] into the antimuonium system ($\mu^- e^+$) in any order of approximation.

There remains one more fundamental possibility for settling the question of whether ν_e and ν_μ are different particles, and this is discussed in the following section.

PROPOSED EXPERIMENT FOR DETECTING THE DIFFERENCE BETWEEN ν_e AND ν_μ

The method discussed below is in essence analogous to that used to determine whether the neutrino and antineutrino (we are referring here to ν_e and $\bar{\nu}_e$) are identical[2,5] or whether the K^0 meson and $\bar{K}^0$ meson are identical.[17] In these cases particle and antiparticle were proved to be distinct when transitions, whose matrix elements would be nonvanishing if the particle and antiparticle were identical, were not observed experimentally. For example the absence of the process $\bar{\nu}_e + Cl^{37} \to A^{37} + \beta^-$ proves that ν_e and $\bar{\nu}_e$ are distinct since the process $\nu_e + Cl^{37} \to A^{37} + \beta^-$ without any doubt does occur.

In our case we are concerned not with the already settled problem about the distinction between neutrino and antineutrino but rather with the distinction between ν_e and ν_μ (or $\bar{\nu}_e$ and $\bar{\nu}_\mu$). If ν_e and ν_μ are different then it is already known which reactions should produce ν_e and $\bar{\nu}_e$ and should not produce ν_μ and $\bar{\nu}_\mu$ (and vice versa).

To settle the question it is necessary to ascertain experimentally whether a beam of $\bar{\nu}_\mu$ is capable of inducing transitions which can definitely be induced by $\bar{\nu}_e$. From the experimental point of view a beam of muon neutrinos is more attractive than a beam of electron neutrinos for the following reasons. The usual intense sources of electron neutrinos are radioactive isotopes. Their very nature makes them incapable of emitting high energy neutrinos. A good source of muon neutrinos is the π-μ decay in which the neutrinos are produced with high energies. It would be of interest to use a high energy antineutrino, say $\gg$ 100 Mev, since the cross section for neutrino induced processes grows rapidly with energy. However at very high energies the intensity of generation of muon neutrinos is reduced due to the relativistic increase in the lifetime of the π mesons and therefore we shall discuss an experiment for a neutrino with energy < 100 Mev.

Now as an example let us consider the reactions (see table, processes 1 — 21)

$$\bar{\nu}_\mu + p \to \mu^+ + n, \tag{a}$$

$$\bar{\nu}_\mu + p \to e^+ + n. \tag{b}$$

The reaction (b), if ν_e and ν_μ are identical, was successfully observed by Reines and Cowan,[4] and if $\nu_e \neq \nu_\mu$, the reaction is unobservable. The reaction (a) is a threshold reaction and therefore can never be observed for ν_μ energies < 100 Mev. The problem is to determine the cross section for reaction (b). When the neutrons from reaction (b) are in the energy region where their detection is possible with good efficiency inside a large scintillation counter containing cadmium, the method of Reines and Cowan is fully applicable. When the event caused by reaction (b) takes place two pulses will appear in the scintillation counter, one corresponding to the release of the positron energy (the neutron receives a small share of the energy) and the other, delayed with respect to the first one, corresponding to the release of the photon energy from the neutron capture in cadmium. To detect the reaction (b) a Reines and Cowan type scintillation counter may be placed in a beam of muon antineutrinos incapable of inducing reaction (a) (for energy reasons) and containing a negligibly small admixture of electron antineutrinos which could cause the "trivial" reaction $\bar{\nu}_e + p \to e^+ + n$.

To clarify the experimental conditions let us discuss the production of neutral leptons of various kinds in cyclic accelerators where protons attain an energy of, say, 700 Bev. The radioactive elements that are produced in the target and in other parts of the accelerator are sources of ν_e and, to a smaller degree, of $\bar{\nu}_e$ of low energy ($\lesssim$ 10 Mev). These electron neutrinos will not give rise to an appreciable background because

a) their energy is low and it is easy to discriminate against them by an analysis of the corresponding pulses from the scintillator;

b) the cross section for the reaction $\bar{\nu}_e + p \to e^+ + n$ is proportional to the square of the energy of the incident antineutrinos and is relatively small at low energies.

Pions of both signs will be produced at the target of the synchrocyclotron. They will give rise to neutral leptons according to the scheme

$$1)\ \pi^+ \to \mu^+ + \nu_\mu, \qquad 2)\ \mu^+ \to e^+ + \nu_e + \bar{\nu}_\mu,$$

$$3)\ \pi^- \to \mu^- + \bar{\nu}_\mu, \qquad 4)\ \mu^- \to e^- + \bar{\nu}_e + \nu_\mu,$$

$$5)\ \mu^- + \text{nucleus} \to \nu_\mu.$$

The admixtures of ν_e and ν_μ in the beam are harmless since it is already known that the neutrino (both ν_μ and ν_e) is incapable of inducing the reaction under study. It is easy to see that "harmful" $\overline{\nu}_e$ come only from the decay 4 of μ^- mesons. However μ^- mesons stopped in a material of high atomic number (it is not difficult to take care of the possibility of mesons stopping in light materials) practically do not decay, and μ-meson decay in flight may be ignored since the mean free path for μ-meson decay is measured in hundreds of meters and it is reasonable to place the detector for reaction (b) at a distance of ≈ 10 m from the target.

It is thus possible to achieve a beam of $\overline{\nu}_\mu$ particles with practically no admixture of $\overline{\nu}_e$. Furthermore the $\overline{\nu}_\mu$ from reaction 2) (stopped μ^+ mesons) will have an average energy of ~35 Mev, and although the $\overline{\nu}_\mu$ from reaction 3) may have a significantly higher energy (decay in flight) their intensity will in general be low.*

The number of $\overline{\nu}_\mu$ produced in reaction 2) may be close to the number of π^+ mesons produced in the target and therefore the number of $\overline{\nu}_\mu$ that present day machines are capable of producing could be equal to 10^{12} sec^{-1}. At the present time models of new accelerators are being discussed, which would be capable in principle of a proton intensity larger by three orders of magnitude. Thus one may think that a flux $\Phi = 10^8\ \overline{\nu}_\mu/\text{cm}^2\ \text{sec}$ at a distance of 10 m from the target may be realistic in the not too distant future. The cross section for reaction (b) was estimated using perturbation theory and found equal to $2 \times 10^{-41}\ \text{cm}^2$ if $\overline{\nu}_e \equiv \overline{\nu}_\mu$, for $\overline{\nu}_e$ energy equal to 35 Mev. If one were to use a scintillation counter of the Reines and Cowan type (1 – 2 m) then the number of events (for $\nu_e \equiv \nu_\mu$) will be ~1 per hour ($\Phi \sim 10^8\ \text{cm}^{-2}\ \text{sec}^{-1}$) for a registration efficiency equal to unity. As was recently shown by Reines and Cowan[4] the efficiency may exceed 0.5. Technically, the registration of one of the events under consideration is less difficult than in the Reines and Cowan experiment since the energy of the emitted β^+ particles is high. Thus the feasibility of the experiment depends on the size of the background; this is difficult to estimate a priori. One can only say that unfortunately the signal-to-background ratio should be considerably lower than in the Reines and Cowan experiment. Attention is called to the fact that the $\overline{\nu}_\mu$ from the reaction 2) are emitted isotropically, in contrast to the neutrons produced in the target. This makes it possible to reduce the difficulties due to the background from the accelerator by placing the $\overline{\nu}_\mu$ detector at an angle of $\gtrsim 90°$ with respect to the direction of the high energy protons incident on the target.

To sum up one could say that an experiment to establish the identity of ν_e and ν_μ, although very difficult, should be seriously considered in the planning of new accelerators. In particular the problem of shielding of the $\overline{\nu}_\mu$ detector from radiation should be looked to in the very first stages of design.

In conclusion the author takes great pleasure in thanking Chou Kuang-Chao, L. B. Okun' and Ya. A. Smorodinskiĭ for numerous discussions, and also E. M. Lipmanov who kindly showed us, prior to publication, the paper in which arguments are presented in favor of the hypothesis of two kinds of neutrino pairs.

---

*The $\overline{\nu}_\mu$ flux from the $\pi^- \to \mu^-$ decay in flight may be appreciable only if the high energy proton beam falls on an external target located several meters away from the massive parts (shield, etc.) of the accelerator.

[1] H. A. Bethe and R. Peierls, Nature **133**, 532 (1934).

[2] B. Pontecorvo, Report PD-205 (1946).

[3] L. W. Alvarez, UCRL Report 328 (1949).

[4] F. Reines and C. L. Cowan, Phys. Rev. **90**, 492 (1953); **113**, 273 (1959).

[5] R. Davis, Phys. Rev. **86**, 976 (1952); Bull. Am. Phys. Soc., Washington meeting (1959).

[6] S. Sakata, Progr. Theor. Phys. **16**, 686 (1946). M. A. Markov, VI Rochester Conf. on High Energy Physics (1956). L. B. Okun', JETP **34**, 469 (1958), Soviet Phys. JETP **7**, 322 (1958).

[7] E. C. G. Sudarshan and R. E. Marshak, Proc. of the Padua-Venice Conf. on Mesons and Newly Discovered Particles (1957).

[8] R. P. Feynman and M. Gell-Mann, Phys. Rev. **109**, 193 (1958).

[9] A. G. W. Cameron, Annual Review of Nuclear Science 1958, p. 306.

[10] B. Pontecorvo, JETP **36**, 1615 (1959), Soviet Phys. JETP **9**, 1148 (1959).

[11] S. Oneda and J. C. Pati, Phys. Rev. Lett. **2**, 125 (1959).

[12] G. Feinberg, Phys. Rev. **110**, 1482 (1958), R. P. Feynman and M. Gell-Mann, Proc. of the VIII Conf. on High Energy Physics, Geneva, 1958.

[13] See, e.g., Berley, Lee, and Bardon, Phys. Rev. Lett. **2**, 357 (1959).

[14] B. Pontecorvo, JETP **33**, 549 (1957), Soviet Phys. JETP **6**, 429 (1958).

[15] Love, Marder, Nadelhaft, Siegel, and Taylor, Phys. Rev. Lett. **2**, 107 (1959).

[16] Goldhaber, Grodzins, and Sunyar, Phys. Rev. **109**, 1015 (1958).

[17] Balandin, Balashov, Zhukov, Pontecorvo, and Selivanov, JETP **29**, 265 (1955), Soviet Phys. JETP **2**, 98 (1956).

Translated by A. M. Bincer
338

SOVIET PHYSICS JETP VOLUME 37(10), NUMBER 6 JUNE, 1960

ON THE THEORY OF NEUTRON BETA DECAY

S. M. BILEN'KIĬ, R. M. RYNDIN, Ya. A. SMORODINSKIĬ, and HO TSO-HSIU

Joint Institute for Nuclear Research

Submitted to JETP editor July 9, 1959

J. Exptl. Theoret. Phys. (U.S.S.R.) 37, 1758-1763 (December, 1959)

Corrections are calculated to various effects in neutron beta decay coming from terms $\sim m/M$ (m and M are the electron and nucleon masses), depending on Gell-Mann "weak magnetism" and proton recoil. It is shown that in electron-neutrino correlation and in the electron asymmetry in the decay of polarized neutrons these corrections reach several percent.

1. INTRODUCTION

As a result of intensive theoretical and experimental investigations in the last few years, the V-A form of the weak interaction has obviously been uniquely established.[1,2,3] Starting with the equality between the μ-decay constant G_μ and the Fermi constant G_F of beta decay, Feynman and Gell-Mann enunciated a proposal on the profound analogy between the vector part of the weak interaction and the nucleon current in electrodynamics. As Gell-Mann showed in a later paper,[4] this leads to the appearance of supplementary terms ("weak magnetism") in the formulas for the effects observed in beta decay. The observation of these corrections in an experiment would greatly strengthen the hypothesis. The corrections connected with the Feynman—Gell-Mann hypothesis for the beta decay of nucleons have been considered in other papers.[5,6]

In the present work we examine the influence of strong interactions on the simplest case of beta decay, the decay of the neutron. A phenomenological analysis of the strong interactions leads (as is known[7]) in the case of the V-A form to the appearance of six form factors which depend, thanks to the locality of the weak interaction, only on the square of the 4-momentum transfer. In examining the matrix element, we take into account only terms of the order m/M (m and M are the electron and neutron masses) and neglect terms of higher order. It is shown that 1) the dependence of the form factors on the 4-momentum transfer can be neglected so that they can be considered constant; 2) besides the ordinary beta-decay constants G and λ, only a constant corresponding to "weak magnetism" enters. The other terms in the amplitude are shown to be second-order.

Essentially, the value of the new constant is determined by the anomalous magnetic moments of the nucleons. Therefore, the final formulas in this approximation contain no undetermined parameters.

Corrections to the effects observed which are obtained here arise both from "weak magnetism" and from the calculation of proton recoil in ordinary matrix elements. Although these corrections are not great and make up, generally speaking, $\sim 0.1\%$ of the fundamental effect, in some cases (electron-neutrino correlation and electron asymmetry in the decay of polarized neutrons) they reach several percent and could be measured if the accuracy of present experiments were increased a few times. The measurement of such effects is essential because it would assure a test of present-day theory to an accuracy of 1%, free of any supposition of nuclear characteristics.

It may be in place here to emphasize the difference between the setup for the verification of the V-A interaction hypothesis and that for the electromagnetic analogy of Feynman and Gell-Mann. The latter predicts a numerical value for the "weak magnetism" effect, the former establishes only the form of the amplitude. The investigation of neutron decay gives sufficient information for the verification of both hypotheses.

If the theory is confirmed by experiment, it can really lead to an understanding of the law of the weak interaction, in particular, one can get an understanding of the ratio of the coupling constants for μ decay and beta decay taking into account various corrections coming from the interaction with the radiation field and the pion field. The work of Berman[8] was devoted to this question.

One must emphasize that as long as the influence of the effects mentioned above on beta decay is not investigated in sufficient theoretical detail it is useless to pose the question of a rigorous test of the V-A theory by looking at nuclear beta decays.

2. THE MATRIX ELEMENT

According to the Feynman—Gell-Mann theory, the neutron beta decay Hamiltonian has the form of a product of the lepton and nucleon "currents." The strong interaction of the nucleons in the matrix element can be taken care of phenomenologically by the introduction of form factors which, from the locality of the lepton interaction, depend only on one invariant, the square of the 4-momentum transfer of the nucleon. Then the most general expression for the matrix element is

$$S = (2\pi)^4 i\delta(n - p - e - \nu)\left[\frac{m}{e_0}\frac{m_\nu}{\nu_0}\frac{M_p}{p_0}\frac{M_n}{n_0}\right]^{1/2} R,$$

$$\begin{aligned} R = {} & (G/\sqrt{2})\,[\bar{u}_e\gamma_\mu(1+\gamma_5)u_\nu] \\ & \times [\bar{u}_p(a_1\gamma_\mu + a_2\sigma_{\mu\nu}k_\nu + ia_3k_\mu + b_1\gamma_\mu\gamma_5 \\ & + b_2\sigma_{\mu\nu}\gamma_5k_\nu + ib_3\gamma_5k_\mu)u_n]. \end{aligned} \tag{1}$$

Here n and p are the 4-momenta of the neutron and proton; ν and e are the 4-momenta of the anti-neutrino and the electron; a_i and b_i are arbitrary functions of the square of the momentum transfer; $k = p - n$, $p_0 = -ip_4$, $n = -in_4$, etc.; and $\sigma_{\mu\nu} = (1/2i) \times (\gamma_\mu\gamma_\nu - \gamma_\nu\gamma_\mu)$. We use the invariant spinor normalization ($\bar{u}u = \pm 1$), and the appearance of one factor in (1) is connected with this. We note also that for an invariant normalization of the spinor u_ν we introduced a neutrino mass m_ν, which in the final results is equal to zero.

The invariance of the theory under time reversal leads to the relation

$$R_{\alpha\beta} = R_{-\beta-\alpha}, \tag{2}$$

where the states $(-\beta)$ and $(-\alpha)$ are obtained from β and α by changing the sign of the spins and of the spatial components of the momenta. The requirement of unitarity of the S matrix to first order in the weak coupling constant gives

$$R_{\alpha\beta} = R^*_{\beta\alpha}. \tag{3}$$

From (2) and (3), the reality of the form factors coming from amplitude (1) follows.

If we limit our consideration to corrections of the order m/M only, then expression (1) simplifies, in an essential way. This happens for the following reasons:

1. If one considers that G invariance[9,10] holds for strong interactions, then

$$a_2 = b_2 = 0. \tag{4}$$

Since in our calculations we want to fix our attention on corrections coming from the neutron-proton mass difference Δ, (4) means that the ratios a_3/a_2 and b_2/b_3 are of the order Δ/M (this is also confirmed by lowest order perturbation theory). Besides this, the terms with b_2 and a_3 are multiplied in the matrix element by a quantity of the order of Δ. Therefore they give only a contribution on the order of $(\Delta/M)^2$ and can be neglected.

2. The term with b_3 is also of the order $(\Delta/M)^2$ since first, k_μ enters in it and second, the matrix element is of the order Δ/M from the γ_5.

3. The dependence of the form factors on k^2 can be neglected in our case (see reference 7). This is connected with the fact that an expansion of the form factors in a series in k^2 (for example, for a_1) has the form $a_1(k^2) = 1 - r^2k^2/6 + \ldots$ Here r represents the dimensions of the nucleon and the corresponding correction is of higher order than Δ/M.

4. Therefore, in the approximation that omits only terms linear in Δ/M, only one additional term determined by the strong interactions (a) is left in the matrix element. In conformity with the Feynman-Gell-Mann hypothesis, by analogy with electrodynamics a_2 should be replaced by $-\mu_0/2M$, where μ_0 is the difference in the anomalous magnetic moments of the proton and neutron.

So the final expression for R takes the form

$$R = \frac{G}{\sqrt{2}}[\bar{u}_e\gamma_\mu(1+\gamma_5)u_\nu]\left[\bar{u}_p\left(\gamma_\mu - \frac{\mu_0}{2M}\sigma_{\mu\nu}k_\nu + \lambda\gamma_\mu\gamma_5\right)u_n\right], \tag{5}$$

where λ is the ratio of the Gamow-Teller and Fermi constants.

To calculate the observed effects with the aid of (5) we use the method of covariant density matrices.[11,12] The density matrix of the initial state has the form

$$\rho_0 = \tfrac{1}{2}(1 + i\gamma_5\gamma_\mu\xi^n_\mu)\Lambda_+(n). \tag{6}$$

Here $\Lambda_+(n) = (n_\mu\gamma_\mu + iM_n)/2iM_n$ is a projection operator, and $\xi^n_\mu = \mathrm{Sp}\, i\gamma_5\gamma_\mu\rho_0$ is the 4-component pseudovector of the neutron polarization, satisfying the condition

$$\xi^n_\mu n_\mu = 0. \tag{7}$$

The degree of polarization is given as $\sqrt{\xi^n_\mu\xi^n_\mu}$.

The density matrix of the final state is equal to

$$\rho = \rho^L_{\alpha\beta}\rho^N_{\alpha\beta}, \tag{8}$$

where

$$\rho^L_{\alpha\beta} = -\Lambda_+(e)O_\alpha\Lambda_-(\nu)\bar{O}_\beta\Lambda_+(e),$$

$$\rho^N_{\alpha\beta} = \Lambda_+(p)N_\alpha\rho_0\bar{N}_\beta\Lambda_+(p).$$

In these formulas

$$\overline{O}_\beta = \gamma_4 O_\beta^+ \gamma_4, \ \overline{N}_\beta = \gamma_4 N_\beta^+ \gamma_4,$$
$$O_\alpha = \gamma_\alpha (1 + \gamma_5), \ N_\alpha = \frac{G}{\sqrt{2}} \left(\gamma_\alpha - \frac{\mu_0}{2M} \sigma_{\alpha\varkappa} k_\varkappa + \lambda \gamma_\alpha \gamma_5\right).$$

Here it must be kept in mind that the matrices in $\rho^{L}_{\alpha\beta}$ act on the spin variables of the leptons, while the matrices in $\rho^{N}_{\alpha\beta}$ act on the spin variables of the nucleons. Furthermore, expression (8) for the density matrices leaves out a common factor coming from the matrix element (1). This factor will be taken into account in the final expressions.

In conclusion we note that the definition of polarization (6) differs from the ordinary one by a factor m/E, which is connected with the choice of a covariant normalization (in particular, with such a definition we get for the polarization 3-vector of the electron in the two-component theory not $-\beta$, but $-p/m$).

3. ELECTRON-NEUTRINO CORRELATION

Let us go now to a consideration of the observed effects. First we look at the electron-neutrino correlation in the decay of an unpolarized neutrino. For this it is necessary to calculate Sp ρ for $\xi^{n}_{\mu} = 0$ and the density of the final states. As we have already noted, we keep terms $\sim \Delta/M$ in these calculations and neglect terms of higher order. The expression for the statistical weight has the following form in the approximation considered:

$$\frac{2}{(2\pi)^5}\left(1 + \frac{3(E - p\cos\theta) - \Delta}{M}\right) pE (E_0 - E)^2 \, dE \, d\Omega. \qquad (9)$$

Here $d\Omega = 2\pi \sin\theta \, d\theta$, θ is the angle between the directions of emission of the electron and the neutrino, E and p are the total energy and momentum of the electron, and E_0 is the maximum energy of the electron, equal, in the approximation used, to

$$E_0 = \Delta - (\Delta^2 - m^2)/2M.$$

The calculations of the expression of the electron-neutrino correlation are very cumbersome, and we give only the final result

$$dW(E, \cos\theta) = A(E)(1 + \beta a(E)$$
$$\times \cos\theta + \beta^2 b(E) \cos^2\theta) \, dE \, d\Omega, \qquad (10)$$

where β is the electron velocity,

$$A(E) = \frac{2G^2}{(2\pi)^4} pE (E_0 - E)^2 \Big\{ 1 + 3\lambda^2 + [3(1 + 3\lambda^2) + 4\lambda\mu] \frac{E}{M}$$
$$- [1 + \lambda^2 + 2\lambda\mu] \frac{m^2}{ME} - 2\lambda(\lambda + \mu)\frac{\Delta}{M}\Big\},$$
$$a(E) = \frac{1 - \lambda^2}{1 + 3\lambda^2} + \frac{1}{(1 + 3\lambda^2)^2} \Big\{ 4\lambda(1 + \lambda^2)(\lambda + \mu)\frac{\Delta}{M}$$
$$+ (1 - \lambda^2)(1 + \lambda^2 + 2\lambda\mu)\frac{m^2}{ME}$$
$$- [8\lambda(1 + \lambda^2)\mu + 3(1 + 6\lambda^2 + 9\lambda^4)] \frac{E}{M}\Big\},$$
$$b(E) = 3\frac{\lambda^2 - 1}{1 + 3\lambda^2}\frac{E}{M},$$

and μ is the difference between the total magnetic moments of the proton and neutron. As is evident from the formulas, the corrections $\sim \Delta/M$ come both from "weak magnetism" and from taking into account proton recoil. It is interesting to note the appearance of $\cos^2\theta$ terms, which are missing in the ordinary e-ν correlation formulas and turn up here because of the inclusion of recoil. The size of the corrections to the ordinary effects is given in Table I. It is evident that the corrections come up to a few percent. This is partially connected with the fact that the term $(1 - \lambda^2)$ in the fundamental process is rather small because of the nearness of λ to unity ($\lambda = 1.2$).

TABLE I. Corrections to e-ν correlation in %

Total electron energy, Mev	From "weak magnetism"	From recoil
0.71	0.4	1.9
0.91	1.4	2.7
1.11	2.4	3.5
1.29	3.3	4.2

4. THE ELECTRON SPECTRUM AND THE PROBABILITY OF DECAY

Integrating (10) over the angle between the electron and neutrino, we get the following expression for the electron spectrum:

$$dW(E) = 4(2\pi)^{-3} G^2 pE (E_0 - E)^2 \{1 + 3\lambda^2$$
$$- 2\lambda(\lambda + \mu)\Delta/M + 2(5\lambda^2 + 2\lambda\mu + 1)$$
$$\times E/M - 2\lambda(\mu + \lambda) m^2/ME\} \, dE. \qquad (11)$$

The corrections to the spectrum are shown to be small (the fundamental process determines the term $1 + 3\lambda^2$) and reach a few tenths of a percent. For example, for the electron energies 0.91, 1.11, and 1.29 Mev, the total corrections are, respectively, 0.3, 0.4, and 0.6%.

From (11) we get the following expression for the total decay probability.

$$W = \frac{4G^2}{(2\pi)^3}\Big\{\frac{m^4}{4}\ln\frac{E_0 + \sqrt{E_0^2 - m^2}}{m}\Big[\Big(1 + 3\lambda^2 - 2\lambda(\lambda + \mu)\frac{\Delta}{M}\Big)E_0$$
$$- \frac{1}{2}(1 + 3\lambda^2)\frac{m^2}{M} - (1 + \lambda^2 - 2\lambda\mu)\frac{E_0^2}{M}\Big] + \sqrt{E_0 - m^2}$$
$$\times\Big[(5\lambda^2 + 1 + 2\lambda\mu)\frac{E_0^5}{30M} + \frac{1}{5}\Big(1 + 3\lambda^2 - 2\lambda(\lambda + \mu)\frac{\Delta}{M}\Big)$$
$$\times\Big(\frac{1}{6}E_0^4 - \frac{3}{4}m^2E_0^2 - \frac{2}{3}m^4\Big) - \Big(\frac{3}{10}\lambda\mu + \frac{1}{15} + \frac{1}{2}\lambda^2\Big)\frac{m^2E_0^3}{M}$$
$$+ \Big(\frac{23}{24}\lambda^2 + \frac{49}{120} - \frac{4}{15}\lambda\mu\Big)\frac{m^4E_0}{M}\Big]\Big\}. \qquad (12)$$

The correction to the probability is small and comes to about 0.2%.

5. ASYMMETRY AND ELECTRON POLARIZATION

Now we look at the asymmetry in the emission of electrons in the decay of a polarized neutron. By a long, but not complicated calculation, one can get the formula given below for the angular distribution of the electrons

$$dW(E, \cos\theta_e) = (1/4\pi) \to (\text{spectrum}) \to [1 + P\beta c(E)\cos\theta_e]\, d\Omega_e, \quad (13)$$

where

$$c(E) = \frac{2\lambda(1-\lambda)}{1+3\lambda^2} + \frac{2(\lambda+\mu)}{(1+3\lambda^2)^2}\Big[(3\lambda^2+2\lambda-1)\frac{\Delta}{3M} - (3\lambda^3+9\lambda^2+5\lambda-1)\frac{E}{3M} - 2\lambda^2(\lambda-1)\frac{m^2}{ME}\Big],$$

P is the degree of polarization of the neutron, and θ_e is the angle between the direction of polarization of the neutron and the momentum of the electron. From Table II it is evident that the corrections to the asymmetry of the electrons come to several percent, which fact, as in the electron-neutrino case, is partially due to the smallness of the basic effect [proportional to $\lambda(\lambda-1)$]. We note that the corrections to the asymmetry of the neutrino, where the basic effect is large, are small.

TABLE II. Corrections to the asymmetry of the electrons in %

Total electron energy, Mev	From "weak magnetism"	From recoil
0.71	1.3	0.3
0.91	1.8	0.5
1.11	2.4	0.6
1.29	3.0	0.8

In conclusion we given the expression for the electron polarization P_e, calculated with the aid of the amplitude (5) (with ordinary normalization):

$$P_e = -\beta\Big(1 + 2\lambda\frac{\lambda+\mu}{1+3\lambda^2}\frac{m^2}{ME}\Big). \quad (14)$$

The corrections to the polarization are small and for energies of 0.71, 0.91, and 1.11 Mev make up, respectively, 0.14, 0.08, and 0.07%.

Finally, we note that, as the calculations show, the radiation corrections, although they change the effective value of the beta-decay constant, have practically no influence on the effect observed by us.

The authors are grateful to Prof. V. Telegdi for his examination of the results of this work.

---

[1] E. C. G. Sudarshan and R. E. Marshak, Phys. Rev. **109**, 1860 (1958).

[2] R. P. Feynman, and M. Gell-Mann, Phys. Rev. **109**, 193 (1958).

[3] Proceedings, 1958 Annual International Conference on High Energy Physics, CERN.

[4] M. Gell-Mann, Phys. Rev. **111**, 362 (1958).

[5] J. Bernstein and R. R. Lewis, Phys. Rev. **112**, 232 (1958).

[6] M. Morita, Bull. Am. Phys. Soc. **4**, 230 D11 (1959).

[7] M. L. Goldberger and S. B. Treiman, Phys. Rev. **111**, 354 (1958).

[8] S. M. Berman, Phys. Rev. **112**, 267 (1958).

[9] T. D. Lee and C. N. Yang, Nuovo cimento **3**, 749 (1956).

[10] S. Weinberg, Phys. Rev. **112**, 1375 (1958).

[11] L. Michel and A. S. Wightman, Phys. Rev. **98**, 1190 (1955).

[12] S. M. Bilen'kiĭ and R. M. Ryndin, JETP **36**, 1609 (1959), Soviet Phys. JETP **9**, 1144 (1959).

Translated by W. Ramsay
339

SOVIET PHYSICS JETP VOLUME 37(10), NUMBER 6 JUNE, 1960

ANALYTICITY AND UNITARITY IN THE SCATTERING OF SCALAR MESONS FROM A STATIC NUCLEON

B. L. IOFFE

Submitted to JETP editor July 10, 1959

J. Exptl. Theoret. Phys. (U.S.S.R.) 37, 1764-1769 (December, 1959)

The uniqueness of the determination of the scattering amplitude from the analyticity and unitarity conditions is considered for the problem of scattering of scalar neutral and charged mesons from a static nucleon in the one-meson approximation. The analysis is carried out by describing the analytic properties of the scattering amplitude on all sheets of the Riemann surface. As a result it is found that the non-unique terms appearing in the solution are characteristic of scattering from virtual or Breit-Wigner levels.

IN the course of the last few years it has been discussed repeatedly (see, for example, references 1 and 2) whether the conditions of analyticity and unitarity (in addition to the data on the mass spectrum) are sufficient for the determination of the amplitude for various physical processes. Castillejo, Dalitz, and Dyson[3] showed that in the problem of the scattering of charged (or neutral) scalar mesons from a static nucleon in the one-meson approximation the conditions of analyticity and unitarity do not determine the scattering amplitude uniquely. One can therefore add certain additional terms to the scattering amplitude without violating these conditions. In the present paper we consider the same problem by a somewhat different method from that employed by the aforementioned authors (we also remark on the scattering of mesons from nucleons in the Lee model). It seems to us that our approach makes the physical meaning of the non-unique terms more apparent.

Let us first consider the scattering of neutral scalar mesons from a static nucleon in the one-meson approximation. It is known that the solution of this problem by the usual methods of field theory leads to a vanishing scattering cross section. We will get a different result if we use only the conditions of analyticity and unitarity.

In the case of a static nucleon only the S wave gives a contribution to the scattering amplitude for scalar mesons. The general expression for the scattering amplitude will therefore be of the form

$$f(\omega) = (e^{2i\delta} - 1)/2ik, \tag{1}$$

where ω and k are the energy and the momentum of the meson ($\hbar = c = 1$), and $k = \sqrt{\omega^2 - \mu^2}$. Since we are using the one-meson approximation, the scattering phase δ is real.

In specifying the analytic properties of $f(\omega)$ in the complex plane ω we shall consider the many-valued function $f(\omega)$ on all sheets of its Riemann surface. This is in contrast to the usual method where $f(\omega)$ is given only on one sheet by introducing a cut in the complex plane. In the one-meson approximation the function $f(\omega)$ has two branch points of second order at $\omega = \mu$ and $\omega = -\mu$, so that the Riemann surface for $f(\omega)$ consists of four sheets. Owing to the requirement of relativistic invariance (for the mesons) the expressions $\sqrt{\omega - \mu}$ and $\sqrt{\omega + \mu}$ cannot enter in $f(\omega)$ separately, but only through the momentum k, i.e., in the combination $\sqrt{\omega^2 - \mu^2}$. Two of the four Riemann sheets, therefore, coincide pairwise, so that the Riemann surface consists of two sheets.

We shall call the first sheet of the Riemann surface that sheet on which $\varphi = \arg\sqrt{\omega^2 - \mu^2}$ varies between the limits $0 < \varphi < \pi$, and the second sheet, that on which $\pi < \varphi < 2\pi$. The values of $f(\omega)$ on the first and second sheets will be denoted by $f_1(\omega)$ and $f_2(\omega)$, respectively. With this definition the first Riemann sheet corresponds to the complex plane of ω with cuts from μ to $+\infty$ and from $-\mu$ to $-\infty$ (here $\arg\sqrt{\omega - \mu}$ varies between the limits 0 and π, and $\arg\sqrt{\omega + \mu}$ between $-\pi/2$ and $\pi/2$), and $f_1(\omega)$ is that value of the amplitude which appears in the usual form of the dispersion relations. For real $\omega > \mu$ the function $f_1(\omega)$ is the physical scattering amplitude.

By the usual method of the theory of many-valued functions (see, for example, reference 4), we introduce, instead of f_1 and f_2, the two functions

$$\varphi_1(\omega) = [f_1(\omega) + f_2(\omega)]/2, \qquad \varphi_2(\omega) = f_1(\omega) f_2(\omega). \tag{2}$$

It is easily seen that $\varphi_1(\omega)$ and $\varphi_2(\omega)$ are single-valued analytic functions and can therefore be defined through their poles, if they vanish at infinity and contain no essential singularities. The functions f_1 and f_2 are given in terms of φ_1 and φ_2 by

$$f_{1,2}(\omega) = \varphi_1 \pm \sqrt{\varphi_1^2 - \varphi_2}, \tag{3}$$

where one of the signs corresponds to f_1, the other to f_2.

We now write down the condition of unitarity. This condition is valid only for physical values of the energy: ω real, $\omega > \mu$, $\arg\sqrt{\omega^2 - \mu^2} = 0$, and is written in the form

$$\operatorname{Im} f_1(\omega) = k\,|f_1(\omega)|^2, \qquad \omega = \omega + i0,\ \omega > \mu. \tag{4}$$

Let us write (4) in terms of the functions φ_1 and φ_2, We note that for $\operatorname{Im}\omega = 0$, $\omega > \mu$,

$$f_2(\omega) = f_1^*(\omega). \tag{5}$$

Indeed, $f_2(\omega)$ differs from $f_1(\omega)$ only by the sign in front of $k = \sqrt{\omega^2 - \mu^2}$. Since $\delta(k)$ in (1) is an odd function of k, $\delta(k) = -\delta(-k)$, and is also real, a change of the sign of k is equivalent to complex conjugation. It follows from (2) and (5) that in the physical region ($\operatorname{Im}\omega = 0$, $\omega > \mu$)

$$\varphi_1(\omega) = \operatorname{Re} f_1(\omega), \qquad \varphi_2(\omega) = |f_1(\omega)|^2. \tag{6}$$

With the help of (6) and (4) we easily obtain the relation

$$\varphi_1^2(\omega) = \varphi_2(\omega) - (\omega^2 - \mu^2)\,\varphi_2^2(\omega). \tag{7}$$

As is evident from its derivation, this relation is valid only in the physical region ($\operatorname{Im}\omega = 0$, $\omega > \mu$). However, since $\varphi_1(\omega)$ and $\varphi_2(\omega)$ are analytic in the entire complex plane, expression (7) can be continued analytically, and we arrive at the result that (7) is valid everywhere. Substituting (7) in (3), we obtain

$$f_{1,2}(\omega) = \varphi_1 \pm i\sqrt{\omega^2 - \mu^2}\,\varphi_2. \tag{8}$$

The upper sign in (8) corresponds to the value of the amplitude on the first sheet, $f_1(\omega)$, the lower sign so that on the second sheet, $f_2(\omega)$. [With the alternative choice of signs formula (4) would not be true.]

Up to now we have not used at all the fact that $f(\omega)$ is the scattering amplitude for neutral mesons. As a consequence of the neutrality of the scattered mesons the scattered amplitude must be invariant under the substitution $\omega \to -\omega$:

$$f(\omega) = f(-\omega), \tag{9}$$

since $\sqrt{\omega^2 - \mu^2}$ does not change under this substitution, relation (9) must be true for $f_1(\omega)$ as well as for $f_2(\omega)$. This means that $\varphi_1(\omega)$ and $\varphi_2(\omega)$ are even functions of ω, i.e., functions of ω^2. Considering that $\varphi_1(\omega)$ and $\varphi_2(\omega)$ must be analytic functions which vanish at infinity [this is seen immediately from (1) and (2)] and satisfy (7), we write down the following general expression for φ_1 and φ_2:*

$$\varphi_1(\omega) = \sum_{i=1}^{n} \alpha_i / (\omega^2 - \lambda_i),$$

$$\varphi_2(\omega) = -i \sum_{i=1}^{N} \varepsilon_i \alpha_i / (\lambda_i^2 - \mu^2)^{1/2} (\omega^2 - \lambda_i^2), \tag{10}$$

where λ_i and α_i are certain (in general complex) constants, $\epsilon_i = \pm 1$, and the root $(\lambda_i^2 - \mu^2)^{1/2}$ must be taken on the first sheet ($0 < \arg(\lambda_i^2 - \mu^2)^{1/2} < \pi$). The N coefficients α_i are not independent but are functions of λ_i; as is seen from (7), they can be determined from the system of N equations

$$\alpha_i \frac{1}{\lambda_i^2 - \mu^2} - 2 \sum_{k \neq i} \frac{\alpha_k}{\lambda_k^2 - \lambda_i^2} \left[1 - \left(\frac{\lambda_i^2 - \mu^2}{\lambda_k^2 - \mu^2} \right)^{1/2} \varepsilon_i \varepsilon_k \right]$$

$$= i \frac{\varepsilon_i}{(\lambda_i^2 - \mu^2)^{1/2}}. \tag{11}$$

It is easily seen by substituting (10) in (8) that the still undetermined constants λ_i correspond to poles of the scattering amplitude which lie either on the first ($\epsilon_i = +1$) or on the second sheet ($\epsilon_i = -1$). On the basis of physical considerations we can make definite assertions regarding the poles on the first sheet: these poles correspond to real physical states; the poles on the second sheet may lie anywhere in the complex plane. Accordingly, we must require, in the neutral theory, that $f_1(\omega)$ have no poles, i.e., all $\epsilon_i = -1$. After substituting (10) in (8) we then obtain for the general expression for the scattering amplitude $f_1(\omega)$

$$f_1(\omega) = \sum_{i=1} [\alpha_i / (\omega^2 - \lambda_i^2)] \left[1 - \sqrt{(\omega^2 - \mu^2)/(\lambda_i^2 - \mu^2)} \right]. \tag{12}$$

As an illustrative example we consider the case of a single real pole† $N = 1$, $\lambda_1^2 \equiv \lambda^2 < \mu^2$. We easily find from (11) that $\alpha = -i(\lambda^2 - \mu^2)^{1/2} = (\mu^2 - \lambda^2)^{1/2}$, and (12) is written as

$$f_1(\omega) = \frac{1}{\omega^2 - \lambda^2} \left[\sqrt{\mu^2 - \lambda^2} + i\sqrt{\omega^2 - \mu^2} \right] = \frac{i}{k + i\alpha}. \tag{13}$$

Expression (13) for the scattering amplitude is of a familiar form: it is the scattering amplitude for a virtual level in ordinary quantum mechanics.

---

*It is assumed in (10) that $\varphi_1(\omega)$ and $\varphi_2(\omega)$ have only simple poles. In principle, some of the poles may, of course, be multiple. The consideration of multiple poles, however, does not introduce anything new in the following discussion, so that we shall leave it out in order to keep the presentation simple.

†λ^2 cannot be real and larger than μ^2. This can be seen without solving equations (11): for $\lambda^2 > \mu^2$ at least one of the functions $\varphi_1(\omega)$, $\varphi_2(\omega)$ would be complex for $\omega^2 > \mu^2$, which would contradict (6) and would lead to a non-zero imaginary part of the scattering amplitude for $\omega^2 < \mu^2$.

For each complex value λ_i^2 there must be another value λ_j^2 which is the complex conjugate of the first one: $\lambda_i^2 = \lambda_j^{2*}$; the coefficients α_i and α_j will also be complex conjugates of each other. This follows immediately from (10), since, according to (6), the functions $\varphi_1(\omega)$ and $\varphi_2(\omega)$ must be real for real $\omega > \mu$. For complex values of λ the simplest expression for the scattering amplitude must, therefore, contain two terms of the sum (12) and can be written after some simple transformations

$$f_1(\omega) = [k(\beta-\beta^*) - \beta\varkappa^* - \beta^*\varkappa] / [k^2 + 2ik\,\mathrm{Im}\,\varkappa - |\varkappa|^2], \quad (14)$$

where $\kappa = (\lambda^2 - \mu^2)^{1/2}$, $\beta = \alpha/\kappa$. [In deriving (14) from (12) one must keep in mind that according to our definition of the root $(\lambda^{2*} - \mu^2)^{1/2} = -\kappa^*$.] The denominator in (14) agrees in the nonrelativistic approximation with the denominator in the Breit-Wigner formula for a resonance, $E - E_0 + i\sqrt{E}\,\Gamma$, $\Gamma > 0$, since $\mathrm{Im}\,\kappa > 0$.

We thus obtain the following result. The conditions of unitarity and analyticity in the one-meson approximation of the neutral scalar theory do not determine the scattering amplitude uniquely. The non-unique terms which appear are characteristic of resonance scattering from virtual (Wigner) or Breit-Wigner levels whose position (and, in the case of Breit-Wigner levels, width) can be arbitrary.

This result agrees with the result of Castillejo, Dalitz, and Dyson[3] that the scattering amplitude can be determined up to an arbitrary number of parameters such that to every two real parameters there corresponds a zero of the scattering amplitude in the physical region. In our solution the presence of zeros of the scattering amplitude follows at once from the presence of virtual and Breit-Wigner resonances. Indeed, let us add a single Breit-Wigner resonance to the scattering amplitude. This resonance, determined by two real parameters (energy and level width), has the property that in going through it the scattering phase changes by π, i.e., the scattering amplitude goes through zero. If there are n Breit-Wigner resonances, the scattering amplitude will have $(n-1)$ zeros on the real axis in the physical region for finite values of ω. If we add a single virtual level, the phase changes by $\pi/2$, but the virtual level is determined by a single parameter, the energy, so that two parameters, i.e., two virtual levels, will again correspond to a zero in the scattering amplitude. Thus we see that in our discussion 2n real parameters give rise to $(2n-1)$ zeros of the scattering amplitude in the physical region.[*]

Let us now turn to the charged theory. All considerations leading to formulas (2) to (8) remain unchanged, the only difference being that the formulas (1) to (8) refer now to both scattering amplitudes: $f_+(\omega)$ for the positive and $f_-(\omega)$ for the negative mesons. The symmetry condition (9) is now written

$$f_+(\omega) = f_-(-\omega) \quad (15)$$

and leads to the corresponding conditions for the functions $\varphi_1^{\pm}(\omega)$ and $\varphi_2^{\pm}(\omega)$:

$$\varphi_1^+(\omega) = \varphi_1^-(-\omega), \quad \varphi_2^+(\omega) = \varphi_2^-(-\omega). \quad (16)$$

In analogy to (10), the functions $\varphi_1(\omega)$ and $\varphi_2(\omega)$ can be expressed as sums over poles,

$$\varphi_1^+ = \sum \alpha_i^+ / (\omega - \lambda_i^+), \quad \varphi_2^+ = \sum \beta_i^+ / (\omega - \lambda_i^+),$$
$$\varphi_1^- = \sum \alpha_i^- / (\omega - \lambda_i^-), \quad \varphi_2^- = \sum \beta_i^- / (\omega - \lambda_i^-) \quad (17)$$

(the summation over i goes from 1 to N), where, according to (16),

$$\lambda_i^+ = -\lambda_i^-, \quad \alpha_i^+ = -\alpha_i^-, \quad \beta_i^+ = -\beta_i^-. \quad (18)$$

Owing to formula (18) it is sufficient to find the general expression for the functions φ_1^+, φ_2^- alone. The unitarity condition for these functions has the form (7). Substituting (17) in this condition, we obtain easily the following equations for the determination of the coefficients α_i^+ and β_i^+ in terms of the locations of the poles λ_i^+:

$$\beta_i^+ = -i(\lambda_i^{+2} - \mu^2)^{-1/2}\varepsilon_i\alpha_i^+,$$
$$2\frac{\alpha_i^+\lambda_i^+}{\lambda_i^{+2} - \mu^2} - 2\sum_{k\neq i}^{N}\frac{\alpha_k^+}{\lambda_i^+ - \lambda_k^+}\left[1 - \left(\frac{\lambda_i^{+2} - \mu^2}{\lambda_k^{+2} - \mu^2}\right)^{1/2}\varepsilon_i\varepsilon_k\right]$$
$$= i\frac{\varepsilon_i}{(\lambda_i^{+2} - \mu^2)^{1/2}}, \quad (19)$$

subject to the condition

$$\sum_{i=1}^{N}\beta_i^+ = -i\sum_{i=1}^{N}\varepsilon_i\alpha_i^+ / (\lambda_i^{+2} - \mu^2)^{1/2} = 0, \quad (19')$$

which guarantees the correct behavior of the function $\varphi_2^+(\omega)$ at infinity $(\varphi_2^+(\omega) \sim 1/\omega^2)$ [the correct behavior of the function $\varphi_1^+(\omega)$ at infinity, $\lim_{\omega\to\infty}\varphi_1^+(\omega) \sim 1/\omega$ is automatically assured by the representation (17)]. As in the case of neutral mesons, $\epsilon_i = +1$ is the condition for the appearance of poles on the first sheet (real poles), while $\epsilon_i = -1$ corresponds to poles on the second sheet.

---

[*] In reference 3, 2n zeros correspond to 2n parameters. The apparent difference from our results is explained by the fact that in the paper of Castillejo, Dalitz, and Dyson the solution containing no additional parameters (with vanishing R function) has two poles of the scattering amplitude on the second sheet. In our case these two poles are included in the number of independent parameters.

Let us consider a very simple example: the scattering amplitude has a real pole at $\omega = 0$ (corresponding to a one-nucleon state) and a pole on the second sheet at $\omega = \lambda$, $\operatorname{Im} \lambda = 0$, $\lambda < \mu$. [There must be at least one pole on the second sheet, otherwise equation (19′) cannot be fulfilled.] The solutions of equations (19) are easily found, and we obtain for the functions φ_1^+ and φ_2^+

$$\varphi_1^+(\omega) = \frac{1}{2}\frac{\lambda}{\mu^2 + \sqrt{\mu^2 - \lambda^2}}\left[\frac{1}{\omega} + \frac{\sqrt{\mu^2 - \lambda^2}}{\mu(\omega - \lambda)}\right],$$

$$\varphi_2^+(\omega) = \frac{1}{2\mu}\frac{\lambda}{\mu^2 + \sqrt{\mu^2 - \lambda^2}}\left[-\frac{1}{\omega} + \frac{1}{\omega - \lambda}\right]. \tag{20}$$

The scattering amplitude for positive mesons has the form

$$f_+(\omega) = \frac{1}{2}\frac{\lambda}{(\mu + \varkappa)\,\omega\,(\omega - \lambda)}\left\{\omega\left(1 + \frac{\varkappa}{\mu}\right) - \lambda + \frac{ik\lambda}{\mu}\right\};$$

$$\varkappa = \sqrt{\mu^2 - \lambda^2}. \tag{21}$$

Close to the real pole

$$f_+(\omega) \approx \lambda / (\mu + \varkappa)\,\omega, \tag{22}$$

and in the neighborhood of the virtual pole

$$f_+(\omega) \approx i\lambda^2 / \mu\,(\mu + \varkappa)(k + i\varkappa). \tag{23}$$

The scattering amplitude near the real pole is usually expressed in terms of the coupling constant g^2: $f(\omega) \approx g^2/\omega$. We see from (22) that

$$g^2 = \lambda / (\mu + \sqrt{\mu^2 - \lambda^2});$$

g^2 cannot exceed unity. This is also in agreement with the results of reference 3.

Our considerations can be immediately applied to the scattering of mesons in the Lee model.[5] In virtue of the fact that in this model the process $N + \theta \rightarrow V$ can occur, while the process $V + \theta \rightarrow N$ is excluded, the scattering amplitude must have one branch point at $\omega = +\mu$, as the branch point at $\omega = -\mu$ must not occur. Therefore, the scattering amplitude is again a two-valued function and can be written in the form (2) or (3). As before, the condition of unitarity has the form (4), so that equations (3) and (4) are also valid in the Lee model. However, relation (8) contradicts the assumption of the presence of only one branch point at $\omega = +\mu$ in the scattering amplitude. From this it follows that the conditions of unitarity and analyticity (including the assumption of the presence of only one branch point) are inconsistent with each other in the Lee model.* This result was also obtained by Ter-Martirosyan,[6] who used the method of Castillejo, Dalitz, and Dyson.

The author expresses his gratitude to K. A. Ter-Martirosyan and A. A. Logunov for valuable comments and to Yu. A. Gol'fand for useful advice.

---

[1] M. Gell-Mann, Proc. of the Sixth Ann. Rochester Conference (1956).

[2] S. Mandelstam, Phys. Rev. **112**, 1344 (1958).

[3] Castillejo, Dalitz, and Dyson, Phys. Rev. **101**, 453 (1956).

[4] R. Courant, Geometric Theory of Functions of a Complex Variable (Russ. Translation) (1934).

[5] T. D. Lee, Phys. Rev. **95**, 1329 (1954).

[6] K. A. Ter-Martirosyan, JETP **37**, 1005 (1959), Soviet Phys. JETP **10**, 714 (1960).

Translated by R. Lipperheide
340

---

*It should however be noted that in the expression for the scattering amplitude in the Lee model calculated with the usual Hamiltonian an additional branch point (of the logarithmic type) occurs at $\omega = \infty$. The problem of the consistency of the analyticity and unitarity relations in the Lee model with account of this singularity cannot apparently be easily solved by the proposed method.

SOVIET PHYSICS JETP VOLUME 37(10), NUMBER 6 JUNE, 1960

ON THE CONNECTION BETWEEN THE OPTICAL CONSTANTS OF METALS AND THEIR MICROSCOPIC CHARACTERISTICS

G. P. MOTULEVICH

P. N. Lebedev Physics Institute, Academy of Sciences, U.S.S.R.

Submitted to JETP editor July 10, 1959

J. Exptl. Theoret. Phys. (U.S.S.R.) **37**, 1770-1774 (December, 1959)

The connection between the optical constants of metals and their microscopic characteristics is considered. It is shown that a combination of measurements of the optical constants of metals in the infrared region over a wide range of wavelengths with measurements of the static conductivity of the same specimens at different temperatures enables one to determine the conduction electron concentration, the electron velocity at the Fermi surface, and the frequency of the interelectronic collisions. A scheme is suggested to process the experimental data, taking into account recent theoretical results.

RECENTLY there have been obtained in a number of papers[1-5] further developments of the theory which connects the optical constants of metals with their most important microscopic characteristics. The new theoretical results have, however, still not yet been taken into consideration when the experimental data are worked out. In particular, the quantum character of the interaction between the conduction electrons and the electromagnetic field and the role of the interelectronic collisions which are shown experimentally to be important even in the near infrared region are not taken into account. The processing of experimental data on the basis of an incomplete theory can lead to erroneous conclusions. It is thus essential to choose a scheme for processing the experimental data which takes recent theoretical results into account at the same time as the metal-optical measurements are continued and broadened. In the scheme for processing the experimental data which is proposed here the measurements of the optical constants must be supplemented by measurements of the conductivity of the same samples at various temperatures. The combination of such measurements enables one to determine the conduction electron concentration, the electron velocity at the Fermi surface, the frequencies of collisions of electrons with phonons and with impurities, and the frequency of interelectronic collisions.

We use in the present paper the following notation: n is the real part of the complex index of refraction; κ the imaginary part of the complex index of refraction, $Z = R + iX$ the surface impedance, N the conduction electron concentration, v the electron velocity at the Fermi surface, $\beta = v/c$, ν^{ee} the frequency of the interelectronic collisions, ν^{ef} the frequency of the electron-phonon collisions, ν^{n} the frequency of the electron-impurity collisions, $\nu_{\text{eff}} = \nu^{ef} + \nu^{ee} + \nu^{n}$ the effective collision frequency, ω the cyclic frequency of light, ω_0 the limiting frequency of the internal photoeffect, λ the wavelength of the light in microns, σ_0 the static conductivity, T the absolute temperature, Θ the Debye temperature, ρ the density, δ the skin depth, $l = v/\nu_{\text{eff}}$ the mean free path, and c and k the velocity of light and Boltzmann's constant. In the following all quantities except λ are expressed in cgs units.

We shall consider a model in which we can introduce for the electrons an effective number of collisions

$$\nu_{\text{eff}} = \nu^{ef} + \nu^{ee} + \nu^{n}. \tag{1}$$

We shall assume that: 1) the conduction electrons can be considered to be a Fermi gas, 2) the Fermi surface is spherical, and 3) the electrons are reflected diffusely from the metal surface. Under these assumptions we find that in the region where the inequalities

$$v/\omega \ll \delta, \ \nu_{\text{eff}}/\omega \ll 1, \ \omega/\omega_0 \ll 1, \tag{2}$$

are satisfied the following relations will be valid for the real and the imaginary part of the surface impedance[6,7]*

---

*In the majority of cases the anomalous skin-effect occurs even at room temperatures when measurements are made on good conductors in the infrared region of the spectrum. We must in that case understand by n and κ their effective values.[7] We shall omit the indices "eff."

$$cX/\pi = 4\varkappa/(n^2+\varkappa^2) = 1.34\cdot 10^{11}(1+p^2G)/\sqrt{N}\lambda, \tag{3}$$

$$cR/\pi = 4n/(n^2+\varkappa^2) = 0.75\beta + 3.54\cdot 10^{-5}\cdot N^{-1/2}(\nu^{ef}+\nu^{ee}+\nu^{n}) - p^2\beta D, \tag{4}$$

where*

$$p = 2.59\cdot 10^{-11}\beta\sqrt{N}\lambda, \quad G = 0.0865 + 0.216q + 0.125q^2,$$
$$D = 0.215 + 0.748q + 0.750q^2 + 0.216q^3,$$
$$q = 2.045\cdot 10^{-5}\nu_{\text{eff}}/\sqrt{N}\beta. \tag{5}$$

As far as the dependence of ν_{eff} on ω and T is concerned we can say the following. According to Gurzhi[2]

$$\nu^{ee}(\omega, T) = \nu_0^{ee}(T)\left[1 + (\hbar\omega/2\pi kT)^2\right], \tag{6}$$

where $\nu_0^{ee}(T)$ is the corresponding classical frequency of the interelectronic collisions which is proportional to T^2. In the near infrared region $\hbar\omega \gg kT$ so that we must use for ν^{ef} the expression obtained from the quantum transport equation[1]

$$\nu^{ef}(T) = \nu_0^{ef}(T)\,\varphi(T), \tag{7}$$

where $\nu_0^{ef}(T)$ is the classical expression for the electron-phonon collision frequency which is valid when $\hbar\omega \ll kT$. The values of the function $\varphi(T)$ were evaluated by Gurzhi.[3] When $T \gg \Theta$, $\varphi(T) \approx 1$ and $\nu^{ef} \approx \nu_0^{ef}$. When $T \lesssim \Theta$, ν^{ef} differs from ν_0^{ef} the more the lower the temperature. When $T \ll \Theta$, $\nu_0^{ef} \to 0$, while $\nu^{ef} \to 0.4\,\nu'(\Theta)$, where $\nu'(\Theta)$ is the classical high temperature electron-phonon collision frequency at $T = \Theta$ [i.e., for $T \gg \Theta$, $\nu_0^{ef} = \nu'(\Theta)T/\Theta$]. The electron-impurity collision frequency ν^n depends neither on ω nor on T.

Substituting (6) and (7) into (4) we obtain

$$4n/(n^2+\varkappa^2) = 0.75\beta + 3.54\cdot 10^{-5}(\nu_0^{ef}\varphi + \nu_0^{ee} + \nu^n)/\sqrt{N} + 1.83\cdot 10^2\nu_0^{ee}/\sqrt{N}T^2\lambda^2 - p^2\beta D. \tag{8}$$

The terms p^2G and $p^2\beta D$ in Eqs. (3) and (8) are small corrections to the main terms. The determination of the microscopic parameters from the measurements of the optical constants can therefore proceed by the method of successive approximations.*

In the first approximation we put in (3) and (8) $p = 0$. We then determine N from (3). Substituting this value for N into (8) we find the dependence of $4n/(n^2+\kappa^2)$ on λ^{-2} which must be a linear dependence in the approximation considered, and the slope of the straight line gives ν_0^{ee} and the intersection with the ordinate axis determines v if ν^{ef}, ν_0^{ee}, and ν^n are known. We can then evaluate the correction terms and find the same microscopic parameters in the next approximation. One can usually limit oneself to the second approximation since the third approximation differs by less than 1% from the second one.

As was stated in the foregoing one must know $\nu_0^{ef}\varphi + \nu_0^{ee} + \nu^n = \nu_0^{ef} + \nu_0^{ee} + \nu^n + \nu_0^{ef}(\varphi - 1)$ in order to determine v. To evaluate this sum we must use measurements of σ_0. If $T \gg \Theta$, then $\varphi \approx 1$ and it is sufficient to measure σ_0 of the sample under investigation at the temperature of the optical experiment, since

$$\nu_0^{ef} + \nu_0^{ee} + \nu^n = 2.53\,(N/\sigma_0)\,10^8. \tag{9}$$

If $T \lesssim \Theta$ it is necessary to determine ν_0^{ef} as well as σ_0. This can be done in two ways: 1) using the temperature dependence of σ_0 of the sample under investigation at low temperatures one can separate off the temperature independent quantity ν^n and after that determine ν_0^{ef}; 2) using the tabulated values of the static conductivity of the pure metal in bulk σ_0^M, and taking into account that

$$\sigma_0^M/\sigma_0 = (\nu_0^{ef} + \nu_0^{ee} + \nu^n)/(\nu_0^{ef} + \nu_0^{ee}),$$

we can also determine ν_0^{ef} and ν^n.†

We noted already in the foregoing that the expressions we gave for R and X are valid only under the condition that the inequalities (2) are satisfied. After the microscopic characteristics of the metal are determined one can easily verify whether the first two inequalities are satisfied.

---

*We shall use for G and D the expressions obtained in referances 6 and 7 by using the classical transport equation. The evaluation of these expressions if one uses the quantum transport equation leads according to Gurzhi[1] to somewhat different coefficients. Taking into account that these terms occur only as corrections we may calculate them with less accuracy and use instead of the complicated quantum expressions the formulae given here using Eq. (1). When, however, these terms are large we must use for them the expressions obtained by Gurzhi.

*The determination of the microscopic characteristics of a metal from optical measurements can be done also using expressions for n, κ, $n^2-\kappa^2$, κ/n, and $\sqrt{n^2+\kappa^2}$.[7] The most rational method is, however, to use the expressions for R and X as the coefficients in the terms with G and D are very small compared with the coefficients in the analogous terms in the expressions for n, κ, and so on.

†If the inequality $\nu_0^{ee} \ll \nu_0^{ef}$ is satisfied we can assume $\sigma_0^M \approx 2.53\times 10^8 N/\nu_0^{ef}$ whence follows that

$$\frac{4n}{n^2+\varkappa^2} = 0.75\beta + 0.896\cdot 10^4\sqrt{N}\,\frac{1}{\sigma_0}\left[1 + (\varphi - 1)\frac{\sigma_0}{\sigma_0^M}\right] + 1.83\cdot 10^2\,\frac{\nu_0^{ee}}{\sqrt{N}T^2\lambda^2} - p^2 3D.$$

If the first two inequalities are satisfied one can use the following criterion to decide whether the third inequality is satisfied: the quantity

$$N = 1.79 \cdot 10^{22} (1 + p^2 G)^2 \left(\frac{4\varkappa\lambda}{n^2 + \varkappa^2} \right)^{-2}$$

may not depend on λ and the dependence of the quantity $M = 4n/(n^2 + \kappa^2) + p^2 \beta D$ on λ must be a quadratic one. The measurements must then be performed in a sufficiently wide range of wavelengths. Experiments show that for a number of metals (Ag, Cu, Al) there exists a wavelength region where this inequality is satisfied.

One can thus determine N, v, and ν_0^{ee} by measuring the optical constants. Nearly all measurements of optical constants are at present performed with polycrystalline samples. The optical measurements determine therefore some average values for these quantities. The microscopic characteristics obtained can be compared with the results of other experiments.

One can determine the quantity ν_0^{ee} from a measurement of the temperature dependence of σ_0 at $T \gg \Theta$. Indeed, in that temperature range $\nu_0^{ef} + \nu^n = a + bT$, $\nu_0^{ee} = gT^2$, where a, b, and g are constants. Separating out the quadratic term in the curve that describes the dependence of σ_0 on T, one can easily obtain ν_0^{ee}. One must note that the contribution of the interelectronic collisions in the quantity $cR/\pi = 4n/(n^2 + \kappa^2)$ is important in the near infrared region, since $\nu^{ee}(\omega)$ is in that frequency region comparable to ν^{ef}, while at the same time the contribution of the interelectronic collisions to the static conductivity is small since $\nu_0^{ee} \ll \nu_0^{ef}$. One finds therefore the magnitude of ν_0^{ee} more reliably from optical measurements than from a measurement of the temperature dependence of σ_0.

The experimentally obtained quantity ν_0^{ee} can also be compared with the theoretical estimate of this quantity carried out by Ginzburg and Silin:[8]

$$\nu_0^{ee} \backsim 2.2 N v \, (kT)^2 E_0^{-4} \, e^4 y \, (\hbar / p_0 r). \tag{10}$$

Here $E_0 = \frac{1}{2} m_{eff} v^2 = 3.07 \times 10^{-27} \sqrt{Nv}$ is the electron energy at the Fermi surface,* e the electron charge, $p_0 = m_{eff} v = 6.15 \times 10^{-27} \sqrt{N/v}$ the electron momentum at the Fermi surface, $r \approx 2 \times 10^{-8}$ for a screened Coulomb field and $y(\hbar/p_0 r)$ some function of $\hbar/p_0 r$ which was evaluated in reference 8.

The quantities N and v obtained by the optical method can be compared with data obtained from the measurement of the electronic specific heat or with data obtained from measuring the surface impedance at radiofrequencies at low temperatures.[7] If we measure the electronic specific heat we obtain the quantity

$$v / \sqrt{N} = 1.44 \cdot 10^{-2} / \sqrt{\gamma} \tag{11a}$$

(here $c_e = \gamma T$ is the electronic specific heat per cm^3). From measurements of the surface impedance in the radio-frequency range we can determine the quantity

$$v / N = 2.53 \cdot 10^8 / (\sigma / l). \tag{11b}$$

Here σ and l refer to the radio-frequency range. If we can neglect anisotropy and consider the electrons in the metal as a Fermi gas rather than a Fermi liquid, then optical measurements, electronic specific heat measurements, and radiofrequency measurements must give the same values for $v/\sqrt{N}$ and v/N. If, however, the anisotropy is important or if there is an important additional correlation between the electrons (Fermi liquid) different experimental methods will, as was shown by Silin[4] lead to different values for these quantities. Such a comparison can thus give us some basis to reach a conclusion about the role of the anisotropy or about the presence of additional correlations, but only in the case where all these measurements are performed on the same samples.

In conclusion I express my gratitude to V. L. Ginzburg, V. P. Silin, and I. L. Fabelinskiĭ for discussing the present paper.

---

*In their paper, as also in reference 7, $N = 2/3mv^2(dy/dE)_0$, where $(dy/dE)_0$ is the density of states near the Fermi surface. Hence

$$m_{eff} = \sqrt{3 (2\pi\hbar)^3 N / 8\pi m v^3} = 6.15 \cdot 10^{-27} \sqrt{N / v^3}.$$

[1] R. I. Gurzhi, JETP **33**, 451, 660 (1957), Soviet Phys. JETP **6**, 352, 506 (1958).

[2] R. I. Gurzhi, JETP **35**, 965 (1958), Soviet Phys. JETP **8**, 673 (1959).

[3] R. I. Gurzhi, Thesis, Inst. Techn. Phys. Acad. Sc. Ukr. S.S.R. (1958).

[4] V. P. Silin, JETP **33**, 1282 (1957), Soviet Phys. JETP **6**, 985 (1958).

[5] L. A. Prozorova, JETP **34**, 14 (1958), Soviet Phys. JETP **7**, 9 (1958).

[6] R. B. Dingle, Physica **19**, 348 (1953).

[7] V. L. Ginzburg and G. P. Motulevich, Usp. Fiz. Nauk **55**, 469 (1955).

[8] V. L. Ginzburg and V. P. Silin, JETP **29**, 64 (1955), Soviet Phys. JETP **2**, 46 (1956).

Translated by D. ter Haar
341

SOVIET PHYSICS JETP VOLUME 37(10), NUMBER 6 JUNE, 1960

ON K_{e4} *DECAY*

L. B. OKUN' and E. P. SHABALIN

Submitted to JETP editor August 10, 1959

J. Exptl. Theoret. Phys. (U.S.S.R.) **37**, 1775-1780 (December, 1959)

The probabilities for K_{e4} decays are computed. Selection rules for the decays and isotopic relations between various K_{e4} decays are determined on the basis of the Sakata model.

1. INTRODUCTION

THIS article is concerned with the K_{e4} decays of the K meson

$$K \to e + \nu + 2\pi, \tag{1}$$

in which, in contrast to the well known K_{e3} decay, not one but two pions are emitted. As yet K_{e4} decays have not been observed experimentally. Theoretical estimates by Oneda,[1] based on a comparison of the available volume in phase space and of the matrix elements for K_{e4} and K_{e3} decays, show that the probability for K_{e4} decay is significantly smaller than the probability for K_{e3} decay.

The K_{e4} decays are of interest since they provide a way to test some of the consequences of the Sakata model[2] for strongly interacting particles. In this model all strongly interacting particles are composed of protons, neutrons, Λ hyperons and their antiparticles. If, in the framework of the Sakata model, it is assumed that the leptonic decays of strange particles are caused by the interaction

$$(\bar{p}\Lambda)(\bar{e}\nu) + (\bar{\Lambda}p)(\bar{\nu}e), \tag{2}$$

then it is easy to obtain the following selection rules governing these decays:[3-5]

$$\Delta Q = \Delta S = \pm 1, \tag{3}$$

$$\Delta T = 1/2, \tag{4}$$

where ΔQ, ΔS, ΔT are the change in charge, strangeness and isotopic spin respectively of the strongly interacting particles.

Below we calculate the probability for K_{e4} decay on the basis of the universal Fermi interaction theory[6] and discuss the consequences of the selection rules (3) and (4).

2. MATRIX ELEMENT FOR THE K_{e4} DECAY

According to the universal V-A interaction theory the Lagrangian density of the interaction (2) responsible for leptonic decays of strange particles and, in particular, for the K_{e4} decay, is given by

$$L = \frac{G}{\sqrt{2}} [\bar{\psi}_e \gamma_\alpha (1 + \gamma_5) \psi_\nu] [\bar{\psi}_p \gamma_\alpha (1 + \gamma_5) \psi_\Lambda] + \text{h.c.}, \tag{5}$$

where the weak interaction coupling constant $G = (1.01 \pm 0.01) m^{-2} \times 10^5$ and m is the proton mass ($\hbar = c = 1$).

Since in the K_{e4} decay a substantial role is played by virtual strong interactions along with the weak interaction (5), we cannot calculate the matrix element for K_{e4} decay with the help of (5); we can only establish its most general form consistent with the usual invariance requirements and using the fact that it is sufficient to consider only lowest order perturbation theory for the weak interactions (see review article by Okun'[7]).

We have

$$M = G V'_\alpha \bar{u}_\nu \gamma_\alpha (1 + \gamma_5) u_e (16 E_1 E_2 E_K)^{-1/2}, \tag{6}$$

where u_e and u_ν are the electron and neutrino spinors and V'_α is a 4-vector constructed in the most general way possible out of the momenta of the strongly interacting particles. It is easy to show that

$$V'_\alpha = (f'_1 k_1 + f'_2 k_2 + f'_3 q)_\alpha, \tag{7}$$

where f'_i are unknown invariant functions of the scalar products $k_1 \cdot k_2$, $k_1 \cdot q$ and $k_2 \cdot q$; k_1 and k_2 are the momentum 4-vectors of the pions, q is the momentum 4-vector of the K meson. We assume that the structures f'_i are weak functions of their arguments and will treat them as constants in the following discussion.

Making use of the momentum conservation law

$$q = k_1 + k_2 + p_e + p_\nu \tag{8}$$

and of the Dirac equation for the electron and the neutrino

$$\hat{p}_\nu u_\nu = 0, \quad \hat{p}_e u_e = m_e u_e \tag{9}$$

and ignoring the mass of the electron, we easily convert Eq. (6) into

$$M = (G/2\sqrt{E_1 E_2 E_K}) V_\alpha [\bar{u}_\nu \gamma_\alpha (1 + \gamma_5) u_e], \tag{10}$$

where

$$V_\alpha = [f_1k_1 + f_2k_2]_\alpha = \tfrac{1}{2}\{(f_1+f_2)(k_1+k_2)_\alpha + (f_1-f_2)$$
$$\times (k_1-k_2)_\alpha\} = \tfrac{1}{2}\{f(k_1+k_2)_\alpha + g(k_1-k_2)_\alpha\}. \qquad (11)$$

3. ISOTOPIC RELATIONS BETWEEN VARIOUS K_{e4} DECAYS

It is easy to verify that the following K_{e4} decays of the $K^\pm$ and K^0 mesons do not violate the law of charge conservation

$$K^+ \to \pi^0 + \pi^0 + e^+ + \nu, \qquad (a)$$
$$K^+ \to \pi^+ + \pi^- + e^+ + \nu, \qquad (b)$$
$$K^0 \to \pi^- + \pi^0 + e^+ + \nu, \qquad (c)$$
$$K^0 \to \pi^+ + \pi^0 + e^- + \tilde{\nu}, \qquad (d)$$
$$K^+ \to \pi^+ + \pi^+ + e^- + \tilde{\nu}. \qquad (e)$$

[Decays of the K^- and $\bar{K}^0$ mesons are easily obtained from (a) – (e) by replacing all particles by antiparticles.]

Let us see what restrictions are imposed on the matrix elements of decays (a) – (e) by the selection rules (3) and (4). First of all it is obvious that for the decays (d) and (e) we have $\Delta Q = -\Delta S = 1$ and consequently these decays are forbidden within the framework of the Sakata model. Next, from the rule $\Delta T = \frac{1}{2}$ it follows that the two pions in the decays (a), (b) and (c) must be in the states with $T = 0$ and $T = 1$ only. It is easy to see that both these states are possible only in (b); in (a) only the state $T = 0$, and in (c) only the state $T = 1$, is possible.

Introducing the amplitudes $V^{(0)}$ and $V^{(1)}$ corresponding to transitions into the states $T = 0$ and $T = 1$ we obtain for the amplitudes of the (a), (b) and (c) decays[8]

$$V_a = V^{(0)}/\sqrt{2}, \quad V_c = V^{(1)}, \quad V_b = -V^{(0)} + V^{(1)}/\sqrt{2} \qquad (12)$$

which shows that they are related.

Since the $T = 0$ state should be even under the exchange of the two pions it corresponds in Eq. (11) to the term

$$V^{(0)} = \tfrac{1}{2} f(k_1+k_2) \qquad (13)$$

The $T = 1$ state corresponds to the term

$$V^{(1)} = \tfrac{1}{2} g(k_1-k_2). \qquad (14)$$

4. PROBABILITY OF K_{e4} DECAY

The differential K_{e4} decay probability is given by

$$dw = \sum_{e,\nu} (2\pi)^4 |M|^2 \delta^4(q-k_1-k_2-p_e-p_\nu)$$
$$\times \frac{d^3k_1}{(2\pi)^3}\frac{d^3k_2}{(2\pi)^3}\frac{d^3p_e}{(2\pi)^3}\frac{d^3p_\nu}{(2\pi)^3}, \qquad (15)$$

where the summation is over the polarizations of the electron and the neutrino. Substituting for M from Eq. (10) and performing the above mentioned summation we obtain

$$dw = \frac{G^2}{2(2\pi)^8 E_k}[2(Vp_e)(Vp_\nu) - V^2(p_ep_\nu)]$$
$$\times \delta(q-k_1-k_2-p_e-p_\nu)\frac{d^3k_1}{E_1}\frac{d^3k_2}{E_2}\frac{d^3p_e}{E_e}\frac{d^3p_\nu}{E_\nu}, \qquad (16)$$

with the 4-vector V given by Eq. (11).

It is convenient to carry out the integrations by the invariant method used by Dalitz in a discussion of the decay $K^+ \to 3\pi + \gamma$.[9] We introduce the new variables

$$Q = k_1 + k_2, \quad R = k_1 - k_2 \quad \text{for pions} \qquad (17)$$
$$F = p_e + p_\nu, \quad L = p_e - p_\nu \quad \text{for leptons} \qquad (18)$$

In terms of these variables the conservation law becomes

$$Q + F = q. \qquad (19)$$

The phase space volume element for the pions will be written as

$$\frac{d^3k_1}{E_1}\frac{d^3k_2}{E_2} = 4\delta(k_1^2-m^2)\,\delta(k_2^2-m^2)\,d^4k_1d^4k_2$$
$$= 4\delta(k_1^2/2+k_2^2/2-m^2)\,\delta(k_1^2-k_2^2)\,d^4k_1\,d^4k_2$$
$$= \delta(Q^2+R^2-4m^2)\,\delta(QR)\,d^4Q\,d^4R, \qquad (20)$$

where m is the pion mass. Analogously for leptons

$$\frac{d^3p_e}{E_e}\frac{d^3p_\nu}{E_\nu} = \delta(F^2+L^2)\,\delta(FL)\,d^4F\,d^4L. \qquad (21)$$

The expression for the total probability now becomes

$$w = \frac{G^2}{2(2\pi)^8E_k}\iint \frac{1}{2}[(VF)^2 - (VL)^2$$
$$- V^2F^2]\,\delta(QR)\,\delta(Q^2+R^2-4m^2)$$
$$\times\,\delta(FL)\,\delta(F^2+L^2)\,d^4Q\,d^4R\,d^4F\,d^4L\,\delta^4(q-F-Q) \qquad (22)$$

The integration over d^4F is trivial because of the $\delta(q-F-Q)$, and the integration over d^4L yields

$$w = \frac{G^2\pi}{(2\pi)^8 3E_K}\int \delta(QR)\,\delta(Q^2+R^2-4m^2)\,[(VF)^2$$
$$- V^2F^2]\,d^4R\,d^4Q. \qquad (23)$$

In order to proceed with the integration it is necessary to specify the structure of the function V. We shall consider the decay (b) for which

$$V_b = \tfrac{1}{2}[fQ + gR/\sqrt{2}]. \qquad (24)$$

The probability for the decay (a) is obtained by setting $g = 0$ in the final answer and dividing by two. For the decay (c) one must take $V_c = gR/2$. The integration over d^4R yields

$$w = \frac{G^2\pi^2}{(2\pi)^8 6E_K} \int \{f^2[(QF)^2 - Q^2F^2]\, X + \frac{g^2}{6}[2Q^2F^2 + (QF)^2]\, X^3\}\, d^4Q. \tag{25}$$

Here $F = q - Q$ and $X = \sqrt{(Q^2 - 4m^2)/Q^2}$. The integration over d^4Q will be performed as follows. Let us write $d^4Q = dQ_0\,|\mathbf{Q}|^2\, d\,|\mathbf{Q}|\, d\Omega$, and let us change from the variable $|\mathbf{Q}|$ to Q_e, the "effective mass" of the two pions

$$Q_e = \sqrt{Q_0^2 - \mathbf{Q}^2} = \sqrt{(E_1 + E_2)^2 - (\mathbf{k}_1 + \mathbf{k}_2)^2} \tag{26}$$

We then get

$$d^4Q = \sqrt{Q_0^2 - Q_e^2}\, Q_e dQ_0\, dQ_e\, d\Omega. \tag{27}$$

By considering the decay in the rest frame of the K meson ($E_K = M$) we find that the integration over $d\Omega$ gives 4π. To integrate over dQ_0 we establish the limits between which Q_0 varies for fixed Q_e. From the equality $Q + F = M$ it follows that

$$Q_0 = (M^2 + Q_e^2 - F^2)/2M. \tag{28}$$

The maximum value of Q_0 is obtained when $F^2 = 0$ when both leptons are emitted in the same direction:

$$Q_{0\,max} = (M^2 + Q_e^2)/2M. \tag{29}$$

The minimum value of Q_0, as can be seen from Eq. (26), is equal to Q_e. The limits of integration over Q_e are simple:

$$2m \leqslant Q_e \leqslant M. \tag{30}$$

As a result of the Q_0 integration we obtain

$$dw = \frac{G^2\pi^3M^7}{48\,(2\pi)^8}\Big\{f^2\Big[\frac{1}{4} - 2\frac{Q^2}{M^2} + 2\frac{Q^6}{M^6} - \frac{1}{4}\frac{Q^8}{M^8} - 3\frac{Q^4}{M^4}\ln\frac{Q^2}{M^2}\Big] \times \sqrt{\frac{Q^2 - 4m^2}{Q^2}} + \frac{g^2}{6}\Big[\frac{1}{4} + 18\frac{Q^4}{M^4} - 16\frac{Q^6}{M^6} - \frac{9}{4}\frac{Q^8}{M^8} + \Big(9\frac{Q^4}{M^4} + 12\frac{Q^6}{M^6}\Big)\ln\frac{Q^2}{M^2}\Big]\sqrt{\Big(\frac{Q^2 - 4m^2}{Q^2}\Big)^3}\Big\}\, d\Big(\frac{Q^2}{M^2}\Big). \tag{31}$$

The above expression gives the spectrum in the "effective mass" of the two pions produced in the K_{e4} decay.

The total decay probability is obtained by integrating this spectrum between the limits $(2m/M)^2$ and 1. This integration cannot be performed all the way in terms of elementary functions and it is therefore useful to consider the integral of (31) in certain simple limiting cases.

1) For $m/M \to 0$ we obtain

$$w = \frac{G^2M^7\pi^3}{(2\pi)^8\cdot 3\cdot 16\cdot 30}\Big[f^2 + \frac{g^2}{4}\Big]. \tag{32}$$

2) For $2m/M \to 1$ we obtain

$$w = \frac{4\sqrt{2M}\,(M - 2m)^{13/2}}{\pi^5\cdot 13\cdot 11\cdot 9\cdot 7\cdot 5\cdot 3}\Big[f^2 + \frac{g^2}{5}\frac{M - 2m}{M}\Big]. \tag{33}$$

The exact value of the probability which is of interest to us lies between the results (32) and (33). A numerical integration yields

$$w = \frac{G^2M^7}{2^{10}\pi^5 360}\{f^2 0{,}0296 + g^2 0{,}0029\}. \tag{34}$$

Since the interference term fg has dropped out we see that the probability for the decay (b) is equal to the sum of twice the probability for the decay (a) plus half the probability for the decay (c).

5. CONCLUSION

The K_{e4} decay probability obtained above may be compared with the probability for K_{e3} decay. The latter, calculated according to the universal Fermi interactions theory, (see, e.g., Okun'[7]) is equal to

$$w_{K_{e3}} = 0{,}58G^2\varkappa^2M^5/768\pi^3,$$

where κ is a dimensionless parameter and M is the K-meson mass.

The constants f and g appearing in the expression for the K_{e4} decay probability have the dimensions of an inverse mass. Considering, for example, the decay (a) and setting $f = \kappa/m_\pi$, κ/m_K, κ/m_N (where m_π, m_K, and m_N are the pion, K-meson and nucleon masses) we obtain for the ratio of the K_{e4} and K_{e3} probabilities

$$\begin{array}{ll} 1.27\cdot 10^{-4} & \text{for } f = \varkappa/m_\pi, \\ 1.02\cdot 10^{-5} & \text{for } f = \varkappa/m_K, \\ 0.28\cdot 10^{-5} & \text{for } f = \varkappa/m_N. \end{array} \tag{35}$$

We see that the K_{e4} decay probability is exceptionally small in comparison with the K_{e3} probability. Therefore a detailed experimental test of the results obtained above apparently will not be possible in the near future. An exception is the verification of the absence of the decay $K^+ \to 2\pi^+ + e^- + \tilde{\nu}$. In photoemulsions this decay should look like an anomalous τ decay. If the presently available statistics of τ decays were increased by an order of magnitude the decay $K^+ \to 2\pi^+ + e^- + \tilde{\nu}$ should be discovered provided that its probability is comparable to the probabilities (35). An observation of this decay would indicate the incorrectness of the Sakata model in the sense indicated above. Of course, not seeing the decay would not constitute proof that the Sakata model is right since the rule $\Delta Q = \Delta S$ may be completely unrelated to it (see, e.g., Oneda[1]).

APPENDIX

As an illustration of the invariant integration method let us consider the integral

$$J = \int \delta(QR)\, \delta(Q^2 + R^2 - 4m^2)\, [(VF)^2 - (V^2F^2)]\, d^4R.$$

Using expression (24) for V we have

$$(VF)^2 - V^2F^2 = \tfrac{1}{4}\{f^2[(QF)^2 - Q^2F^2] + (g^2/2)[(RF)^2 - R^2F^2] + gf\sqrt{2}[(QF)(RF) - (QR)F^2]\}. \qquad \text{(A.1)}$$

In the above expression the first term is independent of R; therefore integrating it is equivalent to multiplication by $2\pi\sqrt{(Q^2 - 4m^2)/Q^2}$, since

$$\int \delta(QR)\, \delta(Q^2 + R^2 - 4m^2)\, d^4R = 2\pi\sqrt{(Q^2 - 4m^2)/Q^2}.$$

The integral

$$\int (RN)\, \delta(QR)\, \delta(Q^2 + R^2 - 4m^2)\, d^4R = 0$$

for an arbitrary vector N. Consequently the third term in (A.1) disappears upon d^4R integration. Finally, since

$$\int (RF)^2\, \delta(QR)\, \delta(Q^2 + R^2 - 4m^2)\, d^4R = \frac{2\pi}{3}[(QF)^2 - Q^2F^2]\sqrt{\left(\frac{Q^2 - 4m^2}{Q^2}\right)^3},$$

it is easy to see that

$$\int [(RF)^2 - R^2F^2]\, \delta(QR)\, \delta(Q^2 + R^2 - 4m^2)\, d^4R = \frac{2\pi}{3}[2Q^2F^2 + (QF)^2]\sqrt{\left(\frac{Q^2 - 4m^2}{Q^2}\right)^3}.$$

In the end we obtain

$$J = \frac{\pi}{2}\left\{f^2[(QF)^2 - Q^2F^2]\sqrt{\frac{Q^2 - 4m^2}{Q^2}} + \frac{g^2}{6}[2Q^2F^2 + (QF)^2]\sqrt{\left(\frac{Q^2 - 4m^2}{Q^2}\right)^3}\right\}.$$

---

[1] S. Oneda, Nucl. Phys. **4**, 21 (1957).

[2] S. Sakata, Progr. Theor. Phys. **16**, 686 (1956).

[3] M. Gell-Mann, Proc. of the Sixth Rochester Conf. on High Energy Nuclear Physics, N. Y., 1956.

[4] L. B. Okun', JETP **34**, 469 (1958), Soviet Phys. JETP **7**, 322 (1958).

[5] Okubo, Marshak, Sudarshan, Teutsch, and Weinberg, Phys. Rev. **112**, 665 (1958).

[6] R. Feynman and M. Gell-Mann, Phys. Rev. **109**, 193 (1958). E. C. Sudarshan and R. E. Marshak, Phys. Rev. **109**, 1860 (1958).

[7] L. B. Okun', Usp. Fiz. Nauk **68**, 449 (1959), Ann. Rev. Nuc. Sci. **9**, 1959.

[8] L. B. Okun', Usp. Fiz. Nauk **61**, 535 (1957) (Appendix II).

[9] R. H. Dalitz, Phys. Rev. **99**, 915 (1955).

Translated by A. M. Bincer
342

SOVIET PHYSICS JETP VOLUME 37(10), NUMBER 6 JUNE, 1960

ON THE CLUSTERING OF NUCLEONS IN LIGHT NUCLEI

V. G. NEUDACHIN, Yu. F. SMIRNOV, and N. P. YUDIN

Institute of Nuclear Physics, Moscow State University

Submitted to JETP editor July 18, 1959

J. Exptl. Theoret. Phys. (U.S.S.R.) 37, 1781-1783 (December, 1959)

The theory of permutation groups is used to demonstrate the equivalence of wave functions of the shell theory with LS coupling, for the states with higher symmetry of the orbital part, and the antisymmetrized wave functions composed of wave functions of nucleon clusters. Very simple examples are considered.

THE question of nucleon clusters in nuclei is quite timely at present. In this connection, it is interesting to segregate the internal coordinates of such clusters so as to investigate the effect of spatial correlation on the nucleons, the interactions between different nuclear models, etc. This question was qualitatively examined by Baz'.[1] It has also been noted[2] that in the theory of shells with LS coupling the wave functions for the oscillator potential, in the case of C^{12} and O^{16}, coincide with the wave functions of the α model; an analogous phenomenon takes place also for the lower excited states of Be^8 with $J = 0^+, 2^+$, and 4^+.[3]

We wish to point out the general fact that for the lowest states of the light nuclei in the LS coupling, when the orbital portion of the wave function has a Young tableau of maximum possible symmetry (for example, for B^{10}, [442]), the wave function of shell theory for the oscillator potential coincides with the antisymmetrized wave function made up of the wave functions of the nucleon clusters (for B^{10} this cluster consists of two α particles plus a deuteron, for Li^7 this is an α particle plus a triton, etc.).

The question of the structure of the wave function of Be^8 was examined by Perring and Skyrme,[2] but very briefly and without use of the theory of permutation groups. The use of group theory yields a general approach to the problem.

Our analysis is based on the following premises.

1. For the state of the system with total orbital momentum L, spin S, isobaric spin T, and a Young tableau for the orbital part of the wave function $[\alpha] \equiv [\alpha_1, \alpha_2, \ldots \alpha_m]$, the total wave function $\psi([\alpha]LST)$ can be constructed in the following manner

$$\psi([\alpha]\,LST) = A\Phi(L\,[\alpha]\,r)\,\chi(ST\,[\widetilde{\alpha}]\,\widetilde{r}). \tag{1}$$

where A is the antisymmetrization operator, r the Yamanochi symbol[4] possible for the given $[\alpha]$, while $[\widetilde{\alpha}]$ and $\widetilde{r}$ are symbols analogous to α and r but for the conjugate representation. Expression (1) is equivalent to the one usually employed[4]

$$\psi([\alpha]\,LST) = \sum_r \Phi(L\,[\alpha]\,r)\,\chi(ST\,[\widetilde{\alpha}]\,\widetilde{r}), \tag{2}$$

but is more convenient for our purposes, since it is possible to go in it from basis functions of the orthogonal representation of the permutation group[4] [which are used in (1) and (2)] to functions constructed with the aid of Weyl operators, i.e., symmetrized by rows of the Young tableau $[\alpha]r$ and antisymmetrized by columns.[5] The construction of these latter functions is much simpler. We shall henceforth deal only with these, and retain the notation of (1).

2. We note that

$$\psi([\alpha]\,LST) = A\Phi(L)\,\chi(ST\,[\widetilde{\alpha}]\,\widetilde{r}) = A\Phi(L\,[\alpha]\,r)\,\chi(ST), \tag{3}$$

i.e., there is no need of constructing $\Phi(L[\alpha]r)$, if the function $\chi(ST[\widetilde{\alpha}]\widetilde{r})$ is constructed, and vice versa. The antisymmetrization operator A will automatically pick out the necessary term from the expansion $\Phi(L)$ in functions of different symmetry (provided the final result is not zero).

3. For the spin-orbit functions, corresponding to the Young tableau with maximum symmetry $[\alpha] = [\alpha_1\alpha_2 \ldots \alpha_m]$ (only α_m can be less than 4), we can write

$$\begin{aligned}\chi(ST\,[\widetilde{\alpha}]\,\widetilde{r}_0) &= \chi(S_1 = 0 T_1 = 0\,[\widetilde{\alpha}_1]\,1234)\,\chi(S_2T_2\,[\widetilde{\alpha}_2]\,5678)\ldots\\ &\times \chi(S_mT_m\,[\widetilde{\alpha}_m]\,n - \alpha_m,\ n - \alpha_m + 1, \ldots, n)\\ &= \sum_{\widetilde{r}} C_{\widetilde{r}}\,\chi(ST[\widetilde{\alpha}]\widetilde{r}).\end{aligned} \tag{4}$$

Equation (4) is correct because the Young tableaux $[\tilde{\alpha}]$ with five cells in each column cannot be realized for the spin-charge portion of the wave function. Equation (4) reflects the specific features of the Young patterns of high asymmetry and is essential to our analysis.

From relations (3) and (4) we have

$$\psi([\alpha]\,LST) = A\Phi(L)\,\chi(S_1T_1[\alpha_1]\,1234)\,\chi(S_2T_2[\alpha_2]\,5678)\ldots$$
$$\times\,\chi(S_mT_m[\alpha_m]\,n-\alpha_m,\ n-\alpha_m+1,\ldots,n). \qquad (5)$$

We next consider two specific examples. We start with Be^8. In the shell theory the orbital wave function of the configuration p^4 with $[\alpha_2] = [4]$ and $L = 0$ contains a polynomial[2] (the exponential factor is not written out)

$$(\mathbf{r}_5\mathbf{r}_6)(\mathbf{r}_7\mathbf{r}_8) + (\mathbf{r}_5\mathbf{r}_7)(\mathbf{r}_6\mathbf{r}_8) + (\mathbf{r}_5\mathbf{r}_8)(\mathbf{r}_6\mathbf{r}_7), \qquad (6)$$

which in accordance with $[\alpha_2] = [4]$ is symmetrical in the coordinates of all four nucleons. If, on the other hand, we consider the configuration s^4p^4 in the state $[4, 4]$, $S = 0$, $T = 0$, and $L = 0$, then according to (1) and (3) it is necessary to construct the orbital part with the aid of the Weyl operator for one of the tableaux of form $[\alpha] = [44]$, for example $[44]\,r_0$. Then the polynomial (6) becomes

$$(\mathbf{r}_5-\mathbf{r}_1)(\mathbf{r}_6-\mathbf{r}_2)(\mathbf{r}_7-\mathbf{r}_3)(\mathbf{r}_8-\mathbf{r}_4) + \ldots \qquad (7)$$

The function $\Phi(L = 0\ [44]\,r_0)$ is obtained by multiplying the latter expression by a function which is symmetrical in the coordinates of all the nucleons, $\exp\{-\nu(r_1^2 + \ldots + r_8^2)/2\}$. $\sum \mathbf{r}^2$ is readily converted to a form corresponding to nucleon clustering.

It now remains to explain, for the case of Be^8, the connection between the polynomial (7) of the shell model and the corresponding expression in the wave function of the α model. The coordinate transformation from the shell model to the α model is linear, therefore the corresponding polynomials in the α model should be of fourth degree. The polynomial

$$(\mathbf{R}_1-\mathbf{R}_2)^4$$
$$(\mathbf{R}_1 = \tfrac{1}{4}(\mathbf{r}_1+\mathbf{r}_2+\mathbf{r}_3+\mathbf{r}_4);\ \mathbf{R}_2 = \tfrac{1}{4}(\mathbf{r}_5+\mathbf{r}_6+\mathbf{r}_7+\mathbf{r}_8))$$

is symmetrical in the coordinates $1\ldots4$ and $5\ldots8$, but is not symmetrical for the permutation of the nucleons between these groups. Therefore the application of the Weyl operator, corresponding to the tableau $[44]$, to this polynomial will yield in the end a non-vanishing function that should coincide with (7), accurate to within a factor, by virtue of the uniqueness of the construction of (7).

In exactly the same manner, for the case of Be^{10}, the sixth-degree shell-function polynomial analogous to (7) and constructed with the aid of the Weyl operator for the tableau $[442]$, will be equivalent to the polynomial $(\mathbf{R}_{\alpha_1} - \mathbf{R}_{\alpha_2})^4(\mathbf{R}_\alpha - \mathbf{R}_{\alpha_1\alpha_2})^2$, which describes the clustering $\alpha\alpha d$. States with $S = 1$ and $T = 0$ will correspond to a "deuteron" in the triplet state, while states with $S = 0$ and $T = 1$ will correspond to the deuteron in the singlet state.

In the case when $L > 0$ or when we consider a d-shell etc. the wave functions are subjected to Talmi transformations,[6] but all the conclusions concerning the properties of the states whose orbital wave function has a Young tableau of maximum possible symmetry remain in force. For the d-shell and higher shells the question of the additional quantum numbers necessary to classify the states may arise. We shall not discuss this question. If the self-consistent potential differs from the oscillator potential, the functions may not coincide, but will still be close to each other (large overlap).

For light nuclei, the most substantial is the α clustering. It can be calculated for α nuclei of the type Be^8, C^{12}, etc by writing down the wave function in the "α representation" and then introducing a certain "compression" of the internal dimensions of the α particles, characterized by a parameter $\epsilon < 1$. The resultant wave function will no longer coincide with the wave function of shell theory, but will represent, with the aid of this one parameter ϵ, the configuration mixing due to α correlation.

Such an α correlation can also be taken into account in other than α nuclei. For example, in B^{10} it is possible to use the parentage technique[4,7] to determine the states of eight nucleons and two nucleons, and then introduce the aforementioned internal compression in the states of the eight nucleons, described by the Young tableau $[4, 4]$. What consequences should result from such an α correlation? First, it should increase the quadrupole moments and the probabilities of quadrupole transitions. This is seen with Be^8 as an example. If $\epsilon \ll 1$, the nucleus will represent a "dumbell" with large asphericity, i.e., a nucleus with "different" α particles. Next, the values of ft should increase somewhat for those cases when a new α cluster appears in β decay in the final nucleus, for example in the decays

$$Li^8 \to Be^{8*}(J^\pi = 2^+), \quad B^{12} \to C^{12}.$$

The technique of the computation in such an α model was developed in principle by Biel.[8]

[1] A. I. Baz', JETP **31**, 831 (1956), Soviet Phys. JETP **4**, 704 (1957).

[2] J. K. Perring and T. H. Skyrme, Proc. Phys. Soc. **A69**, 600 (1956).

[3] K. Wildemuth and Th. Kannelopoulos, Nucl. Phys. **7**, 150 (1958); **9**, 449 (1959).

[4] H. A. Jahn and H. van Wieringen, Proc. Roy. Soc. **A209**, 502 (1951).

[5] H. Weyl, The Theory of Groups and Quantum Mechanics, Methuen, London 1931. L. D. Landau and E. M. Lifshitz, Quantum Mechanics, Addison Wesley, Reading, 1958. H. Weyl, The Classical Groups, Princeton, 1939, (Russ. Transl.) IIL, 1947.

[6] I. Talmi, Helv, Phys. Acta **25**, 185 (1952).

[7] G. Racah, Phys. Rev. **63**, 367 (1943), A. R. Edmonds and B. H. Flowers, Proc Roy. Soc. **A214** 515 (1952).

[8] S. J. Biel, Proc. Phys. Soc. **A70**, 866 (1957).

Translated by J. G. Adashko
343

SOVIET PHYSICS JETP VOLUME 37(10), NUMBER 6 JUNE, 1960

ON THE INTERMEDIATE STATE OF FERROMAGNETIC SUPERCONDUCTORS

G. F. ZHARKOV

P. N. Lebedev Physics Institute, Academy of Sciences, U.S.S.R.

Submitted to JETP editor July 22, 1959

J. Exptl. Theoret. Phys. (U.S.S.R.) **37**, 1784-1788 (December, 1959)

The range of external magnetic field values for which a single domain ferromagnetic ellipsoid can exist in the intermediate state is found. The structure of the intermediate state for the case of a ferromagnetic superconducting plate is examined, using the "unbranched" model.

1. The possibility of observing superconductivity in ferromagnetics has been discussed theoretically from the thermodynamic viewpoint by Ginzburg[1] and the author.[2] Recently, Mattias, Suhl, and Corenzwit[3] discovered experimentally that certain ferromagnetics become superconductors; the specimen they studied was found to be in the intermediate state. The question considered below is this: for what external magnetic fields can a single domain ferromagnetic superconductor in the form of an ellipsoid exist in the intermediate state?

For simplicity we take the ferromagnetic specimen in the form of an ellipsoid of rotation with spontaneous magnetization M_0 directed parallel to the rotation axis. Let the external magnetic field H_0 in which the specimen is situated be also parallel to this axis. The magnetic permeability μ of the specimen we put equal to unity, which corresponds to saturation. As follows from Eq. (9) of reference 2, the thermodynamic potential of such a specimen referred to unit volume is equal to

$$\Phi_n = \Delta - 2\pi M_0^2 (1 - n_1) - M_0 H_0, \tag{1a}$$

$$\Phi_s = H_0^2 / 8\pi (1 - n_1), \tag{1b}$$

where the indices n and s refer respectively to specimens entirely in the normal or superconducting states, $\Delta = \Phi_n^0 - \Phi_s^0 > 0$, Φ_s^0 and Φ_n^0 are the thermodynamic potentials of unit volume of the specimen in the absence of the external magnetic field, $4\pi n_1$ is the demagnetization coefficient along the rotation axis of the specimen. The value of n_1 varies from zero (for a cylinder) to unity (for a plane disc); below we will use n instead of n_1. The field $H_0 > 0$, if it is directed along M_0, and $H_0 < 0$, if it is in the opposite direction to M_0. The latter circumstance apparently occurs only for specimens possessing a definite coercive force H_c, preventing the rotation of M_0 into a direction parallel to the field. Of course, the situation with H_0 and M_0 in opposite directions is not one of thermodynamic equilibrium; however, for $H_0 < H_c$ it can be considered a stable one. We formally include the presence of such a coercive force by considering M_0 as a fixed parameter $M_0 > 0$.

The condition $\Phi_s = \Phi_n$ determines the critical fields*

$$H^{(\pm)} = -4\pi M_0 (1 - n) \pm \sqrt{8\pi\Delta (1 - n)}. \tag{2}$$

In fields $H^{(-)} < H_0 < H^{(+)}$ we have $\Phi_s < \Phi_n$, i.e., it is more advantageous thermodynamically for the specimen to be entirely in the superconducting state. In fields $H_0 > H^{(+)}$ and $H_0 < H^{(-)}$ we have $\Phi_n < \Phi_s$, i.e., it is more advantageous for the specimen to be entirely in the normal state. Remembering that in the normal state the induction

$$B = H_0 + 4\pi M_0 (1 - n) \tag{3}$$

and using (2), we find that it is advantageous for the specimen to be in the normal state for $|B| > \sqrt{8\pi\Delta(1-n)}$. In the case of a cylinder $n = 0$ and the superconducting state is impossible if the induction exceeds the value

$$B_c = \sqrt{8\pi\Delta}. \tag{4}$$

In analogy to the case of ordinary superconductors (see reference 4, Sec. 43), the quantity (4) is the magnitude of the mean microscopic magnetic field for which there is equilibrium between the normal and superconducting phases. For ordinary superconductors such equilibrium occurs in the field

$$H_{\mathrm{cm}} = \sqrt{8\pi\Delta}. \tag{5}$$

It is clear that when $M_0 \rightarrow 0$ the difference between the induction B and the field H disappears and condition (4) then agrees with (5).

---

*In reference 2 there are misprints in Eqs. (12), (13), and (15); in the expressions for H_k the first terms on the right should contain the factor $(1 - n_1)$.

From (3) and (4) it follows that if the external field is in the range

$$H_c^{(-)} \leqslant H_0 \leqslant H_c^{(+)},$$
$$H_c^{(\pm)} = -4\pi M_0 (1-n) \pm \sqrt{8\pi\Delta}, \qquad (6)$$

then the induction in the specimen $|B| \leq B_c$, and the appearance of superconducting regions is possible. In the figure (diagram a) the region of fields for which superconductivity is allowed lies between the straight lines III and IV.

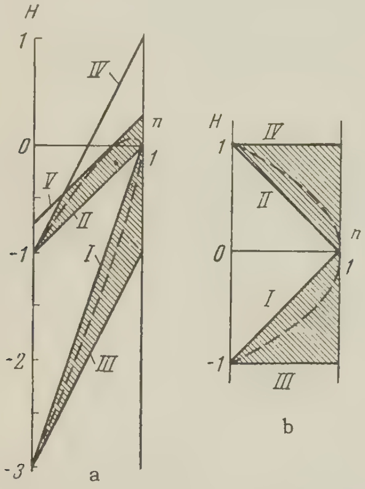

Values of the fields $H_c^{(\pm)}$, $H_e^{(\pm)}$, H' as functions of the coefficient of demagnetization: a – for $4\pi M_0/\sqrt{8\pi\Delta} = 2$, b – for $M_0 = 0$. The straight line I gives $H_e^{(-)}$, II gives $H_e^{(+)}$, III gives $H_c^{(-)}$, IV gives $H_c^{(+)}$, V gives H'; the dotted curve gives $H^{(\pm)}$ (fields plotted in units of $\sqrt{8\pi\Delta}$).

To determine the range of fields in which the specimen will be in the intermediate state, further considerations apply. If the specimen is entirely superconducting, the field at its equator is a maximum and is equal to $H_0/(1-n)$. It is natural that the destruction of superconductivity starts in the field for which the induction $|B_e|$ in the normal layer formed at the equator of the ellipsoid exceeds B_c – the condition of appearance of such a layer can be taken as the same as for a cylinder specimen. Writing $B_e = H_0/(1-n) + 4\pi M_0$, we find that if the external field lies inside the range

$$H_e^{(-)} \leqslant H_0 \leqslant H_e^{(+)}, \quad H_e^{(\pm)} = (-4\pi M_0 \pm \sqrt{8\pi\Delta})(1-n), \qquad (7)$$

then $|B_e| \geq B_c$ and a pure superconducting state is impossible. In the figure, the regions within which a pure superconducting state is impossible are limited by the straight lines II, IV and I, III. Inside the range of fields given by (7), a pure superconducting state is realized (the region between lines I and II in the figure).

It is still necessary to remember that if the field H_0 exceeds the value

$$H' = [\Delta - 2\pi M_0^2 (1-n)]/M_0, \qquad (8)$$

then the thermodynamic potential of the normal state (1a) becomes negative. At the same time the presence of superconducting regions always contributes a positive increment to the potential [which can be seen from (1b)]. This means that in fields $H_0 > H'$ superconductivity disappears, and only the normal phase can exist. With this limitation we find the region of fields in which the superconducting ferromagnetic ellipsoid can exist in an intermediate state. In the figure (diagram a) this region is shaded. The dotted line shows the curves $H^{(\pm)}$ defining the region inside which $\Phi_s \leq \Phi_n$. Diagram b, given for comparison in the figure, corresponds to an ordinary superconductor $M_0 = 0$. In this case the field $H' \to 0$ and the limitation existing for $M_0 \neq 0$ is removed.

It is a noteworthy fact that when $4\pi M_0 > \sqrt{8\pi\Delta}$ a single domain ferromagnetic ellipsoid can only be entirely superconducting because of the coercive force in fields of the opposite direction to the spontaneous magnetization. If the coercive force H_c is not large enough, then when $H_0 > H_c$ rotation of M_0 occurs and part of the superconducting region in the figure is unattainable. The difficulty indicated in obtaining a pure superconducting state is possibly relevant to the experiments of Mattias, Suhl and Corenzwit,[3] where the ferromagnetic specimen was always in the intermediate state.

2. In this section the structure of the intermediate state is determined for a single domain ferromagnetic plate with spontaneous magnetization M_0 perpendicular to its plane. The discussion proceeds in the framework of the so-called "unbranched" model studied by Landau[5] for the case of ordinary superconductors.

We write Maxwell's equation for the plate

$$\operatorname{div} \mathbf{B} = 0, \quad \operatorname{curl} \mathbf{B} = 4\pi \operatorname{curl} \mathbf{M}_0 + (4\pi/c)\,\mathbf{j}_s = 0. \qquad (9)$$

where $\mathbf{B} = \mathbf{H} + 4\pi\mathbf{M}_0$ (the magnetic permeability $\mu = 1$), $\mathbf{j}_s$ is the superconducting current arising at the surface dividing the superconducting from the normal phase. Because this is a surface current and $\operatorname{curl} \mathbf{M}_0 = 0$ everywhere apart from the surface of the specimen, we have put in (9) $\operatorname{curl} \mathbf{B} = 0$, and, as is usual, will take into account the jump in $\mathbf{B}$ in the boundary conditions. These conditions are that on one side of the surface in the superconducting phase $\mathbf{B} = 0$, and on the other side in the normal phase $|\mathbf{B}| = B_c$, where B_c is determined in (4).

Since the equations for the field (9) agree with the analogous equations of Landau[5] (there $\mathbf{H}$ replaces $\mathbf{B}$), all the results of this work concerning the determination of the form of the layers can be directly taken over to our case (with the substitution of B_c for H_c).

To determine the dependence of the thickness of the layers on the external magnetic field H_0 applied perpendicular to the plate, it is necessary to write down the corresponding thermodynamic potential (cf. reference 4, Sec. 44):

$$\Phi = \int dv \left\{ \Phi^0 + w_m - \frac{1}{2}\mathbf{M}\mathbf{H}_0 - \frac{\mathbf{B}\mathbf{H}}{8\pi} \right\},$$

$$w_m = \frac{1}{4\pi}\int_0^B \mathbf{H}d\mathbf{B} = \frac{B^2}{8\pi} - \mathbf{B}\mathbf{M}_0, \qquad \mathbf{M} = \mathbf{M}_0 + \mathbf{M}_s, \tag{10}$$

where $\mathbf{M}_s$ is the part of the total moment of the specimen caused by the superconducting currents flowing at the boundary dividing the normal and superconducting portions.

Let one of the surfaces of the plate be in the yz plane and M_0 be directed along the positive x axis. Calling a_s and a_n the thicknesses of the superconducting and normal layers, respectively, we have $a = a_s + a_n$. Using the theorem on the flow of induction, we obtain the relationship $aH_0 = a_n B_c$; using this in (10) it is possible to eliminate the terms not depending on a. Performing calculations analogous to those of Landau,[4,5] we find for the thermodynamic potential referred to unit surface area of the plate the expression

$$\Phi = C + (B_c^2/4\pi)\, a\, [f(h) \pm \alpha h f_1(h)]. \tag{11}$$

Here, C does not depend on a; $h = |H_0/B_c|$; $\alpha = 4\pi M_0/B_c$; the signs + and − refer to the cases $H_0 < 0$ and $H_0 > 0$ respectively,

$$f(h) = \frac{h^2}{\pi}\left[\ln\frac{\sqrt{\zeta_0}}{2} + \sqrt{\zeta_0+1}\,\ln\frac{1+\sqrt{\zeta_0+1}}{\sqrt{\zeta_0}} + \frac{\sqrt{\zeta_0}}{\pi}J(\zeta_0)\right]$$
$$+ \frac{h^3}{\pi}\left[\ln\frac{1+\sqrt{\zeta_0+1}}{\sqrt{\zeta_0}} + \sqrt{\zeta_0+1}\,\ln\frac{\sqrt{\zeta_0}}{2\sqrt{\zeta_0+1}} - \sqrt{\zeta_0}\ln 2\right],$$

$$f_1(h) = \frac{h^2}{\pi^2}\sqrt{\zeta_0}\,J(\zeta_0), \quad J(\zeta_0) = \int_{\zeta_0}^{\infty}\sqrt{1-\frac{\zeta_0}{\zeta}}\,\tan^{-1}\frac{1}{\sqrt{\zeta}}\,\frac{d\zeta}{\zeta+1},$$
$$\zeta_0 = \frac{1}{4}(1/h - h)^2. \tag{12}$$

For $h \ll 1$

$$f(h) = (h^2/\pi)\{\ln(1/h) - 3\ln 2 + {}^3/_2\} = (h^2/\pi)\ln(0.56/h),$$
$$f_1(h) = h^2/2\pi; \tag{12'}$$

for $1 - h \ll 1$

$$f(h) = \pi^{-1}(1-h)^2\ln 2, \qquad f_1(h) = \pi^{-1}(1-h)\ln 2. \tag{12''}$$

The function f(h) has been tabulated by Lifshitz and Sharvin.[6] Using (12) and reference 6, the corresponding values of $f_1(h)$ can be found.

The complete thermodynamic potential of the specimen, together with the component (11) still contains the term

$$\Phi_1 = (B_c^2/4\pi)(l/a)\Delta_1, \tag{13}$$

accounting for the "surface tension" at the boundary between the normal and superconducting phases. Here l is the thickness of the plate and the coefficient of surface tension is written as $B_c^2\Delta_1/8\pi$. The minimization condition with respect to a of the sum of (11) and (13) gives

$$a = \{l\Delta_1/[f(h) \pm \alpha h f_1(h)]\}^{1/2}. \tag{14}$$

For $\alpha = 0$ we obtain Landau's result.

As remarked above [formula (8)], the presence of superconducting regions in a ferromagnetic for $H_0 > 0$ is possible only in fields $h < h' = 1/2\alpha$, for which $\Phi_n > 0$. It can be considered that $\alpha = 4\pi M_0/\sqrt{8\pi\Delta}$ is large and the field $h' \ll 1$. In this case it is possible to use approximation (12′), and $f(h) > f_1(h)$, and the pole appearing in (14) for $H_0 > 0$ is not attained.

Thus, in fields $0 \le h \le h'$ the dependence of thickness a on h gives the formula

$$a = \{\pi l\Delta_1/h^2[\ln(0.56/h\} - 0.5\,\alpha h]\}^{1/2}.$$

For quite small values of h the logarithmic term predominates and the dependence of a on h is the same as in the case of non-ferromagnetic material. With increasing field for $h \ge h'$ superconductivity collapses and the normal phase is established.

In fields $H_0 < 0$, in the opposite direction to M_0 (as above we assume the presence of a corresponding coercive force), in (14) the + sign should be taken. In the limiting case $(1-h) \ll 1$ we have $f(h) \ll \alpha f_1(h)$ and

$$a = [\pi l\Delta_1/\alpha(1-h)\ln 2]^{1/2},$$

i.e., the dependence is $a \sim (1-h)^{1/2}$ instead of $a \sim (1-h)^{-1}$, occuring for non-ferromagnetics.

The corresponding formulae for $a_s = a(1-h)$ and $a_n = ah$ are obvious.

A discussion of the structure of the intermediate state in the "branched" and filamentary models (cf. Landau[7] and Andrew[8]) will be presented in a later paper.

---

[1] V. L. Ginzburg, JETP **31**, 202 (1956), Soviet Phys. JETP **4**, 153 (1957).

[2] G. F. Zharkov, JETP **34**, 412 (1958), Soviet Phys. JETP **7**, 286 (1958).

[3] Mattias, Suhl, and Corenzwit, Phys. Rev. Letters **1**, 449 (1958).

[4] L. D. Landau and E. M. Lifshitz, Электродинамика сплошных сред, (Electrodynamics of Continuous Media), Gostekhizdat M. (1957).

[5] L. D. Landau, JETP **7**, 371 (1937).

[6] E. M. Lifshitz and Yu. V. Sharvin, Dokl. Akad. Nauk SSSR **79**, 783 (1951).

[7] L. D. Landau, JETP **13**, 377 (1943).

[8] E. R. Andrew, Proc. Roy. Soc. **194A**, 98 (1948).

Translated by K. F. Hulme
344

SOVIET PHYSICS JETP VOLUME 37(10), NUMBER 6 JUNE, 1960

ON THE TWO-CHARGE RENORMALIZATION GROUP IN SCALAR QUANTUM ELECTRODYNAMICS

V. A. SHAKHBAZYAN

Mathematical Institute, Academy of Sciences, U.S.S.R.

Submitted to JETP editor July 24, 1959

J. Exptl. Theoret. Phys. (U.S.S.R.) **37**, 1789-1793 (December, 1959)

The behavior, in the high momentum region, of single-particle Green's functions and of some asymptotic values of the vertex part and the four-vertex diagram in the quantum electrodynamics of zero spin particles is investigated by the renormalization group procedure. It is established that we step out of the weak coupling region in the nonlinear meson field interaction ("four-meson" interaction) earlier than in the electromagnetic interaction.

1. The interaction of scalar particles with the electromagnetic field has been investigated repeatedly. These studies were concerned with the perturbation theory in the interaction picture[1] and with the problem of the partial summing of the perturbation expansions.[2] The divergencies of the S matrix are completely removed by renormalizing the mass and the charge and by introducing an additional "four-meson" compensation term in the effective interaction Lagrangian. The necessity of introducing a "four-meson" compensation term leads to a two-charge formulation of the theory analogous to the procedure used in pseudoscalar meson theory.[3]

In our discussion we use the Duffin-Kemmer formalism.[4] The basic interaction Lagrangian is given by the expression

$$\mathscr{L}^{\text{int}}(x) = e : \bar{\psi}(x)\,\hat{A}\psi(x) : + h : (\bar{\psi}X\psi)^2 :,$$

where $\psi(x)$ and $\bar{\psi}(x)$ are scalar field operators used in the Kemmer formalism,

$$\hat{A} = \sum \Gamma^k A_k,$$

where Γ^k are the five-rowed Kemmer matrices ($k = 0, 1, 2, 3$), X is a five-rowed matrix which satisfies the equation

$$\bar{\psi}(x)\,X\psi(x) = \varphi^*(x)\,\varphi(x),$$

and $\varphi^*(x)$ and $\varphi(x)$ are ordinary scalar field operators.

It is of interest to apply the renormalization group procedure[3] to scalar electrodynamics. In this case the multiplicative renormalization group involves two charges. In another paper[5] the author has derived the group equations, which are of the form

$$G_2 = zG_1, \quad D_2 = z_3 D_1, \quad \Gamma_2 = z^{-1}\Gamma_1, \quad \square_2 = z_4^{-1}\square_1,$$
$$e_2 = z_3^{-1}e_1^2, \quad h_2 = z_4 z^{-2} h_1, \quad d_l^{0\,(2)} = z_3^{-1} d_l^{0\,(1)}. \tag{2}$$

Here G is the meson Green's function,* D is the photon Green's function, Γ is the vertex part, $\square$ is the four-vertex operator describing the interaction of two mesons, h is the second charge, d_l^0 is an arbitrary coefficient in the longitudinal part of the photon Green's function. It should be noted that in the derivation of (2) d_l^0 was assumed to be arbitrary.

The expressions for G, Γ, and $\square$ in the Duffin-Kemmer formalism have a complicated matrix structure. From perturbation theory we find for G

$$G(p) = \frac{1}{m}\,\frac{m^2 a(p) + b(p)(\hat{p}^2 - p^2) + m\hat{p}d_M(p)}{m^2 - p^2} - \frac{1}{m}Y[f(p) - 1],$$
$$Y = 1 - X. \tag{3}$$

We shall not write down the general form of Γ and $\square$. Among all the scalars of the four-vertex function $\square_{\alpha\beta\gamma\delta}$ we shall be interested in the one which goes into the construction of the second invariant charge term. This function is obtained from those parts of $\square_{\alpha\beta\gamma\delta}$ which have the matrix structure $X_{\alpha\beta}X_{\gamma\delta}$. Let us denote this function by $\square_1$. Further below we shall make some remarks on the matrix structure of the different asymptotic values of the vertex part.

The differential equations of Lie for the renormalization group[5] are obtained from (2) in the usual way.[3] The set of scalar functions appearing in the right side of (3) and in the symmetric asymptotic values of the vertex part and of the four-vertex operator $\square$ will be denoted by $s(x, y, e^2, e^2 d_l^0, h)$ (x and y are the dimensionless momentum and mass of the meson[3]). The invariant charges are defined in the following way:

---

*In the following we shall always call the zero-spin particle the "meson."

$$\sigma(x, y, e^2, h) = e^2 d(x, y, e^2, h),$$

$$\rho(x, y, e^2, h) = h\varphi(x, y, e^2, h)$$

$$= d_M^2(x, y, e^2, h, e^2 d_l^0)\,\square_1(x, y, e^2; h, e^2 d_l^0). \tag{4}$$

It is appropriate here to make two remarks about $\rho(x, y, e^2, h)$.

1) Of the four functions, a, b, d_M, f, appearing in (3), only the function d_M is used in the transformation of $h\varphi(x, y, e^2, h)$. The functions b and f, which multiply $(\hat{p}^2 - p^2)$ and Y, respectively, drop out in all internal lines ending in h vertices as a consequence of the specific matrix structure of these vertices (see reference 5). The function a can be chosen equal to d_M in the regions of interest to us, i.e., the ultraviolet and infrared regions. In fact, perturbation calculations in the infrared region give $a = b = d_M$ (see also reference 6). In the ultraviolet region, where $|p^2| \gg m^2$, the function a is not uniquely determined, and can be taken equal to d_M.[5]

2) It is seen from (4) that $h\varphi$ is independent of d_l^0, while $\square_1$ and d_M^2 depend on d_l^0 separately. This can be understood in the following way. $h\varphi$ cannot depend on d_l^0 in virtue of the gauge invariance of the theory, since the second invariant charge appears explicitly in the expression for the transverse Green's function of the photon. On the other hand, the independence of the second invariant charge from the longitudinal gauge of the photon Green's function is not obvious a priori. Generally speaking, we must therefore interpret Eq. (4) as a kind of consistency condition for the gauge invariance and renormalization invariance of the theory. Lowest order (in e^2 and h) perturbation calculations in the ultraviolet region confirm the independence of $h\varphi$ from d_l^0.

2. The ultraviolet and infrared asymptotes of the functions $d(x, y, e^2, h)$, $\varphi(x, y, e^2, h)$, and $s(x, y, e^2, e^2 d_l^0, h)$ are found by solving the Lie differential equations of the renormalization group using the results of perturbation theory. The detailed investigation of the corresponding diagrams leads to the result that in the considered approximation the meson and photon Green's functions and the vertex part do not depend on the second charge ρ. It is therefore sufficient to use the single-charge approximation for the calculation of the momentum asymptotes of the above-mentioned functions.

For $|p^2| \gg m^2$ we have

$$d(x, e^2) = \left(1 - \frac{e^2}{48\pi^2}\ln x\right)^{-1}, \tag{5}$$

$$b(x, e^2, e^2 d_l^0) = x^{e^2 d_l^0/16\pi^2}, \tag{6}$$

$$d_M(x, e^2, e^2 d_l^0) = x^{e^2 d_l^0/16\pi^2}\,[d(x, e^2)]^{-9/2}, \tag{7}$$

$$f(x, e^2, e^2 d_l^0) = x^{3e^2 d_l^0/64\pi^2}\,[d(x, e^2)]^{-9/4}. \tag{8}$$

Formulas (5), (6), and (7) agree with the corresponding expressions obtained by Gor'kov and Khalatnikov.[2]

The vertex part depends on three independent momentum arguments. It can therefore have various asymptotic values in the ultraviolet region. As the most interesting cases we consider the symmetric and the doubly logarithmic asymptotes. The symmetric asymptote of the vertex part can be expressed in terms of scalar functions of the momentum argument:

$$\Gamma^n(p^2, p^2, p^2) = \Gamma^n \Gamma(p^2) - (2p^n/m)\,X\,[f(p^2) - 1]. \tag{9}$$

Here $f(p^2)$ is the same function as in (3), owing to the Ward identity. It is given by formula (8). For $\Gamma(x, e^2, e^2 d_l^0)$ we have

$$\Gamma(x, e^2, e^2 d_l^0) = x^{-e^2 d_l^0/64\pi^2}\,[d(x, e^2)]^{9/4}. \tag{10}$$

We now turn to the doubly logarithmic asymptote of the vertex part. For the case of spinor electrodynamics this asymptote was found by Sudakov[7] and Blank and Shirkov.[8] To obtain it in the scalar electrodynamics, we must derive the explicit form of the doubly logarithmic terms in the second order of perturbation theory. Applying the method of Sudakov to scalar electrodynamics, we find for the vertex operator in second order, with $|k^2| \gg |p^2|$, $|q^2| \gg m^2$,

$$\Gamma^n_{(2)}(p, q, k) = \Gamma^n\left(1 - \frac{e^2}{32\pi^2}\ln\left|\frac{k^2}{p^2}\right|\ln\left|\frac{k^2}{q^2}\right|\right)$$

$$- \left(\frac{e^2}{32\pi^2}\right)\frac{(p^n + q^n)}{m}\,X\ln\left|\frac{k^2}{p^2}\right|\ln\left|\frac{k^2}{q^2}\right|. \tag{11}$$

We therefore seek the logarithmic asymptote of the vertex part in the form

$$\Gamma^n(p, q, k) = \Gamma^n \Gamma(p^2, q^2, k^2)$$

$$- \frac{p^n + q^n}{m}\,X\,\frac{e^2}{32\pi^2}\ln\left|\frac{k^2}{p^2}\right|\ln\left|\frac{k^2}{q^2}\right| f(p^2, q^2, k^2). \tag{12}$$

We limit ourselves to finding $\Gamma(p^2, q^2, k^2)$. The calculation is analogous to that of references 8 and 3. Introducing the dimensionless momenta x, y, z and the dimensionless mass u, which satisfy the conditions $|z| \gg |x|$, $|y| \gg |u|$, we obtain

$$\ln\frac{\Gamma(x,\ y,\ z,\ e^2)}{\Gamma(x_0,\ y_0,\ z_0,\ e^2)} = 3\left(\ln\frac{z}{z_0} - \frac{48\pi^2}{e^2}\ln\frac{d(z,\ e^2)}{d(z_0,\ e^2)}\right)$$
$$+ \frac{3}{2}\ln(x_0y_0)\ln\frac{d(z,\ e^2)}{d(z_0,\ e^2)} + \frac{3}{2}\ln\frac{z}{z_0}\left[\ln\frac{d(x,\ e^2)}{d(x_0,\ e^2)} + \ln\frac{d(y,\ e^2)}{d(y_0,\ e^2)}\right]$$
$$+ \frac{3}{2}\ln\frac{z_0}{y_0}\ln\frac{d(x,\ e^2)}{d(x_0,\ e^2)} - \frac{3}{2}\ln\frac{x}{x_0}\ln\frac{d(y,\ e^2)}{d(y_0,\ e^2)}$$
$$+ \frac{3}{2}\ln\frac{z}{x_0}\ln\frac{d(y,\ e^2)}{d(y_0,\ e^2)}. \qquad (13)$$

For $e^2 \ln z \ll 1$ we have

$$\ln\frac{\Gamma(x,\ y,\ z,\ e^2)}{\Gamma(x_0,\ y_0,\ z_0,\ e^2)} = -\frac{e^2}{32\pi^2}\left[\ln\frac{z}{x}\ln\frac{z}{y} - \ln\frac{z_0}{x_0}\ln\frac{z_0}{y_0}\right]. \qquad (14)$$

We note further that the exponent of the infrared singularity of the Green's function is the same as in spinor electrodynamics, in accordance with the result of the paper of Gor'kov.[6]

3. We now consider the second charge in the theory. As was shown earlier, it does not give any contribution to the single-particle Green's functions and to the vertex part in the considered approximation. The second charge plays a most essential role in the discussion of the four-vertex operator, in particular, of the function $\Box_1$. Let us consider the system of equations for the invariant charges in the ultraviolet region:

$$d\sigma/dz = \sigma D(\sigma,\ \rho), \qquad d\rho/dz = \rho\Phi(\sigma,\ \rho), \qquad (15)$$

where

$$\sigma = e^2 d(z,\ e^2,\ h), \qquad \rho = h\varphi(z,\ c^2,\ h), \qquad z = \ln x,$$
$$D(\sigma,\ \rho) = \left[\frac{\partial}{\partial\xi}d(\xi,\ \sigma,\ \rho)\right]_{\xi=1},$$
$$\Phi(\sigma,\ \rho) = \left[\frac{\partial}{\partial\xi}\varphi(\xi,\ \sigma,\ \rho)\right]_{\xi=1}.$$

From a study of the lowest order diagrams we find

$$d\sigma/dz = d_1\sigma^2, \qquad d\rho/dz = -\varphi_1\sigma^2 - \varphi_2\sigma\rho - \varphi_3\rho^2, \qquad (16)$$

where

$$d_1 = 1/48\pi^2, \qquad \varphi_1 = 3/4\pi^2, \qquad \varphi_2 = 3/16\pi^2,$$
$$\varphi_3 = 5/32\pi^2.$$

The solution of the first equation of (16) is given by (5).

Eliminating z from the two equations, we obtain

$$d\rho/d\sigma = -\varphi_1/d_1 - (\varphi_2/d_1)(\rho/\sigma) - (\varphi_3/d_1)(\rho^2/\sigma^2). \qquad (17)$$

The solution of this equation is

$$\rho = [h/e^2 - a - b\tan(\varphi - \alpha)]\, e^2\exp(c\varphi), \qquad (18)$$

where

$$\varphi = c^{-1}\ln(\sigma/e^2), \quad \tan\alpha = a/b, \qquad a = h/c^2 + 2/3,$$
$$b = 2{,}09, \ c = 0{,}064.$$

We are interested in the values $\sigma^2 \geq e^2$. For finite and non-vanishing h and e^2 we find that $|\alpha| < \pi/2$. For $\varphi = 0$ ($\sigma = e^2$) we have $\rho = h$. Different values of the ratio h/e^2 give rise to different curves, which form the family of curves $\rho(\varphi,\ \alpha)$. For values of φ sufficiently close to $\pi/2 + \alpha$, we leave the region of weak coupling with respect to ρ. We can therefore limit the discussion to that part of the phase plane $(\rho,\ \varphi)$ which corresponds to the variation of φ in the interval $[0,\ \pi/2 + \alpha]$. The figure shows the curves corresponding to the values $h/e^2 = \pm 1,\ \pm 10$. The behavior of each curve is shown from the value $\varphi = 0$ to the first asymptote. The value σ for which $\rho \to \infty$ is given by

$$\sigma_{\rho\to\infty} = e^2\exp\{c(\pi/2 + \alpha)\}. \qquad (19)$$

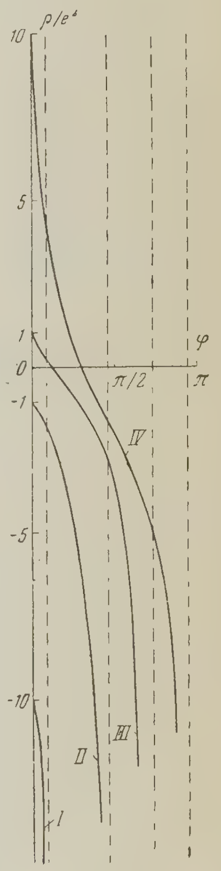

Curve I: $h/e^2 = -10$, Curve II: $h/e^2 = -1$, Curve III: $h/e^2 = 1$, Curve IV: $h/e^2 = 10$; along the abscissa we write the values of $\varphi = c^{-1}\ln(\sigma/e^2)$.

Using (5) we can find a relation between the value of the dimensionless momentum x for $\rho \to \infty$ and e^2 and h:

$$\ln x_{\rho\to\infty} = (48\pi^2/e^2)\,[1 - e^2/\sigma_{\rho\to\infty}]. \qquad (20)$$

It is easily seen that the ratio $e^2/\sigma_{\rho\to\infty}$ varies between the limits

$$e^{-c\pi} < e^2/\sigma_{\rho\to\infty} < 1.$$

Noting further that the value ln x at which $\sigma \to \infty$, is equal to $48\pi^2/e^2$, we find that always $\ln x_{\rho\to\infty} < \ln x_{\sigma\to\infty}$.

We should thus expect that the weak coupling hypothesis for ρ breaks down earlier than for σ. Indeed, the family of asymptotes (19) is bounded from the right by the value $e^2 \exp(c\pi) \approx 1.22\,e^2$. Since $e^2 \ll 1$, the asymptote which is farthest to the right is in the region of values $\sigma_{\rho\to\infty} \ll 1$. For all curves of the family we shall therefore leave the region of weak coupling with respect to ρ before this occurs with respect to σ. For example, for $h/e^2 = 1$ the second invariant charge ρ goes to unity as $\sigma \to 1.15\,e^2$.

The ratio of the logarithms of the dimensionless momenta for which $\rho \sim 1$ and $\sigma \sim 1$, is equal to

$$\ln x_{\rho\sim 1} / \ln x\sigma_{\sigma\sim 1} = 0,13 \qquad (h/e^2 = 1).$$

In conclusion we give the expression for the symmetric asymptote of the function $\square_1$:

$$\square_1 (x, e^2, h, e^2 d_l^0) = x^{-e^2 d_l^0/8\pi^2} [d(x, e^2)]^{5-A/c} (\cos\beta/\sin\alpha) \times [\cos(\varphi+\beta)]^B / \sin(\varphi+\alpha_1), \tag{21}$$

where

$$\tan\beta = (2a+3b^2)/(3ab-2b), \quad \tan\alpha_1 = b/a,$$
$$A = -(9b^2+4)^{-1}, \qquad B = 3b/(9b^2+4).$$

We see with the aid of (7) that the product $\square_1 d_M^2$ is independent of d_l^0.

The author takes this opportunity to express his deep gratitude to D. V. Shirkov, under whose guidance this work has been carried out.

---

[1] M. Neumann and W. H. Furry, Phys. Rev. **76**, 1677 (1949). T. Kinoshita, Progr. Theor. Phys. **5**, 473 (1950). T. Kinoshita and Y. Nambu, Progr. Theor. Phys. **5**, 749 (1950). P. T. Matthews, Phys. Rev. **80**, 292 (1950). D. C. Peaslee, Phys. Rev. **81**, 731 (1952). A. Salam, Phys. Rev. **86**, 731 (1952) and Proc. Roy. Soc. **A211**, 276 (1952).

[2] L. P. Gor'kov and I. M. Khalatnikov, JETP **31**, 1062 (1956), Soviet Phys. JETP **4**, 777 (1957).

[3] N. N. Bogolyubov and D. V. Shirkov, Введение в теорию квантованных полей, (Introduction to the Theory of Quantized Fields), Gostekhizdat (1957).

[4] N. Kemmer, Proc. Roy. Soc. **A173**, 91 (1939).

[5] V. A. Shakhbazyan, Изв. АН Арм. ССР (News, Acad. of Sciences, Armenian S.S.R.), in press.

[6] L. P. Gor'kov, JETP **30**, 790 (1956), Soviet Phys. JETP **3**, 762 (1956).

[7] V. V. Sudakov, JETP **30**, 87 (1956), Soviet Phys. JETP **3**, 65 (1956).

[8] V. Z. Blank and D. V. Shirkov, Dokl. Akad. Nauk SSSR **111**, 1206 (1956) [sic!].

Translated by R. Lipperheide

SOVIET PHYSICS JETP VOLUME 37 (10), NUMBER 6 JUNE, 1960

ON THE SUPERFLUIDITY OF LIQUID He^3

L. P. PITAEVSKIĬ

Institute of Geomagnetism, Ionospherics and Radio-wave Propagation, Academy of Sciences, U.S.S.R.

Submitted to JETP editor July 24, 1959

J. Exptl. Theoret. Phys. (U.S.S.R.) **37**, 1794-1807 (December, 1959)

A thorough investigation is made of the interaction between elementary excitations in a Fermi liquid for large values of the relative angular momentum. It is shown that this interaction is of the nature of an attractive force, so that the suggestion that He^3 is superfluid seems to be justified. Expressions in terms of observable quantities are derived for the asymptotic values of the excitation scattering amplitudes for large values of l. A formula is deduced for the effective mass of an excitation in a Fermi liquid by quantum field theory methods.

1. STATEMENT OF THE PROBLEM

As is well known, liquid He^3 remains non-superfluid down to the lowest temperatures so far reached ($T \gtrsim 0.2°K$).[1] This indicates that the interaction between elementary excitations in liquid He^3 has a repulsive nature, at least at distances of the order of the mean inter-atomic distances. If the opposite were the case, as for electrons in a superconducting metal, atoms of He^3 would form Cooper pairs[2] at sufficiently low temperatures, with a binding energy of the order of the Fermi energy. This would lead to He^3 becoming superfluid at temperatures around the Fermi degeneracy temperature.

There is a special reason why He^3 could go over into the superfluid state at very low temperatures. As Landau has pointed out, for the formation of Cooper pairs in a Fermi system it is sufficient that the interaction between the elementary excitations have an attractive character for any one value of the relative angular momentum l, i.e., that at least one phase of the scattering of one excitation by another should have a positive sign. (We have in mind the case of large l, when the phases are small and positive.) In this case the pairs will be formed with non-zero orbital momentum. Also, Pomeranchuk has remarked that at sufficiently large values of the angular momentum, the excitations should evidently attract one another. This is because large values of the momentum correspond to large distances between the excitations, so that forces should act which are analogous to the van der Waals forces between distant atoms. For identical particles these forces are always attractive, regardless of the properties of the surrounding medium.[3] The existence of such an interaction would lead to the formation of Cooper pairs in He^3 and, as a result, to a transition into a new state which in all probability would be superfluid. Since the interaction is very weak at large distances, a transition into a superfluid state would only be expected at very low temperatures.

This discussion is not in itself rigorous, since the interaction of elementary excitations in a liquid differs substantially from the interaction of isolated atoms or of solute atoms in a dilute solution. The present work is concerned with the detailed study of the interactions between elementary excitations in a Fermi liquid for a large relative angular momentum l. It will be shown that this interaction is indeed of an attractive nature and makes it most likely that He^3 becomes superfluid at very low temperatures. An asymptotic expression for the scattering phase for large l is obtained in terms of observable quantities. Quantum field theory is used for the calculation, and this makes it applicable to the general case without the assumption that the interaction between atoms is weak at small distances, which is obviously not valid for a liquid.

2. LONG-RANGE FORCES

The possibility of separating out, mathematically, the effects due to long-range forces, i.e., forces that fall off with distance according to a power law (and not exponentially), in the same way as van der Waal's forces, is connected with the fact that their existence leads to the appearance in the scattering amplitude of terms with a branch-point singularity in the square of the momentum transfer

$$k^2 = 2p^2(1 - \cos\vartheta)$$

at $k^2 = 0$ (ϑ is the scattering angle and $\mathbf{p}$ the momentum in the center-of-mass system).

One can see this from perturbation theory by calculating the Born scattering amplitude in a field that decreases as r^{-n} at large distances. For example, two identical atoms interact at large* distances as[4]

$$U(r) = -\left(\frac{3}{\pi}\int_0^\infty \alpha^2(i\xi)\,d\xi\right)\frac{1}{r^6}, \tag{1}$$

where $\alpha(\omega)$ is the atomic polarizability ($\hbar = c = 1$). Such an interaction leads to characteristic terms in the scattering amplitude, of the form

$$F(k^2) = k^3\frac{m}{16}\int_0^\infty \alpha^2(i\xi)\,d\xi \tag{2}$$

(m is the atomic mass).

It is precisely such terms that determine the asymptotic behavior of the scattering phases at large l. In fact, terms which do not have a singularity in scattering amplitude at $k^2 = 0$ give an exponential fall off as $l \to \infty$, as can easily be seen by expanding in Legendre polynomials. Terms that have a branch point at $k^2 = 0$ lead, when expanded in Legendre polynomials, to coefficients that decrease according to a power law with increasing l.†

Let us examine, for example, the term in the scattering amplitude

$$F_s = Ak^{2\rho}, \tag{3}$$

where ρ is not a positive integer, and express it in the form

$$F_s = \frac{1}{2ip}\sum_l (2l+1)P_l(\cos\vartheta)\,\eta_l, \qquad \eta_l = e^{2i\delta_l} - 1, \tag{4}$$

where δ_l is the scattering phase.

Using the expansion of $(1 - \cos\vartheta)^\rho$ in Legendre polynomials [see reference 6, p 214, Eq. (12)] we obtain

$$\eta_l = iA2^{\rho+1}p^{2\rho+1}\Gamma(l-\rho)\,\Gamma(\rho+1)/(l+\rho+1)$$
$$\times\Gamma(l+\rho+1)\,\Gamma(-\rho)$$

or as $l \to \infty$

$$\eta_l \approx 2i\delta_l \approx iA(2ep)^{2\rho+1}[\Gamma(\rho+1)/\Gamma(-\rho)]\,l^{-2(\rho+1)}. \tag{5}$$

We are interested in the case $\rho = 3/2$; then

$$\eta_l \approx 2i\delta_l \approx 9iA(ep)^4 l^{-5}. \tag{6}$$

In a similar way it can be shown that the presence of terms in the scattering amplitude of the form

$$A'k^{2n}\ln k^2$$

(n is a positive integer) leads to an expression behaving as $l^{-2(n+1)}$ asymptotically.

From what has been said it is clear that in order to determine the nature of the interaction between the excitations in a Fermi liquid at large l, by quantum field theory, we must pick out those Feynman diagrams of the scattering which have a singularity for small momentum transfer, k, with the smallest power of k.

3. ASYMPTOTIC BEHAVIOR OF THE SCATTERING AMPLITUDE AT LARGE l. APPROXIMATE DISCUSSION

As will be shown below, the problem of determining the scattering amplitude for excitations in a Fermi liquid at large l can be solved quite rigorously in general form. In this section, however, we shall treat this in a simpler way, based on the specific property of helium atoms — the rigidity of their electron shells, which is reflected in the dielectric constant, which is nearly unity. Because of this, the force acting between two distant atoms in liquid He^3 (or between the elementary excitations, in so far as in a Fermi liquid the number of excitations is equal to the number of atoms, since to each atom there corresponds an excitation) is almost exactly equal to the force between two isolated helium atoms.

Because of the rigidity of the electron shells the polarizability of each of the interacting atoms is practically unaltered by the presence of neighboring atoms. Since the dielectric constant is nearly unity, the polarization of the intervening atoms does not alter the force of the interaction between the atoms we are considering. We should point out that although the energy of interaction between atoms in the liquid is, at large distances, close to the interaction energy for isolated atoms, the scattering amplitude for the excitations is not at all similar to that for atoms, since interaction with neighboring atoms has a considerable influence on the excitation motion. This interaction could, in principle, even change the sign of the amplitude. The problem in this section is to express the excitation scattering amplitude, or more precisely its singular part, in terms of the singular part of the scattering amplitude for isolated atoms, given by Eq. (2).

---

*The distances are assumed large compared with the atoms, but small compared with the effective wavelengths in the atomic spectrum.

†We should point out the well known analogy between the discussion here and the investigation by Okun' and Pomeranchuk[5] of the peripheral interaction between elementary particles.

For this purpose we separate the Hamiltonian for the system, $\hat{H}$, into two parts:

$$\hat{H} = \hat{H}_0 + \hat{V}_1,$$

where in $\hat{V}_1$ only the interaction of atoms in the liquid at distances $r \geq r_0$ is included, r_0 being some distance which is much greater than the interatomic distance in liquid helium. All the other interactions are included in $\hat{H}_0$. (The magnitude of r_0 does not enter into the result, so that its exact value is immaterial.) From what has been said at the beginning of the section, it is clear that for helium $\hat{V}_1$ can be taken with sufficient accuracy as a pair interaction between atoms, with an interaction potential given by Eq. (1). As the interaction is weak at large distances, perturbation theory can be used for studying the scattering of excitations related to $\hat{V}_1$. Since all the "long-range" part of the interaction is contained in $\hat{V}_1$, the singularity sought in the scattering amplitude is connected with $\hat{V}_1$; the amplitude determined by $\hat{H}_0$ has no singularity.

For the further discussion we shall use the method for studying the properties of a Fermi liquid developed by Landau,[7] based on quantum field theory. Those parts of Landau's theory which we need will be briefly described.

The Green's function of the system $G_{\alpha\beta}(P)$, represented by a continuous line on a Feynman diagram, will play an important part. The Green's function has the form

$$G_{\alpha\beta}(P) = G(P)\,\delta_{\alpha\beta} = \{a/[\varepsilon - v(p - p_0) + i\delta] + \varphi(P)\}\,\delta_{\alpha\beta} \tag{7}$$

$(\delta = \gamma\epsilon/|\epsilon|,\ \gamma \rightarrow +0)$. Here $\varphi(P)$ is a function that has no singularity at $\epsilon \approx 0$; $p \approx p_0$; P is the 4-momentum vector with components $P\{\epsilon, \mathbf{p}\}$; $\alpha, \beta, \gamma \ldots = 1, 2 \ldots$ are the spin indices, which can take two values; a is the renormalization factor $(0 < a < 1)$.

Another important expression is

$$G(P)\,G(P + K),$$

where $K = K\{\omega, \mathbf{k}\}$ is the 4-momentum transfer vector. For small K this expression can be written

$$G(P)\,G(P+K) \approx i\,\frac{2\pi a^2 \mathbf{l}\mathbf{k}}{\omega - v\,\mathbf{l}\mathbf{k}}\,\delta(\varepsilon)\,\delta(p - p_0) + g(P), \tag{8}$$

where $g(P)$ is a smooth function of P, i.e., it does not contain any δ-function part.

The vertex part $\Gamma_{\alpha\beta,\gamma\delta}(P_1, P_2;\ K)$ is also important in the theory. This is a combination of all diagrams with two entering and two leaving fermion ends, which is related to the transition amplitude of excitations, originally in the states α, P_1; β, P_2 into the states γ, $P_1 + K$; δ, $P_2 - K$ by the relation

$$F_{\alpha\beta,\gamma\delta}(P_1, P_2;\ P_1 + K,\ P_2 - K) = -\frac{m^*}{4\pi}\,a^2\Gamma_{\alpha\beta,\gamma\delta}(P_1, P_2, K) \tag{9}$$

(F is the scattering amplitude and m^* the effective mass).

We shall need the limiting value of the vertex part Γ for $K \rightarrow 0$, i.e., for $\omega \rightarrow 0$ and $k \rightarrow 0$. This value depends on the limit of ω/k for these conditions. We introduce the Landau notation

$$\Gamma^{\omega}_{\alpha\beta,\gamma\delta}(P_1, P_2) = \lim_{\substack{K\to 0\\ k/\omega\to 0}} \Gamma_{\alpha\beta,\gamma\delta}(P_1, P_2;\ K);\ \ \Gamma^{k}_{\alpha\beta,\gamma\delta}(P_1, P_2) = \lim_{\substack{K\to 0\\ \omega/k\to 0}} \Gamma_{\alpha\beta;\gamma\delta}(P_1, P_2; K). \tag{10}$$

As Landau[7] has shown, at the Fermi surface the function $\Gamma^{\omega}_{\alpha\beta,\gamma\delta}(P_1, P_2)$ is simply related to the second variational derivative of the energy of the liquid with respect to the distribution function for elementary excitations $f_{\alpha\beta,\gamma\delta}(\mathbf{p}_1, \mathbf{p}_2)$. That is,

$$f_{\alpha\beta,\gamma\delta}(\mathbf{p}_1, \mathbf{p}_2) = a^2\Gamma^{\omega}_{\alpha\beta,\gamma\delta}(P_1, P_2), \quad \varepsilon_1 = \varepsilon_2 = 0, \quad |\mathbf{p}_1| = |\mathbf{p}_2| = p_0. \tag{11}$$

Γ^k and Γ^{ω} are related by

$$\Gamma^{\omega}_{\alpha\beta,\gamma\delta}(P_1, P_2) = \Gamma^{k}_{\alpha\beta,\gamma\delta}(P_1, P_2) + \frac{a^2 p_0^2}{v\,(2\pi)^3}\int \Gamma^{\omega}_{\alpha\varepsilon,\gamma\zeta}(P_1 Q)\,\Gamma^{k}_{\zeta\beta,\varepsilon\delta}(Q,\ P_2)\,dQ_{\mathbf{q}}. \tag{12}$$

The integration in Eq. (12) is over all directions of the vector $\mathbf{q}$ at the surface of the Fermi sphere.

There are several relations which connect Γ^k and Γ^{ω} with the derivatives of the Green's function with respect to different variables. We give now the derivation of one such relation which we shall require. We introduce into the Hamiltonian of a Fermi liquid an infinitesimal time-independent external field with a potential (per particle),

$$\delta U = \delta U_0 e^{i\mathbf{k}\mathbf{r}} \tag{13}$$

and calculate the change in the Green's function of the liquid under the influence of such a field.* Since the field is considered infinitesimally small, first-order perturbation theory will suffice. The interaction between the particles of the liquid must obviously be calculated exactly. We obtain for the change δG in the G-function the Feynman diagram shown in Fig. 1, where the wavy line repre-

---

*The derivation of (16) and of (26) (of Sec. 5), is due to Landau, who used them in a rigorous derivation of the equality of the numbers of excitations and of particles in a Fermi liquid.

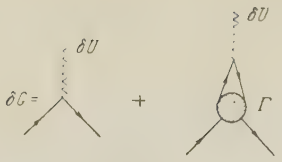

FIG. 1

sents the external field δU and the shaded circle the total vertex part Γ. This relation can be expressed analytically as follows:

$$\delta G(P, K) = \Big\{G(P)\,G(P+K) - \frac{i}{2(2\pi)^4}\,G(P)\int\Gamma_{\alpha\beta,\,\alpha\beta}(P, Q, K)$$
$$\times G(Q)\,G(Q+K)\,d^4Q\,G(P+K)\Big\}\,\delta U, \qquad (14)$$

where the vector K has components $\{0, k\}$, since the field δU is independent of the time. On the other hand, the equilibrium condition

$$\mu + \delta U = \mu_0, \qquad (15)$$

must hold in the external field, where μ is the chemical potential of the system and μ_0 is the chemical potential in the absence of the field.

Let us go to the limit $k \to 0$. From (15) it follows that the chemical potential changes then by an amount $-\delta U_0$. The limit of the left hand side of (14) as $k \to 0$ is $(-\partial G/\partial\mu)\delta U_0$. For the right hand side of (14) we note that the field is constant, so that $\omega = 0$. Using (7) and dividing both sides by $G^2(P)\,\delta U_0$ we finally obtain

$$\frac{\partial G^{-1}(P)}{\partial\mu} = \Big\{1 - \frac{a^2p_0^2}{v2(2\pi)^3}\int\Gamma^k_{\alpha\beta,\,\alpha\beta}(P, Q)\,do_{\mathbf{q}}$$
$$- \frac{i}{2(2\pi)^4}\int\Gamma^k_{\alpha\beta,\,\alpha\beta}(P, Q)\,g(Q)\,d^4Q\Big\}. \qquad (16)$$

The integral with respect to $do_{\mathbf{q}}$ is taken over all directions of the vector **q** at the Fermi surface.

We now return to our problem of determining the singular part of the excitation scattering amplitude. In what follows we shall be concerned with the case of excitations with total spin zero. The corresponding amplitude must be symmetrical with respect to orbital exchange and antisymmetrical in the spin, and since the interaction considered is independent of spin, can be expressed in the form

$$F_{\alpha\beta,\,\gamma\delta} = \{F(2p^2(1-\cos\vartheta))$$
$$+ F(2p^2(1+\cos\vartheta))\}\,\{\delta_{\alpha\gamma}\delta_{\beta\delta} - \delta_{\alpha\delta}\delta_{\beta\gamma}\},$$

where $F(k^2)$ is a function independent of the spin variables. When we later refer to scattering amplitude, we shall mean $F(k^2)$.

As has been shown, we can apply perturbation theory to the "long range" interaction $\hat{V}_1$, since it is small. Since the singularity in the momentum transfer only arises because of $\hat{V}_1$, we need include only those Feynman diagrams in which the whole momentum transfer comes about through $\hat{V}_1$; all the others do not give a singularity, as can easily be shown. We must therefore include the diagrams shown in Fig. 2. The singular part of the scattering amplitude for isolated atoms, $\bar{F}(k^2)$, is represented by a point. As we are concerned with scattering of excitations at the Fermi surface, we must put the energy transfer equal to zero. In addition, since only $\bar{F}(k^2)$ has a singularity at $k^2 = 0$, we can let k tend to zero for all other terms. Using the usual rules for drawing Feynman diagrams and applying Eq. (8), we obtain after simple rearrangement the final expression for $F_s(k^2)$ — the singular part of $F(k^2)$:

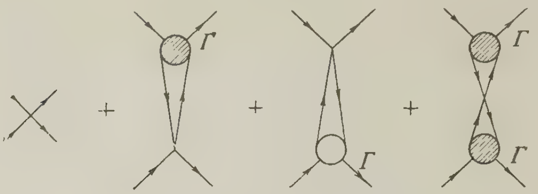

FIG. 2

$$F_s(k^2) = \Big(\frac{m^*}{m}a^2\Big)\Big\{1 - \frac{a^2p_0^2}{v2(2\pi)^3}\int\Gamma^k_{\alpha\beta,\,\alpha\beta}(P, Q)\,do_{\mathbf{q}}$$
$$- \frac{i}{2(2\pi)^4}\int\Gamma^k_{\alpha\beta,\,\alpha\beta}(P, Q)\,g(Q)\,d^4Q\Big\}^2\bar{F}(k^2). \qquad (17)$$

We must make here the following remarks. From the way in which (17) has been derived we have to understand by Γ^k the vertex part Γ^k_0 described by the Hamiltonian $\hat{H}_0$, and not the whole vertex part. As the whole calculation is made in the first Born approximation in $\hat{V}_1$ and the right-hand side of (17) is already of order $\hat{V}_1$, the calculation of the difference between Γ^k and Γ^k_0 would be unnecessary, and we can take as Γ^k in (17) the whole vertex part of the forward scattering.

Rewriting the expression in curly brackets in (17) with the help of (16), we obtain

$$F_s = (m^*/m)\,a^2\,(\partial G^{-1}/\partial\mu)^2\,\bar{F}(k^2). \qquad (18)$$

We need retain only the terms in $\partial G^{-1}/\partial\mu$ which do not tend to zero for $\epsilon \to 0$, $p \to p_0$ since we are only concerned with excitations at the Fermi surface. From (7) we find $(\partial G^{-1}/\partial\mu) = (v/a)(dp_0/d\mu)$ and finally

$$F_s = (m^*/m)\,(v\,dp_0/d\mu)^2\,\bar{F}(k^2). \qquad (19)$$

We see that $F_s(k^2)$ has the same sign as $\bar{F}(k^2)$, i.e., the excitations attract one another at large distances, just as do isolated atoms.

$v\,dp_0/d\mu$ can be expressed in terms of observable quantities. The number of particles per unit volume, N, is related to p_0 by the expression

$$N = (4\pi / 3)\, 2p_0^3 / (2\pi)^3.$$

Hence

$$v \frac{dp_0}{d\mu} = \frac{(2\pi)^3}{8\pi m^* p_0} \frac{dN}{d\mu} = \frac{(2\pi)^2}{8\pi m^*} \left(\frac{8\pi}{3N}\right)^{1/3} \frac{dN}{d\mu}.$$

Expressing $dN/d\mu$ in terms of the compressibility of the liquid,[8] we obtain

$$v\, dp_0 / d\mu = ((2\pi)^2 / 3mm^* c^2)\, (3N / 8\pi)^{2/3} \tag{20}$$

where c is the velocity of sound.

Equations (19) and (20) give the solution of the problem. Using relation (2) for $F(k^2)$ and Eq. (6), we can write down an expression for the asymptotic value of the scattering phase for $l \to \infty$. As was indicated at the beginning of this section, the method used is an approximation relying on the smallness of the polarizability of the atoms of the liquid. This condition is well fulfilled by He^3. In the next section we derive a relation not based on this assumption. The method used is of interest and makes it possible to determine the limits of applicability of the results obtained in this section.

4. EXACT ASYMPTOTIC EXPRESSION FOR THE SCATTERING AMPLITUDE AT LARGE *l*

In order to obtain the more exact relations desired, we must examine in more detail the van der Waals forces between elementary excitations. As is well known (see, for example, reference 9), van der Waals forces are connected with the existence of zero-point fluctuations of long-wave electromagnetic radiation in the medium, i.e., with the exchange of virtual long-wave photons. To separate the effects connected with these photons, we shall divide up the Hamiltonian of the system into two parts, as is done in reference 10:

$$\hat{H} = \int \hat{j} \hat{A}\, dV + \hat{H}_0 = \hat{H}_1 + \hat{H}_0,$$

where the first term ($\hat{j}$ is the 4-vector current of liquid and $\hat{A}$ the electromagnetic vector potential) describes the interaction of the liquid with the long-wave radiation, and all the rest of the energy of the system is contained in $\hat{H}_0$.

The virtual photons will be depicted on the Feynman diagrams by dashed lines, and to each line corresponds a photon propagation function

$$D_{ik}(\Omega_0) = \frac{4\pi}{\varepsilon(|\omega_0|)\, \omega_0^2 - k_0^2} \left(\delta_{ik} - \frac{k_{0i} k_{0k}}{\varepsilon(|\omega_0|)\, \omega_0^2}\right) \tag{21}$$

[$\epsilon(\omega)$ is the complex dielectric constant of the liquid, $\Omega_0 \{\omega_0, k_0\}$ is the 4-vector of energy and momentum of the photon, i, k, $l \ldots = 1, 2, 3$. As in reference 10, we use a vector potential gauge for which $D_{0i} = D_{00} = 0$].

Since only the interaction with long-wave photons is included in $\hat{H}_1$, all integrals over photon lines must be cut off at some maximum wave vector L, such that $Ld \ll 1$, where $d \sim 1/p_0$ is of the order of atomic dimensions. The final answer is independent of L.

As in the previous section, we are interested in those Feynman diagrams which have a singularity in the momentum transfer. These singularities are associated with van der Waals forces and therefore with the exchange of long-wave photons, so that diagrams in which the whole momentum transfer takes place through long-wave photons will have singularities. These are diagrams which can be divided between the ends P_1, $P_1 + K$ and P_2, $P_2 - K$ into two parts connected only by long-wave photon lines. We must limit ourselves to the diagrams with the smallest number of such photon lines since, as can be shown, each extra integration increases the power of k in the singularity, or gives an extra power of the small quantity Ld.

The first of such diagrams is I in Fig. 3. The corresponding matrix element is identically zero, since it is proportional to the square of the electric dipole moment of the He^3 atom in the ground state. Diagram II therefore provides the main contribution to the singular part of the scattering amplitude; this represents the exchange of two virtual photons. We should note that it is just such diagrams which are relevant to the calculation of the van der Waals attraction between isolated atoms.[11] The shaded circles in diagram II represent

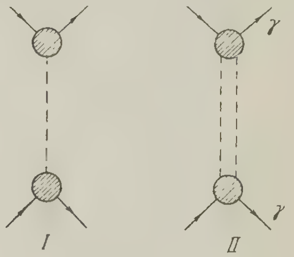

FIG. 3

$$\gamma_{ik\alpha\beta}(\Omega_0, P, K) = \delta_{ik} \delta_{\alpha\beta} \gamma(\Omega_0, P, K),$$

which describes the Compton scattering of a photon by an elementary excitation in a Fermi liquid (P is the original 4-vector of energy and momentum of the excitation, Ω_0 is the original 4-momentum vector of the photon and K the 4-momentum exchange vector).

We first determine the values of the argument for which we need to know γ. We are only interested in scattering of excitations with energy and momentum at the Fermi limit, i.e., with $\epsilon = 0$, $\omega = 0$, $|\mathbf{p}| = p_0$. In addition, since the singularity in diagram III for small k comes from integration over the photon lines, and γ itself does not have a singularity for $k \to 0$ and $\omega = 0$, we can let k in it tend to zero (with the condition $\omega = 0$). Finally we must take into account the fact that the momenta of long-wave photons are in general much smaller than the momenta of Fermi particles ($k_0/p_0 \ll Ld \ll 1$). We can, therefore, always set the wave vector $\mathbf{k}_0$ equal to zero in the arguments of γ.

Thus the only quantity which enters the scattering amplitude is

$$\gamma^k(\Omega_0 P) = \lim_{\substack{k\to 0\\ \omega/k\to 0}} \gamma(\Omega_0,\ P,\ K)$$

with $k_0 = 0$, $\epsilon = 0$, $|\mathbf{p}| = p_0$. This only depends on the photon frequency ω_0 and will be represented by $\gamma^k(\omega_0)$. We shall, in what follows, also require

$$\gamma^\omega(\Omega_0,\ P) = \lim_{\substack{K\to 0\\ k/\omega\to 0}} \gamma(\Omega_0,\ P,\ K)$$

and, correspondingly, its value $\gamma^\omega(\omega_0)$ for $\epsilon = 0$, $|\mathbf{p}| = p_0$, $\mathbf{k}_0 = 0$.

Using these expressions, the scattering amplitude corresponding to diagram II can be written in the form

$$F_s = \left(-\frac{m^*}{4\pi}\right)\frac{-i}{(2\pi)^4}\int [a\gamma^k(\omega_0)]^2 D_{ik}(\omega_0,\ \mathbf{k}_0) \times D_{ik}(\omega_0,\ \mathbf{k}-\mathbf{k}_0)\, d\omega_0\, d^3\mathbf{k}_0. \tag{22}$$

By using the general analytical properties of the Green's functions and of the vertex parts, we can see that the path of integration over ω_0 in (22) can be taken towards the upper half of the imaginary axis. Substituting expression (21) for D_{ik} we then obtain

$$F_s(k^2) = -\frac{4m^*}{(2\pi)^3}\int_0^\infty \left[\frac{a\gamma^k(i\xi)}{\varepsilon(i\xi)\,\xi^2}\right]^2 d\xi \times \int \frac{3\varepsilon^2(i\xi)\,\xi^4 + \varepsilon(i\xi)\,\xi^2\,[k_0^2 + (\mathbf{k}_0-\mathbf{k})^2] + (\mathbf{k}_0,\ \mathbf{k}-\mathbf{k}_0)^2}{[\varepsilon(i\xi)\,\xi^2 + k_0^2]\,[\varepsilon(i\xi)\,\xi^2 + (\mathbf{k}_0-\mathbf{k})^2]}\, d^3\mathbf{k}_0. \tag{22a}$$

We shall be concerned with distances much less than the wavelengths of the spectrum of the liquid, but large compared with interatomic distances. The interaction becomes vanishingly small at large distances, so that in the integral of (22) we can assume

$$k_0 \sim k \gg \omega_0. \tag{23}$$

The integral over k_0 diverges for large k_0, so that we must assume that the expression under the integral in (22) has a cut-off multiplier which is unity for $k_0 \ll L$ and tends to zero for $k_0 \to \infty$.

The calculation of the integral in (22) then reduces to a calculation in terms of k_0 at the poles of the expression in the integral, and can easily be carried through. For the condition (23) the result is

$$F_s(k^2) = k^3\frac{m^*}{16}\int_0^\infty [a\gamma^k(i\xi)/\varepsilon(i\xi)\,\xi^2]^2\, d\xi. \tag{24}$$

Apart from the trivial substitution of m* for m, which is related to the normalization of the amplitude, (24) differs from the scattering amplitude for isolated atoms (2) only in the substitution of $a\gamma^k(\omega)/\epsilon(\omega)\,\omega^2$ for $\alpha(\omega)$. It now remains for us only to express the amplitude $\gamma^k(\omega)$ in terms of observable quantities. This is done in the next section.

5. THE EXPRESSION OF $\gamma^k(\omega)$ IN TERMS OF OBSERVABLE QUANTITIES

We require several equations analogous to (16). To obtain the first of these we again introduce into the interaction Hamiltonian an infinitesimal external field δU, which this time depends only on the time:

$$\delta U = \delta U_0 e^{-i\omega t}. \tag{25}$$

The change in the Green's function due to the influence of such a field is again determined by the diagram of Fig. 1. This field introduced does not represent any real change in the state of the liquid, since the field can be removed from the expression for the ψ-operators by means of a trivial physical transformation of the operators:

$$\hat{\psi} \to \psi \exp\left\{-i\int \delta U\, dt\right\}.$$

Going to the limit $\omega \to 0$ we find that the introduction of our fictitious field produces a multiplication of the ψ-operators by a factor $\exp\{-i\delta U_0 t\}$, i.e., to a change in the origin of particle energy measurement by δU_0. Using this and writing down the analytical expression, represented in Fig. 1, in the limit of $\omega \to 0$ (for the condition $k = 0$) we obtain the required expression

$$\frac{\partial G^{-1}(P)}{\partial\varepsilon} = \left\{1 - \frac{i}{2\,(2\pi)^4}\int \Gamma^{\omega}_{\alpha\beta,\ \alpha\beta}(P,\ Q)\, g(Q)\, d^4Q\right\}. \tag{26}$$

We note that for $\epsilon \approx 0$, $p \approx p_0$ the differential coefficient $\partial G^{-1}/\partial\epsilon$ is just equal to $1/a$.

In a similar way an equation for the D-function can be obtained. The change, δD_{ik}, when the infinitesimal field δU is applied is shown graphically in Fig. 4. As follows from the previous discussion, for a field $\delta U_0 e^{i\mathbf{kr}}$ ($k \to 0$) the function

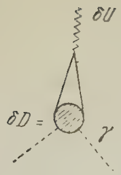

FIG. 4

D_{ik} changes by $-(\partial D_{ik}/\partial\mu)\,\delta U_0$. D_{ik} cannot in general change when a field $\delta U_0 e^{-i\omega t}$ $(\omega \to 0)$ is applied, since a change in the energy reference point does not affect the propagation of photons in the liquid.

Making use of this and diagram III, and going to the limit in a suitable manner, we obtain two other identities:

$$\frac{\partial D_{ik}^{-1}}{\partial\mu} = -\delta_{ik}\left\{4\pi\frac{a^2p_0^2}{(2\pi)^3\,v}\gamma^k(\omega_0) + \frac{i}{(2\pi)^4}\int\gamma^k(\omega_0, Q)\,g(Q)\,d^4Q\right\}, \tag{27}$$

$$0 = -i\,(2\pi)^{-4}\int\gamma^\omega(\omega_0, Q)\,g(Q)\,d^4Q. \tag{28}$$

In (27) D_{ik}^{-1} is the matrix inverse to D_{ik}. As was pointed out in reference 10, with the chosen gauge, D_{ik} satisfies the relation

$$[(\omega_0^2\varepsilon(|\omega_0|) - k_0^2)\,\delta_{il} + k_{0i}k_{0l}]\,D_{lk} = 4\pi\delta_{ik}. \tag{29}$$

It then follows that

$$D_{ik}^{-1} = (4\pi)^{-1}\{[\omega_0^2\varepsilon(|\omega_0|) - k_0^2]\,\delta_{ik} + k_{0i}k_{0k}\}, \tag{30}$$

and the left hand side of (27) can be written in the form

$$\frac{\partial D_{ik}^{-1}}{\partial\mu} = \delta_{ik}\frac{\omega_0^2}{4\pi}\frac{\partial\varepsilon(|\omega_0|)}{\partial\mu} = \delta_{ik}\frac{\omega_0^2}{4\pi}\frac{\partial\varepsilon(|\omega_0|)}{\partial N}\frac{\partial N}{\partial\mu}. \tag{31}$$

Apart from Eqs. (26) – (28), we will require another relation between $\gamma^k(\Omega_0, P)$ and $\gamma^\omega(\Omega_0, P)$. The derivation is completely analogous to that of (12), carried out by Landau.[7] We therefore omit these simple calculations and only give the final result:

$$\gamma^k(\Omega_0, P) = \gamma^\omega(\Omega_0, P) - \frac{a^2p_0^2}{2\,(2\pi)^3v}\int\gamma^k(\Omega_0, Q)\,\Gamma^\omega_{\alpha\beta,\,\alpha\beta}(Q, P)\,do_{\mathbf{q}}$$
$$= \gamma^\omega(\Omega_0, P) - \frac{a^2p_0^2}{2\,(2\pi)^3v}\gamma^k(\omega_0)\int\Gamma^\omega_{\alpha\beta,\,\alpha\beta}(Q, P)\,do_{\mathbf{q}}. \tag{32}$$

(We have assumed $\gamma^k(\Omega_0, Q)$ to depend only on the absolute magnitude of the vector $\mathbf{q}$ and not on its direction, since we can always consider $k_0 = 0$.)

Relations (26) – (28) and (32) make it easy to find $\gamma^k(\omega_0)$. We multiply both sides of (32) by $i\,(2\pi)^{-4}g(P)$, integrate with respect to d^4P and evaluate

$$i\,(2\pi)^{-4}\int\Gamma^\omega g d^4P,\quad i\,(2\pi)^{-4}\int\gamma^k g d^4P,\quad i\,(2\pi)^{-4}\int\gamma^\omega g d^4P$$

by means of (26), (27) and (28) respectively. We then obtain

$$\gamma^k(\omega_0) = -\frac{\omega_0^2}{4\pi a}\frac{v\,(2\pi)^3}{4\pi p_0}\frac{\partial\varepsilon(|\omega_0|)}{\partial\mu} = -\frac{v\omega_0^2}{4\pi a}\frac{\partial\varepsilon(|\omega_0|)}{\partial N}\frac{dp_0}{d\mu}. \tag{33}$$

Substituting (33) into (24) we find the final expression for the scattering amplitude:

$$F_s = \frac{m^*}{16}\int_0^\infty\left[\frac{1}{4\pi\varepsilon(i\xi)}\frac{\partial\varepsilon(i\xi)}{\partial N}\right]^2 d\xi\left(v\frac{dp_0}{d\mu}\right)^2 k^3. \tag{34}$$

We note that the renormalization constant, a, has disappeared as it should. The result is expressed in terms of observable quantities only.

Using (6) we can now write down the asymptotic expression for the scattering phase for $l \to \infty$

$$\delta_l = \frac{9}{32}(ep_0)^4\,m^*\int_0^\infty\left[\frac{1}{4\pi\varepsilon(i\xi)}\frac{\partial\varepsilon(i\xi)}{\partial N}\right]^2 d\xi\left(v\frac{dp_0}{d\mu}\right)^2 l^{-5}. \tag{35}$$

We can see, as follows from the approximate treatment in Sec. 3, that the sign of the phase at large l corresponds to an attraction between the excitations.

From (34) it appears that the amplitude for excitations differs from that for isolated atoms by the replacement of $\alpha(\omega)$ by

$$(v\,4\pi\varepsilon(\omega))\,(\partial\varepsilon(\omega)/\partial N)\,(dp_0/d\mu).$$

As was shown in reference 3, the interaction energy of atoms in a dilute solution is obtained from the interaction energy of the atoms in vacuo by substituting for $\alpha(\omega)$

$$(1/4\pi\varepsilon(\omega))\,(\partial\varepsilon(\omega)/\partial N).$$

The additional factor $v\,dp_0/d\mu$ is connected in our case with the influence of neighboring atoms in the liquid on the scattering of excitations. Equation (34) goes over into (19) if we put in the denominator $\epsilon = 1$ and set $\epsilon - 1 = 4\pi\alpha N$, where $\alpha(\omega)$ is the polarizability of an isolated atom. Both these conditions are quite well fulfilled in liquid helium.

In conclusion we point out again that this investigation makes it seem most likely that liquid He^3 goes into a superfluid state at sufficiently low temperatures. This state will have a number of special properties which it will be most interesting to study.

The author takes this opportunity of thanking Academician L. D. Landau and I. Ya. Pomeranchuk for their valued advice and discussions, and L. P. Gor'kov for a discussion of the problems presented in the appendix.

APPENDIX

DERIVATION OF THE FORMULA FOR THE EFFECTIVE MASS OF ELEMENTARY EXCITATIONS IN A FERMI LIQUID BY THE METHODS OF QUANTUM FIELD THEORY

We shall derive two relations analogous to (16) and (26), which can be of great use in studying the properties of a Fermi liquid. As an example of their application we will obtain an expression for the effective mass of excitations in a Fermi liquid, derived on the basis of a semi-phenomenological theory by Landau.[8]

It is easiest to derive the first relation if we assume that the atoms of the liquid have an infinitesimally small charge e. The final expression will not contain the charge and will hold equally well for uncharged particles. We subject the Fermi liquid to an infinitesimally weak external magnetic field with vector potential

$$\delta \mathbf{A} = \delta \mathbf{A}_0 e^{i\mathbf{kr}}. \tag{36}$$

This corresponds to substituting for $p^2/2m$ in the Hamiltonian of the system $(\mathbf{p} - e\delta\mathbf{A})^2/2m$ or, as $\delta\mathbf{A} \rightarrow 0$, to an extra term in the Hamiltonian

$$\delta U = -(e/m)\,\delta \mathbf{A}\mathbf{p}. \tag{37}$$

If we now go to the limit $\mathbf{k} \rightarrow 0$, then $\delta\mathbf{A}$ becomes the constant vector potential $\delta\mathbf{A}$. By the gauge invariance theorem, all functions that depend on the momentum $\mathbf{p}$ must become functions of $\mathbf{p} - e\delta\mathbf{A}_0$.[12] The Green's function $G(P)$ therefore changes, because of the addition of (37), by the amount

$$\delta G = -e\,(\partial G/\partial \mathbf{p})\,\delta \mathbf{A}_0.$$

On the other hand, this change can be calculated according to the diagram of Fig. 1, bearing in mind that δU is now given by Eq. (37). After going to the limit $\mathbf{k} \rightarrow 0$ (for $\omega = 0$) we obtain the analogous expression*

$$\frac{\partial G^{-1}(P)}{\partial \mathbf{p}} = -\left\{\frac{\mathbf{p}}{m} - \frac{a^2 p_0^2}{2(2\pi)^3 m v}\int \Gamma^k_{\alpha\beta,\,\alpha\beta}(P, Q)\,\mathbf{q}\,do_{\mathbf{q}} - \frac{1}{2(2\pi)^4 m}\int \Gamma^k_{\alpha\beta,\,\alpha\beta}(P, Q)\,g(Q)\,\mathbf{q}\,d^4Q\right\}. \tag{38}$$

Equation (38) can be very convenient in studying general questions in the theory, because the function $G^{-1}(P)$ can also be related to the vertex part through the well known Dyson relation. In addition to the full vertex parts, this relation consists of the "bare" vertex which does not have a direct physical meaning, and its form therefore depends on the actual form of the interaction Hamiltonian. Relation (38) is quite general and is independent of the form of the Hamiltonian.

To derive the second equation we examine the liquid in a coordinate system moving non-uniformly with velocity $\delta\mathbf{V} = \delta\mathbf{V}_0 e^{-i\omega t}$. The transition to such a system denotes a change of velocity operator in the Hamiltonian from $\mathbf{p}/m$ to $\mathbf{p}/m - \delta\mathbf{V}$ or, correspondingly an extra term in the Hamiltonian

$$\delta U = -\delta\mathbf{V}\mathbf{p}.$$

If now ω tends to zero we go over to an inertial coordinate system moving with velocity $\delta\mathbf{V}_0$ relative to the previous one. According to the Galilean transformation (see reference 13) the energy of the system changes by $\delta\mathbf{V}_0\mathbf{p}$, and consequently the Green's function changes by

$$\delta G = -(\partial G/\partial \varepsilon)\,\mathbf{p}\,\delta\mathbf{V}_0.$$

On the other hand, expressing this quantity according to diagram I, we obtain the relation

$$\mathbf{p}\,\frac{\partial G^{-1}(P)}{\partial \varepsilon} = \mathbf{p} - \frac{i}{2(2\pi)^4}\int \Gamma^\omega_{\alpha\beta,\,\alpha\beta}(P, Q)\,g(Q)\,\mathbf{q}\,d^4Q. \tag{39}$$

In order to obtain the formula for the effective mass of the excitations we multiply the right and left hand sides of the inequality (12) by

$$\mathbf{p}_2\,\frac{2\pi a^2}{v}\,\delta(\varepsilon_2)\,\delta(p_2 - p_0) + i\,\mathbf{p}_2 g(P_2),$$

integrate with respect to $d^4P_2/(2\pi)^4$ and express the integrals

$$(2\pi)^{-4}\int \Gamma^k g\,\mathbf{p}_2 d^4P_2 \quad \text{and} \quad (2\pi)^{-4}\int \Gamma^\omega g\,\mathbf{p}_2 d^4P_2$$

by relations (38) and (39). After reduction we obtain

$$-m\,\frac{\partial G^{-1}}{\partial \mathbf{p}} = \mathbf{p}\,\frac{\partial G^{-1}}{\partial \varepsilon} + \frac{a^2 p_0^2 m}{2(2\pi)^3 v}\int \Gamma^\omega_{\alpha\beta,\,\alpha\beta}(P, Q)\,\frac{\partial G^{-1}}{\partial \mathbf{q}}\,do_{\mathbf{q}}.$$

Taking $\mathbf{p} \approx \mathbf{p}_0$, $\epsilon \approx \epsilon_0$

$$\frac{\partial G^{-1}}{\partial \mathbf{p}} \approx -\frac{v}{a}\frac{\mathbf{p}}{p} = -\frac{1}{a}\frac{\mathbf{p}}{m^*}, \quad \frac{\partial G^{-1}}{\partial \varepsilon} \approx \frac{1}{a}.$$

We finally obtain

$$\frac{1}{m} = \frac{1}{m^*} + \frac{p_0}{2(2\pi)^3}\int a^2 \Gamma^\omega_{\alpha\beta,\,\alpha\beta}(Q, P)\cos\vartheta\,do_{\mathbf{q}}, \tag{40}$$

where ϑ is the angle between $\mathbf{p}$ and $\mathbf{q}$; Γ^ω is taken at $\epsilon = 0$, $|\mathbf{p}| = p_0$. With allowance for (11), relation (40) for the effective mass coincides with that obtained by Landau.[8]

---

*The derivation of (38) is quite analogous to the well known derivation of the Ward identity in quantum electrodynamics (see reference 12). This equation can therefore be obtained directly by considering the result of perturbation theory for G(P).

[1] V. P. Peshkov and K. N. Zinov'eva, Usp. Fiz. Nauk **67**, 193 (1959), Soviet Phys.-Uspekhi **2**, 82 (1959).

[2] L. N. Cooper, Phys. Rev. **104**, 1189 (1956).

[3] L. P. Pitaevskiĭ, JETP **37**, 577 (1959), Soviet Phys. JETP **10**, 408 (1960).

[4] L. D. Landau and E. M. Lifshitz, Электродинамика сплошных сред, (Electrodynamics of Continuous Media), GITTL, 1957, p. 478.

[5] L. B. Okun and I. Ya. Pomeranchuk, JETP **36**, 300 (1959), Soviet Phys. JETP **9**, 207 (1959).

[6] Higher Transcendental Functions, McGraw-Hill, New York 1953, Vol II, p. 214.

[7] L. D. Landau, JETP **35**, 97 (1958), Soviet Phys. JETP **8**, 70 (1959).

[8] L. D. Landau, JETP **30**, 1058 (1956), Soviet Phys. JETP **3**, 920 (1957).

[9] E. M. Lifshitz, JETP **29**, 94 (1955), Soviet Phys. JETP **2**, 73 (1956).

[10] I. E. Dzyaloshinskiĭ and L. P. Pitaevskiĭ, JETP **36**, 1797 (1959), Soviet Phys. JETP **2**, 1282 (1959).

[11] I. E. Dzyaloshinskiĭ, JETP **30**, 1152 (1956), Soviet Phys. JETP **3**, 977 (1957).

[12] Schweber, Bethe, and de Hoffmann, Mesons and Fields, I (Russ. Transl.) IIL, 1957, p. 396 [Row, Peterson and Co., N.Y., 1955].

[13] L. D. Landau and E. M. Lifshitz, Механика, (Mechanics), Fizmatgiz. 1958, p. 29.

Translated by R. Berman
346

SOVIET PHYSICS JETP VOLUME 37(10), NUMBER 6 JUNE, 1960

Letters to the Editor

MAXIMUM ATOMIC CROSS SECTIONS FOR NONRESONANCE CHARGE EXCHANGE

N. V. FEDORENKO and V. A. BELYAEV

Leningrad Physico-technical Institute,
Academy of Sciences, U.S.S.R.

Submitted to JETP editor August 14, 1959

J. Exptl. Theoret. Phys. (U.S.S.R.) **37**, 1808-1810 (December, 1959)

THE quantum theory of atomic collisions is still relatively undeveloped. Calculations of excitation, charge exchange, and ionization cross sections have been made only for the simplest cases of atomic collisions with hydrogen and helium. Thus an exposition of the empirical laws of inelastic atomic collisions, based on an analysis of the existing experimental data, has considerable importance for the development of a general theory.

Nonresonance single-electron charge exchange is represented by the equation

$$I^+ + A \to I^0 + A^+ + \Delta E,$$

where ΔE is the resonance defect, defined as the energy difference between the electron-transition levels. The investigations of Hasted[1-4] and our work[5,6] show that with an increase in the absolute value of the resonance defect $|\Delta E|$, the velocity for maximum cross section increases in agreement with the criterion given by H. S. W. Massey. This conclusion has subsequently been extended by Fogel'[7] to two-electron charge exchange with formation of a negative ion.

There is interest also in the factors that affect the maximum cross section $\sigma_{\max}$ for inelastic processes, in particular, nonresonance single-electron charge exchange. Massey's quasi-adiabatic hypothesis makes no definite statement about the size of this cross section. Data on charge-exchange scattering[8,9] show that if $|\Delta E|$ is small, then charge exchange occurs chiefly in "glancing" collisions, i.e., it is not connected with a major interpenetration of the electron shells. Therefore the charge exchange cross section must depend strongly on the features of the outer electron shells of the ion (I^+) and the target atom (A).

A study of the experimental data reveals that $\sigma_{\max}$ is affected by two fundamental factors, the absolute value of the resonance defect and the atomic number N of the target atom. The maximum cross section rises with increasing N but falls with increasing $|\Delta E|$. For the same ion and different atomic targets we find two characteristic cases:

1. If $|\Delta E|$ increases continuously, but N decreases, then $\sigma_{\max}$ falls rapidly, for both factors are acting in the same direction.
2. If both $|\Delta E|$ and N increase, then the two factors oppose one another and $\sigma_{\max}$ increases slowly from atom to atom.

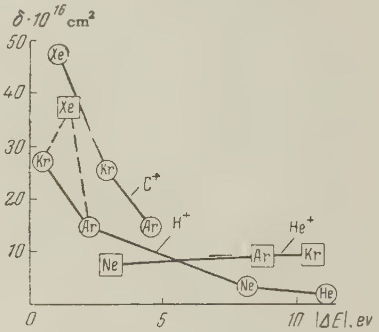

These statements are illustrated in the figure, which shows the dependence of $\sigma_{\max}$ on $|\Delta E|$ for single-electron charge exchange by the ions C^+, He^+, and H^+ in inert gases. Points representing charge-exchange cross sections for the same ion are joined. The figure includes all present-day data on ions for which the maximum of the charge-exchange cross section vs. energy curve has been determined for no less than three inert gases. The first case is illustrated by the C^+ ion (data from Gilbody and Hasted[4]). The He^+ ion (data from Fedorenko, Afrosimov, and Kaminker[6]) illustrates the second. The charge-exchange cross section for the H^+ ion (data from Stedeford and Hasted[3]) generally follows the first case, but it contains a characteristic deviation. The rapid decrease for the sequence Kr, A, Ne, and He results because both factors act to reduce the cross section. However, the uniformity with which $\sigma_{\max}(|\Delta E|)$ decreases is broken by the pair H—Xe. Probably this is connected with the fact that the transition from krypton to xenon is accompanied by an increase in ΔE coupled with an increase in N (second case).

We should note that for charge exchange in inert gases the growth of $\sigma_{\max}$ with increasing N can actually be explained by the greater dimensions of the outer shell of the target atom and by the reduction in the first ionization potential.

Further, it is interesting to note that a growth of $\sigma_{\max}$ with increasing N and decreasing $|\Delta E|$ is also observed[10] for two-electron charge exchange by He$^+$ in inert gases leading to the formation of the metastable He$^-$ ion.

Investigation of electron capture by multiply-charged ions shows that the sign of the resonance defect influences the cross section for such processes. Thus, according to the data of Flaks and Solov'ev,[11] for given velocity and given absolute value of the resonance defect, the cross section for exothermic processes (positive resonance defect) is significantly greater than the cross section for endothermic processes (negative resonance defect). For single-electron charge exchange the effect of the sign of the resonance defect on the cross section is still uncertain; in any case it is less sharply manifested. The squares in the figure represent exothermic charge exchange while the circles represent the endothermic ones.

It should further be mentioned that the values of $|\Delta E|$ displayed in the figure are calculated on the assumption that the electron exchange is between ground states of the atom and the ion. This assumption, to all appearances, is rather reliable for endothermic processes, but less so for exothermic ones, since for exothermic processes there exists the possibility of an excitation of the particles by the internal-energy release.

---

[1] J. B. Hasted, Proc. Roy. Soc. **A205**, 421 (1951).

[2] J. B. Hasted, Proc. Roy. Soc. **A212**, 235 (1952).

[3] J. B. H. Stedeford and J. B. Hasted, Proc. Roy. Soc. **A227**, 466 (1955).

[4] H. B. Gilbody and J. B. Hasted, Proc. Roy. Soc. **A238**, 334 (1957).

[5] N. V. Fedorenko, J. Tech. Phys. (U.S.S.R.) **24**, 2113 (1954).

[6] Fedorenko, Afrosimov, and Kaminker, J. Tech. Phys. (U.S.S.R.) **26**, 1929 (1956), Soviet Phys.-Tech. Phys. **1**, 1861 (1957).

[7] Fogel', Mitin, Kozlov, and Romashko, JETP **35**, 565 (1958).

[8] D. M. Kaminker and N. V. Fedorenko, J. Tech. Phys. (U.S.S.R.) **25**, 2239 (1955).

[9] Carbone, Fuls, and Everhart, Phys. Rev. **102**, 1524 (1956).

[10] Dukel'skiĭ, Afrosimov, and Fedorenko, JETP **30**, 792 (1956).

[11] I. P. Flaks and E. S. Solov'ev, J. Tech. Phys. (U.S.S.R.) **28**, 612 (1958), Soviet Phys.-Tech. Phys. **3**, 577 (1958).

Translated by Ralph Baierlein

POLARIZATION β-γ CORRELATION IN β DECAY OF Co^{60}

V. M LOBASHEV, V. A. NAZARENKO, and
L. I. RUSINOV

Leningrad Physico-technical Institute,
Academy of Sciences, U.S.S.R.

Submitted to JETP editor August 14, 1959

J. Exptl. Theoret. Phys. (U.S.S.R.) **37**, 1810-1811 (December, 1959)

It has been shown by Dolginov[1] and Tolhoek[2] that in β decay of polarized particles one can expect the existence of transverse polarization of the β electrons emitted in the plane perpendicular to the nuclear spin. Dolginov has shown that a study of the polarization of electrons from oriented nuclei is equivalent to a study of the correlation between circularly-polarized photons that follow the β decay and the transversely-polarized electrons. The same reference contains formulas for the expected correlation in the case of allowed β transitions.

We have investigated the correlation between transversely-polarized electrons and circularly-polarized photons in β decay of Co^{60}. A case was investigated in which the electron momentum $\mathbf{p}$ lies in a plane perpendicular to the momentum $\mathbf{k}$ of a photon with circular polarization σ, whereas the spin of the electron $\mathbf{s}$ is antiparallel to $\mathbf{k}$. The degree of circular polarization of the γ quanta coincident with the electrons was determined. Then, according to reference 1, the investigated correlation can be represented in the form

$$W(\sigma) = 1 + A\sigma. \qquad (1)$$

Here $\sigma = \pm 1$, for right-hand and left-hand circular photon polarization respectively. The factor A includes the dependence on the matrix elements of the β transition, level spins, multipolarity of the γ transitions, and electron energy.

Electrons with specified transverse polarization were separated registering the electrons singly scattered at 135° from a bismuth foil (the setup of the experiment is shown in the figure). The circular polarization of the photons was determined from the forward Compton scattering by magnetized iron (see references 3 and 4). An electrolytically prepared Co^{60} source of approximate activity 100 μC, was used. The correlation was determined as the change in counting rate of the coincidences upon reversal of the direction of magnetization in the scattering magnet of the γ polarimeter. The current

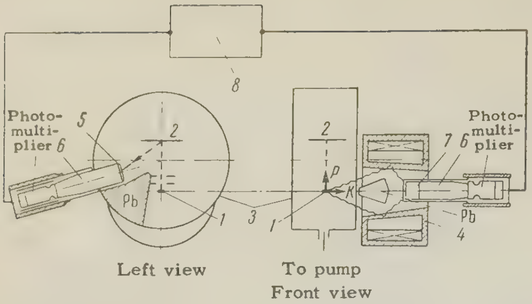

Schematic diagram of the setup: 1 – source, 2 – bismuth scatterer, 3 – vacuum chamber, 4 – scattering magnet, 5 – plastic scintillator, 6 – light pipes, 7 – NaI crystal, 8 – fast-slow coincidence circuit, $\tau = 10^{-8}$ sec.

in the magnet was reversed after 3.5 minutes automatically. The result of the measurement was calculated in the following form

$$\Delta = 2(I_1 - I_2)/(I_1 + I_2), \quad I_{1,2} = R_c / R_\beta R_\gamma; \qquad (2)$$

where R_c, R_β, and R_γ are respectively the counting rates of coincidences, single electron pulses, and photons. The indices 1 and 2 pertain to the direction of the magnetic field from and to the source (see diagram). Measurements with a bismuth electron scatterer 0.4 mg/cm^2 thick yielded $\Delta = (0.50 \pm 0.18)\%$.

As a control experiment, the measurements were repeated with a bismuth scatterer 5 mg/cm^2 thick. Here multiple scattering of the electrons should cause vanishing of the azimuthal scattering asymmetry due to the spin, and the effect should also vanish. Experiment yielded $\Delta = (-0.1 \pm 0.14)\%$; the errors indicated are statistical.

The efficiency of the γ polarimeter was determined from measurements of the β-γ correlation (γ – circularly polarized), in the decay of Co^{60} and Sc^{46}. The efficiency of the β polarimeter was calculated from the used geometry with allowance for multiple scattering in the bismuth foil, according to Sherman[5] and Wegener[6].

The value of A [Eq. (1)], determined with allowance for the background of β-γ coincidences, random coincidences, and efficiencies of both polarimeters, was found to be $A = 0.32 \pm 0.12$. The value of A computed after Dolginov was 0.24.

Thus, within the limits of statistical error, the theoretical and experimental results are found to agree.

In conclusion, the authors consider it their pleasant duty to thank A. Z. Dolginov for discussion and continuous interest in this work, and also to O. V. Saltykovskiĭ, V. S. Andryukevich, and A. V. Kurakin for participation in the preparation of the apparatus and the measurements.

[1] A. Z. Dolginov, JETP **35**, 178 (1958), Soviet Phys. JETP **8**, 123 (1959).

[2] H. A. Tolhoek, Revs. Modern Phys. **28**, 277 (1956).

[3] H. Schopper, Phil. Mag. **2**, 710 (1957).

[4] F. Boehm and A. H. Wapstra, Phys. Rev. **109**, 456 (1958).

[5] N. Sherman, Phys. Rev. **103**, 1601 (1956).

[6] H. Wegener, Z. Physik **151**, 252 (1958).

Translated by J. G. Adashko
348

ON THE FINE STRUCTURE OF THE GIANT RESONANCE

N. A. BURGOV, G. V. DANILYAN, B. S. DOLBILKIN, L. E. LAZAREVA, and F. A. NIKOLAEV

P. N. Lebedev Physics Institute, Academy of Sciences, U.S.S.R.

Submitted to JETP editor August 26, 1959

J. Exptl. Theoret. Phys. (U.S.S.R.) **37**, 1811-1814 (December, 1959)

It has been shown in a number of papers[1-4] that the photonuclear yield curve has breaks in the region of the giant resonance for light nuclei. Their position and magnitude depends on the material. The explanation of such breaks requires the existence of separated narrow resonances in the photon absorption cross section in this energy region. The sum of the integrated cross sections of these resonances is comparable with the total integrated cross section. The data on their width Γ are contradictory. According to the estimates in references 1 – 3, $\Gamma \leq 40$ kev; in reference 5 a much larger width was obtained ($\Gamma \geq 400$ kev).

It is of great interest to look for the existence of such resonances by a direct method. In this connection the fine structure of the giant resonance was investigated by the total absorption method. We give here the preliminary results, obtained this way for carbon.

Figure 1 shows the experimental arrangement. The work was performed with a 30-Mev synchrotron. The x-ray beam with $E_{max} = 28.8$ Mev was collimated by a lead collimator 26 cm long. Behind the collimator was placed a graphite block 60 cm thick (96.6 g/cm^2). The γ-ray spectrum was measured by a pair spectrometer. The magnetic

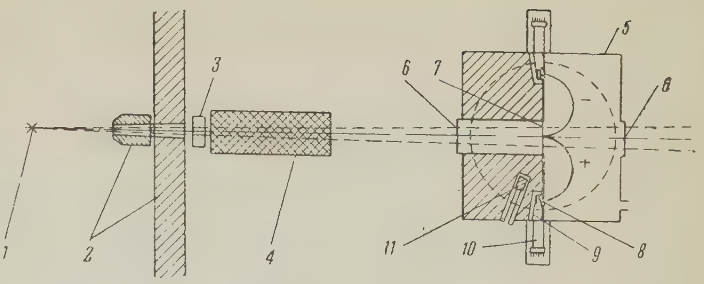

FIG. 1. Experimental setup: 1 – synchrotron target, 2 – lead collimator, 3 – thin-walled ionization chamber–integrator, 4 – graphite absorber, 5 – pair spectrometer chamber, 6 – input and output window of the chamber (aluminum foil of 0.3 and 0.5 mm thickness respectively), 7 – radiator (gold, 10 mg/cm²), 8 – plastic scintillator, 9 – light pipe, 10 – type FEU-33 photomultiplier, 11 – field probe.

field of the spectrometer was stabilized by proton resonance to better than 0.01% (less than ±2 kev at 20 Mev). The resolution of the spectrometer at 9.716 Mev (the γ line associated with capture of thermal neutrons in Cr^{53}) was measured to be 65 kev. According to a calculation the spectrometer resolution did not exceed 110 kev at an energy 20 – 25 Mev.

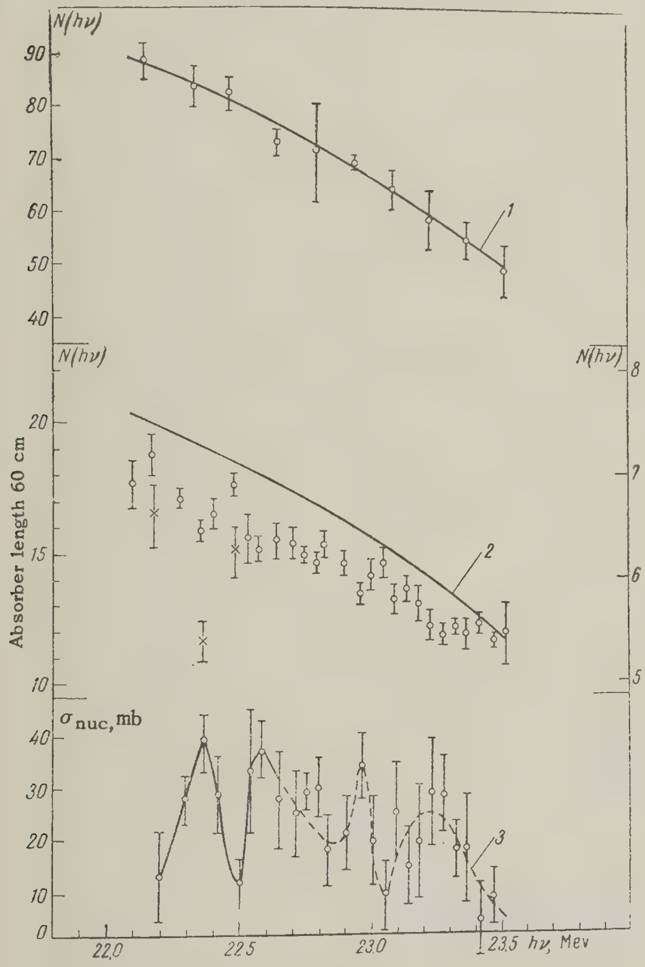

FIG. 2

In Fig. 2 are shown the x-ray spectrum measured without absorber, $N_0(h\nu)$, and with absorber, $N(h\nu)$. All experimental points are referred to an equal γ dose, which was determined by means of a thin-walled ionization chamber and an integrator. The indicated errors are the mean square deviations. Curve 1, $N_0(h\nu)$ was determined by the least squares method. After the absorber the number of photons of a given energy is given by the expression

$$N(h\nu) = N_0(h\nu)\exp \times\{-(\sigma_{\text{pair}}+\sigma_{\text{Compt}})nL\}\exp\{-\sigma_{\text{nuc}}nL\} \qquad (1)$$

(n – number of nuclei per cm³; L – length of the absorber in cm). Curve 2, $N_0(h\nu)\exp\{-(\sigma_{\text{pair}}+\sigma_{\text{Compt}})\}$, was calculated from Curve 1. The difference between the spectrum as measured with the absorber and Curve 2 is due to the nuclear absorption only. In the given geometry the contribution of photons reaching the radiator of the spectrometer after a small angle Compton scattering did not exceed 1%. The increase in the number of photons due to bremsstrahlung of secondary electrons in the absorber did not exceed ~1%. Curve 3 has been obtained from Eq. (1) and shows the nuclear absorption cross section σ_{nuc}.

Despite the large statistical errors, a peak in the cross section shows up in the energy range 22.2 – 22.5 Mev. To check this result the measurements were repeated in this energy interval with an absorber of increased length ($L = 102$ cm). The results obtained this way are indicated in Fig. 2 by crosses. The effect of the nuclear absorption is now more pronounced. The cross sections calculated for $L = 60$ and 102 cm are consistent.

An estimate of the integrated cross section of the peak, made under the assumption that the total cross section in the region 22.2 – 22.5 Mev is due to one resonance, gives 9 Mev-mb. This does not contradict the estimates of references 1 and 6 for the resonances which lie in the energy interval 21 – 23 Mev in carbon. The experimental width of the peak equals ~ 150 kev. Because of the resolution of the apparatus, this implies an actual line width of not more than 100 kev. The mean absorption cross section for the whole interval 22.2 – 23.5 Mev, which equals ~ 22 mb, agrees with the cross sections found in a number of investigations[7-10] for the (γ, n) and (γ, p) reactions in carbon.

The present results indicate that the method employed can be profitably used in the investigation of the fine structure of the giant resonance. The method allows the determination of the location of the different peaks with great accuracy.

Preliminary results for aluminum have been obtained with a similar method in reference 11. The authors of that paper believe that there exists a fine structure but are unable to draw definite conclusions due to large statistical uncertainties.

---

[1] Katz, Haslam, Horsley, Cameron, and Montalbetti, Phys. Rev. **95**, 464 (1954).

[2] J. Goldemberg and L. Katz, Phys. Rev. **95**, 471 (1954).

[3] A. S. Penfold and B. M. Spicer, Phys. Rev. **100**, 1377 (1955).

[4] R. Basile and C. Schuhl, Compt. rend. **240**, 2399 (1955).

[5] C. Tzara, J. Phys. Rad. **17**, 1001 (1956).

[6] L. Katz, Nat. Bur. Standards Photonuclear Conference, Washington (1958).

[7] J. Halpern and A. K. Mann, Phys. Rev. **83**, 370 (1951).

[8] Montalbetti, Katz, and Goldemberg, Phys. Rev. **91**, 659 (1953).

[9] R. Nathans and J. Halpern, Phys. Rev. **93**, 437 (1954).

[10] Barber, George, and Reagan, Phys. Rev. **98**, 73 (1955).

[11] Mihailovic, Pregl, Kernel, and Kregar, Phys. Rev., in press.

Translated by M. Danos
349

THE TEMPERATURE DEPENDENCE OF THE ELASTIC CONSTANTS OF POTASSIUM BROMIDE SINGLE CRYSTALS

S. P. NIKANOROV and A. V. STEPANOV

Leningrad Physico-technical Institute, Academy of Sciences, U.S.S.R.

Submitted to JETP editor August 29, 1959

J. Exptl. Theoret. Phys. (U.S.S.R.) 37, 1814-1815 (December, 1959)

THIS is a continuation of previous work[1] and describes a study of the temperature dependence of the elastic constants of potassium bromide single crystals in the range of temperature from room temperature to the melting point. Using the method of the composite oscillator,[2] measurements were made of Young's modulus and the shear modulus of specimens cut along the [100] and [110] directions; a detailed description of the apparatus and oscillator has been given in reference 1.

The measurements were made on specimens of square cross section for longitudinal oscillations and of circular cross section for torsional oscillations. The dimensions of the crystalline specimens were determined in a comparator with an accuracy of 0.01 mm. The specimens were stuck to a quartz rod using a mixture of water-glass and TU-KH 24-51 phosphate cement; the cementing operation was carried out at 150°C for 15 – 20 minutes. The resonant frequency was determined using Lissajou figures and a type 528 heterodyne wavemeter (accuracy 0.025%) at a fixed temperature. The temperature was measured to an accuracy of 1°C by a platinum-platinum rhodium thermocouple. The fall in temperature along the lengths of the specimens (which ranged from 10 to 16.5 mm) did not exceed 2°C. The method of cutting the specimen insured that the intrinsic frequency of the specimen and that of the three-part oscillator agreed to within 10%. The frequency of the quartz rod differed from the frequency of the three-part oscillator by not more than 2%.

The relative accuracies of the elastic constant measurements

$$s_{11} = 1/E_{[100]},\quad s'_{11} = 1/E_{[110]},\quad s_{44} = 1/G_{[100]}$$

were 1.2, 1.2, and 0.8%, respectively. The error in determining $s_{12} = 2s'_{11} - s_{11} - s_{44}/2$ and the compressibility $\chi = 3(s_{11} + 2s_{12})$, obtained by calculation, is significantly greater.

The values of the elastic constants s_{11}, s'_{11}, s_{44} and s_{12}, and also the compressibility χ, calculated from the formula given above, are given in the table.

Also in the table are data for 730°C; this is the melting point T_m of potassium bromide according to reference data. During the experiments the thermocouple measured the temperature at the contact of the specimens with the quartz rod of the ternary oscillator, which was suspended vertically in the furnace. When the temperature of the upper edge of the specimen reached 728°C

T, °C	$s_{11} \cdot 10^{13}$, cm^2/dyne	$s'_{11} \cdot 10^{13}$, cm^2/dyne	$s_{44} \cdot 10^{13}$, cm^2/dyne	$s_{12} \cdot 10^{13}$, cm^2/dyne	$\chi \cdot 10^{12}$, cm^2/dyne
20	30.1	62.1	195	− 3.4	7
100	32.6	63.7	199	− 4.7	7
200	36.1	63.8	206	− 7.5	6
300	40.3	68.5	213	− 9.8	6
400	45.7	72.0	219	−11.2	7
500	53.5	76.3	226	−13.9	8
600	63.7	82.0	234	−16.7	9
700	75.2	89.3	241	−17.1	12
730	81.3	91.0	244	−21.3	12

the measurements were made (the lower portion of the specimen had a temperature 2° C higher because of the variation of temperature along the length of the furnace). Usually it was difficult to make the measurements because of the frequency drift of the ternary oscillator, which was apparently caused by the specimen starting to melt from the surface, since after such an experiment a droplet had formed at the lower end of the specimen and could be seen after the specimen had been extracted from the furnace. Thus, the temperature 730° C in the table in fact corresponds to a temperature between 728° C and 730° C.

Extrapolating the temperature dependences of $E_{[100]}$, $E_{[110]}$ and $G_{[100]}$, which are nearly linear, to the absolute zero of temperature, the following values were obtained for the elastic constants at $T = 0°$ K: $s_{11} = 24.0 \times 10^{-13}$, $s_{44} = 180 \times 10^{-13}$, $s_{12} = -2.8 \times 10^{-13}$ cm^2/cyne. These values are in close agreement with the values for $T = 0°$ K obtained by Galt.[3]

---

[1] A. V. Stepanov and I. M. Éĭdus, JETP **29**, 669 (1955), Soviet Phys. JETP **2**, 377 (1956).

[2] L. Hunter and S. Siegel, Phys. Rev. **61**, 84 (1942).

[3] J. K. Galt, Phys. Rev. **73**, 1460 (1948).

Translated by K. F. Hulme
350

POLARIZATION OF (d–d) NEUTRONS

P. S. OT-STAVNOV

Submitted to JETP editor July 4, 1959

J. Exptl. Theoret. Phys. (U.S.S.R.) **37**, 1815-1817 (December, 1959)

By now it has been reliably established that certain reactions result in polarized neutrons. They have, however, been insufficiently well investigated. As follows from theory and experiment, the degree of polarization of neutrons depends on the neutron angle of emission and on the energies of the interacting particles.[1–3]

In the present investigation we measured the degree of polarization of (d-d) neutrons at an angle $\varphi = 150°$ laboratory system (this angle is frequently used in experimental physics to obtain monoenergetic neutrons), as a function of the deuteron energy. The degree of polarization was determined by the Lepore method,[4] based on the asymmetry of scattering of polarized particles by the scatterer nuclei.[5] In this case the cross section of the polarized neutrons is given by the formula

$$\sigma(\theta) = \sigma_0(\theta)\,(1 + \mathbf{P}_1(\psi)\,\mathbf{P}_2(\theta)), \tag{1}$$

where $\sigma_0(\theta)$ is the cross section for unpolarized neutrons, $\mathbf{P}_1(\psi)$ is the polarization of the (d-d) neutrons emitted from the target at an angle ψ (c.m.s.), and $\mathbf{P}_2(\theta)$ is the polarization of the neutrons by the scatterer when scattered elastically by an angle θ (c.m.s.).

On changing the left-right asymmetry R in the plane of the (d-d) reaction, we obtain the relation

$$R = N_{el}/N_r = \{1 + P_1(\psi)\,P_2(\theta)\}/\{1 - P_1(\psi)\,P_2(\theta)\}.. \tag{2}$$

The measurements were carried out with a cascade generator. Deuterons d with energies from 400 to 1000 kev were used to bombard a target made of heavy ice. The scatterer was placed 170 cm from the target at an angle $\varphi = 115°$. The experience gained by Levintov et al. in joining a scatterer to a detector[5] was used in this investigation. The scatterer was gaseous He^4, which also served as the detector of scattered neutrons. As can be seen from Fig. 1, the detector-analyzer comprises five counters 1 connected in parallel. Each counter consists of 19×0.1 steel tubes 280 mm long, tungsten polished wires, and telephone insulators. The counters are arranged in a single plane, with a shift

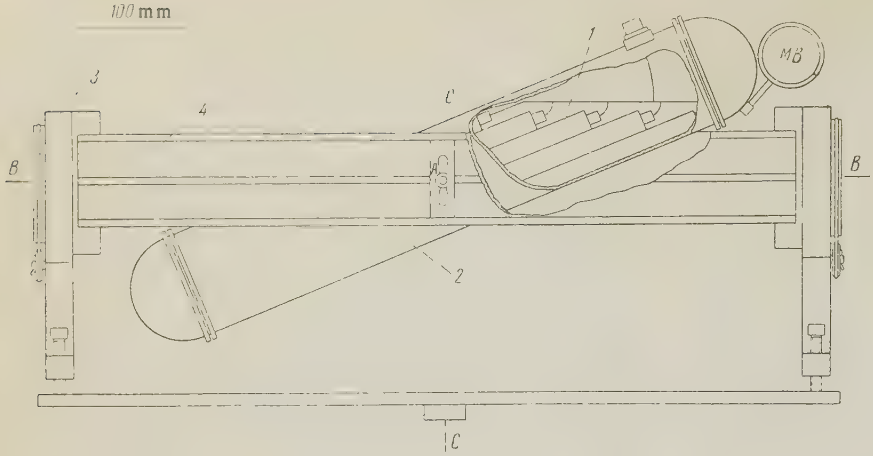

FIG. 1. Overall view of detector-analyzer.

of 40 mm. This shift yields an optimum ratio of effective to working detector volume. The counters are located in cylinder 2 and operate under identical conditions. The cylinder is connected through frame 4 to supports 3 and can be rotated about three axes: AA, BB, CC. Axis AA is perpendicular to the plane of the diagram. The gas pressure in the cylinder was 1 atmos. The scattering angle of the recoil helions was $\alpha = 22.5°$ (laboratory system), corresponding to a neutron scattering angle $\theta = 135°$ (c.m.s.). To pick out recoil helions of specified direction, the Glazkov analyzer scheme was used,[7] in which the tracks along the direction of a counter axis were selected. In this scheme use was made of the dependence of the rise of the leading front of the pulse on the orientation of the recoil-nucleus track relative to the collector electrode. The amplitudes of the selected pulses corresponded to monoenergetic neutrons, emitted by the target at the measured angle.

In the determination of the background, a paraffin stopper was placed in the path of the neutron beam. The background amounted to not more than 5% of the effect and was constant for all deuteron energies, within the limit of the statistics.

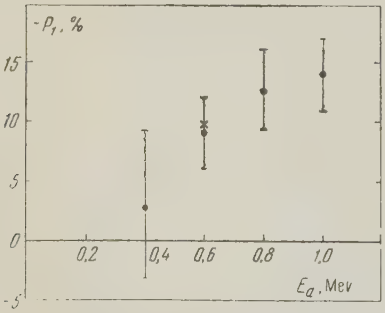

FIG. 2. Dependence of the polarization of (d – d) neutrons on the deuteron energy; ● – experimental points of the present investigation. × – point obtained by Meier et al.[3]

The degree of polarization of (d-d) neutrons, $P_1(\psi)$, was determined from Eq. (2) [$P_2(\theta)$, the degree of polarization of neutrons on He^4, was taken from the paper of Levintov[6]]. The results obtained are shown in Fig. 2. It is obvious that the polarization of (d-d) neutrons increases in absolute magnitude with increasing deuteron energy. This increase has the same character and approximately the same magnitude as obtained in the measurement of the polarization of (d-d) neutrons emitted by the target at angles $\varphi = 47 - 49°$.[2,3,8] Figure 2 shows also the point for $E_d = 0.6$ Mev as calculated by Meier.[3] As can be seen from the diagram, our experimental point is in good agreement with the calculated one. The degree of polarization experimentally obtained by the same authors at $\varphi \approx 105°$ yields a value much lower than calculated. This discrepancy is possibly due to the inaccuracy in the calculation of $P_2(\theta)$ for carbon, which was used by the authors to scatter the polarized neutrons.

The author is grateful to Yu. A. Aleksandrov and N. P. Glazkov for discussing many problems connected with the setup of the experiment.

---

[1] R. I. Blin-Stoyle, Proc. Phys. Soc. **64**, 700 (1951).

[2] Levintov, Miller, Tarumov, and Shamshev, JETP **32**, 375 (1957), Soviet Phys. JETP **5**, 310 (1957).

[3] Meier, Scherrer, and Trumpy, Helv. Phys. Acta **27**, 577 (1954).

[4] I. V. Lepore, Phys. Rev. **79**, 137 (1950).

[5] I. Schwinger, Phys. Rev. **73**, 407 (1948).

[6] Levintov, Miller, and Shamshev, JETP **32**, 274 (1957), Soviet Phys. JETP **5**, 258 (1957).

[7] N. P. Glazkov, Приборы и техника эксперимента (Instrum. and Meas. Engg.), in press.

[8] P. I. Pasma, Nucl. Phys. **6**, 141 (1958).

Translated by J. G. Adashko
351

ON THE MASSES OF THE μ MESON AND THE ELECTRON

Ya. B. ZEL'DOVICH

Institute of Theoretical and Experimental Physics, Academy of Sciences, U.S.S.R.

Submitted to JETP editor September 24, 1959

J. Exptl. Theoret. Phys. (U.S.S.R.) **37**, 1817-1819 (December, 1959)

THE μ meson, the electron, and the neutrino are coupled to the other particles only via the electromagnetic and weak interactions. It is therefore natural to suppose that the masses m_μ and m_e can be expressed in terms of the electromagnetic coupling constant $e = 4.8 \times 10^{-10}$ $g^{1/2}\,cm^{3/2}\,sec^{-1}$, $e^2/\hbar c = \alpha = {}^1/_{137}$, and the universal (see reference 1) weak coupling constant g $= 1.41 \times 10^{-49}$ g cm^5 sec^{-2}, $gc/\hbar^3 = 10^{-5}/M_N^2$, where M_N is the mass of the nucleon. Numerically we have

$$m_\mu = 0.57\sqrt{e^6/gc^4}, \qquad m_e = 0.38\sqrt{e^{10}/gc^6\hbar^2}. \tag{1}$$

Since $e^2/\hbar c$ is dimensionless, these formulas evidently contain an arbitrariness: we can simultaneously change the power of α and the numerical coefficient.*

One can also get an understanding of the structure of the formulas by assuming that the weak interactions involve, in second order, intermediate charged bosons X with spin 1 (see reference 2), so that (see, for example, reference 3)

$$g = 2g_X^2\hbar^2/M_X^2c^2, \tag{2}$$

where g_X (the coupling constant between the fermion current and X) has the same dimensionality as e.

The idea of a connection between the electromagnetic and weak interactions, as put forward by Schwinger[2] and Salam and Ward,[4] leads these authors to the assumption $g_X \equiv e$; to obtain the experimental value of g, one must then set $M_X = 38\,M_N$ (Gell-Mann notes that $M_X \approx M_N/4\alpha$). The μ mesons, electrons, and the neutrino (the "small particle world") are coupled to the other particles only via the electromagnetic field and the field of the X mesons. We assume that the masses of the μ meson and of the electron are due to the interaction with the X field and the photons with the same dimensionless constant $g_X = e = \sqrt{1/137}$ $(\hbar = c = 1)$, so that $m_\mu = m_e = m_\nu = 0$ if there were no interaction (i.e., $g_X = e = 0$). Then the only quantity with the dimensionality of a mass in the "small world" theory is M_X; it is therefore natural to seek an expression for the masses in the form $g_X^2 M_X$. Numerically we have

$$m_\mu = 0.40\,\frac{1}{137}\,M_X = 0.40\,\frac{g_X^2}{\hbar c}\,M_X,$$

$$m_e = 0.27\left(\frac{1}{137}\right)^2 M_X = 0.27\left(\frac{g_X^2}{\hbar c}\right)^2 M_X. \tag{3}$$

If we express M_X in terms of the four-fermion g and $e^2/\hbar c$ according to (2), we obtain the formulas (1).

It was assumed earlier that m_e is somehow due to the electromagnetic interaction (and also to the weak interaction, see reference 2, p. 431), which led to the result that m_μ is "large" and requires a special explanation. For this purpose new interactions were introduced, which show up only in the contribution they give to m_μ. These were interactions either with the neutral σ meson,[2,5,6] or with K mesons,[7] or with the nucleons (Suranyi, as quoted in reference 7).

In the present note we have proposed a mass scale with M_X as the unit, in which the mass of the μ meson is small (of the order of the square of the coupling constant between μ and X), so that there is no need to take recourse to additional interactions. We note that the interaction of X with μ, e, and ν violates the parity conservation principle. This must be taken account of in a theory of masses which depend on the interaction.

The relation $m_e \sim \alpha m_\mu$ was noted earlier:

$$m_\mu = 137\cdot{}^3/_2\, m_e\,[^8], \quad m_\mu = 137\sqrt{2}\ [^9];$$

In a paper, of which he kindly informed the author before publication, Gol'fand[10] assumes that m_e is due to the interaction e-μ and notes that $m_e \sim \alpha m_\mu$.

---

*It may not be accidental that ħ does not enter in the expression for m_μ: this condition fixes the exponent.

---

[1] M. Gell-Mann and R. Feynman, Phys. Rev. **109**, 193 (1958).

[2] J. Schwinger, Ann. of Phys. **2**, 407 (1957).

[3] N. Byers and R. Peierls, Nuovo cimento **10**, 520 (1958).

[4] A. Salam and J. C. Ward, Nuovo cimento **11**, 568 (1959).

[5] W. S. Cowland, Nucl. Phys, **8**, 397 (1958).

[6] J. R. Gatland, Nucl. Phys. **9**, 267 (1958).

[7] G. Marx and K. L. Nagy, Nucl. Phys. **12**, 125 (1959).

[8] H. Fröhlich, Nucl. Phys. 7, 148 (1958).
[9] Y. Nambu, Progr. Theor. Phys. 7, 595 (1952).
[10] Yu. A. Gol'fand, JETP 37, 1493 (1959), Soviet Phys. JETP 10, 1059 (1960).

Translated by R. Lipperheide
352

ON THE CAUSES OF THE PECULIARITIES IN THE PHYSICAL PROPERTIES OF INVAR ALLOYS

E. I. KONDORSKIĬ

Moscow State University

Submitted to JETP editor October 3, 1959

J. Exptl. Theoret. Phys. (U.S.S.R.) 37, 1819-1820 (December, 1959)

As is well known,[1] the physical properties of Invar alloys have a number of peculiarities (low coefficient of thermal expansion, large values of the volume magnetostriction and magnetic susceptibility in the saturation region, etc.). Until now these peculiarities have been explained[2-4] starting from the assumption that the exchange interaction energy between electrons and neighboring ions in these alloys changes rapidly during expansion or compression of the crystalline lattice. Such an explanation can hardly be considered satisfactory. It does not give a direct answer to the question of why these peculiarities are in fact observed in iron-nickel alloys with nickel concentrations from 30 to 45%. From the standpoint of these hypotheses it is impossible to explain the comparatively large changes of the saturation magnetization and specific electrical resistance of alloys with these concentrations under the influence of pressure at low temperatures.[5]

It has been shown[6] that an alloy with face-centered lattice containing 73% Fe, 9% Ni and 18% Cr, which is paramagnetic at room temperature and above, becomes anti-ferromagnetic at a temperature of 40° K. It follows as a probable conclusion that the exchange integral J_1 for neighboring ions of iron in the face-centered lattice is negative, and this allows us to proceed to an explanation of the peculiarities of Invar alloys from a different viewpoint.

Let J_1, J_{12} and J_2, respectively, be the exchange integrals of electrons on neighboring ions of iron, iron and nickel, and nickel. Nickel is ferromagnetic; on increasing the nickel content to 60%, the magnetic moment of iron-nickel alloys increases. Whence it follows that $J_2 > 0$ and $J_{12} > 0$. Taking $J_1 < 0$, it is not difficult to show that, if the nickel concentration c_2 is greater than some critical concentration c_k, then at low temperatures ferromagnetism is energetically favored. If, on the other hand $c_2 < c_k$, then under the same conditions antiferromagnetism is favored. Calculation leads to the conclusion that for a disordered distribution of the ions with antiparallel spins in the crystalline lattice of Fe-Ni alloys

$$c_k = \frac{J_{12} - J_1 - \sqrt{J_{12}^2 - J_1 J_2}}{2J_{12} - J_1 - J_2}$$

for

$$J_2 \approx J_{12} \approx -J_1, \; c_k \approx 0.3. \qquad (1)$$

A disordered distribution of ions with anti-parallel spins is more probable at high than at low temperatures, when grouping of the spins should occur (short-range order). Therefore, between completely ferromagnetic and antiferromagnetic alloys there should be alloys in which a fraction of the ions have antiparallel spins. Calculation shows that similar "hidden" antiferromagnetism should occur for nickel concentrations $c_2 < c_{20} = -J_1/(J_{12} - J_1)$ (for $J_1 \approx -J_{12}$, $c_{20} \approx 0.5$). When $c_2 > c_{20}$, the magnetic moment σ_0 of iron-nickel alloys increases linearly with increasing iron content. When $c_2 \leq c_{20}$, a departure from linearity appears and for c_2 close to c_k a sharp fall of σ_0 starts, because of the increasing number of anti-parallel spins. Data obtained experimentally[7,8] show that the change of σ_0 with increase of iron content in iron-nickel alloys with face-centered lattices occurs in exactly this fashion. We note that the departure from linearity in the σ_0 curve occurs in the range 40 — 50% nickel and on further increasing the nickel content a sharp fall of σ_0 is observed, starting at 36%.

In our view "hidden" antiferromagnetism should be considered as the basic cause of the "anomalies" in the physical properties of Invar alloys. In fact, the presence of antiparallel spins in these alloys explains the comparatively large values of the volume magnetostriction and the para-process susceptibility in strong magnetic fields. Further, as is seen from (1), the transition concentration c_k increases with increase of the absolute value of J_1, which increases most rapidly during hydrostatic compression. The increase of c_k causes a displacement of the steep portion of the σ_0 curve towards the nickel side, which should be accompanied by a stronger decrease of σ_0 for the Invar alloys lying in the transition region. Experimental results[5] confirm this conclusion. Confirmation of the fact that in Invar alloys "hidden" antiferromagnetism occurs is also provided by their large specific electrical resistance, associated in our view with conduction electron scattering at inhomogeneities of the magnetic moment.

Apart from the assumption about the antiferromagnetism of iron in a face-centered lattice, which is supported experimentally, the explanation proposed does not require the artificial assumption that the exchange integrals in these alloys correspond to points lying on the steep portion of the Bethe-Slater curve.

---

[1] R. M. Bozorth, Ferromagnetism, Van Nostrand, N.Y. 1951, (Russ. transl. IIL, 1956).

[2] M. Kornetzki, Z. Physik **98**, 289 (1935).

[3] U. Dehlinger, Z. Metallkunde **28**, 194 (1936).

[4] K. P. Belov, J. Tech. Phys. (U.S.S.R.) 19, 346 (1949); JETP **19**, 1032 (1949).

[5] E. I. Kondorskiĭ and V. L. Sedov, JETP **35**, 845 (1958), Soviet Phys. JETP **8**, 586 (1959).

[6] E. I. Kondorskiĭ and V. L. Sedov, JETP **35**, 1579 (1958), Soviet Phys. JETP **8**, 1104 (1959).

[7] T. S. Marsh, Alloys of Iron and Nickel, N.-J. (1938).

[8] E. I. Kondorskiĭ and L. N. Fedotov, Izv. Akad. Nauk SSSR, Ser. Fiz. **16**, 432 (1952).

Translated by K. F. Hulme
353

CONCENTRATION JUMP IN SLOW EVAPORATION OF A MIXTURE

R. Ya. KUCHEROV and L. É. RIKENGLAZ

Submitted to JETP editor June 12, 1959

J. Exptl. Theoret. Phys. (U.S.S.R.) **37**, 1821-1822 (December, 1959)

In the evaporation (or condensation) of mixtures it is necessary to take into account the difference in the concentration of the liquid and gas phases near the boundary surface. This jump in concentration was investigated only for limiting cases of equilibrium evaporation in vacuo.[1] Yet many problems are connected with the process of slow evaporation, for which the formulas derived for equilibrium are in general incorrect.

In the present work we found the concentration, temperature, and pressure in a gas phase under slow evaporation of the mixture. The following is assumed here: 1) the speed of evaporation is small compared with the speed of evaporation in vacuo, 2) the molecules of all components of the mixture are monatomic, 3) the coefficients of condensation and accommodation are unity, 4) the laws of ideal gases apply to the vapor. The calculations are similar to those given elsewhere by the authors,[2] using the distribution function introduced in reference 3.

For a two-component mixture we obtain

$$\tau_i(0) = 2\left[\tau_{i0} - \frac{p_i(0)}{\sqrt{2\pi m_i kT(0)}}\right],$$

$$Q(0) = 2\left[Q_0 - \sqrt{\frac{2kT(0)}{\pi}} \sum_{i=1}^{2} p_i(0)/\sqrt{m_i}\right]. \qquad (1)$$

Here $\tau_i(0)$ is the flow density of the i-th component of the mixture, τ_{i_0} the flow density of the vapor molecules emitted from the liquid of the i-th component. The remaining symbols are taken from references 2 and 3. Solving (1) for $p_i(0)$ and $T(0)$, we obtain the partial pressures and temperature in the vapor near the surface of the liquid

$$p_i(0) = \left\{\frac{\pi m_i [Q_0 - Q(0)/2]}{\tau_0 - \tau(0)/2}\right\}^{1/2} (\tau_{i0} - \tau_i(0)/2), \qquad (2)$$

$$T(0) = T_0[1 + \tau(0)/2\tau_0 - Q(0)/2Q_0]. \qquad (3)$$

As an example we consider the following problem. Let the vapor over the liquid binary mixture be pumped out and let us find the coefficient of separation of this process, α, as a function of $\tau(0)$, assuming complete mixing in the liquid phase.

By definition

$$\alpha = \tau_1(0)(1-\gamma)/\tau_2(0)\gamma, \qquad (4)$$

where γ is the molar fraction of the first component in the liquid phase. Neglecting the diffusion flow

$$\tau_1(0) = \tau(0)p_1(0)/p(0), \quad \tau_2(0) = \tau(0)p_2(0)/p(0). \qquad (5)$$

After elementary transformations with the aid of (2), (4), and (5) and neglecting terms quadratic in $\tau_i(0)/\tau_{i_0}$, we obtain

$$\alpha = \frac{\tau_{10}(1-\gamma)}{\tau_{20}\gamma}\sqrt{\frac{m_1}{m_2}}\left\{1 + \tau(0)\frac{\sqrt{m_2} - \sqrt{m_1}}{2[\sqrt{m_1}\tau_{10} + \sqrt{m_2}\tau_{20}]}\right\}. \qquad (6)$$

If the solution is ideal, then

$$\tau_{10} = p_{1s}\gamma/\sqrt{2\pi m_1 kT_0}, \quad \tau_{20} = p_{2s}(1-\gamma)/\sqrt{2\pi m_2 kT_0},$$
$$p_s(\gamma) = p_{1s}\gamma + p_{2s}(1-\gamma),$$

where p_{1s} and p_{2s} are respectively the vapor tension of the pure first and second component and $p_s(\gamma)$ is the vapor pressure of the mixture at $T = T_0$. In this case

$$\alpha = \frac{p_{1s}}{p_{2s}}\left\{1 + \frac{\tau(0)}{2p_s}\sqrt{2\pi kT_0}\,(\sqrt{m_2}-\sqrt{m_1})\right\}. \qquad (7)$$

In particular, for a mixture of isotopes $(m_2 - m_1 \ll m_1)$

$$\alpha = \frac{p_{1s}}{p_{2s}}\left[1 + \frac{\tau(0)}{4\tau_0}\,\frac{m_2 - m_1}{m_1}\right]. \qquad (8)$$

Since for isotopes the condensation coefficient a is independent of the concentration, its influence can be readily taken into account. The corresponding calculation yields

$$\alpha = \frac{p_{1s}}{p_{2s}}\left[1 + \frac{2-a}{4a}\,\frac{\tau(0)\sqrt{2\pi m_1 kT_0}}{p_s}\,\frac{m_2 - m_1}{m_1}\right]. \qquad (9)$$

---

[1] L. D. Landau and E. M. Lifshitz, Статистическая физика, (Statistical Physics), M-L, 1951.

[2] R. Ya. Kucherov and L. É. Rikenglaz, JETP **37**, 125 (1959), Soviet Phys. JETP **10**, 88 (1960).

[3] R. Ya. Kucherov and L. É. Rikenglaz, JETP **36**, 1758 (1959), Soviet Phys. JETP **9**, 1253 (1959).

Translated by J. G. Adashko
354

COMPARISON OF EFFECTIVE TEMPERATURES OF SPECTRA OF NEUTRONS EMITTED IN FISSION OF U^{235} AND Pu^{239} BY FAST AND THERMAL NEUTRONS

G. N. SMIRENKIN

Submitted to JETP editor August 6, 1959

J. Exptl. Theoret. Phys. (U.S.S.R.) **37**, 1822-1824 (December, 1959)

FROM an examination of the aggregate of experimental data on the energy distributions of fission neutrons of various nuclei and of the consequences of the evaporation model, it follows that the dependence of the form of the spectrum of the prompt neutrons on the excitation energy of the fissioning nucleus reduces essentially to a change in one parameter — the effective temperature T_{ef}, which determines the exponential drop in the yield of neutrons with energies greater than ~ 2 Mev. Estimates[1,2] show that as the energy E_n of the fission-inducing neutrons is increased by 1 Mev, an increase of 1.5 — 2% in T_{ef} is expected. Direct measurements of the spectra of neutrons emitted during the fission of various nuclei by fast and thermal neutrons[2,3] have shown that the difference in T_{ef} is either substantially less than expected,[3] or is not observed at all.[2]

In the present investigation we used for the determination of dT_{ef}/dE_n the method of threshold indicators, which was successfully used to establish differences in the neutron spectra for the fission of U^{233}, U^{235}, and Pu^{239} by thermal neutrons.[2,4] The investigated fission neutrons were obtained by irradiating the converters with fast and thermal neutrons. Fast neutrons with an average energy of 3.3 ± 0.1 Mev were obtained from the $Be^9(d, n)B^{10}$ reaction. Bombardment by thermal neutrons was in a cavity inside a paraffin block. The converters used were metallic hollow spheres of U^{235} (90% enriched) and Pu^{239} of 50 mm outside diameter and 10 mm thickness. During the neutron bombardment of the spheres a cartridge with a set of activation threshold indicators $Ag^{107}(n, 2n)Ag^{106m}$ was placed in the center of the cavity. After the bombardment we measured the β activities of the silver indicators (N_β) and the intensity of the γ radiation of the fission fragments in the sphere (N_γ). The first quantity determines the fission neutron flux above threshold (9.5 Mev) of the reaction $Ag^{107}(n, 2n)$ Ag^{106m}, while the second determines the number of fissions in the sphere. From the combination $\rho = N_\beta^f N_\gamma^t / N_\beta^t N_\gamma^f$ of these data, obtained in experiments with fast and thermal neutrons, we determined the unknown dT_{ef}/dE_n. To make the corrections for self absorption of γ radiation accurate, the converters were placed during the time of measurement within a lead absorber, which shifted the γ-ray spectrum to the energy range above 1.5 Mev, in which the absorption coefficient is approximately constant.

The experimental values of the ration ρ were 1.95 ± 0.05 for U^{235} and 1.82 ± 0.05 for Pu^{239}. The considerable excess of ρ over unity is due not only to the "hardening" of the spectrum with increasing E_n, but also to the increase in the absolute neutron yield, and also to the difference in the self absorption of γ rays and the neutron value for the detector at the center of the sphere for fissions by fast and thermal neutrons. To exclude these effects we used Peierls' solution of the kinetic equation for a sphere with a cavity. In establishing the connection between ρ and dT_{ef}/dE_n we took into account the contribution of fissions by the fission neutrons and inelastically scattered neutrons, the mean energies of which are less than the mean energy of the source neutrons. After reducing the experimental data we obtained $dT_{ef}/dE_n = 0.008 \pm 0.004$ for U^{235} and $dT_{ef}/dE_n = 0.01 \pm 0.004$ for Pu^{239}. Approximately half of the measurement error is due to inaccuracies in the assumptions concerning the character of the distributions of fissions by fast and slow neutrons.

The results of the experiment are 1.5 — 2 times smaller than the quantity expected from theoretical considerations[1,2] and obtained within the framework of the representation of the nucleus as a degenerate Fermi gas of nucleons. According to this model, the excitation energy is, on the average, distributed equally among all the nucleons, while in the actual case the average number of particles participating in the redistribution of the excitation energy is generally speaking not equal to the total number of particles in the nucleus. As the excitation energy increases the nucleons are imparted thermal motion gradually. Part of the energy is consumed in destroying the shell structure and "evaporation" of the nucleons. Therefore the connection between the nuclear temperature T with the excitation energy E_x will be weaker than the relation $T \sim \sqrt{E_x}$ obtained in the model of degenerate Fermi gas. These considerations, which are due to Stavinskiĭ,[5] are confirmed by the results of the latest measurements of the spectra of inelastically scattered neutrons[6] and α particles.[7] It is possible that a certain discrepancy between the data of the present experiment with computation is also explained by this effect.

The author is grateful to Prof. A. I. Leĭpunskiĭ and Prof. I. I. Bondarenko for interest in this work and for valuable advice. The author is also indebted to Sh. S. Nikolaĭshvili for help in the calculations, and to M. K. Golubeva and N. E. Tokmantseva for participating in the investigation.

---

[1] Bondarenko, Kuz'minov, Kutsaeva, Prokhorova, and Smirenkin, Second UN Conf. on the Peaceful Uses of Atomic Energy, Geneva, 1958, P/2187.

[2] R. B. Leachman, ibid. P/665.

[3] Zamyatin, Safina, Gutnikova, and Ivanova, Атомная энергия, (Atomic Energy) **4**, 374 (1958).

[4] Kovalev, Andreev, Nikolaev, and Gusseĭnov, JETP **33**, 1069 (1957), Soviet Phys. JETP **6**, 825 (1958).

[5] V. S. Stavinskiĭ, Abstract of Dissertation, Moscow Engineering-Physics Inst., 1959.

[6] J. S. Levin and L. Cranberg, Conf. on Neutron Physics by Time-of-flight, Tenn. ORNL-2309, 1956.

[7] Fulbright, Lassen, and Poulsen, Mat.-Fys. Medd. Dan. Vid. Selsk. **31**, No. 10 (1959).

Translated by J. G. Adashko

DEPOLARIZATION OF MUONS IN MU-MESIC ATOMS WITH DEFORMED NUCLEI

D. F. ZARETSKIĬ and V. M. NOVIKOV

Submitted to JETP editor August 21, 1959

J. Exptl. Theoret. Phys. (U.S.S.R.) **37**, 1824-1825 (December, 1959)

POLARIZED muons slowed down and captured at the upper levels of mu-mesic atoms are rarely depolarized.[1] After a cascade transition to the 1s state they are strongly depolarized.[2] The mechanism of depolarization is attributed to the spin-orbit interaction of the muon.[3] However, mu-mesic atoms with deformed nuclei should exhibit an additional depolarization, due to the interaction between the muon and the deformation of the nucleus. We consider here this effect for even-even nuclei.

The Hamiltonian of the muon-nucleus system will be taken in the form

$$H = H_0 + H_R + H_q, \tag{1}$$

where H_0 is the Hamiltonian of the muon in the monopole field of the nucleus, H_R the operator of the rotational energy of the nucleus, and H_q is the operator of the quadrupole interaction between the muon and the nucleus. The diagonalization of the Hamiltonian (1) shows that the quadrupole interaction changes substantially the system eigenfunctions that correspond to the muon in the 2p-states.[4] The changes in the eigenfunctions of the other states can be neglected. In this approximation the muon polarization P in the 1s state can be written in the form

$$P = A_q W_{1/2} \langle \sigma_{2p_{1/2}} \rangle_0 + B_q W_{3/2} \langle \sigma_{2p_{3/2}} \rangle_0,$$

where $W_{1/2}$ and $W_{3/2}$ are the probabilities of the muon passing through the $2p_{1/2}$ and $2p_{3/2}$ states respectively, $\langle \sigma_{2p_{1/2}} \rangle_0$ and $\langle \sigma_{2p_{3/2}} \rangle_0$ are the polarizations of the muon in these states in the absence of quadrupole interactions, and A_q and B_q are factors that take into account the additional depolarization due to the foregoing effect. These are obtained by considering the transitions of the muon from the upper levels to the 1s state through the states described by the eigenfunctions of the Hamiltonian (1), and their values are:

$A_q = 1$

$$B_q = 0.8 \sum_{k=1}^{3} C_k^1 \left[\left(\frac{E_{\mathrm{fs}} - 3E_k}{3E_q} \right)^2 + 2 \right] - 0.6, \tag{2}$$

where

$$C_k^2 = \frac{E_q^2(E_R + E_q - \frac{2}{3}E_{\mathrm{fs}} - E_k)^2}{E_q^2(E_R+E_q-\frac{2}{3}E_{\mathrm{fs}} - E_k)^2 + E_q^2(E_q+\frac{1}{3}E_{\mathrm{fs}} - E_k)^2 + [(\frac{1}{3}E_{\mathrm{fs}} -} \longrightarrow \frac{E_q^2(E_R + E_q - \frac{2}{3}E_{\mathrm{fs}} - E_k)^2}{- E_k)(E_R - \frac{2}{3}E_{\mathrm{fs}} - E_k) - E_q^2]^2},$$

E_k are the eigenvalues of (1), corresponding to the muon in the 2p states and the total momentum of the system $^3/_2$, E_{fs} is the fine structure splitting of the 2p level, E_R the energy of the first rotational level of the nucleus, $E_q = \langle 2p | H_q | 2p \rangle$. It follows from reference 3 that $W_{1/2} \langle \sigma_{2p_{1/2}} \rangle_0 \approx 0$ and $W_{3/2} \langle \sigma_{2p_{3/2}} \rangle_0 \approx {}^1/_6$, and therefore $P \approx B_q/6$. An analysis of (2) shows that B_q differs noticeably from unity when E_q is comparable with E_R or $|E_{fs} - E_R|$. When $E_{fs} \gg E_q \gg E_R$ or $E_R \gg E_q \gg |E_{fs} - E_R|$, we have $B_q \approx 0.6$. When E_q is small compared with the smaller of E_R or $|E_{fs} - E_R|$, we have

$$B_q \approx 1 - \left(\frac{E_q}{E_R}\right)^2 \frac{7E_{\mathrm{fs}}^2 - 6E_{\mathrm{fs}}E_R + 6E_R^2}{(E_{\mathrm{fs}} - E_R)^2}.$$

In a cascade transition of the muon in the 1s state, there is a definite probability that the nucleus will remain with an excited first rotational level,[4] the lifetime of which is $\sim 10^{-9}$ sec, sufficient for the reorientation of the spin of the muon in the 1s state, owing to the fine-structure splitting of the 1s level. The factor that determines the depolarization D_q due to this effect is $D_q = 1 - {}^2/_3 W_b$, where W_b is the probability of excitation of the first rotational level of the nucleus, which in our notation is $W_b = 1 - \sum_{k=1}^{3} C_k^4$. We finally have $P \approx B_q D_q/6$. The values of B_q, D_q, and the quantities that determine them for certain mu-mesic atoms are listed in the table.

Thus, the interaction between the muon and the quadrupole deformation of the nucleus can lead to a considerable additional muon depolarization.

Element	E_{fs}, kev	E_R (kev)	E_q (kev)	B_q	D_q
Gd^{158}	91.5	79	52	0.63	0.61
W^{184}	137	112	43	0.64	0.64
Th^{232}	216	52	83	0.38	0.6
U^{238}	226	44	91	0.38	0.59

---

[1] G. W. Ford and C. J. Mullin, Phys. Rev. **108**, 477 (1957).

[2] Ignatenko, Egorov, Khalupa, and Chultém, JETP **35**, 1131 (1958), Soviet Phys. JETP **8**, 792 (1958).

[3] I. M. Shmushkevich, Nucl. Phys. **11**, 419 (1959).

[4] L. Wilets, Kong. Dansk. Vidensk, Selsk. Mat.-fys. Medd. **29**, 3 (1954).

Translated by J. G. Adashko
356

THE FORMFACTOR AND THE LEPTONIC DECAY PROBABILTY OF THE Λ PARTICLE

HO TSO-HSIU

Joint Institute of Nuclear Research

Submitted to JETP editor August 28, 1959

J. Exptl. Theoret. Phys. (U.S.S.R.) **37**, 1825-1827 (December, 1959)

THE preliminary experimental data on the β and μ decays of the Λ hyperons[1] do not agree with the values given by the elementary theory of the universal (V-A) interaction for the Λ as a point particle: they are about ten times smaller than the theoretical values for the decay probability.[2,3] In this connection it is of interest to estimate the effect of the formfactors due to the strong interactions on the probability of the aforementioned decays.

The matrix element for the leptonic decay of the Λ particle, Λ → p + L + ν, can be written in the form[4]

$$M = \frac{G}{\sqrt{2}} \langle p | V_\alpha + A_\alpha | \Lambda \rangle \langle L | \gamma_\alpha (1 + \gamma_5) | \nu \rangle,$$
$$V_\alpha = f_1 \gamma_\alpha + \frac{f_2}{m_\Lambda} \sigma_{\alpha\beta} k_\beta + \frac{if_3}{m_\Lambda} k_\alpha,$$
$$A_\alpha = g_1 \gamma_\alpha \gamma_5 + \frac{g_2}{m_\Lambda} \sigma_{\alpha\beta} k_\beta \gamma_5 + \frac{ig_3}{m_\Lambda} k_\alpha \gamma_5,$$
$$\sigma_{\alpha\beta} = (1/2i)(\gamma_\alpha \gamma_\beta - \gamma_\beta \gamma_\alpha), \qquad (1)$$

where L denotes either the μ meson or the electron; $k = p_\Lambda - p_p$ is the four-momentum transfer; f_i and g_i are functions of the invariant momentum transfer. If the process is invariant under time reversal, all f's and g's are real.

The probability for the β decay of the Λ particle can be written in the form

$$W_e = (G^2 \varepsilon_e^5 / 60\pi^3) [(f_1^2 + 3g_1^2) \times (1 + \varepsilon_e / m_\Lambda) - 4g_1 g_2 \varepsilon_e / m_\Lambda]. \tag{2}$$

The probability of the μ mesonic decay of the Λ particle is equal to

$$W_\mu = 0.03 \frac{G^2 m_\mu^5}{2\pi^3} \Big[f_1^2 + 3g_1^2 + [f_1^2 + q g_1^2 + f_1(f_1 + 2f_3) - g_1(g_1 + 2g_2)] \frac{m_\mu}{m_\Lambda} - [2g_1(f_1 + 2f_3) + 2g_1(g_1 + 2g_2)] \frac{\varepsilon_\mu - m_\mu}{m_\Lambda} \Big], \tag{3}$$

where ϵ is the maximal energy of the electron or the μ meson. In the calculation we neglected terms of order $\epsilon_e^2/m_\Lambda^2 \sim \epsilon_\mu^2/m_\Lambda^2 \sim 0.02$ and assumed that all f's and g's have a constant value in the interval of integration, since $\langle\gamma^2\rangle k^2 \ll 1$, where $\langle\gamma^2\rangle$ is the square of the "radius" of the Λ particle. It appeared that in the β decay of the Λ particle only the term containing g_2 gives a large correction to the transition probability. The terms with f_3 and g_3 can be neglected, since they are always proportional to the mass of the electron. In the μ mesonic decay the terms with f_2, g_2, and f_3 lead to large corrections. The pseudoscalar term is omitted, because it is of order $(m_\mu/m_\Lambda)^2$. Of course, it will give a sizeable correction if g_3 is large.

Although the present experimental data seem to disagree with the theoretical predictions on the β and μ decay probabilities of the Λ particle, they cannot as yet be regarded as seriously contradicting the theory, since the statistics of the experiments performed thus far are not sufficiently good. Furthermore, as the sign and the order of magnitude of the formfactors are unknown, it is hardly possible to say anything definite about the effect of the formfactors on the β and μ decay probabilities of the Λ particle. It is seen from the above-quoted formulas, however, that, substituting the experimental value in the above formula and setting[1]

$$Gm_N^2 = 1.01 \cdot 10^{-5}, \qquad \frac{\varepsilon_\mu}{m_\Lambda} \sim \frac{\varepsilon_e}{m_\Lambda} \sim \frac{1}{7},$$

$$W_e = \frac{1}{\tau_\Lambda} \cdot \frac{2}{1529} = 5 \cdot 10^6,$$

we obtain for the β decay

$$W_e = 5 \cdot 10^6 = \tfrac{8}{7} \cdot 10^6 [f_1^2 + 3g_1^2 - \tfrac{1}{2} g_1 g_2] \tag{4}$$

or

$$0.42 = f_1^2 + 3g_1^2 - \tfrac{1}{2} g_1 g_2 \tag{5}$$

and for the μ decay

$$W_\mu = \tfrac{1}{6} \cdot 10^6 [f_1^2 + 3g_1^2 + [f_1^2 + qg_1^2 + f_1(f_1 + 2f_3) - g_1(g_1 + 2g_2)] \tfrac{1}{10} - 2[g_1(f_1 + 2f_2) + g_1(g_1 + 2g_2)] (\tfrac{1}{7} - \tfrac{1}{10})]. \tag{6}$$

If we assume that all f's and g's are the same for the β decay and for the μ decay, i.e., that they have the same order of magnitude, we can estimate the μ decay probability. It is equal to $W_\mu \approx \frac{1}{6} W_e = 0.8 \times 10^6$. The ratio $W_\mu/W_e \approx \frac{1}{6}$ is apparently not in violent disagreement with the existing experimental data (up to now two cases of β decay of the Λ particle have been observed, and no case of μ decay[1]).

To determine the role of these formfactors it is necessary to carry out a "complete experiment," which includes measuring the energy spectrum, the angular correlation, the Wu effect, etc. For this we have obtained all necessary formulas.

The author expresses his deep gratitude to Ya. A. Smorodinskiĭ for proposing this problem and discussing the results, and also to S. M. Bilen'kiĭ and R. M. Ryndin for valuable comments.

---

[1] Crawford, Cresti, Good, Kalbfleisch, Stevenson, and Ticho, Phys. Rev. Lett. 1, 377 (1958); Nordin, Orear, Reed, Rosenfeld, Solmitz, Taft, and Tripp, Phys. Rev. Lett. 1, 380 (1958).

[2] R. P. Feynman and M. Gell-Mann, Phys. Rev. 109, 193 (1958); E. C. G. Sudarshan and R. E. Marshak, Proc. of the Padua-Venice Conference (1957) and Phys. Rev. 109, 1860 (1958).

[3] V. M. Shekhter, JETP 35, 458 (1958), Soviet Phys. JETP 8, 316 (1959).

[4] Ya. A. Smorodinskiĭ, Report at the IX All-Union Conference on Nuclear Spectroscopy, in press.

Translated by R. Lipperheide
357

GRAVITATIONAL DAMPING OF SOUND

S. B. PIKEL'NER

Crimean Astrophysical Observatory, Academy of Sciences, U.S.S.R.

Submitted to JETP editor September 3, 1959

J. Exptl. Theoret. Phys. (U.S.S.R.) **37**, 1827-1828 (December, 1959)

THE propagation of sound in a gravitational field is usually considered in the linear approximation.[1,2] It follows from this approximation that the propagation is affected not by the force of gravity itself but by the associated density gradient. The energy flux through a flat or hemispherical surface (in the case of a spherical wave) is found to be constant, and this determines the variation of the amplitude with altitude. However, in the second approximation the sound is related with the flux of matter

$$\int \mathrm{j}\, dV = c^{-2}\int \mathrm{q}\, dV, \quad \mathrm{q} = c\rho v^2 \mathrm{n}$$

(see reference 2, p. 308). It therefore stirs the atmosphere and expands work for this purpose, if the atmosphere is convectively stable. Consequently, the sound-energy flux should decrease in a gravitational field, regardless of whether the sound propagates upwards or downward.

Let us estimate this effect for an isothermal atmosphere, and we shall consider the motion of gas in the sound packet to be adiabatic and the wave to be plane. It can be assumed that the sound lifts a mass $\rho'' = \rho v^2 c^{-2}$ g/cm^3 with a velocity c. An equal mass of atmosphere descends in its place; this descent will be considered isothermal. The density ρ' in the rising adiabatic mass, in which the pressure equals the pressure of the surrounding layers of the atmosphere, is determined from

$$\rho' = \rho_0 \exp(-\mu g z/\gamma R T_0) = \rho_0 \exp(-gz/c^2).$$

The lifting of ρ'' accompanied by stirring is equivalent to the simple lifting of a gas of density

$$\rho''(\rho' - \rho)/\rho' = \rho''(1 - e^{-\alpha z}), \text{ where } \alpha = g(\gamma - 1)c^{-2}$$

The attenuation of the flux is determined by the work of lifting

$$d(\rho v^2)/dz = -\rho'' g(1 - e^{-\alpha z}) = -\rho v^2 g c^{-2}(1 - e^{-\alpha z}),$$

hence

$$\rho v^2 = (\rho v^2)_0 \exp\left\{-\frac{gz}{c^2} f(\alpha z)\right\}, \quad f(\alpha z) = 1 - \frac{1}{\alpha z}(1 - e^{-\alpha z}).$$

Consequently, within the limits of the altitude of a homogeneous atmosphere $[\alpha z < (\gamma - 1)/\gamma]$ the gravitational damping is insignificant, and at large distances it increases exponentially. The variation of the amplitude in a plane wave is of the form

$$v^2 = v_0^2 \exp\left\{\frac{gz}{c^2}(\gamma - f)\right\} \to v_0^2 \exp\left\{\frac{gz}{c^2}(\gamma - 1)\right\} \quad (z \to \infty),$$

and not $v_0^2 \exp(\gamma g z/c^2)$ as obtained in earlier calculations.

If the temperature of the atmosphere increases upward, then the effect should become even stronger. At a convective gradient, its value is zero. Violation of the adiabaticity of the rising flow also reduces the attenuation. In the limiting case, when the element has at all times the same temperature as the ambient atmosphere, the work of stirring is zero. Therefore under astrophysical conditions, when the heat transfer by radiation is very intense, the gravitational damping of this kind is of low effectiveness. This is quite significant, since great importance is ascribed to sound waves from the photosphere in explaining the high temperature of the chromosphere and the corona.

I thank M. A. Isakovich for discussions and valuable remarks.

---

[1] H. Lamb, Hydrodynamics (Russ. Transl. Gostekhizdat, 1947), pp 678 — 681 [Dover, 1945].

[2] L. D. Landau and E. M. Lifshitz Механика сплошных сред, (Mechanics of Continuous Media), Gostekhizdat, 1953, p 317.

Translated by J. G. Adashko
358

LIMITS OF APPLICABILITY OF THE THEORY OF TRANSITION RADIATION

G. M. GARIBYAN and I. Ya. POMERANCHUK

Institute of Physics, Academy of Sciences, Armenian S.S.R.

Submitted to JETP editor September 4, 1959

J. Exptl. Theoret. Phys. (U.S.S.R.) **37**, 1828-1831 (December, 1959)

1. When a charged particle moves from one medium into another there is an adjustment of the fields associated with the particle; as a result part of the field breaks away from the particle, i.e., transition radiation is produced.[1] The basic part of this radiation is emitted in the forward direction (in the direction of motion of the par-

ticle) in the extreme nonrelativistic case.[2] If the particle moves from a vacuum into a medium the spectral distribution of the transition radiation intensity is essentially constant between optical frequencies and the limiting frequency $\omega_{gr} = (\sqrt{\sigma}/2)E/\mu c^2$ where $\sigma = 4\pi Ne^2/m$ and E and μ are the total energy and the rest mass of the particle. It is important to note that transition radiation at a given frequency is not generated instantaneously upon passage through the boundary of the medium; there is a certain time delay, that is to say, a finite region in which the transition photon is produced. One of the basic assumptions in the analysis of transition radiation is that the trajectory of the particle is rectilinear in this region. The production zone for a photon of frequency ω is[2] $(c/\omega)[(\mu c^2/E)^2 + \sigma/2\omega^2]^{-1}$. It is apparent from this expression that the radiation zone can be very large at certain frequencies and that multiple scattering can disturb the radiation process in certain regions of the spectrum.

Thus, whereas the polarization properties of the medium are responsible for the production of transition radiation, multiple scattering (i.e., another property of the medium) can disturb the mechanism by which this radiation is produced.

2. The trajectory of the particle is characterized by the vector **v**t when multiple scattering is neglected, but when scattering is introduced the trajectory is given by some vector **r**(t). The exponentials in the Fourier integrals now contains the term **k·r**(t), which, as shown in reference 3, results in the extra term

$$\frac{1}{2}\omega\int_0^t \theta_t^2\,dt,$$

where θ_t is the multiple scattering angle. As in reference 3 we replace θ_t^2 by the mean-square multiple scattering angle and, for t, substitute the time required for the emission of a photon of frequency ω. The usual formulas for transition radiation no longer apply if this term is of the order of unity or larger:

$$\frac{1}{4}\frac{\omega}{c}\left(\frac{E_s}{E}\right)^2\frac{1}{L}\left[\frac{c/\omega}{(\mu c^2/E)^2 + \sigma/2\omega^2}\right]^2 \gtrsim 1, \qquad (1)$$

where L is the radiation unit of length and $E_s = 21$ Mev. The last expression can be written in the form

$$\frac{\sigma}{2\omega^2}\left(\frac{E}{\mu c^2}\right)^2 - \frac{E_s}{2\mu c^2}\sqrt{\frac{c}{\omega L}}\frac{E}{\mu c^2} + 1 \lesssim 0. \qquad (2)$$

Account must be taken of the fact that ω and E in this expression are not arbitrary, but are governed by the condition $\omega \lesssim (\sqrt{\sigma}/2)E/\mu c^2$.

When $E/\mu c^2 \gtrsim 1$ the left part of Eq. (2) is positive and the roots of this equation are complex when

$$\omega < (8\sigma L/c)(\mu c^2/E_s)^2, \qquad (3)$$

so that it is apparent that multiple scattering does not affect the production of photons of frequencies which satisfy (3) regardless of the energy of the particle. However, if $\omega_{gr} < (8\sigma L/c)(\mu c^2/E_s)^2$ i.e.,

$$E/\mu c^2 < E_1/\mu c^2 = (16L\sqrt{\sigma}/c)(\mu c^2/E_s)^2, \qquad (4)$$

multiple scattering does not affect the emission of transition photons for any frequency.

Suppose now that (4) is not satisfied and that we consider the emission of photons with frequencies which do not satisfy (3). Of the two values of the square root of the relation in (2) (solved with respect to ω) we are interested in the root

$$\omega_1 = (\sigma E/E_s)^{2/3}(L/c)^{1/3}, \qquad (5)$$

which satisfies the condition $\omega_1 \ll \omega_{gr}$. Thus, when

$$\omega_1 \ll \omega < \omega_{gr} \qquad (6)$$

multiple scattering becomes important. Consequently if the relation in (4) is not satisfied the particle emits transition photons with frequencies up to approximately ω_1, in accordance with the usual formula for transition radiation. The energy radiated in this frequency range will be of order

$$I \approx (e^2/c)(\sigma E/E_s)^{2/3}(L/c)^{3/2}, \qquad (7)$$

so that the number of photons is

$$N_2' \approx \frac{1}{137}\frac{2}{\pi}\ln\left[\frac{\sigma E}{E_s}\left(\frac{L}{c}\right)^{1/2}\omega'^{-3/2}\right]. \qquad (8)$$

Thus, the introduction of multiple scattering means in general only that the transition radiation spectrum will contain no frequencies higher than ω_1 (since at these frequencies the conditions for coherent radiation from different parts of the trajectory are violated) so that the number of transition photons remains essentially unchanged.

We may also note in contrast with bremsstrahlung, where multiple scattering has no effect on radiation of photons of maximum energy (close to the energy of the particle), when $E > E_1$ in transition radiation multiple scattering always affects the emission of photons with frequencies close to the limiting frequency.

3. Inasmuch as bremsstrahlung and transition radiation can be generated together in a medium, it is of interest to compare the number of bremsstrahlung and transition photons in corresponding frequency ranges. In making this comparison we must take account of the effects of polarization of the medium and multiple scattering[3-6] on the bremsstrahlung.

If the energy of the particle satisfies the condition given in Eq. (4), the number of bremsstrahlung photons emitted per unit time in the frequency range between optical frequencies and $\omega_{\lim}$ is given by the following expression,[4] which takes account of the effect of the polarization of the medium on the bremsstrahlung:

$$N' = \frac{m}{12\pi^2 LN\hbar}\left(\frac{E_s}{E}\right)^2 \frac{\omega_{\lim}^2}{2}. \qquad (9)$$

The number of bremsstrahlung photons emitted in the transition radiation production zone is

$$N = \frac{1}{137}\frac{1}{6\pi}\frac{c}{L\sqrt{\varepsilon}}\left(\frac{E_s}{\mu c^2}\right)^2 \frac{E}{\mu c^2}. \qquad (10)$$

This number is to be compared with the number of transition photons:[2]

$$N_2' = \frac{1}{137}\frac{2}{\pi}\left[\ln\left(\frac{E}{\mu c^2}\right) - \frac{1}{2}(1 + \ln 2)\right]. \qquad (11)$$

It is apparent from these two expressions that the number of transition photons exceeds the number of bremsstrahlung photons. Even for particles with energies close to E_1 the number of transition photons is larger than the number of bremsstrahlung photons by approximately a factor of $\ln(E/\mu c^2)$.

Now suppose that $E > E_1$. At frequencies lower than ω_1 Eq. (9) still applies, but in place of $\omega_{\lim}$ we must substitute ω_1. As a result, the number of bremsstrahlung photons emitted in the zone for the production of transition photons with frequencies up to approximately ω_1 is

$$N = 1/137 \cdot 12\pi. \qquad (12)$$

However, the number of transition photons is

$$N_2' \approx \frac{1}{137}\frac{2}{3\pi}\ln\left[\frac{L\sqrt{\varepsilon}}{c}\left(\frac{E}{E_s}\right)^2\right]. \qquad (13)$$

Again the number of transition photons is greater than the number of bremsstrahlung photons.

Strictly speaking, the transition radiation should not be compared with the bremsstrahlung computed for multiple scattering in an infinite homogeneous medium. The bremsstrahlung should be computed from formulas in which the effect of the boundary is taken into account.

---

[1] V. L. Ginzburg and I. M. Frank, JETP **16**, 15 (1946).

[2] G. M. Garibyan, JETP **37**, 527 (1959), Soviet Phys. JETP **10**, 372 (1960).

[3] L. D. Landau and I. Ya. Pomeranchuk, Dokl. Akad. Nauk SSSR **92**, 535, 735 (1953).

[4] M. L. Ter-Mikaélyan, Dokl. Akad. Nauk SSSR **94**, 1033 (1954).

[5] A. B. Migdal, Dokl. Akad. Nauk SSSR **96**, 49 (1954).

[6] E. L. Feĭnberg, Usp. Fiz. Nauk **58**, 193 (1956).

Translated by H. Lashinsky
359

ON THE STRUCTURE OF SOLID HYDROGEN

A. A. GALKIN and I. V. MATYASH

Institute of Radiophysics and Electronics, Academy of Sciences, Ukrainian S.S.R.

Submitted to JETP editor October 13, 1959

J. Exptl. Theoret. Phys. (U.S.S.R.) **37**, 1831-1832 (December, 1959)

At present, despite a series of published investigations, the structure of crystalline hydrogen is not uniquely determined. According to Keesom,[1] hydrogen has a hexagonal close-packed structure ($a = 3.75$, $c = 6.11$ A). The work of Kogan, Lazarev, and Bulatova[2-4] showed that the x-ray data are satisfied by both a hexagonal non-close-packed lattice with parameters $a = 3.7$ and $c = 6.42$ and by a tetragonal lattice ($a = 4.5$, $c = 3.68$).

To determine more exactly the structure of crystalline hydrogen, investigations of its nuclear magnetic resonance were undertaken. In this connection, following our suggestion, S. S. Dukhin has calculated the possible anisotropy of the nuclear magnetic resonance of hydrogen single crystals with hexagonal and tetragonal lattices.[5] Neglecting intermolecular broadening for the hexagonal lattice with parameters $a = 3.7$, $c = 6.42$ A, the anisotropy of the second moment relative to the sixfold axis is zero, and relative to the twofold axis amounts to 40%. For the tetragonal lattice with parameters $a = 4.5$, $c = 3.68$, anisotropy is almost absent: it is zero relative to the fourfold axis and less than 10% relative to the twofold axis.

In the present communication are described the results of nuclear magnetic resonance (n.m.r.) experiments performed on a large number of single-crystal and polycrystalline specimens of hydrogen at a temperature of 4.2°K. Since the anisotropy of the n.m.r. line width depends on the angle between the highest order axis of the single crystal and the direction of the constant magnetic field, it would be desirable to have single crystals with previously determined orientation, which presents considerable difficulty. Our experiments were performed on cylindrical specimens obtained with different directions of the temperature gradient relative to the axis. One might think that in these conditions specimens were obtained with different crystallographic directions. The single-crystal specimens were placed in the oscillator circuit and could be rotated only about an axis perpendicular to the constant magnetic field.

By studying the rotation diagram, it was shown that in the single crystals there was no significant (more than 2%) anisotropy of the second n.m.r. moment. The width and shape of the lines at single-crystal specimens agreed quite accurately with the width and shape of the lines of polycrystalline hydrogen.

With complete absence of anisotropy of the rotation diagram, about 10% (5.4 — 6.0 oe) differences in the widths of the lines were observed from measurement to measurement, which is explained by the different concentrations of ortho- and para-hydrogen in the specimens. The absence of anisotropy of the rotation diagram in single crystals of hydrogen favors the choice of the tetragonal lattice.

The agreement of the width and shape of the n.m.r. lines in single-crystal and polycrystalline specimens at the temperature of 4.2° K can be ascribed to the effect of rotational motion "smearing out" the anisotropy.

It appears that some anisotropy of the n.m.r. of hydrogen can be obtained at a temperature below 1.5° K, when to a large extent the rotation of the molecules is hindered and fine structure appears in the lines.

---

[1] Keesom, DeSmedt, and Mooy, Comm. Phys. Univ. Leiden, 209 d (1930).

[2] Kogan, Lazarev, and Bulatova, JETP **31**, 541 (1956), Soviet Phys. JETP **4**, 593 (1957).

[3] Kogan, Lazarev, and Bulatova, JETP **34**, 238 (1958), Soviet Phys. JETP **7**, 165 (1958).

[4] Kogan, Lazarev, and Bulatova, JETP **37**, 678 (1959), Soviet Phys. JETP **10**, 485 (1960).

[5] S. S. Dukhin, JETP **37**, 1486 (1959), Soviet Phys. JETP **10**, 1054 (1960).

Translated by K. F. Hulme
360

POSSIBILITY OF MEASURING THE VELOCITY OF PROPAGATION OF GRAVITATION IN THE LABORATORY

I. L. BERSHTEĬN and M. E. GERTSENSHTEĬN

Submitted to JETP editor July 29, 1959

J. Exptl. Theoret. Phys. (U.S.S.R.) **37**, 1832-1833 (December, 1959)

At present there exists a large body of theoretical work on gravitation, but almost no experimental work. In the present note we want to point out that with modern methods for detecting weak signals against a background of noise it is possible in principle to measure gravitational effects of the first order in v/c (where v is the velocity of the body and c is that of light) under laboratory conditions, although the technical difficulties are extremely great. Below we perform an order-of-magnitude calculation of the following experiment for measuring the velocity of propagation of gravitation.

An alternating gravitational field is produced by a rotating wheel with massive spheres on its rim. We assume that the gravitational field of the spheres is determined by the retarded Newtonian potential, which is correct to terms of the first order in v/c. Stationary detectors (transducers) of alternating gravitational field are located in the plane of the wheel. Independent of their construction, such detectors can be regarded as mechanical oscillators, tuned to the frequency of the alternating gravitational field and having a figure of merit Q.

Consider a pair of detectors located on different but neighboring radii and at several different distances from the center of the wheel. For one sense of rotation of the wheel, the phase shift between the alternating gravitational fields at the detectors will be

$$\varphi_+ = \varphi_0 + \omega\Delta l / c, \quad \varphi_0 \gg \omega\Delta l / c, \qquad (1)$$

where ω is the angular frequency of the field, c is the velocity of propagation of gravitation which in subsequent estimates we assume to be equal to the velocity of light, Δl is the difference of the distances of the detectors from the rim of the wheel, and φ_0 is the phase shift due to the location of the detectors on different radii. For the opposite sense of rotation, the phase difference will be

$$\varphi_- = -(\varphi_0 - \omega \Delta l / c). \qquad (2)$$

The change in the modulus of the phase difference is

$$\Delta\varphi = 2\omega \Delta l / c. \qquad (3)$$

A measurement of this quantity in an experiment (similar, for example, to that performed with the experimental arrangement of Sagnac on radio waves[1]) allows one to determine the velocity of propagation of gravitation. The feasibility of measuring the quantity $\Delta\varphi$ is characterized by the signal-to-noise ratio for the experiment, which can be shown to be equal to

$$\frac{P_s}{P_n} = N \frac{Qm\omega\tau}{kT} \left(\frac{\Delta l}{c}\right)^2 (\Delta g)^2, \quad \Delta g = \frac{1}{4} \frac{\gamma M}{R^2}, \qquad (4)$$

where N is the number of detector pairs at a temperature T, and Δg is the amplitude of the alternating gravitational field. The factor ¼ stems from the conversion from the field calculated according to the law of Newton to the alternating component of the field, and τ is the time of observation.

An estimate calculated according to formula (4) gives $P_s/P_n = 30$. We have assumed the following values: $Q = 10^4$, m = 15 kg, M = 72 kg (lead spheres 25 cm in diameter), 200 m/sec for the rim speed* of the wheel, T = 2° K,† 20.30 m for the distance between the centers of the spheres and the detectors, and $\tau = 10^4$ sec.

We have used here technically admissible parameters for the apparatus; the problem of optimizing the parameters, i.e., maximizing the signal-to-noise ratio, has not been worked out.

In modern radio technique the fundamental limit to the sensitivity of detecting devices has been attained; in the case of mechanical transducers it is necessary to overcome considerable technical difficulties.

---

*With modern materials it is possible to obtain a rim speed considerably greater than 200 m/sec (720 km/hr).

†Maser amplifiers operate at such temperatures.

---

[1] I. L. Bershteĭn, Dokl. Akad. Nauk SSSR 75, 635 (1950).

Translated by J. Heberle

ON THE THEORY OF THE DIRECT NUCLEAR PHOTOEFFECT

Yu. V. ORLOV

Nuclear Physics Institute, Moscow State University

Submitted to JETP editor July 21, 1959

J. Exptl. Theoret. Phys. (U.S.S.R.) 37, 1834-1836 (December, 1959)

THE mechanism of the direct nuclear photoeffect has been proposed by Jensen[1] and by Courant.[2] It has been qualitatively confirmed in a number of experiments[3] and has been treated in a number of papers.[4-6] In these papers the interaction of the emitted nucleon with the daughter nucleus either was disregarded[5] or was treated in too simplified a manner.[4,6] In particular, the spin-orbit interacaction was not taken into account. In connection with the increase in the experimental accuracy it is of interest to investigate the direct photoeffect in a more detailed and rigorous fashion.

In the present work expressions for the cross section of the direct nuclear photoeffect have been obtained in the dipole approximation in the framework of the shell model with jj coupling. The interaction of the emitted nucleon with the daughter nucleus was described by the optical model with a complex potential. The calculation was carried out in the nonrelativistic approximation. Only the case of a closed subshell (with given quantum numbers n, j, l) or of one particle (hole) outside such a subshell were considered. The differential cross section then is given by the formula

$$d\sigma / d\Omega = \sum_{(njl)} (d\sigma / d\Omega)_{njl};$$

$$(d\sigma / d\Omega)_{njl} = (4\varepsilon^2 K / 3Mc^2 k)(2l+1)(2j+1)$$

$$\times \sum_{ILI'L'} (-i)^L i^{L'} (-1)^{I+I'+1} (2L+1)(2L'+1)$$

$$\times (2I+1)(2I'+1) C^{10}_{L0l0} C^{10}_{L'0l0} W(I\,{}^1\!/_2\,1l \mid Lj)$$

$$\times W(I'\,{}^1\!/_2\,1\,l \mid L'j)\, a^{(IL)*}_{njl}\, a^{(I'L')}_{njl} \sum_g [C^{g1}_{11L0} C^{g1}_{11L'0} (1+\cos^2\theta)$$

$$+ C^{g0}_{10L0} C^{g0}_{10L'0} \sin^2\theta]\, X(j1I';\ 1gL';\ IL\,{}^1\!/_2).$$

$$a^{(IL)}_{njl} = [M(E+E_{njl})/\hbar^2] \int_0^\infty \varphi^*_{IL}(r) R_{njl}(r) r^3\, dr. \qquad (1)$$

Here W — Racah coefficients;[7] the quantities X are defined in reference 8; φ_{IL} and R_{njl} — radial parts of the final and initial state wave function of the nucleon respectively; E — energy of the

E, Mev	A_{11}, mb/sterad		B_{11}, mb/sterad		B_{11}/A_{11}	
	$\zeta=0$	$\zeta=-0.15$	$\zeta=0$	$\zeta=-0.15$	$\zeta=0$	$\zeta=-0.15$
3	0.234	0.112	0.111	0.020	0.477	0.175
5	0.101	0.027	0.088	0.067	0.872	2.442
10	0.021	0.016	0.032	0.022	1.495	1.393

emitted nucleon; E_{nj} (> 0) — binding energy of the nucleon in the subshell (nlj); K, k — wave number of the emitted nucleon and the photon respectively; ϵ — "effective charge" of the nucleon, which is eN/A for a proton and $-eZ/A$ for a neutron; θ — angle between the vectors **K** and **k**; $\hbar ck = E + E_{njl}$. The summation has to be performed over the closed subshells. If there exists a particle (or a "hole") in one subshell then the corresponding cross section has to be multiplied by $(2j+1)^{-1}$.

One of the main difficulties connected with a rigorous description of the direct photoeffect consists in the computation of the quantities $a_{njl}^{(IL)}$ since for this purpose one needs to know the wave functions. The simplest case is that where the emitted particle is a neutron. Its interaction with the nucleus is given by a square well (real for the ground state, complex for the final state). Here one can obtain an analytic expression for the $a_{njl}^{(IL)}$. In particular, if one disregards the spin-orbit interaction we have

$$\begin{aligned}
a_{njl}^{(l\,l\pm1)} &\equiv a_{nl}^{(l\pm1)} = [\sqrt{2EU_0R}/(E+E_{nl})]\,\{[h_{l\pm1}^{(2)}(x_f)\\
&+\overset{*}{\eta}_{l\pm1}h_{l\pm1}^{(1)}(x_f)]/[2j_{l\pm1}(x^*)\sqrt{-j_{l-1}(x_0)\,j_{l+1}(x_0)}]\}\\
&\times\{j_l(x_0)\,j_{l\pm1}(x^*)\pm(1-\beta+i\zeta\beta)\,x_0\,(x^{*2}-x_0^2)^{-1}\\
&\times[x_0\,j_{l\pm1}(x^*)\,j_{(l\pm1)-1}(x_0)-x^*\,j_{(l\pm1)-1}(x^*)\,j_{l\pm1}(x_0)]\},\\
x_0 &= \sqrt{2M(U_0-E_{nl})/\hbar^2}\,R,\quad x_f=KR,\\
x &= \sqrt{2M[E+U_f(1+i\zeta)]}\,R/\hbar,
\end{aligned}\tag{2}$$

where $\beta = U_f/U_0$; U_f and U_0 — depth of the potential well for the final and initial state neutron; ζ — parameter of the imaginary part of the potential; R — nuclear radius; j_L and h_L — spherical Bessel and Hankel functions; η_L — amplitude of the incoming spherical wave associated with the emitted nucleon.

In order to determine the influence of the imaginary part of the potential, the cross section for the (γ, n) reaction in C^{12} was evaulated numerically, utilizing (2). We write the cross section in the form

$$d\sigma_{nl}/d\Omega = A_{nl} + B_{nl}\sin^2\theta$$

The values obtained for A_{nl} and B_{nl} for some energies are given in the table for the $1p_{3/2}$ subshell. (The cross section of the direct photoeffect for the $1s_{1/2}$ shell is roughly 10 — 100 times smaller.) The following well parameters were chosen: $U_f = 42$ Mev; $\zeta = 0$ and -0.15.* The value $U_0 \approx 43.7$ Mev was determined from the binding energy of the last neutron,[9] using $R = 1.45\,A^{1/3}$ f. The table illustrates the importance of the effects connected with the absorption of the final state neutrons in the nucleus. The addition of the imaginary part to the potential leads to a decrease of the cross section, as could be expected. It is of interest to point out that the anisotropy is increased considerably at E = 5 Mev for $\zeta = -0.15$ as compared with $\zeta = 0$.

The obtained numerical results evidently are rough and preliminary since the spin-orbit force as well as the energy dependence of the parameters ζ and U_f (which in the energy region 5 — 15 Mev can be considered to be weak[10]) and the finite slope of the nuclear potential have been neglected. Calculations taking into account these details are being performed at present and will be published at a later date.

In conclusion I would like to express my deep gratitude to I. S. Shapiro for his interest in the work, as well as to L. D. Blokhintsev and É. I. Dolinskiĭ who kindly supplied me with some details concerning the wave function of a neutron in a complex well.

---

*In contrast to the case of particle scattering, here ζ has to be taken negative. This is connected with the asymptotic form of the emitted neutron (plane wave plus incoming spherical wave).

---

[1] P. Jensen, Naturwiss. **35**, 190 (1948).

[2] E. D. Courant, Phys. Rev. **82**, 703 (1951).

[3] V. DeSabbata, Nuovo cimento Suppl. **11** No. 2, 225 (1959).

[4] J. Eichler and H. A. Weidenmüller, Z. Physik **152**, 261 (1958).

[5] S. Sueoka, Can. J. Phys. **37**, 232 (1959).

[6] G. M. Shklyarevskiĭ, JETP **36**, 1492 (1959), Soviet Phys. JETP **9**, 1057 (1959).

[7] Biedenharn, Blatt, and Rose, Revs. Modern Phys. **24**, 244 (1952).

[8] A. Simon and T. A. Welton, Phys. Rev. **90**, 1042 (1953).

[9] N. Feather, Adv. Phys. **2**, 141 (1953).

[10] Luk'yanov, Orlov, and Turovtsev, JETP **35**, 750 (1958), Soviet Phys. JETP **8**, 521 (1959); Nucl. Phys. **8**, 325 (1958).

Translated by M. Danos
362

Author Index to Volume 37 (10)

References with L are Letters to the Editor

Abramov, A. I. Variation of Angular Distributions of Neutrons Elastically Scattered from He^3 — 1046L.

Abrikosov, A. A., L. P. Gor'kov, and I. M. Khalatnikov. Analysis of Experimental Data Relating to the Surface Impedance of Superconductors — 132.

Agranovich, V. M. Dispersion of Electromagnetic Waves in Crystals — 307.

Akhiezer, I. A., R. V. Polovin, and N. L. Tsintsadze. Simple Waves in the Chew-Goldberger-Low Approximation — 539.

Akimov, Yu. K., K. S. Marish, O. V. Savchenko, and L. M. Soroko. Measurement of the Polarization of Deuterons in the Reaction $p + p \rightarrow d + \pi^+$ at Proton Energies of 670 Mev — 33.

Alekseeva, K. I. and N. L. Grigorov. Heavy Nuclei Flux in the Primary Cosmic Radiation at a Geomagnetic Latitude of 31° N — 271.

—, S. I. Brikker, N. L. Grigorov, V. S. Murzin, and F. D. Savin. Investigation of Pion Production in Interactions of Cosmic-Ray Protons and α Particles with Carbon Nuclei in the Stratosphere — 422.

Alekseevskiĭ, N. E. and Yu. P. Gaĭdukov. The Anisotropy of Magnetoresistance and the Topology of Fermi Surfaces of Metals — 481.

Alikhanov, R. A. Antiferromagnetism in NiF_2 — 814L.

Alkhazov, D. G., A. P. Grinberg, G. M. Gusinskiĭ, K. I. Erokhina, and I. Kh. Lemberg. Coulomb Excitation of Odd-mass Nuclei by Multiply-Charged Ions — 1086.

Amaglobeli, N. S. and Yu. M. Kazarinov. Elastic Scattering of 630-Mev Neutrons by Protons — 1125.

Andronikashvili, É. L. and D. S. Tsakadze. Experimental Investigation of the Harmonic Oscillations of a Disk in Rotating Helium. II — 397L.

— The Propagation of Oscillations along Vortex Lines in Rotating Helium. II — 227L.

Anikina, M. P. (see Tret'yakov, E. F.) — 656.

Ansel'm, A. A. and V. N. Gribov. On the Possibility of Determining the Amplitude for Charge Exchange Pion-Pion Scattering from an Analysis of the $\pi^- + p = N + \pi^+ + \pi^-$ Reactions near Threshold — 354.

Anton'eva, N. M., A. A. Bashilov, and E. K. Kulakovskiĭ, Radioactive Decay of Ag^{110m} — 1063.

Antonov-Romanovskiĭ, V. V., V. G. Dubinin, A. M. Prokhorov, Z. A. Trapeznikova, and M. V. Fock. Detection of Ionization of Eu^{++} in the SrS-Eu, Sm Phosphor by the Paramagnetic Absorption Method — 1039L.

Antonova, S. F., S. S. Vasilenko, M. G. Kaganskiĭ, and D. L. Kaminskiĭ. Positron Spectrum of Eu^{152} and Eu^{152m} — 477.

Apostolov, D. A. (see Berlovich, É. E.) — 855.

Arkhipov, R. G. and A. I. Shal'nikov. On the Motion of Charges in Liquid Helium — 888.

Artemov, K. P., S. P. Kalinin, and L. N. Samoĭlov. Scattering of 5 — 10 Mev Protons on He^3 — 474.

—, N. A. Vlasov, and L. N. Samoĭlov. Polarization of Neutrons from the $T(p, n)He^3$ Reaction and Protons from the $He^3(n, p)T$ Reaction — 841.

Askar'yan, G. A., L. P. Kotenko, E. P. Kuznetsov, and A. V. Samoĭlov. On Certain Experiments with Metastable Liquids in an X-ray Beam — 1041L.

Astrov, D. N., S. I. Novikova, and M. P. Orlova. Shift in Curie Temperature during Uniform Compression of Manganese and Cobalt Fluorides — 851.

Avakov, G. V. Electron-Electron Scattering and Quantum Electrodynamics at Small Distances — 604L.

Avvakumov, V. I. The Dynamical Character of the Jahn-Teller Effect and Its Influence on the Paramagnetic Resonance of Cu^{2+} — 723.

—, N. S. Garif'yanov, B. M. Kozyrev, and P. G. Tishkov. Paramagnetic Resonance and Paramagnetic Relaxation in Electrolyte Solutions — 1110.

Bagdasar'yan, Z. A. (see Piskunov, A. K.) — 213L.

Baĭer, V. N. Electron-Electron Scattering Cross Section at High Energies — 1057L.

Balandin, M. P. (see Laberrigue-Frolova, J. V.) — 452.

Balashov, V. V., V. G. Neudachin, Yu. F. Smirnov, and N. P. Yudin. Reduced Widths for Nucleon Associations in the Shell Model of the Nucleus — 983.

Balats, L. Ya., (see San'ko, L. A.) — 1.

Balats, M. Ya., P. I. Lebedev, and Yu. V. Obukhov. Production of K^+ Mesons by Cosmic-Ray Protons at 3250 m Above Sea Level — 417.

Baldin, A. M. Optical Anisotropy of Atomic Nuclei — 142.

Bannik, B. P., V. G. Grishin, M. Ya. Danysh, V. B. Lyubimov, and M. I. Podgoretskiĭ. Elastic Scattering of 8.7-Bev Protons by Photoemulsion Nuclei — 1118.

Barabanenkov, Yu. N. On the Solution of the Kinetic Equation for a Plasma in a Variable Magnetic Field — 305.

Barashenkov, V. S. Angular Asymmetry in (πN) Collisions and the $(\pi\pi)$ Interaction — 1038L.

— and V. M. Mal'tsev. Resonance Interaction of Pions — 630L.

—, V. M. Mal'tsev, and É. K. Mikhul. Theoretical Interpretation of Inelastic (pp) and (pn) Collisions at 9 Bev Energy — 1052L.

Barsukov, K. A. Transition Radiation in Waveguides — 787.

Bar'yakhtar, V. G. On the Theory of Magnetic-Moment Relaxation in Ferrodielectric Substances — 493.

Basov, N. G. and A. N. Oraevskiĭ. Use of Slow Molecules in a Maser — 761.

—, B. M. Vul, and Yu. M. Popov. Quantum-mechanical Semiconductor Generators and Amplifiers of Electromagnetic Oscillations — 416L.

Bashilov, A. A. (see Anton'eva, N. M.) — 1063.

Bass, F. G. and M. I. Kaganov. Raman Scattering of Electromagnetic Waves in Ferromagnetic Dielectrics — 986.

Batygin, V. V. and I. N. Toptygin. Inelastic Collisions Between Fast Polarized Particles and Atoms — 975.

Bazhanov, E. B. Spectrum of Photoprotons Produced by

Gamma Rays in the Narrow 82 — 89 Mev Energy Range — 267.
Bedescu, A., K. P. Mitrofanov, A. A. Sorokin, and V. S. Shpinel'. Decay of Te^{131} ($T_{1/2} = 30$ hr) — 221L.
Belousov, A. S., S. V. Rusakov, E. I. Tamm, and P. A. Cerenkov. Search for Particles with Mass between 6 and 25 Electron Masses — 1143.
Belov, K. P. and R. Z. Levitin. Magnetostriction of Antiferromagnetic Nickel Monoxide — 400L.
— and E. P. Svirina. Hall Effect in Ferrites near the Curie Temperature — 862.
—, G. I. Kataev, and R. Z. Levitin. Anomalies in Internal Friction and Modulus of Elasticity in Ferromagnetics Near the Curie Point — 670.
—, M. A. Zaĭtseva, and A. M. Kadomtseva. Features of Magnetic Hysteresis Phenomena in the Systems $Pr_2O_3 \cdot Fe_2O_3$ and $La_2O_3 \cdot Fe_2O_3$ — 825L.
Bel'skiĭ, S. A. and S. V. Starodubtsev. Small Angle Rayleigh Scattering of Co^{60} Gamma Rays — 700L.
Belyaev, V. B., S. S. Gershteĭn, B. N. Zakhar'ev, and S. P. Lomnev. Mesic Molecular Processes in Hydrogen — 1171.
— (see Fedorenko, N. V.) — 1276L.
Berkovich, I. B., A. P. Zhdanov, F. G. Lepekhin, and Z. S. Khokhlova. Nonmesonic Decay of Hyperfragments — 428.
Berlovich, É. E., V. N. Klement'ev, V. G. Fleĭsher, O. V. Larionov, F. Sh. Murtazin, and D. A. Apostolov. Forbidden Transitions in the Deformed Tm^{169} Nucleus — 855.
Bershteĭn, I. L. and M. E. Gertsenshteĭn. Possibility of Measuring the Velocity of Propagation of Gravitation in the Laboratory — 1293L.
Bezuglyĭ, P. A. and A. A. Galkin. Cyclotron Resonance in Indium at 9300 Mcs — 1049L.
Biberman, L. M. and B. A. Veklenko, Radiative Processes Ahead of a Shock-Wave Front — 117.
Bilen'kiĭ, S. M., R. M. Ryndin, Ya. A. Smorodinskiĭ, and Ho Tso-Hsiu. On the Theory of Neutron Beta Decay — 1241.
Birger, N. G. and Yu. A. Smorodin. On a Certain Possibility of Investigation of the Structure of Nucleons and Nuclei — 964.
Blokhintsev, L. D. (see Shapiro I. S.) — 542.
Bogachev, N. P., S. A. Bunyatov, I. M. Gramenitskiĭ, V. B. Lyubimov, Yu. P. Merekov, M. I. Podgoretskiĭ, V. M. Sidorov, and D. Tuvdendorzh. Interaction of 9 Bev Protons with Free and Quasifree Nucleons in Photographic Emulsions — 872.
Bogolyubov, N. N., A. A. Logunov, and D. V. Shirkov. The Method of Dispersion Relations and Perturbation Theory — 574.
Bogoyavlenskiĭ, I. V., V. N. Grigor'ev, and N. S. Rudenko. Effect of Temperature on the Variation of the Isotopic Composition of Liquid Mercury in the Electric Field of a Constant Current — 884.
Bolotovskiĭ, B. M. and A. A. Rukhadze. Field of a Charged Particle in a Moving Medium — 958.
Boos, É. G. and Zh. S. Takibaev. On an Estimate of Energy Characteristics of Shower Producing Particles — 206L.
Borisova, N. L., M. Ya. Kuznetsova, L. N. Kurchatova, V. N. Mekhedov, and L. V. Chistyakov. Recoil Nuclei from the Disintegration of Silver by Fast Protons — 261.
Borovskiĭ, I. B. and I. A. Ovsyannikova. Investigation of X-Ray Spectra of Superconducting CuS — 1033L.
Braginskiĭ, S. I. On the Magnetohydrodynamics of Conducting Fluids — 1005.
Brandt, N. B. and G. A. Ryabenko. Effect of Uniaxial Compression on the Quantum Oscillations of the Magnetic Susceptibility of Bismuth — 278.
—, A. E. Dubrovskaya, and G. A. Kytin. An Investigation of the Quantized Oscillations in the Magnetic Susceptibility of Bismuth at Extremely Low Temperatures — 405L.
Braun, M. A. On the Determination of the Potential in Quantum Field Theory — 582.
Brikker, S. I. (see Alekseeva, K. I.) — 422.
Brish, A. A., M. S. Tarasov, and V. A. Tsukerman. Electric Conductivity of the Explosion Products of Condensed Explosives — 1095.
Brodskiĭ, A. M. and D. D. Ivanenko. On the Connection of Isotopic Spin and Strangeness with the Behavior of Spinors under Inversion — 624L.
Budagov, Yu. A., S. Viktor, V. P. Dzhelepov, P. F. Ermolov, and V. I. Moskalev. Beta Decay of the Negative Muon — 625L.
Bukhvostov, A. P. and I. M. Shmushkevich. Capture of Polarized Muons by Deuterons — 1042L.
Bulatova, R. F., V. S. Kogan, and B. G. Lazarev. Mutual Solubility of Hydrogen and Deuterium at 4.2°K — 1058L.
— (see Kogan, V. S.) — 485.
Bunyatov, S. A. (see Bogachev, N. P.) — 872.
Burgov, N. A., G. V. Danilyan, B. S. Dolbilkin, L. E. Lazareva, and F. A. Nikolaev. On the Fine Structure of the Giant Resonance — 1278L.
Bychkov, Yu. A., L. É. Gurevich, and G. M. Nedlin. Thermoelectric Phenomena in Strong Magnetic Fields in Metals Possessing Various Fermi Surfaces — 377.
Cerenkov, P. A. (see Belousov, A. S.) — 1143.
Chaĭka, M. P. (see Kaliteevskiĭ, N. I.) — 629L.
Cheng P'u-Ying (see Lyubimov, V. B.) — 651.
— (see Zhdanov, G. B.) — 433.
Chernavskiĭ, D. S. (see Emel'yanov, A. A.) — 753.
Chilashvili, G. A. (see Vashakidze, I. Sh.) — 535.
Chistyakov, L. V. (see Borisova, N. I.) — 261.
Chou Kuang-Chao and V. I. Ogievetskiĭ. Electromagnetic Mass of the K Meson — 616L.
— (see Lapidus, L. I.) — 199.
— (see Lapidus, L. I.) — 1213.
Chuev, V. I. (see Vlasov, N. A.) — 844.
Chultém, D. (see Egorov, L. B.) — 1077.
Chuvilo, I. V. On a Certain Possibility of Setting up a System of "Elementary" Particles — 994.
Daĭon, M. I. and V. Kh. Volynskiĭ. On the Measurement of the Momentum of Fast Particles and the Investigation of Nuclear Interaction in the $10^{10} - 10^{12}$ ev Energy Range — 648.
Danilyan, G. V. (see Burgov, N. A.) — 1278L.
Danysh, M. Ya. (see Bannik, B. P.) — 1118.
Darovskikh, V. F., N. P. Kocherov, and N. A. Perfilov. Fragmentation on Bismuth Nuclei — 921.
Dautov, R. A. (see Korepanov, V. D.) — 218L.

Davies, R. and F. Goodman. On Popov's Relation between the Symmetry of Transport Coefficients and Thermodynamics — 828L.
Davydov, A. S. Intensity Rules for Beta Transitions to Different Rotational States of Even-Even Daughter Nuclei — 98.
Degtyarev, I. F. (see Kirenskiĭ, L. V.) — 437.
Delyagin, N. N. Electric Quadrupole Gamma Transitions in Even-even Nuclei — 605L.
— Resonance Scattering of Gamma Quanta on Cd^{114} Nuclei — 837.
Demirkhanov, R. A., T. I. Gutkin, and V. V. Dorokhov. Isotopic Masses and Binding Energies of Nuclei for Masses between 186 and 196 — 866.
Dmitriev, V. A., G. V. Kulikov, and G. B. Khristiansen. Investigation of High-Energy Nuclear-Active Particles at Sea Level — 637.
— (see Vernov, S. N.) — 1050L.
Dolbilkin, B. S. (see Burgov, N. A.) — 0000L.
Dolginov, A. Z. and E. V. Kharitonov. Angular Distribution and Polarization of Beta Particles in Second Forbidden Transitions — 553.
— and A. N. Moskalev. Relativistic Spherical Functions — 1202.
— and I. N. Toptygin. Relativistic Spherical Functions — 1022.
Donets, E. D. (see Perelygin, V. P.) — 1106.
Dorokhov, V. V. (see Demirkhanov, R. A.) — 866.
Dotsenko, B. B. Pionic and Electromagnetic Structure of Nucleons — 1048L.
Druin, V. A., Yu. V. Lobanov, and S. M. Polikanov. Angular Distribution of Fission Fragments in Fission Induced by Heavy Ions — 26.
— (see Mikheev, V. L.) — 612L.
Drukarev, G. F. On the Massey Parameter in the Theory of Atomic Collisions — 603L.
Dubinin, V. G. (see Antonov-Romanovskiĭ, V. V.) — 1039L.
Dubrovskaya, A. E. (see Brandt, N. B.) — 405L.
Dukel'skiĭ, V. M. (see Khvostenko, V. I.) — 465.
Dukhin, S. S. Anomalous Heat Capacity and Nuclear Resonance in Crystalline Hydrogen in Connection with New Data on Its Structure — 1054L.
Dyatlov, I. T. Threshold Momentum Power Series Expansion of the Amplitude of a Reaction Involving the Formation of Low Energy Particles — 947.
Dykman, I. M. and S. I. Pekar. Light Waves in Crystals in the Exciton Absorption Region and the Impurity Photoeffect — 361.
Dzhelepov, B. S., I. F. Uchevatkin, and S. A. Shestopalova. $O^+ - O^+$ Transition in the Decay $Pr^{140} \rightarrow Ce^{140}$ — 611L.
— (see Budagov, Yu. A.) — 625L.
Dzyaloshinskiĭ, I. E. On the Magneto-Electrical Effect in Antiferromagnets — 628L.
—, E. M. Lifshitz, and L. P. Pitaevskiĭ. Van der Waals Forces in Liquid Films — 161.
Egorov, L. B., A. E. Ignatenko, and D. Chultém. Effect of the Hyperfine Structure on Polarization of Negative Muons in Mesic Atoms — 1077.
Él'tekov, V. A. On the Influence of the Pauli Principle and of Short-Range Nuclear Forces on the Absorption of Photons by Nuclei in the Oscillator Model — 830L.
Emel'yanov, A. A. and D. S. Chernavskiĭ. Effect of Viscosity in Multiple Production on the Energy Distribution of Secondary Particles — 753.
Ermolov, P. F. (see Budagov, Yu. A.) — 625L.
Érnst, B. M. (see Lomsadze, Yu. M.) — 955.
Erokhina, K. I. (see Alkhazov, D. G.) — 1086.
Esel'son, B. N. and A. D. Shvets. The Use of a Superconducting Ring for Registering the Phase Transition in Liquid Helium — 228L.
Fadeev, V. M. (see Korepanov, V. D.) — 218L.
Faĭnberg, V. Ya. Application of the Dispersion Relations Method in Quantum Electrodynamics — 968.
Fedorenko, N. V. and V. A. Belyaev. Maximum Atomic Cross Sections for Nonresonance Charge Exchange — 1276L.
Fedotov, P. I. Potential Barrier Criterion and Stars in Emulsions — 674.
— (see Zhdanov, A. P.) — 280.
Fetisov, I. K. and O. B. Firsov. Resonance Charge Exchange of Doubly Charged Ions in Slow Collisions — 67.
Filimonov, V. A. (see Lyul'ka, V. A.) — 1015.
Filimonov, Yu. I. (see Golenetskiĭ, S. V.) — 395L.
Filippova, K. V. (see Guseva, L. I.) — 694.
— (see Volkov, V. V.) — 859.
Filov, R. A. (see Ostroumov, V. I.) — 459.
Firsov, O. B. (see Fetisov, I. K.) — 67.
Fisun, A. N. (see Grishaev, I. A.) — 1031L.
Fleĭsher, V. G. (see Berlovich, É. E.) — 855.
Flerov, G. N. (see Karnaukhov, V. A.) — 901.
— (see Korneev, E. I.) — 29.
— (see Mikheev, V. L.) — 612L.
— (see Perelygin, V. P.) — 1106.
Fock, M. V. (see Antonov-Romanovskiĭ, V. V.) — 1039L.
Fradkin, É. E. (see Kaliteevskiĭ, N. I.) — 629L.
Fremlin, J. H. and J. S. Lille. Nuclear Reactions Induced by Heavy Ions — 229L.
Frolov, G. V. Polarization Effects in the Elastic Scattering of Electrons from Deuterons — 269.
Gadzhiev, S. A. (see Kerimov, B. K.) — 407L.
Gaĭdukov, Yu. P. Topology of the Fermi Surface of Gold — 913.
— (see Alekseevskiĭ, N. E.) — 481.
Galanin, A. D., A. F. Grashin, B. L. Ioffe, and I. Ya. Pomeranchuk. On the Collisions of Nucleons with Large Orbital Angular Momentum — 1179.
Galkin, A. A. and A. P. Korolyuk. Oscillations in the Absorption Coefficient of Sound in Tin at Low Temperature — 219L.
— and I. V. Matyash. On the Structure of Solid Hydrogen — 1292L.
— (see Bezuglyĭ, P. A.) — 1049L.
Gamstemlidze. G. A. On the Critical Mode in Experiments with an Oscillating Disk — 678.
— The Landau Correction Coefficient in the Determination of the Viscosity of a Liquid — 609L.
Gandel'man, G. M. and V. S. Pinaev. Emission of Neutrino Pairs by Electrons and the Role Played by it in Stars — 764.
Gaponov, Yu. V. Second Forbidden Coulomb β-Decay Transitions — 109.
Garibyan, G. M. Transition Radiation Effects in Particle Energy Losses — 372.
— and I. Ya. Pomeranchuk. Limits of Applicability of

the Theory of Transition Radiation — 0000L.
Garif'yanov, N. S. Paramagnetic Resonance in Magnetically Dilute Systems — 1101.
— (see Avvakumov, V. I.) — 1118.
Geĭlikman, B. T. On the Question of Critical Velocities for Flow of He II in Capillaries — 635L.
Gel'man A. P. On the Relativistic Operators for Momentum and Angular Momentum — 339.
Gershman, B. N. Nonresonance Absorption of Electromagnetic Waves in a Magnetoactive Plasma — 497.
Gershteĭn, S. S. (see Belyaev, V. B.) — 1171.
Gertsenshteĭn, M. E. (see Bershteĭn, I. L.) — 1293L.
Getmantsev, G. G. Growth of Electromagnetic Waves in Interpreting Infinite Moving Media — 600.
Ginzburg, N. I. and A. I. Shal'nikov. Destruction of Superconductivity in Thin Films by Field and Current — 285.
Gippius, A. A. (see Vavilov, V. S.) — 15.
Gogichaĭshvili, Sh. M. (see Kucheryaev, A. G.) — 412L.
Gol'danskiĭ, V. I. and M. I. Podgoretskiĭ. Possible Method of Identifying New Transuranic Elements — 223L.
— (see Vasil'kov, R. G.) — 7.
— (see Vasil'kov, R. G.) — 818L.
Gol'din, L. L., G. I. Novikova, N. I. Pirogova, and E. F. Tret'yakov. Alpha Decay of Th^{229}. Interaction of Nuclear Levels — 822L.
— (see Novikova, G. I.) — 663.
— (see Tret'yakov, E. F.) — 656.
Golenetskiĭ, S. V., L. I. Rusinov, and Yu. I. Filimonov. On the Decay Scheme of the Bi^{210} Isomer — 395L.
Gol'fand, Yu. A. On the Introduction of an "Elementary Length" in the Relativistic Theory of Elementary Particles — 356.
— On Lepton Mass — 1059L.
Golitsyn, G. S. Some Problems of the Dynamics and Heating of a Conducting Medium in a Magnetic Field — 756.
Goodman, F. (see Davies R.) — 828L.
Gordon, I. M. Mechanism for the Production of Relativistic Electrons in the Atmospheres of Nonstationary Stars — 608L.
Gor'kov, L. P. The Critical Supercooling Field in Superconductivity Theory — 593.
— Theory of Superconduction Alloys in a Strong Magnetic Field Near the Critical Temperature — 998.
— (see Abrikosov, A. A.) — 132.
Gornyĭ, N. B. Discrete Electron Energy Losses and Secondary Emission from CdO — 242.
Gorshkov, M. M. (see Vavilov, V. S.) — 15.
Govorkov, B. B. (see Vasil'kov, R. G.) — 7.
— (see Vasil'kov, R. G.) — 224L.
— (see Vasil'kov, R. G.) — 818L.
Gramenitskiĭ, I. M. (see Bogachev, N. P.) — 872.
Granovskiĭ, Ya. I. On the Calculation of the Interaction Constant in a Nonlinear Theory — 135.
— The Electromagnetic Interaction in the Heisenberg Theory — 314.
Grashin, A. F. (see Galanin, A. D.) — 1179.
— (see Kirillov-Ugryumov, V. G.) — 907.
Grebenshchikov, S. E. (see Raĭzer, M. D.) — 398L.
Grechukhin, D. P. On the Nucleon + Core Model of the Nucleus with a Vibrational Excitation Spectrum of the Core — 730.
Gribov, V. N. (see Ansel'm, A. A.) — 354.
Grigor'ev, E. L. and N. A. Mitin. Elastic Scattering of 390-Mev π^+ Mesons from Protons — 1123.
— and N. A. Mitin. Polarization of Recoil Protons Produced in Elastic Scattering at 307 Mev — 295.
Grigor'ev, V. N. (see Bogoyavlenskiĭ, I. V.) — 884.
Grigorov, N. L. and M. A. Kondrat'eva. Investigation of a Shower Consisting of 200,000 Particles and Recorded in a Nuclear Photographic Plate — 489.
— and V. Ya. Shestoperov. On Certain Singularities in the Interaction with Light Nuclei of Particles with Energies $E \geq 2 \times 10^{12}$ ev — 816L.
— (see Alekseeva, K. I.) — 271.
— (see Alekseeva, K. I.) — 422.
Grinberg, A. P. (see Alkhazov, D. G.) — 1086.
Grishaev, N. A., A. N. Fisun, A. S. Litvinenko, V. M. Grizhko, B. I. Shramenko, and I. N. Onishchenko. Measurement of Energy Loss of Fast Electrons Penetrating through Matter — 1031L.
Grishin, V. G. (see Bannik, B. P.) — 1118.
Grizhko, V. M. (see Grishaev, N. A.) — 1031L.
Gurevich, A. V. The Influence of Collisions between Electrons on Their Velocity Distribution in Gases and in Semiconductors in an Electric Field — 215L.
Gurevich, I. I., B. A. Nikol'skiĭ, and L. V. Surkova. Three-Electron Decay of the Muon — 225L.
Gurevich, L. É. and I. P. Ipatova. Faraday Effect in Semiconductors on Free Carriers in a Strong Magnetic Field — 943.
— and G. M. Nedlin. Thermoelectric Coefficients of Metals in Strong Magnetic Fields and the Effect of Drag of Electrons by Photons — 546.
— (see Bychkov, Yu. A.) — 377.
Gurevich, V. L. Ultrasonic Absorption in Metals in a Magnetic Field I. — 51.
— Ultrasonic Absorption in Metals in a Magnetic Field. II — 1190.
Guseva, L. I., B. F. Myasoedov, N. I. Tarantin, and K. V. Filippova. Cross Section for Production of Cm^{240} by Irradiation of Th^{232} with C^{12} and C^{13} Ions — 694.
— (see Volkov, V. V.) — 859.
Gusinskiĭ, G. M. (see Alkhazov, D. G.) — 1086.
Gutkin, T. I. (see Demirkhanov, R. A.) — 866.
Gutman, I. I. A Generally Covariant Method of Successive Approximations in General Relativity — 1162.
Ho Tso-Hsiu. The Formfactor and the Leptonic Decay Probability of the Λ Particle — 1288L.
— (see Bilen'kiĭ, S. M.) — 1241.
Ignatenko, A. E. (see Egorov, L. B.) — 1077.
Inopin, E. V. and B. I. Tishchenko. Scattering of Electrons by Light Nonspherical Nuclei — 932.
Ioffe, B. L. Analyticity and Unitarity in the Scattering of Scalar Mesons from a Static Nucleon — 1245.
— Capture of μ^--Mesons by Light Nuclei — 113.
— (see Galanin, A. D.) — 1179.
Iogansen, L. V. Effect of Interaction on the Phase Motion of Electrons in a Synchrotron — 211L.
— and M. S. Rabinovich. Coherent Electron Radiation in the Synchrotron II — 83.
Ipatova, I. P. (see Gurevich, L. É.) — 943.

Isaev, P. S. (see Zlatev, I. S.) — 519.
— (see Zlatev, I. S.) — 826L.
Ishmukhametov, B. Kh. (see Vlasov, K. B.) — 531.
Ivanenko, D. D. and N. V. Mitskevich. Taking Account of the Gravitational Energy — 618L.
— (see Brodskiĭ, A. M.) — 624L.
Ivanenko, I. P. On the Theory of the Passage of the Nuclear Cascade Through the Atmosphere — 744.
Ivanov, V. G., V. T. Osipenkov, N. I. Petrov, and V. A. Rusakov. Cross Sections for Elastic Scattering of 195-Mev Positive Pions by Carbon and Lithium Nuclei — 615L.
— (see Petrov, N. I.) — 682.
Ivanova, N. S., V. I. Ostroumov, and Yu. V. Pavlov. Production of Multi-Charged Particles on Photographic Emulsion Nuclei by 280-Mev Positive Pions — 1137.
Kadmenskiĭ, S. G. (see Rapoport, L. P.) — 929.
Kadomtsev, B. B. Convective Pinch Instability — 780.
— On Equilibrium of a Plasma Under Helical Symmetry — 962.
— On the Stability of a Low Pressure Plasma — 1167.
Kadomtseva, A. M. (see Belov, K. P.) — 825L.
Kaganov, M. I. and V. M. Tsukernik. Nonresonance Absorption of Oscillating Magnetic Field Energy by a Ferromagnetic Dielectric — 587.
— (see Bass, F. G.) — 986.
— (see Lifshitz, I. M.) — 392L.
Kaganskiĭ, M. G. (see Antonova, S. F.) — 477.
Kalinin, S. P. (see Artemov, K. P.) — 474.
Kaliteevskiĭ, N. I., M. P. Chaĭka, I. Kh. Pacheva, and É. E. Fradkin — 629L.
Kaminskiĭ, D. L. (see Antonova, S. F.) — 477.
Kaplan, E. G. Classification of Molecular Terms with Respect to Total Nuclear Spin — 747.
Karamyan, A. S. and A. A. Pleve. Production of Compound Nuclei by Bombardment of V and Nb with O^{16}, C^{12}, and C^{13} Ions — 467.
Karnaukhov, V. A., V. I. Khalizev, and G. N. Flerov. Emitters of Alpha Particles with Energies of About 9 and 12 Mev — 901.
Kataev, G. I. (see Belov, K. P.) — 870.
Kazantsev, A. P. Motion of Charged Particle in a Rotating Magnetic Field — 1036L.
Kazarinov, Yu. M. (see Amaglobeli, N. S.) — 1125.
Keldysh, L. V. Kinetic Theory of Impact Ionization in Semiconductors — 509.
Kel’man, V. M., R. Ya. Metskhvarishvili, B. K. Preobrazhenskiĭ, V. A. Romanov, and V. V. Tuchkevich. Multipolarities of Gamma Transitions in Tm^{169} — 456.
Kerimov, B. K., A. I. Mukhtarov, and S. A. Gadzhiev. Polarization Effects in the $\pi^0 \rightarrow e^- + e^+ + \gamma$ Decay — 407L.
Khabakhpashev, A. G. and É. M. Tsenter. Measurement of the Lifetime of the First Excited State of Ne^{21} — 705.
— (see Tsenter, É. M.) — 806L.
Khaĭkin, M. S. Cyclotron Resonance on Tin — 1044L.
Khalatnikov, I. M. (see Abrikosov, A. A.) — 132.
Khalizev, V. I. (see Karnaukhov, V. A.) — 901.
Kharitonov, E. V. (see Dolginov, A. Z.) — 553.
Kharitonov, Yu. I. (see Sliv, L. A.) — 819L.
Khokhlov, Yu. K. On the Theory of the Nuclear Moment of Inertia — 808L.
Khokhlova, Z. S. (see Berkovich, I. B.) — 428.
Khrenov, B. A. (see Vernov, S. N.) — 891.
Khristiansen, G. B. (see Dmitriev, V. A.) — 637.
— (see Vernov, S. N.) — 848.
— (see Vernov, S. N.) — 891.
— (see Vernov, S. N.) — 1050L.
Khvostenko, V. I. and V. M. Dukel’skiĭ. Formation of Negative Hydrogen Ions on an Incandescent Tungsten Surface — 465.
Kirenskiĭ, L. V., M. K. Savchenko, and I. F. Degtyarev. On the Magnetization Process in Ferromagnets — 437.
Kirillov, V. D. Energy Lost to Radiation in a Gas-Discharge Plasma — 812L.
Kirillov-Ugryumov, V. G., L. P. Kotenko, E. P. Kuznetsov, F. M. Sergeev, and A. F. Grashin. Elastic Scattering of 5 — 22 Mev π^+-Mesons on Carbon — 907.
Kirzhnits, D. A. The Energy of a Compressed Imperfect Fermi Gas — 414L.
Klement’ev, V. N. (see Berlovich, É. E.) — 855.
Klepikov, N. P. Minimal Error in the Experimental Observation of Asymmetry — 810L.
Klimontovich, Yu. L. Relativistic Transport Equations for a Plasma I. — 524.
Kobzarev, I. Yu. (see Shalamov, Ya. Ya.) — 622L.
Kochelaev, B. I. Contribution to the Theory of Spin-Lattice Relaxation of Nuclear Spins in Ionic Crystals — 171.
Kocherov, N. P. (see Darovskikh, V. F.) — 921.
Kogan, V. S., B. G. Lazarev, and R. F. Bulatova. Diffraction of X-rays by Polycrystalline Samples of Hydrogen Isotopes — 485.
— (see Bulatova, R. F.) — 1058L.
Kokin, A. A. and G. V. Skrotskiĭ. Theory of Paramagnetic Resonance in Systems Containing Two Kinds of Magnetic Moments — 342.
— (see Skrotskiĭ, G. V.) — 572.
Kolesnikov, N. N. and A. P. Krylova. The Proton Subshell Z = 100 — 389L.
Kolganova, É. D. (see Vaĭsenberg, A. O.) — 231L.
Komar, A. P. (see Vorob’ev, A. A.) — 386L.
— (see Vorob’ev, A. A.) — 1032L.
Komarov, V. V. (see Vasil’ev, S. S.) — 1034L.
Kompaneets, A. S. Propagation of a Strong Electromagnetic-Gravitational Wave in Vacuo — 1218.
Kondorskiĭ, E. I. On the Causes of the Peculiarities in the Physical Properties of Invar Alloys — 1284L.
— Theory of the Stability of Magnetic States of Ferromagnetic Materials in the Magnetization Process — 790.
Kondrat’eva, M. A. (see Grigorov, N. L.) — 489.
Konstantinov, O. V. and V. I. Perel’. Quantum Theory of Spatial Dispersion of Electric and Magnetic Susceptibilities — 560.
Konyukov, M. V. Nonlinear Langmuir Electron Oscillations in a Plasma — 570.
Kopaleĭshvili, T. I. (see Mamasakhlisov, V. I.) — 93.
(see Mamasakhlisov, V. I.) — 807L.
— (see Vashakidze, I. Sh.) — 535.
Kopylov, G. I. Identification of Particles in High Energy Stars — 393L.
Kopylova, D. D., Yu. B. Korolevich, N. I. Petukhova,

and M. I. Podgoretskiĭ. On the Mechanism of Capture of Stopped K^- Mesons — 203.
Kopylovskiĭ, B. D. (see Vavilov, V. S.) — 15.
Korepanov, V. D., R. A. Dautov, and V. M. Fadeev. Measurements of the Transverse Proton Relaxation Time in Aqueous Solutions of Paramagnetic Salts by Spin-echo Method — 218L.
Korneev, E. I., V. S. Skobkin, and G. N. Flerov. Fission of Th^{232} by Thermal Neutrons — 29.
Korolev, V. A. (see Vorob'ev, A. A.) — 386L.
— (see Vorob'ev, A. A.) — 1032L.
Korolevich, Yu. B. (see Kopylova, D. K.) — 203.
Korolyuk, A. P. (see Galkin, A. A.) — 219L.
Koshelyaev, G. V. (see Vasil'ev, S. S.) — 1034L.
Kotenko, L. P. (see Askar'yan, G. A.) — 1041L.
— (see Kirillov-Ugryumov, V. G.) — 907.
Kovrizhnykh, L. M. Effect of Inelastic Collisions on the Velocity Distribution of Electrons — 347.
— Oscillations of an Electron-Ion Plasma — 1198.
— Stability of a Hollow Gas Conductor in a Magnetic Field — 65.
— Velocity Distribution of Electrons in a Strong Electric Field — 989.
Kozyrev, B. M. (see Avvakumov, V. I.) — 1110.
Kresnin, A. A. On the Polarization of the Electrons in Bremsstrahlung Processes — 621L.
Krestnikov, Yu. S., A. G. Meshkovskiĭ, Ya. Ya. Shalamov, V. A. Shebanov, and I. Yu. Kobzarev. The $\mu \to e + \gamma$ and $\mu \to e + \nu + \overline{\nu} + \gamma$ Decays — 622L.
Krylova, A. P. (see Kolesnikov, N. N.) — 389L.
Kucherov, R. Ya. and L. É. Rikenglaz. Concentration Jump in Slow Evaporation of a Mixture — 1285L.
— and L. É. Rikenglaz. On Hydrodynamic Boundary Conditions for Evaporation and Condensation — 88.
Kucheryaev, A. G., Yu. K. Szhenov, and Sh. M. Gogichaĭshvili. Measurements of Nuclear Magnetic Moments in the Alkali Earths by Molecular Beam Magnetic Resonance — 412L.
Kulakovskiĭ, E. K. (see Anton'eva, N. M.) — 1063.
Kul'chitskiĭ, L. A. and V. Presperin. Fast Photoneutrons from Be^9, C^{12}, and Al^{27} — 1082.
Kulikov, G. V. (see Dmitriev, V. A.) — 637.
— (see Vernov, S. N.) — 848.
Kulikovskiĭ, A. G. and G. A. Lyubimov. On the Paper of V. A. Belokon': "The Permanent Structure of Shock Waves with Joule Dissipation" — 835L.
Kurchatova, L. N. (see Borisova, N. I.) — 261.
Kurushin, A. I. Paramagnetic Absorption and Rotation of Plane of Polarization for Certain Salts in the Microwave Band — 209L.
Kutsaeva, L. S. (see Kuz'minov, B. D.) — 290.
Kuz'minov, B. D., L. S. Kutsaeva, V. G. Nesterov, L. I. Prokhorova, and G. N. Smirenkin. Some Features of the Spontaneous Fission of U^{238} — 290.
Kuznetsov, E. P. (see Askar'yan, G. A.) — 1041L.
— (see Kirillov-Ugryumov, V. G.) — 907.
Kuznetsov, V. P. On Electromagnetic Corrections in $\mu - e$ Decay — 784.
Kuznetsova, M. Ya. (see Borisova, N. I.) — 261.
Kytin, G. A. (see Brandt, N. B.) — 405L.
Laberrigue-Frolova, J. V., M. P. Balandin, and S. Z. Otvinovskiĭ. On the Absorption of π^+ Mesons with Energies of About 50 Mev by Carbon Nuclei — 452.
Landau, L. D. On the Analytic Properties of Vertex Parts in Quantum Field Theory — 45.
Lapidus, L. I. and Chou Kuang-Chao. Dispersion Relations for the Scattering of Gamma Quanta by Nucleons — 1213.
— and Chou Kuang-Chao. On the Problem of Investigating the Interaction between Pions and Hyperons — 199.
Larionov, O. V. (see Berlovich, É. E.) — 855.
Larkin, A. I. Passage of Particles through a Plasma — 186.
Lazarev, B. G., A. I. Sudovtsev, and E. E. Semenenko. Superconductivity of Beryllium and its Low-Temperature Polymorphism — 1035L.
— (see Bulatova, R. F.) — 1058L.
— (see Kogan, V. S.) — 485.
Lazareva, L. E. (see Burgov, N. A.) — 1278L.
Lebedev, P. I. (see Balats, M. Ya.) — 417.
Lebedev, S. V., S. L. Mandel'shtam, and G. M. Rodin. Shortwave Radiation from a Vacuum Spark — 248.
Lemberg, I. Kh. (see Alkhazov, D. G.) — 1086.
Lend'el, V. I. (see Lomsadze, Yu. M.) — 955.
Lepekhin, F. G. (see Berkovich, I. B.) — 428.
Levitin, R. Z. (see Belov, K. P.) — 670.
— (see Belov, K. P.) — 400L.
Lifshitz, E. M. (see Dzyaloshinskiĭ, I. E.) — 161.
Lifshitz, I. M. and M. I. Kaganov. Electron Resonance in Crossed Electric and Magnetic Fields — 392L.
Lille, J. S. (see Fremlin, J. H.) — 229L.
Lipmanov, É. M. On Two Types of Neutrinos, the Isotopic Spin of Leptons, and the Universal Four-Fermion Interaction — 750.
Litvinenko, A. S. (see Grishaev, A. N.) — 1031L.
Lobanov, Yu. V. (see Druin, V. A.) — 26.
Lobashev, V. M., V. A. Nazarenko, and L. I. Rusinov. Polarization β-γ Correlation in Decay of Co^{60} — 1277L.
Logunov, A. A. (see Bogolyubov, N. N.) — 574.
Lomnev, S. P. (see Belyaev, V. B.) — 1171.
Lomsadze, Yu. M., V. I. Lend'el, and B. M. Érnst. On the Anomalous Magnetic Moment of Nucleons in Chew's Method — 955.
Los', F. S. On the Phase of the Scattered Wave (A Reply to V. V. Malyarov) — 836L.
Luk'yanov, S. Yu. and I. M. Podgornyĭ. Magnetic Trap with Field Increasing toward Periphery — 18.
Lysov, B. A. Polarization Effects in the Direct Transition of $\mu^+\mu^-$ into an Electron-Positron Pair — 404L.
Lyubimov, G. A. (see Kulikovskiĭ, A. G.) — 835L.
Lyubimov, V. B., P. M. Markov, É. N. Tsyganov, Cheng P'u-Ying, and M. G. Shafranova. Elastic Proton-Proton Scattering at 8.5 Bev — 651.
— (see Bannik, B. P.) — 1118.
— (see Bogachev, N. P.) — 872.
Lyuboshitz, V. L. Polarization Phenomena in Radiative Collisions of Two Electrons — 1221.
Lyul'ka, V. A. and V. A. Filimonov. Contribution of Three-Particle Forces to the Binding Energy of Hyper-Nuclei — 1015.
Mak, A. A. Concentration of Charged Particles in Plasma of Spark-discharge Channel — 1055L.
Maksimenko, V. M. (see Zhdanov, G. B.) — 442.
Maksimov, M. Z Range-Energy Relation for Some

Substances — 90.
Mal'tsev, V. M. (see Barashenkov, V. S.) — 630L.
— (see Barashenkov, V. S.) — 1052L.
Mamasakhlisov, V. I. and T. I. Kopaleĭshvili. Inelastic Scattering of Nucleons of Mg^{24} and Si^{28} Nuclei — 93.
— and T. I. Kopaleĭshvili. On the Rotational Levels of Li^7 — 807L.
Mandel'shtam, S. L. (see Lebedev, S. V.) — 248.
Manenkov, A. A. (see Piskunov, A. K.) — 213L.
Marek, I. and I. Ulehla. Concerning Anomalous Equations for Spin ½ Particles — 1051L.
Marish, K. S. (see Akimov, Yu. K.) — 33.
Markov, P. K. (see Lyubimov, V. B.) — 651.
— (see Zhdanov, G. B.) — 433.
Matinyan, S. G. Parity Conservation in Strong Interactions of Strange Particles — 736.
Matyash, I. V. (see Galkin, A. A.) — 1292L.
Mekhedov, V. N. (see Borisova, N. L.) — 261.
Merekov, Yu. P. (see Bogachev, N. P.) — 872.
Meshkovskiĭ, A. G. and Ya. Ya. Shalamov. Inelastic Interaction of π^+ Mesons with Light Nuclei in the Energy Region 80 — 300 Mev — 697.
— (see Krestnikov, Yu. S.) — 622L.
Metskhvarishvili, R. Ya. (see Kel'man, B. M.) — 456.
Migdal, A. B. Superfluidity and the Moments of Inertia of Nuclei — 176.
Mikaélyan, L. A. and P. Ya. Spivak. Measurement of the Degree of Longitudinal Polarization of Beta Particles — 831L.
Mikhaĭlov, G. V. Effect of Pressure on the Raman Spectrum of Oxygen — 1114.
Mikheev, V. L., N. K. Skobelev, V. A. Druin, and G. N. Flerov. Spontaneous Fission of Am^{241} — 612L.
Mikhul, É. K. (see Barashenkov, V. S.) — 1052L.
Mishakova, A. P. and B. A. Nikol'skiĭ. Angular Distribution of Shower Particles in Explosion Showers Produced by High-Energy Cosmic-Ray Particles — 1130.
— (see Tumanyan, V. A.) — 253.
Mitin, N. A. (see Grigor'ev, E. L.) — 295.
— (see Grigor'ev, E. L.) — 1123.
Mitrofanov, K. P. (see Bedescu, A.) — 221L.
Mitsek, A. I. (see Turov, E. A.) — 801.
Mitskevich, N. V. (see Ivanenko, D. D.) — 618L.
Moĭseev, S. S. On the Distribution Function for Dissipative Processes in a Rarefied Relativistic Gas — 391L.
Moskalev, A. N. (see Dolginov, A. Z.) — 1202.
Moskalev, V. I. (see Budagov, Yu. A.) — 625L.
Motulevich, G. P. On the Connection between the Optical Constants of Metals and their Microscopic Characteristics — 1249.
Mukhtarov, A. I. (see Kerimov, B. K.) — 407L.
Murtazin, F. Sh. (see Berlovich, E. É.) — 855.
Murzin, V. S. (see Alekseeva, K. I.) — 422.
Myasoedov, B. F. (see Guseva, L. I.) — 694.
— (see Volkov, V. V.) — 859.
Nazarenko, V. A. (see Lobashev, V. M.) — 1277L.
Nedlin, G. M. (see Bychkov, Yu. A.) — 377.
— (see Gurevich, L. É.) — 546.
Nesterov, V. G. (see Kuz'minov, B. D.) — 290.
Neudachin, V. G., Yu. F. Smirnov, and N. P. Yudin. Clustering of Nucleons in Light Nuclei — 1256.
—, I. B. Teplov, and A. F. Tulinov. Use of the (d, p) Reaction to Excite States with Large Spins — 387L.
— (see Balashov, V. V.) — 983.
Nikanorov, S. P. and A. V. Stepanov. The Temperature Dependence of the Elastic Constants of Potassium Bromide — 1280.
Nikolaev, F. A. (see Burgov, N. A.) — 1278L.
Nikol'skiĭ, B. A. (see Gurevich, I. I.) — 225L.
— (see Mishakova, A. P.) — 1130.
Nikol'skiĭ, S. I. (see Zatsepin, G. T.) — 138.
Nosov, V. G. On the Determination of Nuclear Deformation from the Alpha-decay Fine Structure — 631L.
Novikov, V. M. (see Zaretskiĭ, D. F.) — 1287L.
Novikova, G. I., E. A. Volkova, L. L. Gol'din, D. M. Ziv, and E. F. Tret'yakov. Radioactive Decay of Ac^{227} and Excited Levels of Fr^{223} and Th^{227} — 663.
— (see Gol'din, L. L.) — 822L.
— (see Tret'yakov, E. F.) — 656.
Novikova, S. I. (see Astrov, D. N.) — 851.
Nurushev, S. B. Determination of the p-p Scattering Matrix at 90° — 212L.
Obukhov, Yu. V. (see Balats, M. Ya.) — 417.
Ogievetskiĭ, V. I. and I. V. Polubarinov. Wave Equations with Zero and Nonzero Rest Masses — 335.
— (see Chou Kuang-Chao) — 616L.
Ogloblin, A. A. (see Vlasov, N. A.) — 39.
— (see Vlasov, N. A.) — 844.
Oiglane, H. Note on a Baryon Scheme — 394L.
Okun', L. B. and E. P. Shabalin. On K$_{e4}$ Decay — 1252.
Onishchenko, I. N. (see Grishaev, I. A.) — 1031L.
Oraevskiĭ, A. N. (see Basov, N. G.) — 761.
Orfanov, I. V. (see Yurasova, V. E.) — 689.
Orlov, Yu. V. On the Theory of the Direct Nuclear Photoeffect — 1294L.
Orlova, M. P. (see Astrov, D. N.) — 851.
Osipenkov, V. T. (see Ivanov, V. G.) — 615L.
Ostroumov, V. I. and R. A. Filov. Knock-On Alpha Particles Produced by Fast Nucleons — 459.
— (see Ivanova, N. S.) — 1137.
Otstavnov, P. S. Polarization of (d-d) Neutrons — 1281L.
Otvinovskiĭ, S. Z. (see Laberrigue-Frolova, J. V.) — 452.
Ovsyannikova, I. A. (see Borovskiĭ, I. B.) — 1033L.
Pacheva, I. Kh. (see Kaliteevskiĭ, N. I.) — 629L.
Pavlov, Yu. V. (see Ivanova, N. S.) — 1137.
Pekar, S. I. (see Dykman, I. M.) — 361.
Peletminskiĭ, S. V. Coupled Magnetoelastic Oscillations in Antiferromagnetics — 321.
— (see Volkov, D. V.) — 121.
Perel', V. I. (see Konstantinov, O. V.) — 560.
Perelygin, V. P., E. D. Donets, and G. N. Flerov. Experiments in the Production of a New Fermium Isotope — 1106.
Perfilov, N. A. and Z. I. Solov'eva. Angular Distribution of Long-range Alpha Particles — 824L.
— (see Darovskikh, V. F.) — 921.
Peshkov, V. P. (see Zinov'eva, K. N.) — 22.
Peterkop, R. K. On the Inclusion of Exchange in the Theory of Collisions — 834L.
Petrov, N. I., V. G. Ivanov, and V. A. Rusakov. Inelastic Scattering and Absorption of (195 ± 15)-Mev Positive Pions by Carbon and Lithium Nuclei — 682.
— (see Ivanov, V. G.) — 615L.
Petrov, Yu. V. Possibility of Investigating the Levels of

the Compound Nucleus Produced by Interaction between Slow Neutrons and Isomers — 833L.
Petukhova, N. I. (see Kopylova, D. K.) — 203.
Pikel'ner, S. B. Gravitational Attenuation of Sound — 1290L.
Piliya, A. D. Excitation of Vibrational Levels in Nuclei by Charged Particles — 1018.
— On the Cross Section for Compound-Nucleus Formation by Charged Particles — 413L.
Pinaev, V. S. (see Gandel'man, G. M.) — 764.
Pirkin, I. A. (see Tsenter, É. M.) — 806L.
Pirogova, N. I. (see Gol'din, L. L.) — 822L.
— (see Tret'yakov, E. F.) — 656.
Piskunov, A. K., A. A. Manenkov, and Z. A. Bagdasar'yan. Paramagnetic Resonance in Potassium Ozonide — 213L.
Pitaevskiĭ, L. P. Attraction of Small Particles Suspended in a Liquid at Large Distances — 408L.
— On the Superfluidity of Liquid He^3 — 1267.
— (see Dzyaloshinskiĭ, I. E.) — 161.
Pleshivtsev, N. V. Sputtering of Copper by Hydrogen Ions Possessing Energies up to 50 kev — 878.
— (see Yurasova, V. E.) — 689.
Pleve, A. A. (see Karamyan, A. S.) — 467.
Podgoretskiĭ, M. I. (see Bannik, B. P.) — 1118.
— (see Bogachev, N. P.) — 872.
— (see Gol'danskiĭ, V. I.) — 223L.
— (see Kopylova, D. K.) — 203.
Podgornyĭ, I. M. (see Luk'yanov, S. Yu.) — 18.
Podlubnyĭ, L. I. The Non-Additivity of London-Van der Waals Forces — 633L.
Polikanov, S. M. (see Druin, V. A.) — 26.
Polovin, R. V. (see Akhiezer, I. A.) — 539.
Polubarinov, I. V. (see Ogievetskiĭ, V. I.) — 335.
Pomanskiĭ, A. A. (see Zatsepin, G. T.) — 138.
Pomeranchuk, I. Ya. (see Galanin, A. D.) — 1179.
— (see Garibyan, G. M.) — 1290L.
Pontecorvo, B. Electron and Muon Neutrinos — 1236.
Popov, V. S. On the Theory of the Relativistic Transformations of the Wave Functions and Density Matrix of Particles with Spin — 794.
Popov, Yu. M. (see Basov, N. G.) — 416L.
Popova, A. M. (see Vasil'ev, S. S.) — 1034L.
Preobrazhenskiĭ, B. K. (see Kel'man, V. M.) — 456.
Presperin, V. (see Kul'chitskiĭ, L. A.) — 1082.
Prokhorov, A. M. (see Antonov-Romanovskiĭ, V. V.) — 1039L.
Prokhorova, L. I. (see Kuz'minov, B. D.) — 290.
Pustovoĭt, V. I. On Linear Theories of Gravitation — 619L.
Rabin, N. V. (see Vaĭsenberg, A. O.) — 231L.
Rabinovich, E. M. (see Zel'dovich, Ya. B.) — 924.
Rabinovich, M. S. (see Iogansen, L. V.) — 83.
Raĭzer, M. D. and S. E. Grebenshchikov. Localization of a High-Frequency Induction Discharge — 398L.
Raĭzer, Yu. P. Condensation of a Cloud of Vaporized Matter Expanding in Vacuum — 1229.
— Residual Ionization of a Gas Expanding in Vacuum — 411L.
— Simple Method for Computing the Mean Range of Radiation in Ionized Gases at High Temperatures — 769.
Rapoport, L. P. and S. G. Kadmenskiĭ. Distribution of the Density of Protons in a Nucleus with a Given Angular Momentum — 929.
Regirer, S. A. On Convective Motion of a Conducting Fluid between Parallel Vertical Plates in a Magnetic Field — 149.
Rikenglaz, L. É. (see Kucherov, R. Ya.) — 1285L.
— (see Kucherov, R. Ya.) — 88.
Ritus, V. I. Angular and Polarization Analyses of Reactions of the Type $a + b \rightarrow a' + b' + c'$ — 153.
Rodin, G. M. (see Lebedev, S. V.) — 248.
Romanov, V. A. (see Kel'man, V. M.) — 456.
Romanovskiĭ, E. A. Excitation of Nuclear Vibrational and Rotational States in the Scattering of Charged Particles — 59.
— Excitation of Rotational States of Nonaxial Nuclei in Alpha-particle Scattering — 606L.
Rudakov, L. I. and R. Z. Sagdeev. Oscillations of an Inhomogeneous Plasma in a Magnetic Field — 952.
Rudenko, N. S. (see Bogoyavlenskiĭ, I. V.) — 884.
Rukhadze, A. A. (see Bolotovskiĭ, B. M.) — 958.
Rumer, Yu. B. A Simple Model in the Theory of Superconductivity — 409L.
Rusakov, S. V. (see Belousov, A. S.) — 1143.
Rusakov, V. A. (see Ivanov, V. G.) — 615L.
— (see Petrov, N. I.) — 682.
Rusinov, L. I. (see Golenetskiĭ, S. V.) — 395L.
— (see Lobashev, V. M.) — 1277L.
Rus'kin, V. I. π^--p Interaction at 1.4 Bev — 74.
Ryabenko, G. A. (see Brandt, N. B.) — 278.
Ryndin, R. M. (see Bilen'kiĭ, S. M.) — 1241.
Sagdeev, R. Z. (see Rudakov, L. I.) — 952.
Samoĭlov, A. V. (see Askar'yan, G. A.) — 1041L.
Samoĭlov, I. M. Capture Mechanism in Betatrons — 504.
Samoĭlov, L. N. (see Artemov, K. P.) — 841.
— (see Artemov, K. P.) — 474.
Sanikidze, D. G. Hydrodynamics of Solutions of Strange Particles in Helium II near the λ Point — 226L.
San'ko, L. A., Zh. S. Takibaev, Ts. I. Shakhova, and L. Ya. Balats. Angular Distribution of Shower Particles in Stars Produced by High-Energy Particles — 1.
Savchenko, M. K. (see Kirenskiĭ, L. V.) — 437.
Savchenko, O. V. (see Akimov, Yu. K.) — 33.
Savin, F. D. (see Alekseeva, K. I.) — 422.
Semenenko, E. E. (see Lazarev, B. G.) — 1035L.
Sergeev, F. M. (see Kirillov-Ugryumov, V. G.) — 907.
Shabalin, E. P. (see Okun', L. B.) — 1252.
Shafranov, V. D. Equilibrium of a Plasma Toroid in a Magnetic Field — 775.
Shafranova, M. G. (see Lyubimov, V. B.) — 651.
— (see Zhdanov, G. B.) — 433.
Shakhbazyan, V. A. On the Two-charge Renormalization Group in Scalar Quantum Electrodynamics — 1263.
Shakhova, Ts. I. (see San'ko, L. A.) — 1.
Shalamov, Ya. Ya. (see Krestnikov, Yu. S.) — 622L.
— (see Meshkovskiĭ, A. G.) — 697.
Shal'nikov, A. I. (see Arkhipov, R. G.) — 888.
— (see Ginzburg, N. I.) — 285.
Shapiro, I. S. and L. D. Blokhintsev. Circular Polariza-

tion of Gamma Quanta Emitted by a Nucleus after μ^- Capture — 542.
Shcherbakova, M. N. (see Zhdanov, G. B.) — 442.
Shebanov, V. A. (see Shalamov, Ya. Ya.) — 622L.
Shelepin, L. A. Contribution to the Theory of Relativistically Invariant Equations — 1153.
Shestopalova, S. A. (see Dzhelepov, B. S.) — 611L.
Shestoperov, V. Ya. (see Grigorov, N. L.) — 816L.
Shirkov, D. V. On Taking the Coulomb Effects into Account in the Theory of Superconductivity — 127.
— (see Bogolyubov, N. N.) — 574.
Shirokov, M. I. On a Symmetry in τ^0 Decay — 232L.
Shmelev, V. P. Application of the Variational Principle for the Determination of the Binding Energy of a Proton-Electron-Positron System — 325.
Shmushkevich, I. M. (see Bukhvostov, A. P.) — 1042L.
Shpinel', V. S. (see Bedescu, A.) — 221L.
Shramenko, B. I. (see Grishaev, N. A.) — 1031L.
Shvets, A. D. (see Esel'son, B. N.) — 228L.
Sidorov, V. M. (see Bogachev, N. P.) — 872.
Silin, V. P. Collective Losses of Fast Electrons in Passage through Matter — 192.
— (see Zharkov, V. N.) — 102.
Skobelev, N. K. (see Mikheev, V. L.) — 612L.
Skobkin, V. S. (see Korneev, E. I.) — 29.
Skobov, V. G. Scattering of Low-energy Electron by Short-range Potential in Strong Magnetic Field — 1039L.
Skrotskiĭ, G. V. and A. A. Kokin. On the Influence of Coherent Magnetic Dipole Radiation on Magnetic Resonance — 572.
— (see Kokin, A. A.) — 342.
Sliv, L. A. and Yu. I. Kharitonov. Calculation of Energy Levels of Te^{206} and Bi^{210} Nuclei — 819L.
Smirenkin, G. N. Comparison of Effective Temperatures of Spectra of Neutrons Emitted in Fission of U^{235} and P^{239} by Fast and Thermal Neutrons — 1286L.
— (see Kuz'minov, B. D.) — 290.
Smirnit-skiĭ, V. A. (see Vaĭsenberg, A. O.) — 231L.
Smirnov, Yu. F. (see Balashov, V. V.) — 983.
— (see Neudachin, V. G.) — 1256.
Smorodin, Yu. A. (see Birger, N. G.) — 964.
Smorodinskiĭ, Ya. A. (see Bilen'kiĭ, S. M.) — 1241.
Solov'ev, L. D. and G. N. Tentyukova. Numerical Solution of Static Dispersion Relations of the Photoproduction P-Wave — 634L.
Solov'eva, V. I. (see Vernov, S. N.) — 1050L.
Solov'eva, Z. I. (see Perfilov, N. A.) — 824L.
Solyakin, G. E. (see Vorob'ev, A. A.) — 386L.
Sorokin, A. A. (see Bedescu, A.) — 221L.
Soroko, L. M. (see Akimov, Yu. K.) — 33.
Spivak, P. Ya. (see Mikaélyan, L. A.) — 831L.
Starodubtsev, S. V. (see Bel'skiĭ, S. A.) — 700.
Stepanov, A. V. (see Nikanorov, S. P.) — 1280L.
Stepanova, A. A. (see Zhuravlev, N. N.) — 627L.
Stolyarova, G. S. (see Tumanyan, V. A.) — 253.
Strel'tsov, V. N. (see Zhdanov, G. B.) — 433.
Strugal'skiĭ, Z. S. (see Vernov, S. N.) — 848.
Strutinskiĭ, V. M. Angular Anisotropy of Gamma Quanta that Accompany Fission — 613L.
Sudovtsev, A. I. (see Lazarev, B. G.) — 1035L.
Surkova, L. V. (see Gurevich, I. I.) — 225L.
Svirina, E. P. (see Belov, K. P.) — 862.
Svirskiĭ, M. S. (see Vonsovskiĭ, S. V.) — 1060L.
Szhenov, Yu. K. On the Mechanism of Surface Ionization of Atoms of the Alkali Earth Metals — 239.
— (see Kucheryaev, A. G.) — 412L.
Takibaev, Zh. S. (see Boos, É. G.) — 206L.
— (see San'ko, L. A.) — 1.
Tamm, E. I. (see Belousov, A. S.) — 1143.
Tarantin, N. I. (see Guseva, L. I.) — 694.
— (see Volkov, V. V.) — 859.
Tarasov, Yu. A. On the Stability of Plane Poiseuille Flow of a Plasma of Finite Conductivity in a Magnetic Field — 1209.
Tarasov, M. S. (see Brish, A. A.) — 1095.
Tentyukova, G. N. (see Solov'ev, L. D.) — 634L.
Teplov, I. B. (see Neudachin, V. G.) — 387L.
Ter-Martirosyan, K. A. Incompatibility of the Conditions of Analyticity and Unitarity in the Lee Model — 714.
Ternov, I. M. and V. S. Tumanov. Effect of Vacuum Fluctuations on the Polarization of Electrons Moving in a Magnetic Field — 809L.
Ternovskiĭ, F. F. Effect of Multiple Scattering on Pair Production by High-Energy Particles in a Medium — 718.
— Pair Production in Collisions between Charged Particles — 565.
Tishchenko, B. I. (see Inopin, E. V.) — 939.
Tishkov, P. G. (see Avvakumov, V. I.) — 1110.
Titts, T. On the Methods of Born and Pais for Finding Phase Shifts — 207L.
Toptygin, I. N. (see Batygin, V. V.) — 975.
— (see Dolginov, A. Z.) — 1022.
Trapeznikova, Z. A. (see Antonov-Romanovskiĭ, V. V.) — 1039L.
Tret'yakov, E. F., M. P. Anikina, L. L. Gol'din, G. I. Novikova, and N. I. Pirogova. The Spectrum of Internal Conversion Electrons accompanying Alpha Decay of U^{233}, and the Level Scheme of Th^{229} — 656.
— (see Gol'din, L. L.) — 822L.
— (see Novikova, G. I.) — 663.
Tret'yakova, M. I. (see Zhdanov, G. B.) — 433.
— (see Zhdanov, G. B.) — 442.
Tsakadze, D. S. (see Andronikashvili, É. L.) — 227L.
— (see Andronikashvili, É. L.) — 397L.
Tsekhmistrenko, Yu. V. Two-particle Excitations of Superfluid Fermi Systems — 829L.
Tsenter, É. M., A. G. Khabakhpashev, and I. A. Pirkin. Gamma Rays from a Po-O^{18} Neutron Source — 806L.
— (see Khabakhpashev, A. G.) — 705.
Tsintsadze, N. L. (see Akhiezer, I. A.) — 539.
Tsukerman, V. A. (see Brish, A. A.) — 1095.
Tsukernik, V. M. (see Kaganov, M. I.) — 587.
Tsyganov, É. N. (see Lyubimov, V. B.) — 651.
Tuchkevich, V. V. (see Kel'man, V. M.) — 456.
Tulinov, A. F. (see Neudachin, V. G.) — 387L.
Tumanov, V. S. (see Ternov, I. M.) — 809L.
Tumanyan, V. A., G. S. Stolyarova, and A. P. Mishakova. On Direct Production of Electron-Positron Pairs by High-Energy Electrons — 253.
Turov, E. A. and A. I. Mitsek. On the Theory of the Temperature Dependence of Ferromagnetic Anisotropy — 801.

Tuvdendorzh, D. (see Bogachev, N. P.) — 872.
Uchevatkin, I. F. (see Dzhelepov, B. S.) — 611L.
Ulehla, I. (see Marek, I.) — 1051L.
Urbakh, V. Yu. The Radiative Correction to the Mass of the Electron in Nonlinear Electrodynamics — 208L.
Ustinova, A. K. Angular Correlation in Internal Conversion, Including Effects of Screening and of the Finite Size of the Nucleus — 216L.
Vaĭsenberg, A. O. Space Asymmetry of Low Energy Positrons from $\pi^+ - \mu^+ - e^+$ Decay — 401L.
—, V. A. Smirnit-skiĭ, É. D. Kolganova, and N. V. Rabin. Energy Dependence of the Spatial Asymmetry of Positrons in $\pi^+ \rightarrow \mu^+ \rightarrow e^+$ Decay — 231L.
Vaks, V. G. On Theories with an Indefinite Metric — 332.
Valiev, K. A. Theory of Spin-Lattice Quadrupole Relaxation in Liquid Solutions of Diamagnetic Salts — 77.
Vashakidze, I. Sh., T. I. Kopaleĭshvili, and G. A. Chilashvili. Resonance Scattering of Gamma Quanta by Mg^{24} — 535.
Vasilenko, S. S. (see Antonova, S. F.) — 477.
Vasil'ev, S. S., V. V. Komarov, G. V. Koshelyaev, and A. M. Popova. Angular Distributions of Alpha Particles from the Reaction $C^{12}(p, p'3\alpha)$ — 1034L.
Vasil'kov, R. G. and B. B. Govorkov. Total Cross Section of Photoproduction of π^0 Mesons on Protons at Low Energies — 224L.
—, B. B. Govorkov, and V. I. Gol'danskiĭ. Photoproduction of π Mesons on Hydrogen by γ Quanta with Energy between the Threshold and 240 Mev — 7.
—, B. B. Govorkov, and V. I. Gol'danskiĭ. Photoproduction of π^0 Mesons from Carbon Near Threshold — 818L.
Vavilov, V. S., A. A. Gippius, M. M. Gorshkov, and B. D. Kopylovskiĭ. Radiative Recombination in Germanium Crystals Bombarded by Fast Electrons — 15.
Veklenko, B. A. (see Biberman, L. M.) — 117.
Vernov, S. N., V. A. Dmitriev, V. I. Solov'eva and G. B. Khristiansen. Energy of the Electron-photon Component of Extensive Atmospheric Showers — 1050L.
—, B. A. Khrenov, and G. B. Khristiansen. Investigation of the High Energy μ-Meson Flux in Extensive Atmospheric Showers — 891.
—, G. V. Kulikov, Z. S. Strugalskiĭ, and G. B. Khristiansen. On the Microstructure of the Core of Extensive Air Showers — 848.
Viktor, S. (see Budagov, Yu. A.) — 625L.
Vinokurov, V. M., M. M. Zaripov, and N. R. Yafaev. Fine Structure in the Paramagnetic Resonance Spectrum of Natural Sapphire — 220L.
Vlasov, K. B. and B. Kh. Ishmukhametov. Rotation of the Plane of Polarization of Elastic Waves in Magnetically Polarized Magnetoelastic Media — 531.
Vlasov, N. A. and A. A. Ogloblin. (d, t) Reactions on Li^6, Li^7, and Be^9 Nuclei — 39.
—, S. P. Kalinin, A. A. Ogloblin, and V. I. Chuev. The (d, t) Reaction on C^{12}, F^{19}, and Al^{27} Nuclei — 844.
— (see Artemov, K. P.) — 841.
Vol'f, Yu. Dispersion Relations for Inelastic Processes Involving K Mesons — 980.
Volkov, D. V. and S. V. Peletminskiĭ. On the Lagrangian Formalism for Spin Variables — 121.
Volkov, T. F. Ion Oscillations in a Plasma — 302.
Volkov, V. V., L. I. Guseva, B. F. Myasoedov, N. I. Tarantin, and K. V. Filippova. Cross Section for Production of Fm^{250} in the Reactions $Pu^{241}(C^{13}, 4n)Fm^{250}$ and $U^{238}(O^{16}, 4n)Fm^{250}$ — 859.
Volkova, E. A. (see Novikova, G. I.) — 663.
Volynskiĭ, V. Kh. (see Daĭon, M. I.) — 648.
Vonsovskiĭ, S. V. and M. S. Svirskiĭ. Effect of Exchange Interaction on the Superconductor Transition Temperature — 1060L.
Vorob'ev, A. A., A. P. Komar, and V. A. Korolev. Measurement of the Intensity Ratio of Transitions to the First Excited Levels of the Daughter Nuclei in the Decay of U^{238} and U^{234} — 1032L.
—. A. P. Komar, V. A. Korolev, and G. E. Solyakin. Alpha Spectrum of the Natural Samarium Isotope Mixture — 386L.
Vul, B. M. (see Basov, N. G.) — 416L.
Wang Ling, Transition Probabilities between Rotational States of Non-Axial Odd Nuclei — 821L.
Wrzecionko, J. Ultraviolet Asymptotic Value for the Interaction of K Mesons with Baryons — 69.
Yafaev, N. R. (see Vinokurov, V. M.) — 220L.
Yakovlev, L. G. Calculation of Phase Integrals in the Covariant Formulation of the Theory of Multiple Production of Particles — 741.
Yankov, V. V. Dynamics of a Conducting Gaseous Sphere in a Quasi-Stationary Electromagnetic Field — 158.
Yudin, N. P. (see Balashov, V. V.) — 983.
— (see Neudachin, V. G.) — 1256.
Yurasova, V. E., N. V. Pleshivtsev, and I. V. Orfanov. Directed Emission of Particles from a Copper Single Crystal Sputtered by Bombardment with Ions up to 50 Kev Energy — 689.
Zaikin, D. A. Ground States of Nonspherical Odd Nuclei According to the Independent Particle Model — 381.
Zaĭtseva, M. A. (see Belov, K. P.) — 825L.
Zakhar'ev, B. N. (see Belyaev, V. B.) — 1171.
Zaretskiĭ, D. F. Radiative Capture of Neutrons — 772.
— and V. M. Novikov. Muon Depolarization in Mesic Atoms with Deformed Nuclei — 1287L.
Zaripov, M. M. (see Vinokurov, V. M.) — 220L.
Zastavenko, L. G. A Method for Calculation of Phase Volumes — 939.
Zatsepin, G. T., S. I. Nikol'skiĭ, and A. A. Pomanskiĭ. Decay Processes in the Development of Nuclear Cascades in the Atmosphere — 138.
Zavaritskiĭ, N. V. Investigation of Thermal Properties of Superconductors. III. Anisotropy of Thermal Conductivity of Gallium — 1069.
Zel'dovich, Ya. B. On the Masses of the Muon and the Electron — 1283L.
— The Number of Elementary Baryons and the Universal Baryon Repulsion Hypothesis — 403L.
— and E. M. Rabinovich. On the Conditions of Applicability of Statistical Formulas to a Degenerate Fermi Gas — 924.
Zharkov, G. F. On the Intermediate State of Ferromagnetic Superconductors — 1259.
Zharkov, V. N. and V. P. Silin. Theory of Weak Solutions of He^4 in Liquid He^3 — 102.
Zhdanov, A. P. and P. I. Fedotov. Results of a Study of

the Disintegration of Carbon Nuclei by 660-Mev Protons — 280.
— (see Berkovich, I. B.) — 428.
Zhdanov, G. B., V. M. Maksimenko, M. I. Tret'yakova, and M. N. Shcherbakova. Nuclear Interactions of 8.7-Bev Protons in Photographic Emulsions — 442.
—, P. K. Markov, V. N. Strel'tsov, M. I. Tret'yakova, Cheng P'u-Ying, and M. G. Shafranova. Secondary Stars Created by the Interaction of 8.7 Bev Protons with Photoemulsion Nuclei — 433.
Zhirnov, N. I. Quasiclassical Solutions of the Radial Dirac Equations — 1148.
Zhizhin, E. D. Scattering of a Proton by a Nucleon in the One-Meson Approximation — 707.
Zhumartbaev, M. T. Absorption of Sound and the Width of Shock Waves in Relativistic Hydrodynamics — 711.
Zhuravlev, N. N., A. A. Stepanova, and N. I. Zyuzin. On the Superconductivity of the Compound BiPt — 627L.
Zil'berman, G. E. On the Zone Energy Spectrum in the Presence of a Magnetic Field — 1029.
Zinov'eva, K. N. and V. P. Peshkov. Phase Diagram for Liquid He^3-He^4 Solutions — 22.
Ziv, D. M. (see Novikova, G. I.) — 663.
Zlatev, I. S. and P. S. Isaev. Dispersion Relations for the Virtual Compton Effect — 519.
— and P. S. Isaev. Use of Dispersion Relations for a Test of Quantum Electrodynamics at Small Distances — 826L.
Zyuzin, N. I. (see Zhuravlev, N. N.) — 627L.

Analytic Subject Index to Volume 37 (10)

References with L are Letters to the Editor. Items are listed under the following categories:

Acoustics
Astrophysics
Atomic and Molecular Beams
Atomic Mass and Abundance
Atomic Structure and Spectra
Biographical Material
Cosmic Radiation
Crystalline State
Dielectrics and Dielectric Properties
Diffraction
Diffusion
Elasticity and Plasticity
Electrical Conductivity and Resistance
Electrical Discharges
Electrical Properties
Electromagnetic Theory and Electrodynamics
Electrons and Positrons
Elementary Particle Interactions
Field Theory
Films, Properties
Fluid Dynamics
Gamma Rays
Gases
Helium, Liquid
Imperfections in Solids
Ionization
Ions
Ions and Electrons, Mobility
Liquids
Luminescence
Magnetic Properties
Magnetic Resonance
Mathematical Methods
Mechanics
Mesons and Hyperons
Methods and Instruments
Microwaves
Miscellaneous
Molecular Structure and Spectra
Neutrino
Nuclear Fission
Nuclear Moments and Spin
Nuclear Photoeffects
Nuclear Reactions, General
Nuclear Reactions Induced by α Particles and He^3
Nuclear Reactions Induced by Deuterons and Tritons
Nuclear Reactions Induced by Mesons
Nuclear Reactions Induced by Neutrons
Nuclear Reactions Induced by Protons
Nuclear Spectra
Nuclear Structure Theory
Optical Properties
Quantum Electrodynamics
Quantum Mechanics
Radiation
Radioactivity
Range and Energy Loss of Particles
Relativity and Gravitation
Scattering, General
Scattering of α Particles
Scattering of Deuterons
Scattering of Electrons and Positrons
Scattering of Mesons
Scattering of Neutrons
Scattering of Protons
Semiconductors
Spectra, General
Statistical Mechanics and Thermodynamics
Superconductivity
Thermal Properties
X-rays

Absorption of Radiation (see Radiation)
Acoustics
- Absorption of Sound and the Width of Shock Waves in Relativistic Hydrodynamics. M. T. Zhumartbaev — 711.
- Anomalies in Internal Friction and Modulus of Elasticity in Ferromagnetics near the Curie Point. K. P. Belov, G. I. Kataev, and R. Z. Levitin — 670.
- Coupled Magnetoelastic Oscillations in Antiferromagnetics. S. V. Peletminskiĭ — 321.
- Gravitational Attenuation of Sound. S. B. Pikel'ner — 1290L.
- Oscillations in the Absorption Coefficient of Sound in Tin at Low Temperatures. A. A. Galkin and A. P. Korolyuk — 219L.
- Ultrasonic Absorption in Metals in a Magnetic Field. V. L. Gurevich — 1190.

Afterglow (see Electrical Discharges)
Alloys (see Crystalline State)
Annihilation (see Electrons and Positrons)
Antiferroelectric Phenomena (see Dielectrics and Dielectric Properties)
Antiferromagnetism (see Magnetic Properties)
Arcs (see Electric Discharges)
Astrophysics
- Emission of Neutrino Pairs by Electrons and the Role Played by it in Stars. G. M. Gandel'man and V. S. Pinaev — 764.
- Gravitational Attenuation of Sound. S. B. Pikel'ner — 1290L.

Mechanism for the Production of Relativistic Electrons in the Atmospheres of Nonstationary Stars. I. M. Gordon — 608L.
Residual Ionization of a Gas Expanding in Vacuum. Yu. P. Raĭzer — 411L.

Atomic and Molecular Beams
Experiments in the Production of a New Fermium Isotope. V. P. Perelygin, E. D. Donets, and G. N. Flerov — 1106.
Measurements of Nuclear Magnetic Moments in the Alkali Earths by Molecular Beam Magnetic Resonance. A. G. Kucheryaev, Yu. K. Szhenov, and Sh. M. Gogichaĭshvili — 412L.
Nuclear Reactions Induced by Heavy Ions. J. H. Fremlin and J. S. Lille — 229L.
Use of Slow Molecules in a Maser. N. G. Basov and A. N. Oraevskiĭ — 761.

Atomic Mass and Abundance
Effect of Temperature on the Variation of the Isotopic Composition of Liquid Mercury in the Electric Field of a Constant Current. I. V. Bogoyavlenskiĭ, V. N. Grigor'ev, and N. S. Rudenko — 884.
Experiments in the Production of a New Fermium Isotope. V. P. Perelygin, E. D. Donets, and G. N. Flerov — 1106
Isotopic Masses and Binding Energies of Nuclei for Masses between 186 and 196. R. A. Demirkhanov, T. I. Gutkin, and V. V. Dorokhov — 866.
Possible Method of Identifying New Transuranic Elements. V. I. Gol'danskiĭ and M. I. Podgoretskiĭ — 223L.

Atomic Structure and Spectra
Effect of Pressure on the Raman Spectrum of Oxygen. G. V. Mikhaĭlov — 1114.
Forbidden Transitions in the Deformed Tm^{169} Nucleus. É. E. Berlovich, V. N. Klement'ev, V. G. Fleĭsher, O. V. Larionov, F. M. Murtazin, and D. A. Apostolov — 855.
Maximum Atomic Cross Sections for Nonresonance Charge Exchange. N. V. Fedorenko and V. A. Belyaev — 1276L.
On the Determination of Nuclear Deformation from the Alpha-Decay Fine Structure. V. G. Nosov — 631L.
On the Inclusion of Exchange in the Theory of Collisions. R. K. Peterkop — 834L.
Optical Anisotropy of Atomic Nuclei. A. M. Baldin — 142.
Quasiclassical Solutions of the Radial Dirac Equations. N. I. Zhirnov — 1148.
Radiative Processes Ahead of a Shock-Wave Front. L. M. Biberman and B. A. Veklenko — 117.
The Proton Subshell $Z = 100$. N. N. Kolesnikov and A. P. Krylova — 389L.

Auger Effect (see Atomic Structure and Spectra)
Barkhausen Effect (see Magnetic Properties)
Biographical Material
Academician Nikolaĭ Nikolaevich Bogolyubov (On the Occasion of His Fiftieth Birthday) — 235.
Boson Theory (see Radiation)
Broadening of Spectral Lines (see Atomic Structure and Spectra; Spectra, General)
Capture Cross Sections (see Electrons and Positrons; Nuclear Reactions, General; Radiation)
Cerenkov Effect (see Radiation)
Chemiluminescence (see Luminescence)
Cold Emission (see Electrical Properties)
Compton Effect (see Radiation)
Conductivity, Electrical (see Electrical Conductivity and Resistance)

Cosmic Radiation
Angular Distribution of Shower Particles in Explosion Showers Produced by High-energy Cosmic-ray Particles. A. P. Mishakova and B. A. Nikol'skiĭ — 1130.
Angular Distribution of Shower Particles in Stars Produced by High-energy particles. L. A. San'ko, Zh. S. Takibaev, Ts. I. Shakhova, and L. Ya. Balats — 1.
Decay Processes in the Development of Nuclear Cascades in the Atmosphere. G. T. Zatsepin, S. I. Nikol'skiĭ, and A. A. Pomanskiĭ — 138.
Energy of the Electron-photon Component of Extensive Atmospheric Showers. S. N. Vernov, V. A. Dmitriev, V. I. Solov'eva, and G. B. Khristiansen — 1050L.
Heavy Nuclei Flux in the Primary Cosmic Radiation at a Geomagnetic Latitude of 31° N. K. I. Alekseeva and N. L. Grigorov — 271.
Investigation of a Shower Consisting of 200,000 Particles and Recorded in a Nuclear Photographic Plate. N. L. Grigorov and M. A. Kondrat'eva — 489.
Investigation of High-energy Nuclear-active Particles at Sea Level. V. A. Dmitriev, G. V. Kulikov, and G. B. Khristiansen — 637.
Investigation of Pion Production in Interactions of Cosmic-ray Protons and α Particles with Carbon Nuclei in the Stratosphere. K. I. Alekseeva, S. I. Brikker, N. L. Grigorov, V. S. Murzin, and F. D. Savin — 422.
Investigation of the High Energy Meson Flux in Broad Atmospheric Showers. S. N. Vernov, B. A. Khrenov, and G. B. Khristiansen — 891.
Mechanism for the Production of Relativistic Electrons in the Atmospheres of Nonstationary Stars. I. M. Gordon — 608L.
On an Estimate of Energy Characteristics of Shower Producing Particles. É. G. Boos and Zh. S. Takibaev — 206L.
On Certain Singularities in the Interaction with Light Nuclei of Particles with Energies $E \geq 2 \times 10^{12}$ ev. N. L. Grigorov and V. Ya. Shestoperov — 816L.
On the Measurement of the Momentum of Fast Particles and the Investigation of Nuclear Interaction in the $10^{10} - 10^{12}$ ev Energy Range. M. I. Daĭon and V. Kh. Volynskiĭ — 648.
On the Microstructure of the Core of Extensive Air Showers. S. N. Vernov, G. V. Kulikov, Z. S. Strugal'skiĭ, and G. B. Khristiansen — 848.
On the Theory of the Passage of the Nuclear Cascade Through the Atmosphere. I. P. Ivanenko — 744.
Production of K^+ Mesons by Cosmic-ray Protons at 3250 m Above Sea Level. M. Ya. Balats, P. I. Lebedev, and Yu. V. Obukhov — 417.

Cosmology (see Relativity and Gravitation)
Critical Potentials (see Atomic Structure and Spectra)
Cross Section (see Electrons and Positrons; Nuclear Reactions, General; Scattering, General)

- **Crystal Counters** (see Methods and Instruments)
- **Crystalline** State (see also Electrical Properties; Magnetic Properties; Semiconductors; etc.)
  - Anomalous Heat Capacity and Nuclear Resonance in Crystalline Hydrogen in Connection with New Data on Its Structure. S. S. Dukhin — 1054L.
  - Contribution to the Theory of Spin-lattice Relaxation of Nuclear Spins in Ionic Crystals. B. I. Kochelaev — 171.
  - Diffraction of X-rays by Polycrystalline Samples of Hydrogen Isotopes. V. S. Kogan, B. G. Lazarev, and R. F. Bulatova — 485.
  - Discrete Electron Energy Losses and Secondary Emission from CdO. N. B. Gornyĭ — 242.
  - Dispersion of Electromagnetic Waves in Crystals. V. M. Agranovich — 307.
  - Electron Resonance in Crossed Electric and Magnetic Fields. I. M. Lifshitz and M. I. Kaganov — 392L.
  - Magnetostriction of Antiferromagnetic Nickel Monoxide. K. P. Belov and R. Z. Levitin — 400L.
  - Mutual Solubility of Hydrogen and Deuterium at 4.2°K. R. F. Bulatova, V. S. Kogan, and B. G. Lazarev — 1058L.
  - Nonresonance Absorption of Oscillating Magnetic Field Energy by a Ferromagnetic Dielectric. M. I. Kaganov and V. M. Tsukernik — 587.
  - On the Structure of Solid Hydrogen. A. A. Galkin and I. V. Matyash — 1292L.
  - On the Superconductivity of the Compound BiPt. N. N. Zhuravlev, A. A. Stepanova, and N. I. Zyuzin — 627L.
  - On the Zone Energy Spectrum in the Presence of a Magnetic Field. G. E. Zil'berman — 1029.
  - Paramagnetic Resonance in Magnetically Dilute Systems. N. S. Garif'yanov — 1101.
  - Radiative Recombination in Germanium Crystals Bombarded by Fast Electrons. V. S. Vavilov, A. A. Gippius, M. M. Gorshkov, and B. D. Kopylovskiĭ — 15.
  - Rotation of the Plane of Polarization of Elastic Waves in Magnetically Polarized Magnetoelastic Media. K. B. Vlasov and B. Kh. Ishmukhametov — 531.
  - Superconductivity of Beryllium and its Low-Temperature Polymorphism. B. G. Lazarev, A. I. Sudovtsev, and E. E. Semenenko — 1035L.
  - Theory of Superconducting Alloys in a Strong Magnetic Field Near the Critical Temperature. L. P. Gor'kov — 998.
  - Thermoelectric Coefficients of Metals in Strong Magnetic Fields and the Effect of Drag of Electrons by Phonons. L. É. Gurevich and G. M. Nedlin — 546.
  - Topology of the Fermi Surface of Gold. Yu. P. Gaĭdukov — 913.
  - Ultrasonic Absorption in Metals in a Magnetic Field. II. V. L. Gurevich — 1190.
- **Diamagnetism** (see Magnetic Properties)
- **Dielectrics and Dielectric Properties**
  - Light Waves in Crystals in the Exciton Absorption Region and the Impurity Photoeffect. I. M. Dykman and S. I. Pekar — 361.
  - Quantum Theory of Spatial Dispersion of Electric and Magnetic Susceptibilities. O. V. Konstantinov and V. I. Perel' — 560.
  - Raman Scattering of Electromagnetic Waves in Ferromagnetic Dielectrics. F. G. Bass and M. I. Kaganov — 986.
- **Diffraction**
  - Diffraction of X-rays by Polycrystalline Samples of Hydrogen Isotopes. V. S. Kogan, B. G. Lazarev, and R. F. Bulatova — 485.
- **Diffusion**
  - Effect of Temperature on the Variation of the Isotopic Composition of Liquid Mercury in the Electric Field of a Constant Current. I. V. Bogoyavlenskiĭ, V. N. Grigor'ev, and N. S. Rudenko — 884.
- **Elasticity and Plasticity**
  - Anomalies in Internal Friction and Modulus of Elasticity in Ferromagnetics Near the Curie Point. K. P. Belov, G. I. Kataev, and R. Z. Levitin — 670.
  - Coupled Magnetoelastic Oscillations in Antiferromagnetics. S. V. Peletminskiĭ — 321.
  - Magnetostriction of Antiferromagnetic Nickel Monoxide. K. P. Belov and R. Z. Levitin — 400L.
  - Rotation of the Plane of Polarization of Elastic Waves in Magnetically Polarized Magnetoelastic Media. K. B. Vlasov and B. Kh. Ishmukhametov — 531.
  - The Temperature Dependence of the Elastic Constants of Potassium Bromide Single Crystals. S. P. Nikanorov and A. V. Stepanov — 1280L.
  - Theory of the Stability of Magnetic States of Ferromagnetic Materials in the Magnetization Process. E. I. Kondorskiĭ — 790.
- **Electrical Breakdown** (see Dielectrics and Dielectric Properties; Electrical Discharges)
- **Electrical Conductivity and Resistance**
  - Effect of Temperature on the Variation of the Isotopic Composition of Liquid Mercury in the Electric Field of a Constant Current. I. V. Bogoyavlenskiĭ, V. N. Grigor'ev, and N. S. Rudenko — 884.
  - Electron Resonance in Crossed Electric and Magnetic Fields. I. M. Lifshitz and M. I. Kaganov — 392L.
  - Hall Effect in Ferrites Near the Curie Temperature. K. P. Belov and E. P. Svirina — 862.
  - The Anisotropy of Magnetoresistance and the Topology of Fermi Surfaces of Metals. N. E. Alekseevskiĭ and Yu. P. Gaĭdukov — 481.
  - Thermoelectric Phenomena in Strong Magnetic Fields in Metals Possessing Various Fermi Surfaces. Yu. A. Bychkov, L. É. Gurevich, and G. M. Nedlin — 377.
  - Topology of the Termi Surface of Gold. Yu. P. Gaĭdukov — 913.
- **Electrical Discharges**
  - Concentration of Charged Particles in Plasma of Spark-Discharge Channel. A. A. Mak — 1055L.
  - Convective Pinch Instability. B. B. Kadomtsev — 780.
  - Dynamics of a Conducting Gaseous Sphere in a Quasi-Stationary Electromagnetic Field. V. V. Yankov — 158.
  - Effect of Inelastic Collisions on the Velocity Distribution of Electrons. L. M. Kovrizhnykh — 347.
  - Energy Lost to Radiation in a Gas-Discharge Plasma. V. D. Kirillov — 812L.
  - Equilibrium of a Plasma Toroid in a Magnetic Field. V. D. Shafranov — 775.
  - Growth of Electromagnetic Waves in Interpenetrating

Infinite Moving Media. G. G. Getmantsev — 600.
Ion Oscillations in a Plasma. T. F. Volkov — 302.
Localization of a High-Frequency Induction Discharge. M. D. Raĭzer and S. E. Grebenshchikov — 398L.
Magnetic Trap with Field Increasing toward Periphery. S. Yu. Luk'yanov and I. M. Podgornyĭ — 18.
Nonlinear Lagmuir Electron Oscillations in a Plasma. M. V. Konyukov — 570.
Nonresonance Absorption of Electromagnetic Waves in a Magnetoactive Plasma. B. N. Gershman — 497.
On Equilibrium of a Plasma Under Helical Symmetry. B. B. Kadomtsev — 962.
On the Magnetohydrodynamics of Conducting Fluids. S. I. Braginskiĭ — 1005.
Oscillations of an Electron-ion Plasma. L. M. Kovrizhnykh — 1198.
Oscillations of an Inhomogeneous Plasma in a Magnetic Field. L. I. Rudakov and R. Z. Sagdeev — 952.
Relativistic Transport Equations for a Plasma. I. Yu. L. Klimontovich — 524.
Shortwave Radiation from a Vacuum Spark. S. V. Lebedev, S. L. Mandel'shtam, and G. M. Rodin — 248.
Simple Method for Computing the Mean Range of Radiation in Ionized Gases at High Temperature. Yu. P. Raĭzer — 769.
Stability of a Hollow Gas Conductor in a Magnetic Field. L. M. Kovrizhnykh — 65.
The Influence of Collisions between Electrons on Their Velocity Distribution in Gases and in Semiconductors in an Electric Field. A. V. Gurevich — 215L.

Electrical Properties (see also Dielectrics and Dielectric Properties; Electrical Conductivity and Resistance; Semiconductors; Superconductivity)
An Investigation of the Quantized Oscillations in the Magnetic Susceptibility of Bismuth at Extremely Low Temperatures. N. B. Brandt, A. E. Dubrovskaya, and G. A. Kytin — 405L.
Analysis of Experimental Data Relating to the Surface Impedance of Superconductors. A. A. Abrikosov, L. P. Gor'kov, and I. M. Khalatnikov — 132.
Cyclotron Resonance in Indium at 9300 Mcs. P. A. Bezuglyĭ and A. A. Galkin — 1049L.
Electric Conductivity of the Explosion Products of Condensed Explosives. A. A. Brish, M. S. Tarasov, and V. A. Tsukerman — 1095.
Electron Resonance in Crossed Electric and Magnetic Fields. I. M. Lifshitz and M. I. Kaganov — 392L.
Measurement of Energy Loss of Fast Electrons Penetrating Through Matter. N. A. Grishaev, A. N. Fisun, A. S. Litvinenko, V. M. Grizhko, B. I. Shramenko, and I. N. Onishchenko — 1031L.
On the Connection between the Optical Constants of Metals and Their Microscopic Characteristics. G. P. Motulevich — 1249.
The Anisotropy of Magnetoresistance and the Topology of Fermi Surfaces of Metals. N. E. Alekseevskiĭ and Yu. P. Gaĭdukov — 481.
Thermoelectric Phenomena in Strong Magnetic Fields in Metals Possessing Various Fermi Surfaces. Yu. A. Bychkov, L. É. Gurevich, and G. M. Nedlin — 377.
Velocity Distribution of Electrons in a Strong Electric Field. L. M. Kovrizhnykh — 989.

Electrodynamics (see Electromagnetic Theory and Electrodynamics)

Electromagnetic Theory and Electrodynamics
Attraction of Small Particles Suspended in a Liquid at Large Distances. L. P. Pitaevskiĭ — 408L.
Capture Mechanism in Betatrons. I. M. Samoĭlov — 504.
Coherent Electron Radiation in the Synchrotron. II. L. V. Iogansen and M. S. Rabinovich — 83.
Collective Losses of Fast Electrons in Passage Through Matter. V. P. Silin — 192.
Convective Pinch Instability. B. B. Kadomtsev — 780.
Dispersion of Electromagnetic Waves in Crystals. V. M. Agranovich — 307.
Dynamics of a Conducting Gaseous Sphere in a Quasi-stationary Electromagnetic Field. V. V. Yankov — 158.
Effect of Inelastic Collisions on the Velocity Distribution of Electrons. L. M. Kovrizhnykh — 347.
Effect of Multiple Scattering on Pair Production by High-Energy Particles in a Medium. F. F. Ternovskiĭ — 718.
Electron Resonance in Crossed Electric and Magnetic Fields. I. M. Lifshitz and M. I. Kaganov — 392L.
Equilibrium of a Plasma Toroid in a Magnetic Field. V. D. Shafranov — 775.
Field of a Charged Particle in a Moving Medium. B. M. Bolotovskiĭ and A. A. Rukhadze — 958.
Growth of Electromagnetic Waves in Interpenetrating Infinite Moving Media. G. G. Getmantsev — 600.
Ion Oscillations in a Plasma. T. F. Volkov — 302.
Limits of Applicability of the Theory of Transition Radiation. G. M. Garibyan and I. Ya. Pomeranchuk — 1290L.
Localization of a High-frequency Induction Discharge. M. D. Raĭzer and S. E. Grebenshchikov — 398L.
Magnetic Trap with Field Increasing toward Periphery. S. Yu. Luk'yanov and I. M. Podgornyĭ — 18.
Motion of Charged Particle in a Rotating Magnetic Field. A. P. Kazantsev — 1036L.
Nonlinear Langmuir Electron Oscillations in a Plasma. M. V. Konyukov — 570.
Nonresonance Absorption of Electromagnetic Waves in a Magnetoactive Plasma. B. N. Gershman — 497.
Convective Motion of a Conducting Fluid between Parallel Vertical Plates in a Magnetic Field. S. A. Regirer — 149.
On Equilibrium of a Plasma Under Helical Symmetry. B. B. Kadomtsev — 962.
On the Magneto-electrical Effect in Antiferromagnets. I. E. Dzyaloshinskiĭ — 628L.
On the Magnetohydrodynamics of Conducting Fluids. S. I. Braginskiĭ — 1005.
On the Solution of the Kinetic Equation for a Plasma in a Variable Magnetic Field. Yu. N. Barabanenkov — 305.
On the Stability of a Low Pressure Plasma. B. B. Kadomtsev — 1167.
On the Stability of Plane Poiseuille Flow of a Plasma of Finite Conductivity in a Magnetic Field. Yu. A. Tarasov — 1209.
Oscillations of an Electron-Ion Plasma. L. M. Kovrizhnykh — 1198.
Oscillations of an Inhomogeneous Plasma in a Magnetic

Field. L. I. Rudakov and R. Z. Sagdeev — 952.
  Polarization Phenomena in Radiative Collisions of Two Electrons. V. L. Lyuboshitz — 1221.
  Propagation of a Strong Electromagnetic-gravitational Wave in Vacuo. A. S. Kompaneets — 1218.
  Quantum Theory of Spatial Dispersion of Electric and Magnetic Susceptibilities. O. V. Konstantinov and V. L. Perel’ — 560.
  Raman Scattering of Electromagnetic Waves in Ferromagnetic Dielectrics. F. G. Bass and M. I. Kaganov — 986.
  Simple Waves in the Chew-Goldberger-Low Approximation. I. A. Akhiezer, R. V. Polovin, and N. L. Tsintsadze — 539.
  Stability of a Hollow Gas Conductor in a Magnetic Field. L. M. Kovrizhnykh — 65.
  The Radiative Correction to the Mass of the Electron in Nonlinear Electrodynamics. V. Yu. Urbakh — 208L.
  Thermoelectric Coefficients of Metals in Strong Magnetic Fields and the Effect of Drag of Electrons by Phonons. L. É. Gurevich and G. M. Nedlin — 546.
  Transition Radiation Effects in Particle Energy Losses. G. M. Garibyan — 372.
  Transition Radiation in Waveguides. K. A. Barsukov — 787.
  Ultrasonic Absorption in Metals in a Magnetic Field. I. V. L. Gurevich — 51.
  Use of Slow Molecules in a Maser. N. G. Basov and A. N. Oraevskiĭ — 761.

Electron Diffraction (see Scattering of Electrons and Positrons)

Electron-Optical Effects (see Optical Properties)

Electron Optics (see Methods and Instruments)

Electrons and Positrons (see also Electromagnetic Theory and Electrodynamics; Elementary Particle Interaction; Scattering of Electrons and Positrons)
  Application of the Variational Principle for the Determination of the Binding Energy of a Proton-Electron-Positron System. V. P. Shmelev — 325.
  Discrete Electron Energy Losses and Secondary Emission from CdO. N. B. Gornyĭ —242.
  Dispersion of Electromagnetic Waves in Crystals. V. M. Agranovich — 307.
  Effect of Inelastic Collisions on the Velocity Distribution of Electrons. L. M. Kovrizhnykh — 347.
  Effect of Multiple Scattering on Pair Production by High-Energy Particles in a Medium. F. F. Ternovskiĭ — 718.
  Effect of Vacuum Fluctuations on the Polarization of Electrons Moving in a Magnetic Field. I. M. Ternov and V. S. Tumanov — 809L.
  Inelastic Collisions Between Fast Polarized Particles and Atoms. V. V. Batygin and I. N. Toptygin — 975.
  Measurement of the Degree of Longitudinal Polarization of Beta Particles. L. A. Mikaélyan and P. Ya. Spivak — 831L.
  Mechanism for the Production of Relativistic Electrons in the Atmospheres of Nonstationary Stars. I. M. Gordon — 608L.
  On Direct Production of Electron-positron Pairs by High-energy Electrons. V. A. Tumanyan, G. S. Stolyarova, and A. P. Mishakova — 253.
  On Lepton Mass. Yu. A. Gol’fand — 1059L.
  On the Inclusion of Exchange in the Theory of Collisions. R. K. Peterkop — 834L.
  On the Solution of the Kinetic Equation for a Plasma in a Variable Magnetic Field. Yu. N. Barabanenkov — 305.
  Pair Production in Collisions Between Charged Particles. F. F. Ternovskiĭ — 565.
  Polarization Effects in the Direct Transition of $\mu^+\mu^-$ into an Electron-positron Pair. B. A. Lysov — 404L.
  Polarization Effects in the $\pi^0 \rightarrow e^- + e^+ + \gamma$ Decay. B. K. Kerimov, A. I. Mukhtarov, and S. A. Gadzhiev — 407L.
  Polarization Phenomena in Radiative Collisions of Two Electrons. V. L. Lyuboshitz — 1221.
  Scattering of Low-energy Electron by Short-range Potential in Strong Magnetic Field. V. G. Skobov — 1039L.
  Search for Particles with Mass between 6 and 25 Electron Masses. A. S. Belousov, S. V. Rusakov, E. I. Tamm, and P. A. Cerenkov — 1143.
  Space Asymmetry of Low-energy Positrons from $\pi^+ - \mu^+ - e^+$ Decay. A. O. Vaĭsenberg — 401L.
  The Spectrum of Internal Conversion Electrons Accompanying Alpha Decay of U^{233}, and the Level Scheme of Th^{229}. E. F. Tret’yakov, M. P. Anikina, L. L. Gol’din, G. I. Novikova, and N. I. Pirogova — 656.
  Theory of Superconducting Alloys in a Strong Magnetic Field Near the Critical Temperature. L. P. Gor’kov — 998.
  Thermoelectric Coefficients of Metals in Strong Magnetic Fields and the Effect of Drag of Electrons by Phonons. L. É. Gurevich and G. M. Nedlin — 546.
  Three-Electron Decay of the Muon. I. I. Gurevich, B. A. Nikol’skiĭ, and L. V. Surkova — 225L.
  Ultrasonic Absorption in Metals in a Magnetic Field. I. V. L. Gurevich — 51.

Electrons, Scattering (see Scattering of Electrons and Positrons)

Electrons, Secondary (see Electrical Properties)

Electrostriction (see Dielectrics and Dielectric Properties)

Elementary Particle Interactions
  Angular Asymmetry in (πN) Collisions and ($\pi\pi$) Interaction. V. S. Barashenkov — 1038L.
  Angular Distribution of Shower Particles in Stars Produced by High-energy Particles. L. A. San’ko, Zh. S. Takibaev, Ts. I. Shakhova, and L. Ya. Balats — 1.
  Angular Distributions of Alpha Particles from the Reaction C^{12} (p, p′3α). S. S. Vasil’ev, V. V. Komarov, G. V. Koshelyaev, and A. M. Popova — 1034L.
  Capture of μ^--Mesons by Light Nuclei. B. L. Ioffe — 113.
  Contribution of Three-particle Forces to the Binding Energy of Hypernuclei. V. A. Lyul’ka and V. A. Filimonov — 1015.
  Contribution to the Theory of Spin-lattice Relaxation of Nuclear Spins in Ionic Crystals. B. I. Kochelaev — 171.
  Decay Processes in the Development of Nuclear Cascades in the Atmosphere. G. T. Zatsepin, S. I. Nikol’skiĭ, and A. A. Pomanskiĭ — 138.

Dispersion Relations for Inelastic Processes Involving K Mesons. J. Wolf — 980.
Dispersion Relations for the Virtual Compton Effect. I. S. Zlatev and P. S. Isaev — 519.
Effect of Interaction on the Phase Motion of Electrons in a Synchrotron. L. V. Iogansen — 211L.
Effect of Viscosity in Multiple Production on the Energy Distribution of Secondary Particles. A. A. Emel'yanov and D. S. Chernavskiĭ — 753.
Elastic Scattering of 8.7 Bev Protons by Photoemulsion Nuclei. B. P. Bannik, V. G. Grishin, M. Ya. Danysh, V. B. Lyubimov, and M. I. Podgoretskiĭ — 1118.
Elastic Scattering of 630-Mev Neutrons by Protons. N. S. Amaglobeli and Yu. M. Kazarinov — 1125.
Elastic Scattering of 390-Mev π^+ Mesons from Protons. E. L. Grigor'ev and N. A. Mitin — 1123.
Electromagnetic Mass of the K Meson. Chou Kuang-Chao and V. I. Ogievetskiĭ — 616L.
Electron and Muon Neutrinos. B. Pontecorvo — 1236.
Electron-Electron Scattering and Quantum Electrodynamics at Small Distances. G. V. Avakov — 604L.
Electron-Electron Scattering Cross Section at High Energies. V. N. Baĭer — 1057L.
Emitters of X-particles with Energies of About 9 and 12 Mev. V. A. Karnaukhov, V. I. Khalizev, and G. N. Flerov — 901.
Identification of Particles in High Energy Stars. G. I. Kopylov — 393L.
Inelastic Collisions Between Fast Polarized Particles and Atoms. V. V. Batygin and I. N. Toptygin — 975.
Interaction of 9-Bev Protons with Free and Quasifree Nucleons in Photographic Emulsions. N. P. Bogachev, S. A. Bunyatov, I. M. Gramenitskiĭ, V. B. Lyubimov, Yu. P. Merekov, M. I. Podgoretskiĭ, V. M. Sidorov, and D. Tuvdendorzh — 872.
Investigation of High-energy Nuclear-active Particles at Sea Level. V. A. Dmitriev, G. V. Kulikov, and G. B. Khristiansen — 637.
Measurement of the Degree of Longitudinal Polarization of Beta Particles. L. A. Mikaélyan and P. Ya. Spivak — 831L.
Nonmesonic Decay of Hyperfragments. I. B. Berkovich, A. P. Zhdanov, F. G. Lepekhin, and Z. S. Khokhlova — 428.
Note on a Baryon Scheme. H. Oiglane — 394L.
Nuclear Interactions of 8.7-Bev Protons in Photographic Emulsions. G. B. Zhdanov, V. M. Maksimenko, M. I. Tret'yakova, and M. N. Shcherbatova — 442.
On a Certain Possibility of Investigation of the Structure of Nucleons and Nuclei. N. G. Birger and Yu. A. Smorodin — 964.
On a Certain Possibility of Setting up a System of "Elementary" Particles. I. V. Chuvilo — 994.
On a Symmetry in τ^0 Decay. M. I. Shirokov — 232L.
On an Estimate of Energy Characteristics of Shower Producing Particles. É. G. Boos and Zh. S. Takibaev — 206L.
On Direct Production of Electron-positron Pairs by High-energy Electrons. V. A. Tumanyan, G. S. Stolyarova, and A. P. Mishakova — 253.
On Electromagnetic Corrections in μ-e Decay. V. P. Kuznetsov — 784.
On K_{e4} Decay. L. B. Okun' and E. P. Shabalin — 1252.
On Lepton Mass. Yu. A. Gol'fand — 1059L.
On the Absorption of π^+ Mesons with Energies of About 50 Mev by Carbon Nuclei. J. V. Laberrrigue-Frolova, M. P. Balandin, and S. Z. Otvinovskiĭ — 452.
On the Anomalous Magnetic Moment of Nucleons in Chew's Method. Yu. M. Lomsadze, V. I. Lend'el, and B. M. Érnst — 955.
On the Calculation of the Interaction Constant in a Nonlinear Theory. Ya. I. Granovskiĭ — 135.
On the Collisions of Nucleons with Large Orbital Angular Momentum. A. D. Galanin, A. F. Grashin, B. L. Ioffe, and I. Ya. Pomeranchuk — 1179.
On the Determination of the Potential in Quantum Field Theory. M. A. Braun — 582.
On the Introduction of an "Elementary Length" in the Relativistic Theory of Elementary Particles. Yu. A. Gol'fand — 356.
On the Massey Parameter in the Theory of Atomic Collisions. G. F. Drukarev — 603L.
On the Measurement of the Momentum of Fast Particles and the Investigation of Nuclear Interaction in the $10^{10}-10^{12}$ ev Energy Range. M. I. Daĭon and V. Kh. Volynskiĭ — 648.
On the Possibility of Determining the Amplitude for Charge Exchange Pion-pion Scattering from an Analysis of the $\pi^- + p = N + \pi^+ + \pi^-$ Reactions near Threshold. A. A. Ansel'm and V. N. Gribov — 354.
On the Problem of Investigating the Interaction between Mesons and Hyperons. L. I. Lapidus and Chou Kuang-Chao — 199.
On the Theory of Neutron Beta Decay. S. M. Bilen'kiĭ, R. M. Ryndin, Ya. A. Smorodinskiĭ, and Ho Tso-Hsiu — 1241.
On Two Types of Neutrinos, the Isotopic Spin of Leptons, and the Universal Four-fermion Interaction. É. M. Lipmanov — 750.
Parity Nonconservation in Strong Interactions of Strange Particles. S. G. Matinyan — 736.
Passage of Particles through a Plasma. A. I. Larkin — 186.
Photoproduction of Neutral π Mesons on Hydrogen by γ Quanta with Energy between the Threshold and 240 Mev. R. G. Vasil'kov, B. B. Govorkov, and V. I. Gol'danskiĭ — 7.
Photoproduction of π^0 Mesons from Carbon near Threshold. R. G. Vasil'kov, B. B. Govorkov, and V. I. Gol'danskiĭ — 818L.
π^--p Interaction at 1.4 Bev. V. I. Rus'kin — 74.
Pionic and Electromagnetic Structure of Nucleons. B. B. Dotsenko — 1048L.
Polarization Effects in the Direct Transition of $\mu^+\mu^-$ into an Electron-Positron Pair. B. A. Lysov — 404L.
Potential Barrier Criterion and Stars in Emulsions. P. I. Fedotov — 674.
Production of K^+ Mesons by Cosmic-ray Protons at 3250 m above Sea Level. M. Ya. Balats, P. I. Lebedev, and Yu. V. Obukhov — 417.
Relativistic Spherical Functions. A. Z. Dolginov and I. N. Toptygin — 1022.
Resonance Interaction of Pions. V. S. Barashenkov and V. M. Mal'tsev — 630L.

Results of a Study of the Disintegration of Carbon Nuclei by 660-Mev Protons. A. P. Zhdanov and P. I. Fedotov — 280.
Scattering of a Proton by a Nucleon in the One-Meson Approximation. E. D. Zhizhin — 707.
Secondary Stars Created by the Interaction of 8.7-Bev Protons with Photoemulsion Nuclei. G. B. Zhdanov, P. K. Markov, V. N. Strel'tsov, M. I. Tret'yakova, Cheng P'u-Ying, and M. G. Shafranova — 433.
Space Asymmetry of Low-energy Positrons from π^+-μ^+-e^+ Decay. A. O. Vaĭsenberg — 401L.
The Electromagnetic Interaction in the Heisenberg Theory. Ya. I. Granovskiĭ — 314.
The Formfactor and the Leptonic Decay Probability of the Particle. Ho Tso-Hsiu — 1288L.
The $\mu \rightarrow e + \gamma$ and $\mu \rightarrow e + \nu + \overline{\nu} + \gamma$ Decays. Yu. S. Krestnikov, A. G. Meshkovskiĭ, Ya. Ya. Shalamov, V. A. Shebanov, and I. Yu. Kobzarev — 622L.
The Number of Elementary Baryons and the Universal Baryon Repulsion Hypothesis. Ya. B. Zel'dovich — 403L.
Theoretical Interpretation of Inelastic (pp) and (pn) Collisions at 9 Bev Energy. V. S. Barashenkov, V. M. Mal'tsev, and É. K. Mikhul — 1052L.
The Ultraviolet Asymptotic Value for the Interaction of K Mesons with Baryons. J. Wrzecionko — 69.
Three-electron Decay of the Muon. I. I. Gurevich, B. A. Nikol'skiĭ, and L. V. Surkova — 225L.

Elements (see Atomic Mass and Abundance)
Energy Loss of Particles (see Range and Energy Loss)
Energy States of Atoms (see Atomic Structure and Spectra)
Energy States of Nucleus (see Nuclear Reactions; Nuclear Spectra; Nuclear Structures)
Evaporation (see Liquids)
Excitation of Atoms (see Atomic Structure and Spectra)
Excitation of Nucleus (see Nuclear Reactions; Nuclear Spectra; Nuclear Structure)
Faraday Effect (see Optical Properties)
Ferroelectric Phenomena (see Dielectrics and Dielectric Properties)
Field Emission (see Electrical Properties)
Field Theory
Analyticity and Unitarity in the Scattering of Scalar Mesons from a Static Nucleon. B. L. Ioffe — 1245.
Concerning Anomalous Equations for Spin $\frac{1}{2}$ Particles. I. Marek and I. Ulehla — 1051L.
Dispersion Relations for Inelastic Processes Involving K Mesons. Yu. Vol'f — 980.
Dispersion Relations for the Scattering of Gamma Quanta by Nucleons. L. I. Lapidus and Chou Kuang-Chao — 1213.
Dispersion Relations for the Virtual Compton Effect. I. S. Zlatev and P. S. Isaev — 519.
Effect of Multiple Scattering on Pair Production by High-energy Particles in a Medium. F. F. Ternovskiĭ — 718.
Electronic Mass of the K Meson. Chou Kuang-Chao and V. I. Ogievetskiĭ — 616L.
Incompatibility of the Conditions of Analyticity and Unitarity in the Lee Model. K. A. Ter-Martirosyan — 714.
On Electromagnetic Corrections in μ-e Decay. V. P. Kuznetsov — 784.
On the Analytic Properties of Vertex Parts in Quantum Field Theory. L. D. Landau — 45.
On the Calculation of the Interaction Constant in a Nonlinear Theory. Ya. I. Granovskiĭ — 135.
On the Collisions of Nucleons with Large Orbital Angular Momentum. A. D. Galanin, A. F. Grashin, B. L. Ioffe, and I. Ya. Pomeranchuk — 1179.
On the Connection of Isotopic Spin and Strangeness with the Behavior of Spinors under Inversion. A. M. Brodskiĭ and D. D. Ivanenko — 624L.
On the Determination of the Potential in Quantum Field Theory. M. A. Braun — 582.
On the Lagrangian Formalism for Spin Variables. D. V. Volkov and S. V. Peletminskiĭ — 121.
On the Masses of the Muon and the Electron. Ya. B. Zel'dovich — 1283L.
On the Superfluidity of Liquid He^3. L. P. Pitaevskiĭ — 1267.
On the Theory of Neutron Beta Decay. S. M. Bilen'kiĭ, R. M. Ryndin, Ya. A. Smorodinskiĭ, and Ho Tso-Hsiu — 1241.
On Theories with an Indefinite Metric. V. G. Vaks — 332.
Parity Nonconservation in Strong Interactions of Strange Particles. S. G. Matinyan — 736.
Pionic and Electromagnetic Structure of Nucleons. B. B. Dotsenko — 1048L.
Scattering of a Proton by a Nucleon in the One-Meson Approximation. E. D. Zhizhin — 707.
The Electromagnetic Interaction in the Heisenberg Theory. Ya. I. Granovskiĭ — 314.
The Formfactor and the Leptonic Decay Probability of the Particle. Ho Tso-Hsiu — 1288.
The Non-additivity of London-Van der Waals Forces. L. I. Podlubnyĭ — 633L.
The Radiative Correction to the Mass of the Electron in Nonlinear Electrodynamics. V. Yu. Urbakh — 208L.
The Ultraviolet Asymptotic Value for the Interaction of K Mesons with Baryons. J. Wrzecionko — 69.
Two-particle Excitations of Superfluid Fermi Systems. Yu. V. Tsekhmistrenko — 829L.
Wave Equations with Zero and Nonzero Rest Masses. V. I. Ogievitskiĭ and I. V. Polubarinov — 335.
Films, Properties
Collective Losses of Fast Electrons in Passage through Matter. V. P. Silin — 192.
Destruction of Superconductivity in Thin Films by Field and Current. N. I. Ginzburg and A. I. Shal'nikov — 285.
Van der Waals Forces in Liquid Films. I. E. Dzyaloshinskiĭ, E. M. Lifshitz, and L. P. Pitaevskiĭ — 161.
Fine Structure (see Atomic Structure and Spectra)
Fission of Nucleus (see Nuclear Fission)
Fluid Dynamics
Absorption of Sound and the Width of Shock Waves in Relativistic Hydrodynamics. M. T. Zhumartbaev — 711.
Convective Pinch Instability. B. B. Kadomtsev — 780.
Effect of Viscosity in Multiple Production on the En-

- ergy Distribution of Secondary Particles. A. A. Emel'yanov and D. S. Chernavskiĭ — 753.
- Equilibrium of a Plasma Toroid in a Magnetic Field. V. D. Shafranov — 775.
- Experimental Investigation of the Harmonic Oscillations of a Disk in Rotating Helium. II. E. L. Andronikashvili and D. S. Tsakadze — 397L.
- Nonlinear Langmuir Electron Oscillations in a Plasma. M. V. Konyukov — 570.
- Convective Motion of a Conducting Fluid between Parallel Vertical Plates in a Magnetic Field. S. A. Regirer — 149.
- On Equilibrium of a Plasma under Helical Symmetry. B. B. Kadomtsev — 962.
- On the Magnetohydrodynamics of Conducting Fluids. S. I. Braginskiĭ — 1005.
- On the Paper of V. A. Belokon': "The Permanent Structure of Shock Waves with Joule Dissipation". A. G. Kulikovskiĭ, and G. A. Lyubimov — 835L.
- On the Stability of a Low-pressure Plasma. B. B. Kadomtsev — 1167.
- On the Stability of Plane Poiseuille Flow of a Plasma of Finite Conductivity in a Magnetic Field. Yu. A. Tarasov — 1209.
- Radiative Processes Ahead of a Shock-wave Front. L. M. Biberman and B. A. Veklenko — 117.
- Simple Waves in the Chew-Goldberger-Low Approximation. I. A. Akhiezer, R. V. Polovin, and N. L. Tsintsadze — 539.
- Some Problems of the Dynamics and Heating of a Conducting Medium in a Magnetic Field. G. S. Golitsyn — 756.
- Superfluidity and the Moments of Inertia of Nuclei. A. B. Migdal — 176.
- The Landau Correction Coefficient in the Determination of the Viscosity of a Liquid. G. A. Gamtsemlidze — 609L.

Galvanomagnetic Effect (see Magnetic Properties)

Gamma Rays
- Angular Anisotropy of Gamma Quanta that Accompany Fission. V. M. Strutinskiĭ — 613L.
- Angular Correlation of Internal Conversion, Including Effects of Screening and of the Finite Size of the Nucleus. A. K. Ustinova — 216L.
- Electric Quadrupole Gamma Transitions in Even-even Nuclei. N. N. Delyagin — 605L.
- Gamma Rays from a Po—O^{18} Neutron Source. É. M. Tsenter, A. G. Khabakhpashev, and I. A. Pirkin — 806L.
- Measurement of the Lifetime of the First Excited State of Ne^{21}. A. G. Khabakhpashev and É. M. Tsenter — 705.
- Multipolarities of Gamma Transitions in Tm^{169}. V. M. Kel'man, R. Ya. Metskhvarishvili, B. K. Preobrazhenskiĭ, V. A. Romanov, and V. V. Tuchkevich — 456.
- Optical Anisotropy of Atomic Nuclei. A. M. Baldin — 142.
- Radioactive Decay of Ag^{110m}. N. M. Anton'eva, A. A. Bashilov, and E. K. Kulakovskiĭ — 1063.
- Resonance Scattering of Gamma Quanta by Mg^{14}. I. Sh. Vashakidze, T. I. Kopaleĭshvili, and G. A. Chilashvili — 535.
- Search for Particles with Mass between 6 and 25 Electron Masses. A. S. Belousev, S. V. Rusakov, E. I. Tamm, and P. A. Cerenkov — 1143.
- Small Angle Rayleigh Scattering of Co^{60} Gamma Rays. B. A. Bel'skiĭ and S. V. Starodubtsev — 700.
- The Spectrum of Internal Conversion Electrons Accompanying Alpha Decay of U^{233}, and the Level Scheme of Th^{229}. E. F. Tret'yakov, M. P. Anikina, L. L. Gol'din, G. I. Novikova, and N. I. Pirogeva — 656.

Gases
- Condensation of a Cloud of Vaporized Matter Expanding in Vacuum. Yu. P. Raĭzer — 1229.
- Effect of Pressure on the Raman Spectrum of Oxygen. G. V. Mikhaĭlov — 1114.
- Formation of Negative Hydrogen Ions on an Incandescent Tungsten Surface. V. I. Khvostenko and V. M. Dukel'skiĭ — 465.
- Maximum Atomic Cross Sections for Nonresonance Charge Exchange. N. V. Fedorenko and V. A. Belyaev — 1276L.
- On Hydrodynamic Boundary Conditions for Evaporation and Condensation. R. Ya. Kucherov and L. É. Rikenglaz — 88.
- Radiative Processes Ahead of a Shock-wave Front. L. M. Biberman and B. A. Veklenko — 117.
- Residual Ionization of a Gas Expanding in Vacuum. Yu. P. Raĭzer — 411L.

Gravitation (see Relativity and Gravitation)

Gyromagnetization (see Magnetic Properties)

Hall Effect (see Electrical Conductivity and Resistance; Semiconductors)

Helium, Liquid
- Experimental Investigation of the Harmonic Oscillations of a Disk in Rotating Helium. II. E. L. Andronikashvili and D. S. Tsakadze — 397L.
- Hydrodynamics of Solutions of Strange Particles in Helium II near the λ-Point. D. G. Sanikidze — 226L.
- On the Critical Mode in Experiments with an Oscillating Disk in Helium II. G. A. Gamtsemlidze — 678.
- On the Motion of Charges in Liquid Helium II. R. G. Arkhipov and A. I. Shal'nikov — 888..
- On the Question of Critical Velocities for Flow of He II in Capillaries. B. T. Geĭlikman — 635L.
- On the Superfluidity of Liquid He^3. L. P. Pitaevskiĭ — 1267.
- Phase Diagram for Liquid He^3-He^4 Solutions. K. N. Zinov'eva and V. P. Peshkov — 22.
- The Propagation of Oscillations along Vortex Lines in Rotating Helium II. É. L. Andronikashvili and D. S. Tsakadze — 227L.
- The Use of a Superconducting Ring for Registering the Phase Transition in Liquid Helium. B. N. Esel'son and A. D. Shvets — 228L.
- Van der Waals Forces in Liquid Films. I. E. Dzyaloshinskiĭ, E. M. Lifshitz, and L. P. Pitaevskiĭ — 161.

High Voltage Tubes and Machines (see Methods and Instruments)

Hyperfine Structure (see Atomic Structure and Spectra; Nuclear Moments and Spin)

Hyperons (see Mesons and Hyperons)

Imperfections in Solids
- Fine Structure in the Paramagnetic Resonance Spec-

trum of Natural Sapphire. V. M. Vinokurov, M. M. Zaripov, and N. R. Yafaev — 220L.
On the Superconductivity of the Compound BiPt. N. N. Zhuravlev, A. A. Stepanova, and N. I. Zyuzin — 627L.
Theory of the Stability of Magnetic States of Ferromagnetic Materials in the Magnetization Process. E. I. Kondorskiĭ — 790.
Inelastic Scattering (see Nuclear Reactions; Scattering)
Instruments (see Methods and Instruments)
Internal Conversion (see Nuclear Spectra)
Ionization (see also Electrical Discharges; Range and Energy Loss of Particles)
Alpha Spectrum of the Natural Samarium Isotope Mixture. A. A. Vorob'ev, A. P. Komar, V. A. Korolev, and G. E. Solyakin — 386L.
Formation of Negative Hydrogen Ions on an Incandescent Tungsten Surface. V. I. Khvostenko and V. M. Dukel'skiĭ — 465.
Kinetic Theory of Impact Ionization in Semiconductors. L. V. Keldysh — 509.
Maximum Atomic Cross Sections for Nonresonance Charge Exchange. N. V. Fedorenko and V. A. Belyaev — 1276L.
On the Mechanism of Surface Ionization of Atoms of the Alkali Earth Metals — Yu. K. Szhenov — 239.
On Certain Singularities in the Interaction with Light Nuclei of Particles with Energies $E \geq 2 \times 10^{12}$ ev. N. L. Grigorov and V. Ya. Shestoperov — 816L.
Radiative Processes Ahead of a Shock-wave Front. L. M. Biberman and B. A. Veklenko — 117.
Shortwave Radiation from a Vacuum Spark. S. V. Lebedev, S. L. Mandel'shtam, and G. M. Rodin — 248.
Simple Method for Computing the Mean Range of Radiation in Ionized Gases at High Temperatures. Yu. P. Raĭzer — 769.
Ionization Potentials of Atoms (see Atomic Structure and Spectra)
Ions (see also Electrical Discharges)
Emitters of α-Particles with Energies of about 9 and 12 Mev. V. A. Karnaukhov, V. I. Khalizev, and G. N. Flerov — 901.
Experiments in the Production of a New Fermium Isotope. V. P. Perelygin, E. D. Donets, and G. N. Flerov — 1106.
Maximum Atomic Cross Section for Nonresonance Charge Exchange. N. V. Fedorenko and V. A. Belyaev — 1276L.
Measurements of the Transverse Proton Relaxation Time in Aqueous Solutions of Paramagnetic Salts by the Spin-Echo Method — 218L.
Paramagnetic Resonance in Magnetically Dilute Systems. N. S. Garif'yanov — 1101.
Resonance Charge Exchange of Doubly Charged Ions in Slow Collisions. I. K. Fetisov and O. B. Firsov — 67.
Sputtering of Copper by Hydrogen Ions Possessing Energies up to 50 kev. N. V. Pleshivitsev — 878.
Ions and Electrons, Mobility
Hall Effect in Ferrites Near the Curie Temperature. K. P. Belov and E. P. Svirina — 862.
On the Motion of Charges in Liquid Helium II. R. G. Arkhipov and A. I. Shal'nikov — 888.
Velocity Distribution of Electrons in a Strong Electric Field. L. M. Kovrizhnykh — 989.
Isomers, Nuclear (see Nuclear Spectra)
Isotopes (see Atomic Mass and Abundance; Radioactivity)
Kerr Effect (see Optical Properties)
Liquid Helium (see Helium, Liquid)
Liquids
Concentration Jump in Slow Evaporation of a Mixture. R. Ya. Kucherov and L. É. Rikenglaz — 1285L.
Experimental Investigation of the Harmonic Oscillations of a Disk in Rotating Helium II. E. L. Andronikashvili and D. S. Tsakadze — 397L.
Theory of Weak Solutions of He^4 in Liquid He^3. V. N. Zharkov and V. P. Silin — 102.
Van der Waals Forces in Liquid Films. I. E. Dzyaloshinskiĭ, E. M. Lifshitz, and L. P. Pitaevskiĭ — 161.
Luminescence
Detection of Ionization of Eu^{++} in the SrS-Eu, Sm Phosphor by the Paramagnetic Absorption Method. V. V. Antonov-Romanovskiĭ, V. G. Dubinin, A. M. Prokhorov, Z. A. Trapeznikova, and M. V. Fock — 1039L.
Magnetic Fields (see Electromagnetic Theory and Electrodynamics)
Magnetic Properties
An Investigation of the Quantized Oscillations in the Magnetic Susceptibility of Bismuth at Extremely Low Temperatures. N. B. Brandt, A. E. Dubrovskaya, and G. A. Kytin — 405L.
Anomalies in Internal Friction and Modulus of Elasticity in Ferromagnetics Near the Curie Point. K. P. Belov, G. I. Kataev, and R. Z. Levitin — 670.
Antiferromagnetism in NiF_2. R. A. Alikhanov — 814L.
Coupled Magnetoelastic Oscillations in Antiferromagnetics. S. V. Peletminskiĭ — 321.
Effect of Uniaxial Compression on the Quantum Oscillations of the Magnetic Susceptibility of Bismuth. N. B. Brandt and G. A. Ryabenko — 278.
Features of Magnetic Hysteresis Phenomena in the Systems $Pr_2O_3 \cdot Fe_2O_3$ and $La_2O_3 \cdot Fe_2O_3$. K. P. Belov, M. A. Zaĭtseva, and A. M. Kadomtseva — 825L.
Hall Effect in Ferrites Near the Curie Temperature. K. P. Belov and E. P. Svirina — 862.
Magnetostriction of Antiferromagnetic Nickel Monoxide. K. P. Belov and R. Z. Levitin — 400L.
Nonresonance Absorption of Oscillating Magnetic Field Energy by a Ferromagnetic Dielectric. M. I. Kaganov and V. M. Tsukernik — 587.
On the Causes of the Peculiarities in the Physical Properties of Invar Alloys. E. I. Kondorskiĭ — 1284L.
On the Intermediate State of Ferromagnetic Superconductors. G. F. Zharkov — 1259.
On the Magnetization Process in Ferromagnets. L. V. Kirenskiĭ, M. K. Savchenko, and I. F. Degtyarev — 437.
On the Magneto-electrical Effect in Antiferromagnets. I. E. Dzyaloshinskiĭ — 628L.
On the Paper of V. A. Belokon': "The Permanent Structure of Shock Waves with Joule Dissipation." A. G. Kulikovskiĭ, and G. A. Lyubimov — 835L.
On the Theory of Magnetic-moment Relaxation in Ferroelectric Substances. V. G. Bar'yakhtar — 493.
On the Theory of the Temperature Dependence of Fer-

  - romagnetic Anisotropy. E. A. Turov and A. I. Mitsek — 801.
  - Oscillations in the Absorption Coefficient of Sound in Tin at Low Temperatures. A. A. Galkin and A. P. Korolyuk — 219L.
  - Paramagnetic Resonance in Magnetically Dilute Systems. N. S. Garif'yanov — 1101.
  - Quantum Theory of Spatial Dispersion of Electric and Magnetic Susceptibilities. O. V. Konstantinov and V. I. Perel' — 560.
  - Raman Scattering of Electromagnetic Waves in Ferromagnetic Dielectrics. F. G. Bass and M. I. Kaganov — 986.
  - Rotation of the Plane of Polarization of Elastic Waves in Magnetically Polarized Magnetoelastic Media. K. B. Vlasov and B. Kh. Ishmukhametov — 531.
  - Scattering of Low-energy Electron by Short-range Potential in Strong Magnetic Field. V. G. Skobov — 1039L.
  - Shift in Curie Temperature During Uniform Compression of Manganese and Cobalt Fluorides. D. N. Astrov, S. I. Novikova, and M. P. Orlova — 851.
  - The Anisotropy of Magnetoresistance and the Topology of Fermi Surfaces of Metals. N. E. Alekseevskiĭ and Yu. P. Gaĭdukov — 481.
  - Theory of Paramagnetic Resonance in Systems Containing Two Kinds of Magnetic Moments. A. A. Kokin and G. V. Skrotskiĭ — 342.
  - Theory of the Stability of Magnetic States of Ferromagnetic Materials in the Magnetization Process. E. I. Kondorskiĭ — 790.
  - Thermoelectric Phenomena in Strong Magnetic Fields in Metals Possessing Various Fermi Surfaces. Yu. A. Bychkov, L. É. Gurevich, and G. M. Nedlin — 377.

Magnetic Resonance
  - Anomalous Heat Capacity and Nuclear Resonance in Crystalline Hydrogen in Connection with New Data on Its Structure. S. S. Dukhin — 1054L.
  - Coupled Magnetoelastic Oscillations in Antiferromagnetics. S. V. Peletminskiĭ — 321.
  - Cyclotron Resonance in Indium at 9300 Mcs. P. A. Bezuglyĭ and A. A. Galkin — 1049L.
  - Cyclotron Resonance in Tin. M. S. Khaĭkin — 1044L.
  - Electron Resonance in Crossed Electric and Magnetic Fields. I. M. Lifshitz and M. I. Kaganov — 392L.
  - Fine Structure in the Paramagnetic Resonance Spectrum of Natural Sapphire. V. M. Vinokurov, M. M. Zaripov, and N. R. Yafaev — 220L.
  - Measurements of the Transverse Proton Relaxation Time in Aqueous Solutions of Paramagnetic Salts by the Spin-echo Method. V. D. Korepanov, R. A. Dautov, and V. M. Fadeev — 218L.
  - Nonresonance Absorption of Oscillating Magnetic Field Energy by a Ferromagnetic Dielectric. M. I. Kaganov and V. M. Tsukernik — 587.
  - On the Influence of Coherent Magnetic Dipole Radiation on Magnetic Resonance. G. V. Skrotskiĭ and A. A. Kokin — 572.
  - On the Structure of Solid Hydrogen. A. A. Galkin and I. V. Matyash — 1292L.
  - Paramagnetic Resonance and Paramagnetic Relaxation in Electrolyte Solutions. V. I. Avvakumov, N. S. Garif'yanov, B. M. Kozyrev, and P. G. Tishkov — 1110.
  - Paramagnetic Resonance in Magnetically Dilute Systems. N. S. Garif'yanov — 1101.
  - Raman Scattering of Electromagnetic Waves in Ferromagnetic Dielectrics. F. G. Bass and M. I. Kaganov — 986.
  - The Dynamical Character of the Jahn-Teller Effect and its Influence on the Paramagnetic Resonance of Cu^{++}. V. I. Avvakumov — 723.
  - Theory of Paramagnetic Resonance in Systems Containing Two Kinds of Magnetic Moments. A. A. Kokin and G. V. Skrotskiĭ — 342.
  - Theory of Spin-lattice Quadrupole Relaxation in Liquid Solutions of Diagmagnetic Salts. K. A. Valiev — 77.

Magneto-Optical Effects (see Optical Properties)

Magnetoresistance (see Electrical Conductivity and Resistance; Semiconductors)

Magnetostriction (see Magnetic Properties)

Mathematical Methods
  - A Method for Calculation of Phase Volumes. L. G. Zastavenko — 939.
  - Angular and Polarization Analyses of Reactions of the Type $a + b \to a' + b' + c'$. V. I. Ritus — 153.
  - Application of the Dispersion Relations Method in Quantum Electrodynamics. V. Ya. Faĭnberg — 968.
  - Calculation of Phase Integrals in the Covariant Formulation of the Theory of Multiple Production of Particles. L. G. Yakovlev — 741.
  - Classification of Molecular Terms with Respect to Total Nuclear Spin. E. G. Kaplan — 747.
  - Contribution to the Theory of Relativistically Invariant Equations. L. A. Shelepin — 1153.
  - Equilibrium of a Plasma Toroid in a Magnetic Field. V. D. Shafranov — 775.
  - Growth of Electromagnetic Waves in Interpenetrating Infinite Moving Media. G. G. Getmantsev — 600.
  - Incompatibility of the Conditions of Analyticity and Unitarity in the Lee Model. K. A. Ter-Martirosyan — 714.
  - On the Analytic Properties of Vertex Parts in Quantum Field Theory. L. D. Landau — 45.
  - On the Conditions of Applicability of Statistical Formulas to a Degenerate Fermi Gas. Ya. B. Zel'dovich and E. M. Rabinovich — 924.
  - On the Cross Section for Compound-nucleus Formation by Charged Particles. A. D. Piliya — 413L.
  - On the Determination of the Potential in Quantum Field Theory. M. A. Braun — 582.
  - On the Introduction of an "Elementary Length" in the Relativistic Theory of Elementary Particles. Yu. A. Gol'fand — 356.
  - On the Lagrangian Formalism for Spin Variables. D. V. Volkov and S. V. Peletminskiĭ — 121.
  - On the Methods of Born and Pais for Finding Phase Shifts. T. Titts — 207L.
  - On the Relativistic Operators for Momentum and Angular Momentum. A. P. Gel'man — 339.
  - On the Theory of the Relativistic Transformations of the Wave Functions and Density Matrix of Particles with Spin. V. S. Popov — 794.
  - Quantum Theory of Spatial Dispersion of Electric and Magnetic Susceptibilities. O. V. Konstantinov and V. I. Perel' — 560.

Quasiclassical Solutions of the Radial Dirac Equations. N. I. Zhirnov — 1148.
Relativistic Spherical Functions. II. A. Z. Dolginov and I. N. Toptygin — 1022.
Relativistic Spherical Functions III. A. Z. Dolginov and A. N. Moskalev — 1202.
The Method of Dispersion Relations and Perturbation Theory. N. N. Bogolyubov, A. A. Logunov, and D. V. Shirkov — 574.
Threshold Momentum Power Series Expansion of the Amplitude of a Reaction Involving the Formation of Low Energy Particles. I. T. Dyatlov — 947.
Wave Equations with Zero and Nonzero Rest Masses. V. I. Ogievetskiĭ and I. V. Polubarinov — 335.

Measurements (see Methods and Measurements)

Mechanics
Paramagnetic Absorption and Rotation of Plane of Polarization for Certain Salts in the Microwave Band. A. I. Kurushin — 209L.
Paramagnetic Resonance in Potassium Ozonide. A. K. Piskunov, A. A. Manenkov, and Z. A. Bagdasar'yan — 213L.

Mechanics, Quantum (see Quantum Mechanics)

Mechanics, Quantum — Atomic Structure and Spectra (see Atomic Structure and Spectra)

Mechanics, Quantum — of Solid Bodies (see Crystalline State)

Mechanics, Statistical (see Statistical Mechanics and Thermodynamics)

Meson Field Theory (see Field Theory)

Mesons and Hyperons (see also Cosmic Radiation; Elementary Particle Interactions; Nuclear Reactions Induced by Mesons; Scattering of Mesons)
Analyticity and Unitarity in the Scattering of Scalar Mesons from a Static Nucleon. B. L. Ioffe — 1245.
Angular Distribution of Shower Particles in Stars Produced by High-energy Particles. L. A. San'ko, Zh. S. Takibaev, Ts. I. Shakhova, and L. Ya. Balats — 1.
Capture of μ^- Mesons by Light Nuclei. B. L. Ioffe.
Capture of Polarized Muons by Deuterons. A. P. Bukhvostov and I. M. Shmushkevich — 1042L.
Decay Processes in the Development of Nuclear Cascades in the Atmosphere. G. T. Zatsepin, S. I. Nikol'skiĭ, and A. A. Pomanskiĭ — 138.
Effect of the Hyperfine Structure on Polarization of Negative Muons in Mesic Atoms. L. B. Egorov, A. E. Ignatenko, and D. Chultém — 1077.
Effect of Viscosity in Multiple Production on the Energy Distribution of Secondary Particles. A. A. Emel'yanov and D. S. Chernavskiĭ — 753.
Elastic Scattering of 5 — 22 Mev π^+ Mesons on Carbon. V. G. Kirillov-Ugryumov, L. P. Kotenko, E. P. Kuznetsov, F. M. Sergeev, and A. F. Grashin — 907.
Elastic Scattering of 390-Mev π^+ Mesons from Protons. E. L. Grigor'ev and N. A. Mitin — 1123.
Electromagnetic Mass of the K Meson. Chou Kuang-Chao and V. I. Ogievetskiĭ — 616L.
Energy Dependence of the Spatial Asymmetry of Positrons in $\pi^+ \rightarrow \mu^+ \rightarrow e^+$ Decay. A. O. Vaĭsenberg, V. A. Smirnit-skiĭ, É. D. Kolganova, and N. V. Rabin —231L.
Inelastic Collisions between Fast Polarized Particles and Atoms. V. V. Batygin and I. N. Toptygin — 975.
Inelastic Interaction of π^+ Mesons with Light Nuclei in the Energy Region 80 — 300 Mev. A. G. Meshkovskiĭ and Ya. Ya. Shalamov — 697.
Inelastic Scattering and Absorption of (195 ± 15)-Mev Positive Pions by Carbon and Lithium Nuclei. N. I. Petrov, V. G. Ivanov and V. A. Rusakov — 682.
Interaction of 9-Bev Protons with Free and Quasifree Nucleons in Photographic Emulsions. N. P. Bogachev, S. A. Bunyatov, I. M. Gramenitskiĭ, V. B. Lyubimov, Yu. P. Merekov, M. I. Podgoretskiĭ, V. M. Sidorov, and D. Tuvdendorzh — 872.
Investigation of the High-energy μ-Meson Flux in Extensive Atmospheric Showers. S. N. Vernov, B. A. Khrenov, and G. B. Khristiansen — 891.
Nonmesonic Decay of Hyperfragments. I. B. Berkovich, A. P. Zhdanov, F. G. Lepekhin, and Z. S. Khokhlova — 428.
Note on a Baryon Scheme. H. Oiglane — 394L.
Nuclear Interactions of 8.7-Bev Protons in Photographic Emulsions. G. B. Zhdanov, V. M. Maksimenko, M. I. Tret'yakova, and M. N. Shcherbakova — 442.
On a Certain Possibility of Setting up a System of "Elementary" Particles. I. V. Chuvilo — 994.
On a Symmetry in τ^0 Decay. M. I. Shirokov — 232L.
On an Estimate of Energy Characteristics of Shower Producing Particles. É. G. Boos and Zh. S. Takibaev — 206L.
On Certain Singularities in the Interaction with Light Nuclei of Particles with Energies $E \geq 2 \times 10^{12}$ ev. N. L. Grigorov and V. Ya. Shestoperov — 816L.
On Electromagnetic Correction in μ-e Decay. V. P. Kuznetsov — 784.
On K_{e4} Decay. L. B. Okun' and E. P. Shabalin — 1252.
On the Anomalous Magnetic Moment of Nucleons in Chew's Method. Yu. M. Lomsadze, V. I. Lend'el, and B. M. Érnst — 955.
On the Connection of Isotopic Spin and Strangeness with the Behavior of Spinors under Inversion. A. M. Brodskiĭ and D. D. Ivanenko — 624L.
On the Mechanism of Capture of Stopped K^- Mesons. D. K. Kopylova, Yu. B. Korolevich, N. I. Petukhova, and M. I. Podgoretskiĭ — 203.
On the Problem of Investigating the Interaction between π Mesons and Hyperons. L. I. Lapidus and Chou Kuang-Chao — 199.
Parity Nonconservation in Strong Interactions of Strange Particles. S. G. Matinyan — 736.
Photoproduction of Neutral π Mesons on Hydrogen by γ Quanta with Energy between the Threshold and 240 Mev. R. G. Vasil'kov, B. B. Govorkov, and V. I. Gol'danskiĭ — 7.
Photoproduction of π^0 Mesons from Carbon near Threshold. R. G. Vasil'kov, B. B. Govorkov, and V. I. Gol'danskiĭ — 818L.
π^--p Interaction at 1.4 Bev. V. I. Ruskin — 74.
Polarization Effects in the Direct Transition of $\mu^+\mu^-$ into an Electron-Positron Pair. B. A. Lysov — 404L.
Polarization Effect in the $\pi^0 \rightarrow e^- + e^+ + \gamma$ Decay. B. K. Kerimov, A. I. Mukhtarov, and S. A. Gadzhiev — 407L.

Production of K^+ Mesons by Cosmic-ray Protons at 3250 m Above Sea Level. M. Ya. Balats, P. I. Lebedev, and Yu. V. Obukhov — 417.
Resonance Interaction of Pions. V. S. Barashenkov and V. M. Mal'tsev — 630L.
The Formfactor and the Leptonic Decay Probability of the Λ Particle. Ho Tso-Hsiu — 1288L.
The $\mu \rightarrow e + \gamma$ and $\mu \rightarrow e + \nu + \overline{\nu} + \gamma$ Decays. Yu. S. Krestnikov, A. G. Meshkovskiĭ, Ya. Ya. Shalamov, V. A. Shebanov, and I. Yu. Kobzarev — 622L.
The Number of Elementary Baryons and the Universal Baryon Repulsion Hypothesis. Ya. B. Zel'dovich — 403L.
The Ultraviolet Asymptotic Value for the Interaction of K Mesons with Baryons. J. Wrzecionko — 69.
Three-electron Decay of the Muon. I. I. Gurevich, B. A. Nikol'skiĭ, and L. V. Surkova — 225L.
Total Cross Section of Photoproduction of π^0 Mesons on Protons at Low Energies. R. G. Vasil'kov and B. B. Govorkov — 224L.

Metals (see Crystalline State)

Metastable Atoms (see Atomic Structure and Spectra)

Methods and Instruments
Alpha Spectrum of the Natural Samarium Isotope Mixture. A. A. Vorob'ev, A. P. Komar, V. A. Korolev, and G. E. Solyankin — 386L.
Capture Mechanism in Betatrons. I. M. Samoĭlov — 504.
Electric Conductivity of the Explosion Products of Condensed Explosives. A. A. Brish, M. S. Tarasov, and V. A. Tsukerman — 1095.
Experiments in the Production of a New Fermium Isotope. V. P. Perelygin, E. D. Donets, and G. N. Flerov — 1106.
Gamma Rays from a Po-O^{18} Neutron Source. É. M. Tsenter, A. G. Khabakhpashev, and I. A. Pirkin — 806L.
Localization of a High-Frequency Induction Discharge. M. D. Raĭzer and S. E. Grebenshchikov — 398L.
Minimal Error in the Experimental Observation of Asymmetry. N. P. Klepikov — 810L.
Muon Depolarization in μ-Mesic Atoms with Deformed Nuclei. D. F. Zaretskiĭ and V. M. Novikov — 1287L.
On Certain Experiments with Metastable Liquids in an X-ray Beam. G. A. Askar'yan, L. P. Kotenko, E. P. Kuznetsov, and A. V. Samoĭlov — 1041L.
On Certain Singularities in the Interaction with Light Nuclei of Particles with Energies $E \geq 2 \times 10^{12}$ ev. N. L. Grigorov, and V. Ya. Shestoperov — 816L.
On the Measurement of the Momentum of Fast Particles and the Investigation of Nuclear Interaction in the $10^{10} - 10^{12}$ ev Energy Range. M. I. Daĭon and V. Kh. Volynskiĭ — 648.
Possibility of Measuring the Velocity of Propagation of Gravitation in the Laboratory. I. L. Bershteĭn and M. E. Gertsenshteĭn — 1293L.
Quantum-mechanical Semiconductor Generators and Amplifiers of Electromagnetic Oscillators. N. G. Basov, B. M. Vul, and Yu. M. Popov — 416L.
Search for Particles with Mass between 6 and 25 Electron Masses. A. S. Belousov, S. V. Rusakov, E. I. Tamm, and P. A. Cerenkov — 1143.
Use of Slow Molecules in a Maser. N. G. Basov and A. N. Oraevskiĭ — 761.
Use of the (d, p) Reaction to Excite States with Large Spins. V. G. Neudachin, I. B. Teplov, and A. F. Tulinov — 387L.

Microwaves
Fine Structure in the Paramagnetic Resonance Spectrum of Natural Sapphire. V. M. Vinokurov, M. M. Zaripov, and N. R. Yafaev — 220L.
Growth of Electromagnetic Waves in Interpenetrating Infinite Moving Media. G. G. Getmantsev — 600.
Paramagnetic Absorption and Rotation of Plane of Polarization for Certain Salts in the Microwave Band. A. I. Kurishin — 209L.
Raman Scattering of Electromagnetic Waves in Ferromagnetic Dielectrics. F. G. Bass and M. I. Kaganov — 986.
Use of Slow Molecules in a Maser. N. G. Basov and A. N. Oraevskiĭ — 761.

Miscellaneous
Condensation of a Cloud of Vaporized Matter Expanding in Vacuum. Yu. P. Raĭzer — 1229.
Directed Emission of Particles from a Copper Single Crystal Sputtered by Bombardment with Ions up to 50 Kev Energy. V. E. Yurasova, N. V. Pleshivtsev, and I. V. Orfanov — 689.

Molecular Structure and Spectra
Classification of Molecular Terms with Respect to Total Nuclear Spin. E. G. Kaplan — 747.
Mesic Molecular Processes in Hydrogen. V. B. Belyaev, S. S. Gershteĭn, B. N. Zakhar'ev, and S. P. Lomnev — 1171.
The Dynamical Character of the Jahn-Teller Effect and Its Influence on the Paramagnetic Resonance of Cu^{++}. V. I. Avvakumov — 723.

Moments, Nuclear (see Nuclear Moments and Spin)

Neutrino
Electron and Muon Neutrinos. B. Pontecorvo — 1236.
Emission of Neutrino Pairs by Electrons and the Role Played by it in Stars. G. M. Gandel'man and V. S. Pinaev — 764.
On Two Types of Neutrinos, the Isotopic Spin of Leptons, and the Universal Four-Fermion Interaction. É. M. Lipmanov — 750.
Second-forbidden Coulomb β-Decay Transitions. Yu. V. Gaponov — 109.

Neutrons (see Elementary Particle Interactions)

Nuclear Fission
Angular Anisotropy of Gamma Quanta that Accompany Fission. V. M. Strutinskiĭ — 613L.
Angular Distribution of Fission Fragments in Fission Induced by Heavy Ions. V. A. Druin, Yu. V. Lobanov, and S. M. Polikanov — 26.
Comparison of Effective Temperatures of Spectra of Neutrons Emitted in Fission of U^{235} and P^{239} by Fast and Thermal Neutrons. G. N. Smirenkin — 1286L.
Cross Section for Production of Fm^{250} in the Reactions $Pu^{241}(C^{13}, 4n)Fm^{250}$ and $U^{238}(O^{16}, 4n)Fm^{250}$. V. V. Volkov, L. I. Guseva, B. F. Myasoedov, N. I. Tarantin, and K. V. Filippova — 859.
Experiments in the Production of a New Fermium Isotope. V. P. Perelygin, E. D. Donets, and G. N. Flerov — 1106.

Fission of Th^{232} Induced by Thermal Neutrons. E. I. Korneev, V. S. Skobkin, and G. N. Flerov — 29.

Fragmentation on Bismuth Nuclei. V. F. Darovskikh, N. P. Kocherov, and N. A. Perfilov — 921.

Some Features of the Spontaneous Fission of U^{238}. B. D. Kuz'minov, L. S. Kutsaeva, V. G. Nesterov, L. I. Prokhorova, and G. N. Smirenkin — 290.

Spontaneous Fission of Am^{241}. V. L. Mikheev, N. K. Skobelev, V. A. Druin, and G. N. Flerov — 612L.

Nuclear Moments and Spin

Clustering of Nucleons in Light Nuclei. V. G. Neudachin, Yu. F. Smirnov, and N. P. Yudin — 1256.

Excitation of Vibrational Levels in Nuclei by Charged Particles. A. D. Piliya — 1018.

Measurements of Nuclear Magnetic Moments in the Alkali Earths by Molecular Beam Magnetic Resonance. A. G. Kucheryaev, Yu. K. Szhenov, and Sh. M. Gogichaĭshvili — 412L.

Measurement of the Polarization of Deuterons in the Reaction $p + p \rightarrow d + \pi^+$ at Proton Energies of 670 Mev. Yu. K. Akimov, K. S. Marish, O. V. Savchenko, and L. M. Soroko — 33.

Nuclear Moments of the Odd Isotopes of Gadolinium. N. I. Kaliteevskiĭ, M. P. Chaĭka, I. Kh. Pacheva, and É. E. Fradkin — 629L.

On the Theory of the Nuclear Moment of Inertia. Yu. K. Khokhlov — 808L.

Optical Anisotropy of Atomic Nuclei. A. M. Baldin — 142.

Radioactive Decay of Ag^{110m}. N. M. Anton'eva, A. A. Bashilov, and E. K. Kulakovskiĭ — 1063.

The Spectrum of Internal Conversion Electrons Accompanying Alpha Decay of U^{233} and the Level Scheme of Th^{229}. E. F. Tret'yakov, M. P. Anikina, L. L. Gol'din, G. I. Novikova, and N. I. Pirogova — 656.

Use of the (d, p) Reaction to Excite States with Large Spins. V. G. Neudachin, I. B. Teplov, and A. F. Tulinov — 387L.

Nuclear Photoeffects

Fast Photoneutrons from Be^9, C^{12} and Al^{27}. L. A. Kul'chitskiĭ and V. Presperin — 1082.

On Certain Singularities in the Interaction with Light Nuclei of Particles with Energies $E \geq 2 \times 10^{12}$ ev. N. L. Grigorov and V. Ya. Shestoperov — 816L.

On the Fine Structure of the Giant Resonance. N. A. Burgov, G. V. Danilyan, B. S. Dolbilkin, L. E. Lazareva, and F. A. Nikolaev — 1278L.

On the Influence of the Pauli Principle and of Short-Range Nuclear Forces on the Absorption of Photons by Nuclei in the Oscillator Model. V. A. Él'tekov — 830L.

On the Theory of the Direct Nuclear Photoeffect. Yu. V. Orlov — 1294L.

Optical Anisotropy of Atomic Nuclei. A. M. Baldin — 142.

Spectrum of Photo Protons Produced by Gamma Rays in the Narrow 82 — 89 Mev Energy Range. E. B. Bazhanov — 267.

Nuclear Reactions, General

Angular and Polarization Analyses of Reactions of the Type $a + b \rightarrow a + b' + c'$. V. I. Ritus — 153.

Angular Distribution of Long-range Alpha Particles, Connected with the Fission Forces. N. A. Perfilov and Z. I. Solov'eva — 824L.

Circular Polarization of Gamma Quanta Emitted by a Nucleus after μ^- Capture. I. S. Shapiro and L. D. Blokhintsev — 542.

Coulomb Excitation of Odd-mass Nuclei by Multiply-charged Ions. D. G. Alkhazov, A. P. Grinberg, G. M. Gusinskiĭ, K. I. Erokhina, and I. Kh. Lemberg — 1086.

Cross Section for Production of Cm^{240} by Irradiation of Th^{232} with C^{12} and C^{13} Ions. L. I. Guseva, B. F. Myasoedov, N. I. Tarantin, and K. V. Filippova — 694.

Cross Section for Production of Fm^{250} in the Reactions $Pu^{241}(C^{13}, 4n)Fm^{250}$ and $U^{238}(O^{16}, 4n)Fm^{250}$. V. V. Volkov, L. I. Guseva, B. F. Myasoedov, N. I. Tarantin, and K. V. Filippova — 859.

Emitters of α-Particles with Energies of About 9 and 12 Mev. V. A. Karnaukhov, V. I. Khalizev, and G. N. Flerov — 901.

Excitation of Vibrational Levels in Nuclei by Charged Particles. A. D. Piliya — 1018.

Experiments in the Production of a New Fermium Isotope. V. P. Perelygin, E. D. Donets, and G. N. Flerov — 1106.

Fragmentation on Bismuth Nuclei. V. F. Darovskikh, N. P. Kocherov, and N. A. Perfilov — 921.

Gamma Rays from a Po-O^{18} Neutron Source. É. M. Tsenter, A. G. Khabakhpashev, and I. A. Pirkin — 806L.

Measurement of the Intensity Ratio of Transitions to the First Excited Levels of the Daughter Nuclei in the Decay of U^{238} and U^{234}. A. A. Vorob'ev, A. P. Komar, and V. A. Korolev — 1032L.

Muon Depolarization in μ-Mesic Atoms with Deformed Nuclei. D. F. Zaretskiĭ and V. M. Novikov — 1287L.

Nuclear Reactions Induced by Heavy Ions. J. H. Fremlin and J. S. Lille — 229L.

On the Cross Section for Compound-Nucleus Formation by Charged Particles. A. D. Piliya — 413L.

On the Determination of Nuclear Deformation from the Alpha-Decay Fine Structure. V. G. Nosov — 631L.

On the Mechanism of Capture of Stopped K^- Mesons. D. K. Kopylova, Yu. B. Korolevich, N. I. Petukhova, and M. I. Podgoretskiĭ — 203.

Production of Compound Nuclei by Bombardment of V and Nb with O^{16}, C^{12}, and C^{13} Ions. A. S. Karamyan and A. A. Pleve — 467.

Scattering of Electrons by Light Nonspherical Nuclei. E. V. Inopin and B. I. Tishchenko — 932.

Threshold Momentum Power Series Expansion of the Amplitude of a Reaction Involving the Formation of Low-energy Particles. I. T. Dyatlov — 947.

Nuclear Reactions Induced by Alpha Particles and He^3.

Excitation of Rotational States of Nonaxial Nuclei in Alpha-Particle Scattering. E. A. Romanovskiĭ — 606L.

Gamma Rays from a Po—O^{18} Neutron Source. É. M. Tsenter, A. G. Khabakhpashev, and I. A. Pirkin — 806L.

Nuclear Reactions Induced by Deuterons and Tritons

(d, t) Reactions on Li^6, Li^7, and Be^9 Nuclei. N. A. Vlasov and A. A. Ogloblin — 39.

The (d,t) Reaction on C^{12}, F^{19}, and Al^{27} Nuclei.

  - N. A. Vlasov, S. P. Kalinin, A. A. Ogloblin, and V. I. Chuev — 844.
  - Use of the (d, p) Reaction to Excite States with Large Spins. V. G. Neudachin, I. B. Teplov, and A. F. Tulinov — 387L.

- **Nuclear Reactions Induced by Mesons**
  - Capture of μ^- Mesons by Light Nuclei. B. L. Ioffe — 113.
  - Capture of Polarized Muons and Deuterons. A. P. Bukhvostov and I. M. Shmushkevich — 1042L.
  - Circular Polarization of Gamma Quanta Emitted by a Nucleus after μ^- Capture. I. S. Shapiro and L. D. Blokhintsev — 542.
  - Inelastic Scattering and Absorption of (195 ± 15)-Mev Positive Pions by Carbon and Lithium Nuclei. N. I. Petrov, V. G. Ivanov, and V. A. Rusakov — 682.
  - Nonmesonic Decay of Hyperfragments. I. B. Berkovich, A. P. Zhdanov, F. G. Lepekhin, and Z. S. Khokhlova — 428.
  - On the Absorption of π^+ Mesons with Energies of About 50 Mev by Carbon Nuclei. J. V. Laberrigue-Frolova, M. P. Balandin, and S. Z. Otvinovskiĭ — 452.
  - Production of Multiply-charged Particles on Photographic Emulsion Nuclei by 280-Mev Positive Pions. N. S. Ivanova, V. I. Ostroumov, and Yu. V. Pavlov — 1137.
- **Nuclear Reactions Induced by Neutrons**
  - Comparison of Effective Temperatures of Spectra of Neutrons Emitted in Fission of U^{235} and Pu^{239} by Fast and Thermal Neutrons. G. N. Smirenkin — 1286L.
  - Polarization of Neutrons from the $T(p, n)He^3$ Reaction and Protons from the $He^3(n, p)T$ Reaction. K. P. Artemov, N. A. Vlasov, and L. N. Samoĭlov — 841.
  - Possibility of Investigating the Levels of a Compound Nucleus Produced by Interaction between Slow Neutrons and Isomers. Yu. V. Petrov — 833L.
  - Radiative Capture of Neutrons. D. F. Zaretskiĭ — 772.
- **Nuclear Reactions Induced by Protons**
  - Angular Distribution of Shower Particles in Stars Produced by High-energy Particles. L. A. San'ko, Zh. S. Takibaev, Ts. I. Shakhova, and L. Ya. Balats — 1.
  - Fragmentation on Bismuth Nuclei. V. F. Darovskikh, N. P. Kocherov, and N. A. Perfilov — 921.
  - Interaction of 9-Bev Protons with Free and Quasifree Nucleons in Photographic Emulsions. N. P. Bogachev, S. A. Bunyatov, I. M. Gramenitskiĭ, V. B. Lyubimov, Yu. P. Merekov, M. I. Podgoretskiĭ, V. M. Sidorov, and D. Tuvdendorzh — 872.
  - Knock-on Alpha Particles Produced by Fast Nucleons. V. I. Ostroumov and R. A. Filov — 459.
  - Nuclear Interactions of 8.7-Bev Protons in Photographic Emulsions. G. B. Zhdanov, V. M. Maksimenko, M. I. Tret'yakova, and M. N. Shcherbakova — 442.
  - Polarization of Neutrons from the $T(p, n)He^3$ Reaction and Protons from the $He^3(n, p)T$ Reaction. K. P. Artemov, N. A. Vlasov, and L. N. Samoĭlov — 841.
  - Potential Barrier Criterion and Stars in Emulsions. P. I. Fedotov — 674.
  - Production of Multiply-charged Particles on Photographic Emulsion Nuclei by 280-Mev Positive Pions. N. S. Ivanova, V. I. Ostroumov, and Yu. V. Pavlov — 1137.
  - Recoil Nuclei from the Disintegration of Silver by Fast Protons. N. L. Borisova, M. Ya. Kuznetsova, L. N. Kurchatova, V. N. Mekhedov, and L. V. Chistyakov — 261.
  - Results of a Study of the Disintegration of Carbon Nuclei by 660-Mev Protons. A. P. Zhdanov and P. I. Fedotov — 280.
  - Total Cross Section of Photoproduction of π^0 Mesons on Protons at Low Energies. R. G. Vasil'kov and B. B. Govorkov — 224L.
  - Use of the (d, p) Reaction to Excite States with Large Spins. V. G. Neudachin, I. B. Teplov, and A. F. Tulinov — 387L.
- **Nuclear Scattering** (see Scattering)
- **Nuclear Spectra**
  - Alpha Decay of Th^{229}. Interaction of Nuclear Levels. L. L. Gol'din, G. I. Novikova, N. I. Pirogova, and E. F. Tret'yakov — 822L.
  - Application of the Variational Principle for the Determination of the Binding Energy of a Proton-Electron-Positron System. V. P. Shmelev — 325.
  - Calculation of Energy Levels of Te^{206} and Bi^{210} Nuclei. L. A. Sliv and Yu. I. Kharitonov — 819L.
  - Comparison of Effective Temperatures of Spectra of Neutrons Emitted in Fission of U^{235} and Pu^{239} by Fast and Thermal Neutrons. G. N. Smirenkin — 1286L.
  - Coulomb Excitation of Odd-mass Nuclei by Multiply-charged Ions. D. G. Alkhazov, A. P. Grinberg, G. M. Gusinskiĭ, K. I. Erokhina, and I. Kh. Lemberg — 1086.
  - Effect of the Hyperfine Structure on Polarization of Negative Muons in Mesic Atoms. L. B. Egorov, A. E. Ignatenko, and D. Chultém — 1077.
  - Electric Quadrupole Gamma Transitions in Even-even Nuclei. N. N. Delyagin — 605L.
  - Experiments in the Production of a New Fermium Isotope. V. P. Perelygin, E. D. Donets, and G. N. Flerov — 1106.
  - Gamma Rays from a $Po\text{-}O^{18}$ Neutron Source. É. M. Tsenter, A. G. Khabakhpashev, and I. A. Pirkin — 806L.
  - Intensity Rules for Beta Transitions to Different Rotational States of Even-even Daughter Nuclei. A. S. Davydov — 98.
  - Measurement of the Intensity Ratio of Transitions to the First Excited Levels of the Daughter Nuclei in the Decay of U^{238} and U^{234}. A. A. Vorob'ev, A. P. Komar, and V. A. Korolev — 1032L.
  - Measurement of the Lifetime of the First Excited State of Ne^{21}. A. G. Khabakhpashev and É. M. Tsenter — 705.
  - Multipolarities of Gamma Transitions in Tm^{169}. V. M. Kel'man, R. Ya. Metskhvarishvili, B. K. Preobrazhenskiĭ, V. A. Romanov, and V. V. Tuchkevich — 456.
  - $0^+ - 0^+$ Transition in the Decay $Pr^{140} \rightarrow Ce^{140}$. B. S. Dzhelepov, I. F. Uchevatkin, and S. A. Shestopalova — 611L.
  - On the Decay Scheme of the Bi^{210} Isomer. S. V. Golenetskiĭ, L. I. Rusinov, and Yu. I. Filimonov — 395L.
  - On the Nucleon + Core Model of the Nucleus with a Vibrational Excitation Spectrum of the Core. D. P. Grechukhin — 730.
  - On the Rotational Levels of Li^7. V. I. Mamasakhlisov

and T. I. Kopaleĭshvili — 807L.
Optical Anisotropy of Atomic Nuclei. A. M. Baldin — 142.
Positron Spectrum of Eu^{152} and Eu^{152m}. S. F. Antonova, S. S. Vasilenko, M. G. Kaganskiĭ, and D. L. Kaminskiĭ — 477.
Production of Compound Nuclei by Bombardment of V and Nb with O^{16}, C^{12}, and C^{13} Ions. A. S. Karamyan and A. A. Pleve — 467.
Radiative Capture of Neutrons. D. F. Zaretskiĭ — 772.
Radioactive Decay of Ac^{227} and Excited Levels of Fr^{223} and Th^{227}. G. I. Novikova, E. A. Volkova, L. L. Gol'din, D. M. Ziv, and E. F. Tret'yakov — 663.
Resonance Scattering of Gamma Quanta by Mg^{24}. I. Sh. Vashakidze, T. I. Kopaleĭshvili, and G. A. Chilashvili — 535.
Resonance Scattering of Gamma Quanta on Cd^{114} Nuclei. N. N. Delyagin — 837.
The (d, t) Reaction on C^{12}, F^{19}, and Al^{27} Nuclei. N. A. Vlasov, S. P. Kalinin, A. A. Ogloblin, and V. I. Chuev — 844.
The Spectrum of Internal Conversion Electrons Accompanying Alpha Decay of U^{233} and the Level Scheme of Th^{229}. E. F. Tret'yakov, M. P. Anikina, L. L. Gol'din, G. I. Novikova, and N. I. Pirogova — 656.
Transition Probabilities between Rotational States of Non-Axial Odd Nuclei. Wang Ling — 821L.
Nuclear Structure Theory
Angular Distribution and Polarization of Beta Particles in Second Forbidden Transitions. A. Z. Dolginov and E. V. Kharitonov — 553.
Angular Distribution of Long-range Alpha Particles Connected with the Fission Process. N. A. Perfilov and Z. I. Solov'eva — 824L.
Calculation of Energy Levels of Te^{206} and Bi^{210} Nuclei. L. A. Sliv and Yu. I. Kharitonov — 819L.
Clustering of Nucleons in Light Nuclei. V. G. Neudachin, Yu. F. Smirnov, and N. P. Yudin — 1256.
Contribution of Three-particle Forces to the Binding Energy of Hypernuclei. V. A. Lyul'ka and V. A. Filimonov — 1015.
Distribution of the Density of Protons in a Nucleus with a Given Angular Momentum. L. P. Rapoport and S. G. Kadmenskiĭ — 929.
Electric Quadrupole Gamma Transitions in Even-even Nuclei. N. N. Delyagin — 605L.
Excitation of Rotational States of Nonaxial Nuclei in Alpha-particle Scattering. A. E. Romanovskiĭ — 606L.
Excitation of Vibrational Levels in Nuclei by Charged Particles. A. D. Piliya — 1018.
Ground States of Nonspherical Odd Nuclei According to the Independent-particle Model. D. A. Zaikin — 381.
Measurement of the Lifetime of the First Excited State of Ne^{21}. A. G. Khabakhpashev and É. M. Tsenter — 705.
On a Certain Possibility of Investigation of the Structure of Nucleons and Nuclei. N. G. Birger and Yu. A. Smorodin — 964.
On the Nucleon + Core Model of the Nucleus with a Vibrational Excitation Spectrum of the Core. D. P. Grechukhin — 730.
On the Rotational Levels of Li^{7}. V. I. Mamasakhlisov and T. I. Kopaleĭshvili — 807L.
On the Theory of the Nuclear Moment of Inertia. Yu. K. Khokhlov — 808L.
Radioactive Decay of Ac^{227} and Excited Levels of Fr^{223} and Th^{227}. G. I. Novikova, E. A. Volkova, L. L. Gol'din, D. M. Ziv, and E. F. Tret'yakov — 663.
Reduced Widths for Nucleon Associations in the Shell Model of the Nucleus. V. V. Balashov, V. G. Neudachin, Yu. F. Smirnov, and N. P. Yudin — 983.
Resonance Scattering of Gamma Quanta by Mg^{14}. I. Sh. Vashakidze, T. I. Kopaleĭshvili, and G. A. Chilashvili — 535.
Scattering of 5 — 10 Mev Protons on He^{3}. K. P. Artemov, S. P. Kalinin, and L. N. Samoĭlov — 474.
Superfluidity and the Moments of Inertia of Nuclei. A. B. Migdal — 176.
The Energy of a Compressed Imperfect Fermi Gas. D. A. Kirzhnits — 414L.
The Spectrum of Internal Conversion Electrons Accompanying Alpha Decay of U^{233} and the Level Scheme of Th^{229}. E. F. Tret'yakov, M. P. Anikina, L. L. Gol'din, G. I. Novikova, and N. I. Pirogova — 656.
Transition Probabilities between Rotational States of Nonaxial Odd Nuclei. Wang Ling — 821L.
Optical Instruments (see Methods and Instruments)
Optical Properties
Faraday Effect in Semiconductors on Free Carriers in a Strong Magnetic Field. L. É. Gurevich and I. P. Ipatova — 943.
Light Waves in Crystals in the Exciton Absorption Region and the Impurity Photoeffect. I. M. Dykman and S. I. Pekar — 361.
Measurement of Energy Loss of Fast Electrons Penetrating through Matter. N. A. Grishaev, A. N. Fisun, A. S. Litvinenko, V. N. Grizhko, B. I. Shramenko, and I. N. Onishchenko — 1031L.
On the Connection between the Optical Constants of Metals and their Microscopic Characteristics. G. P. Motulevich — 1249.
Simple Method for Computing the Mean Range of Radiation in Ionized Gases at High Temperatures. Yu. P. Raĭzer — 769.
Pair Production (see Electrons and Positrons)
Phosphors and Phosphorescence (see Luminescence; Semiconductors)
Photoconductivity (see Electrical Conductivity and Resistance)
Photodisintegration (see Nuclear Photoeffects)
Photoelectric Effect (see Electrical Properties)
Photography and Photographic Emulsions (see Methods and Instruments; Optical Properties)
Photometry (see Methods and Instruments; Optical Properties)
Photons (see Radiation)
Photovoltaic Effect (see Electrical Properties; Semiconductors)
Piezoelectric Effect (see Dielectrics and Dielectric Properties)
Polarization, Electrical (see Dielectrics and Dielectric Properties)
Positrons (see Electrons and Positrons)
Probability (see Mathematical Methods)

Protons (see Elementary Particle Interactions)
Quantum Electrodynamics (see also Field Theory)
Application of the Dispersion Relations Method in Quantum Electrodynamics. V. Ya. Faĭnberg — 968.
Dispersion Relations for the Scattering of Gamma Quanta by Nucleons. L. I. Lapidus and Chou Kuang-Chao — 1213.
Dispersion Relations for the Virtual Compton Effect. I. S. Zlatev and P. S. Isaev — 519.
Effect of Multiple Scattering on Pair Production by High-energy Particles in a Medium. F. F. Ternovskiĭ — 718.
Effect of Vacuum Fluctuations on the Polarization of Electrons Moving in a Magnetic Field. I. M. Ternov and V. S. Tumanov — 809L.
Electron-electron Scattering and Quantum Electrodynamics at Small Distances. G. V. Avakov — 604L.
Numerical Solution of Static Dispersion Relations of the Photoproduction P Wave. L. D. Solov'ev and G. N. Tentyukova — 634L.
On Electromagnetic Corrections in μ-e Decay. V. P. Kuznetsov — 784.
On the Masses of the Muon and the Electron. Ya. B. Zel'dovich — 1283L.
On the Polarization of the Electrons in Bremsstrahlung Processes. A. A. Kresnin — 621L.
On the Two-charge Renormalization Group in Scalar Quantum Electrodynamics. V. A. Shakhbazyan — 1263.
Pair Production in Collisions between Charged Particles. F. F. Ternovskiĭ — 565.
Passage of Particles through a Plasma. A. I. Larkin — 186.
Polarization Effects in the Direct Transition of $\mu^+\mu^-$ into and Electron-positron Pair. B. A. Lysov — 404L.
Polarization Effects in the $\pi^0 \rightarrow e^- + e^+ + \gamma$ Decay. B. K. Kerimov, A. I. Mukhtarov, and S. A. Gadzhiev — 407L.
Polarization Phenomena in Radiative Collisions of Two Electrons. V. L. Lyuboshitz — 1221.
The Method of Dispersion Relations and Perturbation Theory. N. N. Bogolyubov, A. A. Logunov, and D. V. Shirkov — 574.
Use of Dispersion Relations for a Test of Quantum Electrodynamics at Small Distances. I. S. Zlatev and P. S. Isaev — 826L.
Quantum Mechanics
Application of the Variational Principle for the Determination of the Binding Energy of a Proton-Electron-Positron System. V. P. Shmelev — 325.
Concentration of Charged Particles in Plasma of Spark-discharge Channel. A. A. Mak — 1055L.
Contribution to the Theory of Relativistically Invariant Equations. L. A. Shelepin — 1153.
On the Conditions of Applicability of Statistical Formulas to a Degenerate Fermi Gas. Ya. B. Zel'dovich and E. M. Rabinovich — 924.
On the Lagrangian Formalism for Spin Variables. D. V. Volkov and S. V. Peletminskiĭ — 121.
On the Phase of the Scattered Wave (a Reply to V. V. Malyarov). F. S. Los' — 836L.
On the Relativistic Operators for Momentum and Angular Momentum. A. P. Gel'man — 339.
On the Theory of the Relativistic Transformations of the Wave Functions and Density Matrix of Particles with Spin. V. S. Popov — 794.
Quantum Theory of Spatial Dispersion of Electric and Magnetic Susceptibilities. O. V. Konstantinov and V. L. Perel' — 560.
Quasiclassical Solutions of the Radial Dirac Equations. N. I. Zhirnov — 1148.
Resonance Charge Exchange of Doubly Charged Ions in Slow Collisions, I. K. Fetisov and O. B. Firsov — 67.
The Dynamical Character of the Jahn-Teller Effect and its Influence on the Paramagnetic Resonance of Cu^{++}. V. I. Avvakumov — 723.
The Energy of a Compressed Imperfect Fermi Gas. D. A. Kirzhnits — 414L.
The Non-additivity of London-Van der Waals Forces. L. I. Podlubnyĭ — 633L.
Quenching of Radiation (see Radiation)
Radar (see Methods and Instruments; Radiation)
Radiation (see also Range and Energy Loss of Particles)
Coherent Electron Radiation in the Synchrotron. II. L. V. Iogansen and M. S. Rabinovich — 83.
Energy Lost to Radiation in a Gas-discharge Plasma. V. D. Kirillov — 812L.
Field of a Charged Particle in a Moving Medium. B. M. Bolotovskiĭ and A. A. Rukhadze — 958.
Limits of Applicability of the Theory of Transition Radiation. G. M. Garibyan and I. Ya. Pomeranchuk — 1290L.
Mechanism for the Production of Relativistic Electrons in the Atmospheres of Nonstationary Stars. I. M. Gordon — 608L.
Nonresonance Absorption of Electromagnetic Waves in a Magnetoactive Plasma. B. N. Gershman — 497.
On the Polarization of the Electrons in Bremsstrahlung Processes. A. A. Kresnin — 621L.
Radiative Processes Ahead of a Shock-wave Front. L. M. Biberman and B. A. Veklenko — 117.
Raman Scattering of Electromagnetic Waves in Ferromagnetic Dielectrics. F. G. Bass and M. I. Kaganov — 986.
Shortwave Radiation from a Vacuum Spark. S. V. Lebedev, S. L. Mandel'shtam, and G. M. Rodin — 248.
Simple Method for Computing the Mean Range of Radiation in Ionized Gases at High Temperatures. Yu. P. Raĭzer — 769.
Use of Slow Molecules in a Maser. N. G. Basov and A. N. Oraevskiĭ — 761.
Radioactivity
Angular Correlation in Internal Conversion, Including Effects of Scattering and of the Finite Size of the Nucleus. A. K. Ustinova — 216L.
Angular Distribution and Polarization of Beta Particles in Second Forbidden Transitions. A. Z. Dolginov and E. V. Kharitonov — 553.
Alpha Decay of Th^{229}. Interaction of Nuclear Levels. L. L. Gol'din, G. I. Novikova, N. I. Pirogova, and E. F. Tret'yakov — 822L.
Beta Decay of the Negative Muon. Yu. A. Budagov, S. Viktor, V. P. Dzhelepov, P. F. Ermolov, and V. I. Moskalev — 625L.

Cross Section for Production of Cm^{240} by Irradiation of Th^{232} with C^{12} and C^{13} Ions. L. I. Guseva, B. F. Myasoedov, N. I. Tarantin, and K. V. Filippova — 694.
Decay of Te^{131} ($T_{1/2} = 30$ Hours). A. Bedescu, K. P. Mitrofanov, A. A. Sorokin, and V. S. Shpinel' — 221L
Emitters of α-Particles with Energies of about 9 and 12 Mev. V. A. Karnaukhov, V. I. Khalizev, and G. N. Flerov — 901.
Experiments in the Production of a New Fermium Isotope. V. P. Perelygin, E. D. Donets, and G. N. Flerov — 1106.
Forbidden Transitions in the Deformed Tm^{169} Nucleus. É. E. Berlovich, V. N. Klement'ev, V. G. Fleĭsher, O. V. Larionov, F. Sh. Murtazin, and D. A. Apostolov — 855.
Gamma Rays from a $Po-O^{18}$ Neutron Source. É. M. Tsenter, A. G. Khabakhpashev, and I. A. Pirkin — 806L.
Intensity Rules for Beta Transitions to Different Rotational States of Even-even Daughter Nuclei. A. S. Davydov — 98.
Measurement of the Degree of Longitudinal Polarization of Beta Particles. L. A. Mikaélyan and P. Ya. Spivak — 831L.
Polarization β-γ Correlation in Beta Decay of Co^{60}. M. I. Lobashev, V. A. Nazarenko, and L. I. Rusinov — 1277L.
Positron Spectrum of Eu^{152} and Eu^{152m}. S. F. Antonova, S. S. Vasilenko, M. G. Kaganskiĭ, and D. L. Kaminskiĭ — 477.
Radioactive Decay of Ac^{227} and Excited Levels of Fr^{223} and Th^{227}. G. I. Novikova, E. A. Volkova, L. L. Gol'din, D. M. Ziv, and E. F. Tret'yakov — 663.
Radioactive Decay of Ag^{110m}. N. M. Anton'eva, A. A. Bashilov, and E. K. Kulakovskiĭ — 1063.
Second Forbidden Coulomb Beta-decay Transitions. Yu. V. Gaponov — 109.
The Proton Subshell $Z = 100$. N. N. Kolesnikov and A. P. Krylova — 389L.
The Spectrum of Internal Conversion Electrons Accompanying Alpha Decay of U^{233} and the Level Scheme of Th^{229}. E. F. Tret'yakov, M. P. Anikina, L. L. Gol'din, G. I. Novikova, and N. I. Pirogova — 656.
Transition Radiation Effects in Particle Energy Losses. G. M. Garibyan — 372.
Transition Radiation in Waveguides. K. A. Barsukov — 787.

Range and Energy Loss of Particles
Collective Losses of Fast Electrons in Passage through Matter. V. P. Silin — 192.
Field of a Charged Particle in a Moving Medium. B. M. Bolotovskiĭ and A. A. Rukhadze — 958.
Limits of Applicability of the Theory of Transition Radiation. G. M. Garibyan and I. Ya. Pomeranchuk — 1290L.
Measurement of Energy Loss of Fast Electrons Penetrating through Matter. N. A. Grishaev, A. N. Fisun, A. S. Litvinenko, V. M. Grizhko, B. I. Shramenko, and I. N. Onishchenko — 1031L.
On Certain Singularities in the Interaction with Light Nuclei of Particles with Energies $E \geq 2 \times 10^{12}$ ev. N. L. Grigorov and V. Ya. Shestoperov — 816L.
Range-energy Relation for Some Substances. M. Z. Maksimov — 90.
Transition Radiation Effects in Particle Energy Losses. G. M. Garibyan — 372.

Rectifiers (see Electrical Conductivity and Resistance;

Relativity and Gravitation
A Generally Covariant Method of Successive Approximations in General Relativity. I. I. Gutman — 1162.
Absorption of Sound and the Width of Shock Waves in Relativistic Hydrodynamics. M. T. Zhumartbaev — 711.
Contribution to the Theory of Relativistically Invariant Equations. L. A. Shelepin — 1153.
On Linear Theories of Gravitation. V. I. Pustovoĭt — 619L.
On the Distribution Function for Dissipative Processes in a Rarefied Relativistic Gas. S. S. Moĭseev — 391L.
Possibility of Measuring the Velocity of Propagation of Gravitation in the Laboratory. I. L. Bershteĭn and M. E. Gertsenshteĭn — 1293L.
Propagation of a Strong Electromagnetic-gravitational Wave in Vacuo. A. S. Kompaneets — 1218.
Relativistic Spherical Functions. II. A. Z. Dolginov and I. N. Toptygin — 1022.
Relativistic Spherical Functions, III. A. Z. Dolginov and A. N. Moskalev — 1202.
Taking Account of the Gravitational Energy. D. D. Ivanenko and N. V. Mitskevich — 618L.

Resistance, Electrical (see Electrical Conductivity and

Resonance Radiation (see Radiation)

Scattering, General (see also Elementary Particle Interactions; Nuclear Reactions; Range and Energy Loss of Particles)
Analyticity and Unitarity in the Scattering of Scalar Mesons from a Static Nucleon. B. L. Ioffe — 1245.
Dispersion Relations for the Scattering of Gamma Quanta by Nucleons. L. I. Lapidus and Chou Kuang-Chao — 1213.
Inelastic Scattering of Nucleons on Mg^{24} and Si^{28} Nuclei. V. I. Mamasakhlisov and T. I. Kopaleĭshvili — 93.
Excitation of Nuclear Vibrational and Rotational States in the Scattering of Charged Particles. E. A. Romanovskiĭ — 59.
Excitation of Rotational States of Nonaxial Nuclei in Alpha-particle Scattering. E. A. Romanovskiĭ — 606L.
Maximum Atomic Cross Sections for Nonresonance Charge Exchange. N. V. Fedorenko and V. A. Belyaev — 1276L.
Nuclear Reactions Induced by Heavy Ions. J. H. Fremlin and J. S. Lille — 229L.
On the Inclusion of Exchange in the Theory of Collisions. R. K. Peterkop — 834L.
On the Methods of Born and Pais for Finding Phase Shifts. T. Titts — 207L.
On the Phase of the Scattered Wave (A Reply to V. V. Malyarov). F. S. Los' — 836L.
Optical Anisotropy of Atomic Nuclei. A. M. Baldin — 142.
Raman Scattering of Electromagnetic Waves in Ferromagnetic Dielectrics. F. G. Bass and M. I. Kaganov — 986.

Resonance Charge Exchange of Doubly Charged Ions in Slow Collisions. I. K. Fetisov and O. B. Firsov — 67.
Scattering of a Proton by a Nucleon in the One-meson Approximation. E. D. Zhizhin — 707.

Scattering of Alpha Particles
Alpha Spectrum of the Natural Samarium Isotope Mixture. A. A. Vorob'ev, A. P. Komar, V. A. Korolev, and G. E. Solyakin — 386L.
Excitation of Nuclear Vibrational and Rotational States in the Scattering of Charged Particles. E. A. Romanovskiĭ — 59.
Excitation of Rotational States of Nonaxial Nuclei in Alpha-particle Scattering. E. A. Romanovskiĭ — 606L.

Scattering of Deuterons
Capture of Polarized Muons by Deuterons. A. P. Bukhvostov and I. M. Shmushkevich — 1042L.
Measurement of the Polarization of Deuterons in the Reaction $p + p \rightarrow d + \pi^+$ at Proton Energies of 670 Mev. Yu. K. Akimov, K. S. Marish, O. V. Savchenko, and L. M. Soroko — 33.

Scattering of Electrons and Positrons (see also Electrons and Positrons)
Electron-Electron Scattering Cross Section at High Energies. V. N. Baĭer — 1057L.
Inelastic Collision between Fast Polarized Particles and Atoms. V. V. Batygin and I. N. Toptygin — 975.
Measurement of Energy Loss of Fast Electrons Penetrating through Matter. N. A. Grishaev, A. N. Fisun, A. S. Litvinenko, V. M. Grizhko, B. I. Shramenko, and I. N. Onishchenko — 1031L.
On the Inclusion of Exchange in the Theory of Collisions. R. K. Peterkop — 834L.
Polarization β-γ Correlation in Beta Decay of Co^{60}. M. I. Lobashev, V. A. Nazarenko, and L. I. Rusinov — 1277L.
Polarization Effects in the Elastic Scattering of Electrons from Deuterons. G. V. Frolov — 369.
Scattering of Electrons by Light Nonspherical Nuclei. E. V. Inopin and B. I. Tishchenko — 932.
Scattering of Low-energy Electron by Short-range Potential in Strong Magnetic Field. V. G. Skobov — 1039L.

Scattering of Mesons (see also Nuclear Reactions Induced by Mesons)
Cross Sections for Elastic Scattering of 195-Mev Positive Pions by Carbon and Lithium Nuclei. V. G. Ivanov, V. T. Osipenkov, N. I. Petrov, and V. A. Rusakov — 615L.
Dispersion Relations for Inelastic Processes Involving K Mesons. J. Wolf — 980.
Elastic Scattering of 5 — 22 Mev π^+ Mesons on Carbon. V. G. Kirillov-Ugryumov, L. P. Kotenko, E. P. Kuznetsov, F. M. Sergeev, and A. F. Grashin — 907.
Elastic Scattering of 390 Mev π^+ Mesons from Protons. E. L. Grigor'ev and N. A. Mitin — 1123.
Inelastic Collisions between Fast Polarized Particles and Atoms. V. V. Batygin and I. N. Toptygin — 975.
Inelastic Interaction of π^+ Mesons with Light Nuclei in the Energy Region 80 — 300 Mev. A. G. Meshkovskiĭ and Ya. Ya. Shalamov — 697.
Inelastic Scattering and Absorption of (195 ± 15)-Mev Positive Pions by Carbon and Lithium Nuclei. N. I. Petrov, V. G. Ivanov, and V. A. Rusakov — 682.
π^--p Interaction at 1.4 Bev. V. I. Rus'kin — 74.
Polarization of Recoil Protons Produced in Elastic Scattering at 307 Mev. E. L. Grigor'ev and N. A. Mitin — 295.
Resonance Interaction of Pions. V. S. Barashenkov and V. M. Mal'tsev — 630L.

Scattering of Neutrons (see also Nuclear Reactions Induced by Neutrons)
Elastic Scattering of 8.7-Bev Protons by Photoemulsion Nuclei. B. P. Bannik, V. G. Grishin, M. Ya. Danysh, V. B. Lyubimov, and M. I. Podgoretskiĭ — 1118.
On the Collisions of Nucleons with Large Orbital Angular Momentum. A. D. Galanin, A. F. Grashin, B. L. Ioffe, and I. Ya. Pomeranchuk — 1179.
Polarization of (d-d) Neutrons. P. S. Otstavnov — 1281L.
Variation of Angular Distributions of Neutrons Elastically Scattered from He^3. A. I. Abramov — 1046L.

Scattering of Protons (see also Nuclear Reactions Induced by Protons)
Angular Distribution of Shower Particles in Stars Produced by High-energy Particles. L. A. San'ko, Zh. S. Takibaev, Ts. I. Shakhova, and L. Ya. Balats — 1.
Determination of the p-p Scattering Matrix at 90°. S. B. Nurushev — 212L.
Elastic Proton-Proton Scattering at 8.5 Bev. V. B. Lyubimov, P. K. Markov, É. N. Tsyganov, Cheng P'u-Ying, and M. G. Shafranova — 651.
Elastic Scattering of 630-Mev Neutrons by Protons. N. S. Amaglobeli and Yu. M. Kazarinov — 1125.
Interaction of 9-Bev Protons with Free and Quasifree Nucleons in Photographic Emulsions. N. P. Bogachev, S. A. Bunyatov, I. M. Gramenitskiĭ, V. B. Lyubimov, Yu. P. Merekov, M. I. Podgoretskiĭ, V. M. Sidorov, and D. Tuvdendorzh — 872.
Nuclear Interactions of 8.7-Bev Protons in Photographic Emulsions. G. B. Zhdanov, V. M. Maksimenko, M. I. Tret'yakova, and M. N. Shcherbakov — 442.
On the Collisions of Nucleons with Large Orbital Angular Momentum. A. D. Galanin, A. F. Grashin, B. L. Ioffe, and I. Ya. Pomeranchuk — 1179.
Scattering of 5 — 10 Mev Protons on He^3. K. P. Artemov, S. P. Kalinin, and L. N. Samoĭlov — 474.
Theoretical Interpretation of Inelastic (pp) and (pn) Collisions at 9 Bev Energy. V. S. Barashenkov, V. M. Mal'tsev, and É. K. Mikhul — 1052L.
Use of the (d, p) Reaction to Excite States with Large Spins. V. G. Neudachin, I. B. Teplov, and A. F. Tulinov — 387L.

Scattering of Radiation (see Radiation)
Scintillation Counters (see Methods and Instruments)
Secondary Emission (see Electrical Properties)
Semiconductors
Electron Resonance in Crossed Electric and Magnetic Fields. I. M. Lifshitz and M. I. Kaganov — 392L.
Faraday Effect in Semiconductors on Free Carriers in a Strong Magnetic Field. L. É. Gurevich and I. P. Ipatova — 943.

Kinetic Theory Impact Ionization in Semiconductors. L. V. Keldysh — 509.
Quantum-mechanical Semiconductor Generators and Amplifiers of Electromagnetic Oscillations. N. B. Basov, B. M. Vul, and Yu. M. Popov – 416L.
Radiative Recombination in Germanium Crystals Bombarded by Fast Electrons. V. S. Vavilov, A. A. Gippius, M. M. Gorshkov, and B. D. Kopylovskiĭ — 15.
The Influence of Collisions between Electrons on their Velocity Distribution in Gases and in Semiconductors in an Electric Field. A. V. Gurevich — 215L.

Solid State (see Crystalline State)
Solutions (see Liquids)
Sound (see Acoustics)
Spallation (see Nuclear Reactions)
Spark Discharge (see Electrical Discharges)
Spectra, Atomic (see Atomic Structure and Spectra)
Spectra, General
Concentration of Charged Particles in Plasma of Spark-discharge Channel. A. A. Mak — 1055L.
Gamma Rays from a Po-O^{18} Neutron Source. É. M. Tsenter, A. G. Kahabakhpashev, and I. A. Pirkin — 806L.
Shortwave Radiation from a Vacuum Spark. S. V. Lebedev, S. L. Mandel'shtam, and G. M. Rodin — 248.
Spectra, Nuclear (see Nuclear Spectra)
Spectroscopy Technique (see Methods and Instruments)
Spinor Fields (see Field Theory)
Stark Effect (see Atomic Structure and Spectra)
Statistical Mechanics and Thermodynamics
Classification of Molecular Terms with Respect to Total Nuclear Spin. E. G. Kaplan — 747.
Collective Losses of Fast Electrons in Passage through Matter. V. P. Silin — 192.
Condensation of a Cloud of Vaporized Matter Expanding in Vacuum. Yu. P. Raĭzer — 1229.
Concentration Jump in Slow Evaporation of a Mixture. R. Ya. Kucherov and L. É. Rikenglaz — 1285L.
Distribution of the Density of Protons in a Nucleus with a Given Angular Momentum. L. P. Rapoport and S. G. Kadmenskiĭ — 929.
Effect of Inelastic Collisions on the Velocity Distribution of Electrons. L. M. Kovrizhnykh — 347.
On Hydrodynamic Boundary Conditions for Evaporation and Condensation. R. Ya. Kucherov and L. É. Rikenglaz — 88.
On Popov's Relation between the Symmetry of Transport Coefficients and Thermodynamics. R. Davies and F. Goodman — 828L.
On the Distribution Function for Dissipative Processes in a Rarefied Relativistic Gas. S. S. Moĭseev — 391L.
Oscillations of an Inhomogeneous Plasma in a Magnetic Field. L. I. Rudakov, and R. Z. Sagdeev — 952.
Relativistic Transport Equations for a Plasma. I. Yu. L. Klimontovich — 524.
Shift in Curie Temperature During Uniform Compression of Manganese and Cobalt Fluorides. D. N. Astrov, S. I. Novikova, and M. P. Orlova — 851.
Theory of Weak Solutions of He^4 in Liquid He^3. V. N. Zharkov and V. P. Silin — 102.
Statistical Methods (see Mathematical Methods)
Superconductivity
A Simple Model in the Theory of Superconductivity. Yu. B. Rumer — 409L.
Analysis of Experimental Data Relating to the Surface Impedance of Superconductors. A. A. Abrikosov, L. P. Gor'kov, and I. M. Khalatnikov — 132.
Destruction of Superconductivity in Thin Films by Field and Current. N. I. Ginzburg and A. I. Shal'nikov — 285.
Effect of Exchange Interaction on the Superconductor Transition Temperature. S. V. Vonsovskiĭ and M. S. Svirskiĭ — 1060L.
Investigation of Thermal Properties of Superconductors, III. Anisotropy of Thermal Conductivity of Gallium. N. V. Zavaritskiĭ — 1069.
Investigation of X-ray Spectra of Superconducting CuS. I. B. Borovskiĭ and I. A. Ovsyannikova — 1033L.
On Taking the Coulomb Effect into Account in the Theory of Superconductivity. D. V. Shirkov — 127.
On the Intermediate State of Ferromagnetic Superconductors. G. F. Zharkov — 1259.
On the Superconductivity of the Compound BiPt. N. N. Zhuravlev, A. A. Stepanova, and N. I. Zyuzin — 627L.
On the Zone Energy Spectrum in the Presence of a Magnetic Field. G. E. Zil'berman — 1029.
Superconductivity of Beryllium and Its Low-temperature Polymorphism. B. G. Lazarev, A. I. Sudovtsev, and E. E. Semenenko — 1035L.
The Critical Supercooling Field in Superconductivity Theory. L. P. Gor'kov — 293.
The Use of a Superconducting Ring for Registering the Phase Transition in Liquid Helium. B. N. Esel'son and A. D. Shvets — 228L.
Two-particle Excitations of Superfluid Fermi-Systems. Yu. V. Tsekhmistrenko — 829L.
Ultrasonic Absorption in Metals in a Magnetic Field. I. V. L. Gurevich — 51.
Thermal Properties
Anomalous Heat Capacity and Nuclear Resonance in Crystalline Hydrogen in Connection with New Data on Its Structure. S. S. Dukhin — 1054L.
Concentration Jump in Slow Evaporation of a Mixture. R. Ya. Kucherov and L. É. Rikenglaz — 1285L.
Magnetostriction of Antiferromagnetic Nickel Monoxide. K. P. Belov and R. Z. Levitin — 400L.
Shift in Curie Temperature During Uniform Compression of Manganese and Cobalt Fluorides. D. N. Astrov, S. I. Novikova, and M. P. Orlova — 851.
The Use of a Superconducting Ring for Registering the Phase Transition in Liquid Helium. B. N. Esel'son and A. D. Shvets — 228L.
Thermoelectric Phenomena in Strong Magnetic Fields in Metals Possessing Various Fermi Surfaces. Yu. A. Bychkov, L. É. Gurevich, and G. M. Nedlin — 377.
Thermionic Emission (see Electrical Properties)
Thermodynamics (see Statistical Mechanics and Thermodynamics)
Thermoelectric Effect (see Electrical Properties; Semiconductors)
Total Cross Sections (see Electrons and Positrons; Nuclear Reactions)
Uncertainty Principle (see Quantum Mechanics)

Vacuum Tubes (see Methods and Instruments)
Viscosity (see Liquids)
Wave Mechanics (see Quantum Mechanics)
Work Function (see Electrical Properties)
X-rays
- Anomalous Heat Capacity and Nuclear Resonance in Crystalline Hydrogen in Connection with New Data on Its Structure. S. S. Dukhin — 1054L.
- Diffraction of X-rays by Polycrystalline Samples of Hydrogen Isotopes. V. S. Kogan, B. G. Lazarev, and R. F. Bulatova — 485.
- Investigation of X-ray Spectra of Superconducting CuS. I. B. Borovskiĭ and I. A. Ovsyannikova — 1033L.
- Optical Anisotropy of Atomic Nuclei. A. M. Baldin — 142.

ERRATA TO VOLUME 9

On page 868, column 1, item (e) should read:

(e). Ferromagnetic weak solid solutions. By way of an example, we consider the system Fe-Me with A2 lattice, where Me = Ti, V, Cr, Mn, Co, and Ni. For these the variation of the moment m with concentration c is

$$dm/dc = (Nd)_{Me} \mp 0.642 \ \{8\ (2.478 - R_{Me}) + 6\,|\,2.861 - R_{Me}\,| \mp [\,8\,(2.478 - R_{\mathrm{Fe}}) + 6\,(2.861 - R_{\mathrm{Fe}})]\},$$

where the signs – and + pertain respectively to ferromagnetic and paramagnetic Me when in front of the curly brackets, and to metals of class 1 and 2 when in front of the square brackets. The first term and the square brackets are considered only for ferromagnetic Me. We then have dm/dc = −3 (−3.3) for Ti, −2.6 (−2.2) for V, −2.2 (−2.2) for Cr, −2 (−2) for Mn, 0.7 (0.6) for Ni, and 1.2 (1.2) for Co; the parentheses contain the experimental values.

ERRATA TO VOLUME 10

Page	Reads	Should Read
224, Ordinate of figure	10^{23}	10^{29}
228, Column 1, line 9 from top	3.6×10^{-2} mm/min	0.36 mm/min
228, Column 1, line 16 from top	0.5 mm/sec	0.05 mm/min
329, Third line of Eq. (23a)	+(1/4 cosh r +...	+1/4(cosh r +...
413, Table II, line 2 from bottom	−0.0924 ±	−1.0924 ±
413, Table II, line 3 from bottom	+1.8730 ±	+0.8370 ±
479, Fig. 7, right, 1st line	92 hr	9.2 hr
499, Second line of Eq. (1.8)	$+\tilde{k}\sin^2\alpha/\omega_N^2 + \langle c^2\tilde{k}^2 \ldots$	$+\left(\tilde{k}/\omega_H\right)^2 \sin^2\alpha\ \langle c^2\tilde{k}^2 \ldots$
648, Column 1, line 18 from top	18 × 80 mm	180 × 80 mm
804, First line of Eq. (17)	$-{}^1/_3\,(\alpha_x^2\alpha_y^2 + \ldots$	$\ldots - 3\,(\alpha_x\alpha_y^2 + \ldots$
967, Column 1, line 11 from top	$\sigma(N', \pi) \approx 46\,(N', N')$	$\sigma(N', \pi) > \sigma(N', N')$
976, First line of Eq. (10)	$= \frac{e^2}{3r^2c^4}$	$= \frac{e^2}{3\hbar^2c^2}$
978, First line of Eq. (23)	$\Big[\frac{(2\gamma^2 - 1)^2}{(\gamma^2 - 1)\sin^4(\theta/2)}$	$\Big[\frac{(2\gamma^2 - 1)^2}{(\gamma^2 - 1)^2\sin^4(\theta/2)}$